PATTERNS AND IMPLICATIONS OF STASIS IN TRILOBITES.

Submitted for the degree of Ph.D.

by

Timothy McCormick B.Sc. (Aston University).

Department of Geology & Applied Geology,
University of Glasgow.

ABSTRACT

Stasis may be operationally defined as the occurrence of little or no evolutionary change during an interval of geological time, and is an important consequence of punctuated equilibria. Studies of stasis in the fossil record of necessity address only morphological stasis, and that only in the subset of phenotypic characters preservable in the fossil record. Stasis in single characters may be recognised in fossil taxa by lack of significant change in mean value through an interval of geological time; stasis in multiple characters may be recognised by overlap in morphospace occupation by taxa where morphospace occupation is calculated by multivariate techniques. No quantitative definition is placed on such stasis because of the lack of comparable data on non-static (*i.e.* rapidly evolving) taxa to provide the alternative. Proposed explanations for stasis include: developmental and genetic constraints; environment fidelity; selection of generalist phenotypes in fluctuating environments; stabilising selection (including stabilising species selection); developmental canalisation; effects due to population size and distribution.

Mean generic and specific durations (in myr.) of trilobites originating in the stratigraphical systems Cambrian-Carboniferous of England, Scotland and Wales are, respectively: Cambrian (4.42, 2.13); Ordovician (10.89, 2.06); Silurian (10.34, 3.54), Devonian (4.19, 1.12), Carboniferous, (14.82, 5.74). Distributions of both generic and specific durations are highly positively skewed. Study of the species composition of the longest duration genera (those whose durations exceed the 90% quantile value for the system in which they originated) suggests that species stasis played an important role in the Cambrian and Carboniferous; no clear pattern is revealed for the interval Silurian-Devonian inclusive. Chronostratigraphical range charts are presented for species and genera from England, Scotland and Wales. Study of the durations of Ordovician Laurentian genera in relation to their position on the palaeoslope shows that longest duration genera are eurytopic; their wide geographical and environmental dispersal enabled them to avoid localised factors which caused extinction in more endemic genera.

Taxonomy-independent phylogenetic and morphometric analysis of selected long duration shape conservative genera from the middle to upper Ordovician and Silurian shows that disassociated mosaic evolution in some characters is abundant in all three, superimposed on an almost invariant body plan. *Achatella* Delo, 1935 had a duration of about 22 myr. (upper Llanvirn - Hirnantian, time scale of Tucker *et al.* 1990). Nine species (three new) and one form under open nomenclature have been diagnosed. *Calyptaulax* Cooper, 1930 had a duration of about 25 myr. (lower Llanvirn - upper Rawtheyan, time scale of Tucker *et al.* 1990). Two subgenera are diagnosed, each of duration about 20 myr. (time scale of Tucker *et al.* 1990). The nominate subgenus is well resolved on the cladogram, and five species have been diagnosed. *Calyptaulax*

(Calliops) is unresolved on the cladogram because of a disassociated mosaic pattern of "peripheral" character evolution; ten species have been diagnosed. A sixteenth species could not be assigned to a subgenus. *Acernaspis* Campbell, 1967 had a duration of about 11 myr. (lower Llandovery - Wenlock, time scale of Harland *et al.* 1989). Eighteen species have been diagnosed, three of them new. Several stratigraphical samples of *Ananaspis* Campbell, 1967 have been studied and an hypothesis that this genus arose through neoteny from *Acernaspis* has been confirmed, although not a further hypothesis that progressive neoteny continued throughout the existence of *Ananaspis*. Four *Ananaspis* species have been diagnosed, one of which is new. This does not constitute a complete survey of *Ananaspis*.

The disassociated mosaic pattern of peripheral character states probably reflects differing degrees of developmental canalisation at different levels of phenotypic organisation. The basic body plan is strongly canalised, whereas at "peripheral" levels, less strong canalisation allows emergence of superficial characteristics. This, combined with eurytopic distribution, may keep the taxa adapted to their (various) environments without need for more major evolutionary change.

DECLARATION

This thesis is the result of research carried out between September 1990 and January 1995 in the Department of Geology & Applied Geology, University of Glasgow, under the supervision of Dr. Alan W. Owen.

This thesis is the result of my own independent research and any published or unpublished material used by me has been given full acknowledgement in the text.

Timothy McCormick
February 1995.

ACKNOWLEDGEMENTS

This research project was devised and supervised by Dr. Alan Owen of the Dept. of Geology & Applied Geology, University of Glasgow - the man whose door is always open. His encyclopaedic knowledge of trilobite systematics and Palaeozoic stratigraphy, together with his endless patience have been more than invaluable.

Thanks are due to the technical staff of the department, among whom special mention must be made of Douglas Maclean who produced the large numbers of photographic prints I required, producing excellent results from my often less than excellent photography; and Jim Kavanagh for providing computing support (including on one occasion rescuing some accidentally deleted files - always take backups, people). Roddy Morrison rapidly and efficiently provided whatever materials were necessary at whatever time.

The following people kindly allowed access to, and where necessary, loan of, specimens in their care (in alphabetical order):
Prof. J. Bergström (Naturhistoriska Riksmuseum, Stockholm); Dr. D. L. Bruton (Paleontologisk Museum, Oslo); Dr. E. N. K. Clarkson (Grant Institute of Geology, Edinburgh); Dr. L. R. M. Cocks (The Natural History Museum, London); F. Collier (Museum of Comparative Zoology, Harvard University); M. Dorling (Sedgwick Museum, Cambridge); Dr. D. A. T. Harper (University College, Galway); Dr. H. C. Ivimey-Cook (British Geological Survey, Keyworth); Dr. A. Jeram (Ulster Museum, Belfast); M. Jewkes (Hunterian Museum, Glasgow University); A. Koller (Carnegie Museum, Pittsburgh); Dr. C. Labandeira (United States National Museum, Washington DC); E. Landing (New York State Museum); Dr. R. M. Owens (National Museum of Wales, Cardiff); Dr. I. W. Rohlf (Royal Scottish Museum, Edinburgh); Dr. M. P. Smith (Lapworth Museum, Birmingham University); Dr. S. Tunnicliff (Trinity College, Dublin); J. Waddington (Royal Ontario Museum, Toronto); R. D. White (Peabody Museum of Natural History, Yale University).

No thanks at all to the Canadian Geological Survey.

I have benefited greatly from discussions with a number of palaeontologists who generously gave of their time, enthusiasm, and experience (in alphabetical order):
Dr. D. L. Bruton (who even lent me his office for a few days); Dr. N. D. L. Clark; Dr. R. A. Fortey; Dr. N. C. Hughes; Dr. J. K. Ingham; Dr. V. Jaanusson; Dr. K. G. Johnson; Dr. A. W. A. Rushton; Dr. P. R. Sheldon.

In the course of my travels a number of thoroughly excellent people gave me a free place to kip (alphabetical order again):
Fred and Martha Collier (Boston, Mass - "The home for itinerant paleontologists"); Nigel Hughes (Washington DC); Ian and Maddie McCormick (London, several occasions); Betsey Robinson (Boston, Mass).

Thanks to all the other postgrads (and one or two undergrads too) too numerous to name who fought the battle to keep me (reasonably) sane during the long dark days of writing up, and for keeping me smiling (most of the time).

Thanks to my parents for their support - they know I think more of them than I ever say.

NERC research studentship GT4/90/GS/52 is gratefully acknowledged.

So anyway, there was this bunch of trilobites that refused to evolve like they should have done ...

CONTENTS

Page

APPENDICES.

LIST OF FIGURES

LIST OF TABLES

LIST OF PLATES

CHAPTER ONE

INTRODUCTION.

1. 1. Introduction.

> "And what of species? Can a species die of old age? Has any species died out because it has grown old, going peacefully in its sleep, as it were? ... do some species survive for a very long time because of good genes or good luck?"
>
> Ward (1992)

Recognition of the importance and predominance of stasis in the fossil record was perhaps the most important aspect to emerge from the punctuated equilibria debate which was begun by Eldredge and Gould (1972). The questions surrounding the phenomenon of morphological stasis in the fossil record are perhaps best illustrated by the so-called "living fossils".

The term "living fossil" was first coined by Darwin (1859) in the *Origin of Species*. The term is used to refer to extant representatives of taxa that have survived with relatively little change over a long span of geological time (Fisher 1990). Living fossils provided a problem for Darwin. Under his theory of evolution through the action of natural selection, species should exhibit gradual and continuous change through geological time, and fossils should exhibit the same sort of continuous change through the stratigraphical record. Darwin was able to explain away the sudden appearance of new species in the fossil record (such as occurs after the biotic crises at the Permo-Triassic and Cretaceous-Tertiary boundaries, both levels of faunal replacement which were well-known in Darwin's day) as an artefact caused by the incomplete nature of deposition in the geological record. However the phenomenon of living fossils, which appeared to show no evolution at all for long time periods, troubled Darwin, and provided ammunition for his contemporary critics (Ward 1992).

The measurement of rates of evolution in the fossil record was pioneered by G. G. Simpson (e.g. 1953) who recognised that there are essentially three ways to measure such rates:

(i) Genetic rates. Simpson envisaged measurement of the rate at which gene frequencies change within an evolving population. In Simpson's day the necessary techniques were only beginning to be developed (Ward 1992). Today, as well as measuring rates of gene frequencies, rates of nucleotide substitutions within genes can also be measured. These rates can be measured over successive generations of living organisms in the laboratory, or alternatively the cumulative divergence between contemporaneous taxa can be measured to provide an "evolutionary distance" between them (Fisher 1990).

(ii) Morphological rates. These are rates at which individual morphological characters, or complexes of characters, change. More recently developed techniques allow subdivision of morphological variation into "size" and "shape" variation (see for example discussion of principal component analysis in Chapter 4 of this study).

(iii) Taxonomic rates. The study of taxonomic rates of evolution involves measurement of rates of origination and extinction of taxa. In the case of phyletic evolution as envisaged by Darwin and the neo-Darwinians (see for example Hoffman 1989), high rates of taxonomic evolution result in large numbers of taxa of short duration. However, where production of new taxa through lineage splitting (cladogenesis) is considered to play a role (as for example by the proponents of the punctuated equilibria model of evolution, e.g. Eldredge and Gould 1972; Gould and Eldredge 1993) then taxonomic origination rates will include two components: a lineage transformation component and a lineage splitting component, the relative contributions of which are difficult to quantify (Fisher 1990).

Simpson (1944, 1953) argued for three discrete rates of evolution, based on his observations of morphological and taxonomic rates:

(i) A fast rate, exhibited by a relatively small number of the taxa in any sufficiently inclusive group ("Tachytely");

(ii) An intermediate rate, exhibited by the majority of taxa in any sufficiently inclusive group ("Horotely");

(iii) A slow rate, exhibited by a relatively small number of the taxa in any sufficiently inclusive group ("Bradytely"). Taxa exhibiting this slowest rate of evolution may show little or no change through time at all (Fisher 1990; Ward 1992).

For example, Simpson (1953) showed that mammals tend to have relatively high rates of taxonomic evolution, with genera lasting on average around 8 myr., whereas bivalve molluscs show much lower rates, with genera lasting on average around 80 myr. Simpson's discrete multi-modality of evolution rates has more recently been shown to be flawed (Gingerich 1983; Stanley 1985) but the terminology and concept of differing rates of evolution is still informally used (Fisher 1990).

So it has been known since Darwin's time (and even before) that there are, and have been in the past, taxa which have evolved only very slowly or effectively not at all. Under the neo-Darwinian model of evolution, the question which arises is: why should some taxa evolve at such a low rate (Ward 1992)?

Under the punctuated equilibria model of evolution (Eldredge and Gould 1972) the majority of change in a lineage is concentrated in geologically brief periods of speciation, with little or no change occurring between speciation events. The degree of morphological change exhibited by a lineage in a given time interval is then related to the number of speciation events which have occurred. According to this view, living fossils and long-term static taxa belong to lineages in which few speciation events have taken place (Ward 1992). Stanley (1979) characterised living fossils as follows:

(i) organisms which have survived for relatively long periods of geological time represented by only one or a few species, often as sole survivors of previously diverse taxa;

(ii) they must today exhibit primitive morphological characters, having undergone little evolutionary change since dwindling to low diversity at some time in the past.

Therefore, under the punctuated equilibria model of evolution, the question which arises is: why have these static taxa undergone so few speciation events (Ward 1992)?

1. 2. Definition of Stasis and its Recognition in the Fossil Record.

The term "stasis" tends to be used rather loosely by palaeontologists. The Concise Oxford Dictionary of Earth Sciences (1990) defines stasis as follows: "Period of little or no evolutionary change". Maynard Smith (1983: 11) defined the term in a very similar way, except that he concentrated on the morphological aspect: "period ... during which little or no morphological change takes place". Hoffman (1989: 115 - writing with particular reference to the punctuated equilibria model) spoke of a "very long period of evolutionary stasis, when the species remains in homeostasis with its environment and essentially does not evolve, thus maintaining its identity and even individuality". The word "stasis" is therefore used, rather informally, to refer to a lack of evolutionary change through some time interval. It has not normally been considered to be a process in its own right.

Levinton (1983) drew a distinction between what he termed "species stasis", the maintenance of the species phenotype without change for a significant period of time, and "character stasis", a lack of change in individual characters through time, noting that species stasis implies character stasis for all characters. Hoffman (1989) argued that true evolutionary stasis (*i.e.* species stasis of Levinton 1983) cannot be tested in the fossil record, since the data on evolution in fossils consists only of a small sample of preservable phenotypic characters for each taxon. There is always the possibility that the non-preservable soft parts of the phenotype underwent considerable change which is

completely undetectable in the fossil record. Hoffman (1989) quoted the examples of extant snail species which differ only in the anatomy of the foot or digestive tract, and extant spider species which differ only in their genital structures, characters unpreservable in the fossil record. Further, it is of course impossible to draw inferences about changes in a fossil species' gene pool, and rarely possible to draw inferences about the relative frequencies of different phenotypes within the fossil taxon, on the basis of the small subset of phenotypic characters preserved (Hoffman 1989). Behavioural stasis and plasticity, such as that studied in extant plethodontid salamanders by Wake *et al.* (1983), is similarly impossible to detect in the fossil record.

Thus any test of stasis in fossil taxa can focus only on morphological stasis, and even then only on the subset of morphological characters which are preservable. In testing whether a taxon has undergone morphological stasis (either in all preservable characters or only in a subset of them), it is necessary first to define morphological stasis. Hoffman (1989) noted that stasis must not simply be equated with the persistence of a certain phenotype within the boundaries set by a taxonomist for recognition of that taxon, since this would just mean that every taxon remains in stasis throughout its entire duration. Lande (1986) arbitrarily defined morphological stasis in a single measurable character, as measured in a stratigraphical series of populations, as a deviation of the mean value of that character of less than two standard deviations from the mean value shown by the stratigraphically earliest population. Lande considered such a definition to coincide more or less with the limits set on subspecies disparity by modern zoologists. Hoffman (1989) however considered such a definition to be too highly dependent on the amount of variation shown by the earliest population. Hoffman also noted that sample size at each stratigraphical level becomes critical under such a definition, since if the samples are too small then a statistical test may be unable to reject a null hypothesis that the means of two samples vary by less than two standard deviations (or whatever criterion is being used), whatever the actual observed mean values are. A further complicating factor is added by the fact that samples in the fossil record tend to be lumped, containing individuals which may have existed many generations apart, and this may act to diminish the true amount of variation between successive populations (Hoffman 1989).

Foote (1989, 1990, 1991a, perimeter-based Fourier analysis; 1991b, principal component analysis) and Labandeira and Hughes (1994, nonmetric multidimensional scaling) demonstrated that multivariate analyses of form can be used to quantify morphospace occupation in invertebrate fossils and hence estimate morphological similarity or disparity between specimens and groups of specimens. This approach has the advantage over "single character" approaches of allowing of combinations of many

characteristics of the preserved phenotype to be studied simultaneously. In the present study, multivariate morphometrics have been undertaken on samples of fossils selected from stratigraphically and geographically separate locations, and principal component analysis (PCA) has been used to erect a morphospace in which the samples can be objectively compared and contrasted. This study is therefore entirely independent of existing taxonomy. In this way, the pitfall noted by Hoffman (1989) of simply equating stasis to the persistence of a phenotype within the boundaries set by a taxonomist for recognition of that species, is avoided.

No attempt has been made here to attach an explicit quantitative definition to morphological stasis in phylogenetic and morphometric terms. This is because of the difficulty encountered in defining an adequate "cut-off" between "stasis" and "non-stasis" (see Hoffman's comments on Lande's quantitative definition of morphological stasis, above), and also because such a cut-off would be highly arbitrary and artificial. Further, a quantitative multivariate definition of "stasis" requires an alternative of "non-stasis", and no comparable morphometric data for such rapidly evolving taxa yet exist. Rather, "stasis" is used herein as a notional concept, recognised in the fossil record by an apparent absence of significant morphological change through a significant period of geological time. Such a definition is necessarily subjective, but there does appear to be general agreement among palaeontologists as to what constitutes morphological stasis.

That stasis is common in the fossil record is not disputed, although proponents of neo-Darwinism and punctuated equilibria may argue over its relative abundance. What is now becoming a topic of debate is the mechanism governing stasis, and its implications for evolutionary theory (Hoffman 1989).

1. 3. Proposed Explanations for Stasis.

What discussion of the phenomenon of stasis there has been in the literature has been almost entirely of a theoretical nature and has taken place in an almost complete absence of data concerning the nature of stasis in the fossil record. The proposed mechanisms can be grouped into a number of broad categories (Table 1. 1) which are briefly discussed below. It is important to note that these categories are in no way mutually exclusive, and stasis may ultimately be controlled by a combination of the listed factors. Indeed, some of the factors overlap with one another to greater or lesser degrees.

1. 3. 1. Developmental and Genetic Constraints.

Developmental constraints were defined by Maynard Smith *et al.* (1985) as "a bias in the appearance of phenotypic variants in a species, where the bias has no relation

Table 1. 1. Proposed mechanisms for stasis.

Mechanism	**Intrinsic/Extrinsic to organism**	**Predicted Variability Patterns**
Developmental constraints	Intrinsic	Low intraspecific morphological variation.
Climate fidelity	Extrinsic	No predicted pattern
Stabilising selection	Extrinsic	Low intraspecific morphological and genetic variability.
Stabilising species selection	Extrinsic	No predicted pattern
Developmental canalisation	Intrinsic	Low intraspecific morphological variation, high genetic variation.
Homeostasis due to population size	Extrinsic	Low intraspecific morphological and genetic variability.

whatsoever to the species' adaptive requirements". Such occurrences seem to reflect intrinsic controls on an organism's ontogenetic development. It has been envisaged that such controls could cause stasis by imposing a resistance to change in phenotypic development which allows minor adjustments to be made but not major shifts (Hoffman 1989), in spite of the more or less constant state of flux within the genome (Schopf 1981).

Such internal controls would arise partly as a result of the past history of the evolving population, and partly as a result of the processes and controls which govern individual development. The constraints arising from the past evolutionary history of the population were termed "initial conditions" by Hoffman (1989) and include such factors as: the nature of phenotypic variation within the population (which is underlain by, but not exclusively determined by, the nature of variation in the genome); the pattern of individual ontogenetic development; the nature of the organism-environment interaction. These constraints provide the "starting point" on which natural selection acts. Constraints arising from the processes and controls on individual development were termed "boundary" conditions by Hoffman (1989). Again, variation in the genome, the pattern of ontogenetic development, and the nature of the interaction between the developing organism and the environment are probably important (Hoffman 1989).

Such constraints may allow continuous variation in the development of the phenotype, or they may allow only discontinuous variation (Maynard Smith 1983). Constraints allowing continuous variation in the phenotype do not explain stasis (*i.e.* they may serve to constrain the morphological "direction" in which changes are possible, but they do not explain cases of stasis, where little or no change occurs). Maynard Smith (1983) therefore considered constraints which cause discontinuous variation in the phenotype to be potentially more important in controlling stasis. Maynard Smith noted that there are essentially two ways of achieving this:

(i) Continuous variation in some genome variable, on eventually crossing a threshold value, might cause a discrete shift in some other parameter controlling phenotypic development.

(ii) Introduction of some new element for genetic regulation which changes the way in which genes are activated.

Considering the genome as a whole, such a process of discontinuous variation could operate through the "cohesive genotype" of Mayr (1982). Each gene must be viewed as a member of its "genetic milieu"; *i.e.* it's environment of neighbouring, highly interlinked and interacting genes. It is possible that major mutations within the genome

could be compensated by shifts in the cohesion of the whole, so that in spite of the change, there may be no alteration in the consequent phenotype. Such a cohesive genome could maintain morphological stasis in the phenotype in spite of significant gene mutations. To overcome the cohesion, some major "genetic revolution" may be required which would cause the breakdown of the current genomic cohesion and a shift to a new balanced system (Mayr 1982). This revolution may not require a major (e.g. chromosomal) mutation; a small point mutation may be enough, if it is the *right* small point mutation.

Hoffman (1989) considered that the occurrence of extensive intraspecific variation in morphological characters as measured in extant and fossil organisms indicates that developmental constraints alone cannot provide an explanation for stasis at the species level. Lande (1986) expressed a similar opinion, and also noted that measurable characters in extant populations display rapid and significant response to artificial selection.

1. 3. 2. Environment Fidelity.

A conceptually simple way to maintain stasis in a lineage over long time periods is to hold the environment in which the organism lives, or at least those aspects of the environment which have a selective impact on the organism in question, constant. It is considered infeasible by many workers to expect the physical environment to remain constant for the kinds of time spans involved in morphological stasis (Hoffman 1982). However during times of global or local environmental change, rather than remaining in the same place and adapting to the new conditions, organisms tend to track the habitat to which they are already adapted by a process of population growth in favourable areas and population decline in unfavourable ones. In this way, fluctuations in selection pressures due to the changing environment are reduced unless the favourable habitat is completely closed off (either because of elimination or occupation by a competing species), or the organism is somehow prevented from tracking it (Lande 1986; Hoffman 1989). Hoffman (1989) gave the example of migration by benthonic invertebrate faunas inhabiting the North American continental shelf to track habitats moving in response to glacial episodes.

Sheldon (1990) suggested that in widely fluctuating environments (on geological timescales) selection might favour lineages with "all-purpose" hard part morphologies which are relatively immune to the environmental perturbations. Such lineages could experience a widely fluctuating environment as "stable" (with respect to their environmental needs) until some threshold in environmental conditions is reached. The model goes on to suggest that in less widely fluctuating environments, organisms need

not be generalists and can be more specialised, but this has the effect of causing them to be more sensitive to minor environmental fluctuations (which may be too minor to be recorded in the geological record), and thus more prone to cladogenesis or extinction (Figure 1. 1). The model therefore predicts stasis in widely fluctuating environments, such as near shore shallow marine environments, and more continuous phyletic evolution in narrowly fluctuating environments, such as the deep offshore benthonic environment.

1. 3. 3. Effects of Stabilising Selection.

Neo-Darwinian evolutionary scientists have traditionally viewed stabilising selection as the major cause of morphological stasis (Charlesworth *et al.* 1982; Hoffman 1989). Assuming that those aspects of the environment which have a selective impact on the organisms in question remain approximately constant over a relatively long time span, the early stages of adaptation towards an adaptive peak will see directed selection in a lineage as certain traits are consistently selected. Subsequently, as the population approaches the adaptive peak, individuals whose phenotypes are closest to the population mean are the fittest, so that the early directed selection is replaced by a stabilising selection which holds the population in stasis until the relevant aspects of the environment undergo some change (Hoffman 1989).

It is helpful here to consider the "environment" in terms of two primary components (Maynard Smith 1983). An organism's "physical environment" is characterised by palaeobiologists in terms of a relatively small number of physical parameters. For example in marine organisms, which form the vast majority of the fossil record, these may be: temperature, salinity, nature of the substrate (in benthonic organisms), oxygen abundance. Other factors such as homogeneity or heterogeneity of the environment may play a contributory role. An organism's "biological environment" is made up by the other organisms with which the organism interacts, such as competitors for resources, predators, prey, and parasites; *i.e.* all the other constituents of the ecosystem on which the organism in question imposes selection pressures, and which impose selection pressures on the organism in question. Both of these environmental components may play a role in imposing stabilising selection pressures (see for example Brett and Baird 1992; Morris *et al.* 1992).

Barnard (1984) pointed out that descriptions such as that given above for stabilising selection imply that the organism-environment interaction is a one-way relationship in which the environment is considered to already exist before the organism is inserted into it. In reality, the organism and the environment are co-evolved. Organisms change their physical and biological environment to varying degrees by constructing shelters,

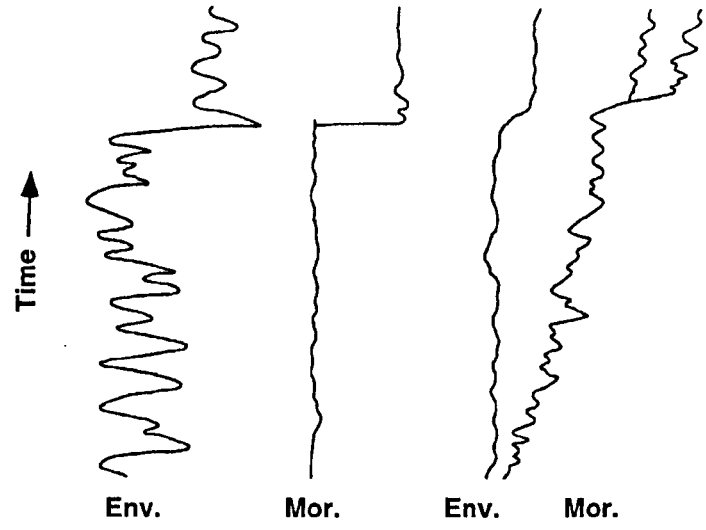

Figure 1. 1. Model to illustrate the hypothesis of Sheldon (1990) that persistent phyletic evolution is more characteristic of narrowly fluctuating environments (right) whereas stasis tends to prevail in more widely fluctuating environments (left). Env.= some long term aspect of the environment, such as sea level or temperature; Mor.= some aspect of hard part morphology. Redrawn from Sheldon (1990).

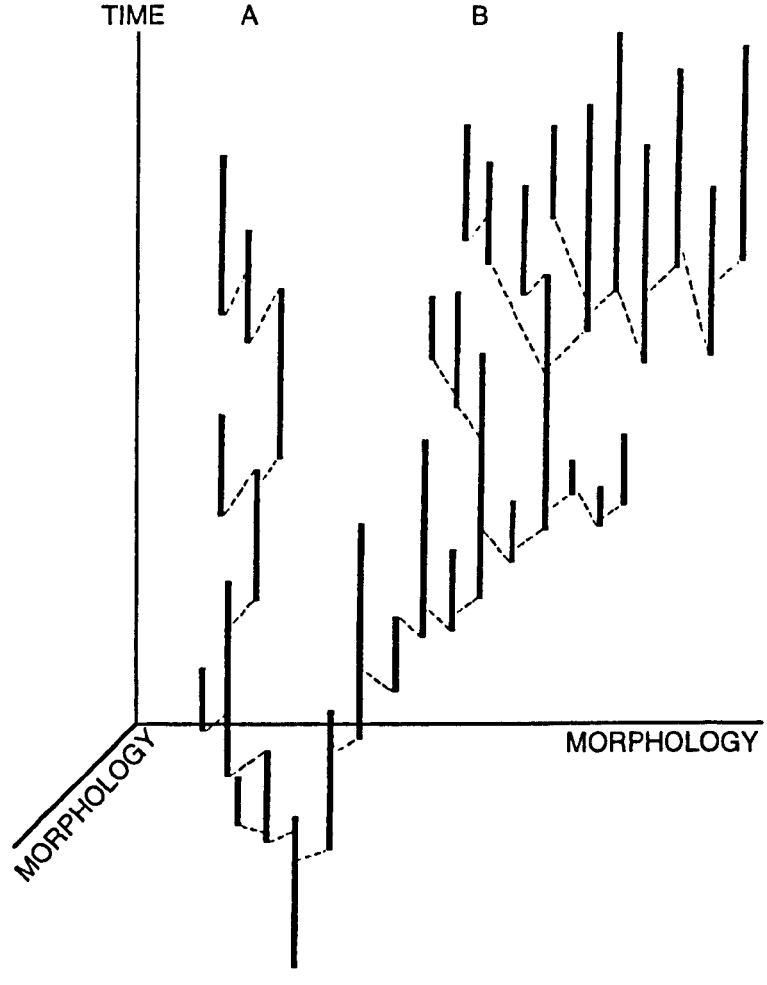

Figure 1. 2. Three dimensional sketch showing approximate morphological stability (A) and morphological trend (B) as a result of differential success of speciation events. Morphological change depicted on the horizontal axes, time on the vertical axis. Dashed lines represent speciation events. From Eldredge and Gould (1972: figure 5-10).

producing waste, and imposing selection pressures on the other organisms in their ecosystem which prey on them or are preyed on by them. Stasis may then be due to the attainment of a co-adapted equilibrium between the organism and its environment (Barnard 1984; Hoffman 1989).

An empirical observation which has already been mentioned provides a major problem for stabilising selection as a mechanism for stasis: the abundant observed morphological variation in extant and fossil populations and species (Lande 1986; Hoffman 1989).

It has been suggested that stasis in a species may result if the environment imposes selection pressures which act in different "directions" in different parts of the geographical range of the species, so that the conflicting selection pressures somehow cancel each other out (Maynard Smith 1983). However, Maynard Smith (1983) considered that this would be more likely to result in sympatric speciation with the ancestral species giving rise to two descendent species in different parts of its geographical range.

1. 3. 4. Approximate Net Stasis Maintained by Stabilising Species Selection.

As part of their description of the punctuated equilibria model, Eldredge and Gould (1972) extended their idea of rapid speciation and stasis through allopatric speciation to account for long term trends and stasis in the fossil record. They considered multiple "explorations" of new environments by peripheral isolates (Figure 1. 2). The speciation events themselves are not directional or adaptational with respect to the past evolutionary history of the lineage. Some of the speciations are "successful" in that they result in new species well fitted to the environmental niche they are exploring. Other speciations are "unsuccessful" in that they are not well fitted to the niche and the new species consequently does not survive for long. Differential success of randomly "directed" speciations can therefore result in a long-term trend if the environment is changing in a directed manner (Figure 1. 2 B).

Alternatively, if the environment is approximately stable through time, or is fluctuating within narrow bands, then approximate net stasis can be maintained. Note that the speciation events are still considered non-adaptational and non-directed with respect to the past history of the lineage. It is the differential survival of randomly derived species which maintains the stasis (Figure 1. 2 A).

1. 3. 5. Developmental Canalisation and Developmental Plasticity.

The ability of an organism to develop the "normal" adult phenotype (*i.e.* one not too dissimilar from that of the previous generation) under a variety of environmental conditions is a selective advantage, since it allows the organism to remain fitted to an environment which is subject to slight environmental shifts without requiring genetically-based changes to the organism's phenotype, and this ability to remain on the same developmental pathway, but inability to enter it if the environment shifts too far from the "norm", has been termed "developmental canalisation" (Hoffman 1982). In this way, genetic variation can be accumulated over time within a population without being expressed in the phenotype, and therefore being invisible to natural selection. At times of environmental stress, this canalisation can break down so that the accumulated genetic variation becomes expressed as phenotypic variation, on which natural selection can act (Hoffman 1982, 1989; Stearns 1982; Wake *et al.* 1983).

Developmental canalisation can be contrasted with its opposite case, developmental plasticity, which refers to the ability of a single genome to produce highly variable phenotypes under variable environmental regimes. In reality there is probably a range of intermediates between these two end member conditions, such that organisms vary in their degree of canalisation (Hoffman 1982, 1989).

1. 3. 6. Effects of Population Size and Distribution.

Eldredge and Gould (1972) originally envisaged rapid speciation events as occurring in small isolated populations according to the allopatric speciation model of Mayr (1942). Under this model, small peripheral populations which are reproductively isolated from other populations of their species by some physical barrier are small enough for genetic mutations to become fixed in the population's gene pool. Correspondingly, large populations within which there is abundant gene flow should not be susceptible to such processes. Such large populations should at the same time be under the influence of stabilising selection (in a constant environment) as described above, which promotes stasis.

More recently, the recognition of sympatric speciation and clines in the fossil record has shown that rapid evolution is not necessarily restricted to small populations, but is also possible in larger populations. Indeed, Maynard Smith (1983) pointed out that if rate of evolution is controlled by the rate of mutation giving rise to genetic and thus phenotypic variation, then evolutionary events should occur more often in large widespread populations than in small isolated ones. This observation is based on the recognition of abundant variation, both genetic and morphological, in extant large populations of organisms (Maynard Smith 1983; Lande 1986; Hoffman 1989).

Purely on the matter of population distribution, it has been demonstrated that organisms with cosmopolitan distributions are far less vulnerable to extinction than organisms which are endemic to one particular region, which could more easily be made extinct by processes such as habitat destruction (e.g. Sheehan and Coorough 1990; Robertson *et al.* 1991; Owen and Robertson in press). Similarly, organisms which are generalists in terms of their environmental requirements (eurytopic organisms) are less prone to extinction through habitat destruction than organisms which have very narrow environmental requirements (stenotopic organisms) (e.g. Owen *et al.* in press). However, these facts merely explain why some taxa escape extinction for long time periods without addressing the question as to why some taxa should exhibit such little net morphological change throughout their history.

1. 4. This Study.

This study is an examination of long-term morphological stasis in the fossil record of the Trilobita. There are a number of reasons why the trilobites lend themselves to such a study:

(i) They formed part of the original foundation for punctuated equilibria, the model which first highlighted the importance of stasis in the fossil record (Eldredge and Gould 1972).

(ii) They have previously been used in a number of case studies of both punctuational change (e.g. Eldredge and Gould 1972, punctuation and stasis in numbers of dorso-ventral lens files in *Phacops rana* ; Henry and Clarkson 1975 and Henry 1980, punctuational trend towards better fit of cephalic margin with the pygidium during enrollment in *Placoparia*; Fortey 1985, punctuation and stasis in Balnibarbiinae through the Arenig of Spitsbergen; Owen and Ingham 1988, punctuational changes in the distribution of fringe pits in *Onnia* from the type Onnian of south Shropshire) and gradualistic change (e.g. Kaufmann 1933, both punctuation and gradualism in pygidial proportions in *Olenus* from the upper Cambrian of southern Sweden; Engel and Morris 1983, gradualistic net decrease in number of pygidial ribs in *Weberiphillipsia* from the Carboniferous of Australia; Fortey 1985, gradual anterior migration of visual surfaces in *Pricyclopyge*, both gradualistic and punctuational evolution in a single lineage in *Carolinites* in the Arenig of Spitsbergen; Sheldon 1987, 1988, gradualistic net increase in numbers of pygidial ribs with reversals accompanied by net size increase in eight lineages in the Llandeilian of central Wales; Feist and Clarkson 1989, progressive reduction and ultimate loss of eyes in late Devonian Tropidocoryphine trilobites from southern France). Clarkson (1988) and Fortey and Owens (1990) have reviewed many of these examples.

(iii) High preservation potential of hard parts means that the Trilobita have a good fossil record world-wide, representing a wide spectrum of marine environments from shallow subtidal to deep water slope environments.

(iv) Relatively complex hard part morphology means that there are a lot of structures available for morphometric study per specimen. Presence of well defined landmarks on the exoskeleton make the trilobites especially well suited to morphometric study.

(v) Preservation of successive growth stages in some taxa has enabled links between phylogenetic and ontogenetic patterns to be recognised.

This study looks at two aspects of stasis. The first may be termed "genus stasis" and refers to long-duration genera which remain morphologically stable throughout their history. The second may be termed "species stasis" and refers to long-duration species within genera. The study can be considered to consist of two parts:

1. A "broad brush" study of the occurrence of long-term morphological stasis in the trilobite fossil record, as revealed by analysis of published taxonomic data (Chapter 2). This analysis has the following aims:
   (i) to evaluate the distribution of taxon durations (genera and species) and hence establish, in general terms, the relative frequency of long term morphological stasis as compared with more "normal" taxon durations;
   (ii) to highlight trilobite genera and species which have unusually long durations;
   (iii) to see whether particular periods in geological time or particular palaeoenvironmental settings are characterised by greater or lesser abundance of long-term morphological stasis.

2. Three case studies based on detailed analysis of morphological variation in long-duration, apparently morphologically stable trilobite lineages (chapters 3 to 7). These analyses have the following aims:
   (i) to demonstrate the maintenance of long-term morphological stasis in the lineages under study, independently of the pre-existing taxonomy applied to them;
   (ii) To define the amount of variation (both intraspecific and interspecific) which occurs within the broad phenomenon of "stasis";
   (iii) To determine whether, within the confines of net stasis, changes occur which are "directed" in time (*i.e.* a trend) or are completely random with

respect to the previous evolutionary history of the lineage; further to determine whether groups of morphological characters show simple group patterns of change, or whether they show more complex, disassociated "mosaic" patterns of change.

Effort has been made to study morphology of the fossils entirely independently of the existing taxonomic definitions of species within the genera under study. As Sheldon (1987) noted, the application of binomial taxonomy tends to submerge actual morphological variation in an evolving lineage, and tends to promote the impression of punctuation and stasis (see also Hoffman's 1989 comment on the inadequacy of defining stasis by equating it with the persistence of a certain phenotype used by a taxonomist to recognise that taxon, above). To achieve this, phylogenetic and morphometric techniques have been applied to stratigraphically and geographically separate samples of fossils. Chapter 3 describes the stratigraphical successions from which the samples were obtained. Chapter 4 describes the techniques used in obtaining and analysing morphometric data from the fossils. Chapters 5 to 7 describe the results of phylogenetic and morphometric studies on the genera. The particular genera studied are:

Achatella Delo, 1935. Ordovician System, upper Llanvirn to topmost Ashgill Series. Known from the Baltic and Laurentian faunal provinces. Chapter 5.

Calyptaulax Cooper, 1930. Ordovician System, Llanvirn to Ashgill Series. Known from the Baltic, Laurentian, and Avalonian faunal provinces. Chapter 6.

The *Acernaspis* Campbell, 1967 - *Ananaspis* Campbell, 1967 lineage. *Acernaspis* : Silurian System, Llandovery to Wenlock Series; known from Laurentia, Avalonia, Baltica and Siberia. *Ananaspis* : Wenlock and Ludlow Series; known from Baltica and Kazakhstan. Chapter 7.

The study is based largely on material housed in existing museum collections, supplemented by samples collected during fieldwork in Girvan, the Pentland Hills and the Oslo Region.

Chapter 8 draws together conclusions from the earlier chapters and discusses their implications in constraining the proposed mechanisms for stasis.

Specimens utilised in this study are housed in the following institutions: British Geological Survey (BGS); Geological Survey of Ireland (GSI); Geological Survey of

Sweden (SGU); Grant Institute, Edinburgh University (GIG); Hunterian Museum, Glasgow University (GLAHM); James Mitchell Museum, University College Galway (JMM); Lapworth Museum, Birmingham University (LM); Museum of Comparative Zoology, Harvard (MCZ); National Museum of Wales, Cardiff (NMW); Naturhistoriska Riksmuseum (RM); New York State Museum (NYSM); Paleontologisk Museum, Oslo (PMO); Peabody Museum of Natural History, Yale University (YPM); Royal Ontario Museum (ROM); Royal Scottish Museum (RSM); Sedgwick Museum, Cambridge University (SM); The Natural History Museum, London (BM); Trinity College, Dublin (TCD); Ulster Museum, Belfast (UM); United States National Museum (USNM).

CHAPTER TWO

A SURVEY OF CHRONOSTRATIGRAPHICAL RANGES OF TRILOBITE SPECIES AND GENERA FROM MAINLAND BRITAIN.

2. 1. Introduction.

A survey of the chronostratigraphical ranges of trilobite genera and species from mainland Britain (*i.e.* England, Scotland and Wales) was undertaken, with the following aims:

(i) to study patterns of stasis through time as revealed by taxonomy in British trilobites, in particular to determine whether particular time intervals are characterised by the occurrence of longer periods of stasis;

(ii) to highlight the long-ranging, morphologically stable species and genera (in so far as they are reflected by traditional taxonomy).

(iii) to establish, at least in general terms, the extent of stasis in the trilobite fossil record, or at least the degree of variation in chronostratigraphical ranges within species and genera as traditionally depicted.

In chapters 5 (morphometric and phylogenetic analysis of *Achatella* Delo) and 6 (morphometric and phylogenetic analysis of *Calyptaulax* Cooper) where dates have been placed on the Ordovician chronostratigraphy, the high-precision U-Pb dates of Tucker *et al.* (1990) have been used, as they are herein considered to supersede the dates given by Harland *et al.* (1989) for the Ordovician System. This means that the dates for some horizons in these chapters vary slightly from dates given for the corresponding horizons in the trilobite range charts in this chapter, in which the dates of Harland *et al.* (1989) have been used throughout for consistency. Attempting to insert the dates of Tucker *et al.* (1990) for the Ordovician System in between the dates of Harland *et al.* (1989) for the Cambrian and Silurian systems in this chapter would have resulted in slight discontinuities in dates at both the base and top of the Ordovician, since Tucker *et al.* (1990) gave dates for the Cambrian/Ordovician and Ordovician/Silurian boundaries of about 513 Ma and 441 Ma respectively, while Harland *et al.* (1989) gave dates of about 510 Ma and 439 Ma respectively.

2. 2. Compilation of Trilobite Chronostratigraphical Ranges.

A published compilation of stratigraphical ranges of trilobite species from the Palaeozoic of the British Isles has been calibrated against an absolute time scale, so that the chronostratigraphical ranges of the species and genera (expressed in absolute time) could be analysed. The range compilation used was that of Thomas *et al.* (1984).

Thomas *et al.* (1984) presented a number of stratigraphical range charts for trilobite species from Britain and Ireland for the Cambrian to Carboniferous systems (the interval during which trilobites occur in British strata). They plotted the stratigraphical ranges in terms of biostratigraphical intervals (usually biozones, although for the Carboniferous they used stratigraphical stages instead, Thomas *et al.* 1984: fig. 29). In general, they showed the species ranges as beginning and ending at biostratigraphical interval

boundaries or at convenient fractional parts of intervals (e.g. 1/4 of the way through an interval, 1/2 way through, 1/3 way through etc.). This was done deliberately to avoid any impression of spurious precision (R. M. Owens, pers. comm.). Occasionally, Thomas *et al.* felt justified in drawing the ranges to a greater precision (e.g. their charts for Llanvirn - Ashgill species, Thomas *et al.* 1984: figs. 10-11, 14, 17-18).

2. 2. 1. Method for Compilation of Chronostratigraphical Ranges.

A data base has been created containing the ranges of all trilobite species from mainland Britain (*i.e.* England, Scotland and Wales) as extracted from Thomas *et al.* (1984). Trilobite species listed by them as only occurring at a single locality (Thomas *et al.* 1984: pp. 16-17, 45-48, 57-58, 63, 69) were included. However, those species listed by them as only being known from single specimens were not included since this would greatly increase the size of the data base by including monotypic species which may be of dubious validity. Since the purpose of this analysis is to highlight species and genera with long durations, the exclusion of monotypic taxa, which by definition have a duration of zero myr., makes little difference to the results. Species for which the start and end of the range could not be fixed to within a precision of one biostratigraphical interval as used by Thomas *et al.* (1984) were similarly not included. This left 971 species of trilobites from Cambrian - middle Carboniferous strata of Britain, 252 of which are only known from single localities, for inclusion in the data base. These species represent a total of 359 genera, 40 of which are only known from single localities.

In order to calculate the chronostratigraphical ranges of the trilobite species, the biostratigraphical intervals used by Thomas *et al.* (1984) were first numbered sequentially in ascending stratigraphical order from 1 (non-trilobite zone, basal Cambrian, Thomas *et al.* 1984: fig. 2) to 90 (Arnsbergian Stage, middle Carboniferous, Thomas *et al.* 1984: fig. 29). Then the stratigraphical levels at which each of the trilobite species has its first and last appearance were extracted from the charts with the greatest precision they would allow and recorded as a number between 0 and 90 (this number is hereinafter referred to as the "biozone number"). For example, a species whose first appearance is at the upper boundary of the first biostratigraphical interval (= non-trilobite zone, basal Cambrian) was assigned a biozone number of 1 for its time of first appearance. A species which becomes extinct half way through the 39th biostratigraphical interval (=*D. anceps* Zone, Ashgill Series) was assigned a biozone number of 38.5 for its time of last appearance. For species listed by Thomas *et al.* as only occurring at a single locality, the locality was assigned to a biostratigraphical interval, and the species occurrence was placed in the middle of that biostratigraphical interval. In this way, each of the 971 species was assigned two biozone numbers, one for its time of first appearance and one for its time of last appearance.

The first and last appearance times of the genera were then worked out from their constituent species: the time of first appearance of a genus is equal to the time of first appearance of its stratigraphically earliest member species; the time of last appearance of a genus is equal to the time of last appearance of its stratigraphically latest member species. Thus each of the 359 genera was also assigned two biozone numbers recording its times of first and last appearance in the stratigraphical record.

The relative appearance and disappearance times of the species and genera (expressed in biozone numbers) were then converted into absolute dates of first and last appearance (in Ma before present) with reference to the time scale of Harland *et al.* (1989). Harland *et al.* gave dates for stratigraphical stage boundaries (Harland *et al.* 1989: fig. 1. 7). For this study, dates for boundaries between the biostratigraphical intervals used by Thomas *et al.* (1984) and for key levels within those biostratigraphical intervals (where necessary) were derived by simple interpolation from the stage boundary dates of Harland *et al.* (1989). For the purposes of this interpolation, all biozones within a stage were assumed to be of equal duration. The calculated ages of the boundaries between the biostratigraphical intervals are shown in Table 2. 1.

Once the absolute dates (in Ma) of the relevant stratigraphical horizons had been derived, the times of first and last appearance of the 971 species and 359 genera (expressed in biozone numbers) could be converted to absolute dates in Ma. To accomplish this, a computer program entitled "calibrator()" was specially written. This program, written in "S" to run on AT & T's "S" software system running on a Sun workstation, simply takes a file containing the times of first and last appearance for each taxon (in biozone numbers) and, by reference to a calibration file containing the information reproduced in Table 2. 1, outputs a file containing the corresponding absolute dates in Ma. Documentation for "calibrator()" is given in Appendix 1. In this way, the times of first and last appearance for each species and genus, in Ma, were obtained. Calculating the chronostratigraphical range for each taxon (in myr) was then a simple matter of subtracting its time of last appearance (in Ma) from its time of first appearance (in Ma). The data bases containing the names and times of first and last appearance (both in biozone numbers and in Ma) of the 971 species and 359 genera are given in Appendix 2.

This method of calibrating the stratigraphical ranges - *i.e.* expressing the times of first and last appearance of each taxon in terms of relative stratigraphical level (the biozone number) and then converting these relative levels into absolute dates - was used since it makes the stratigraphical information easy to recalibrate against other time scales as they become available at future times. All that is required is the construction of a new calibration file from which "calibrator()" reads absolute dates.

Table 2. 1. Biozone numbers for the biostratigraphical intervals used by Thomas *et al.* (1984) and corresponding dates of boundaries calculated from the time scale of Harland *et al.* (1989). Dates in bold type are given by Harland *et al.* (1989: figure 1. 7). Dates in plain type are interpolated from those of Harland *et al.* as described in the text.

Biostratigraphical interval	Biozone number	Date (Ma)
	90	**328.3**
Arnsbergian	89	**331.1**
Pendleian	88	**332.9**
Brigantian	87	**336.0**
Asbian	86	**339.4**
Holkerian	85	**342.8**
Arundian	84	**345.0**
Chadian	83	**349.5**
Courceyan		
	82	**362.5**
Wocklumeria Stufe	81	363.63
Clymenia Stufe	80	364.75
Platyclymenia Stufe	79	365.88
Cheiloceras Stufe	78	**367.0**
C. holzapfeli	77	372.2
M. cordatum	76	**377.4**
P. lunulicosta	75	378.25
M. terebratum	74	379.1
M. molarium	73	379.95
C. crispiforme	72	**380.8**
P. jugleri	71	383.4
A. lateseptatus	70	**386.0**
S. wenkenbachi	69	388.2
M. zorgensis	68	**390.4**
A. hunsrueckianum	67	399.45
M. hercynicus		
	66	**408.5**
Downton	65	**410.7**
Bohemograptus	64	412.9
leintwardinensis	63	**415.1**
incipiens	62	418.07
scanicus	61	421.03
nilssoni	60	**424.0**
ludensis	59	424.7
nassa	58	**425.4**
lundgreni	57	**426.1**
ellesae	56	426.82
linnarssoni	55	427.53
rigidus	54	428.25
riccartonensis	53	428.97
murchisoni	52	429.68
centrifugus	51	**430.4**
crenulata	50	430.95
griestoniensis	49	431.5
crispus	48	432.05
turriculatus	47	**432.6**
sedgwickii	46	434.03
convolutus	45	435.47
gregarius	44	**436.9**
cyphus	43	437.43
atavus	42	437.95
acuminatus	41	438.48
persculptus	40	**439.0**

Biostratigraphical interval	Biozone number	Date (Ma)
	40	**439.0**
extraordinarius	39	**439.5**
anceps	38	**440.6**
complanatus	37	442.27
linearis	36	443.66
clingani	35	**449.7**
foliaceus	34	463.1
gracilis	33	**467.0**
teretiusculus	32	**468.6**
murchisoni	31	**472.7**
artus	30	**476.1**
hirundo	29	479.48
gibberulus	28	482.86
nitidus	27	486.24
deflexus	26	489.62
approximatus	25	**493.0**
sedgwickii	24	496.4
pusilla	23	499.8
incipiens	22	503.2
tenellus	21	506.6
flabelliforme		
	20	**510.0**
Acerocare	19	510.68
scarabaeoides	18	511.37
minor	17	512.05
praecursor	16	512.73
Leptoplastus & Eurycare	15	513.42
spinulosa	14	**514.1**
Olenus & obesus	13	515.65
pisiformis	12	**517.2**
laevigata	11	519.37
brachymetopa	10	521.53
nathorsti & lundgreni	9	523.7
punctuosus	8	525.87
parvifrons	7	528.03
fissus	6	**530.2**
gibbus	5	532.13
pinus	4	534.07
insularis	3	**536.0**
protolenid - strenuellid	2	**554**
olenellid	1	**560**
non-trilobite	0	**570**

This compilation of taxonomic ranges involves several assumptions which should be made explicit at this point:

(i) It is assumed that the Harland *et al.* (1989) time scale is an accurate and precise time scale for the Palaeozoic. This time scale was used since it is the most recently published single time scale which covers the whole of the Palaeozoic. Parts of the Palaeozoic time scale have since been modified: e.g. the U-Pb dates of Compston *et al.* (1992), Cooper *et al.* (1992), Bowring *et al.* (1993) and Isachsen *et al.* (1994) for the Cambrian System (which tend to shorten the duration of the Cambrian somewhat relative to Harland *et al.* 1989); the U-Pb dates of Tucker *et al.* (1990) and Compston and Williams (1992) for the Ordovician System.

(ii) As noted above, it is assumed that biozones within stratigraphical stages are of equal duration for the purposes of interpolating dates for biozone boundaries.

(iii) As noted above, it is implicit in the range charts provided by Thomas *et al.* (1984) that taxon ranges begin and end either at the boundaries between their biostratigraphical intervals, or at convenient fractional parts within biostratigraphical intervals.

(iv) The compilation is based on stratigraphical ranges assigned by Thomas *et al.* (1984). Work done subsequently has modified and refined the stratigraphical ranges of some taxa: e.g. the work of Fortey and Owens (1987) on Arenig trilobites of South Wales.

(v) The compilation uses taxonomic knowledge as it was in 1984. Work done subsequently has refined the taxonomy of a number of the taxa included. See for example Morris (1988).

These assumptions mean that the results presented here are relatively "broad brush" and should be used only to show broad patterns, but they are nonetheless useful for that purpose.

2. 2. 2. Results.

A simple summary of the chronostratigraphical range data for species and genera of trilobites from mainland Britain (England, Wales and Scotland) is given in Table 2. 2. Figure 2. 1 shows histograms of chronostratigraphical ranges and survivorship plots for the whole set of genera and species. Histograms of chronostratigraphical ranges of genera and species originating within each stratigraphical system (Cambrian - Carboniferous) are shown in Figures 2. 2 and 2. 3 respectively. For purposes of constructing the histograms, taxa which are only known from a single locality, and which therefore have a chronostratigraphical range of zero myr, were arbitrarily assigned a range of 0.001 myr so that they would fall within the first class on the histograms (zero values would otherwise form a unique class of their own on the histograms).

Table 2. 2. Summary of chronostratigraphical range data for genera and species from each of the stratigraphical systems Cambrian - Carboniferous in England, Scotland and Wales. Stratigraphical ranges extracted from Thomas *et al.* (1984) and calibrated against the time scale of Harland *et al.* (1989).

System	Genera	Species
Cambrian:		
Number of taxa:	90	190
Mean duration (myr):	4.42	2.13
Median (myr)	2.17	0.725
75% quantile (myr)	7.12	2.82
90% quantile (myr)	11.96	4.5
Max. duration (myr):	21.0	19.5
Most durable taxon:	*Olenellus* Billings	*Callavia callavei* (Lapworth)
Ordovician:		
Number of taxa:	193	531
Mean duration (myr):	10.89	2.06
Median (myr)	6.04	0.87
75% quantile (myr)	16.89	2.9
90% quantile (myr)	28.84	6.28
Max. duration (myr):	79.8	26.2
Most durable taxon:	*Proetus* Steininger	*Atractopyge petiolulata* Tripp
(Laurentian Ordovician from Sloan 1991):		
Number of taxa:	318	-
Mean duration (myr):	10.61	-
Median (myr)	5.87	-
75% quantile (myr)	16.2	-
90% quantile (myr)	28.76	-
Max. duration (myr):	56.4	-
Most durable taxon:	*Shumardia* Billings	-

Table 2. 2. Continued.

System	Genera	Species
Silurian:		
Number of taxa:	40	149
Mean duration (myr):	10.34	3.54
Median (myr)	6.68	2.15
75% quantile (myr)	11.61	5.17
90% quantile (myr)	19.87	7.99
Max. duration (myr):	52.2	13.9
Most durable taxon:	*Cornuproetus* Richter & Richter	*Dalmanites myops* (König)
Devonian:		
Number of taxa:	15	32
Mean duration (myr):	4.19	1.12
Median (myr)	1.13	1.13
75% quantile (myr)	2.25	1.7
90% quantile (myr)	17.45	2.25
Max. duration (myr):	29.2	3.5
Most durable taxon:	*Typhloproetus* Richter	*Scutellum flabelliferum* (Goldfuss)
Carboniferous:		
Number of taxa:	21	69
Mean duration (myr):	14.82	5.74
Median (myr)	13.0	3.4
75% quantile (myr)	26.5	9.03
90% quantile (myr)	29.6	13.0
Max. duration (myr):	29.6	26.5
Most durable taxon:	*Archegonus* Burmeister	*Carbonocoryphe colei* (McCoy)
	Brachymetopus McCoy	*Namuropyge discors* (McCoy)
	Eocyphinium Reed	

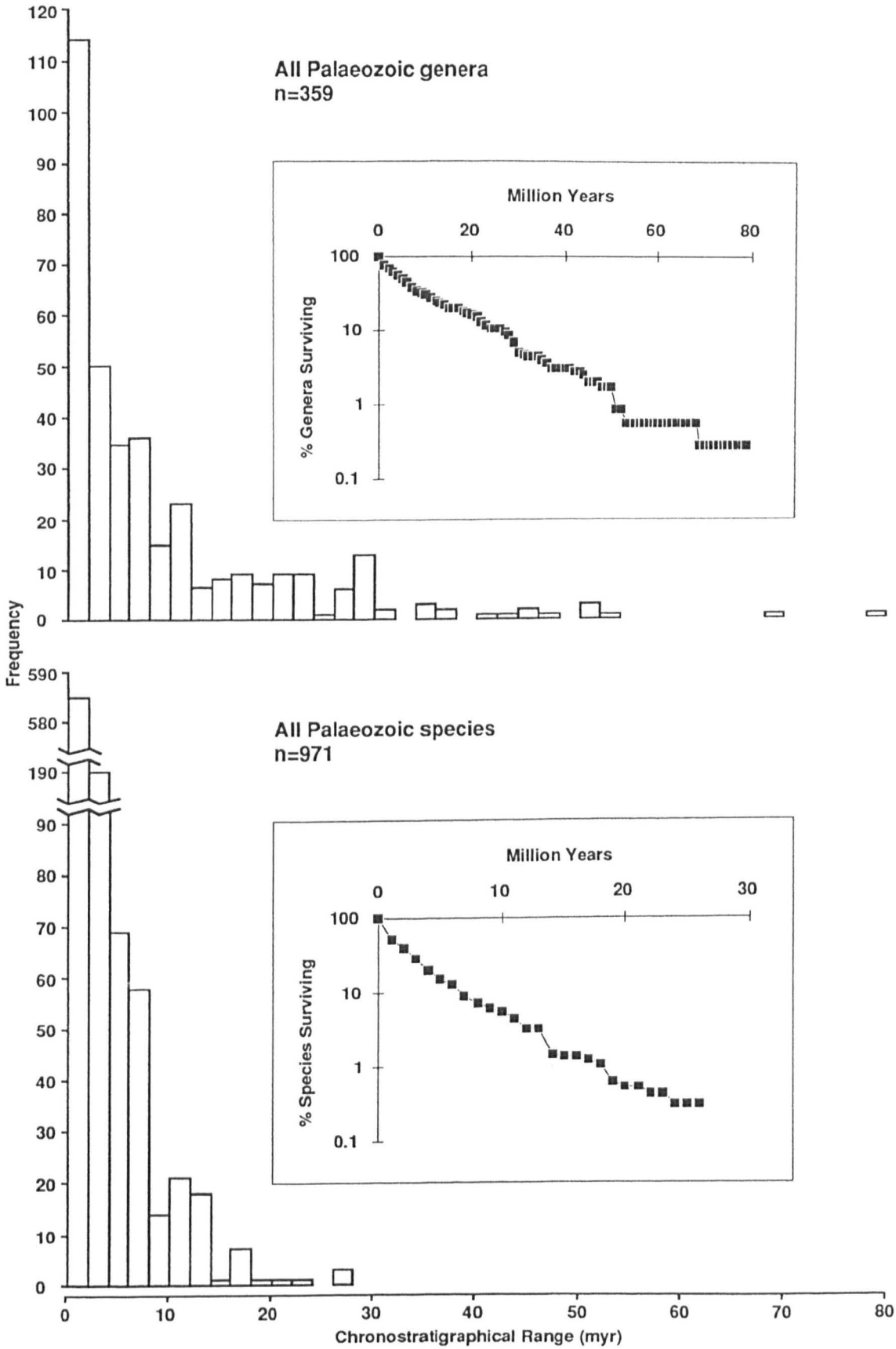

Figure 2. 1. Histograms of chronostratigraphical ranges and survivorship plots for genera and species of trilobites from the Palaeozoic (Cambrian - Carboniferous) of England, Scotland and Wales. Stratigraphical ranges extracted from Thomas *et al.* (1984) and calibrated against the time scale of Harland *et al.* (1989).

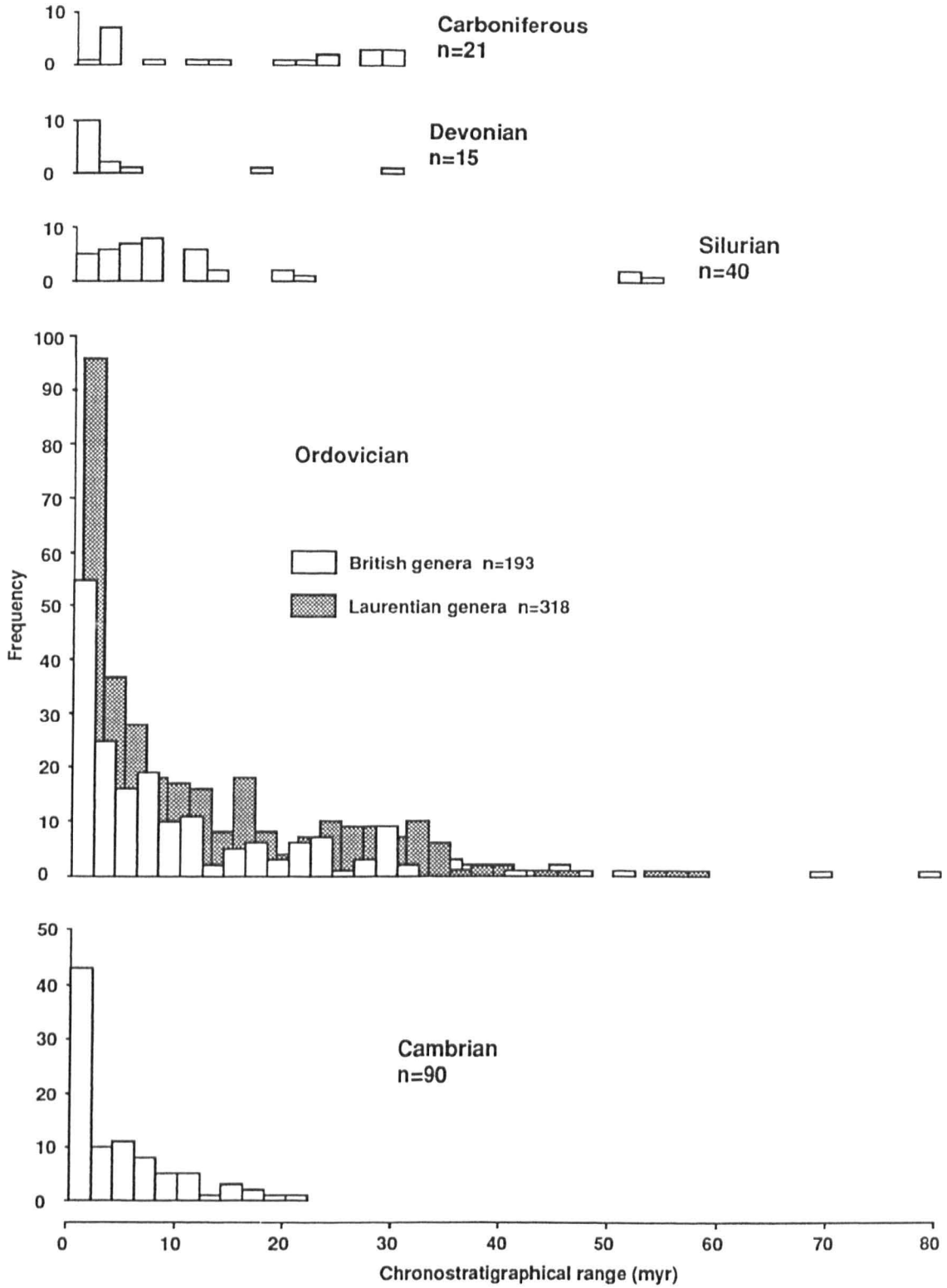

Figure 2. 2. Histograms of chronostratigraphical ranges of trilobite genera originating in each of the stratigraphical systems of England, Scotland and Wales. Stratigraphical ranges of genera extracted from Thomas *et al.* (1984) and calibrated against the time scale of Harland *et al.* (1989). Histogram of chronostratigraphical ranges of Ordovician genera from the Laurentian Province extracted from Sloan (1991) shown for comparison with the British Ordovician genera. Class intervals for Sloan's data as for the British data, but classes moved slightly to the right on the histogram for clarity.

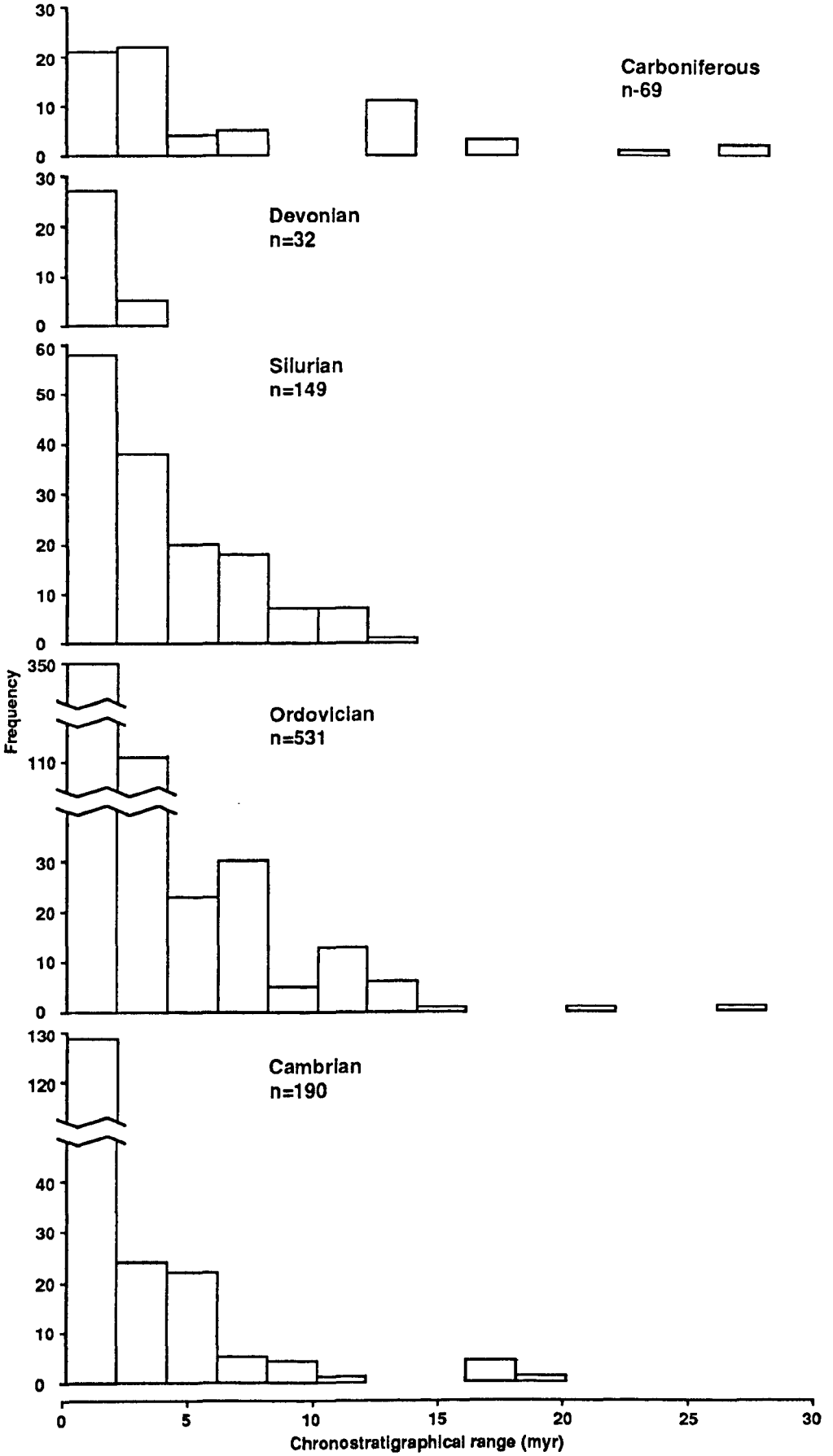

Figure 2. 3. Histograms of chronostratigraphical ranges of trilobite species originating in each of the stratigraphical systems of England, Scotland and Wales. Compiled as in Figure 2. 2.

Table 2. 2 shows that mean duration of genera increases from the Cambrian to the Ordovician (from about 4.4 to about 10.9 myr) and then remains approximately constant for the Ordovician and Silurian (at between 10 and 11 myr). Devonian genera have comparatively low mean duration (about 4.2 myr), while that for Carboniferous genera is much greater (about 14.8 myr). The mean duration of species is approximately constant for Cambrian and Ordovician species (just over 2 myr), and slightly higher for both Silurian and Devonian species (about 3.5 myr). Carboniferous species, like Carboniferous genera, exhibit high mean duration (about 5.7 myr).

Sloan (1991) provided chronostratigraphical ranges for 318 trilobite genera from the Ordovician of North America, Greenland, Spitsbergen, NW and SW Scotland, and N and NW Ireland (*i.e.* the Laurentian Province). Sloan calculated his Ordovician chronostratigraphy from Sweet's (1984) Composite Standard Section for the interval Whiterockian to end Ordovician, which Sloan extrapolated to the base of the Ordovician, combined with three high precision dates from the North American Ordovician. A summary of results extracted from Sloan's (1991) table 2 is included in Table 2. 2 herein for comparison with the results for English, Scottish and Welsh trilobites, and a histogram of Sloan's calculated chronostratigraphical ranges is included in Figure 2. 2 for comparison with the British data. It can be seen that the data on Laurentian genera are comparable with that for British genera (318 Ordovician Laurentian genera have mean duration of approximately 10.6 myr, compared with 10.9 for British genera, Table 2. 2).

It is immediately apparent that the distributions of chronostratigraphical ranges (for all genera and species as well as for genera and species originating within each stratigraphical system) are all positively skewed, with the smallest class exhibiting by far the greatest frequency in all histograms except those for Silurian and Carboniferous genera (Figure 2. 2) and Carboniferous species (Figure 2. 3) (*i.e.* the majority of chronostratigraphical ranges are short, with longer ranges being very rare). The histograms of Ordovician, Silurian, Devonian and Carboniferous genera, as well as those for Cambrian, Ordovician and Carboniferous species show isolated cases at the long end of the range spectrum, which reflect taxa with unusually long chronostratigraphical ranges.

A number of survivorship diagrams have been constructed from the data. Plots constructed for all 359 genera and all 971 species are shown in Figure 2. 1. Plots for the species and genera originating within each stratigraphical system are shown in Figures 2. 4 - 2. 13. Survivorship diagrams are reversed cumulative plots of longevity data (Stanley 1979). The abscissa axis shows taxon duration in millions of years. The ordinate axis shows the number of taxa surviving to each successive interval on the abscissa,

expressed (in this case) as a percentage of the starting number and plotted on a logarithmic scale. The result is a monotonically descending line, down and to the right, which shows how the number of taxa surviving for a given duration decreases as the duration in question is increased. Note that all of the survivorship plots presented here include taxa taken from a broad stratigraphical interval and lumped together in each diagram. For example, the plots shown in Figure 2. 1 include all genera and species from the Palaeozoic of England, Scotland and Wales. The plots on Figures 2. 4 - 2. 13 include all species and genera originating within the stratigraphical system in question. The horizontal axis on these plots therefore represents *duration* in millions of years, not elapsed time after some starting point. If one wanted to be able to pick off certain stratigraphical intervals, one would need to construct a cohort survivorship diagram in which the whole data set of taxa was decomposed into cohorts containing taxa which originated at more or less the same time (or at least within the same biozone). A series of such plots could then be produced, one for each cohort. The time axis on such a plot would then represent time elapsed since the origination of the cohort. Raup (1978) and Foote (1988) have used such cohort survivorship diagrams. This has not been done here since the purpose of this chapter is to study taxonomic durations rather than to pinpoint individual events in the fossil record. Also, since a number of taxonomic range charts have been constructed (Figures 2. 4 - 2. 13) the information which could be obtained from a cohort survivorship diagram can be obtained with equal (perhaps greater) facility from those.

If the observed taxon durations on a survivorship plot define a straight line (when the ordinate axis is plotted as a logarithmic scale), this indicates that the probability of extinction of taxa remains constant irrespective of the actual durations of the taxa; taxa which have existed for a long time are just as likely to go extinct as those which have only existed for a short time (Van Valen 1973; Foote 1988). It can be shown that if a plot of survivorship data at the species level is a straight line, then corresponding plots made from higher level taxonomic data must be curved concave-up; *i.e.* higher level taxa which have survived for a long time are less likely to become extinct than ones which have only been in existence for a shorter time. This tends to occur since higher level taxa which have been in existence for a longer time will tend to have more member species than ones which have existed for a shorter time. Clearly all member species must go extinct for the higher level taxon to go extinct (Raup 1978).

Both survivorship plots in Figure 2. 1 approximate to straight lines until the number of surviving taxa has fallen to about 1% of the starting number (this 1% level equates to about 3 genera and 9 species), at which point both lines become markedly stepped. If a straight line is placed on the first 99% of taxa (*i.e.* the straight line representing constant probability of extinction irrespective of taxon duration, see above), it is seen that the

long-duration 1% of taxa fall markedly to the right of this line on both the genus and species survivorship plots; *i.e.* these 1% of longest-duration taxa survived for longer than constant probability of extinction with duration predicts. The plots therefore suggest that these longest-duration taxa do not represent just the tail end of a continuous spectrum of ranges; rather they are qualitatively different.

It is of interest to study the specific composition of the longest duration genera, to see how many member species they have and what the durations of those member species are. As end members of a spectrum of possibilities, it could be postulated that long duration genera consist either of a large number of member species, each of which may itself only have a relatively short duration (*i.e.* the species exhibited relatively rapid evolution), or alternatively that long duration genera consist of only a relatively small number of very long duration species (*i.e.* the species showed long term stasis). In order to study this, genera whose chronostratigraphical range exceeds the 90% quantile value for the stratigraphical system in which they originated have been extracted from the data set and their durations and number of constituent species have been tabulated. The results are summarised in Table 2. 3.

In the Cambrian, it can be seen from Table 2. 3 that almost all of the long duration genera have between one and four member species (the exception being *Ptychagnostus* with 10 member species). The mean number of species per genus for all of the Cambrian genera in the data set (those whose chronostratigraphical range does not exceed the 90% quantile value as well as those which do) is 2.2. The mean duration for all Cambrian species is 2.13 myr. (from Table 2. 2). Thus it can be seen that in general the long duration Cambrian genera listed in Table 2. 3 do not have significantly more species than other Cambrian genera, but the durations of their species are usually greater than those of other Cambrian species. Therefore it appears that long generic duration in the Cambrian was a result of long specific duration, rather than possession of large numbers of short-lived member species (*i.e.* species stasis rather than rapid evolution played the important role). It should be noted that the very longest duration species and genera in the Cambrian are those from the Comley Series, and taxonomic durations may be affected by poor biostratigraphical control on these strata (see Section 2. 3).

In the Ordovician, Table 2. 3 shows that several genera possess relatively large numbers of member species (e.g. *Calymene*, 16 spp., *Illaenus*, 13 spp., *Remopleurides*, 14 spp., *Stenopareia*, 15 spp.). However, these are not necessarily the longest ranging genera of all. Also, there are very long ranging genera which possess comparatively few species (e.g. *Ceratocephala*, 4 spp., *Miraspis*, 3 spp.). The mean number of member species for all Ordovician genera in the data set is 3.1, and the mean duration of all Ordovician species in the data set is 2.06 myr (from Table 2. 2). The durations of the member

Table 2. 3. Genera whose chronostratigraphical ranges exceed the 90% quantile value for the system in which they originated. Columns are: genus name, chronostratigraphical range, number of member species (excluding those only known from single specimens), range of shortest-duration member species, range of longest-duration member species, mean range of member species.

		----------Included species----------			
Genus	Range	No. spp.	Min.	Max.	Mean
Cambrian genera (90% quantile = 11.96 myr).					
Callavia	19.5	2	6.0	19.5	12.75
Micragnostus	15.0	4	0.4	11.9	8.18
Olenelloides	18.0	1	18.0	18.0	18.00
Olenellus	21.0	4	0	18.0	13.50
Parabolinella	15.0	3	0	6.8	2.41
Ptychagnostus	12.9	10	0	4.30	1.99
Serrodiscus	18.0	3	4.5	9.0	6.00
Shumardia	14.3	3	3.4	4.1	3.82
Strenuella	12.0	4	0	4.5	2.25
Ordovician genera (90% quantile = 28.84 myr).					
Ampyx	31.2	6	0	10.1	3.22
Calymene	34.6	16	0	6.5	1.75
Ceratocephala	44.6	4	0	2.1	0.73
Cybeloides	29.6	3	0	4.7	1.55
Decoroproetus	50.5	10	0	13.3	4.32
Dionide	36.3	4	0	2.0	1.02
Flexicalymene	36.3	9	0	8.7	2.76
Geragnostus	41.7	3	0	11.3	6.04
Harpidella	34.5	10	0	2.0	0.67
Hemiarges	43.8	10	0	13.3	2.71
Illaenus	68.5	13	0	3	0.86
Lonchodomas	29.0	11	0	3.9	1.03
Miraspis	48.0	3	0	7.3	2.44
Pharostoma	35.2	3	0.1	0.7	0.37
Primaspis	29.0	9	0	5.5	2.19
Proetus	79.8	10	0	9.4	4.58
Remopleurides	29.8	14	0	6.3	1.26
Sphaerexochus	44.6	6	0	7.5	1.95
Stenopareia	30.5	15	0	13.3	1.79
Silurian genera (90% quantile = 19.87 myr).					
Acanthopyge	50.3	2	0	5.0	2.49
Cheirurus	20.8	2	4.4	7.5	5.95
Cornuproetus	52.2	3	1.7	2.2	1.85
Cyphaspis	50.7	2	1.7	7.9	4.82
Devonian genera (90% quantile = 17.45 myr).					
Typhloproetus	29.2	2	0	1.1	0.57
Carboniferous genera (90% quantile = 29.6 myr).					
Archegonus	29.6	9	0	13.0	6.50
Brachymetopus	29.6	4	6.5	17.5	12.50
Eocyphinium	29.6	5	0	13.0	4.58

species of the longest duration Ordovician genera show a wide spread to either side of this mean species duration. There is thus no clear pattern in the Ordovician data to show whether the long duration genera are characterised by possession of large numbers of species (*i.e.* rapid evolution) or small numbers of species (*i.e.* stasis).

In the Silurian, four genera have durations greater than the 90% quantile value for the system. The mean number of member species for all Silurian genera in the data set is 1.88, and the mean duration of all Silurian species is 3.54 myr (from Table 2. 2). Therefore, long generic duration in the Silurian does not appear to have been a result of rapid evolution leading to large numbers of member species, but neither does extreme specific stasis appear to have been important.

Because of the relatively small number of Devonian genera known, only one exceeds the 90% quantile value for the system. It has only two member species one of which is only known from a single horizon.

In the Carboniferous, Table 2. 3 shows that the longest duration genera have relatively high numbers of member species (the mean number of member species for all Carboniferous genera in the data set is 3.24). The mean durations of the member species are close to or higher than the mean duration of all Carboniferous species (5.74 myr from Table 2. 2). Therefore the long duration Carboniferous genera appear to be composed of relatively high numbers of reasonably static species.

2. 3. Range Charts for Trilobite Species and Genera from England, Scotland and Wales.

A number of chronostratigraphical range charts have been constructed from the chronostratigraphical range data calculated above, and are presented as Figures 2. 4 - 2. 8 (chronostratigraphical ranges of trilobite species originating in each stratigraphical system Cambrian - Carboniferous) and 2. 9 - 2. 13 (chronostratigraphical ranges of trilobite genera originating in each stratigraphical system Cambrian - Carboniferous). These charts have been plotted to illustrate changing patterns of stasis (as reflected by existing taxonomy) with time. They will be briefly considered below. Note that the purpose of this brief review is to show the broad pattern of stasis through time and highlight those taxa showing unusually long chronostratigraphical ranges, rather than exhaustively to analyse each successive interval of the stratigraphical record.

The size at which the charts are reproduced does not allow the individual taxa to be named on the charts; rather the taxa are numbered (from 1 to 971 for species; from 1 to 359 for genera) and the taxon names are given with their numbers in Appendix 2. Where species or genera are named below, their number on the relevant chart and in Appendix 2

is given in brackets. In using these charts, the assumptions noted in subsection 2.2.1. should be borne in mind. Where stratigraphical and taxonomic work carried out since the publication of Thomas *et al.* (1984) may make a difference to the charts, it is noted in the text.

Cambrian species (Figure 2. 4). The longest durations of any Cambrian species are in the Comley Series (lower Cambrian). This may be influenced by the rather poor biostratigraphical control available for lower Cambrian strata: Comley Series biozones are rather vague broad subdivisions based on local distributions of trilobites which are often difficult to identify or classify (Thomas *et al.* 1984). In the Comley Series, the species *Callavia callavei* (2), *Olenelloides armatus* (8), *Olenellus intermedius* (10), *O. lapworthi* (11) and *O. reticulatus* (14) are notable for their especially long ranges. There is a general trend towards shorter ranges throughout the remaining part of the Cambrian, with Merioneth Series species showing the shortest ranges of all. Merioneth Series biozones are assemblage zones finely subdivided on the basis of local ranges of olenids, giving a resolution as fine as that anywhere else in the Palaeozoic (Thomas *et al.* 1984). Marked exceptions to the generally short duration of Merioneth trilobite species are *Shumardia alata* (181), *Niobella homfrayi homfrayi* (182) and *Psilocephalinella innotata* (183), all of which continue into the Ordovician (they and *Beltella nodifer* (187) are the only four Cambrian species to do so). Extinctions followed by radiations are apparent at the base of the St. David's Series and at the *nathorsti / brachymetopa* biozone boundary.

The survivorship plot for Cambrian species is slightly stepped and approximates to a concave-up curve for most of its length. This suggests that probability of extinction decreased slightly with increased duration, *i.e.* long-ranging taxa were less likely to become extinct. However, the long-ranging taxa on the survivorship plot are almost exclusively those from the Comley Series, so the difference may lie in the fact that they are lower Cambrian species rather than in the fact that they are long-ranging species.

Ordovician species (Figure 2.5). The chronostratigraphy used is that of Fortey *et al.* (in press), and all stratigraphical assignments made by Thomas *et al.* (1984) have been converted accordingly. The mixed graptolite - trilobite zonal scheme used for the Tremadoc gives a reasonably fine-scale zonation. Many Tremadoc species show moderately long ranges. The top of the Tremadoc is marked by an extinction with no species ranging through into the Arenig. The Arenig itself appears to have been a time of remarkable stability judging by the near uniformity of species ranges. Four species range through an extinction at the base of the *hirundo* Zone, *Placoparia cambriensis cambriensis* (239), *Selenopeltis inermis macropthalmus* (245), *Agerina perplexa* (249) and *Ampyx salteri* (250). The first two of these together with *Pricyclopyge binodosa* (256) and *P. prisca* (258) are the only four species to continue into the Llanvirn.

Figure 2. 4. Chronostratigraphical ranges of trilobite species originating in the Cambrian of England, Scotland and Wales. Stratigraphical ranges extracted from Thomas *et al.* (1984) and callibrated against the timescale of Harland *et al.* (1989). Inset shows the survivorship plot for the species.

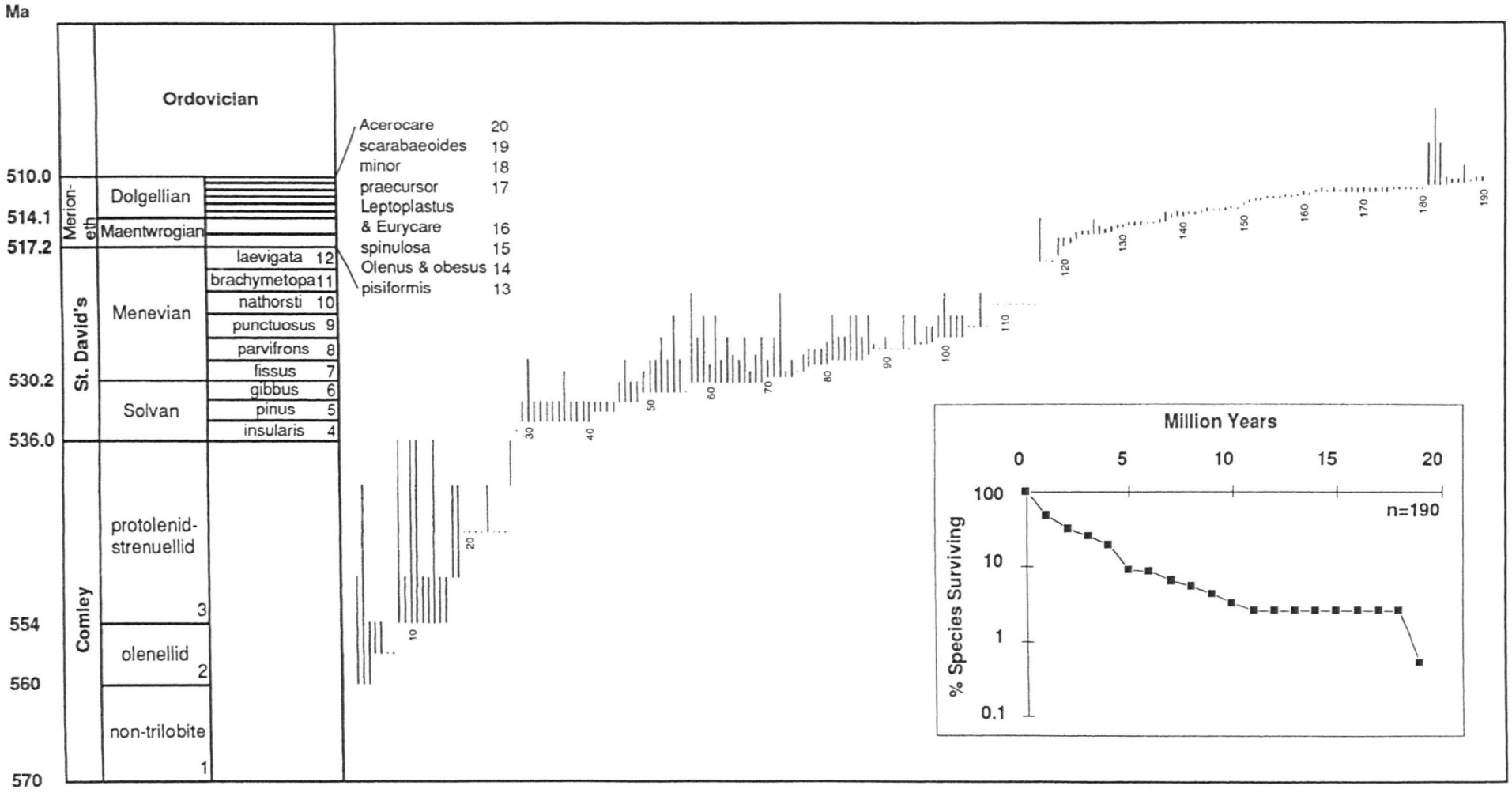

Figure 2. 5 (a). Chronostratigraphical ranges of trilobite species originating in the Ordovician of England, Scotland and Wales. Constructed as in Figure 2. 4. Chronostratigraphy after Fortey *et al.* (in press). Divisions within the Caradoc are considered to be substages.

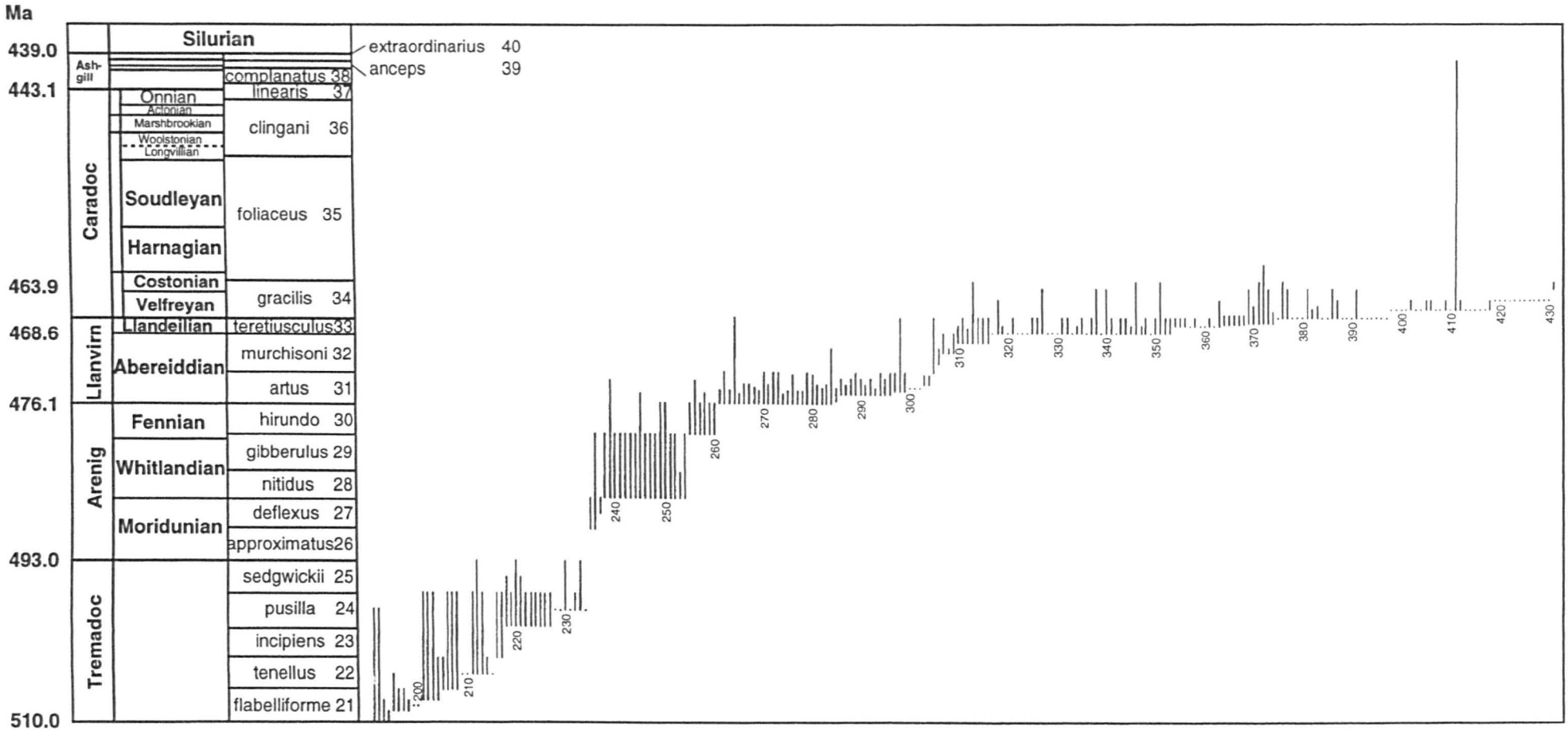

Figure 2. 5 (b). Chronostratigraphical ranges of trilobite species originating in the Ordovician of England, Scotland and Wales, continued. Constructed as in Figure 2. 4. Inset shows the survivorship plot for the species.

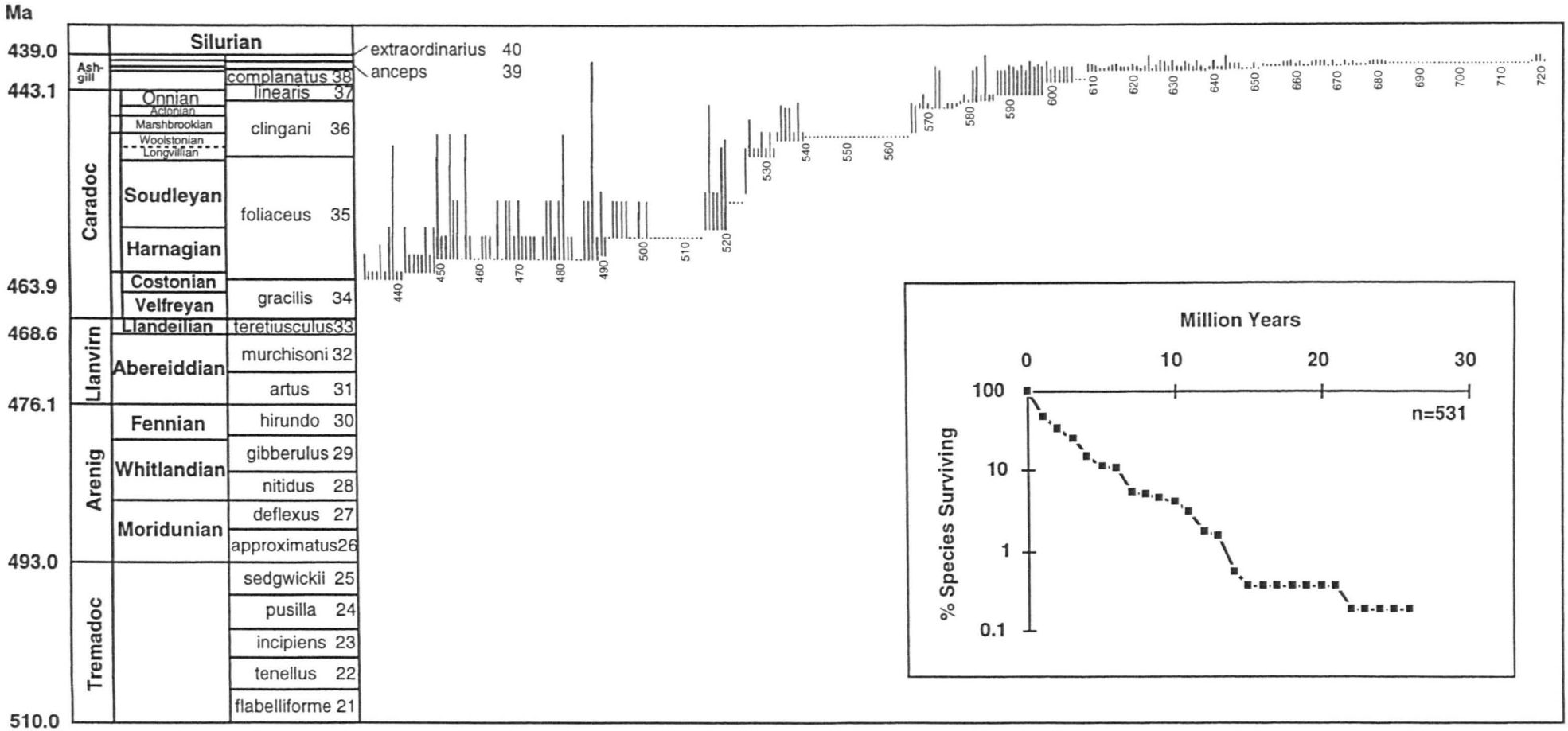

The Llanvirn Series is a time of relatively shorter ranges, particularly so in the Llandeilian Stage. In the Abereiddian, the following species stand out as having long ranges: *Bettonia chamberlaini* (264), *Platycoryphe vulcani* (284), *Ogyginus corndensis* (298) and *Metopolichas patriarchus* (305). In the Llandeilian, ranges are generally short, the following species standing out as having slightly longer ranges: *Thulincola barbara* (318), *Decoroproetus fearnsidesi pristinus* (327), *Segmentagnostus mccoyii* (338), *Cnemidopyge nuda nuda* (340), *Primaspis simulatrix* (346), *P. whitei* (351), *Remopleurides vulgaris* (363), *Ogygiocarella angustissima* (369), *Spirantyx calvarina* (371), *Platycalymene duplicata duplicata* (372), *Marrolithus favus favus* (373), *Marrolithoides arcuatus* (376), *Cnemidopyge bisecta* (377), *Trinucleus fimbriatus* (381), *Homalopteon murchisoni* (386), *Nobiliasaphus powysensis* (391).

The Caradoc is again a time of rather poor species survivability, particularly so the early Caradoc. One remarkable exception appears to be *Atractopyge petiolulata* (411) which ranges through into *anceps* Zone (Rawtheyan Stage) strata; however, the taxonomy of this species requires revision and more than one species may well be represented within the quoted stratigraphical range (A. W. Owen pers. comm.). Caradoc species which originated at the base of *foliaceus* Zone or later (Figure 2. 5 (b)) show slightly better survivability than their lowermost Caradoc predecessors. *Parabasilicus powisii* (439), *Hemiarges angustifrons* (450), *Stenopareia balclatchiensis* (453), *Calyptaulax brongniartii* (457), *Amphilichas planus* (481), *Toernquistia translata* (488) and *Decoroproetus calvus* (516) all stand out as having particularly long ranges.

The zonation of the Ashgill is very precise compared with the rest of the Palaeozoic, consisting of assemblage zones based on brachiopods and trilobites, some of which (trinucleids in particular) are particularly sensitive biostratigraphical indicators (Thomas *et al.* 1984). In the Ashgill, almost all specific ranges are short, and most of those species that did survive for most of the duration of the Ashgill are ones which originated in the Caradoc. Time scales published since that of Harland *et al.* (1989) show the Ashgill Series as significantly longer than is shown on Figure 2. 5; e.g. Tucker *et al.* show a duration of about 8 myr. (Tucker *et al.* 1990: figure 4); Compston and Williams (1992) give a comparable duration; compare the duration of 4.1 myr. given by Harland *et al.* 1989: figure 1.7. However, even if the duration of the Ashgill is thus considered to be twice as long as shown in Figure 2. 5, this still means that the species durations are very short compared with those elsewhere in the Palaeozoic. The Ashgill therefore appears to have been a time of considerable biological stress, although the short species durations may also to some extent reflect the large amount of taxonomic work which has been done on Ashgill trilobites (e.g. McNamara 1975, 1979; Price 1973, 1974, 1980; Whittington 1962-1968). No species range from the Ordovician into the Silurian.

The survivorship curve for Ordovician species approximates to a straight line for about 99% of the species although with some stepping. If a straight line is placed on these 99% of species, it can be seen that the extremely long duration 1% lie well to the right of this line on the plot, suggesting that their ranges are much longer than a model of constant probability of extinction with time predicts.

Silurian species (Figure 2. 6). It took a while for trilobites to re-establish themselves after the end Ordovician extinction event, with no species being known in Britain during the first two biozones of the Rhuddanian. The upper Rhuddanian and Aeronian interval seems to have been a time of some environmental persistence judging by the specific ranges, although with a marked extinction and subsequent radiation at the *convolutus - sedgwickii* boundary. *Calymene planicurvata* (739) is notable for its long chronostratigraphical range. A number of species pass through from the Aeronian into the Telychian. Within the Telychian, there are radiations at the base of the stage, and at the bases of the *griestoniensis* and *crenulata* zones. None of the new *crenulata* Zone species survived beyond the top of the *crenulata* zone. *Proetus latifrons* (775), *Cheirurus centralis* (777), *Prantlia grindrodi* (778), *Acastocephala macrops* (779), *Sphaerexochus mirus* (780), *Staurocephalus susanae* (782) and *Encrinurus tuberculatus* (783) all have notably long ranges.

There is a further radiation at the base of the Wenlock, and also within the Wenlock at the base of *riccartonensis* Zone. A number of Wenlock trilobites show good survivability, probably suggestive of settled environmental conditions. *Proetus concinnus* (797), *Delops nobilis marri* (810), *Odontopleura ovata* (811), *Raphiophorus parvulus* (812), *Heliocephalus coronatus* (817) and *Dalmanites myops* (824) are notable for their long ranges. The base of the *lundgreni* Zone is marked by another radiation. Of the species which originated at this level, *Leonaspis coronata* (838), *Acaste downingiae* (841), *Acaste inflata* (842) and *Decoroproetus scrobiculatus* (847) have notably long ranges. Within the Ludlow, a number of long ranges are evident, with *Homalonotus knightii* (860) and *Acastella minor* (862) most notable. No species pass from the Silurian into the Devonian.

The survivorship curve for Silurian species approximates a straight line for about 95% of the species. The few very long-ranging species fall well to the left of a straight line defined by the 95% of shorter range species *i.e.* their ranges are not so long as constant probability of extinction would suggest.

Devonian species (Figure 2. 7). Few lower Devonian species are known. In the middle Devonian, there is a radiation at the base of the *molarium* Zone, but all species which

Figure 2. 6. Chronostratigraphical ranges of trilobite species originating in the Silurian of England, Scotland and Wales. Constructed as in Figure 2. 4. Inset shows the survivorship plot for the species.

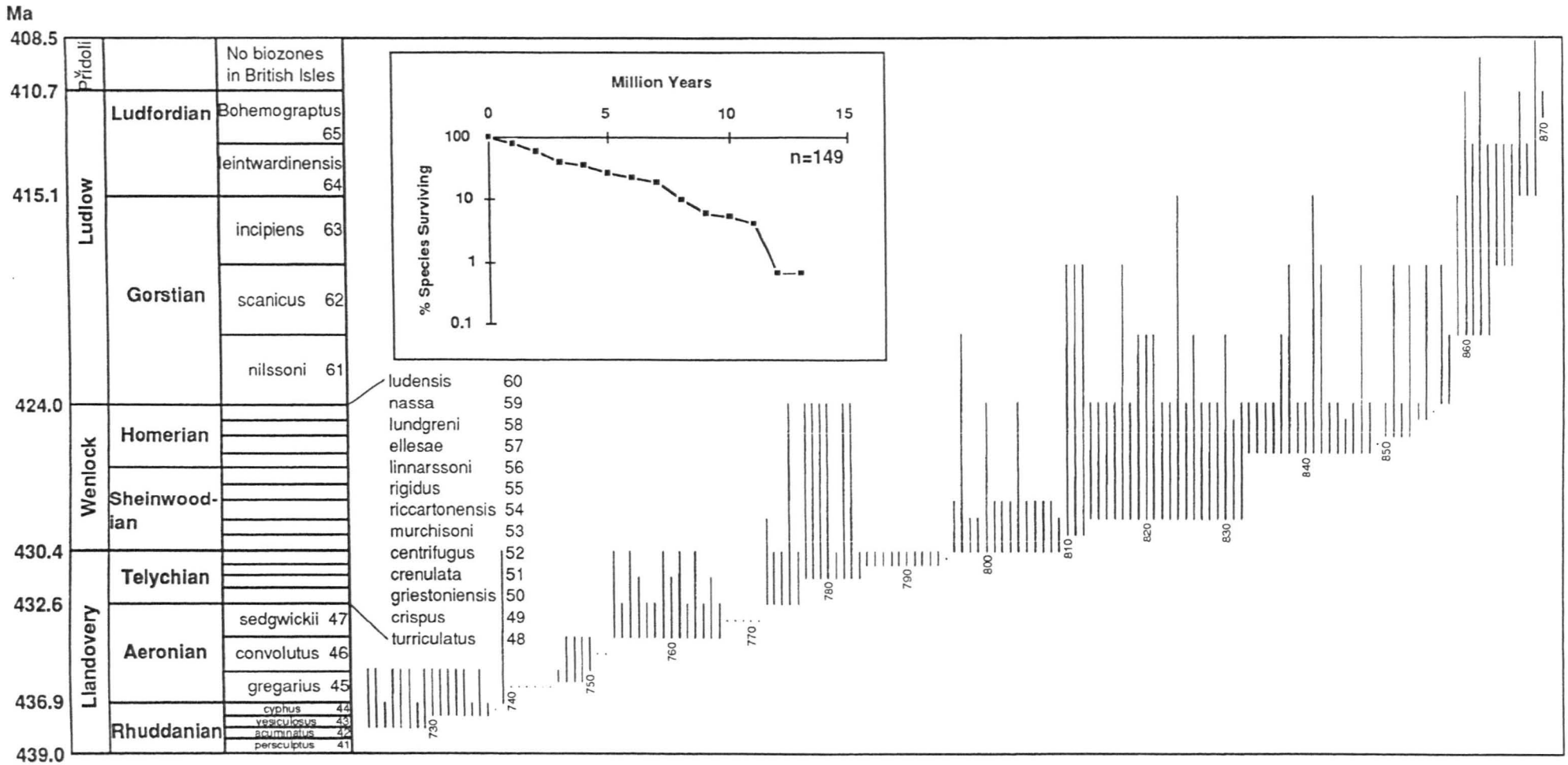

Figure 2. 7. Chronostratigraphical ranges of trilobite species originating in the Devonian of England, Scotland and Wales. Constructed as in Figure 2. 4. Inset shows the survivorship plot for the species.

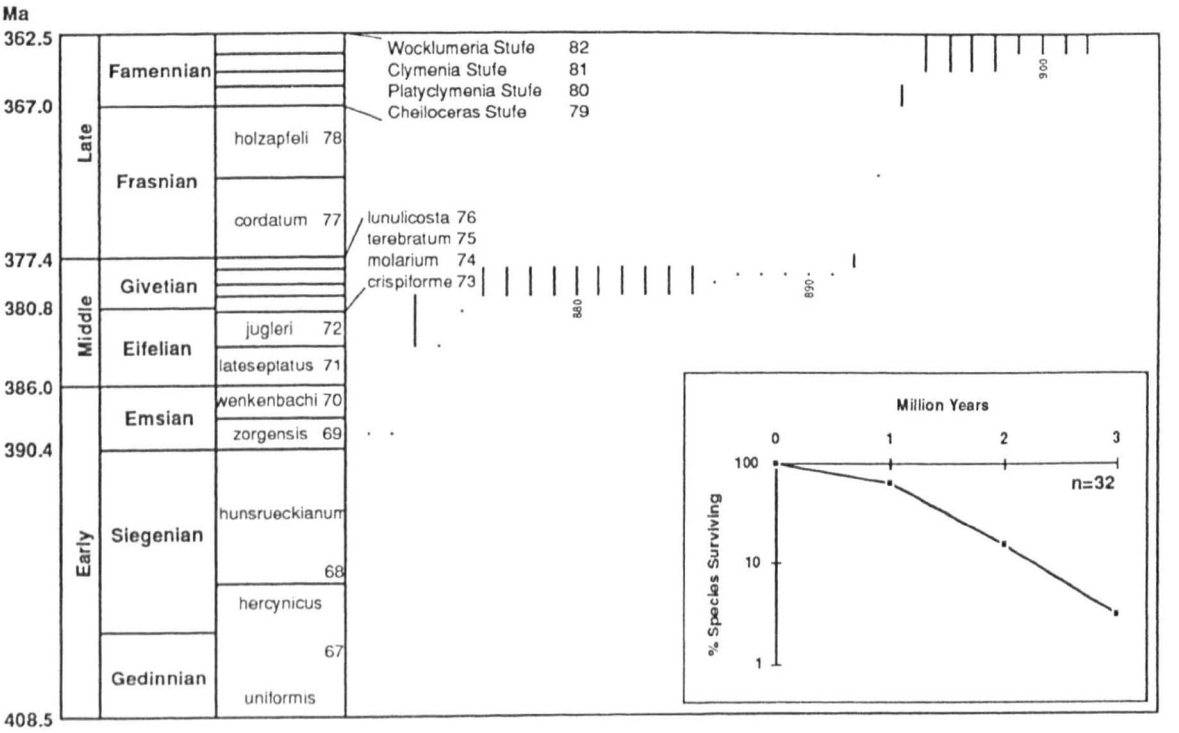

Figure 2. 8. Chronostratigraphical ranges of trilobite species originating in the Carboniferous of England, Scotland and Wales. Constructed as in Figure 2. 4. Inset shows the survivorship plot for the species.

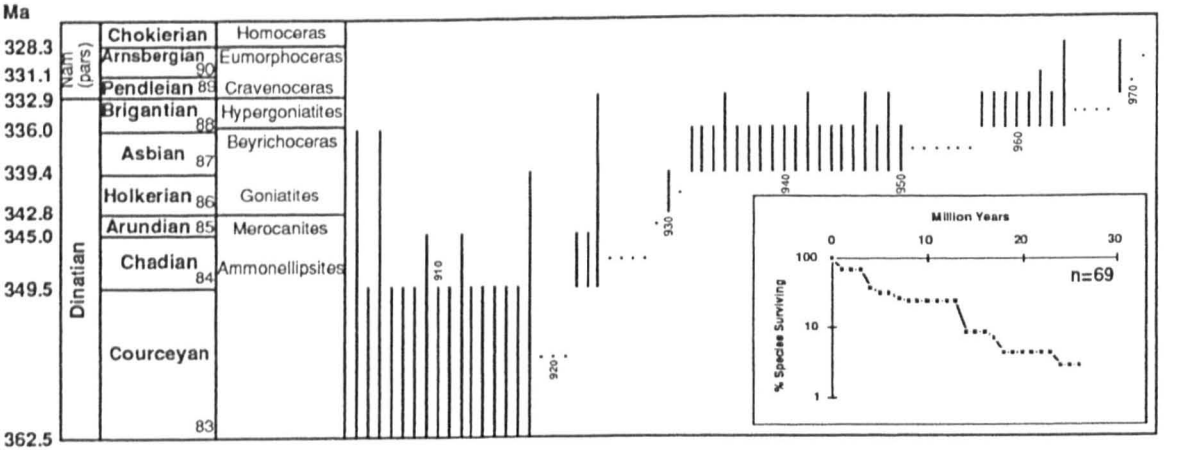

originated at this level have relatively short ranges. The upper Devonian has minor radiations at the base of the *Clymenia* and *Wocklumeria* zones. The Devonian appears to have been a time of short specific ranges. No species pass up from the Devonian into the Carboniferous.

Carboniferous species (Figure 2. 8). Thomas *et al.* (1984) noted that several of the species on their range charts for the Carboniferous may be synonymous; they also considered that some material presently incorporated into the same species may ultimately prove to belong in more than one species.

There are a number of long-ranging species in the Courceyan. *Carbonocoryphe colei* (903), *Namuropyge discors* (905), *Bollandia globiceps* (909), *Brachymetopus maccoyi* (912) and *Phillibolina worsawensis* (918) stand out as having particularly long ranges. A small number of species are present in the Chadian, of which *Cummingella laticaudata* (924) has a particularly long range. The Asbian and Brigantian stages both have radiations at their bases, but specific ranges do not approach those seen in the Courceyan.

The survivorship curve for Carboniferous species is markedly stepped. This appears to reflect the fact that Thomas *et al.* (1984) depicted the ranges of all Carboniferous species on their range chart (*i.e.* those known from more than one locality) as beginning and ending at stage boundaries (Thomas *et al.* 1984: figure 29), and is exacerbated by the fact that the stage durations as given by Harland *et al.* (1989) have a discrete distribution: the Courceyan is long (13 myr.), the Arundian, Pendleian and Arnsbergian are short (between 1.8 and 2.8 myr.), and the Chadian, Holkerian, Asbian and Brigantian are intermediate in duration (between 3.1 and 4.5 myr.) (Figure 2. 8).

Cambrian genera (Figure 2. 9). A number of long generic ranges are apparent within the Comley Series: *Callavia* (1), *Olenellus* (4), *Olenelloides* (8) and *Serrodiscus* (10) stand out as having particularly long generic ranges. No genera pass from the Comley Series into the St. David's Series. There are a number of long-ranging genera within the St. David's Series, the longest being *Ptychagnostus* (34) and *Hypagnostus* (38). The only genus which passes from the St. David;'s Series into the Merioneth Series is *Grandagnostus* (57). Within the Merioneth Series *Micragnostus* (78), *Parabolinella* (79) and *Shumardia* (86) have notably long ranges. These three genera and four others, *Niobella* (84), *Psilocephalinella* (85), *Beltella* (87) and *Dichelepyge* (90) are the only ones that range up from the Cambrian into the Ordovician.

Ordovician genera (Figure 2. 10). A number of extremely long durations are apparent among genera originating in the Ordovician. In the Tremadoc, *Illaenus* (94) and *Geragnostus* (95) have remarkably long ranges. Within the Arenig, *Ampyx* (116) is

Figure 2. 9. Chronostratigraphical ranges of trilobite genera originating in the Cambrian of England, Scotland and Wales. Constructed as in Figure 2. 4. Inset shows the survivorship plot for the genera.

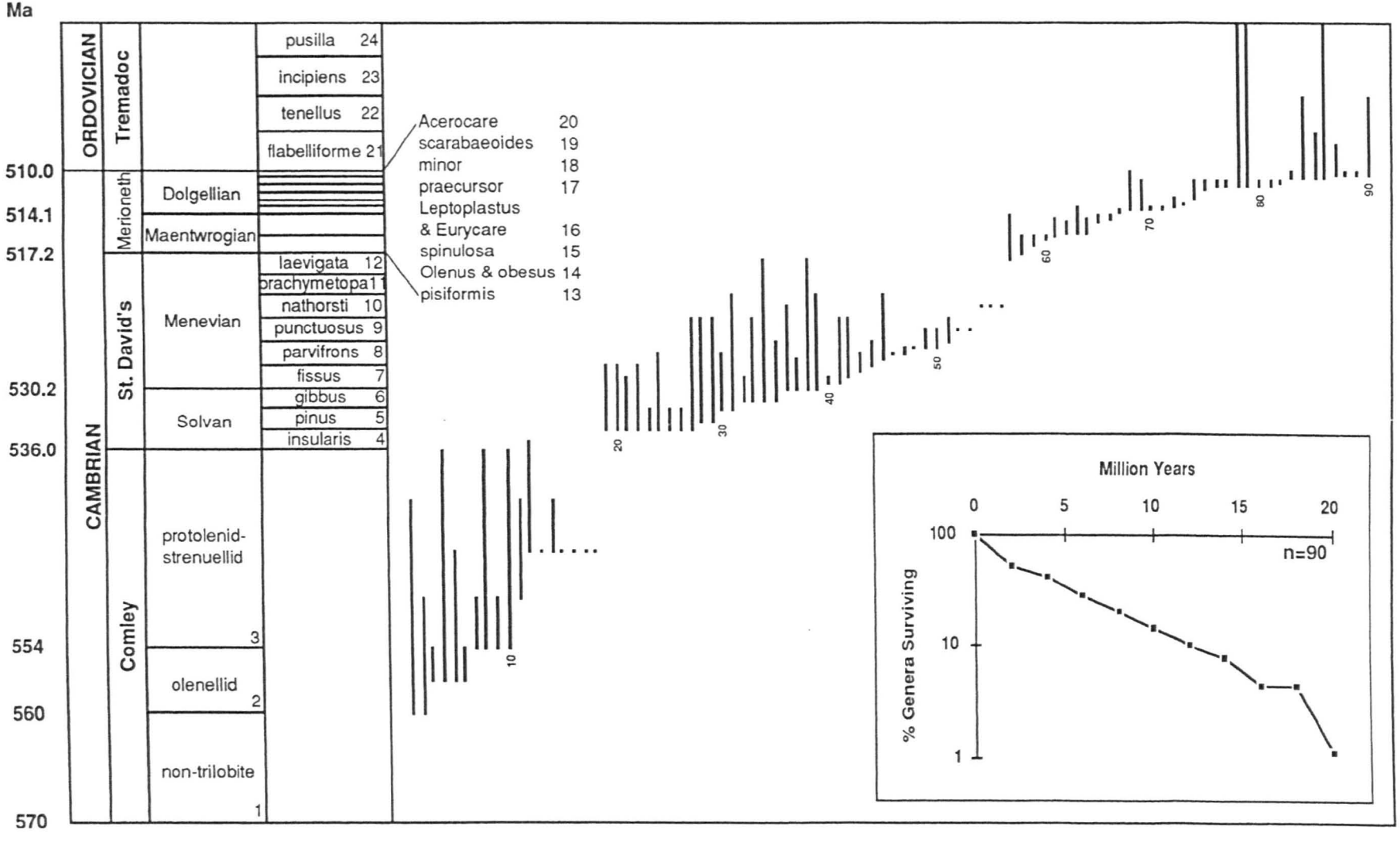

Figure 2. 10. Chronostratigraphical ranges of trilobite genera originating in the Ordovician of England, Scotland and Wales. Constructed as in Figure 2. 4. Chronostratigraphy after Fortey *et al.* (in press.). Divisions within the Caradoc are considered to be substages. Inset shows the survivorship plot for the genera.

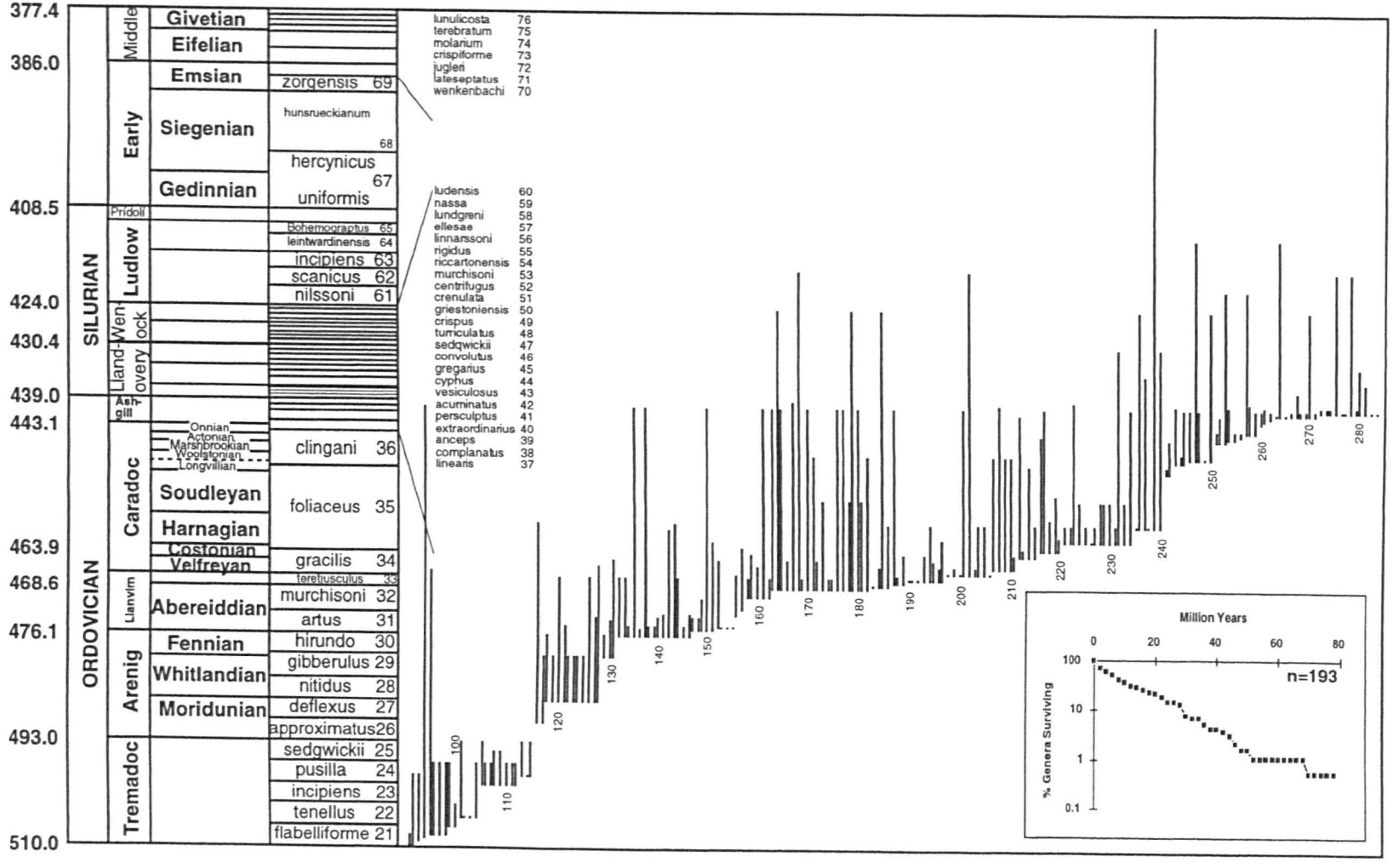

most notable. *Dionide* (135), *Flexicalymene* (137), *Prionocheilus* (=*Pharostoma*) (150) and *Remopleurides* (161) stand out in the Abereiddian. A number of genera with extremely long ranges originated within the Llandeilian: *Calyptaulax* (163), *Ceratocephala* (164), *Ceraurinella* (165), *Cybeloides* (167), *Decoroproetus* (168), *Encrinuroides* (170), *Eobronteus* (171), *Lonchodomas* (176), *Primaspis* (177), *Sphaerexochus* (179), *Sphaerocoryphe* (180), *Xylabion* (182) and *Hemiarges* (185).

Within the Caradoc, the following long ranging genera originated: *Atractopyge* (187), *Gravicalymene* (201), *Miraspis* (202), *Arthrorhachis* (208), *Brongniartella* (212), *Kloucekia* (217), *Diacanthaspis* (223), *Stenopareia* (232), *Harpidella* (236), *Otarion* (237), *Proetus* (239), *Scotoharpes* (240), *Calymene* (247), *Cyphoproetus* (250) and *Platylichas* (253).

Genera which originated within the Ashgill have short generic durations in general, marked exceptions being: *Acidaspis* (257), *Encrinurus* (264) (Ordovician examples probably do not in fact belong in this genus; they are probably better placed within *Erratencrinurus*, A. W. Owen pers. comm.), *Staurocephalus* (270), *Raphiophorus* (275) and *Leonaspis* (278) all of which continued into the Silurian.

Silurian genera (Figure 2. 11). Chronostratigraphical ranges of genera which originated within the Rhuddanian and Aeronian stages are mostly relatively short; *Acernaspis* (285), *Youngia* (289), *Eophacops* (290), *Bumastus* (292) and *Dalmanites* (293) stand out as having slightly longer ranges. In the Telychian, *Cheirurus* (296) and *Warburgella* (300) are notable. Three genera with exceptionally long ranges originated within the Sheinwoodian Stage of the Wenlock Series: *Cornuproetus* (301), *Acanthopyge* (309), *Cyphaspis* (313). All three range up into the Middle Devonian. Only three new genera originated in the Ludlow, and none of them lasted beyond the end of the Silurian. The three Wenlock genera mentioned above are the only Silurian genera which pass up into the Devonian.

Devonian genera (Figure 2. 12). Generic durations within the Devonian are relatively short, paralleling specific durations (see above). The longest ranging genus is the Late Devonian *Typhloproetus* (338) which ranges through into the upper Dinantian (Carboniferous) and is the only Devonian genus to range up from the Devonian into the Carboniferous.

Carboniferous genera (Figure 2. 13). Generic ranges within the Carboniferous more or less parallel the pattern seen in Carboniferous species (see above). The longest ranging genera are those which originated within the Courceyan Stage, almost all of which lasted throughout the Dinantian: *Archegonus* (339), *Bollandia* (340), *Brachymetopus* (341),

Figure 2. 11. Chronostratigraphical ranges of trilobite genera originating in the Silurian of England, Scotland and Wales. Constructed as in Figure 2. 4. Inset shows the survivorship plot for the genera.

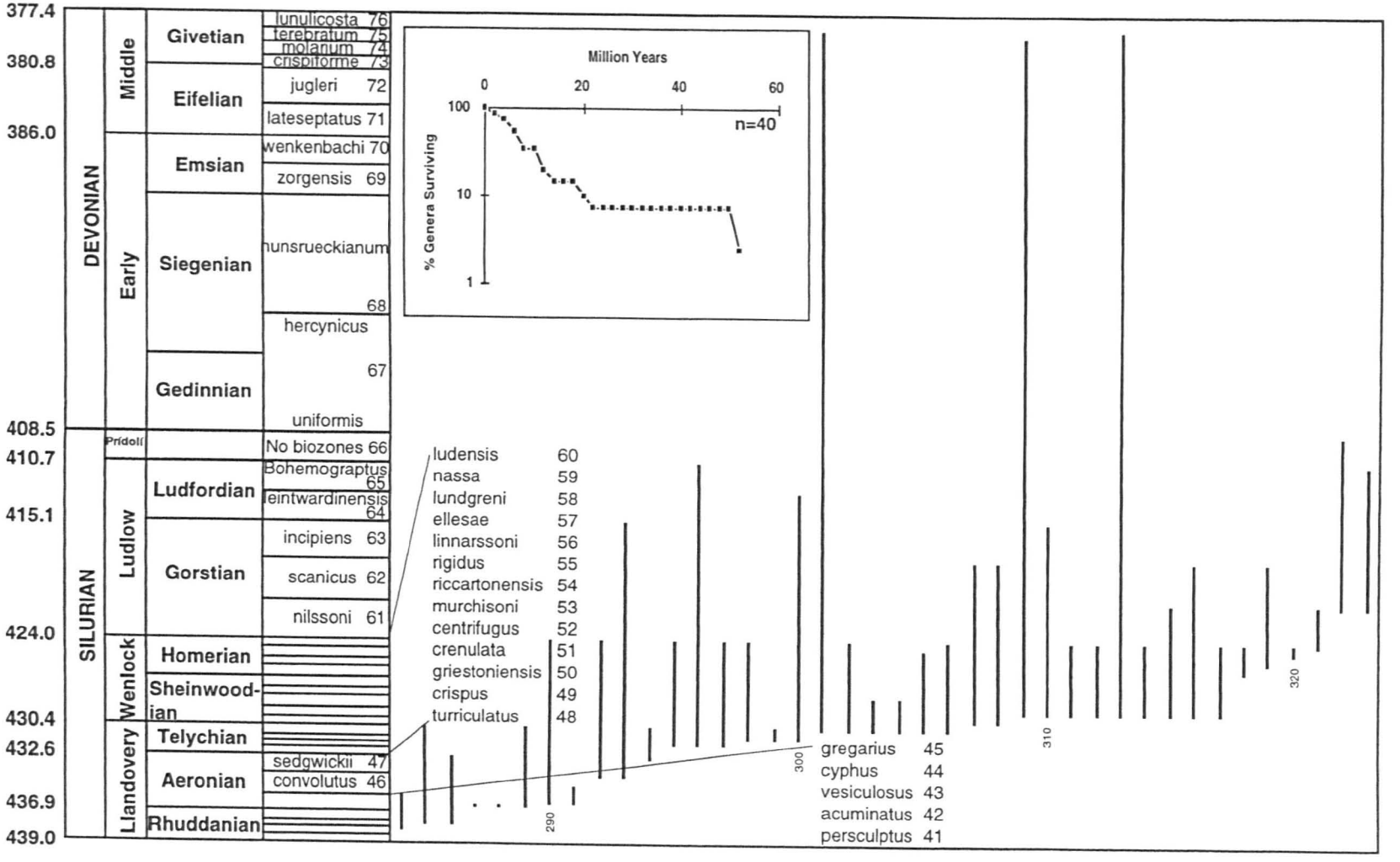

Figure 2. 12. Chronostratigraphical ranges of trilobite genera originating in the Devonian of England, Scotland and Wales. Constructed as in Figure 2. 4. Inset shows the survivorship plot for the genera.

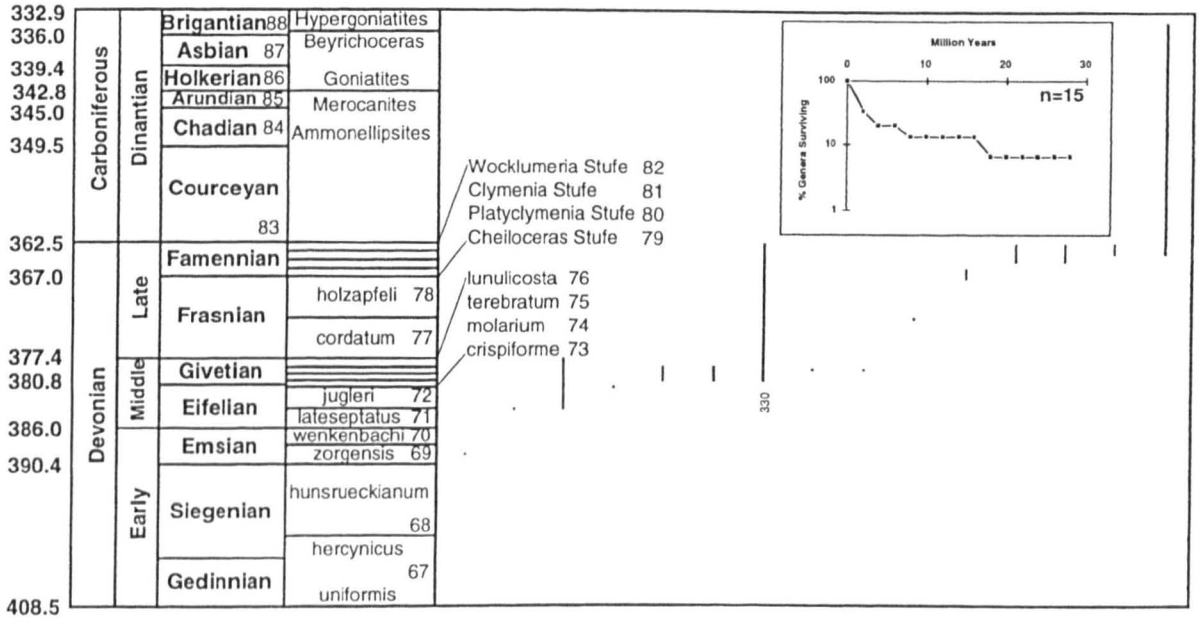

Figure 2. 13. Chronostratigraphical ranges of trilobite genera originating in the Carboniferous of England, Scotland and Wales. Constructed as in Figure 2. 4. Inset shows the survivorship plot for the genera.

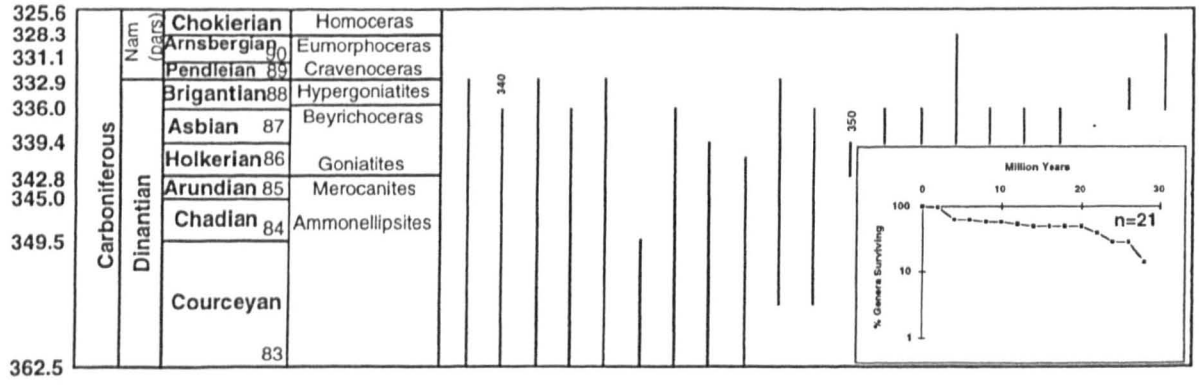

Carbonocoryphe (342), *Eocyphinium* (343), *Namuropyge* (345), *Phillibolina* (346), *Phillipsia* (347), *Cummingella* (348), *Cyrtoproetus* (349). Genera which originated later in the Dinantian have much shorter ranges. Only two late Dinantian genera, *Paladin* (353) and *Particeps* (359) range up into the Namurian.

2. 4. Relationship between Generic Duration and Environment.

Fortey (1980) found that the chronostratigraphical ranges of Ordovician genera could be related to their location on the marine palaeoslope as indicated by their occurrence in the fossiliferous sections of the early Ordovician Valhallfonna Fm. of northern Spitsbergen. Fortey found that genera whose durations were in excess of 50 myr. tended to be confined to one of two sites on the palaeoslope: (i) the shallow water environment associated with carbonate mounds at the edge of the carbonate platform, characterised by the illaenid-cheirurid trilobite association of Fortey (1975); (ii) the deep water lower slope low oxygen environment characterised by deposition of black graptolitic shales and the occurrence of the olenid trilobite association of Fortey (1975). Fortey (1980) attributed long generic ranges in the former environment to the temporally persistent nature of the shelf edge environment with high resource predictability. Conversely Fortey attributed long ranges in the latter environment to the stressed nature of that environment, to which a small number of genera became well adapted. Sites on the palaeoslope intermediate between these shallow water and deep water environments (*i.e.* the upper slope, characterised by the nileid trilobite association of Fortey 1975) were found by Fortey (1980) to be sites of more rapid generic turnover. Fortey considered that this intermediate palaeoslope environment may have been an important source of recruitment to the shallower and deeper water environments.

As part of this study, a simple experiment was undertaken to study the effect of environment on genus longevity, using the longevity data provided by Sloan (1991). Shaw and Fortey (1977) assigned lithological formations from the Llanvirn to Caradoc interval in North America to postulated broad depositional environments. Each formation was assigned to the "shelf" environment, the "shelf edge" environment, or the "slope" environment, these environments being defined as follows:

"Shelf": the range of water depths from the extreme near shore environment to the inner edge of the carbonate mounds of the "shelf edge" environment;

"Shelf Edge": the carbonate mound structures at the edge of the continental shelf commonly characterised by the deposition of pale coloured pure limestones;

"Slope": the range of water depths beyond the edge of the carbonate mounds characterised by the deposition of proximal argillaceous limestones grading distally into dark basinal shales.

In some cases, Shaw and Fortey (1977) felt justified in subdividing these classes (e.g. inner and outer shelf, upper and lower slope). For each formation, as well as stating the postulated depositional environment, Shaw and Fortey listed the trilobite genera associated based on a survey of the literature.

It was originally intended to use the information given by Shaw and Fortey (1977) to assign North American trilobite genera to a position on the palaeoslope in a similar way to that used by Fortey (1980) for Spitsbergen trilobites, and then extract the durations of the genera from Sloan (1991) to see how generic longevity varied with position on the palaeoslope. However, it rapidly became clear on attempting this that many of the genera occurred in different environments at different times or simultaneously. Therefore, the genera listed by Shaw and Fortey (1977) were placed in a set of environmental groupings as follows:

Shelf: the trilobite genera restricted to the range of shelf environments inshore of the shelf edge carbonates;

Shelf Edge: the trilobite genera restricted to the shelf edge carbonates;

Slope: the trilobite genera restricted to the slope beyond the shelf edge;

Shelf and Shelf Edge: the trilobite genera occurring in both of these environments but not found on the slope;

Shelf Edge and Slope: the trilobite genera occurring in both of these environments but not found on the shelf;

Shelf and Slope: the trilobite genera occurring in both of these environments but not found on the shelf edge;

General: the trilobite genera found in all three environmental groupings.

The experiment was undertaken using two sets of genera:

(i) All of the Ordovician genera listed by Shaw and Fortey (1977). Since many genera arose in one environment and then spread into others, there are relatively high numbers of genera in the "composite" environmental groupings, *i.e.* those that contain more than one environmental range.

(ii) Genera from Llanvirn strata only, grouped according to their environmental occurrences in the Llanvirn (*i.e.* disregarding the rest of the Ordovician entirely). There are fewer genera to consider (those from the Llanvirn only) but this is offset by the fact that dealing only with the Llanvirn interval reduces the effects of genera arising in one environment and later colonising others; *i.e.* there is less reliance on the "composite" environmental groupings. This can thus be considered a "snap shot" of the situation in the Llanvirn.

The results are shown in Figure 2. 14. Figure 2. 14 A shows the results using the durations (from Sloan 1991) of all Ordovician genera listed by Shaw and Fortey (1977)

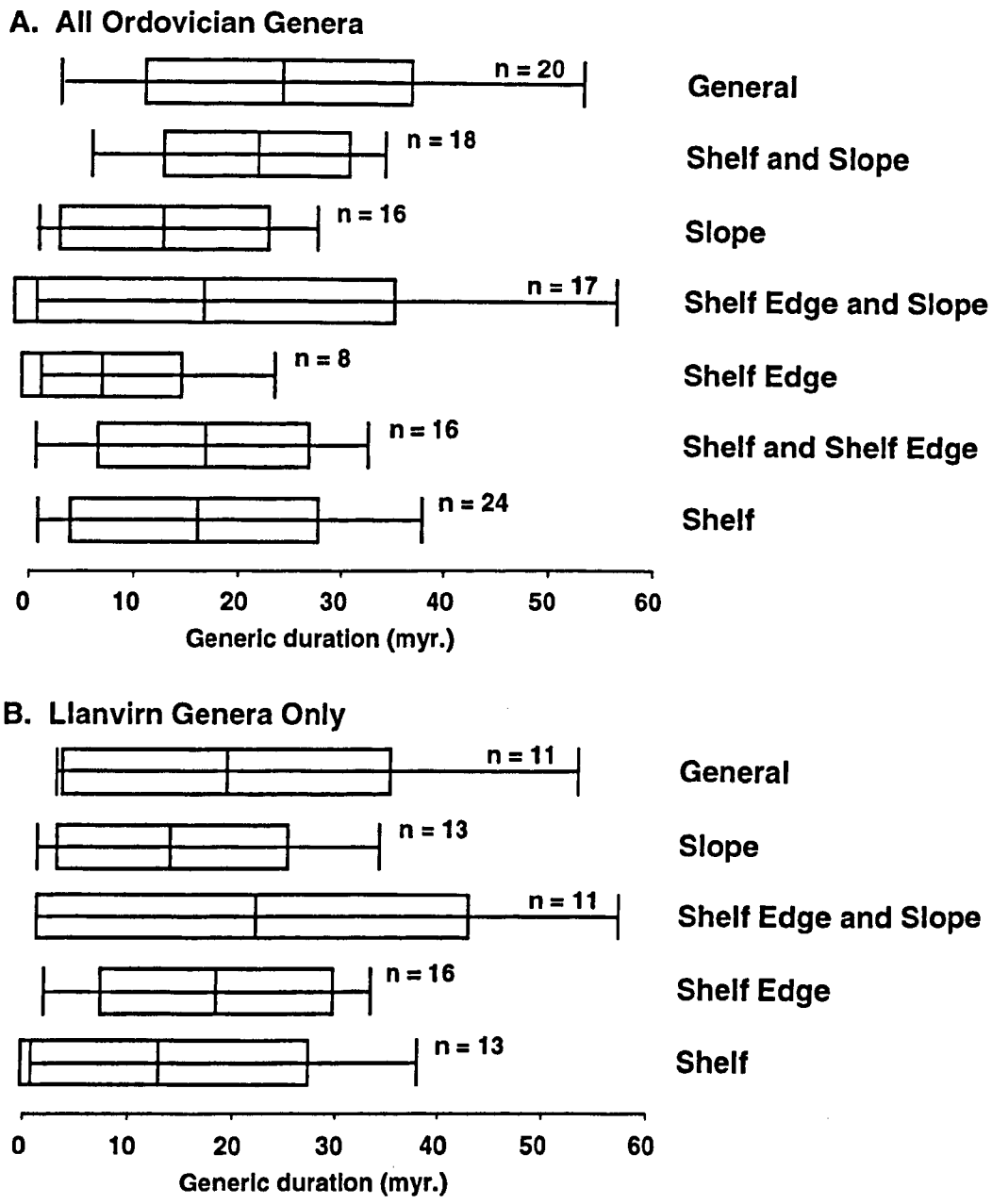

Figure 2. 14. Dice diagrams summarising the durations of trilobite genera from the Laurentian Province, grouped according to faunal affinities extracted from Shaw and Fortey (1977). For each group, the mean duration (vertical bar), range of durations (horizontal bar) and one standard deviation to either side of the mean value (open rectangle) are shown. Generic chronostratigraphical ranges extracted from Sloan (1991). A: all Ordovician genera listed by Shaw and Fortey (1977); B: Llanvirn genera listed by Shaw and Fortey only.

(experiment (i) above). The results are plotted as "dice diagrams" (Jones 1988) in which, for each group, the horizontal bar shows the range of values, the vertical bar shows the mean value, and the open rectangle shows one standard deviation to either side of the mean value. It can be seen from Figure 2. 14 A that the greatest mean durations are exhibited by generalist genera and by those occurring in both the shelf and slope environments. Greatest durations of all are shown by genera which lived in both the shelf edge and slope environments and by generalists. Lowest mean durations are shown by genera restricted to the shelf edge environment.

The Llanvirn "snap shot" shows a not dissimilar result, Figure 2. 14 B. The greatest mean durations are exhibited by genera which lived in both the shelf edge and slope environments, with the generalists and the genera restricted to the shelf edge carbonate environment approximately next equal. The greatest durations of all are shown by genera which lived in both the shelf edge and slope environments and by generalists (in fact the same genera which show the greatest durations in Figure 2. 14 A).

Two interesting points arise from these experiments:

(i) The longest durations are exhibited by genera which are not restricted to one particular palaeoenvironment. The generalists (genera found at all positions on the palaeoslope) and the genera which occur in both the shelf edge and slope environments appear to be most successful in terms of duration. It is probable that genera which were endemic to particular palaeoenvironments were prone to extinction through locally occurring detrimental events (e.g. anoxia) or failing to keep up with locally-acting selection pressures which were imposed either by the physical environment (e.g. changes in nutrient supply due to changing patterns of oceanic circulation and/or connectivity with the open ocean) or by the biological environment (e.g. appearance of new predators and/or parasites, increased competition for resources etc.). Genera which were more geographically and environmentally cosmopolitan were able to survive these events by virtue of their widespread distribution.

(ii) The relatively short durations of genera which were restricted to the shelf edge carbonate environment is something of a surprise, since this environment is generally considered to be relatively stable and persistent in time. It is probable that the relatively short generic durations reflect high rates of taxonomic turnover, probably driven by intense selection pressures imposed by the biological environment in this ecologically complex setting. This result appears to be at odds with that of Fortey (1980) who considered the shelf edge setting to be a site characterised by long generic durations (see above). In spite of this pattern at the generic level, the shelf edge environment is known to be a site of longevity at higher taxonomic levels (e.g. Fortey 1975: "illaenid-cheirurid association").

2. 5. Conclusions.

In a study of the calibrated chronostratigraphical ranges of 359 genera and 971 species of trilobites from the Cambrian to Carboniferous interval in England, Scotland and Wales, the following results were found. Of 90 Cambrian genera, the mean duration is 4.42 myr., and the longest duration is exhibited by *Olenellus* Billiings (21 myr.). Of 190 Cambrian species, the mean duration is 2.13 myr., and the longest duration is exhibited by *Callavia callavei* (Lapworth) (19.5 myr.). Of 193 Ordovician genera, the mean duration is 10.89 myr., the longest duration genus being *Proetus* Steininger (79.8 myr.). Of 531 Ordovician species, the mean duration is 2.06 myr., the longest duration being that of *Atractopyge petiolulata* Tripp (26.2 myr.; however, as noted earlier, the taxonomy of this species is in need of revision). The results for Ordovician genera are comparable with those derived by Sloan (1991) for Laurentian genera. In the Silurian, 40 genera have mean duration 10.34 myr., the longest duration being that of *Cornuproetus* Richter and Richter (52.2 myr.). Of 149 species, the mean duration is 3.54 myr., and the most durable species is *Dalmanites myops* (König) (13.9 myr.). The mean duration for 15 Devonian genera is 4.19 myr., the most durable genus being *Typhloproetus* Richter (29.2 myr.). The mean duration for 32 Devonian species is 1.12 myr., the longest duration being exhibited by *Scutellum flabelliferum* (Goldfuss) (3.5 myr.). Of 21 Carboniferous genera, the mean duration is 14.82 myr., and the most durable genera are *Archegonus* Burmeister, *Brachymetopus* McCoy, and *Eocyphinium* Reed (all 29.6 myr.). The mean duration for 69 Carboniferous species is 5.74 myr., and the maximum duration is exhibited by *Carbonocoryphe colei* (McCoy) and *Namuropyge discors* (McCoy) (both 26.5 myr.).

It does not appear from the calibrated range charts (Figures 2. 4 to 2. 13) that the commonness of stasis is stratigraphically controlled; *i.e.* in each stratigraphical interval there appear to be long-ranging taxa and short-ranging taxa occurring together, although some intervals are characterised by a predominance of very short-ranging taxa (e.g. Merioneth Series species and genera, Figures 2. 4 and 2. 9; Ashgill species, Figure 2. 5 (b)). These may reflect times of increased environmental stress.

The generic survivorship curves presented in Figures 2. 10 (Ordovician), 2. 11 (Silurian) and 2. 12 (Devonian) are curved concave-up, indicating that the longest duration genera have durations which are longer than a model of constant probability of extinction would predict (see subsection 2. 2. 2.). Raup (1978) explained why this might occur. Clades which have been in existence for a long time tend to have more member taxa than ones which have only been in existence for a short time. Therefore these clades have a lower probability of final extinction than clades which have only existed for a short time.

The species survivorship plots for the Cambrian (Figure 2. 4) and Ordovician (Figure 2.5 (b)) are also curved concave-up. This may reflect a species-level analogue of the case outlined above for genera. The longest-duration species may have more member populations which are geographically and/or ecologically widespread (either by virtue of their long past history, or simply because they are intrinsically widely adaptable) and therefore a lower probability of extinction than species which have existed for only a short time and may be more confined in their geographical and ecological distribution.

The longest duration taxa appear to be those which are cosmopolitan in their environmental distribution (Figure 2. 14). This widespread distribution probably enabled them to avoid localised factors which caused extinction in taxa which were more restricted in their occurrence.

CHAPTER THREE

STRATIGRAPHICAL FRAMEWORK.

3. 1. Introduction.

This chapter gives the stratigraphical context for the trilobite genera studied in chapters 5, 6 and 7. Stratigraphy has been dealt with as a separate chapter rather than including it within the individual chapters on *Achatella*, *Calyptaulax* and *Acernaspis* in order to avoid repetition: *Achatella* and *Calyptaulax* co-occur at many localities in the upper Ordovician of NW Scotland and North America, so discussing stratigraphy within each chapter would lead to unavoidable duplication of information.

The stratigraphy of each geographical area from which samples were studied is briefly described. The purpose is to provide a broad stratigraphical framework on which to view the samples in terms of lithology and depositional environment of the host rock, faunal association, and presence/absence of post-mortem transport of the organisms' remains. The geographical areas are arbitrarily described in approximate order of increasing remoteness from Glasgow. The chronostratigraphical scheme used for the Ordovician System is that of Fortey *et al.* (in press). For the Silurian System, the scheme of Cocks *et al.* (1992) is used. The stratigraphical columns are illustrated in the order which is most convenient for illustration. The following stratigraphical abbreviations have been used throughout the chapter: Fm. (Formation); Mbr. (Member); Gp. (Group).

3. 2. Llanvirn to Wenlock Succession of the Girvan District, SW Scotland.

The Ordovician and Silurian strata of the Girvan district have long been studied for their shelly fossils. The history of stratigraphical and palaeontological work in the area was summarised by Cocks and Toghill (1973). The Ordovician and Silurian outcrop of the district can be divided into three main geographical areas. The Craighead Inlier is a NE-plunging asymmetrical anticline with Ordovician rocks at its core. The inlier is bounded by Old Red Sandstone and Carboniferous rocks. The "Main Outcrop" lies to the south of the Girvan valley and consists of steeply-inclined Ordovician (best exposed along the Stinchar and Penwhapple valleys) and Silurian (best exposed along Penwhapple Valley) strata which are locally inverted. The Ordovician outcrop merges to the south with the main Southern Uplands outcrop. Where the Main Outcrop intersects the coast, it is referred to as the "Girvan Foreshore". Ingham (1978, 1992) provided a comprehensive overview of the Ordovician cover sequence (overlying the Ballantrae Volcanic Complex). Harper (1982) reviewed the stratigraphy of the Drummuck Gp. in the Craighead Inlier. Cocks and Toghill (1973) revised the Silurian stratigraphy of the district. Correlations of the Ordovician rocks of the Girvan district are shown in Figure 3. 1. Correlations of the Silurian rocks are shown in Figure 3. 2.

Ordovician cover sequence of Girvan. The Ordovician cover sequence rests unconformably on the Ballantrae Volcanic Gp. (Arenig and older). The oldest post-

Figure 3. 1. Correlation of the upper Ordovician rocks of the Girvan district (columns 1 - 4) and Tract 2 of the Northern Belt of the Southern Uplands (column 5). Ordovician chronostratigraphy after Fortey *et al.* (in press). Formations from which specimens of *Achatella* were used for morphometrics marked with an x; formations from which specimens of *Calyptaulax* were used for morphometrics marked with an open square.

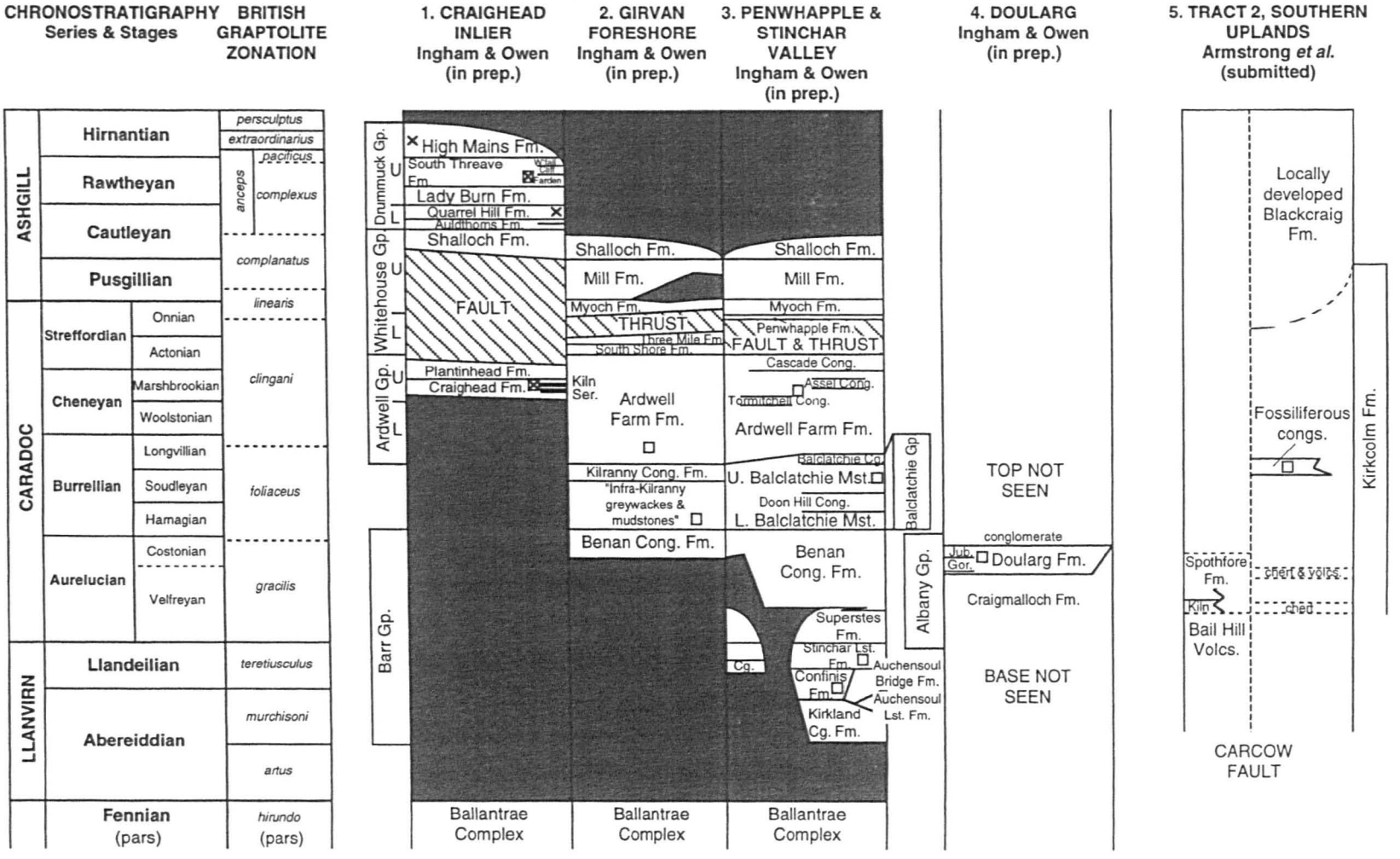

Figure 3. 2. Correlation of the Silurian rocks of the Girvan district (columns 1 - 3) and the North Esk Inlier, Pentland Hills (column 4). Silurian chronostratigraphy after Cocks *et al.* (1992). Formations from which specimens of *Acernaspis* were used for morphometrics marked with a filled square.

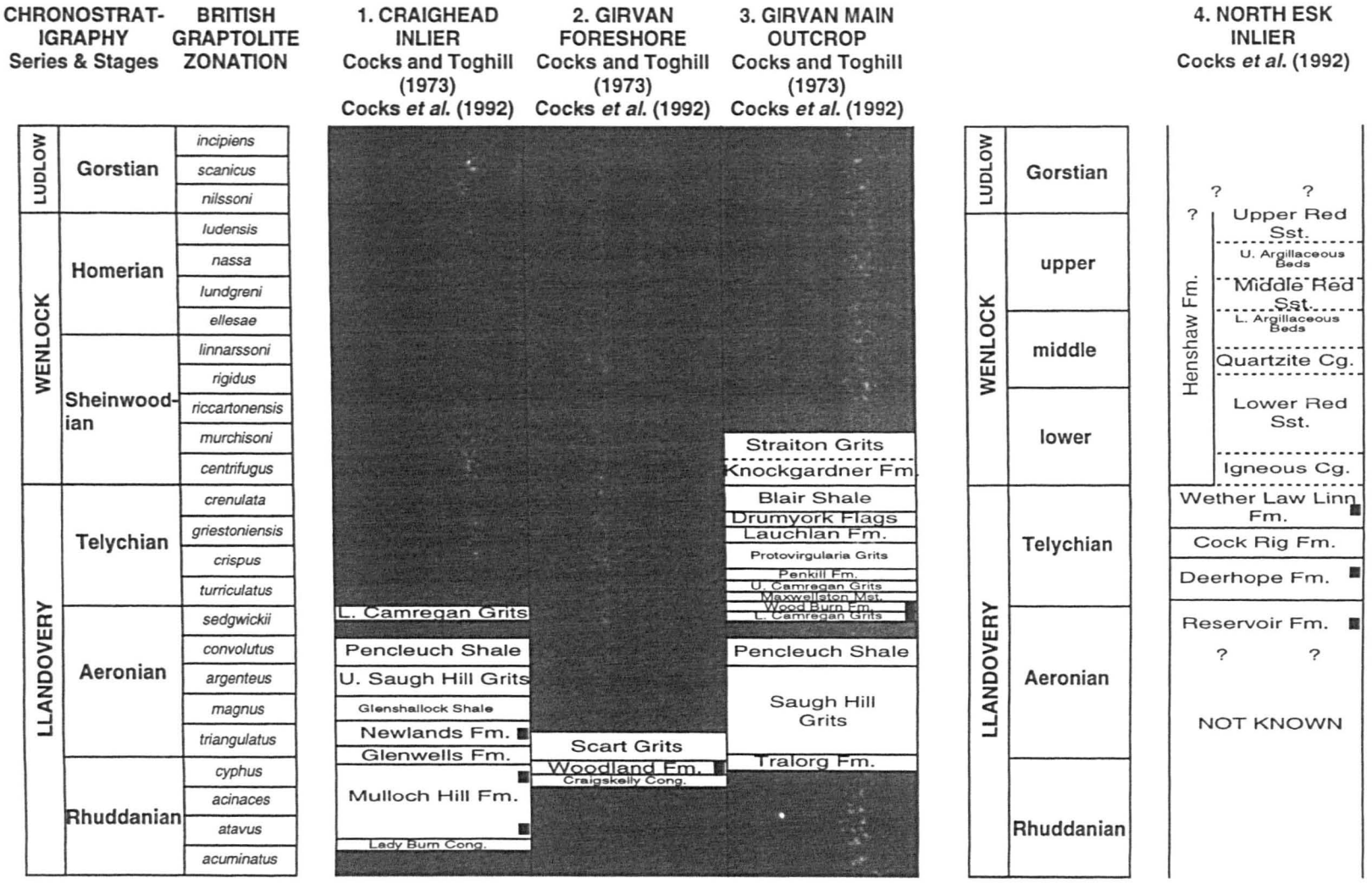

Ballantrae rocks outcrop in the Stinchar Valley, and the strata young progressively towards the north. The Barr Gp. is a transgressive sequence of conglomerates, shallow water sandstones and limestones deposited over an irregular Ballantrae surface (Ingham 1978). Tripp (1993) listed the trilobite associations known from the Barr Gp. The overlying Balclatchie and Ardwell groups are distal mudstones and turbidites with locally developed conglomerates and stratigraphically confined slumping which indicates a palaeoslope direction deepening towards the SE (Ingham 1978). The upper Ardwell Gp. in the Craighead Inlier is represented by the complex interdigitating limestone facies of the Craighead Fm. (Ingham 1992) which contains two mudstone tongues (Sericoidea and Kiln mudstones) which have been interpreted as representing brief deeper water interludes (Williams 1962; Tripp 1980b), and the graptolitic siltstones and shales of the Plantinhead Fm. The succeeding Whitehouse Gp. is a lithologically diverse unit with a basal "limestone flysch" unit (Ingham 1978) and increasing siliciclastic component upwards. Pelagic and deep water benthonic trilobites from the Whitehouse Gp. were listed by Ingham and Williams *in* Bassett *et al.* (1974: 58), and Ingham (1978) interpreted the group as having been deposited on the slopes of a submarine fan prograding towards the SE. The stratigraphy of the lower four formations of the Drummuck Gp. (Auldthorns, Quarrel Hill, Lady Burn and South Threave formations) was revised by Harper (1982) who considered them to represent another prograding submarine fan on the basis of the lithologies, sedimentary structures and faunal associations. The uppermost formation of the Drummuck Gp. is the High Mains Fm. (included within the Drummuck Gp. for the first time by Ingham and Owen in prep.) which represents a regressive sandstone facies developed as a result of the glacio-eustatic sea-level fall at the top of the Ordovician (Owen 1986; Harper 1981, 1988).

Ordovician formations yielding material included in the present study.

Confinis Fm. Fine grained, calcareous friable sandstones, fining upwards slightly and containing a rich shelly fauna: trilobites listed by Tripp (1962, 1993) and Williams (1962), described by Tripp (1962); brachiopods listed and described by Williams (1962). Trilobites referable to the shallow water illaenid-cheirurid association of Fortey (1975) (Ingham 1978). Deposited in shallow water, detrital content probably locally derived (Williams 1962; Ingham 1978).

Stinchar Limestone Fm. Basal rubbly limestones passing up into thickly bedded limestones with rare mudstone partings, and finally into platy and decalcified limestones in the topmost levels. Richly fossiliferous, especially in the topmost platy parts: trilobites listed by Tripp (1967, 1993) and Williams (1962), described by Tripp (1967); brachiopods listed and described by Williams (1962). Trilobites referable to the shallow water illaenid-cheirurid association of Fortey (1975) in lower part of formation (Ingham 1978; Ingham and Tripp 1991), a somewhat deeper water association in the upper part (Tripp 1993).

Separation Sandstone Member, Doularg Fm. Fifteen cm thickness of bedded calcareous silty mudstones separating the underlying Gorse Mbr. (poorly bedded mudstones with limestone nodules) from the overlying Jubilation Mbr. (calcareous silty mudstones), exposed in Plantation Burn on the north slope of Doularg Hill (Ingham and Tripp 1991). The member yields a sparse fauna (the overlying Jubilation Mbr. is much more fossiliferous), whose trilobites were listed and described by Ingham and Tripp (1991). Ingham and Tripp (1991) interpreted the Gorse Mbr. as representing an "outer neritic" environment, and the Jubilation Mbr. as representing a somewhat deeper water environment, characterised by a nileid (Fortey 1975) trilobite association. The Separation Sandstone Mbr. is probably intermediate between these two environments.

Upper Balclatchie Gp. Dark green and grey mudstones with locally developed conglomerates. Mudstones yield a trilobite fauna dominated by raphiophorids and remopleuridids with many inarticulate brachiopods (Ingham 1978). Trilobites listed by Williams (1962) and listed and described by Tripp (1980a); brachiopods listed and described by Williams (1962). Deposition was probably on the lower slope in euxinic conditions, and the associated conglomerates are probably slide conglomerates (Williams 1962).

"Infra-Kilranny greywackes and mudstones". Fossiliferous shales, siltstones and mudstones, described by Williams (1962). Trilobites listed by Williams (1962) and listed and described by Tripp (1980a); brachiopods listed and described by Williams (1962). Interpreted as distal turbidites by Williams (1962).

Ardwell Farm Fm. Fine greywackes composed of laminated green-grey siltstones and mudstones, with locally developed conglomeratic horizons and stratigraphically confined slump structures (Ingham 1978). Graptolitic fauna known from throughout the formation (Ingham 1978); stratigraphically localised shelly faunas also known (Tripp 1980a). Trilobites listed by Williams (1962) and listed and described by Tripp (1980a). Faunas probably accumulated by rapid bottom currents which carried the material some way from its original location (Ingham 1978).

Kiln Mudstone, Craighead Fm. Upper of two mudstone tongues developed within a complex of limestone facies. Mudstones described by Williams (1962) and by Tripp (1980b). Kiln mudstone contains an abundant and diverse entrained shelly fauna: trilobites listed and described by Tripp (1954, 1980b), also listed by Williams (1962); brachiopods listed and described by Williams (1962).

Quarrel Hill Fm. Series of mudflows consisting of bedded green mudstones with occasional thin sandstone interbeds, the mudstones being locally highly fossiliferous with an abundant and diverse entrained fauna described by Harper (1982). The mudflows were probably emplaced with force since they contain debris up to pebble size (Harper 1982).

The Quarrel Hill Crinoid Bed. A unit of coarse green sandstone between 15 and 20cm thick which occurs near the summit of the Quarrel Hill Fm. containing at least eight laterally persistent shelly laminae (Harper 1982). Fossils occur as broken fragments dominated by brachiopod and crinoid fragments, with trilobite fragments being rare (Harper 1982).

Lady Burn Starfish Beds, South Threave Fm. Three highly fossiliferous sandstone beds occurring near the top of the lowest Farden Mbr. of the South Threave Fm. The beds yield abundant and diverse faunas described by Harper (1981a, 1982). Much of the material is relatively complete. Goldring and Stephenson (1972) suggested that the fauna was entombed as a result of shallow water turbulence which concentrated and redeposited the fauna. Harper (1982) preferred rapid downslope movement and burial of the fauna, especially in light of the evidence of slope instability elsewhere in the Ordovician succession of Girvan (e.g. Ingham 1978).

High Mains Fm. Massively bedded fine to medium grained homogeneous grey quartzitic sandstones, from which two distinct shelly faunas have been recovered: a stratigraphically lower fauna dominated by a small number of small, opportunistic brachiopod species; and a stratigraphically higher fauna dominated by a more diverse set of brachiopods belonging to the *Hirnantia* fauna (Harper 1981, 1988). The trilobites from throughout the formation are relicts of the Rawtheyan North American fauna (Owen 1986). The formation is considered to have been deposited as channel fills on the outer shelf and upper slope during the end-Ordovician regressive phase (Owen 1986; Harper 1988).

Llandovery sequence of Girvan. Lower Llandovery strata both overlap and overstep the upper Ordovician towards the SW in the Girvan district (Harper 1988). Transgression at the base of the Llandovery is marked both by lithologies and by associated brachiopod communities (Cocks and Toghill 1973). In the Craighead Inlier the earliest Silurian formations (Lady Burn Conglomerate and Mulloch Hill Fm.) contain in ascending order a low-diversity *Cryptothyrella* community, a high-diversity *Cryptothyrella* community, and a *Clorinda* community overlain by the graptolitic shales of the Glenwells Fm (Cocks and Toghill 1973). The foreshore Silurian sequence (the Woodland Fm.) contains, in ascending stratigraphical order, a *Stricklandia* community , then a *Clorinda* community, followed by graptolite-bearing shales overlain by the unfossiliferous Scart Grits (Cocks and Toghill 1973). The next sequence of shelly fossil communities occur in the Aeronian of the Craighead Inlier with the Newlands Fm. which contains, in ascending order, a *Stricklandia* community and then a *Clorinda* community indicating a shelf-edge environment in the Craighead Inlier, while in the Main Outcrop the contemporaneous formation is the turbiditic (and generally unfossiliferous) Saugh Hill Grits (Cocks and Toghill 1973). In the lower Telychian of the Main Outcrop, the Lower Camregan Grits

and the Wood Burn Fm. contain, in ascending order, a mixed *Lingula - Eocoelia* community, an *Eocoelia* community, a *Pentamerus* community, and a *Clorinda* community overlain by the graptolitic Maxwellston Mudstone, another transgressive sequence (Cocks and Toghill 1973). The Silurian sequence at Girvan therefore represents a transgressive sequence which follows the short-lived regression at the end of the Ordovician.

Silurian formations yielding material included in the present study.

Mulloch Hill Fm. Interbedded shales, siltstones and sandstones, containing an abundant and diverse shelly fauna. Howells (1982) listed and described the trilobites. Cocks and Toghill (1973) noted that the brachiopods belong to a high-diversity *Cryptothyrella* community representing a relatively shallow water depositional environment.

Woodland Fm. Massive or bedded grey and purple flaggy siltstones and shales, yielding rich shelly faunas: Cocks and Toghill (1973) reported diverse brachiopod faunas as both life and death assemblages representing the *Stricklandia* and *Clorinda* communities, grading up into graptolitic facies in the stratigraphically highest levels (see above).

Newlands Fm. Bedded calcareous siltstones with occasional sandstones weathering to a distinctive bright buff colour. The mode of deposition of the formation is unclear: massive bedding of much of the unit suggests deposition by turbidity currents, but Cocks and Toghill (1973) noted that pentamerids can sometimes be found in life position. Extremely fossiliferous in terms of shelly faunas (see faunal lists of Cocks and Toghill 1973) which represent *Stricklandia* and *Clorinda* communities indicating deposition on the outer shelf. Aeronian age (Cocks and Toghill 1973; Cocks *et al.* 1992).

Lower Camregan Grits. Fine to medium-grained red-brown sandstones bedded on a 10 - 60 cm scale, some beds exhibiting graded bedding and sole markings. Shelly fossils representing a relatively shallow water low diversity *Eocoelia* community listed by Cocks and Toghill (1973).

Wood Burn Fm. Hard, pale-coloured siltstones and sandstones which grade upwards into softer blue-grey siltstones and shales. Shelly fossils listed by Cocks and Toghill (1973): brachiopods belonging to a *Pentamerus* community in the lower part of the formation, *Clorinda* Community at stratigraphically higher levels, indicating deepening water conditions. Correlates with *sedgwickii* Zone (Cocks and Toghill 1973; Cocks *et al.* 1992).

3. 3. Upper Ordovician Succession of the Northern Belt of the Southern Uplands of Scotland.

Ordovician and Silurian rocks occur as a set of fault-bounded NE - SW trending tracts extending from the North Sea in the NE to the Irish Sea coast south of Girvan, in the SW. The three northernmost tracts (tracts 1-3) are collectively known as the Northern Belt. The Northern Belt is bounded to the north by the Southern Upland Fault and to the south by the Orlock Bridge - Kingledores Fault. To the north of the Southern Upland Fault lies the Midland Valley of Scotland with its Devonian and Carboniferous cover and a chain of Silurian Inliers, the underlying Ordovician rocks only being exposed at the western end near Girvan. To the south of the Orlock Bridge - Kingledores Fault lie tracts 4 to 6 (collectively known as the Central Belt) which comprise Ordovician and Silurian sediments. The complex tectonic history of the region is still under debate and there have been a number of suggested mechanisms since the model of an accretionary prism was proposed by McKerrow *et al.* (1977) and Leggett *et al.* (1979) to explain the well-known stratigraphical pattern exhibited by the Lower Palaeozoic strata in which each tract youngs to the NW but the set of tracts as a whole youngs to the SE. A review of these models is beyond the scope of this study. A summary of the various proposed models is given by McKerrow (1987).

Ordovician stratigraphy within the Northern Belt begins with an Arenig sequence of volcanics, shales and cherts which may be of ocean floor origin (Clarkson *et al.* 1992). Within Tract 2, greywackes occur containing fossiliferous conglomerates and mudstones. The fossils are of Caradoc age and are very similar to those found in the upper Balclatchie and lower Ardwell groups at Girvan (Clarkson *et al.* 1992; Owen and Clarkson 1992). These fossils are known from several localities in the Kirkcolm Fm. described by Peach and Horne (1899), some of which have recently been relocated (Clarkson *et al.* 1992; Owen and Clarkson 1992). Figure 3. 1 shows the correlation of the Ordovician rocks of Tract 2.

Localities yielding material included in the present study.

Duntercleuch and Kilbucho, both within the fossiliferous conglomerates of the Kirkcolm Fm. (see Clarkson *et al.* 1992 for maps and detailed description of the localities). The shelly faunas found at both localities (and at the other shelly fossil localities in the Caradoc greywackes of the Southern Uplands) are fairly shallow water faunas entrained within mass flow deposits derived from a shallow shelf area to the north (Clarkson *et al.* 1992). Faunal lists are given by Clarkson *et al.* (1992).

3. 4. Silurian Succession of the North Esk Inlier, Pentland Hills.

The North Esk Inlier is the largest (at about 6km in length by about 2.5km in width at its widest point) and most westerly of the three Silurian Inliers in the Pentland Hills, just to

the south of Edinburgh. The inlier is fault-bounded to the north by Upper Old Red Sandstone and bordered elsewhere by Lower Old Red Sandstone which succeeds the Silurian sediments with angular unconformity. Within the inlier, about 1500m of Silurian strata forming a more or less continuous succession are steeply inclined or vertical, striking NE - SW. The strata young towards the NW (Tipper 1976; Robertson 1989). The stratigraphy of the Silurian of the Pentland Hills was summarised by Robertson (1989). Correlation of the rocks of the North Esk Inlier is shown in Figure 3. 2.

Robertson (1989) interpreted the mudstones, siltstones, sandstones and conglomerates of the Reservoir, Deerhope and Cock Rig formations as representing differing lithofacies within a submarine fan. Robertson considered the overlying Wether Law Linn Fm. to have been deposited in shallow marine conditions, with the upper beds representing a restricted lagoon or coastal embayment. The topmost beds of the Wether Law Linn Fm. are reddened, heralding the onset of continental sedimentation, and the succeeding red beds of the Henshaw Fm. probably represent a prograding alluvial fan with siltstone horizons developed at some levels possibly representing periodic development of a playa lake (Robertson 1989).

Formations yielding material included in the present study.

Reservoir Fm. Laterally continuous red, green and brown mudstones and shales with interbedded sandstones some of which exhibit sole markings (groove, prod and skip marks) indicating deposition by palaeocurrents from the east (Robertson 1989). Fossils rare in the formation, except within the upper part which includes the well-known Eurypterid and Starfish Beds in Gutterford Burn (Tipper 1976; Robertson 1989). Faunal lists given by Mykura and Smith (1962). Interpreted by Robertson (1989) as distal turbidite deposits characteristic of the outer submarine fan environment.

Deerhope Fm. Fossiliferous red and grey laminated mudstones, siltstones and shales (Robertson 1989). Rich well preserved fossil assemblages in finer grained sediments especially in the more micaceous siltstones near the top of the formation; the Deerhope Coral Bed is one particularly fossiliferous locality. Faunal lists were provided by Mykura and Smith (1962) (whole formation) and Robertson (1989) (Deerhope Coral Bed). The formation was interpreted by Robertson (1989) as probably representing background pelagic sedimentation at the fringe of the submarine fan.

Wether Law Linn Fm. Highly fossiliferous calcareous mudstones, siltstones and fine sandstones, subdivided by Robertson into three members primarily on faunal grounds (see faunal lists and distributions in Robertson 1989). Robertson interpreted his Lower Mbr. as representing an open marine sublittoral

environment, his Middle Mbr. as representing a storm-affected shoal or barrier island, and his Upper Mbr. as representing a restricted lagoon or coastal embayment (Robertson 1989: figure 19).

3. 5. Caradoc and Ashgill Successions of Northern England.

The Ordovician of northern England can be broadly subdivided into three groups: the structurally complex Skiddaw Slate Gp. of early Ordovician age (precise time interval uncertain); the Borrowdale Volcanic Gp. of essentially subaerial andesitic volcanics; and the overlying upper Ordovician Dent Gp. (= lowest member of the Windermere Supergroup as defined by Kneller *et al.* 1994; = Coniston Limestone Gp. of previous authors) which is generally considered to have been deposited in relatively shallow water and for which good regional correlations are available. These three groups are widely distributed across the entire area of northern England (Williams *et al.* 1972). The lithostratigraphy of the Windermere Supergroup has recently been revised by Kneller *et al.* (1994). For this study, fossils from several horizons within the Dent Gp. of the eastern English Lake District and the Cross Fell Inlier have been used. Figure 3. 3 (columns 1 and 2) shows the correlations of the upper Ordovician rocks.

Upper Ordovician of the Eastern Lake District. The Dent Gp. is up to 150m thick in the Lake District and consists mainly of calcareous mudstones with locally developed nodular limestones (Williams *et al.* 1972). Lithologies were described by Kneller *et al.* (1994). The group charts the southerly transgression by a shallow shelf sea over the underlying Borrowdale Volcanic Gp (Moseley 1978). The basal part of the succession (Longsleddale Mbr, Stile End Fm., Kneller *et al.* 1994) is probably fluviatile in origin (McNamara and Fordham 1981), with progressively deepening water conditions being represented with progressively increasing stratigraphical height. Volcanics (rhyolites and rhyolitic ashes) are developed at two levels (Yarlside and Appletreeworth formations). The youngest Ordovician rocks are the bioturbated calcareous siltstones of the Ashgill Fm. (Kneller *et al.* 1994) which contain a *Hirnantia* brachiopod fauna. Much of the Dent group is fossiliferous. McNamara and Fordham (1981) recognised three substrate-dependant trilobite associations in the group: a low diversity proetid association which occurs within sandstones and calcareous siltstones (e.g. Stile End Fm.); an illaenid association which occurs within mudstones (e.g. isolated occurrences within the Applethwaite and Torver members of the Kirkley Bank Fm.); and a calymenid association which occurs within interbedded argillaceous limestones and calcareous mudstones (e.g. majority of the Applethwaite Mbr.).

Formations yielding material included in the present study.

Applethwaite Mbr., Kirkley Bank Fm. Blue-grey calcareous mudstones with nodules and impersistent beds of argillaceous limestone. The basal part is dominated by

Figure 3. 3. Correlation of the upper Ordovician rocks of the eastern Lake District, Cross Fell Inlier, south Shropshire (northern area), Arenig-Bala area, Berwyn Hills and Haverfordwest area. Ordovician chronostratigraphy as in Figure 3. 1. Formations from which specimens of *Calyptaulax* were used for morphometrics marked with an open square.

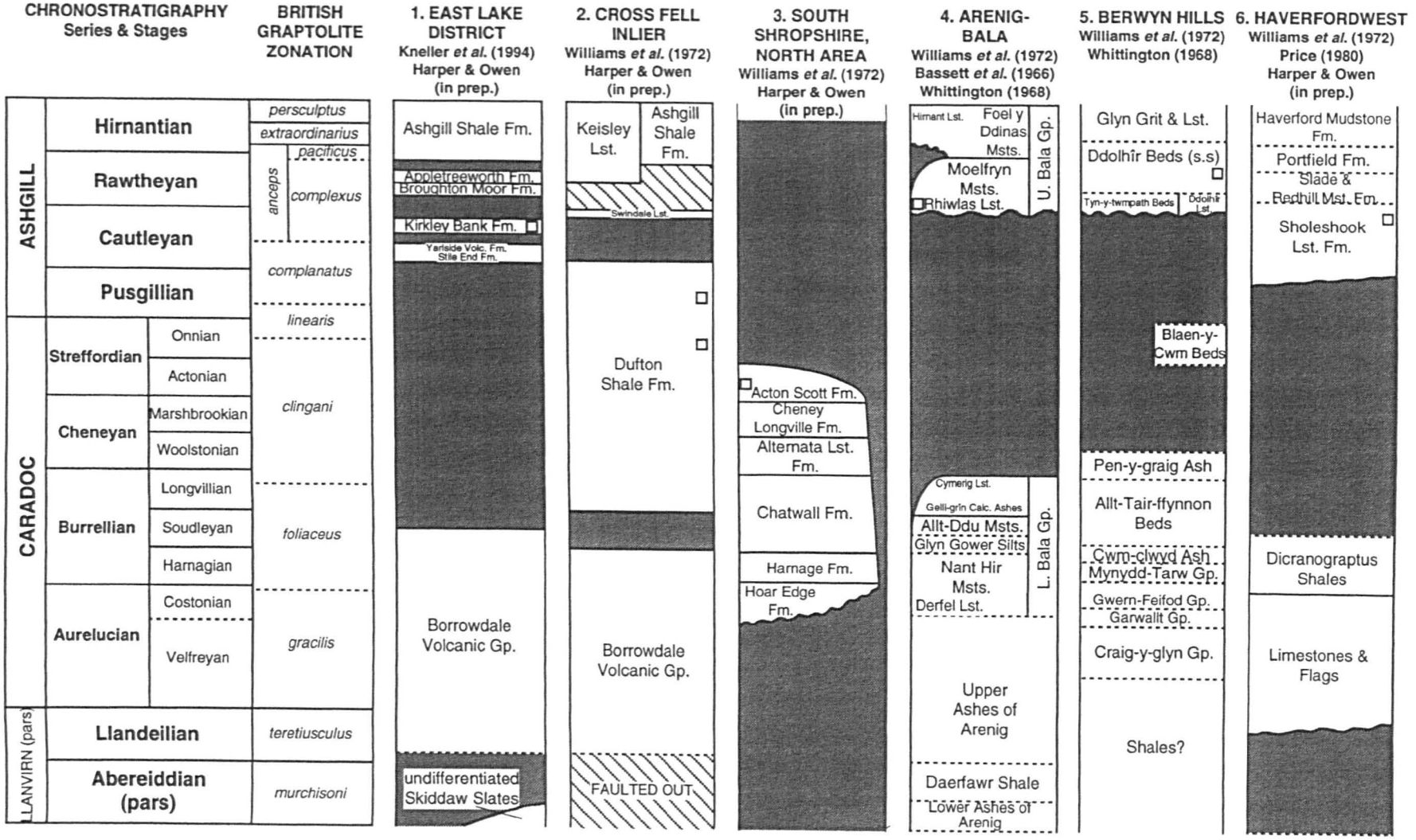

limestone beds, upper parts having higher mudstone component (Ingham *et al.* 1978). The formation contains a diverse trilobite fauna whose main components were listed by Ingham *et al.* (1978). Two trilobite associations were identified and described by McNamara and Fordham (1981) (see above). McNamara and Fordham (1981) interpreted the member as having been deposited in relatively deep water away from the direct influence of fluviatile input, though with occasional higher energy episodes; Kneller *et al.* (1994) interpreted these as storm-affected horizons.

Upper Ordovician of the Cross Fell Inlier. The middle Caradoc to upper Ashgill succession of the Cross Fell Inlier also charts a southerly transgression over the Borrowdale Volcanic Gp. The stratigraphy of the area was described by Dean (1959, 1962) who also provided locality maps. Ingham *et al.* (1978) provided a brief review of the area.

Formations yielding material included in the present study.

Dufton Shale Fm. Thick sequence of dark grey shales and mudstones with occasional nodular limestones. Shelly faunas known from several levels which collectively range in age from Longvillian to lowest Cautleyan (Williams *et al.* 1972; Ingham *et al.* 1978). Fossils from the Onnian part of the sequence exposed in Pus Gill and from the Pusgillian part of the sequence exposed in Swindale Beck have been used for morphometrics.

3. 6. Caradoc Succession of South Shropshire.

The stratigraphy of the highly fossiliferous type Caradoc area in south Shropshire was described in a number of works by Dean (e.g. Dean 1958, 1960) who also provided maps of the area. More recently, Hurst (1979a, 1979b) revised and formalised the upper Caradoc lithostratigraphy of the area. The history of work in the area was outlined by Williams *et al.* (1972) as well as by Hurst. The stratigraphy of the area is shown in Figure 3. 3. The Caradoc of south Shropshire can be geographically subdivided into a northern region and a southern region, there being minor differences relating to diachronism and facies changes between the two; also the sequence extends up into the Onnian in the southern region but only into the Actonian in the northern region (Dean 1958; Williams *et al.* 1972). The lithology consists in the main of calcareous sandstones, siltstones, mudstones and shales containing abundant shelly fossils and considered to have been deposited in a shallow shelf sea (Williams *et al.* 1972). Hurst (1979a, b) considered the upper 300m of the succession from the Alternata Limestone Fm. upwards to be a transgressive sequence deposited on the western margin of the midland craton, and recognised seven vertically arranged facies consistent with a transgression from proximal shelf (e.g. mixed coquinoid and sand and silt facies of Cheney Longville Fm.)

to distal shelf (e.g. bioturbated mud facies of Onny Shale Fm., only preserved in the southern part of south Shropshire where it overlies the Acton Scott Fm. and therefore not shown on Figure 3. 3) environments, together with associated benthic faunal communities (from shallow water *Bancroftina robusta* association to deep water *Onniella broeggeri - Sericoidea homolensis* association). Hurst (1979a) listed the relative abundances of the different elements of the faunas collected from the upper Caradoc succession.

Formations yielding material included in the present study.

Acton Scott Fm. Siltstones and calcareous siltstones grading up into hard calcareous sandstones in the northern part of the area of outcrop. Facies development described by Hurst (1979a). Shelly faunas listed by Dean (1958) and Hurst (1979a, b). Trilobites described by Dean (1960 - 63).

3. 7. Wenlock Succession of the Dudley-Walsall Area.

Stratigraphy of the Dudley-Walsall area is shown in Figure 3. 4, based on the review by Cocks *et al.* (1992). The stratigraphy of the area was described by Bassett (1974) who reviewed the history of work in the Wenlock of the Welsh borders and provided palaeogeographical maps. Thomas (1978-1981) described trilobites from the Wenlock of the area and Bassett (1977) described the articulate brachiopods.

The Wenlock successions of the Welsh borders were deposited in a shallow shelf sea and therefore contain an abundant and diverse trilobite fauna (Thomas 1978). In Shropshire, the Wenlock sediments can be broadly characterised as "Wenlock Shale" (represented in the Dudley-Walsall area by the Coalbrookdale Fm.) and "Wenlock Limestone" (represented by the Much Wenlock [Dudley] Limestone Fm.). Bassett (1974) considered the sequence to have been deposited in a transgressive regime, the sea advancing southwards across a shoreline which was directed approximately NE-SW across the English Midlands and to the north of which successive facies belts developed: shallow water arenaceous sediments proximally, passing into shelf edge limestones and then into a broad area of deposition of calcareous shales and siltstones yielding a mixed shelly and graptolitic fauna distally. During the late Wenlock, carbonate deposition went on over a broad shallow marine area which included much of the Welsh borders (Bassett 1974: text-figs. 7-8).

Formations yielding material included in the present study.

Much Wenlock Limestone Fm., Dudley. About 62m thickness of pure pale coloured limestones with well developed carbonate mound facies. Extremely abundant and diverse shelly faunas. Trilobites described by Thomas (1978-1981), brachiopiods described by Bassett (1977).

Figure 3. 4. Correlation of the Silurian rocks of the Dudley-Walsall area of the English Midlands (column 1), Denbigh-Conway area of North Wales (column 2) and Killary Harbour area of Co. Galway (column 3). Silurian chronostratigraphy as in Figure 3. 2. Formations from which specimens of *Acernaspis* were used for morphometrics marked with a filled square; formations from which specimens of *Ananaspis* were used for morphometrics marked with a filled circle.

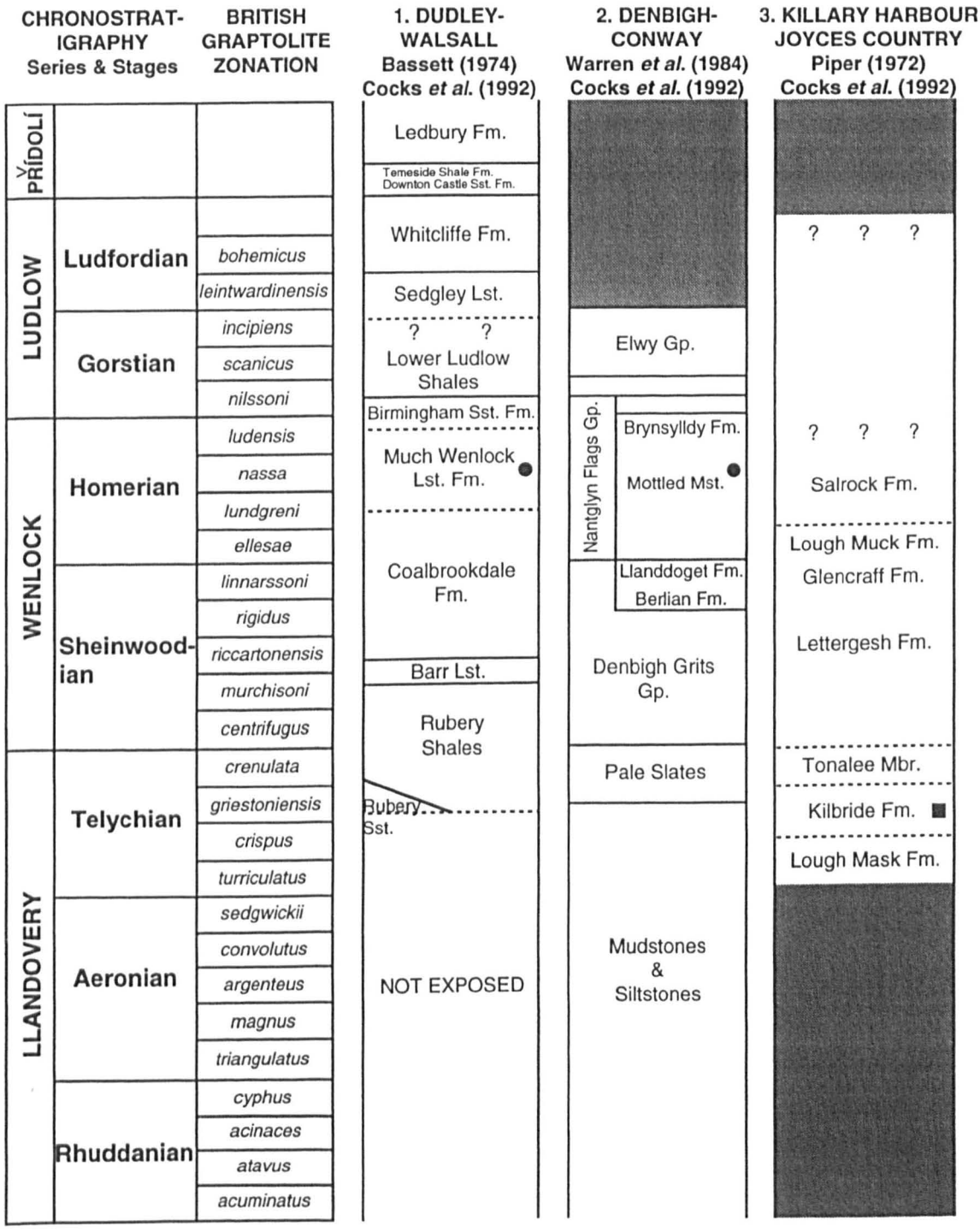

3. 8. Ashgill Successions of North Wales.

Fossils from the Ashgill of the Bala district and the Berwyn Hills have been used in this study. The correlations of these rocks are shown in Figure 3. 3.

Ashgill succession of the Bala district. The Caradoc and Ashgill stratigraphy of the Bala district of north Wales was reviewed by Bassett *et al.* (1966). Bassett *et al.* also provided locality and geological maps and reviewed past work in the area. Whittington (1962 - 1968) described the trilobites of the region and Williams (1963) described the Caradoc brachiopods. The Ashgill rocks are all assigned to the Upper Bala Gp (Williams 1972). Fossiliferous horizons are only known from the base and top of the Upper Bala Gp. succession, in the Rhiwlas Limestone and Foel y Ddinas Msts. respectively (stratigraphical terminology of Williams *et al.* 1972 used in the absence of more formally defined lithostratigraphical formation names). The Hirnant Limestone is locally developed about 25m below the top of the unit and is possibly the youngest Ordovician shelly assemblage known in Britain (Williams *et al.* 1972; fauna listed by Bassett *et al.* 1966).

Formations yielding material included in the present study.

Rhiwlas Limestone. Muddy, impersistent limestone member at the base of the Moelfryn Msts. between about 1.5 and 3m thick (Bassett *et al.* 1966) containing the richest trilobite fauna in the Bala district (see faunal lists of Bassett *et al.* 1966 and Whittington 1968). Price (1980) noted that the Rhiwlas Limestone probably represents a similar depositional environment to the Sholeshook Limestone in south Wales, *i.e.* upper part of slope in a location intermediate between the platform edge and the basin.

Ashgill succession of the Berwyn Hills, north central Wales. Relatively little systematic work has been done in the Berwyn Hills area since that of the Geological Survey in the 1920s (Williams *et al.* 1972). Most of the Ashgill in the area is assigned to the Ddolhîr Beds (stratigraphical terminology of Williams *et al.* 1972 used in the absence of more formally defined lithostratigraphical formation names), which locally contain a rich shelly fauna; the trilobites were described by Whittington (1962 - 1968). The fauna suggests a Rawtheyan age for the formation although the correlation is not unequivocal (Williams *et al.* 1972). The Ddolhîr Beds are overlain by a thin series of grits and locally developed limestones known as the Glyn Grits (Williams *et al.* 1972).

Formations yielding material included in the present study.

Ddolhîr Beds. Locally contain a rich shelly fauna. Whittington (1968) noted that the trilobite fauna is similar to that of the Rhiwlas Limestone in the Bala district, and this probably indicates a similar depositional environment (see above).

3. 9. Ashgill Succession of Haverfordwest.

The correlation of the Ashgill rocks of Haverfordwest and surrounding area is given in Figure 3. 3. The stratigraphy and history of work in the area were reviewed by Williams *et al.* (1972). The fossiliferous Sholeshook Lst. Fm. is overlain by the Slade and Redhill Mst. Fm. which is generally unfossiliferous above its lower part (Williams *et al.* 1972). The St. Martin's Cemetery Beds contain a *Hirnantia* fauna and the overlying Cartlett Beds span the Ordovician-Silurian boundary (Williams *et al.* 1972).

Formations yielding material included in the present study.

Sholeshook Limestone Fm. Lithologically variable formation of calcareous mudstones, sandstones and siltstones whose stratigraphy and correlation was discussed by Price (1973, 1980). The formation yields a rich and diverse shelly fauna: descriptions and stratigraphical ranges of the trilobites were given by Price (1973, 1974, 1980). Price considered the Sholeshook Limestone Fm. to have been deposited in a middle to upper basin slope environment since it contains a mixed assemblage of trilobites including some elements characteristic of the shelf edge carbonate environment (illaenid-cheirurid association of Fortey 1975) and other elements characteristic of the slope environment.

3. 10. Wenlock Succession of the Denbigh-Conway District.

The Silurian stratigraphy of the Denbigh-Conway district is shown in Figure 3. 4. The stratigraphy of this area has most recently been described by Warren *et al.* (1984) who also reviewed the history of systematic work in the area, provided locality maps and listed the shelly and graptolitic faunas, much of which they illustrated. The Wenlock - lower Ludlow sequence consists in the main of mudstones, characterised by Warren *et al.* (1984) as either striped, ribbon banded, or mottled, with subordinate sandstones, siltstones and carbonates. Warren *et al.* (1984) interpreted the sandstones of the lower Wenlock Denbigh Grits Gp. as the products of nearshore slides and turbidity currents. Warren *et al.* considered the various mudstone and siltstone facies of the Nantglyn Flags Gp. to represent deeper water, quieter conditions, with periodic temporary shallowing events which allowed recolonisation of the area by shelly faunas which are only present in the mottled mudstone facies. The sandstones of the Ludlow Elway Gp. are probably distal turbidites (Warren *et al.* 1984).

Formations yielding material included in the present study.

Upper Mottled Mudstone, lower Nantglyn Flags Gp. Massively bedded, irregularly fractured mottled and goethite-veined calcareous silty mudstones, exhibiting penecontemporaneous slumping and sliding. Rich but relatively low diversity graptolitic and autochthonous shelly fauna. Warren *et al.* (1984) listed the faunas as well as describing the petrography of the mudstone in detail. The shelly fauna probably represents a relatively deep water, low oxygen environment.

3. 11. Ordovician Succession of the Grangegeeth District, Eastern Ireland.

The geology and history of stratigraphical and palaeontological work in the Grangegeeth district, between Slane, Co. Meath and Collon, Co. Louth, eastern Ireland was reviewed by Romano (1980). The importance of the trilobite fauna in constraining the location of the Iapetus Suture during the early Caradoc was demonstrated by Owen *et al.* (1992), and the trilobite fauna and its strong affinity to that of Girvan was described in detail by Romano and Owen (1993). The Caradoc stratigraphy of the area is shown in Figure 3. 5.

The Caradoc and Ashgill succession of the region is subdivided into two groups, the Grangegeeth Gp. and the Mellifont Abbey Gp. (Romano 1980). The Grangegeeth Gp. is a transgressive siliciclastic sequence of Caradoc age which rests unconformably on a dominantly volcaniclastic basement (the Slane Gp.) which is at least partly of Llanvirn age (Romano 1980; Romano and Owen 1993). The Grangegeeth Gp. is about 1400m thick and subdivided into the Collon, Knockerk and Fieldstown formations (Romano and Owen 1993). The overlying Mellifont Abbey Gp. consists of basinal black shales and cherts (Broomfield Fm.) and banded mudstones (Oriel Brook Fm.). The lower of the two formations yields poorly preserved graptolites which were listed by Harper (1952).

Formations yielding material included in the present study.

Knockerk House Sandstone Mbr. of the Knockerk Fm. Massive green-grey volcanic sandstones with subordinate tuffaceous shales which become more common with increasing stratigraphical height (Romano 1980; Romano and Owen 1993). Especially fossiliferous in the basal part with abundant brachiopods which are commonly current-orientated on bedding surfaces, and rarer trilobites (listed and described by Romano and Owen 1993).

3. 12. Caradoc and Ashgill Succession of the Pomeroy Inlier, Co. Tyrone.

The Pomeroy Inlier, which lies about 80km west of Belfast, is about 5.6km in length (north - south) and about 4km wide (east - west) at its widest point (see maps of Mitchell

Figure 3. 5. Correlation of the Ordovician rocks of the Grangegeeth area of eastern Ireland and the Pomeroy Inlier, Co. Tyrone. Ordovician chronostratigraphy as in Figure 3. 1. Formations from which specimens of *Achatella* were used for morphometrics marked with an x; formations from which specimens of *Calyptaulax* were used for morphometrics marked with an open square.

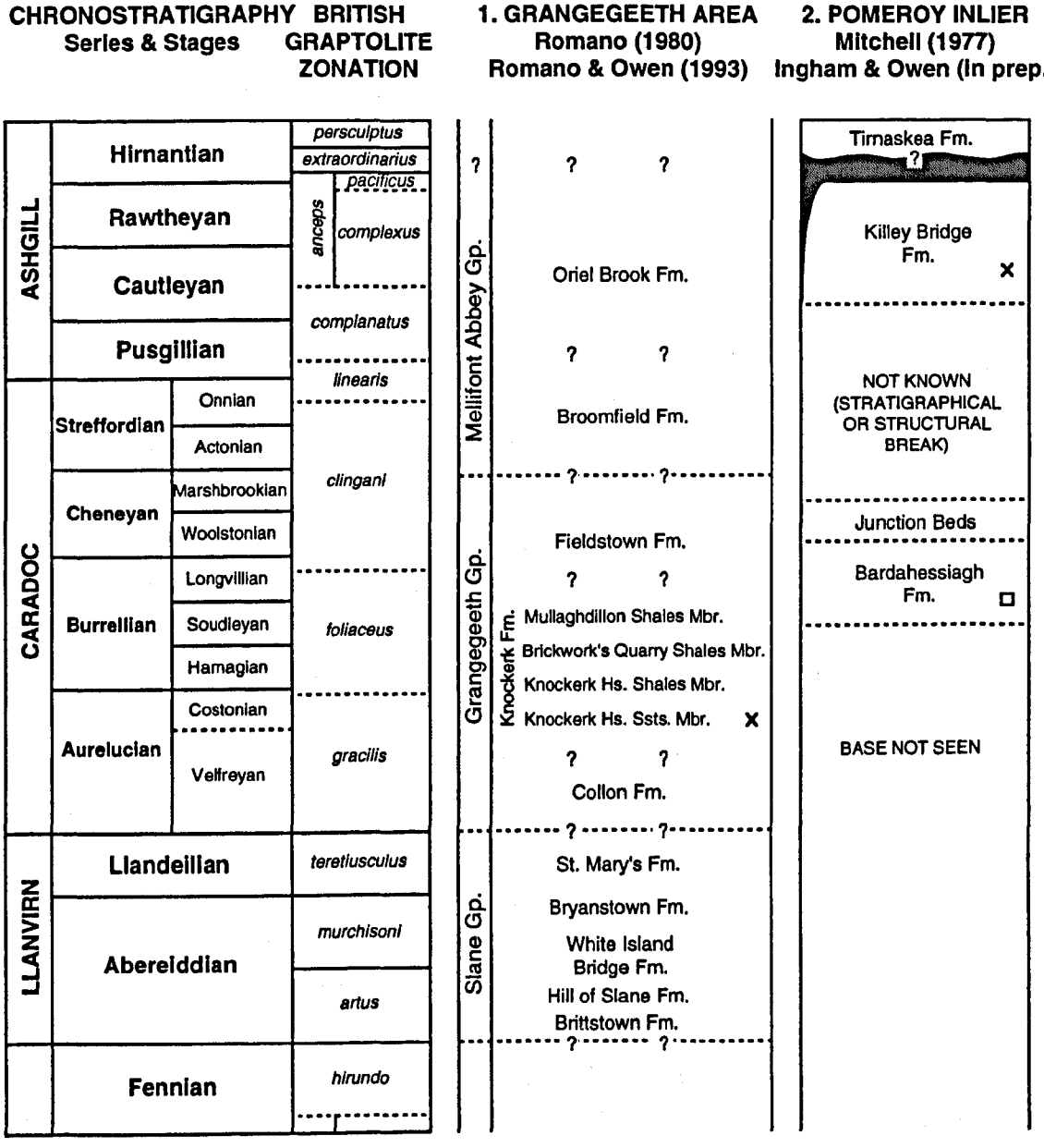

1977). The Ordovician cover sequence within the inlier is of late Caradoc to latest Ashgill age and is mainly composed of calcareous mudstones and siltstones which are often micaceous. These are overlain by graptolitic Silurian sediments. The outcrop of the Ordovician is generally poor (Mitchell 1977), although excavations recently carried out by the Belfast Museum have lead to a substantial improvement in the sampling of the sequence, and to the discovery of the outcrop of the Junction Beds (previously only known from loose blocks, e.g. Mitchell 1977). The Caradoc and Ashgill stratigraphy of the Pomeroy Inlier is shown in Figure 3. 5.

Formations yielding material included in the present study.

Bardahessiagh Fm. Fine-grained grey micaceous sandstones with rare coarse conglomerate beds. Loose blocks which occur on the southern slopes of Craigbardahessiagh are more richly fossiliferous than the *in situ* outcrops, yielding a diverse shelly fauna dominated by brachiopods. The brachiopods were listed and described by Mitchell (1977) who considered the formation to be middle Caradoc in age.

Killey Bridge Fm. Lead-grey micaceous flaggy mudstones and siltstones with thin calcareous horizons and rare sandstone lenses containing the most varied Ordovician fauna of the inlier: brachiopods suggestive of a Cautleyan age were listed and described by Mitchell (1977); the trilobites *Tretaspis* and *Cryptolithus* also occur throughout the formation (Mitchell 1977). Mitchell used size-frequency histograms to assess the depositional environment at each of the main fossiliferous localities within the formation and demonstrated that the faunas within the mudstones and siltstones were more or less unaffected by water currents (and therefore probably *in situ*) while those within more arenaceous lithologies appeared to have been current-transported. A lower basin slope depositional environment is likely.

3. 13. Llandovery Succession of Co. Galway.

The stratigraphy of the Killary Harbour and Joyces Country area, Co. Galway is shown in Figure 3. 4. The stratigraphy was most recently revised by Laird and McKerrow (1970) and by Piper (1972).

The upper Llandovery strata chart a northerly marine transgression over a Llandeilian basement (Piper 1972; Cocks *et al.* 1992). The unfossiliferous sandstones of the Lough Mask Fm. were interpreted by Piper (1972) as being of fluvial origin, and they are succeeded by up to 340m of fossiliferous sandstones and siltstones of the Kilbride Fm. which show a general fining up trend. The conformably overlying Tonalee Mbr. (terminology of Cocks *et al.* 1992) represents even deeper marine conditions (Piper 1972). The succeeding Lettergesh Fm. marks the incoming of turbidite facies which

continue in the Glencraff Fm., with the overlying Lough Muck Fm. and Salrock Fm. recording a regression marked by the deposition of shallow marine and estuarine sediments (Piper 1972).

Formations yielding material included in the present study.

Kilbride Fm. Fossiliferous sandstones and siltstones within which Piper (1972) identified four subdivisions showing an overall fining up trend. Piper interpreted this formation as representing shallow marine conditions, the lower part of the formation having been deposited in a tidal lagoon and successively higher parts representing successively more offshore sites affected to increasingly lesser extent by wave and current activity. Brachiopods from the topmost subdivision are assignable to the *Clorinda* community (Piper 1972). Shelly faunas were described by Doyle (1989).

3. 14. Middle to Upper Ordovician and Lower Silurian Succession of the Oslo Region.

The Oslo Region was defined by Størmer (1953) as an area between 40 and 75km wide and about 220km long with the city of Oslo lying at its eastern edge, within which Lower Palaeozoic rocks crop out in eleven districts within a NNE - SSW trending graben (see Worsley *et al.* 1983 and Owen *et al.* 1990 for regional maps). The total thickness of lower Palaeozoic marine sediments is about 1250m (Worsley *et al.* 1983). The region is a classic area for Ordovician stratigraphy and palaeontology. In the southern-most districts of the region (e.g. Skien-Langesund, Eiker-Sandsvær) the lower Palaeozoic successions are gently tilted, while in the other districts they have been subjected to varying degrees of folding and faulting. The successions consist in the main of alternating shales or mudstones and limestones, with sandstones being rare except in the latest Ordovician. The stratigraphy and history of work in the Ordovician of the Oslo Region were reviewed by Owen *et al.* (1990) and the stratigraphy of the Silurian was reviewed by Worsley *et al.* (1983). Figures 3. 6 and 3. 7 show the chronostratigraphy of the Ordovician and Silurian of the Oslo Region respectively.

Caradoc and Ashgill sedimentation in the Oslo Region. The Cambrian and Ordovician sediments of the Oslo Region were deposited in a stable continental shelf environment characterised by low rates of clastic sediment supply and deposition (Worsley *et al.* 1983). In the Caradoc a series of NNE - SSW trending facies belts developed: shallow marine carbonates with local carbonate mounds in the northernmost and southernmost districts, passing laterally into more distal shelf muddy environments exposed in the more easterly districts. The Caradoc sequences are generally fossiliferous. The Ashgill is characterised by a regional regression (probably of glacio-eustatic origin, Worsley *et al.* 1983) which resulted in subaerial exposure and consequent cessation of deposition in the

Figure 3. 6. Correlation of the Ordovician rocks of the Oslo Region. The districts are arranged approximately south (1) to north (7). Ordovician chronostratigraphy as in Figure 3. 1. Correlations after Owen *et al.* (1990). Formations from which specimens of *Achatella* have been used for morphometrics marked with an x; formations from which specimens of *Calyptaulax* have been used for morphometrics marked with an open square.

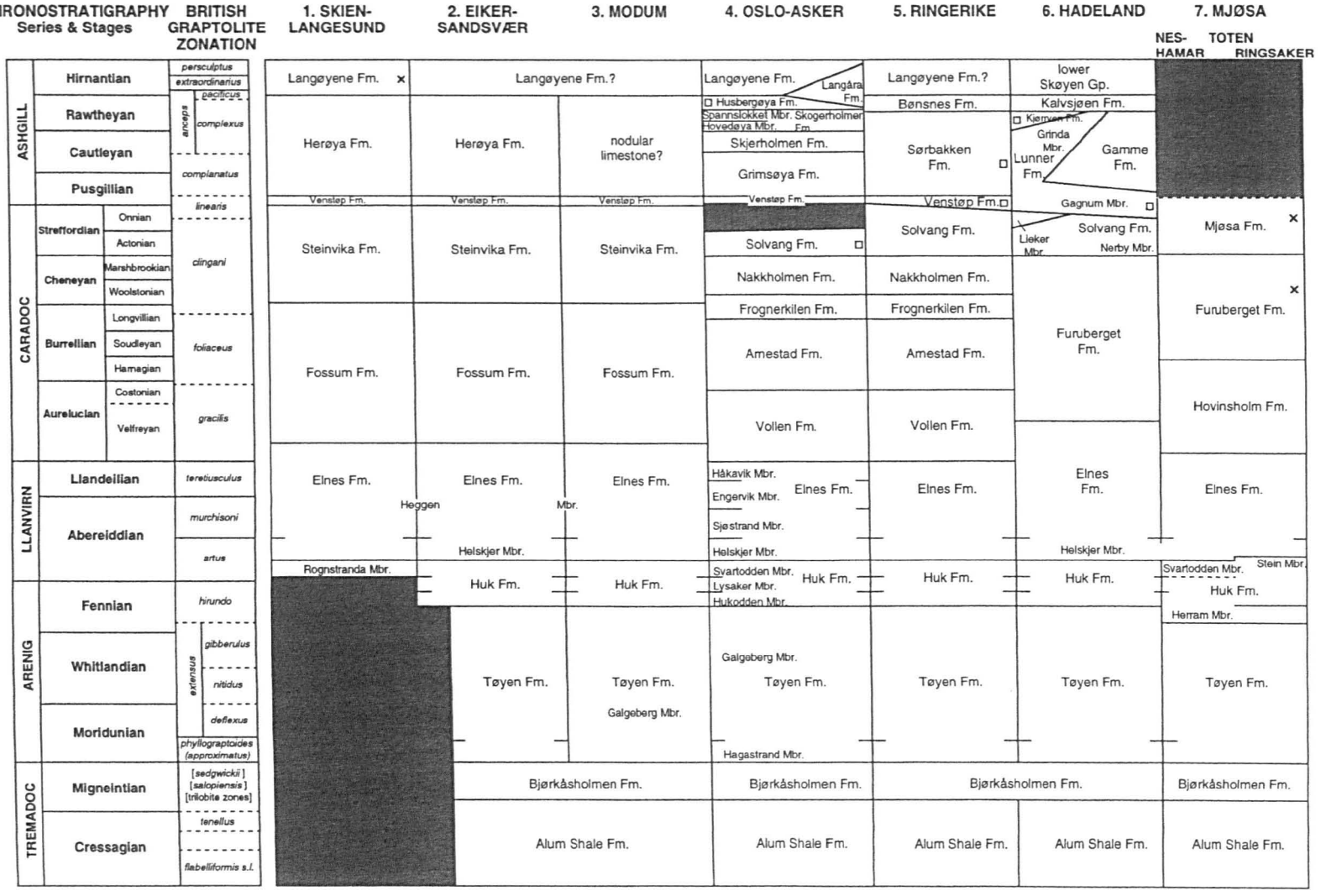

Figure 3. 7. Correlation of the Silurian rocks of the Oslo Region. Silurian chronostratigraphy as in Figure 3. 2. Correlations after Worsley *et al.* (1983). Formations from which specimens of *Acernaspis* were used for morphometrics marked with a filled square.

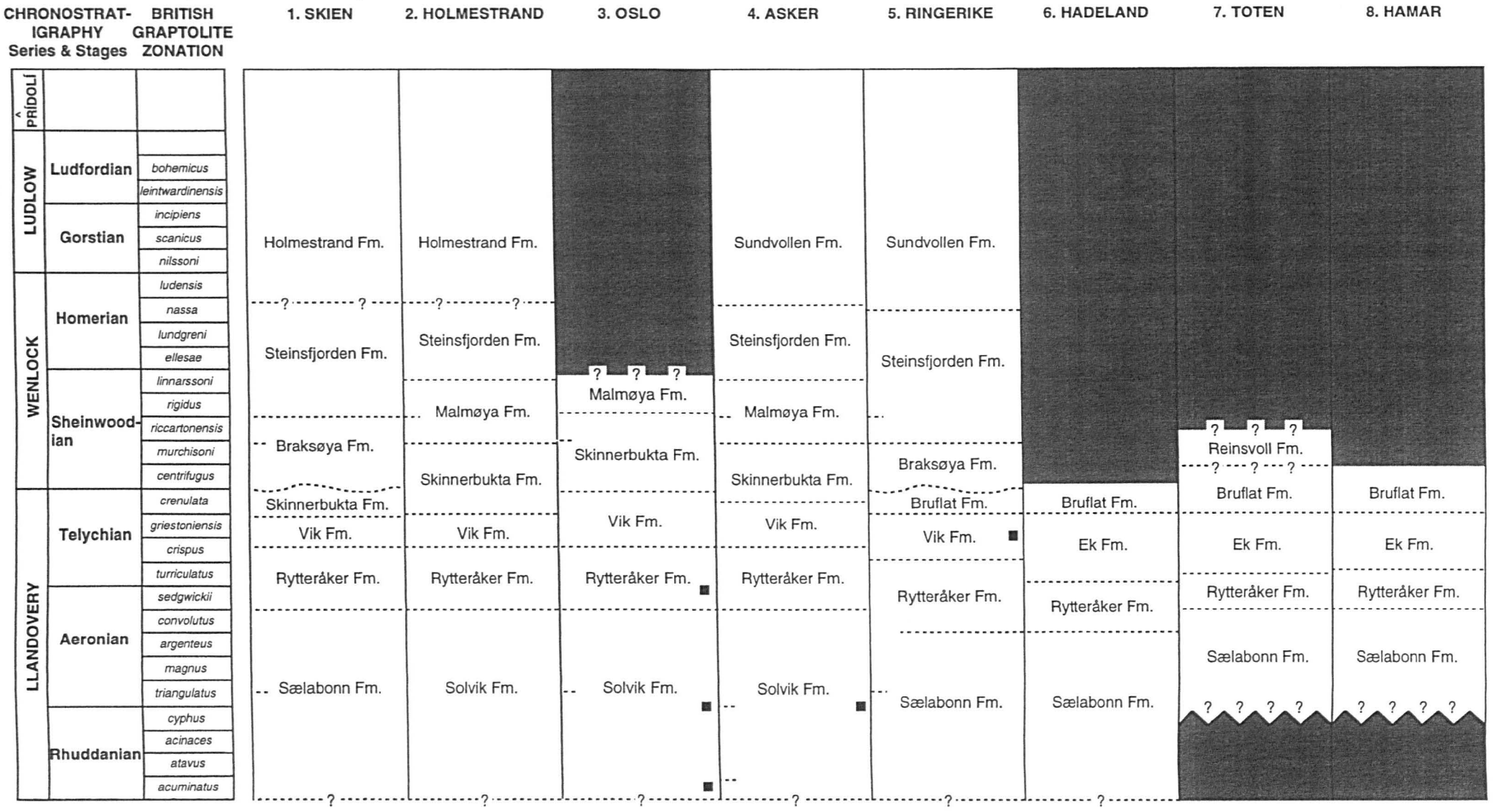

northernmost district (Mjøsa) in the early Ashgill and migration of shallow marine facies towards the SW (*i.e.* from Hamar into Hadeland and Ringerike). The successions in all still submerged districts become clastic-dominated towards the top of the Ashgill as this regression continued.

Ordovician formations yielding material included in the present study.

Furuberget Fm. Predominantly shales with interbedded limestones and calcareous siltstones with cross bedding which indicates deposition on a palaeoslope sloping down towards the east. The stratigraphy and lithologies of the formation were described by Owen *et al.* (1990) and references therein. The Furuberget Fm. has been subdivided into two zones on the basis of calcareous algae: the lower "Coelosphaeridium zone" and the higher "Cyclocrinus zone" (e.g. Størmer 1953; Skjeseth 1963). The formation yields a diverse shelly fauna, particularly so the limestone horizons, which Spjeldnæs (1982) considered to have been transported in from the west (*i.e.* upslope). See references within Owen *et al.* (1990) for descriptions of the faunas.

Mjøsa Fm. Varied limestone facies, tending to be more shaley in the northern part of the Mjøsa district, around Ringsaker, than further south. Carbonate mounds occur locally. The formation contains a diverse fauna and algal flora: see references in Owen *et al.* (1990) for descriptions of the biota, stratigraphy and lithologies.

Solvang Fm. Lithology consists in the main of nodular limestones, bedded limestones and calcareous shales, with (in Oslo-Asker) distinctive laterally continuous bioclastic limestone horizons occurring near the top of the formation. The detailed lithology and internal stratigraphy of the formation was described by Owen *et al.* (1990) and references therein. The Solvang Fm. is one of the most fossiliferous formations in the Oslo Region, yielding abundant and diverse shelly faunas on which much descriptive work has been done. For the most part the formation is of late Caradoc age, although in Ringerike it is probably of basal Ashgill age in its uppermost levels (Owen *et al.* 1990).

Venstøp Fm. Dark, locally graptolitic shales with occasional limestone concretions. Shelly faunas from the formation are of high abundance but low diversity (Owen *et al.* 1990). Brachiopods (including abundant inarticulates), trilobites (including *Tretaspis*, *Flexicalymene* and *Primaspis*, the former two locally in great abundance), gastropods and bivalves are all common and are commonly preserved in articulated condition suggesting that deposition was in low energy conditions with little transport of the fauna. Early Ashgill age.

Husbergøya Fm. Predominantly shales with sandy calcareous beds becoming progressively more common higher in the formation, the top of the formation being marked by a bedded sandstone up to 5m thick (Owen *et al.* 1990 and references therein). The fauna of the formation occurs in both the shales and the

topmost sandstone beds and is sparse but relatively diverse, including brachiopods assignable to the *Onniella* association and trilobites assignable to the *Tretaspis* association (Brenchley and Cocks 1982; Owen *et al.* 1990 and references therein). The formation has been interpreted as having been deposited in an outer shelf environment (Brenchley and Cocks 1982).

Langøyene Fm. Predominantly sandstones with subordinate limestone horizons. A number of depositional environments have been recognised within the formation ranging from intertidal channels to high-energy inner shelf; the unit as a whole has been interpreted as having been deposited in a wave and storm dominated shallow sea (Brenchley and Cocks 1982; Owen *et al.* 1990). Several faunal associations are known from the formation. In the basal part a moderately diverse brachiopod dominated *Hirnantia* fauna is found. Elsewhere associations consisting only of trace fossils are found (Owen *et al.* 1990 and references therein). The Langøyene Fm. marks the maximum extent of the end Ordovician regression in the Oslo Region.

Sørbakken Fm. Characterised by grey, nodular bedded limestones with interbedded thinner calcareous shales (see Owen *et al.* 1990 and references therein for detailed description). The formation yields a diverse shelly fauna.

Lunner Fm. Another shale dominated unit which is about 185m thick in its type area around Lunner, Hadeland, and thinning towards the NW where it is divided into two tongues separated by the intervening nodular limestones of the Gamme Fm. Details of lithology and internal stratigraphy were given by Owen *et al.* (1990) and references therein. Diverse shelly faunas are known from the Grinda and Gagnum members as well as from the main Lunner Fm. to the south.

Kjørrven Fm. Interbedded dark grey limestones, calcareous siltstones and shales, the frequency of the limestones increasing towards the top of the formation. The Kjørrven Fm. yields a very diverse shelly fauna of Rawtheyan age (Owen *et al.* 1990).

Lower Silurian sedimentation in the Oslo Region. Shales and siltstones of the Rhuddanian Solvik Fm. directly overlie the high energy sandstones of the Langøyene Fm. in Oslo-Asker with no basal conglomerate. The shales drape and partially infill the channels in the Langøyene Fm. surface, but contain graptolites and distal shelf benthonic faunas, suggesting that the transgression which occurred at the beginning of the Silurian was rapid and on a large scale (Worsley *et al.* 1983). It has been suggested that this transgression was, like the preceding regression, of glacio-eustatic origin (Brenchley and Newall 1980). Marine depositional environments were probably re-established early on in the Rhuddanian after the end-Ordovician regression over most of the Oslo Region. The distal shelf shale facies of the Solvik Fm. pass laterally westwards into the more proximal Sælabonn Fm. (Worsley *et al.* 1983). From the late Aeronian, the diachronous

development of carbonate facies (Rytteråker Fm.) resulted from the submergence of the clastic source areas to the north and west. Ringerike, Hadeland and Skien were relatively close to the shore at this time while Holmestrand and Oslo-Asker were more distal (Worsley *et al.* 1983). During the Telychian subsidence of the northern districts lead to deposition of graptolitic shales there (Ek Fm.) while shallower water, more calcareous deposition went on further south (Vik Fm.). Bentonites in the Ek, Vik and Bruflat formations reflect occasional volcanic activity at this time. Subsequent shallowing and high sedimentation rates in the northern districts lead to sandstone progradation towards the east and SE (Bruflat Fm.), while in more southerly districts deepening lead to deposition of graptolitic shales (Skinnerbukta Fm.). These contrasting environmental developments reflect local differential tectonic movements at this time (Worsley *et al.* 1983).

Wenlock sedimentation was characterised by the establishment of a stable carbonate platform on which NW - SE trending carbonate facies developed with little supply of clastic sediment (Worsley *et al.* 1983). In the early Wenlock, the districts of Ringerike and Skien were in a marginal marine location as evidenced by the development of carbonate mounds, while marly sedimentation in Holmestrand and basinal shale deposition in Oslo-Asker indicates that these areas were progressively more distal. Fluctuations in sea level caused some migration of the facies during the late Sheinwoodian and early Homerian. In the late Homerian renewed large scale regression (possibly eustatic sea level fall, McKerrow 1979) caused clastic progradation eventually resulting in deposition of continental red beds in Ringerike, Asker, Holmestrand and Skien (Worsley *et al.* 1983).

Silurian formations yielding material included in the present study.

Solvik Fm. Predominantly dark grey shales with thin siltstone and limestone interbeds. Diverse shelly faunas are known from the formation, with some brachiopod faunas *in situ* and others reworked (Worsley *et al.* 1983 and references therein). Worsley *et al.* (1983) interpreted the lower part of the formation as having been deposited in a quiet muddy environment below normal wave base, and the upper part as representing a slightly shallower environment with occasional wave and current reworking of the sea floor. The formation essentially represents a more distal environment than the contemporaneous Sælabonn Fm.

Rytteråker Fm. Thickly bedded biosparitic limestones with calcareous nodules and small carbonate mounds locally developed. Abundant pentamerid brachiopods. Lithologies and faunas discussed by Worsley *et al.* (1983). Depositional environment probably a shallow carbonate shelf throughout the Oslo Region, with high energy shoals which were periodically emergent developed in Hadeland and Ringerike.

Vik Fm. Red and green-grey shales with subordinate marls and nodular bioclastic limestones. The formation was probably deposited in deeper water than the underlying Rytteråker Fm., with slightly shallower marl banks developed in the middle part of the formation containing a rich and diverse shelly fauna which Worsley *et al.* (1983) considered characteristic of Benthic Assemblage zone 3 of Boucot (1975). Sparse shelly faunas are known from the lower and upper parts of the formation.

3. 15. Upper Ordovician Succession of the Siljan District, Central Sweden.

The Siljan region is situated immediately to the north of Lake Siljan, Dalarna. Palaeozoic rocks in the area occur as a complex ring structure of down-faulted sediments surrounding a central uplifted stock of the Sub-Jotnian Dala Granite, the whole structure having a diameter of between five and 18km (Jaanusson 1982). The Ordovician succession is about 100m thick and consists mainly of carbonate rocks which are overlain by Silurian graptolitic shales. The structure is interpreted as a probable hyper-velocity impact crater, and melt samples from the central granite have given an integrated K-Ar age of 361.9 ± 1.1Ma for this impact (Jaanusson 1982).

Upper Ordovician (Harjuan) stratigraphy of the area is given in Figure 3. 8. The sequence consists in the main of calcilutites and argillaceous limestones with occasional mudstones, shales and calcareous sandstones representing a shallow continental shelf depositional environment. Many of the levels are highly fossiliferous (Jaanusson 1982). Stromatactis-bearing carbonate mounds are developed within the Ashgill and are known collectively as the Boda Limestone (similar mounds developed within the upper Caradoc are collectively known as the Kullsberg Limestone).

Formations yielding material included in the present study.

Boda Limestone. About 24 approximately mushroom-shaped carbonate mounds, up to 1000m in diameter and 100-140m thick, flanked by fossiliferous bedded stromatactis-bearing argillaceous limestones. The mounds have no obvious organic framework; their petrography was described by Jaanusson (1982) who noted that mound cores and mound flank sediments are hosts to a rich and diverse fauna.

3. 16. Middle Ordovician Succession of Northern Estonia.

Ordovician rocks outcrop as a continuous belt across the Baltic region extending from the island of Öland in the SW to Lake Ladoga (St. Petersburg District) in the E. The complete sequence of the Ordovician is exposed in northern Estonia as a belt about 40 to 45km wide and about 300km long as almost flat-lying strata (Männil 1990). The basal

Figure 3. 8. Correlation of the Llanvirn - Ashgill strata of the Siljan district, central Sweden (column 1) and the Northern Estonian Confacies Belt (column 2). Ordovician chronostratigraphy as in Figure 3. 1. Formations from which specimens of *Achatella* were used for morphometrics marked with an x.

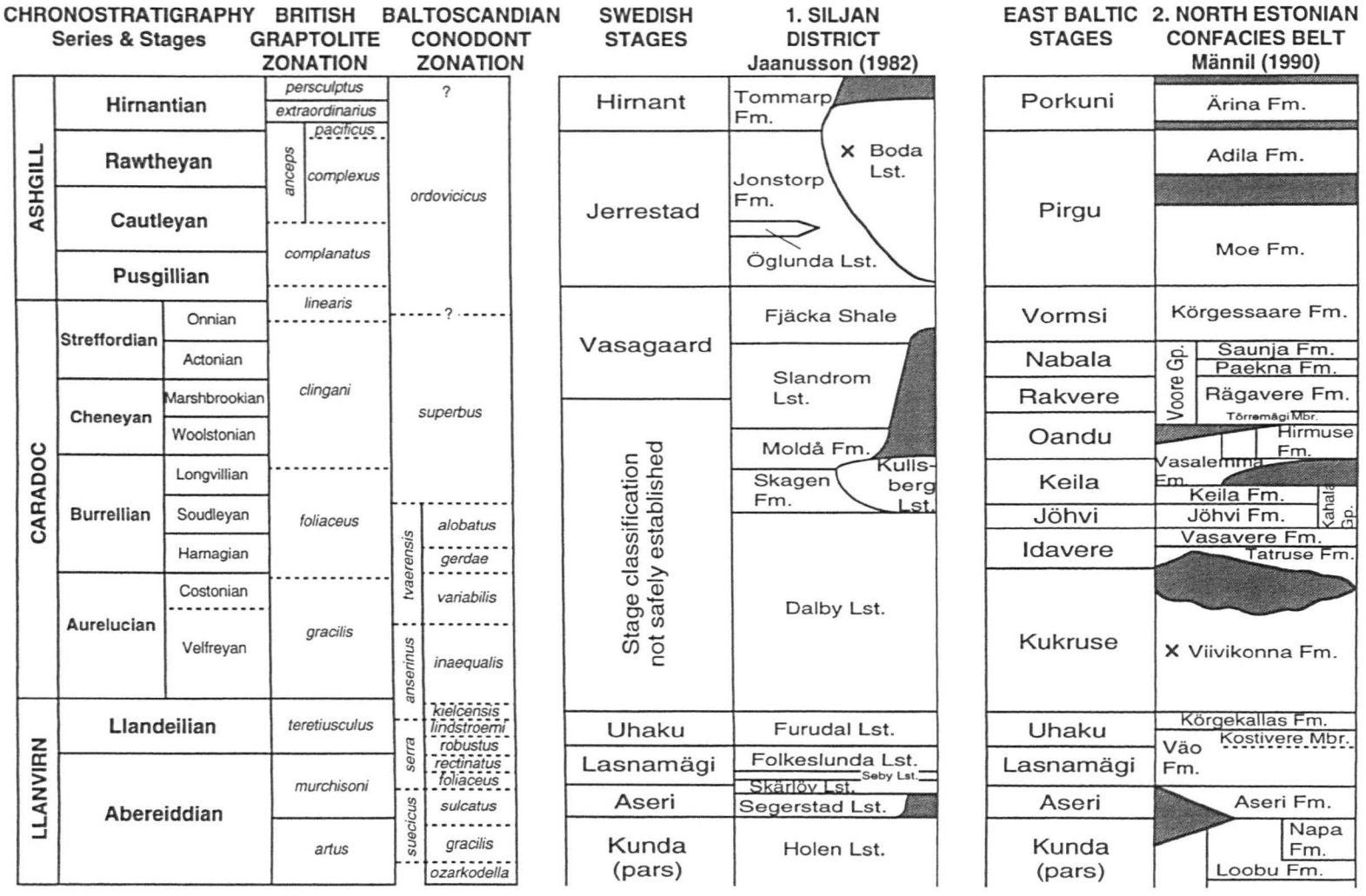

(Tremadoc) part of the succession is of silty sandstones and graptolitic argillites and this is overlain by a succession of shallow water shelf carbonate sediments, mainly calcarenites. The succession is between 70 and 180m thick, the thickest part being in the middle of the area of outcrop. The Ordovician stratigraphy of Estonia was summarised by Männil (1990) who also reviewed the history of systematic work in the region. Ordovician Chronostratigraphy of the northern belt of Estonia is shown in Figure 3. 8.

The base of the Viru Series (middle Ordovician) is marked in the northern Estonian belt by major faunal changes, particularly so in trilobites: the appearance of *Neoasaphus* and the pterygometopids *Estoniops* and *Chasmops* as well as a marked increase in the diversity of illaenids and asaphids (Aru 1990). The Viru Series rocks consist of a succession of highly fossiliferous shallow marine shelf carbonates, the various stages and substages being defined on the basis of shelly faunas. The definitions and international correlations of the stages were described by Männil (1990), and the pattern of trilobite diversity was discussed by Aru (1990).

Formations yielding material included in the present study.

Kukruse Stage (C_{II}). Alternating bioturbated yellow argillaceous limestone and kukersite beds (kukersite = a rock consisting of about 25-65% organic material, 15-50% terrigenous material, and 15-50% calcareous material such as skeletal remains etc.) of the Viivikonna Fm. Lithologies and abundant and diverse shelly fauna discussed by Kórts and Einasto (1990).

3. 17. Llandovery and Wenlock Succession of Gotland.

Gotland has long been recognised as a classic region for Silurian palaeontology (Cocks *et al.* 1992). Hede (1960) and Manten (1971) provided reviews of Gotland stratigraphy, Manten providing a detailed sedimentological analysis of the succession and listing the faunas. The correlations of the strata have been most recently refined by the ostracode work of Martinsson (1962, 1967), the conodont work of Fåhraeus (1967), and the brachiopod work of Bassett and Cocks (1974). The chronostratigraphy of Gotland is shown in Figure 3. 9.

The upper Llandovery-Ludlow succession of Gotland consists of a continuous sequence of marls and carbonates (finely crystalline nodular or oolitic limestones) in which carbonate mounds are developed at a number of horizons. In the lowest of these, in the Upper Visby Fm., corals are the most important reef builders, while in the later ones (Högklint Fm., Slite Fm., Halla Fm., Klinteberg Fm., Hemse Gp.) stromatoporoids are most important. Manten (1971) considered the sporadic development of carbonate mounds to reflect fluctuating water depths within the succession.

Figure 3. 9. Correlation of the Silurian rocks of Gotland (column 1), the Barrandian Basin, Bohemia (column 2) and Anticosti Island, Québec (column 3). Silurian chronostratigraphy as in Figure 3. 2. Formations from which specimens of *Acernaspis* were used for morphometrics marked with a filled square; formations from which specimens of *Ananaspis* were used for morphometrics marked with a filled circle.

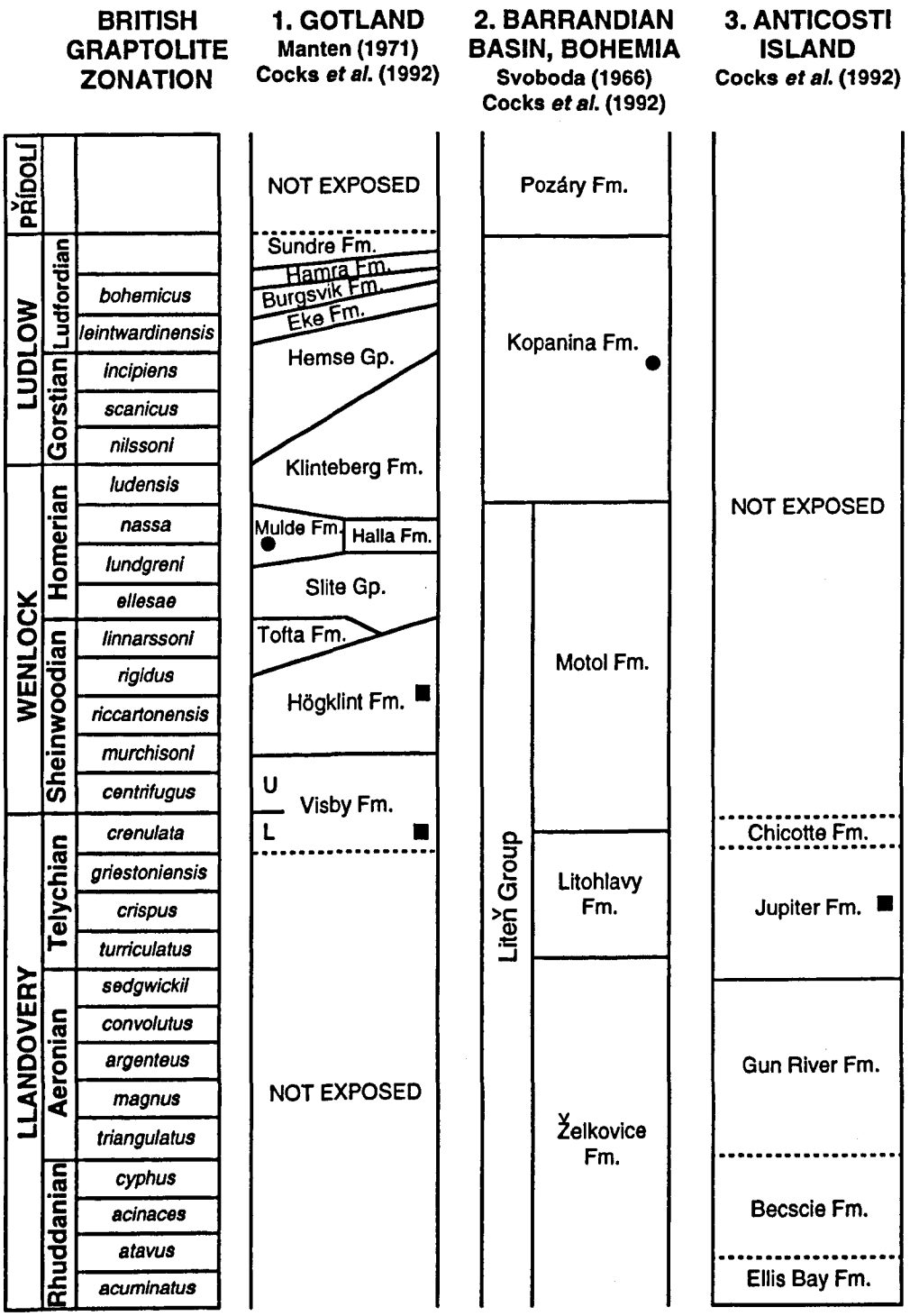

Formations yielding material included in the present study.

Lower Visby Fm. Thinly-bedded soft blue-grey marls alternating with pale grey, finely crystalline marly limestones. Manten (1971) described the sediments in detail and also listed the faunas. Wenlock age (Bassett and Cocks 1974).

Högklint Fm. Finely crystalline blue-grey or brownish-grey bedded limestones, some marly or oolitic, in which huge stromatoporoid-supported carbonate mounds up to 2km in diameter are developed. Manten (1971) described the sedimentology of the mounds and host sediments and listed the highly abundant and diverse shelly faunas present in both. Manten considered the Högklint mounds to have grown in shallower water than the upper Visby mounds. Bassett and Cocks (1974) assigned a *riccartonensis* Zone age to the formation.

Mulde Fm. Interbedded soft blue-grey marls and finely crystalline blue-grey marly limestones weathering a brownish colour. No reefs are developed in the Mulde Fm. Highly fossiliferous. Sedimentology was described by Manten (1971) who also listed the fauna.

3. 18. Ludlow Succession of the Barrandian Basin, Bohemia.

The "Barrandian" Prague Basin of Bohemia takes its name from the author of a series of middle nineteenth century monographs on the geology and palaeontology of the region, Joachim Barrande (Cocks *et al.* 1992). The basin is a synclinorium occupying the central and SW part of Bohemia. The basin fill comprises altered and unaltered complexes of latest Proterozoic and Palaeozoic (Cambrian to Devonian) volcanic, sedimentary and metamorphic rocks, partly covered by Carboniferous and Permian sediments of the central Bohemian coalfields, and partly covered by Upper Cretaceous psammites and marls. The basin fill can be subdivided into the latest Proterozoic complex, which occupies the whole area of the Barrandian Basin, and the Palaeozoic succession which rests unconformably on the Proterozoic and occupies only the central part of the basin. Granites and related igneous rocks intrude the complexes (Svoboda 1966). The Silurian chronostratigraphy of the Barrandian Basin is shown in Figure 3. 9. Svoboda (1966) and Chlupáč *et al.* (1984) provided summaries of the stratigraphy of the basin, the former also giving maps.

The Silurian of the Barrandian Basin has a maximum thickness of about 500m where it is best developed in the central part of the basin. Silurian rocks rest conformably on the uppermost Ordovician Kosov Fm. The Llandovery and Wenlock Liteň Gp. consists mainly of dark graptolitic shales with shelly faunas almost totally absent, in the upper part of which (Motol Fm.) calcareous facies are developed which are contemporaneous with the appearance of basaltic volcanics in the northern part of the basin (Svoboda 1966). These varied carbonate facies continue up into the Ludlow Kopanina Fm. in the north of the basin and contain abundant and diverse shelly faunas, while in southern parts of the

Barrandian a contemporaneous shaley facies with interbedded limestones and tuffaceous horizons yielding abundant graptolites is developed (Svoboda 1966). The carbonate facies of the northern areas are zoned on trilobites, while the shaley facies of the southern areas are zoned on graptolites.

The overlying Pozáry Fm. (Přídolí Stage) is more uniform than the underlying Ludlow rocks, consisting of about 40m of dark flaggy and bituminous limestones with marly shale intercalations. Slump breccias are developed at some levels. Development of paler bioclastic limestones containing a more abundant shelly fauna in the highest levels of the formation indicate a general shallowing at the end of the Silurian.

Formations yielding material included in the present study.

Kopanina Fm., carbonate facies (*P. f. communis* Zone). In the carbonate facies, the zone of *Phacops fecundus communis* consists of nodular or tabular dense limestones and crinoidal limestones which yield an abundant and diverse shelly fauna. The lithology and fauna were discussed by Svoboda (1966).

3. 19. Middle to Upper Ordovician Successions of North America.

The Appalachian Basin: New York State and Ontario. Middle and upper Ordovician stratigraphy of New York State and Ontario is shown in Figure 3. 10. Shaw (1968) and Shaw and Fortey (1977) discussed the depositional environment of the limestones, dolomites, sandstones and shales of the Day Point, Crown Point and Valcour limestones (terminology of Ross *et al.* 1982 used in the absence of more formally defined lithostratigraphical formation names), concluding that they represent a shallow water shelf environment, with periodic development of carbonate mounds (e.g. in Crown Point Limestone and basal Valcour Limestone). Trilobite faunas are listed in both of these papers, and described by Shaw (1968).

Shaw and Fortey (1977) considered the limestones of the Black River Gp. to be a shallow water transgressive sequence and listed the trilobite fauna. The overlying Trenton Gp. of New York and Ontario consists of about 260m thickness of strata consisting predominantly of fossiliferous dark coloured limestones and black shales. The area has long been famous for its palaeontology. Fisher *in* Ross *et al.* (1982) reviewed the history of work in the area and discussed its correlation. Titus and Cameron (1976) carried out a detailed environmental analysis of the lower Trenton Gp. and recognised a transgressive sequence of lithologies and faunas representing a range of depositional environments from lagoonal to relatively deep water offshore shelf. There is a transitional facies (Dolgeville Shale) between these shelf limestones and the laterally equivalent black graptolitic Utica and Frankfort Shales (Figure 3. 10). Titus and Cameron listed the faunas associated with each of their depth related benthic

Figure 3. 10. Correlation of the upper Arenig to Ashgill rocks of Ontario (columns 1 and 2), New York (columns 3 - 5) and Tennessee (column 6). Ordovician chronostratigraphy as in Figure 3. 1. Formations from which specimens of *Achatella* were used for morphometrics marked with an x; formations from which specimens of *Calyptaulax* were used for morphometrics marked with an open square.

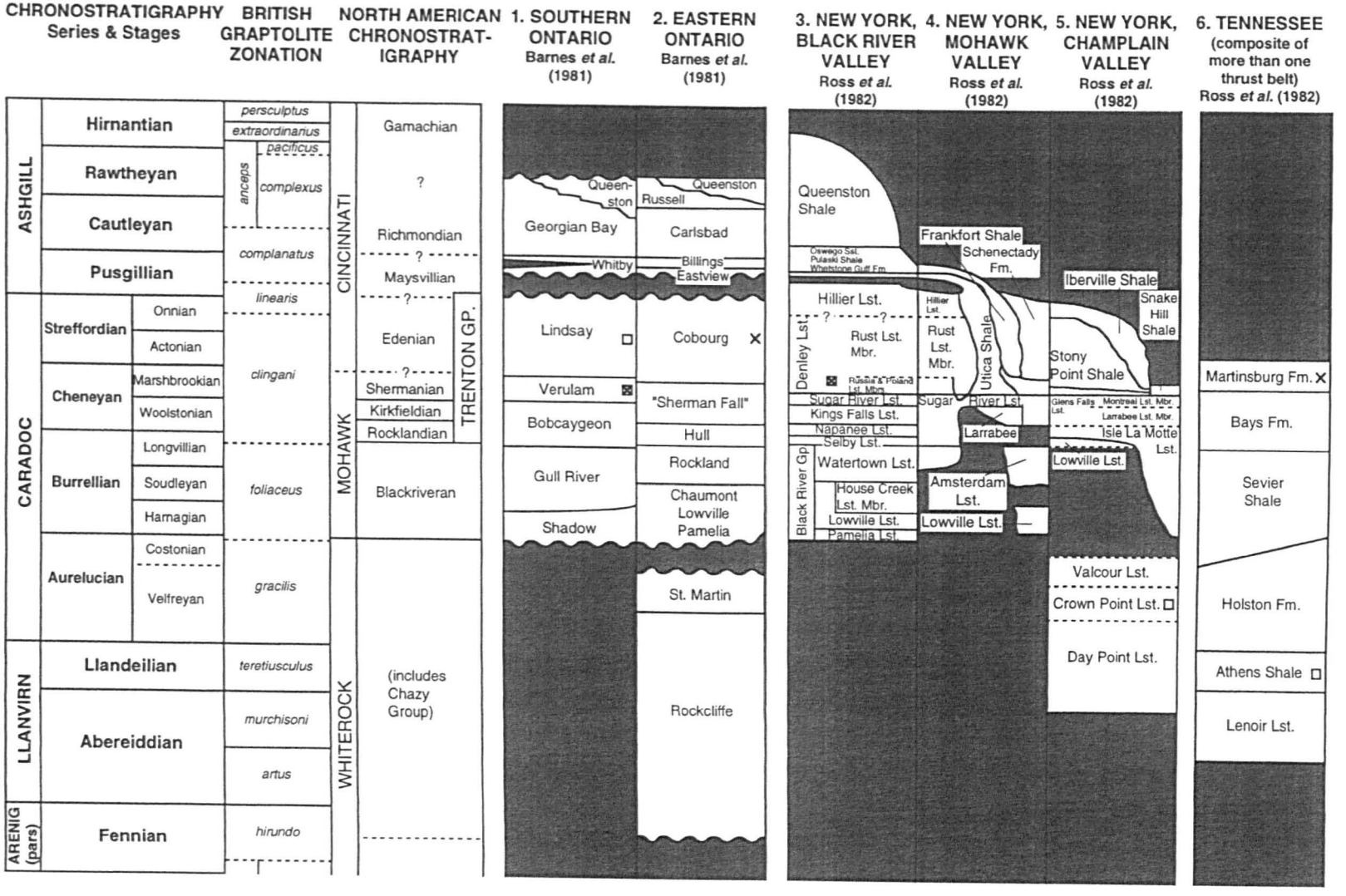

communities. The Blackriveran - Edenian carbonate sequence is terminated in New York and Ontario by a short hiatus, followed by a series of black, grey and red shales probably representing lower slope depositional conditions (Barnes *et al.* 1981).

Formations in New York and Ontario yielding material included in the present study.

Crown Point Fm. Fine-grained blue-grey silty limestones with thin dolomite intercalations. Stromatoporoid-supported carbonate mounds widely developed. Lithology and faunas discussed by Shaw (1968). Trilobites described by Shaw (1968), listed by Shaw and Fortey (1977).

Trenton Gp. carbonates. Napanee and Kings Falls limestones and correlatives interpreted by Titus and Cameron (1976) as a transgressive sequence from lagoonal to shallow offshore shelf environments. Sugar River Limestone and correlatives (Verulam Fm.) interpreted as having been deposited in slightly deeper water, further offshore, characterised by the deposition of thin bedded calcarenites and calcareous shales. Associated fauna listed by Titus and Cameron (1976) and described by them as a high diversity *Trematis* -dominated community. These are overlain by the still deeper water offshore shelf facies of the Denley Limestone and correlatives (Lindsay and Cobourg formations), represented by dark grey fossiliferous silty bioclastic limestones yielding a low diversity shelly fauna. Titus and Cameron (1976) described the lithology and listed the faunas; Shaw and Fortey (1977) listed the trilobites.

Correlative Strata Elsewhere in the Appalachian Basin from which Fossils have been used. Middle to upper Ordovician stratigraphy of central Tennessee is shown in Figure 3. 10. Middle and early upper Ordovician strata of the Appalachian Basin grade eastward from stable carbonate platform deposits (e.g. Stones River and Nashville groups of Tennessee and southern Virginia) through more shaley and silty deposits of the platform margin (e.g. Holston and Effna formations and their correlatives) into slope shales and turbidites (Milici and de Witt 1988). Shaw and Fortey (1977) noted that the term "Athens Shale" has been widely used in the past for many "basinal" (*i.e.* slope) facies of general middle Ordovician age. Filling of the basin during the late middle Ordovician was followed eventually by onlapping of the upper Ordovician Martinsburg Shale.

Formations in Tennessee yielding material included in the present study.

"Athens Shale". Dark platy shales, interpreted by Shaw and Fortey (1977) as representing the lower slope depositional environment. Shaw and Fortey listed the trilobites.

Martinsburg Shale. Calcareous shales with interbedded fossiliferous limestones and siltstones (Milici and de Witt 1988). Interpreted by McBride (1972) and Stephens and Wright (1981) as a mixed sequence of turbidites and pelagic shales.

Central Midcontinent Region of the United States. Lithostratigraphy of the upper Ordovician of the central midcontinent region was reviewed by Bunker *et al.* (1988) and is shown in Figure 3. 11. Following deposition of the very pure and well sorted late Whiterockian - early Mohawkian St. Peter Sandstone (terminology of Ross *et al.* 1982 used in the absence of more formally defined lithostratigraphical formation names) and the shales of the Glenwood Fm., the Platteville and Decorah formations are shallow marine platform carbonates, the latter formation exhibiting significant lateral facies variations with varying shale component (Bunker *et al.* 1988). The Decorah Fm. is succeeded by a fossiliferous transgressive carbonate sequence analogous to the Trenton Gp. of New York. This sequence occurs as the Galena Gp. in Iowa, SE Minnesota, E Nebraska and NW Missouri; as the Kimmswick Limestone in E and central Missouri; and as the "Viola" Fm. in Kansas and W Nebraska. The carbonate sequence is succeeded by the interbedded shales and carbonates of the Maquoketa Gp., which spread westward over the region and represent the distal expression of the Queenston Delta Complex of the Appalachian Basin.

Formations yielding material included in the present study.

Galena Gp. carbonates. Skeletal wackestones and packstones and dolomites. Bunker *et al.* (1988) noted that the limestones and dolomites may form complex facies patterns, but that these are mainly of secondary diagenetic origin rather than reflecting original depositional patterns. Lithology and palaeogeography are discussed by Bunker *et al.* (1988). Highly fossiliferous, yielding abundant and diverse shelly faunas.

Maquoketa Gp. Brown, organic rich shales with interbedded limestones and phosporites. Lithologies and facies variations discussed by Witzke (1983) and by Bunker *et al.* (1988).

Upper Mohawkian and Cincinnatian Rocks of The Cincinnati Region. The "Cincinnati Region" is the type area for the upper Ordovician Cincinnatian Series of North America, and occupies an area covering the joint borders of Ohio, Indiana and Kentucky. Sweet and Bergström (1971) reviewed the lithostratigraphy of the region, which is shown in Figure 3. 11. The bioclastic carbonate facies of the Lexington Limestone (terminology of Ross *et al.* 1982 used in the absence of more formally defined lithostratigraphical formation names) grade both laterally and vertically into grey shales characteristic of the typical Cincinnatian Series (Sweet and Bergström 1971). Stratigraphy of the Cincinnatian Series was recently revised by Mitchell and Bergström (1991).

Figure 3. 11. Correlation of the upper Arenig - Ashgill rocks of SE Minnesota (column 1), Iowa (column 2), the Cincinnati Region (column 3), the Percé area, Gaspé Peninsula (column 4) and the Mackenzie district, NW Territories (column 5). Ordovician chronostratigraphy as in Figure 3. 1. Formations from which specimens of *Achatella* were used for morphometrics marked with an x; formations from which specimens of *Calyptaulax* were used for morphometrics marked with an open square.

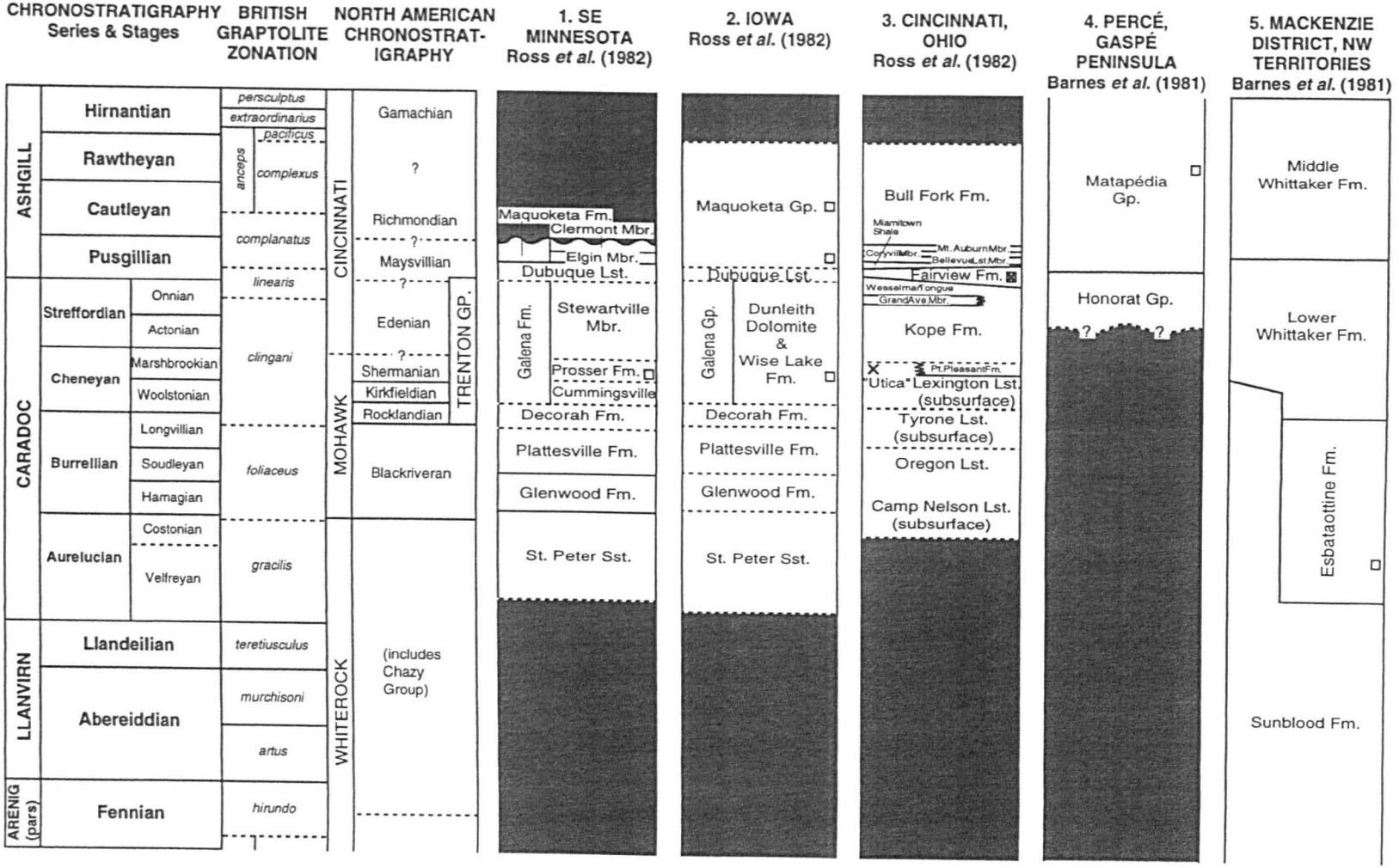

The Cincinnatian succession itself is about 228m thick in northern parts of the Cincinnati Region, thinning to about 200m in the southern part, and consists of grey silty shales with laterally discontinuous biomicrosparitic limestones (Sweet and Bergström 1971).

Formations yielding material included in the present study.

"Utica" Shale. In part correlative with the Utica Shale as used in New York State. Brown to dark grey laminated silty mudstones and shales with some thin shell layers and dark argillaceous limestone and siltstone interbeds (Mitchell and Bergström 1991). Moderately abundant graptolite fauna, but only sparse benthonic fauna, with *Triarthrus* and *Cryptolithus* fragments forming a major element. Lithology and main faunal elements listed by Mitchell and Bergström (1991).

Maysvillian, Cincinnati. Grey or green grey silty shales with laterally discontinuous biomicrosparitic limestones. The rocks in the southern part of the region are more silt-rich and more calcareous than those in the northern part. Although a number of formations are recognised, they are principally biostratigraphical units and few are distinguishable on the basis of any lithological variation from the above pattern (Sweet and Bergström 1971).

Upper Ordovician Succession of the Percé area, Gaspé Peninsula, Québec. The upper Ordovician and lower Silurian stratigraphy of the Percé area was reviewed by Lespérance (1988). The succession consists predominantly of limestones collectively termed the Matapédia Gp. In the Percé area, the Matapédia Gp. occurs in two distinct structural belts: the structurally complex northern belt, known as the "Grande Coupe Beds", consisting of calcilutites and shales with rare calcarenites; and the structurally more simple southern belt consisting of Ashgill to Llandovery carbonates with subordinate clastics and assigned to the Pabos and White Head formations (see maps and stratigraphical columns of Lespérance 1988; also fossil localities given by Cooper 1930).

In this study, fossils from localities within the Grande Coup Beds have been used. The correlation of the succession is shown in Figure 3. 11.

Formations yielding material included in the present study.

Undivided Grande Coup Beds of the Matapédia Gp. Locally varying proportions of calcilutites and shales with rare calcarenites. Abundant and diverse faunas generally indicating relatively deep water conditions (benthic assemblage 6 position of Boucot 1975; Lespérance 1988) although with local accumulations of fossils assignable to Boucot's (1975) benthic assemblage 4 in storm deposits (Lespérance 1988). All faunas of Rawtheyan age (Lespérance 1988).

Ordovician Succession of the Mackenzie Mountains District, Western Canada. Ordovician stratigraphy of the eastern part of the south Nahanni River area is shown in Figure 3. 11. The succession consists of a series of carbonate facies (limestones and dolomites) containing abundant shelly faunas (Ludvigsen 1975; Chatterton and Ludvigsen 1976). Ludvigsen (1975) considered the lower part of the sequence (Broken Skull and Sunblood formations) to represent the shallow subtidal and occasionally intertidal part of a carbonate platform, with intermittent deeper water conditions occurring in the Esbataottine Fm. giving rise locally to highly diverse trilobite faunas in the lower part of that formation. A prolonged transgression in the late Caradoc ("Trentonian") lead to the widespread deposition of bioclastic limestones of the Whittaker Fm. again containing abundant trilobites. Ordovician stratigraphy, facies and faunas of the region were described by Ludvigsen (1975, 1978, 1979a). Chatterton and Ludvigsen (1976) and Chatterton (1980) provided maps for the Esbataottine Fm. localities and described the trilobite faunas.

Formations yielding material included in the present study.

Esbataottine Fm. Homogeneous sequence of biomicritic and microbiosparitic limestones, generally thin bedded and weathering a grey-buff colour (Chatterton and Ludvigsen 1976). Chatterton and Ludvigsen recognised four trilobite biofacies which they considered to be related to fluctuating water depth (in order of progressive deepening: *Bathyurus* biofacies, *Isotelus* biofacies, *Calyptaulax - Ceraurinella* biofacies, and *Dimeropyge* biofacies) and whose constituents they listed and described. They considered the formation to have been deposited in quiet water conditions on a wide carbonate shelf in environments ranging from the littoral to deep sub-littoral, the associations including *Calyptaulax* originating from near the deeper end of this spectrum (Chatterton and Ludvigsen 1976).

3. 20. Silurian Succession of Anticosti Island.

A continuous and uninterrupted succession of almost horizontal upper Ordovician - lower Silurian strata is exposed on Anticosti Island, Québec (Bolton 1971; Barnes 1988). The upper Ordovician consists of alternating laterally persistent calcareous and argillaceous units (Bolton 1971), and these are conformably overlain by a more lithologically variable Llandovery succession of carbonates and shales, which Barnes (1988) interpreted as having been deposited on the stable outer part of a carbonate platform. The lithological and faunal variation across the Ordovician-Silurian boundary was discussed by Barnes (1988) who also provided a map of the island. A geological map was given by Bolton (1971) who reviewed the stratigraphy and lithologies of the entire succession, as well as listing the main elements of the faunas. Lespérance and Letendre (1981, 1982) described trilobites from the succession. Figure 3. 9 shows the Silurian succession of Anticosti Island.

Formations yielding material included in the present study.

Jupiter Fm. Argillaceous brown, grey and blue-grey fossiliferous limestones, occasionally lithographic, with interbedded shales. Carbonate mounds composed of granular limestone 1.5 - 2.5m in height locally define the basal horizons of the formation. The lithologies were described by Bolton (1971) who also listed the most characteristic components of the fauna. Trilobites were described by Lespérance and Letendre (1981, 1982).

CHAPTER FOUR

MORPHOMETRIC TECHNIQUES

4. 1. Introduction.

The field of morphometrics has been defined as "the analysis of biological homology as well as geometric change" (Bookstein *et al.* 1985). Morphometrics is relevant in assessing phylogenetic relationships between geographically and stratigraphically separate samples of organisms, ontogenetic trajectories and their potential for producing evolutionary change through heterochrony, relative importance of anagenetic and cladogenetic patterns in the evolutionary history of one or more clades, and ecophenotypic effects (Kitchell 1990). Importance is placed on analytical procedures which determine which measurable parameters of an organism contribute to intraspecific characterisation, and to interspecific discrimination in time and space (Kitchell 1990). Marcus (1990) distinguished so-called "traditional" morphometric methods (*i.e.* those which have been available to morphometric workers for the last 20 to 30 years) which generally consider biological form by means of distances measured between homologous landmarks on a set of organisms, from the so-called "new morphometrics" which places emphasis on landmark (coordinate) data and statistical methods which take account of the geometrical relationships between landmarks (e.g. the methods of Bookstein 1982). The "traditional" methods include the techniques of principal component analysis (PCA), principal coordinate analysis, factor analysis, discriminant analysis, canonical variate analysis, and multivariate analysis of variance.

Kitchell (1990) noted the historical problem that quantitative data on morphological change within and between taxa, and in time and space, have not been available in sufficient quantity to adequately address the questions and hypotheses which abound in palaeobiology; this problem being in large part due to the difficult and time-consuming nature of the job of accurately collecting such data. Recent advances in computer technology have made the acquisition of large amounts of quantitative data on morphology much faster and more accurate. Further, this technology has greatly increased the speed with which these large data sets can be analysed to provide meaningful results (Kitchell 1990).

The purpose of this chapter is to describe the computer-aided data acquisition and analysis techniques used in the morphometric analysis of the trilobite genera studied in chapters 5 - 7. Section 4. 2 describes the philosophy employed in selection of material for study, both in the field and from established museum collections. Section 4. 3 describes the method by which morphometric data were acquired from the specimens, and the form the data take. Section 4. 4 outlines the mathematical technique of principal component analysis (PCA) and describes the way in which it was employed as the primary tool for studying morphometric variation between specimens from different stratigraphical and geographical localities.

4. 2. Selection of Study Material.

Field collecting for this study was undertaken in the Ordovician and Silurian succession of the Girvan district, SW Scotland and in the Silurian succession of the North Esk Inlier, Pentland Hills. A small amount of collecting was also done in the Ordovician and Silurian succession of the Oslo Region, Norway. In the field, care was taken to collect all sufficiently well preserved cephala and pygidia assignable to the genera under study (*i.e. Achatella, Calyptaulax, Acernaspis, Ananaspis*), regardless of size. For these purposes, "sufficiently well preserved" means specimens which are not markedly distorted, which are preserved with sufficient detail to permit identification and accurate location of the required morphological landmarks, and which, while not necessarily being 100% complete, are complete enough to allow location of the sagittal axis of symmetry so that the location of structures which are not preserved on one side of the specimen can be inferred from their location on the other side.

In selection of material housed in established museum collections, care was taken to identify, so far as possible, all locations within the collections where specimens referable to the genera under consideration might be stored. In the case of systematically arranged collections, this meant taking into consideration all junior synonyms under which material might be stored. In practice, this usually involved checking drawers labelled with the currently assigned name (*i.e. Achatella, Calyptaulax, Acernaspis,* and *Ananaspis*), and then checking neighbouring drawers labelled with other names under which it was known that the genera of interest might have been stored in the past. For example, in selecting specimens of *Achatella* from a systematically arranged collection, drawers labelled as containing *Pterygometopus, Phacops* and *Chasmops* would also be checked since it was known that species now assigned to *Achatella* have previously been placed or mis-identified within these genera. In the case of collections arranged in other ways (*e.g.* stratigraphical, geographical, or by collector) liaison with curators familiar with the collection was helpful in locating material. To be included in the morphometric study, specimens from museum collections had to meet the twin criteria of being sufficiently well preserved and sufficiently well localised, both geographically and stratigraphically. Unfortunately, many museum specimens which were collected in the nineteenth century, while often being of superb preservational quality, fail to meet this second criterion and so could not be included in the morphometric study. The museum collections from which specimens have been used are listed in the acknowledgements at the beginning of this thesis.

If inferences as to the variation within and between populations of organisms are to be drawn from samples taken from those populations, it is important that the samples be, so far as is possible, random samples from their respective populations (Marcus 1990). In the case of specimens collected in the field, the material used herein does represent

random samples with the caveat that only sufficiently well preserved specimens could be used for morphometrics. In the case of specimens selected from museum collections, again, all sufficiently well preserved specimens were used. It can be argued that older museum collections (for example those collected in the nineteenth and early twentieth centuries, before statistical considerations came to the fore in field studies) probably do not represent strictly random samples from their populations, since the collector probably retained only the best-preserved material. However this means that the collector's strategy was not dissimilar to that employed by the worker collecting material for morphometric analysis: any specimen which a nineteenth or early twentieth century collector felt was too poorly preserved to be retained probably would have been unusable for morphometrics.

4. 3. Morphometric Data Acquisition.

Since the genera under study are usually preserved as disassociated sclerites, cephala from given individuals generally could not be associated with their corresponding pygidia, and so cephala and pygidia have been treated separately for morphometrics. Thoracic segments and hypostomes are not common for the genera studied, and in any case possess few measurable characters; these sclera have therefore not been used for morphometrics. Because pygidia of the genera under study can be adequately characterised by a much more reduced set of measurements than can cephala, different (though analogous) techniques were developed for obtaining measurements from them.

Internal moulds, occasional testate specimens, and silicified specimens were used for morphometrics. Where the ends of measurements fall in furrows, the measurements were made to the deepest point in the furrow, since this point is coincident on testate and non-testate specimens when viewed in dorsal view (Shaw 1957). It was decided to use a single orientation measurement system (*i.e.* one in which all measurements are made with the specimen in a single standard orientation, defined below) rather than making measurements normal to the surface of the sclerite, since the former method has the advantage of yielding measurements which approximate to the visual impression of the sclerite, while the latter method requires repeated re-orientation of the specimen (Shaw 1957; Temple 1975).

Data acquisition from cephala. Morphometric data were obtained from cephala and cranidia using a semi-automated method consisting of the following steps:

(i) the cephalon or cranidium was photographed in a standard orientation;

(ii) an enlarged photographic print was made (usually 10x original size);

(iii) the enlarged print was placed on a digitising tablet and the Cartesian coordinates of landmarks on the sclerite were captured; a measurement made from the specimen at the time of photography was used to scale the coordinate system;

(iv) distances between landmarks on the sclerite in the X (transverse) and Y (sagittal and exsagittal) directions were calculated from the landmark coordinates.

Photography was done using a Nikon FM2 camera and Ilford "Pan-F" 50 ASA black and white film which has good resolving properties allowing for production of high quality enlargements (Siveter 1990). Specimens which were to be reproduced on plates were darkened with photographer's opaque and then lightly whitened with either magnesium oxide or ammonium chloride prior to photographing, as recommended by Siveter (1990). The specimen was placed on a plasticene mount which allowed for its precise orientation. For cephala and cranidia which were being photographed for measurement, a standard orientation was defined after Shaw (1957: 194) and Temple (1975: 463): *i.e.* with the chord to the palpebral lobes placed horizontal. The specimen was photographed at x1/2, x1 or x2 magnification depending on its size. Either prior to or just after photography a measurement was made on the specimen itself in standard orientation using a moving stage microscope to allow correct scaling of the coordinate system for digitising landmarks (see below). Where possible, the sagittal distance from the anteriormost extremity of the specimen to the deepest point in the occipital furrow was used for this measurement, since it was obtainable for virtually all specimens used.

An enlarged (x10) photographic print was made. The print was fixed on a GTCO "Macintizer ADB" digitising tablet in such a way that a transverse line traced across the image of the sclerite ran precisely transversely across the tablet. The tablet was connected to a Macintosh II computer running NIH "Image" software. "Image" is an image analysis package which allows capture of XY coordinates and linear, angular and area measurements, as well as supporting many more sophisticated image analysis tools not used in this study. A measurement made on the specimen at the time of photography (see above) was used to set the scaling factor for the coordinate system used by "Image", so that X and Y coordinates of landmarks captured from the enlarged print, and linear measurements derived from them, would correspond to coordinates and measurements on the specimen itself. Cartesian coordinates of landmarks on the sclerite were then captured from the digitising tablet. The landmarks used for each genus studied are described in the relevant chapters.

A number of angular measurements were also made from the cephala and cranidia using "Image". These described the angles at which the lateral glabellar furrows diverged from the sagittal line, and also the angle at which the sagittal line intersected a transverse line traced across the sclerite. This latter angle (the "deformation angle") provided a useful check on the degree of tectonic distortion of the specimen: obviously it should equal 90° in an undistorted cephalon. Cephala and cranidia for which this angle deviated by more than 10° from orthogonality were rejected from the morphometric analysis.

Finally linear distances between landmarks in the transverse X and longitudinal Y directions were calculated from the coordinates obtained above. Since the coordinate system was scaled with respect to a measurement made from the specimen itself (see above) these linear distances equate to distances on the specimen itself. In deriving distances in the transverse X and longitudinal Y directions, this method mimics the action of the moving stage microscope (see below).

Precision and reproducibility of the method. The limit to the precision with which NIH "Image" can measure linear distances and Cartesian coordinates is imposed by the resolving power of the computer screen, *i.e.* the actual distance (on the specimen) represented by the distance on the computer screen from one pixel to the next. In digitising from a print which has been enlarged 10x, "Image" can measure to a precision of 0.05 mm, a precision comparable with the finest precision of the moving stage microscope (see below) or vernier callipers.

The main sources of error in the procedure probably lie in the following: orientating the specimen for photography; enlarging the photographic print; digitising the coordinates of the landmarks. In order to test the reproducibility of the measurements, a test was undertaken. A single cephalon of *Calyptaulax (Calliops) brongniartii* was photographed 20 times in standard orientation (see above), with the specimen being removed from the photographic stage and replaced in standard orientation for each photograph. Twenty enlarged (x10) prints were made from the photographs. Ten measurements were then made from each of the 20 enlargements using the digitising tablet. The data are given in Appendix 5 (morphometric data), and are summarised in Table 4. 1. The measurements are after Shaw (1957) and Temple (1975), and are described fully in Chapter 6 (Figure 6. 9 and Table 6. 4). It can be seen from Table 4. 1 that the reproducibility of the measurements is good, with most measurements varying by less than 3% from the median value over the 20 trials.

Advantages of this method over the moving stage microscope. It was originally intended to make measurements from cephala and cranidia of the trilobite genera under study using the moving stage microscope, as was done for pygidia (see below). However, upon attempting this, it soon became clear that using the moving stage microscope to obtain the large number of measurements required to adequately describe the structure of the cephalon of these trilobites (e.g. 38 measurements derived from the locations of 49 landmarks are used to describe the cephalon of *Achatella*, see Chapter 5) was not feasible if a statistically useful (*i.e.* large) number of specimens were to be utilised. Therefore, the photographic technique described above was developed to handle these large numbers of specimens. This technique has the following advantages over using the moving stage

Table 4. 1. Results of making 10 measurements from each of 20 enlarged photographic prints of a single cephalon of *Calyptaulax (Calliops) brongniartii* using the digitising tablet. Between each photograph, the specimen was removed from the photographic stage and replaced in standard orientation. The measurements are described in Chapter 6 (see Figure 6. 9 and Table 6. 4).

Measurement	Mean value	Median value	Minimum value	Maximum value	% variation of median
B	8.10	8.11	8.02	8.16	± 1.1%
b5	4.00	4.01	3.94	4.09	± 2.0%
b32	2.51	2.51	2.45	2.57	± 2.4%
k5	7.40	7.40	7.31	7.52	± 1.6%
k32	7.18	7.17	7.08	7.29	± 1.7%
k21	4.65	4.64	4.55	4.79	± 3.2%
k10	3.80	3.81	3.72	3.90	± 2.4%
J	11.57	11.55	11.47	11.77	± 1.9%
C1	4.04	4.04	3.98	4.11	± 1.7%
C2	8.67	8.64	8.59	8.78	± 1.6%

Table 4. 2. Results of making four measurements on a single pygidium of *Ananaspis stokesii* using the moving stage microscope. The pygidium was measured 20 times. Between each set of measurements, the specimen was removed from the microscope stage and replaced in standard orientation. The measurements are described in Chapter 7 (see Figure 7. 5 and Table 7. 2).

Measurement	Mean value	Median value	Minimum value	Maximum value	% variation of median
Y1	3.69	3.70	3.60	3.80	± 2.7%
Z1	4.54	4.55	4.40	4.70	± 3.3%
W	10.76	10.75	10.65	10.85	± 0.9%
X	3.15	3.15	3.05	3.20	± 3.2%

microscope:

(i) Increased speed of data acquisition. It is impractical to borrow large numbers of specimens from museum collections, especially those housed overseas. It is preferable to spend a short time at the museum in question and make use of the specimens on site. When using the moving stage microscope to measure the specimens, it can take 45 minutes or longer to capture the coordinates of the 49 landmarks used to describe the cephalon of *Achatella* (for example), and this imposes a serious limit on the number of specimens it is possible to measure in a given time. Using the method described above however, it is necessary only to photograph the specimens in standard orientation, for later digitisation. It is easily possible to photograph 100 specimens per day.

The actual process of capturing the coordinates is also much faster using this method. To capture coordinates of the 49 landmarks noted above using the enlarged print on the digitising tablet takes only about 15 minutes.

(ii) The method uses an image of the specimen. This has a number of advantages over methods using direct measurement from the specimen itself: it is much easier to identify and mark the line of sagittal symmetry on an image than it is on the specimen itself, and hence to use this symmetry to derive the locations of landmarks not preserved on one or other side of the exoskeleton; it allows measurement of angular relationships (not possible with the moving stage microscope); if it is decided at some time after the original data has been collected that some additional data are required from each specimen, it is necessary only to go back to the photograph rather than to obtain the specimen again; some shape analysis procedures begin from a pictorial representation of the specimen (e.g. Fourier outline methods such as that of Foote 1989).

(iii) This method is less prone to errors, since capture of the coordinates from the digitising tablet by the computer is automatic and requires no intermediate step of writing down the numbers and then transferring them to a computer file.

Data acquisition from pygidia. Morphometric data were captured from pygidia of the study genera using a moving stage microscope because of the relatively small number of measurements (commonly three or four) required to characterise the pygidium. Morphometric description of a pygidium could be accomplished in about three minutes. The moving stage microscope is a standard binocular microscope equipped with a stage which is able to move in two perpendicular horizontal directions (X and Y) under the control of geared wheels. Vernier scales along two adjacent sides of the moving stage register its current location in the X and Y directions. A cross hair in one of the eyepieces

is used to accurately target the landmark whose XY coordinates are required, and the coordinates are read from the vernier scales. Pygidia were placed on a plasticene mount and orientated in standard orientation as defined by Shaw (1957: 194) and Temple (1975: 463), *i.e.* with the ventral margin of the pygidial border placed horizontal. Measurements were then made directly from the specimen. The measurements used to characterise pygidia of each study genus are listed in the relevant chapters.

Precision and reproducibility of the method. The vernier scales on the moving stage microscope allow measurement of coordinates and linear distances to a precision of 0.1 mm (possibly to 0.05 mm where the vernier scale reading is seen to fall precisely between two successive increments).

The main sources of error in this procedure probably lie in the following: orientating the specimen on the microscope stage; taking the measurements. In order to test the reproducibility of the measurements a test was undertaken. A single pygidium of *Ananaspis stokesii* was measured 20 times in standard orientation, with the specimen being removed from the microscope stage and replaced in standard orientation each time. Four measurements were made. The data are given in Appendix 5 and summarised in Table 4. 2. The measurements are after Shaw (1957) and are described in Chapter 7 (Figure 7. 5 and Table 7. 2). It can be seen from Table 4. 2 that the reproducibility of the measurements is good, with all measurements varying by 3.3% or less from the median value over 20 trials.

4. 4. Principal Component Analysis.

The morphometric data captured from the trilobite cephala and pygidia consists of a large number of measurements made on a large number of specimens. For example, 36 measurements (taking into account those which are duplicated on the left and right sides of the animal) were made on cephala of *Calyptaulax* derived from the locations of 49 landmarks (see Chapter 6; not all of these measurements were used in the cranidium data set described in Chapter 6). It is intended to study the variation among the measured specimens, in order to attempt to recognise any systematic patterns in time or space. In the simplest multivariate case where only two measurements have been made on each specimen a simple way to study variation among such specimens would be to plot a bivariate graph of the two variables. Each specimen would be represented by a single data point on the graph, and patterns of variation among the specimens should be readily apparent. However this is clearly not possible with a data set consisting of specimens on which 36 measurements have been made; this would require each specimen to be represented by a single data point on a graph plotted in 36 dimensions! A way around this problem is to reduce the dimensionality of the data set, *i.e.* to reduce the 36 (or however many there are) variables down to just two or three which can be readily plotted

on a graph. A way of doing this is to use the data transformation known as principal component analysis (PCA).

Principal component analysis is a model-free and distribution-free technique for rigidly transforming multivariate data (Marcus 1990) in such a way that the dimensionality of the data can be significantly reduced. The mathematics of PCA are reviewed by Davis (1986), and its use with palaeobiological data is described by Temple (1982) and Marcus (1990). Temple (1982) noted that PCA can be used in three types of palaeobiological situations:

(i) Morphological analysis of one or more samples consisting of specimens on which a number of morphological measurements have been made. It is this type of analysis which is undertaken in this study. The particular power of PCA lies in the fact that it enables the size component of variation within and between samples to be separated from shape variation (Harper and Ryan 1990). Examples of PCA used in this way include the following: Temple (1975a) studied variation in the cephalic proportions of Llandovery calymenids, demonstrating a spectrum of variation and possible sexual dimorphism; Foote (1989, 1991a) used the procedure to ordinate twelve Fourier coefficients generated by perimeter-based Fourier analysis of trilobite cranidia in an investigation of trilobite morphospace occupation; Foote (1991b) applied PCA to the coordinates of eight landmarks on the test of blastoids sampled from Ordovician to Permian strata in order to compare patterns of morphological and taxonomic diversity in time.

(ii) Numerical taxonomy, in which the data consist of several taxa on each of which the states of a number of morphological attributes have been coded (often merely as presence/absence data). The technique is able to separate from a large set of characters those that are taxonomically most important (Temple 1982). Examples of PCA used in this way include: Temple and Tripp (1979), who applied the method to the taxonomy of encrinurine trilobites; Temple (1981) applied it to British and Irish species of Trinucleidae.

(iii) Distribution studies in which the data consist of several samples or sample localities at each of which the frequency of occurrence, or presence/absence, of several taxa has been recorded. Examples of PCA used in this way include Harper and Ryan's (1990) ordination of the data on upper Llanvirn palaeocommunities from Wales presented by Williams *et al.* (1981).

The technique works by defining new variables known as principal components (PCs) which are linear combinations of the original observed variables (Marcus 1990). If the original observed data (*i.e.* the measurements made on the specimens) form a matrix [d]

of n rows (one for each specimen) and m columns (one for each measured variable) the specimens can be graphically plotted as data points in an m-dimensional space. Figure 4.1 shows such a plot for two-dimensional data (*i.e.* m=2). Although it is of course not possible to construct an m-dimensional graph where m>3, the technique which follows is still mathematically applicable for such multivariate data. It is possible to define a new axis through the data such that variance along this axis is greater than variance along any other direction through the data; this axis is called the first principal component (PC1). For the two-dimensional example in Figure 4. 1, PC1 is marked. There is also one other PC in this two-dimensional example (PC2, perpendicular to PC1) which is the direction of least variance through the data. In an m-dimensional example, m such mutually orthogonal PC axes can be traced. PC1 is the axis summarising the largest component of variance in the data set; PC2 summarises the next largest component; PC3 the next; and so on down to PCm which summarises the most invariant component. In mathematical terms, the magnitude and orientation respectively of these PC axes are given by numerical quantities called eigenvalues and eigenvectors which are calculated from a similarity matrix [s] (which can be either a variance-covariance matrix or a correlation matrix) which itself is calculated from the original observed data matrix [d] (Davis 1986 discusses calculation of eigenvalues, eigenvectors, and variance-covariance and correlation matrices).

The m observed variables can now be transformed into PC variables by projecting each data point onto each of the PC axes (projections of some data points onto PC1 are shown as lines orthogonal to PC1 in the two-dimensional example illustrated in Figure 4. 1). The position at which the data point projects onto a given PC axis is its "principal component score" on that axis. Since there are as many PC axes as original variables (m), each specimen is now represented by m PC scores as well as m observed values.

It is possible to tell what proportion of the total variance in the data set each PC summarises by studying the eigenvalues. Further it is possible to tell what effect each of the original m variables had in the calculation of each of the PC axes by studying the eigenvectors; these vectors contain m elements called "principal component loadings". By studying the eigenvalues it can usually be seen that the first three or four principal component axes account for the vast majority of the variance in the data set. Indeed, in the case of the morphometric data gathered for this study, the first three principal component axes commonly account for around 95% of the total variance in the data. This means that although there are as many PC axes as there are original variables (m), all but the first three or four account for a proportion of the total variation which is so close to zero that they can be effectively ignored. Thus the number of variables required to describe the variance in the data set has been significantly reduced.

Figure 4. 1. Scatter plot illustrating how principal component axes relate to bivariate data. Projections of several data points onto PC1 are shown. Data in this case are paired skull measurements in mm made on the rodent *Zygodontomys* sampled from a single locality, and given by Marcus (1990: appendix 1). Figure after Marcus (1990: figure 6A).

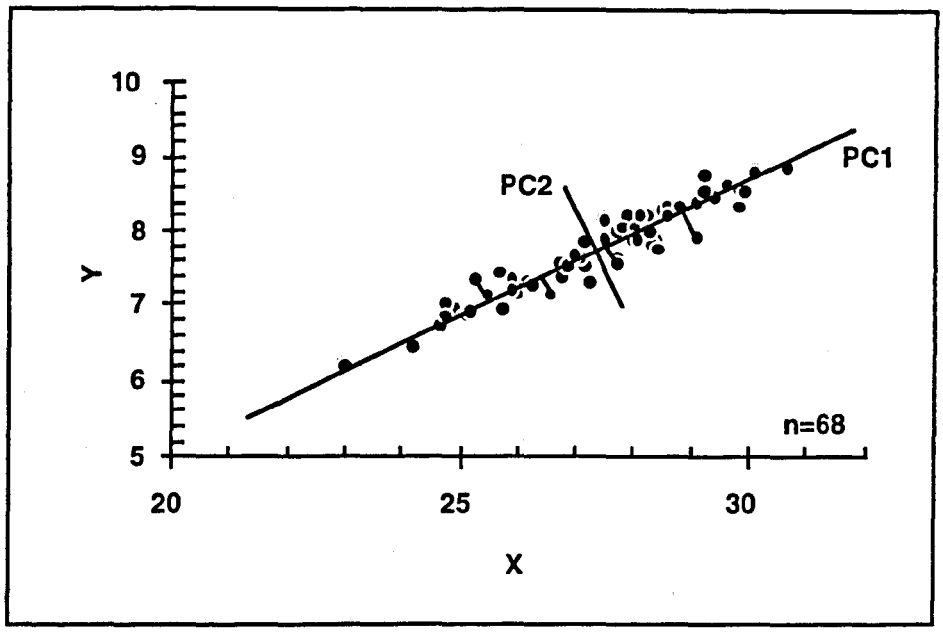

Table 4. 3. Eigenvalue and eigenvector output from the principal component analysis of the *Calyptaulax* pygidium data set.

Principal component analysis of *Calyptaulax* pygidium data set.
192 cases.

EigenValues

	Values	Variance Proportion	Cumulative Variance Proportion
e1	2.948	73.7	73.7
e2	0.884	22.1	95.8
e3	0.135	3.4	99.2
e4	0.033	0.8	100

EigenVectors

	V1	V2	V3	V4
W	0.539	-0.25	-0.804	-0.019
Z1	0.566	-0.144	0.407	0.702
Y1	0.57	-0.045	0.414	-0.708
Axial segs.	0.253	0.956	-0.129	0.067

Example of the use of PCA. To study the morphometric variance (or lack thereof) among trilobites sampled from different stratigraphical and geographical localities, PCA has been applied to sets of linear measurements made from cephala, cranidia and pygidia using the methods described in Section 4. 3. PCA was undertaken using the computer program Odesta "Data Desk" version 3.0 running on a Macintosh II computer. For this example of the use of PCA, measurements made on pygidia of the pterygometopid trilobite *Calyptaulax* will be used, as this data set contains few enough dimensions (*i.e.* four) to produce results presentable on a single page. The *Calyptaulax* pygidium data set and the measurements made on pygidia of *Calyptaulax* are described in Chapter 6, and the data are given in Appendix 5.

The observed data consist of four measurements made on each pygidium; all four measurements were obtainable for a total of 192 pygidia. PCA is unable to cope with missing data values, so all measurements must be available for all specimens included in the analysis. Out of 256 *Calyptaulax* pygidia measured, 192 met this criterion. Choosing which variables to utilise in a PCA of morphometric data involves a compromise between using measurements which are obtainable for a statistically useful number of specimens, and measurements which describe the structure of the sclerite in question with sufficient completeness. Thus the observed data is in the form of a matrix, [d], 192 rows x 4 columns. As a starting point for PCA, it is necessary to calculate the similarity matrix [s] from the data in [d]. It is from this similarity matrix [s] that the eigenvalues and eigenvectors used to orientate the PC axes are calculated. In all PCA undertaken for this study, the correlation matrix (rather than the variance-covariance matrix) has been used as the similarity matrix [s]; Temple (1982) noted that in his experience analyses based on the variance-covariance matrix and analyses based on the correlation matrix do not differ greatly in their results. Many texts describing PCA (e.g. Davis 1986, Marcus 1990) emphasise that it is important that all variables involved in a PCA have similar magnitudes. Variables with magnitudes much greater than the other variables in the data set tend to adversely affect the result of the PCA. The usual way around this problem is to standardise all of the variables so they have means of zero and variances of 1 (Davis 1986). This standardisation step is implicit in the calculation of the correlation matrix [s] from the observed data matrix [d].

The eigenvalues, eigenvectors and PC scores calculated for the *Calyptaulax* pygidium data set are given in Appendix 6, and the eigenvalues and eigenvectors are also reproduced in Table 4. 3. Since there are four original variables, there are also four eigenvalues e1 - e4 (as well as the eigenvalues themselves, the proportions they represent of the total variance in the data set are given), four eigenvectors (each consisting of four elements, the principal component loadings), and 4 x 192 PC scores (not reproduced in Table 4. 3). On studying the list of eigenvalues, it is seen that PC1 accounts for 73.7%

of the total variance in the data set, PC2 for 22.1% and PC3 for 3.4%, so that the vast majority of the variance in the data, 99.2%, is accounted for by these three PC axes. The remaining PC axis only accounts for the remaining 0.8% of the total variance. Therefore, if only the first three PCs are retained, the dimensionality of the *Calyptaulax* pygidium data set is reduced from four dimensions to three with only a 0.8% loss in variance. More highly dimensional data sets (e.g. the *Calyptaulax* cranidium data set which is based on 36 variables) can be similarly reduced to three dimensions with minimal loss of variance (commonly around a 5% loss).

Referring to the eigenvector list resulting from the PCA calculation (Table 4. 3) it is notable that most principal component loadings on PC1 (the elements of eigenvector 1) are similar and all show the same (positive) sign. This means that the correlations of this PC with all original variables (the measurements made on the specimens) has the same sign. So the first PC reflects variance due to the size of the specimens, and this PC can therefore be referred to as a "size component" (Temple 1982; Marcus 1990). Notice that the relationship of the subsequent PCs to the original variables is more complex: all subsequent eigenvectors (from eigenvector 2 onwards) contain elements with a mixture of positive and negative signs, indicating that the correlations of these PCs with the original variables run in different directions for different variables. These three subsequent PCs are therefore referred to as "shape components" (Marcus 1990). By studying the PC loadings contained within the eigenvectors, it is possible to pick out those variables which have greatest effect in the calculation of the PC scores. For example, it can be seen that the number of axial rings is most heavily weighted on PC2; W (which describes the width of the pygidium) is most heavily weighted on PC3. These variables are therefore worthy of further study to see if they exhibit systematic patterns of variation within the data set.

By comparing the amount of variance accounted for by the size component PC1 (73.7% in the above case) with that accounted for by the shape components PC2 - PC4 (100 - 73.7 = 26.3%) it is clear that the vast majority of variance in the original data set just summarises size information. This is usually the case with biological data sets (Marcus 1990) and, as will be seen in subsequent chapters, is particularly the case with the highly shape-conservative organisms studied herein. Shape discontinuities in morphospace occupation by the pygidia can now be studied from plots of the specimens ordinated against PC2 and PC3. See for example Figures 6. 15, 6. 17 and 6. 18 on which the *Calyptaulax* pygidia are ordinated on the second and third principal component axes calculated by the method described above. Subsequent PCs (*i.e.* PC4 in this case) can also be plotted. This has not in general been done in this study since PCs from four onwards generally summarise minute amounts of variance in the original data set.

CHAPTER FIVE

A PHYLOGENETIC AND MORPHOMETRIC ANALYSIS OF *ACHATELLA* DELO, 1935.

5. 1. Introduction.

Achatella (Suborder Phacopina, Family Pterygometopidae, Subfamily Pterygometopinae) is known from rocks of Llanvirn to Hirnantian age belonging to the Baltic and Laurentian faunal provinces, a total duration of some 22.5 myr (Time scale of Tucker *et al.* 1990). The Pterygometopinae are typically a Baltic group, and *Achatella* is the only member of the subfamily to be represented in Laurentia. The first appearance of the genus is in strata of the Uhaku (C_{Ic}) Stage (Llandeilian) of northern Estonia, where it was probably derived from the lower Ordovician *Pterygometopus* (McNamara 1980; Ludvigsen and Chatterton 1982). The genus remained restricted to Baltica throughout the Llandeilian and early Caradoc (Jaanusson and Ramsköld 1993) and made its first appearance in Laurentia in late middle Caradoc (Kirkfieldian-Shermanian) strata of eastern North America and Scotland (Tripp 1954; Ludvigsen and Chatterton 1982; Sloan 1991). Throughout the rest of the Ordovician *Achatella* occurs in rocks of eastern North America (Ontario, Québec, New York, Missouri and Illinois), Scotland (Craighead Inlier) and Norway (Oslo Region). The latest occurrences of the genus are in Hirnantian rocks of the Craighead Inlier, Girvan (High Mains Fm., Owen 1986) and Ringerike, Oslo region (Langøyene Fm., herein). The genus is typical of continental shelf clastic and shelf-edge carbonate mound deposits. Figure 5. 1 shows the stratigraphical range of *Achatella* and its phylogenetic relationship to the other Pterygometopidae as suggested by Ludvigsen and Chatterton (1982).

Throughout the long duration of the genus, all species look superficially very similar and this has given many workers problems in making specific identifications. However it has been noted that, in spite of the conservatism of the basic body plan, there is variation between species in what might be termed "peripheral" characters. Jaanusson and Ramsköld (1993) noted variation in the lengths of genal spines, detailed position of the anterior of the eye, development of the preglabellar furrow, and shape of the outer portion of the pygidial pleural area. The long duration of the genus together with superficial similarity of all member species lead to the choice of this genus for a detailed morphological analysis.

Detailed phylogenetic and morphometric analysis has been undertaken on specimens of *Achatella* belonging to twenty stratigraphically and geographically separate samples. These samples are described in Section 5. 2. Section 5. 3 presents a cladistic analysis of the genus, which was done in order to construct a phylogenetic framework for *Achatella*, and also as a means of studying patterns of change of character states within the genus. This analysis included consideration of some characters which are not amenable to morphometric analysis. Section 5. 4 presents a morphometric analysis which assesses the degree of shape conservatism in *Achatella* and highlights the amount and pattern of variation in those characters which do show change. A

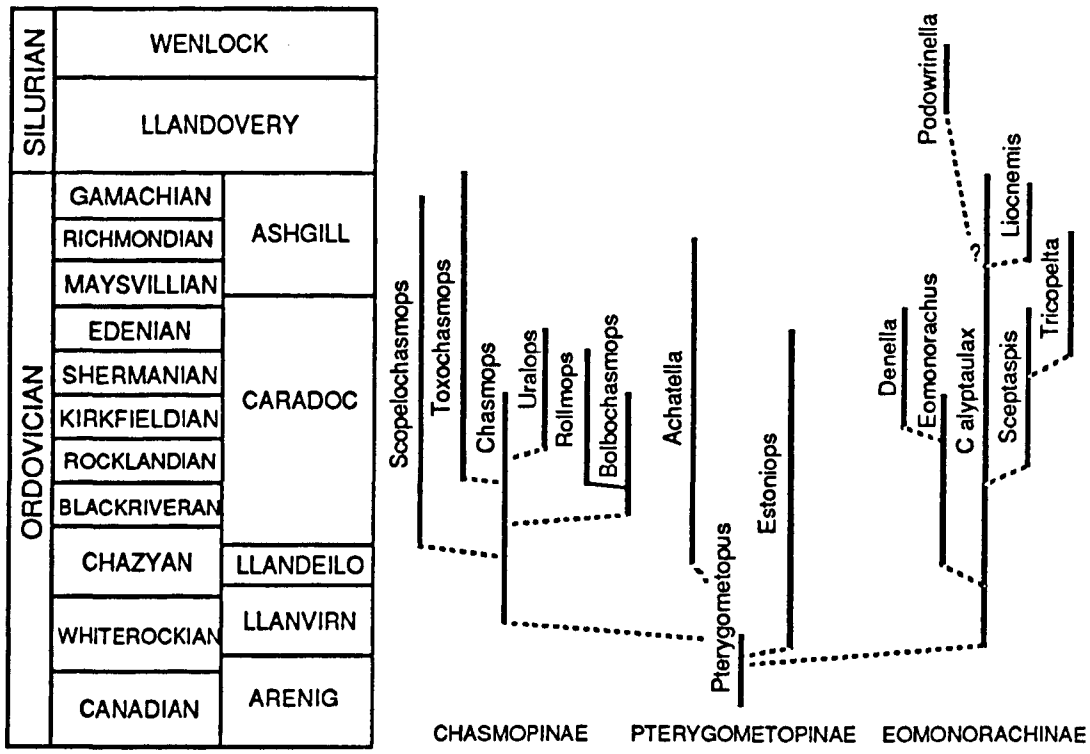

Figure 5. 1. Stratigraphical ranges and possible phylogeny of genera of three of the constituent subfamilies of the Pterygometopidae, as defined by Ludvigsen and Chatterton (1982). The fourth subfamily, the Monorakinae, is too poorly known to be included. Redrawn with slight modification from Ludvigsen and Chatterton (1982).

systematic revision of the genus is presented in Section 5. 5. Section 5. 6 draws conclusions both about the systematics of *Achatella* itself, and also about its implications for the wider question of stasis.

5. 2. Material.

Twenty stratigraphically and geographically separate samples from which specimens of *Achatella* were available were studied. The samples, which together account for the full temporal and geographical range of the genus, are listed below. Locality names and numbers in square brackets refer to the locality list in Appendix 3. Names in curly brackets give the species to which the specimens are currently assigned. The rather small size of some of the samples reflects the rarity of specimens complete enough for morphometric study. While *Achatella* often occurs in Caradoc and Ashgill faunas of Baltica and Laurentia, it is typically a minor constituent and is rarely undistorted and undamaged because of its fragile nature. Note that "material" below refers to specimens complete enough and undistorted enough for morphometrics, and does not include disassociated visual surfaces which are included in Figures 5. 5 and 5. 25.

Girvan District

1. KILN. Specimens from the Kiln Mudstone at Craighead Quarry, Girvan [loc. 12]. Craighead Fm., middle *clingani* Zone (Tripp 1980b). {*Achatella consobrina* Tripp, 1954}. Material: six cephala, five pygidia and two hypostomes.
2. QHILL. From the east brow of Quarrel Hill, Girvan [loc. 13]. Quarrel Hill Fm., Lower Drummuck Group (Cautleyan, probably *anceps* Zone, Harper 1982). {*Achatella retardata* (Reed, 1914); also *Achatella quarrelensis* (Reed, 1930)}. Material: two cephala and 15 pygidia.
3. CRINBED. From the "Crinoid Bed" (Harper 1982, p. 263), Quarrel Hill, Girvan [loc. 14]. Upper part of Quarrel Hill Fm., Lower Drummuck Group (Cautleyan, probably *anceps* Zone, Harper 1982). {*Achatella* sp.}. Material: two incomplete cranidia, only one of which is suitable for morphometrics, and three pygidia.
4. STARBED. Specimens from the "Starfish Beds", Lady Burn, Girvan (Harper 1982, p. 266) [loc. 15]. Lower part of South Threave Fm., Upper Drummuck Group (late Rawtheyan, upper *anceps* Zone, Harper 1982). {*Achatella retardata* (Reed, 1914)}. Material: seven cephala and cranidia, eight pygidia and a hypostome.
5. HIGHMAIN. From trench at High Mains Farm, Girvan [loc. 16]. High Mains Fm., Hirnantian (Owen 1986). {*Achatella* cf. *truncatocaudata* of Owen 1986}. Material: three cranidia and five pygidia.

Eastern Ireland

6. KNOCK. Specimens from Grangegeeth crossroads [loc. 46] and Collon Quarry [loc. 47], Knockerk House Sandstone Member, Grangegeeth Group, eastern

Ireland. Early Caradoc (Romano and Owen 1993). {*A. truncatocaudata* ? of Romano and Owen 1993}. Material: two cephala, one very poorly preserved and unsuitable for morphometrics.

Co. Tyrone

7. KILLEY. Specimens from Little River, Pomeroy district, Co. Tyrone, Northern Ireland [loc. 49]. Lower part of Killey Bridge Fm. (Cautleyan, lower *anceps* Zone, Tunnicliff 1980). {*Achatella truncatocaudata* (Portlock, 1843}. Material: 14 cephala and cranidia, 53 pygidia and five hypostomes.

Oslo Region

8. FURUBERG. Specimens from Furuberg [loc. 51], Furuberget Formation, Mjøsa district, Norway (*clingani* Zone, Owen *et al.* 1990). {*Achatella* sp.}. Material: three cephala.
9. MJØSA. From Furuberg [loc. 51] and Bergevika [loc. 52], Mjøsa Formation, Mjøsa district, Norway (upper Caradoc, upper *clingani* - lower *linearis* Zones, Owen *et al.* 1990). {*Achatella* sp.}. Material: two cephala and a pygidium.
10. LANGØYENE. Single specimen from Lilleklostret, Skien-Langesund district [loc. 66]. Langøyene Formation (Hirnantian, Owen *et al.* 1990). {*Achatella* sp.}.

Siljan, Sweden

11. ?BODA. A single specimen described and figured by Warburg (1925). She noted that although it probably comes from the Ashgill Upper Leptaena Limestone (=Boda Limestone) at Osmundsberget, there is a possibility it is from the Caradoc Lower Leptaena Limestone (=Kullsberg Limestone) at Sinksjön. Jaanusson and Ramsköld (1993) considered it to belong to the former horizon, and it is treated as such herein. {*Pterygometopus schmidti* Warburg, 1925}.

Estonia, Northern Belt

12. KUKRUSE. Specimens from limestones of the Kukruse Stage C2 (lower Caradoc, *gracilis* Zone, Fortey *et al.*, in prep.), Estonia. Exact localities unknown. {*Achatella kuckersianus* (Schmidt, 1881)}. Material: four cephala and three pygidia.

Eastern North America

13. TRENTON. Specimens from the Trenton Limestone, Trenton Falls, New York [loc. 93]. Trenton Group, Shermanian-Edenian (Ross *et al.* 1982). {*A. achates* (Billings, 1860)}. Material: 3 cephala and cranidia, 1 pygidium.
14. UTICA. Single specimen from the Utica Shale of Cincinnati, Ohio. Exact locality unknown. Upper Shermanian (Ross *et al.* 1982). {*A. achates* (Billings, 1860)}.
15. LORRAINE. Specimens from the "Lorraine Group" at Columbia, Tennessee (Martinsburg Shale of current usage). Exact locality unknown. Upper Shermanian (Ross *et al.* 1982). {*A. achates* (Billings, 1860)}. Material: 2

cephala, 3 pygidia.

16. PROSSER. Two fragmentary cephala from the Prosser Fm. at Duck Creek Quarry, Wisconsin [loc. 98]. Shermanian (Ross *et al.* 1982). {*Pterygometopus schmidti* Warburg, 1925}.
17. CINC. Specimens from the Maysvillian of Cincinnati, Ohio. Exact localities unknown (?Fairmount). Maysvillian (Ross *et al.* 1982). {*Achatella carleyi* (Meek, 1873)}. Material: 8 cephala and cranidia, 8 pygidia.
18. VERULAM. Specimens from Canada Cement Co. [loc. 96] and McCarthy Bros. [loc. 94] Quarries, southern Ontario. Verulam Fm., Shermanian (Barnes *et al.* 1981). {*A. achates* (Billings, 1860)}. Material: 5 cephala and cranidia.
19. HULL. Specimens from "Hull, Quebec", exact locality unknown. Trenton Group, Shermanian-Edenian (Barnes *et al.* 1981). {*A. achates* (Billings, 1860)}. Material: 3 cephala and cranidia.
20. COBOURG. Single specimen from the Cobourg Fm., Shermanian-Edenian, Ottawa, Ontario. Exact locality unknown. {**Holotype** of *A. achates* (Billings, 1860)}. Coded from illustration in Ludvigsen and Chatterton (1982).

Figure 5. 2 summarises the stratigraphical and geographical distribution of the samples.

Table 5. 1 summarises the lithologies and postulated depositional environments of the strata from which the stratigraphical samples were obtained. Note that all units in which *Achatella* is present and in which the fauna is considered to be autochthonous represent relatively shallow marine environments: shallow water clastics, mid-shelf clastics and carbonates, shelf-edge carbonate mounds. *Achatella* tends to be associated with trilobite assemblages assignable to the shallow-water illaenid-cheirurid and slightly deeper water nileid associations of Fortey (1975).

5. 3. Phylogenetic Analysis.

In order to construct a phylogenetic framework for subsequent work on *Achatella*, and also to highlight patterns of morphological character states and character combinations in the genus, phylogenetic analysis has been undertaken. A two stage process was used for this. In the first instance, in keeping with the "taxonomy-independent" nature of the present work, the 20 stratigraphical samples were used as the operational taxonomic units (OTU's), and the resulting "sample-based" cladogram used to identify a set of species. These species then became the OTU's for a second cladistic analysis.

Choice of ancestral taxon. Ludvigsen and Chatterton (1982) considered *Pterygometopus* Schmidt, 1881, from the Arenig of Baltica, to be ancestral to all other pterygometopids. For the present analysis, Whittington's (1950) description and illustrations of the genotype specimen of *P. sclerops* (an enrolled complete individual;

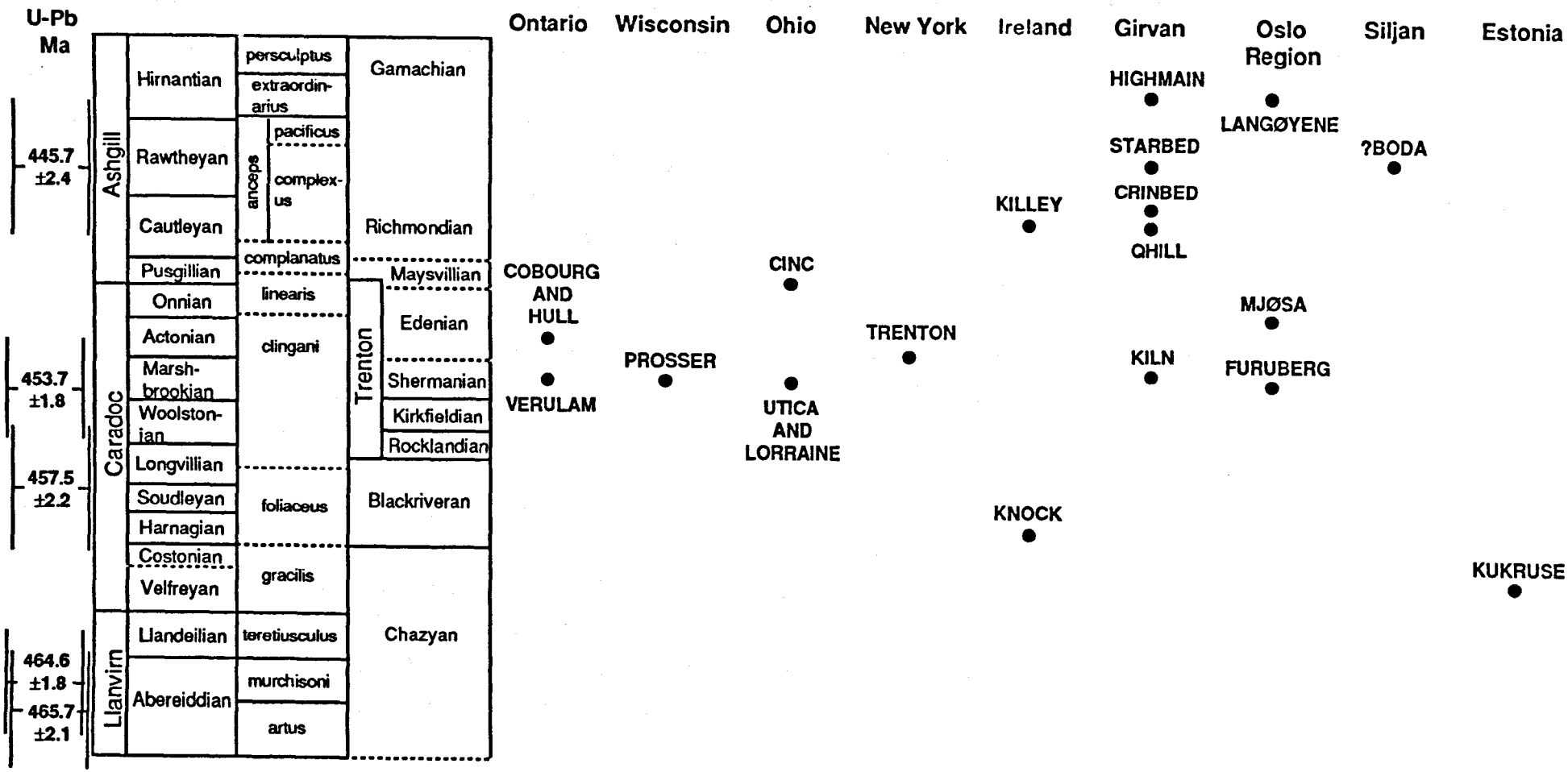

Figure 5. 2. Summary of the stratigraphical and geographical locations of the samples of *Achatella* used. Stratigraphy based on Fortey *et al.* (in press) and Ross *et al.* (1982). Stratigraphical locations of samples based on references in the text. U-Pb dates are those of Tucker *et al.* (1990).

Table 5. 1. Summary of the lithologies, faunas and postulated depositional environments of the rocks associated with the stratigraphical samples of *Achatella*. NB: "slope" refers to basin slope (not continental slope) and probably represents maximum water depth of 200m or less.

Stratigraphical Sample	Unit and Age	Lithology	Fauna	Environment of Deposition	Reference
KILN	Kiln Mudstone, Craighead Fm., Craighead Inlier, Girvan. (upper Caradoc).	Tongue of blue-grey calc. mudsts. and siltstones within a complex of clastic and algal limestones.	Rich and abundant allochthonous shelly fauna. Trilobites of Fortey's (1975) illaenid-cheirurid association.	Brief transgression within shallow water carbonate succession.	Tripp (1954, 1980b); Williams (1962).
QHILL	Quarrel Hill Fm., Craighead Inlier, Girvan (upper Cautleyan).	Bedded green msts. with subsidiary sst. beds forming a series of mudflow sheets.	Abundant allochthonous shelly fauna: low diversity trilobite assemblage.	Mudflow sheets emplaced with force, carrying entrained debris. Middle shelf environment.	Harper (1982).
CRINBED	Quarrel Hill Crinoid Bed, upper Quarrel Hill Fm., Craighead Inlier, Girvan (upper Cautleyan).	Laterally persistent 15-20cm thick coarse green sst. with shelly laminae and conglomeratic base.	Allochthonous assemblage of brachiopods, comminuted debris, crinoid ossicles.	Regressive event within the Quarrel Hill Fm.	Harper (1982).
STARBED	Lady Burn Starfish Beds, South Threave Fm. (upper), Craighead Inlier, Girvan (upper Rawtheyan).	Fossiliferous, calcareous green-grey sandstones.	Abundant and diverse allochthonous shelly fauna: trilobites represent a mixture of shelf and upper slope assemblages.	Sediment and organisms of relatively shallow provenance, transported rapidly downslope by turbulence.	Ingham (1978); Harper (1982).

Table 5. 1. Continued.

Stratigraphical Sample	Unit and Age	Lithology	Fauna	Environment of Deposition	Reference
HIGHMAIN	High Mains Fm., Craighead Inlier, Girvan. (Hirnantian).	Fine-to-medium grained grey massively bedded sandstones.	Allochthonous fauna: *Hirnantia* fauna brachiopods in upper part, opportunistic brachiopods in lower part; rare relict Rawtheyan trilobites.	Regressive facies deposited as channel fills on outer shelf and upper slope.	Harper (1981, 1988); Owen (1986).
KNOCK	Knockerk House Sst. Mbr., Knockerk Fm., eastern Ireland. (lower Caradoc).	Massive green-grey volcanic sandstones with tuffaceous shales.	Rich ?autochthonous fauna of brachiopods and trilobites, trinucleids very abundant.	Relatively deep water, outer shelf.	Romano (1980); Romano & Owen (1993).
KILLEY	Killey Bridge Fm., Pomeroy Inlier, Co. Tyrone. (Cautleyan).	Grey flaggy micaceous mudsts. and siltstones with calc. horizons and rare sst. lenses.	Rich autochthonous shelly fauna. Trilobite assoc. dominated by *Tretaspis* and *Cryptolithus*.	Lower slope deposition.	Mitchell (1977).
FURUBERG	Upper Furuberget Fm., Oslo Region (upper Caradoc).	Shales with interbedded lsts. and calc. siltstones.	Diverse allochthonous shelly fauna of trilobites and brachiopods in the lst. bands.	Relatively deep water, outer shelf environment.	Owen *et al.* (1990).

Table 5. 1. Continued.

Stratigraphical Sample	Unit and Age	Lithology	Fauna	Environment of Deposition	Reference
MJØSA	Mjøsa Fm., Oslo Region (upper Caradoc).	Varied suite of massive bioclastic lsts. with calc. ssts. and mudsts; *Solenopora* bioherms locally developed.	Diverse autochthonous shelly and graptolitic fauna. *Solenopora* bioherms with associated corals.	Shallow marine deposition on an extensive carbonate platform.	Owen *et al.* (1990).
LANGØYENE	Langøyene Fm., Oslo Region (Hirnantian).	Suite of coarse sst. facies, many as channel fills.	Moderately diverse allochthonous assemblage dominated by brachiopods of *Hirnantia* fauna; relict Rawtheyan trilobites.	Range of environments from intertidal channels to high energy inner shelf. Wave and storm dominated shallow sea.	Owen *et al.* (1990).
?BODA	Boda Lst., Siljan district, Sweden (Ashgill).	Carbonate mounds hosted by stromatactis-bearing argillaceous lsts.	Rich and diverse autochthonous shelly fauna in mound cores and on mound flanks. Trilobites of Fortey's (1975) illaenid-cheirurid association.	Bioherms in a shallow carbonate sea.	Jaanusson (1982).
KUKRUSE	Kukruse Stage C_{II}, Estonia (lower Caradoc, *gracilis* Zone).	Yellow or buff argillaceous lsts. and kukersite beds.	Abundant and diverse autochthonous shelly fauna: trilobites suggesting Fortey's (1975) nileid association.	Shallow water open shelf depositional environment.	Männil (1990).

Table 5. 1. Continued.

Stratigraphical Sample	Unit and Age	Lithology	Fauna	Environment of Deposition	Reference
TRENTON	Trenton Lst., Trenton Gp., Trenton Falls, N.Y. (Shermanian-Edenian).	Dark grey fossiliferous silty bioclastic limestones.	Low diversity autochthonous shelly fauna: trilobites of Fortey's (1975) illaenid-cheirurid association.	Relatively deep water offshore shelf environment.	Titus & Cameron (1976); Shaw & Fortey (1977).
UTICA	"Utica Shale", Cincinnati, Ohio (Upper Shermanian).	Brown to dark grey laminated msts. and shales with dark argillaceous lst. and siltstone interbeds.	Moderately abundant graptolites, sparse benthonic fauna: *Triarthrus* and *Cryptolithus* fragments.	Lower slope depositional environment.	Shaw & Fortey (1977); Mitchell & Bergström (1991).
LORRAINE	Martinsburg Shale, Tennessee. (Upper Shermanian).	Calc. shales with interbedded fossiliferous lsts. and siltstones.	Allochthonous assemblage of shelly fragments.	Lower slope deposition, mixed sequence of turbidites and pelagic shales.	Twenhofel (1954); Milici & de Witt (1988).
PROSSER	Prosser Fm., Duck Creek, Wisconsin. (Shermanian).	Pale grey bioclastic limestones.	Abundant and diverse autochthonous assemblage of shelly fossils.	Relatively deep water offshore shelf environment.	Ross *et al.* (1982); Bunker *et al.* (1988).
CINC	Maysvillian (Fairmount), Cincinnati Region. (Maysvillian).	Grey or green-grey silty shales with laterally discontinuous biomicrosparitic lst bed.	Allochthonous assemblages of shelly fragments.	Lower slope.	Twenhofel (1954);

Table 5. 1. Continued.

Stratigraphical Sample	Unit and Age	Lithology	Fauna	Environment of Deposition	Reference
VERULAM	Verulam Fm., Trenton Gp., South Ontario. (Shermanian).	Thinly bedded calcarenites and calcareous shales.	Rich and diverse autochthonous shelly fauna. Trilobites of Fortey's (1975) illaenid-cheirurid association.	Middle shelf depositional environment, relatively deep water.	Titus and Cameron (1976); Barnes *et al.* (1981).
HULL	Trenton Gp. (?Verulam Fm.), Hull, Québec. (Shermanian-Edenian).	As above.	As above.	As above.	As above.
COBOURG	Cobourg Fm., Ottawa, Ontario. (Shermanian-Edenian).	Dark grey fossiliferous silty bioclastic limestones.	Low diversity autochthonous shelly fauna: trilobites of Fortey's (1975) illaenid-cheirurid association.	Relatively deep water offshore shelf environment.	As above.

Whittington 1950 pp 538-540; pls. 68 figs 17-20 and 69 figs. 1-4) from the Expansus Limestone (Arenig) of Västanå, Östergötland, Sweden, were used to define ancestral character states, *P. sclerops* being the only well-described species of that genus.

5. 3. 1. Characters Used.

The original data matrix for this study was to have included morphological characters from the cephalon, thorax and pygidium of the trilobite. However, thoraxes and pygidia were not available for several of the samples, either from collecting in the field or in museum collections. This resulted in a large amount of missing data in the matrix. Since the data already appear to be very "noisy" even when characters from the cephalon alone are used (see below), it was decided to exclude characters based on the thorax and pygidium from the analysis. Thus, the analysis presented here relies only on characters on the cephalon of *Achatella*. It is worth noting that all pygidia of the genus are very similar, the small differences visible between pygidia being of only minor importance in taxonomy. All known thoraxes of *Achatella* are identical.

Since the analysis is of members of a single genus, all of which are extremely similar in appearance, there was virtually no problem in recognition of homologous characters. The only character for which there is a slight note of caution in this respect is character 11 which describes the anteriormost extremity of the palpebral lobe (see list of characters below).

All characters used are on the exterior of the exoskeleton. From close comparison between parts and counterparts of specimens (where both were present), it was ascertained that some characters could be coded successfully from the internal mould if the counterpart was unavailable (as it was for several samples). This was done where necessary and appropriate. In cases where it was not felt that the internal mould could be used the character was coded as "missing".

A great deal of morphometric data has been obtained on *Achatella*. However, the high degree of morphometric similarity between the samples (see Section 5.4) means that few measurements show well defined discontinuities between samples, which could be used to unequivocally define separate character states for cladistic analysis. For this reason, although several of the characters listed below could be defined in numerical terms (for example, as a measurement expressed as a percentage of the total cephalic length), only three have quantitative definitions explicitly attached. The others are expressed qualitatively.

All characters are defined as undirected and unordered, and are polarised 0 to 1 (to 2 where applicable) where 0 is the ancestral state expressed by *Pterygometopus*. The

simplicity of the coding (0 or 1 in almost all cases) is a result of the similarity between the various samples.

List of characters.

Figure 5. 3 shows the location on the cephalon of the characters used in phylogenetic analysis of *Achatella.*

1. Narrowest point on the glabella.

Point on the glabella at which the width (tr.), measured from the deepest point in the left axial furrow to the corresponding point in the right, is a minimum. This feature does not vary among specimens of *Achatella*, but can be used to separate the genus from the supposed ancestor.

Ancestor comparison. The glabella of *P. sclerops* is narrowest across L2.

States. 0: glabella narrowest across L2; 1: glabella narrowest across L1.

2. Relative lengths of glabellar lobes.

The relative lengths (exsag.) of the lateral glabellar lobes can again be used to separate *Achatella* (in which L3 is much longer than L2, which itself is of equal length to, or slightly shorter than, L1) from *Pterygometopus.*

Ancestor comparison. L3, L2 and L1 are all of approximately equal (exsag.) length in *P. sclerops.*

States. 0: L1, L2 and L3 of approximately equal (exsag.) length; 1: L3 much longer than L1, which is slightly longer than, or equal to, L2.

3. Inflation of frontal glabellar lobe.

When the cranidium is studied in lateral view, the frontal lobe is seen to be either confluent with the central body of the glabella, or inflated to a level above it. This fact is here used to define two character states. No attempt is made to separate degrees of inflation, e.g. "moderately inflated" from "highly inflated".

Ancestor comparison. The frontal lobe of *P. sclerops* is not inflated.

States. 0: not inflated; 1: inflated.

4. Anterior embayment on frontal glabellar lobe.

Some samples of *Achatella* (as well as *P. sclerops*) possess a slight antero-medial indentation on the frontal lobe, here termed the "anterior embayment".

Ancestor comparison. P. sclerops possesses an embayment.

States. 0: possessing an embayment; 1: no embayment present.

5. Independent convexity of central area of glabella.

In some samples of *Achatella*, the lateral glabellar lobes are confluent with the central

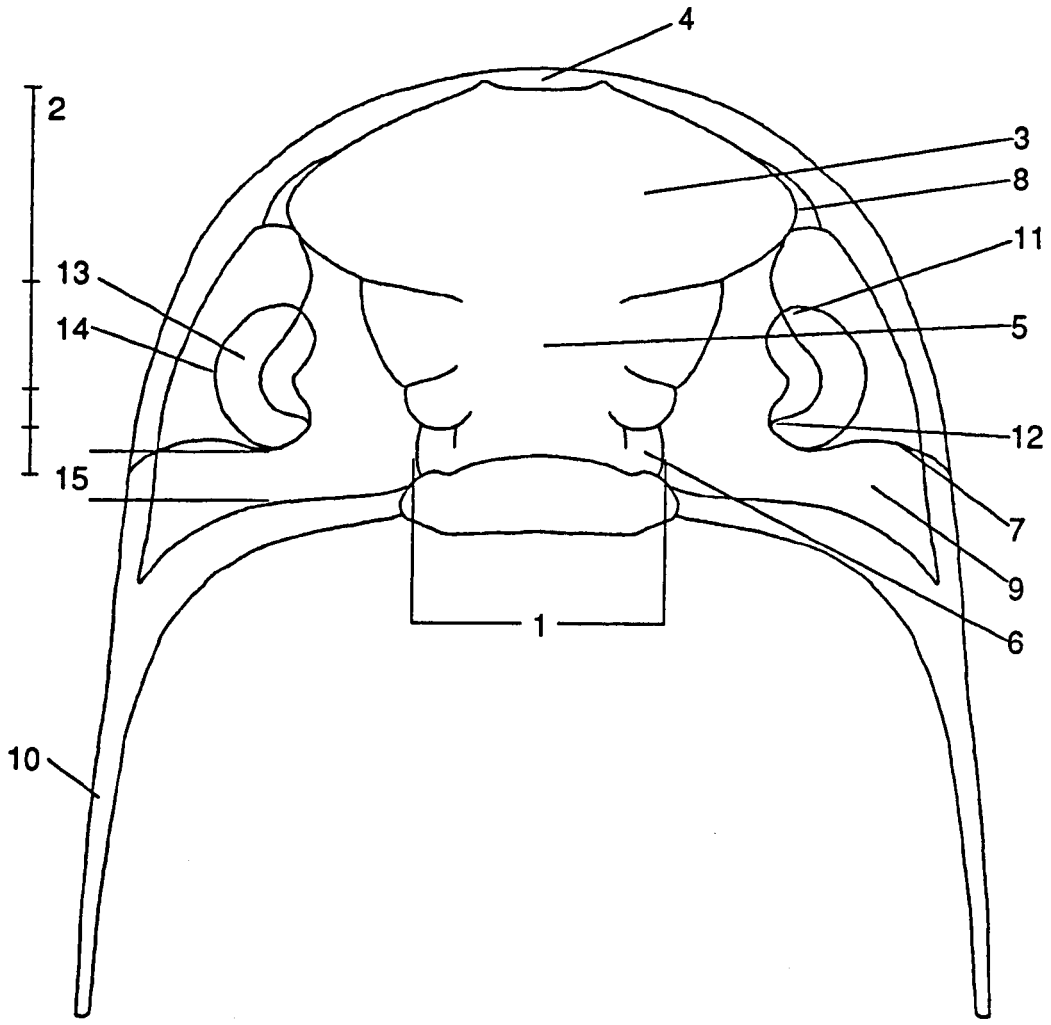

Figure 5. 3. Location on the cephalon of characters used in the cladistic analysis of *Achatella*. See text for explanation of characters.

area of the glabella. In others, however, the central area is inflated to a level slightly higher than the lateral parts, so that a distinct break in slope delimits the lateral lobes from the central area.

Ancestor comparison. In *P. sclerops*, the lateral lobes are confluent with the central area.

States. 0: central area not at a higher level than the lateral lobes; 1: central area inflated to a level above the laterals.

6. Distal node on L1.

In some specimens, the distal portion of L1 occurs as a separate node, delimited from the proximal part of the lobe by a posteriorly-directed bifurcation from the S1 furrow.

Ancestor comparison. There is a node on L1 in *P. sclerops.*

States. 0: Node present; 1: No node present on L1.

7. Furrow for posterior branch of facial suture.

Some specimens possess a furrow confining the postero-lateral branch of the facial suture.

Ancestor comparison. P. sclerops has such a furrow.

States. 0: furrow present; 1: no furrow present.

8. Nature of the preglabellar furrow.

In most samples of *Achatella*, the preglabellar furrow is well defined mesially, but dies out laterally. However, in specimens from the Kukruse Stage of Estonia, the furrow is seen to continue around the lateral extremity of the frontal glabellar lobe, inside the path of the facial suture, and join the dorsal furrow posteriorly (Jaanusson and Ramsköld 1993).

Ancestor comparison. The preglabellar furrow is present both anteriorly and laterally in *P. sclerops.*

States. 0: furrow present anteriorly and laterally; 1: furrow present anteriorly only.

9. Sculpture on fixigena.

There is variation in the nature of sculpture on the fixigenae. Specimens belonging to some samples display a sculpture of scattered, small tubercles, whereas others have fine pits.

Ancestor comparison. There is coarse, densely-packed granulation on the fixigenae of *P. sclerops.*

States. 0: scattered small tubercles; 1: fine pits.

10. Genal Spines.

There is variation in the nature of the genal angle among the samples. Whereas most

specimens of *Achatella* possess long slender genal spines, two of the samples contain specimens with rather short spines, and there are two anomalous samples whose members lack genal spines altogether and have rounded genal angles instead. This character is here coded according to total length of cephalon (measured from the anteriormost point to the posteriormost extremity of the genal spine, or the genal angle where there is no spine) expressed as a percentage of the preoccipital glabellar length. Figure 5. 4 shows the values of this percentage for the stratigraphical samples for which it is measurable. It can be seen that the character can be coded as possessing three states: less than 150% (the two anomalous stratigraphical samples whose specimens possess no genal spines mentioned above); between 150% and 200% (the two samples whose members possess short genal spines); and greater than 200% (all of the other samples). Each of the percentage ranges used in coding this character therefore approximates closely with the visual impression of "no spines", "short spines" or "long spines" which one obtains when studying the specimens.

Ancestor comparison. P. sclerops possesses rounded genal angles with no spines (*i.e.* the total cephalic length is less than 150% of the preoccipital glabellar length).

States. 0: < 150% (*i.e.* no genal spines present); 1: between 150% and 200% (*i.e.* short genal spines); 2: > 200% (*i.e.* long genal spines).

11. Anteriormost point of palpebral lobe.

The anteriormost and posteriormost extremities of the palpebral lobes, seen in dorsal view, are used to define the location of the front and back of the eye. In most samples of *Achatella*, the anterior point is adjacent to the distal end of S3. In some, however, it is located slightly to the posterior of the distal end of S3.

Ancestor comparison. P. sclerops has a wing-like anterior extension to the eye, extending forwards to a point opposite the distal end of S3 (Whittington 1950: plate 69 fig. 3, and text-fig. 3). Here, this is assumed to be homologous with the anteriormost extremity of the palpebral lobe in *Achatella.*

States. 0: anterior extremity of palpebral lobe located opposite distal extremity of S3; 1: anterior extremity of palpebral lobe located a little behind distal extremity of S3.

12. Posteriormost point of palpebral lobe.

In most specimens of *Achatella*, the posteriormost extremity of the palpebral lobe is located opposite L1. In a few, however, it is significantly further forward, adjacent to the anterior part of L2, or even as far forward as S2.

Ancestral comparison. This point in *P. sclerops* is opposite L1.

States. 0: posterior extremity of palpebral lobe located opposite L1; 1: posterior extremity of palpebral lobe located opposite anterior part of L2.

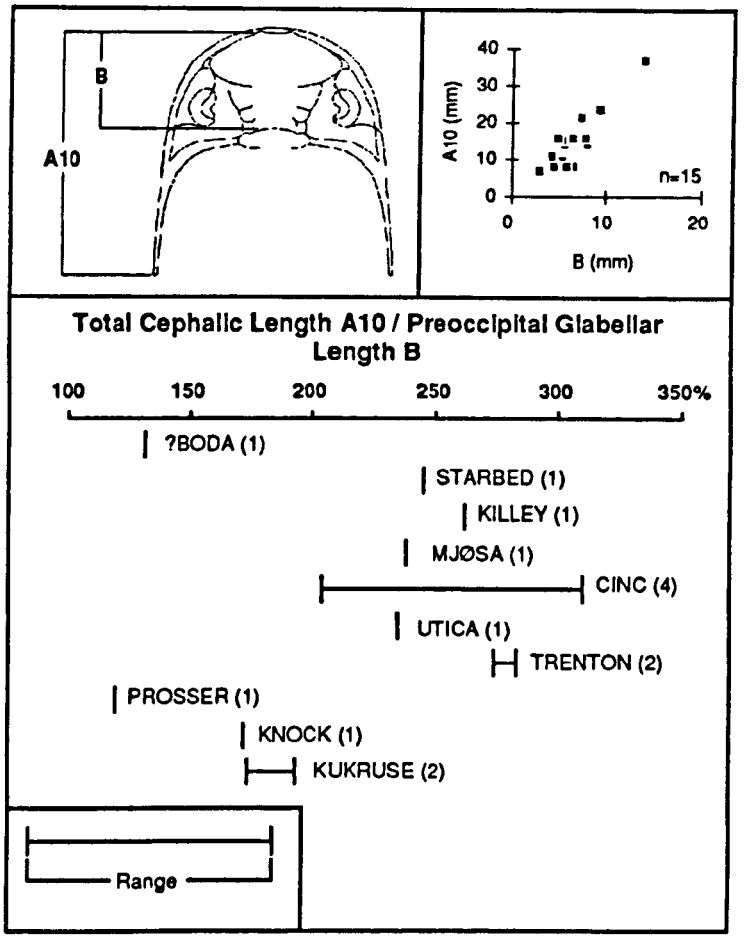

Figure 5. 4. Variation in the ratio total length of cephalon (A10) / preoccipital glabellar length (B), expressed as a percentage, for stratigraphical samples of *Achatella*. Total range and number of measurable specimens shown for each sample. Inset shows a bivariate scatter plot of A10 against B.

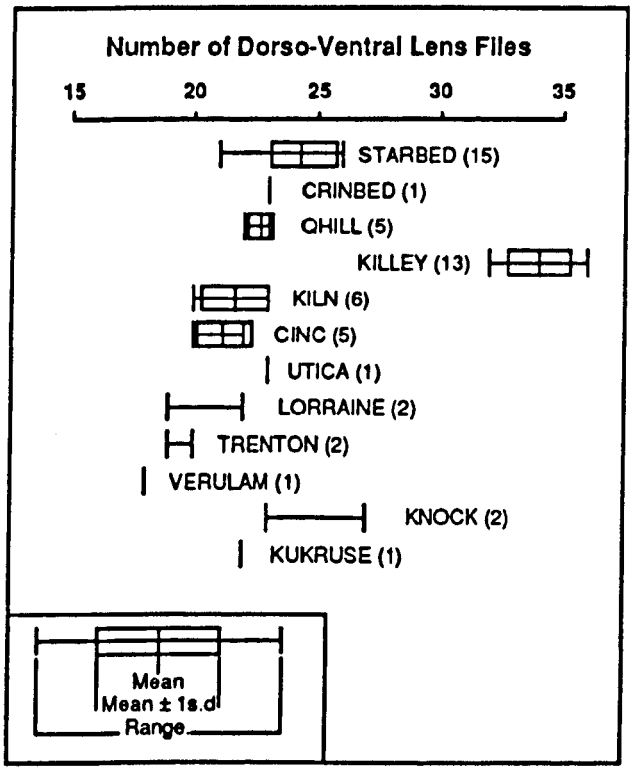

Figure 5. 5. Variation in the number of dorso-ventral lens files in the visual surface of stratigraphical samples of *Achatella*. Total range of values and number of countable specimens shown for each sample, mean value and one standard deviation to either side of the mean shown for samples containing five or more countable specimens.

13. Number of lens files.

The number of dorso-ventral lens files in the visual surface of *Achatella* can range from 18 to 36 (Figure 5. 5). There is a great deal of overlap between most of the samples, in the range 18 - 27. However the sample KILLEY is very different, having a range of 32 - 36, not overlapping at all with the other samples. This fact forms the basis for the coding of this character.

Ancestral comparison. Whittington (1950) describes *P. sclerops* as having from 23 to 27 files.

States. 0: 18 - 27 files; 1: 32 - 36 files.

14. Presence of a subocular furrow.

Jaanusson and Ramsköld (1993) define the "subocular furrow" as a narrow, almost horizontal platform bearing a distinct furrow and delineating the base of the visual surface. They note the lack of this feature in *Achatella* from the Kukruse Stage, Estonia, while it is present in all other pterygometopines.

Ancestor comparison. P. sclerops possesses a subocular furrow.

States. 0: subocular furrow present; 1: no subocular furrow.

15. Length of postocular area.

There is variation between samples whose member specimens possess a relatively short postocular area, and samples whose members possess a relatively long postocular area. This character is coded according to the mean postocular length of specimens in the sample, measured from the posteriormost extremity of the palpebral lobe to the deepest point of the posterior border furrow, expressed as a percentage of the preoccipital glabellar length (Figure 5. 6). Placing a discontinuity at 25% (*i.e.* separating samples whose mean value is less than 25% from samples whose mean value is greater than 25%) separates samples whose specimens give the visual impression of having a long postocular area from those appearing to have short postocular areas. However, it can be seen from Figure 5. 6 that this discontinuity is placed somewhat arbitrarily, the mean values for the samples TRENTON, VERULAM and HULL only falling slightly below 25%, the mean value for MJØSA only falling slightly above 25%. The total ranges of several samples cross the 25% discontinuity.

Ancestor comparison. The postocular area in *P. sclerops* is long (a value of 26% for the holotype specimen).

States. 0: mean value > 25% (*i.e.* possessing a long postocular area); 1: mean value < 25% (*i.e.* possessing a short postocular area).

5. 3. 2. Results.

The input data matrix for the cladistic analysis is shown in Table 5. 2. The analysis was performed using the PAUP computer program, version 3.0i, running on an Apple

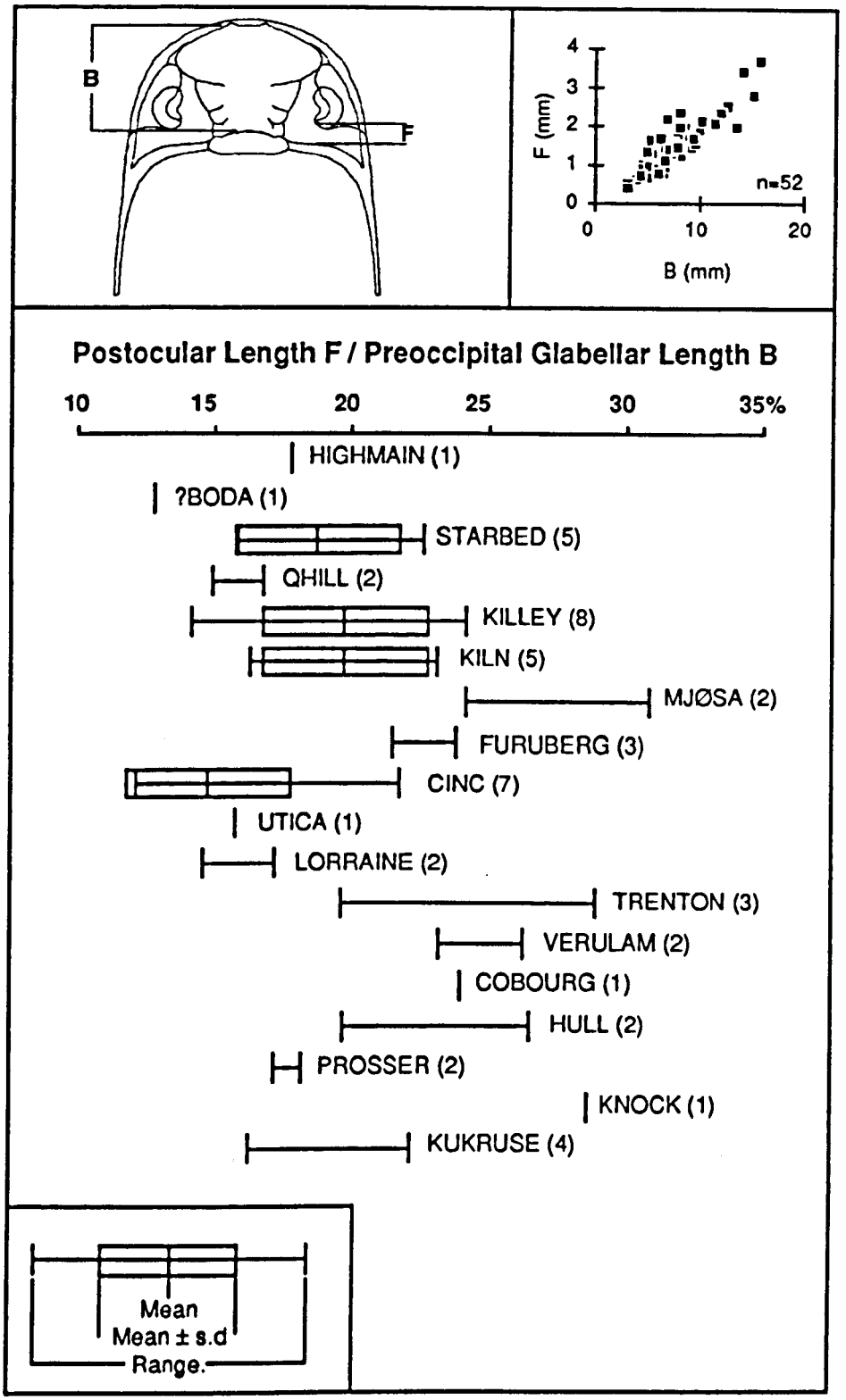

Figure 5. 6. Variation in the ratio postocular length (F) / preoccipital glabellar length (B), expressed as a percentage, for stratigraphical samples of *Achatella*. Total range of values and number of measurable specimens shown for each sample. Mean and one standard deviation to either side of the mean shown for samples containing five or more measurable specimens. Inset shows a bivariate scatter plot of F against B.

Table 5. 2. Character states for cladistic analysis of *Achatella* stratigraphical samples. See Section 5. 2 for description of the samples. *P. sclerops* (the supposed ancestor) is placed at the top of the table. Samples of *Achatella* subsequently entered in random order.

Sample	1	2	3	4	5	6	7	8	9	10	11	12	13	14	15
PSCLEROPS	0	0	0	0	0	0	0	0	0	0	0	0	0	0	0
HIGHMAIN	1	1	1	1	1	0	1	?	?	?	?	?	?	?	?
PROSSER	1	1	0	0	0	0	1	1	?	0	1	0	0	0	1
KNOCK	1	1	0	1	1	0	0	1	1	1	0	1	0	0	0
QHILL	1	1	1	1	1	0	1	1	0	?	0	0	0	0	1
CINC	1	1	0	0	0	0	1	1	?	2	1	0	0	0	1
STARBED	1	1	1	1	1	0	1	1	0	2	0	0	0	0	1
COBOURG	1	1	0	0	0	0	1	1	?	2	1	1	?	0	1
CRINBED	1	1	1	0	1	1	?	1	?	?	?	?	0	0	?
KILLEY	1	1	0	0	1	1	1	1	0	2	0	0	1	0	1
TRENTON	1	1	0	0	0	0	1	1	1	2	1	1	0	0	1
UTICA	1	1	0	0	0	0	1	1	?	2	1	0	0	0	1
VERULAM	1	1	0	0	0	0	1	1	1	2	1	1	0	0	1
LORRAINE	1	1	0	0	0	0	1	1	0	?	1	0	0	0	1
HULL	1	1	0	0	0	0	1	1	1	?	1	0	?	0	1
MJØSA	1	1	0	0	0	0	0	1	1	2	0	0	?	?	0
KILN	1	1	0	0	0	0	0	1	0	2	1	0	0	0	1
KUKRUSE	1	1	0	1	0	0	0	0	1	1	0	0	0	1	1
LANGØYENE	1	1	1	1	1	0	?	?	?	?	?	?	?	?	?
?BODA	1	1	0	0	0	0	1	1	1	0	0	0	?	0	1
FURUBERG	1	1	0	0	0	0	0	1	1	?	0	0	?	0	1

Table 5. 3. Character states for cladistic analysis of *Achatella* species. *P. sclerops* (the supposed ancestor) is placed at the top of the table.

Species	1	2	3	4	5	6	7	8	9	10	11	12	13	14	15
P. sclerops	0	0	0	0	0	0	0	0	0	0	0	0	0	0	0
A. achates	1	1	0	0	0	0	1	1	1	2	1	1	0	0	1
A. kuckersiana	1	1	0	1	0	0	0	0	1	1	0	0	0	1	1
A. sp. A	1	1	0	1	1	0	0	1	1	1	0	1	0	0	0
A. sp. B	1	1	0	0	0	0	0	1	1	2	0	0	?	0	1
A. consobrina	1	1	0	0	0	0	0	1	0	2	1	0	0	0	1
A. truncatocaudata	1	1	0	0	1	1	1	1	0	2	0	0	1	0	1
A. cf. *truncatocaudata*	1	1	1	0	1	1	?	1	?	?	?	?	0	0	?
A. retardata	1	1	1	1	1	0	1	1	0	2	0	0	0	0	1
A. schmidti	1	1	0	0	0	0	1	1	1	0	0	0	?	0	1
A. sp. C	1	1	0	0	0	0	1	1	?	0	1	0	0	0	1

Macintosh II. Due to the number of OTU's and the amount of missing data, it was not feasible to use the branch and bound search algorithm (this was attempted once, but aborted when it still had not reached a final solution after three and a half hours). Instead a heuristic search using tree bisection-reconnection branch swapping (TBR) was carried out. The PAUP nexus file is given in Appendix 4.

The analysis found 330 most parsimonious trees of length 26 steps. The strict consensus tree has a consistency index (Rohlf's CI(1), Rohlf 1982) of 0.358, and is shown in Figure 5. 7. The tree is not well resolved, especially at node 4. In part this is undoubtedly due to some of the separate samples actually comprising the same species (allowing for missing data), for example STARBED and QHILL. However, the high number of equally parsimonious trees found, and the low consistency index, suggest other possible reasons. Either the characters used are not sufficient to resolve the phylogeny within the genus, or characters are appearing and disappearing within the genus in a very complex mosaic pattern.

The genus *Achatella* is defined by two synapomorphies at node 1 on Figure 5. 7 (character 1, state 1; character 2, state 1) and subdivides into groupings which occur in approximately correct stratigraphical order. The lower Caradoc samples KNOCK and KUKRUSE are separated from the upper Caradoc samples FURUBERG and MJØSA by a synapomorphy at node 2 (character 10, state 1). Middle Caradoc and later samples are grouped together above node 3 but there is no unequivocal synapomorphy for this group. Rather, they are grouped on the basis of overall similarity in their character states. Similarly, node 4, above which the middle Caradoc and later samples are grouped, node 5 which groups some Trenton Group samples from North America, node 6 which groups Cautleyan and later samples from Laurentia and Baltica, and node 7 which groups upper Cautleyan and later forms from Laurentia and Baltica do not represent unequivocal synapomorphies. To highlight the way in which individual characters trace through the cladogram, the consensus tree was examined using the MacClade program, version 2.1, again running on a Macintosh II. The character tracings are shown in Figure 5. 8. It is immediately apparent from this figure that there is a complex pattern of character states in the *Achatella* plexus. Clearly the characters are changing state in the cladogram in a complex mosaic pattern (particularly so characters 4, 5, 7, 10 and 12, see Figure 5. 8).

It is possible that inclusion of more characters could improve the resolution of the cladogram. However, the characters used do convey virtually all of the variation expressed on the cephalon of *Achatella*. The only extra cephalic information that could be added relates to sculpture (on glabella and librigenae). However, this is indifferently preserved in many specimens so that it would have to be coded as "missing" in many

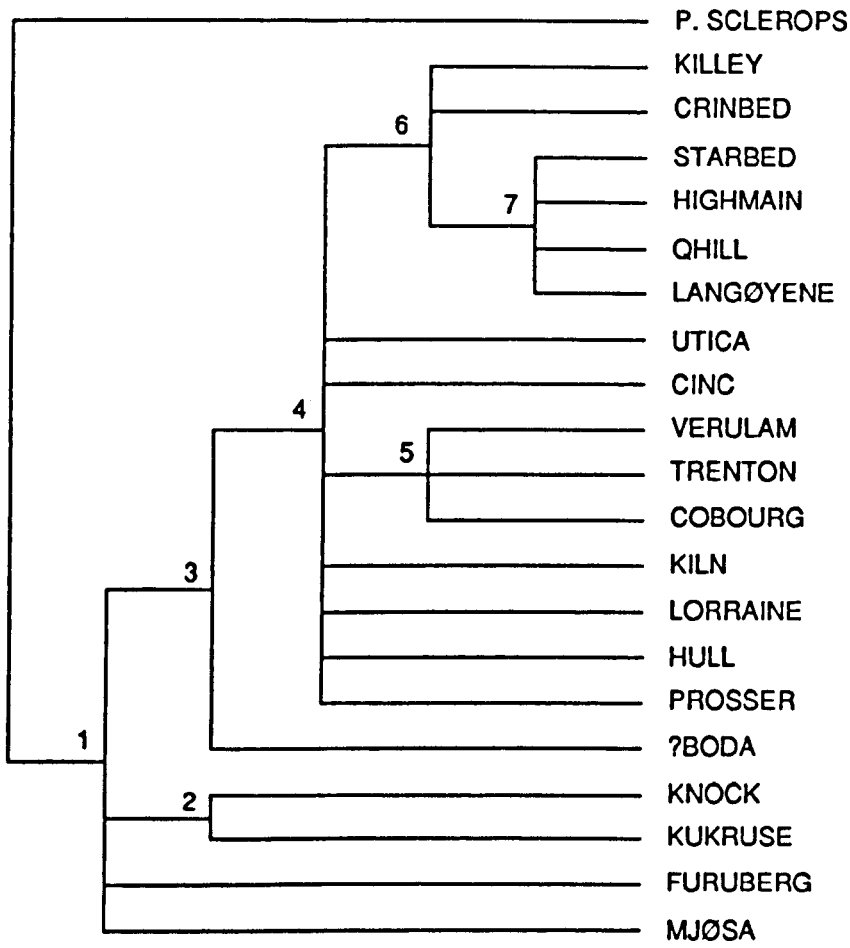

Figure 5. 7. Strict consensus tree for stratigraphical samples of *Achatella*, based on 330 trees. Length 26 steps and consistency index 0.358.

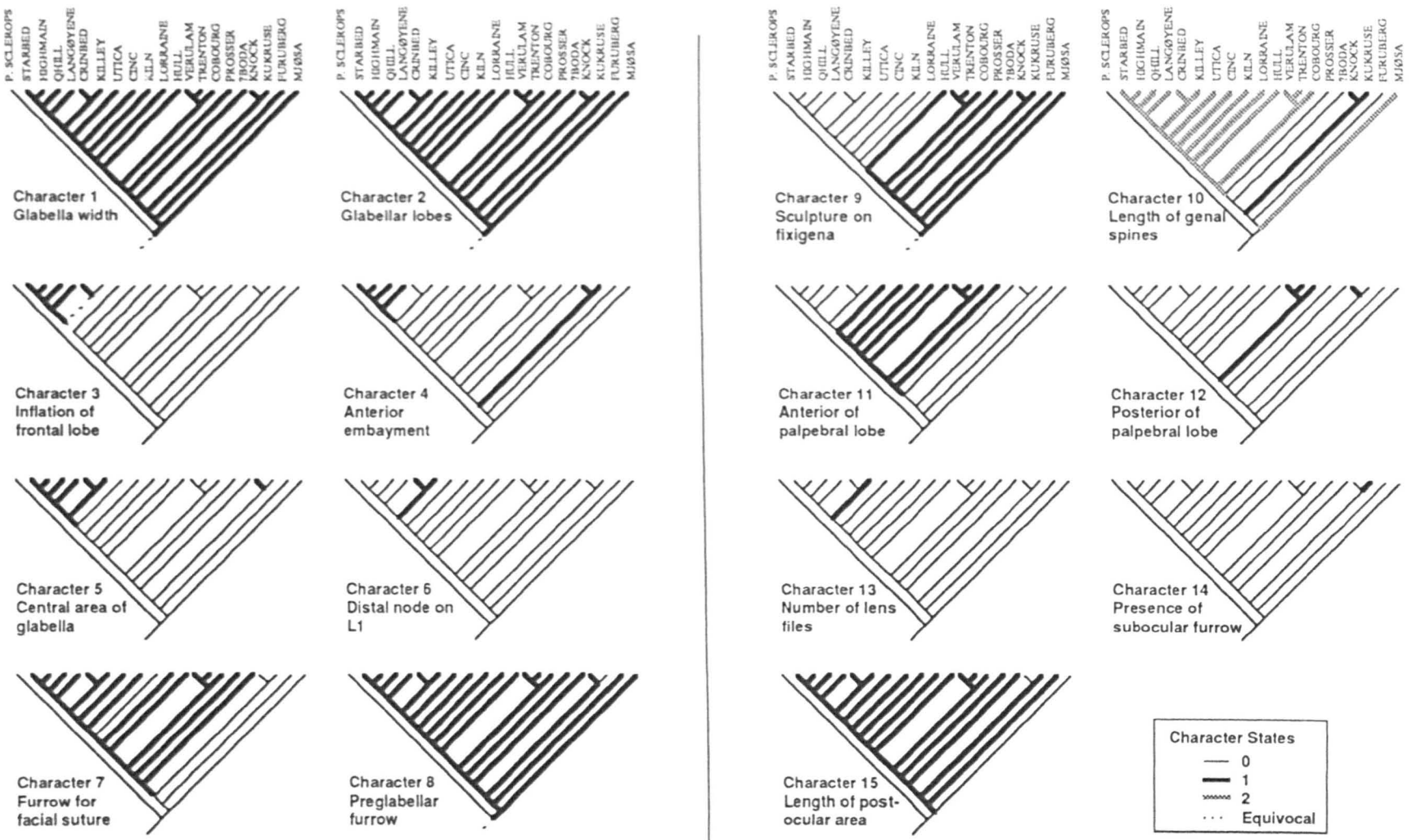

Figure 5. 8. Character state traces through the strict consensus tree for stratigraphical samples of *Achatella*.

cases, and it was found by experimentation that its inclusion only added to the noise in the data set. As has already been mentioned, addition of thoracic and pygidial characters also adds to the noise. It is felt that the choice and coding of the characters is not at fault. However, the amount of missing data in the matrix is a cause for some concern, and this is addressed below (but note from Figure 5. 8 that it is not necessarily the characters with most missing data which show the most complex patterns).

The second step in the phylogenetic analysis was to group the stratigraphical samples together into species and subject these species to cladistic analysis in order to remove some of the missing data in the input matrix and to attempt to obtain a species-based phylogeny. The assignment of stratigraphical samples to species was done on the basis of:

1. The clustering exhibited by the sample-based cladogram (Figure 5. 7);
2. Morphometrics (see next section);
3. Stratigraphical and geographical affinity.

The samples are assigned to species as follows:

1. *P. sclerops* (Dalman, 1827) = The genotype specimen figured by Whittington (1950).
2. *A. achates* (Billings, 1860) = UTICA, VERULAM, TRENTON, COBOURG, LORRAINE, HULL, and CINC.
3. *A. kuckersiana* (Schmidt, 1881) = KUKRUSE.
4. *A.* sp. A = KNOCK.
5. *A.* sp. B = MJØSA and FURUBERG.
6. *A.* sp. C = PROSSER.
7. *A. consobrina* Tripp, 1954 = KILN.
8. *A. truncatocaudata* (Portlock, 1843) = KILLEY.
9. *A.* cf. *truncatocaudata* (Portlock, 1843) = CRINBED
10. *A. retardata* (Reed, 1914) = STARBED, HIGHMAIN, QHILL, and LANGØYENE.
11. *A. schmidti* (Warburg, 1925) = ?BODA.

The input data matrix is shown in Table 5. 3. The characters are the same as those used for the sample-based cladistics above and as before they are treated as undirected and unordered, polarised from 0 to 1 (to 2 where applicable). Because of the smaller number of taxa in this data set, and the smaller quantity of missing data, it was feasible to run a branch and bound search on this matrix. The PAUP nexus file is given in Appendix 4.

The analysis found 74 most parsimonious trees of length 26 steps. The strict consensus

tree has a consistency index (Rohlf's CI(1)) of 0.279, and is shown in Figure 5. 9. The tree is very poorly resolved. Genus *Achatella* is defined by two synapomorphies (character 1, state 1; character 2, state 1) at node 1, and subdivides into a lower Caradoc clade defined by one synapomorphy at node 2 (character 10, state 1) and a Cautleyan - Rawtheyan clade defined above node 3 but which has no defining synapomorphy. Rather, these three taxonomic units are grouped together by virtue of their overall similarity across the full set of characters. As before, the MacClade computer program has been used to trace individual characters through the cladogram and highlight the complex mosaic pattern of character states (Figure 5. 10).

5. 3. 3. Conclusions from Phylogenetic Analysis.

Some conclusions can be drawn from the phylogenetic analysis of *Achatella* :

1. Nine species are defined. In stratigraphical order, they are *A. kuckersiana* (Schmidt, 1881), *A.* sp. A, *A.* sp. B, *A. achates* (Billings, 1860), *A.* sp. C, *A. consobrina* Tripp, 1954, *A. truncatocaudata* (Portlock, 1843), *A. schmidti* (Warburg, 1925) and *A. retardata* (Reed, 1914). A further form, *A.* cf. *truncatocaudata* is recognised for specimens which are closely similar to, but not identical with, one of the named species.
2. Both the stratigraphical sample based cladogram (Figure 5. 7) and the species based cladogram (Figure 5. 9) exhibit complex mosaic evolution, which results in a poorly resolved tree with a relatively low consistency index. Few species or clades are defined by synapomorphies. Rather, most species are defined by shared possession of a set of character states.
3. In spite of the mosaic pattern of most character states in the cladograms, the fact that subclades occur in approximately correct stratigraphical order in the sample based tree (Figures 5. 7 and 5. 8) and also in the species based tree (Figures 5. 9 and 5. 10) suggests that there is some overall temporal trend in the character state data. A set of broad species groups can be recognised: (i) early Caradoc "*kuckersiana* - type" species (*A. kuckersiana* and *A.* sp. A), characterised by short genal spines and the lack of a mesial anterior embayment on the frontal glabellar lobe (Plate 5. 1, figs. 8, 10, 13-14; Plate 5. 2, figs. 1-2); (ii) middle and upper Caradoc "*achates* - type" species (*A. achates*, *A.* sp. C, *A. consobrina*) of Laurentia which have an anterior embayment on the frontal lobe, usually possess long genal spines (although these may be secondarily lost), frontal and lateral glabellar lobes which are confluent with the middle area of the glabella, and have the anteriormost point of the palpebral lobe set slightly behind the distal extremity of S3 (Plate 5. 1, figs. 1-5; Plate 5. 2, figs. 8, 14-16); (iii) the approximately contemporaneous Norwegian form *A.* sp. B which is very similar to the "*achates* - type" with the important distinction of having the anterior of the eye opposite the distal end of S3 (Plate 5. 1, fig. 15; Plate 5. 2, figs. 3-7);

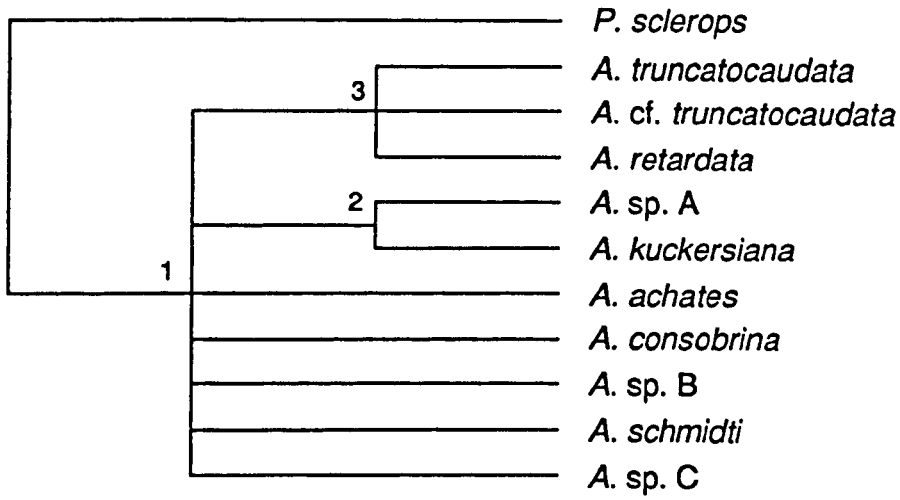

Figure 5. 9. Strict consensus tree for species of *Achatella*, based on 74 trees. Length 26 steps and consistency index 0.279.

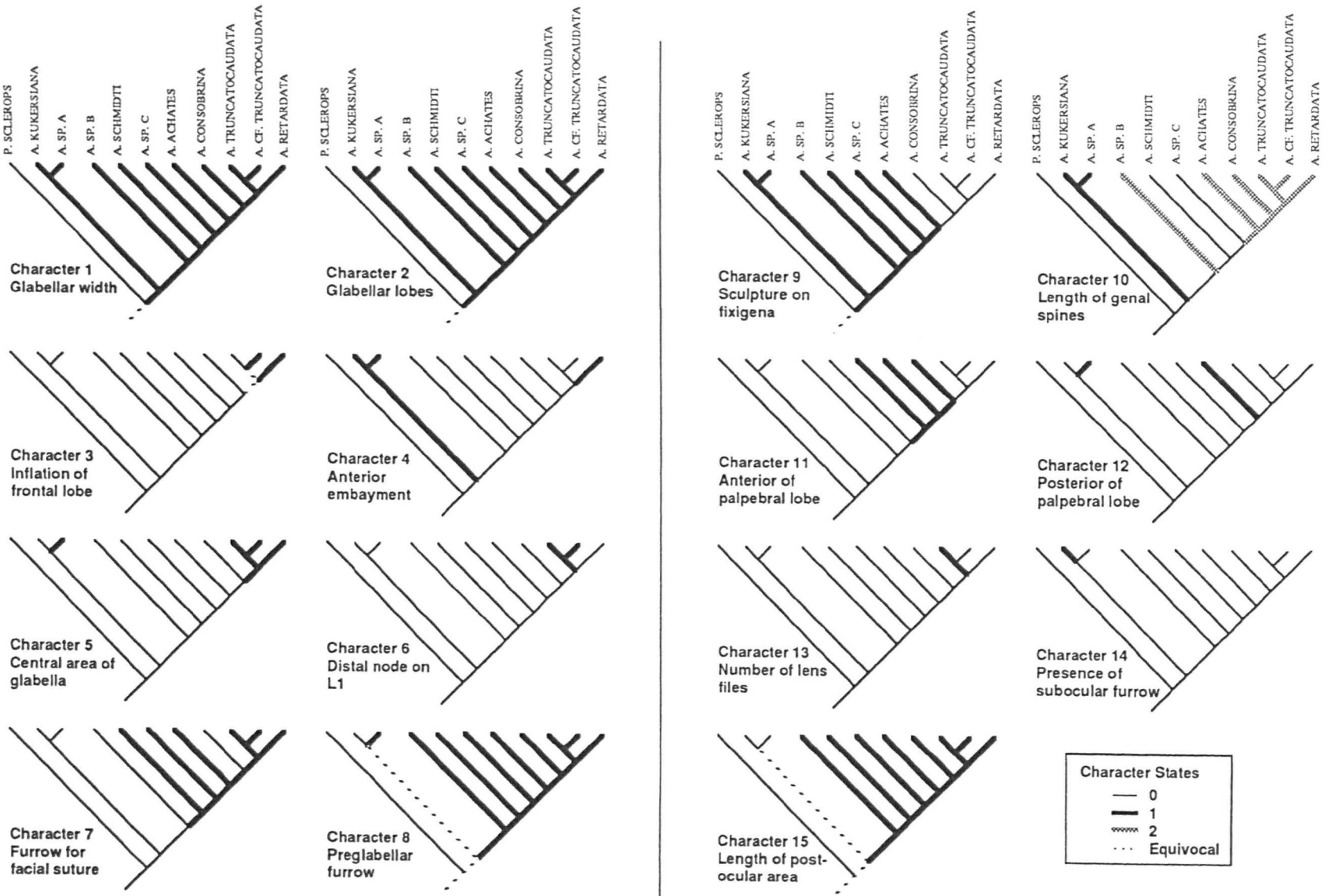

Figure 5. 10 Character state traces through the strict consensus tree for species of *Achatella*.

(iv) the unusual Boda Limestone form *A. schmidti*, similar to *A.* sp. B but with the genal spines secondarily lost (Plate 5. 3, figs. 16-17); (v) the Cautleyan variant *A. truncatocaudata* which in many ways is similar to the "*achates* - type" but has unusually long (exsag.) eyes with their anteriormost extremity located opposite the distal end of S3, an independent convexity to the central area of the glabella, and no distal node on L1 (Plate 5. 3, figs. 1, 3, 5-6); (vi) the Rawtheyan and Hirnantian *A. retardata* characterised by its inflated frontal lobe with no anterior embayment, inflated central area of the glabella, and anteriormost point of the palpebral lobe opposite the distal end of S3 (Plate 5. 3, figs. 11, 14; Plate 5. 4, figs. 1-4, 8, 10). This is the latest *Achatella* species.

These groupings are recognised on the basis of shared possession of sets of character states, rather than individual synapomorphies, and the complex mosaic pattern of individual character states is overlain as "noise" over this underlying broad spatial and temporal pattern.

5. 4. Morphometric Analysis.

Detailed morphometrics have been undertaken on the exoskeleton of *Achatella*. The aims of this analysis were to determine whether the genus really is morphologically stable throughout its duration, and if so, to determine how strictly controlled this shape conservatism is both in terms of temporal variation and interpopulational variation in a single time plane. Characters which do show variation, either temporal or geographical, were to be identified, and assessed as to whether the changes are systematic or non-systematic, reversible or non-reversible, and also whether characters vary as single or correlated complexes of characters. Hence it was hoped to infer causal mechanisms for the observed changes, and the selection pressures involved.

A set of measurements were defined which together describe the shape of the cephalon and pygidium. Since thoraxes and hypostomes are not known in large numbers for most species of the genus, they have not been used for morphometrics. To test the hypothesis of stasis, the measurements have been subjected to principal component analysis (PCA, see Chapter 4). To study variation in individual characters in more detail, uni- and multivariate techniques of data representation have been used.

Altogether, some 200 specimens belonging to the 20 stratigraphical samples already described have been studied, of which 67 cephala and cranidia, 103 pygidia, and 76 individual eyes have been morphometrically analysed.

5. 4. 1. Measurements Used.

All measurements were made on internal moulds of the exoskeleton, and a single

orientation method was used for measuring both cephala and pygidia, as described in chapter 4. The horizontal plane for measurement of cephala of *Achatella* was defined as in Shaw (1957: 194) and Temple (1975: 463) *i.e.*: with the chord of the palpebral surface horizontal. The horizontal plane for pygidia was also defined as in Shaw (1957: 194) and Temple (1975: 463) *i.e.*: with the ventral margin of the pygidial border horizontal. Measurements whose defining end points are in furrows were made to the deepest points in the furrows. Where a bilaterally symmetrical structure was missing on one side of the specimen but present on the other, the original symmetry was used to derive the full transverse measurement as described in Chapter 4.

Figure 5. 11 shows the full set of measurements made on cephala and pygidia of *Achatella*. Measurements are based on those of Shaw (1957), Temple (1975) and Ramsköld (1988). The measurements are formally defined in Table 5. 4.

5. 4. 2. Results.

The morphometric data on *Achatella* are listed in Appendix 5. In order to test the hypothesis of stasis in the genus, PCA was used. Since not all measurements were obtainable for every specimen, the data were organised into three data sets, in order to maximise the amount of information available to PCA. The three data sets are:

1. *Glabella data set.* This consists of all specimens for which the following set of measurements was obtainable:

b5 (left and right)	b!5 (left and right)
b32 (left and right)	b!32 (left and right)
b21 (left and right)	b!21 (left and right)
b10 (left and right)	b!10 (left and right)
k5	k33
k32	k22
k21	k11
k10	k00
B	

These measurements completely describe the structure of the glabella. All of the above measurements were obtainable for 66 specimens.

2. *Cephalon data set.* This set consists of specimens for which a full set of measurements describing the form of the cephalon was obtainable. Due to limitations imposed by missing data, this set is somewhat smaller than that for the glabella, and some stratigraphical samples, for which only incomplete cephala were available, cannot be represented. The data set uses all of the measurements used in the glabella data set

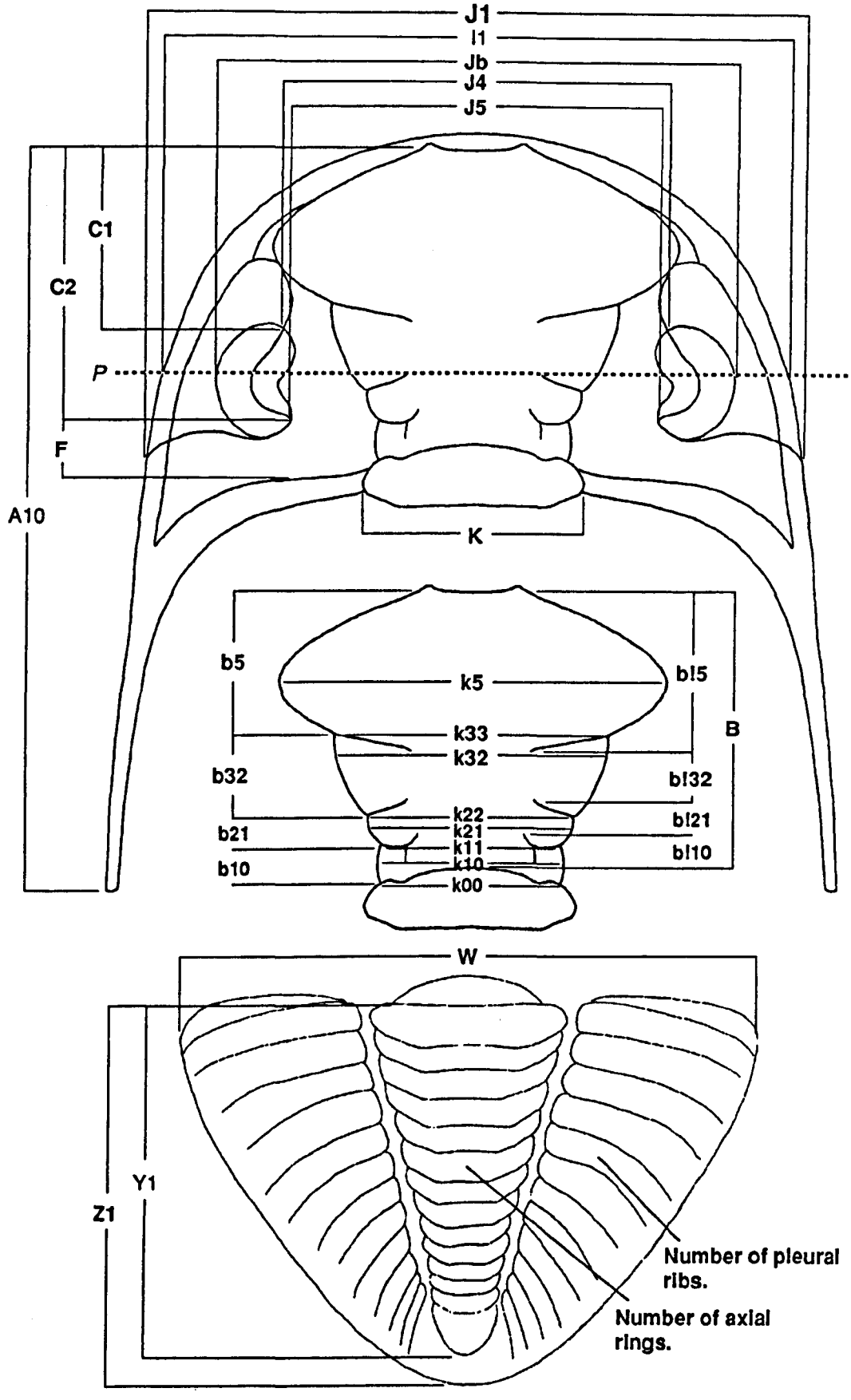

Figure 5. 11. Measurements made on glabellae, cephala and pygidia of *Achatella.* All measurements made on internal casts with the specimen orientated in dorsal view (see text). Measurements used in principal components analysis (PCA) in bold type. The dotted line *PP* is the line which bisects the lengths (exsag.) of the left and right palpebral lobes. See Table 5. 4 for formal definitions of the measurements.

Table 5. 4. Definitions of measurements made on the exoskeleton of *Achatella*. For each measurement an abbreviated name (in bold), a formal name (in italics), and a full definition are given. See Figure 5. 11 for illustrative diagram.

CEPHALA

A10: *Total cephalic length.* Exsag. length of cephalon as measured from the anteriormost extremity of the frontal lobe to the distal extremity of the genal spine. (Anterior of frontal lobe is used rather than anteriormost point of cephalon because the preglabellar region in *Achatella* is very narrow (sag. and exsag.) and often damaged even in well preserved specimens). Left and right side.

B: *Preoccipital glabellar length.* Sag. length of glabella as measured from the anteriormost extremity of the frontal lobe to the deepest point in the occipital furrow.

I1: *Mid. palpebral cephalic width.* Width (tr.) of cephalon as measured along a line which bisects the lengths (exsag.) of the left and right palpebral lobes.

Jb: *Width (tr.) between eye bases.* Width (tr.). measured along the line which bisects the lengths (exsag.) of the left and right palpebral lobes, from the outermost extremity of the basal part of the left eye to the corresponding point on the right side. The width measured between the basal parts of the eyes is used rather than across the palpebral lobes because the topmost extremities of the turret-like eyes of *Achatella*, and hence that part of the palpebral lobes adjacent to them are rarely preserved.

J1: *Cranidial width across distal extremity of facial suture.* Width (tr.) of cranidium as measured from the point at which the posterior branch of the facial suture meets the cephalic margin on the left hand side to the corresponding point on the right hand side.

J4: *Pre-palpebral cranidial width.* Width (tr.) of cranidium from anteriormost point of left palpebral lobe to anteriormost point of right palpebral lobe.

J5: *Post-palpebral cranidial width.* Width (tr.) of cranidium from posteriormost point of left palpebral lobe to posteriormost point of right palpebral lobe.

b5: *Distal length of frontal lobe.* Length (exsag.) of frontal lobe as measured from a point opposite the anteriormost extremity of the frontal lobe to the distal extremity of S3. Left and right side.

b32: *Distal length of L3.* Length (exsag.) of L3 as measured from the distal extremity of S3 to a point opposite the distal extremity of S2. Left and right side.

b21: *Distal length of L2.* Length (exsag.) of L2 as measured from the distal extremity of S2 to a point opposite the distal extremity of S1. Left and right side.

b10: *Distal length of L1.* Length (exsag.) of L1 as measured from the distal extremity of S1 to a point opposite the distal extremity of S0. Left and right side.

Table 5. 4. Continued.

b!5: *Proximal length of frontal lobe.* Length (exsag.) of frontal lobe as measured from a point opposite the anteriormost extremity of the frontal lobe to the proximal extremity of S3. Left and right side.

b!32: *Proximal length of L3.* Length (exsag.) of L3 as measured from the proximal extremity of S3 to a point opposite the proximal extremity of S2. Left and right side.

b!21: *Proximal length of L2.* Length (exsag.) of L2 as measured from the proximal extremity of S2 to a point opposite the proximal extremity of S1. Left and right side.

b!10: *Proximal length of L1.* Length (exsag.) of L1 as measured from the proximal extremity of S1 to the deepest point of S0 on the sagittal line. Left and right side.

k5: *Width (tr.) of frontal lobe.* Maximum width (tr.) of frontal lobe as measured from left branch of facial suture to corresponding point on right branch.

k32: *Width (tr.) of glabella across L3.* Width (tr.) of glabella across widest point of L3 lobes (*i.e.* just to posterior of distal end of S3 furrows), measured from deepest point in left axial furrow to corresponding point in right axial furrow.

k21: *Width (tr.) of glabella across L2.* Width (tr.) of glabella across widest point of L2 lobes measured from deepest point in left axial furrow to corresponding point in right axial furrow.

k10: *Width (tr.) of glabella across L1.* Width (tr.) of glabella across widest point of L1 lobes measured from deepest point in left axial furrow to corresponding point in right axial furrow.

k33: *Width (tr.) of glabella across S3.* The transverse measurement from the point of intersection of the left hand S3 furrow with the left axial furrow, to the corresponding point on the right hand side.

k22: *Width (tr.) of glabella across S2.* The transverse measurement from the point of intersection of the left hand S2 furrow with the left axial furrow, to the corresponding point on the right hand side.

k11: *Width (tr.) of glabella across S1.* The transverse measurement from the point of intersection of the left hand S1 furrow with the left axial furrow, to the corresponding point on the right hand side.

k00: *Width (tr.) of glabella across S0.* The transverse measurement from the point of intersection of the left branch of the occipital furrow with the left axial furrow, to the corresponding point on the right hand side.

K: *Width (tr.) of occipital ring.* Width (tr.) of occipital ring across widest point, measured from deepest point in left axial furrow to corresponding point in right axial furrow.

Table 5. 4. Continued.

C1: *Longitudinal position of anterior of eye.* Exsag. distance from a point opposite the anteriormost extremity of the frontal lobe to the anteriormost extremity of the palpebral lobe as seen in dorsal view. Left and right side.

C2: *Longitudinal position of posterior of eye.* Exsag. distance from a point opposite the anteriormost extremity of the frontal lobe to the posteriormost extremity of the palpebral lobe as seen in dorsal view. Left and right side.

F: *Postocular length.* Exsag. distance from the posteriormost extremity of the palpebral lobe as seen in dorsal view to the deepest point in the posterior border furrow. Left and right side.

PYGIDIA

W: *Pygidial width.* Width (tr.) of pygidium measured across the widest point.

Z1: *Pygidial length.* Length (sag.) of pygidium measured from the deepest point in the articulating furrow to the posteriormost extremity of the pygidium.

Y1: *Length of pygidial axis.* Length (sag.) of pygidial axis measured from the deepest point in the articulating furrow to the posteriormost extremity of the axis.

Number of axial rings. Number of distinct rings making up the pygidial axis, excluding the articulating facet at the anterior of the pygidium.

Number of pleural ribs. Number of pleural ribs making up the pleural region of the pygidium, excluding the articulating facet at the anterior of the pleural field.

plus the following:

J1	C1 (left and right)
J4	C2 (left and right)
J5	F (left and right)
Jb	
K	

All of the above measurements were obtainable for 45 specimens.

3. *Pygidium data set.* This set includes all pygidia for which the following measurements were obtainable:

W	Z1
Number of axial rings	Number of pleural ribs

All of the above measurements were obtainable for 59 specimens.

The PCA results will be considered before moving on to uni- and bivariate plots. In the following plots, symbols are used to represent specimens from the different stratigraphical samples. Figure 5. 12 lists the symbols used.

PCA on glabella data set. The principal components (PCs) of the 25 measurements used for the glabella data set were calculated (see Chapter 4 for discussion of PCA). The resultant eigenvalues and eigenvectors are given in Appendix 6, and the PC scores are given in Appendix 7. PC1 summarises 89.3% of the total variance in the data set, PC2 summarises 3.3%, and PC3 2.2%. Figure 5. 13 shows the 66 specimens comprising the glabella data set ordinated on the first three PCs. According to PCA theory, PC1 should represent the "direction of maximum variance through the data set" (Chapter 4), and this is commonly taken to represent specimen size in palaeontological data. Notice from Figure 5. 13 that specimens belonging to the KILLEY sample tend to have negative scores on PC1, and it can be seen from inspection of Figure 5. 14 that these specimens are usually larger than specimens from other samples. In fact the Pearson correlation coefficient relating score on PC1 to preoccipital glabellar length B for each specimen is r=-0.991. The eigenvector values relating to PC1 are all virtually identical (Appendix 6) which means that all measurements are weighted roughly equally in the PCA calculation (no single variable has greater effect than any other). Since PC1 accounts for 89.3% of total variance in the data set, and describes nothing more than overall size of the specimens, it is clear that all of the glabellae measured are very similar in structure.

PCs 2 and 3 together describe 5.5% of the variance in the data set *i.e.*: most of the

Symbol	Stratigraphical Horizon	Sample Name
□	Langøyene Fm.	LANGØYENE
■	High Mains Fm.	HIGHMAIN
○	Starfish Beds	STARBED
⊠	?Boda Limestone	?BODA
⊕	Crinoid Bed	CRINBED
⊖	Quarrel Hill Fm.	QHILL
●	Killey Bridge Fm.	KILLEY
▽	Kiln Mudstone	KILN
▪	Maysvillian, Cinc.	CINC
✳	Cobourg Beds	COBOURG
⌖	Hull, Quebec	HULL
⋆	Verulam Fm.	VERULAM
△	Utica Shale, Cinc.	UTICA
▲	Lorraine Gp.	LORRAINE
–	Trenton Ls., N. Y.	TRENTON
⊠	Prosser Fm.	PROSSER
↖	Mjøsa Fm.	MJØSA
↗	Furuberget Fm.	FURUBERG
◆	Knockerk Hs. Mbr.	KNOCK
ı	Kukruse	KUKRUSE

Figure 5. 12. Diagram showing symbols used to represent the different stratigraphical samples on morphometric plots. Samples listed in approximate stratigraphical order.

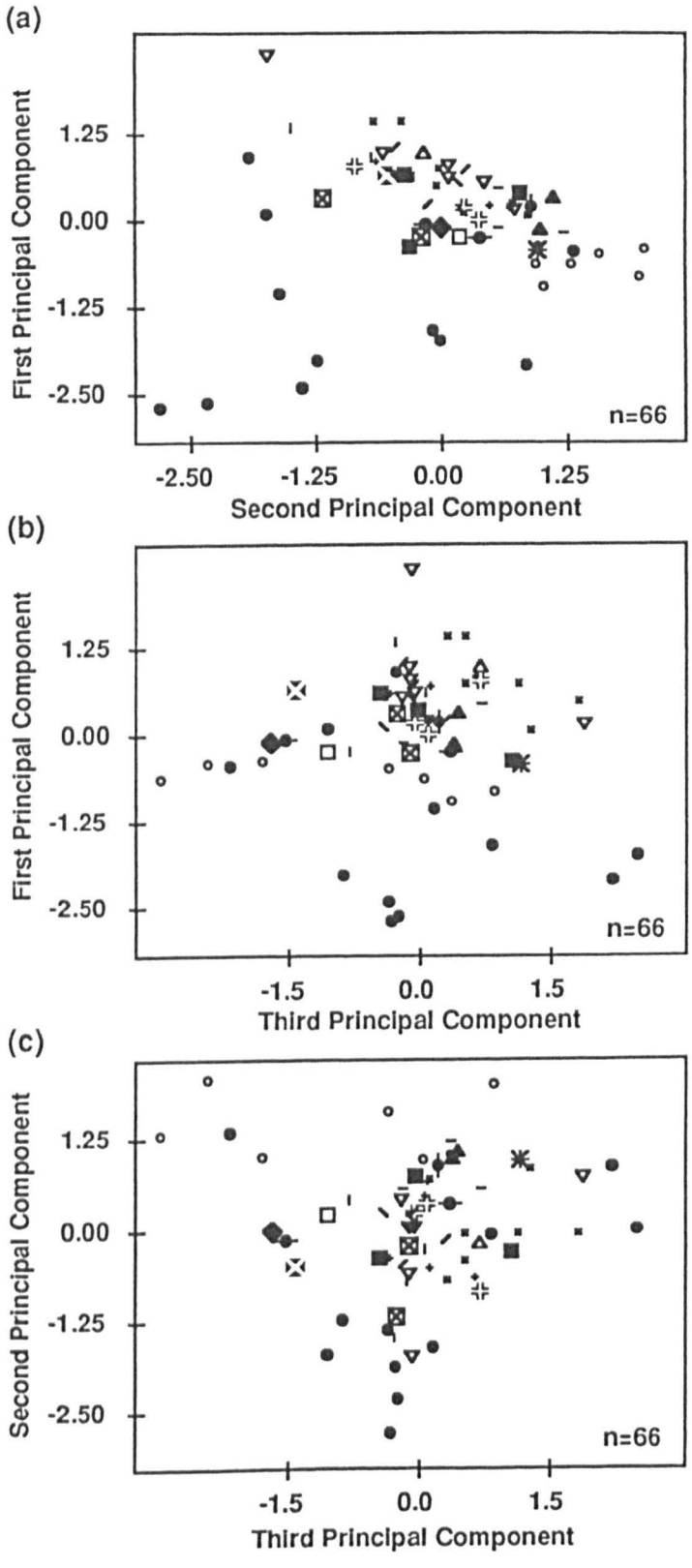

Figure 5. 13. Glabellae of *Achatella* ordinated along the first three principal component axes calculated from the glabella measurement scheme. Symbols as in Figure 5. 12.

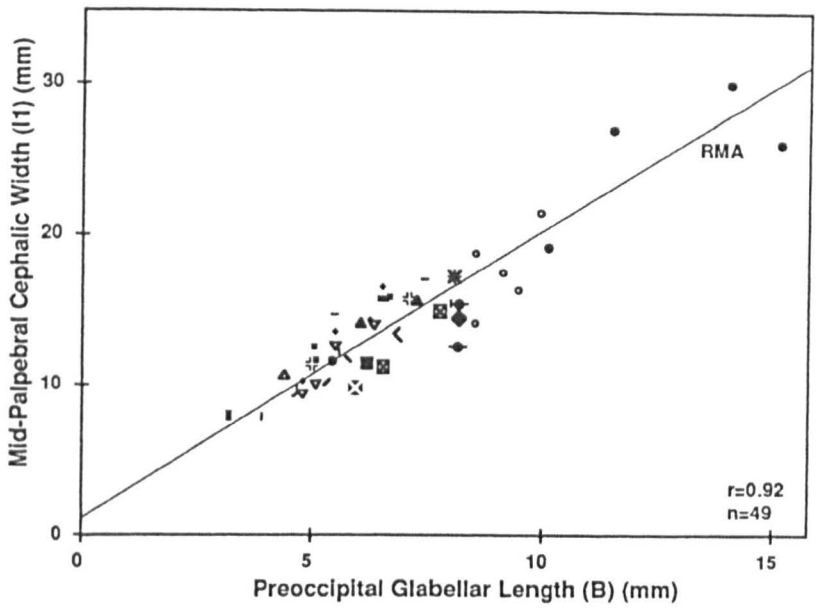

Figure 5. 14. Bivariate scatter plot of mid-palpebral cephalic width (I1) against preoccipital glabellar length (B) for cephala of *Achatella*. Plotting symbols as in Figure 5. 12. Best fit line to the data calculated by the reduced major axis method.

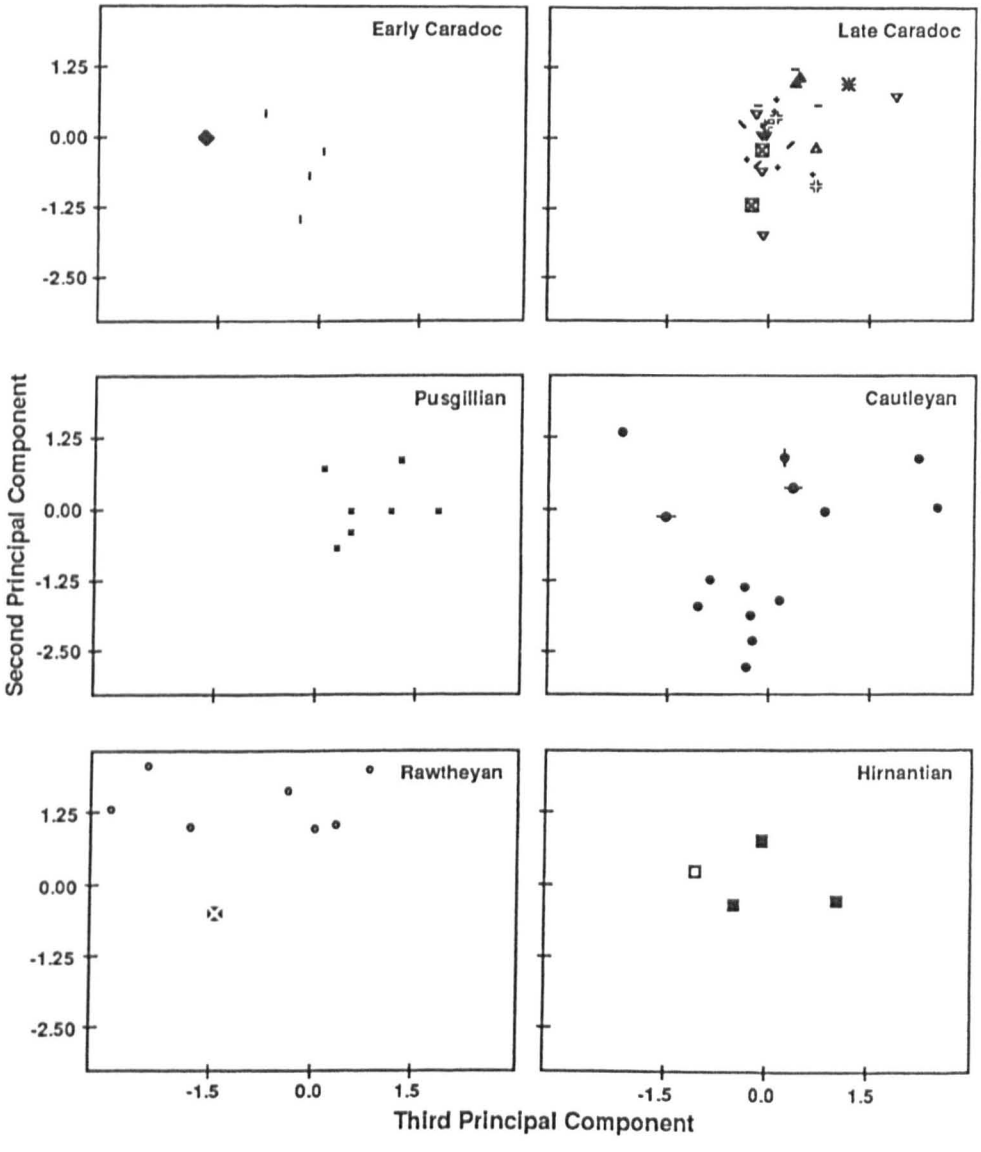

Figure 5. 15. Glabellae of *Achatella* ordinated along the second and third principal component axes and grouped into six broad time intervals to illustrate changing morphospace occupation with time. Symbols as in Figure 5. 12.

remaining variance when specimen size (PC1) is ignored. It can be seen from Figure 5. 13 (c) that specimens are not well sorted with respect to PC2 and PC3. This is clarified in Figure 5. 15, in which the samples are grouped into six time windows. Note that the time intervals used in the figure are just broadly descriptive ones: although specimens from the KILN, VERULAM, TRENTON and MJØSA samples are all of broadly late Caradoc age, there is no suggestion that they are precisely contemporaneous. There is wide overlap in the fields of morphospace occupied by the various stratigraphical samples, so that no one sample is separable from the others. In fact, if one considers the "envelope" defined by the 11 specimens from the KILLEY sample, it can be seen that all of the other samples fall, either wholly or partly, within it. Notice also that the 27 late Caradoc specimens (assigned to 4 named species) occupy a much more restricted region of morphospace than the 14 Cautleyan specimens (assigned to 2 named species), and even than the 11 KILLEY specimens.

In spite of the overlap in fields, it can still be seen that most of the stratigraphical samples do occupy definite regions in the morphospace. For example, specimens from the CINC sample all lie in the area -1.0<PC2<+1.25, 0<PC3<+1.7, and STARBEDS specimens are all in the area defined by PC2>1.0.

By examination of the eigenvector lists (Appendix 6), it can be inferred that the measurements having most effect on PC2 are b10 and b!10 (measurements describing the length of the L1 glabellar lobe). The variable having most effect on PC3 is b5 which describes the length (exsag.) of the frontal lobe. In order to determine whether these variations are systematic, or are randomly scattered throughout the data, these variables must be examined more closely, and this will be discussed below.

PCA on cephalon data set. PCs of the 36 variables used in the cephalon data set were calculated. The resulting eigenvalues and eigenvectors are given in Appendix 6 and the PC scores are given in Appendix 7. PC1 summarises 90.0% of the total variance, PC2 summarises 3.1%, PC3 summarises 2.0%. The 45 specimens are ordinated on the first three PCs in Figure 5. 16. PC1 sorts the specimens with respect to size, as in the previous data set (compare Figure 5. 16 with Figure 5. 14): the Pearson correlation coefficient relating score on PC1 to glabellar length (B) is r=-0.99 and all eigenvector values for PC1 are almost identical. Again, it can be seen from Figure 5. 16 (c) that the specimens are not well sorted with respect to PC2 and PC3. In Figure 5. 17, the samples are grouped into the same six time windows used for the glabella data. A high degree of overlap exists between the fields occupied by the stratigraphical samples, and the envelope defined by the KILLEY specimens encompasses the variation in almost all of the other samples. Exceptions to this are the specimens from the STARBEDS and HIGHMAIN samples, which lie in a region of morphospace not occupied by other

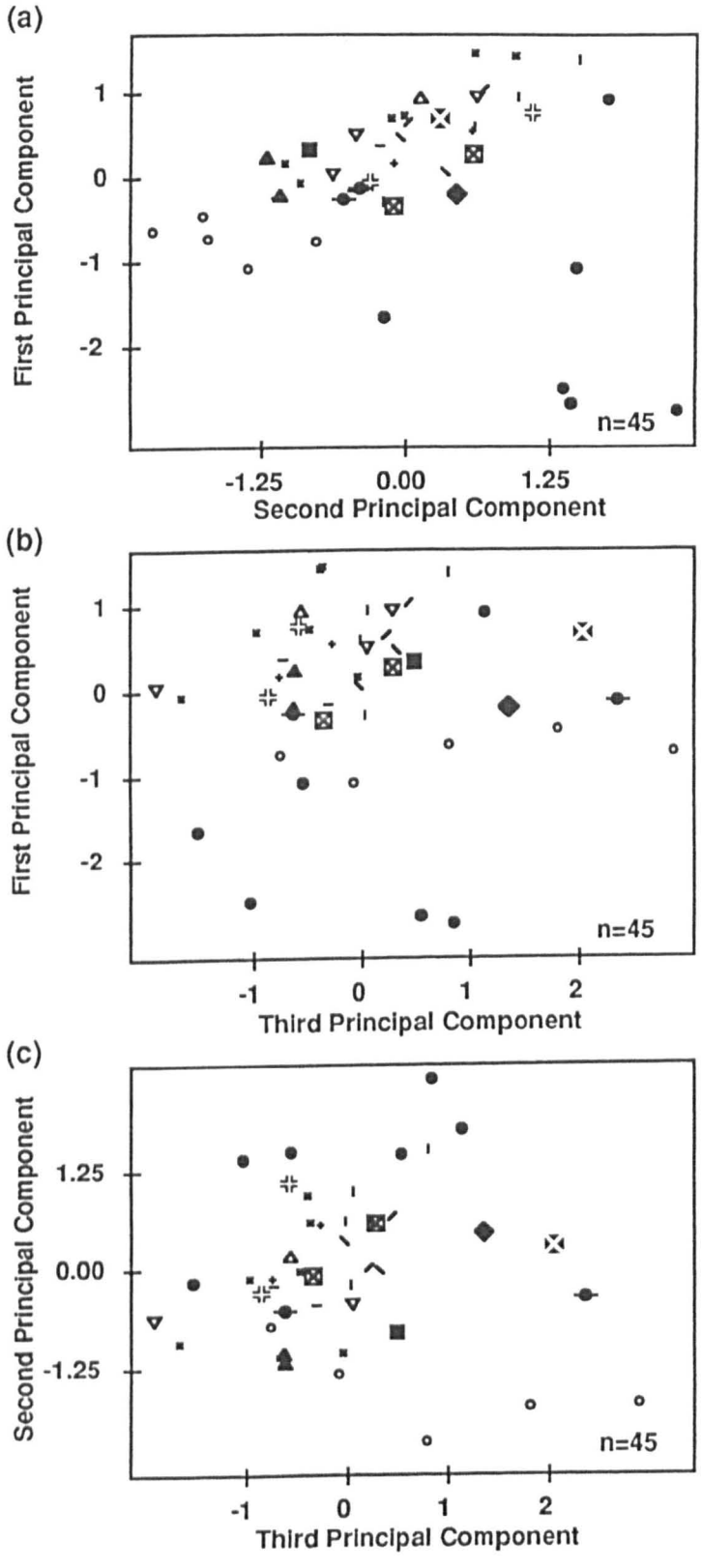

Figure 5. 16. Cephala of *Achatella* ordinated along the first three principal component axes calculated from the cephalon measurement scheme. Symbols as in Figure 5. 12.

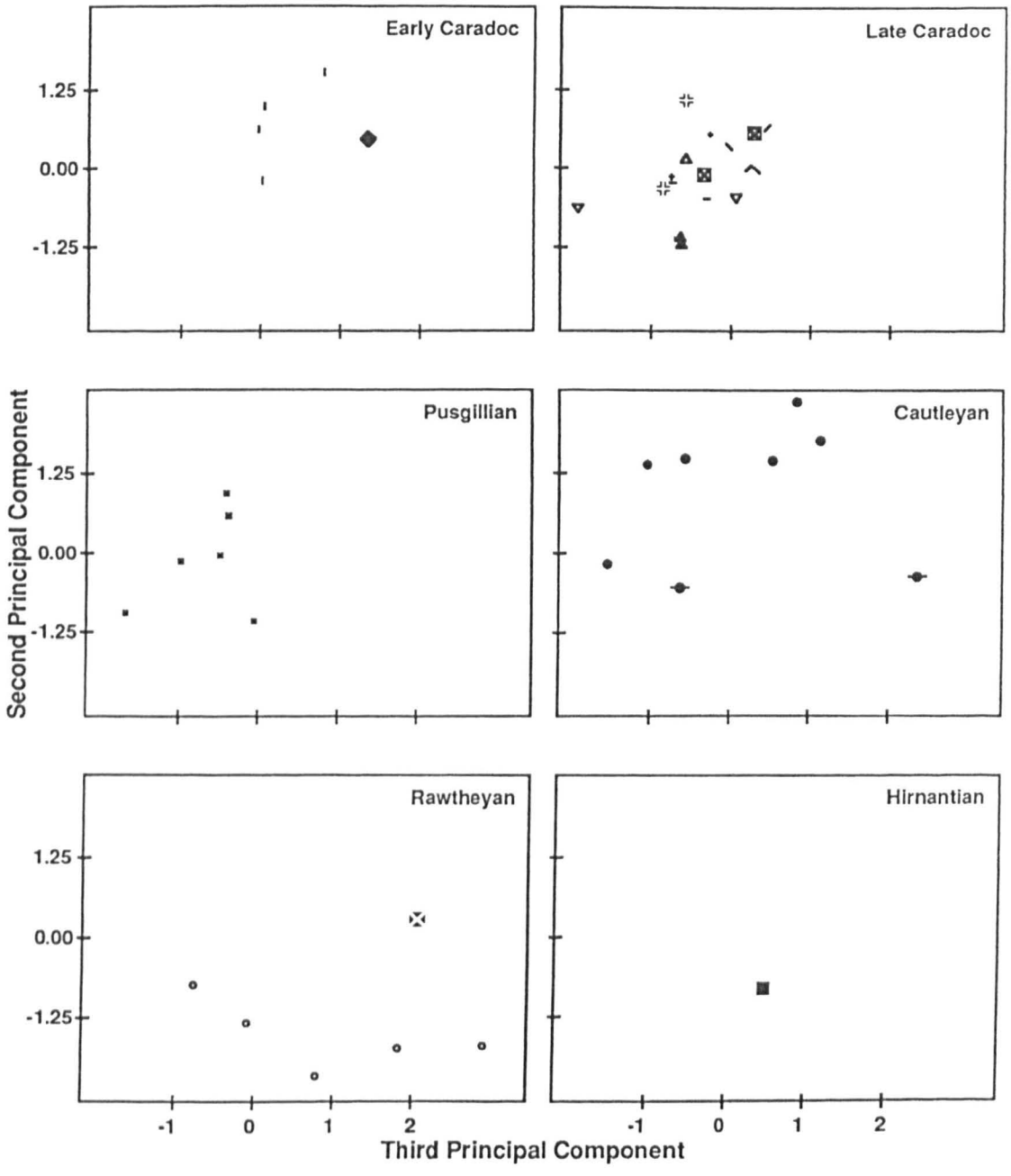

Figure 5. 17. Cephala of *Achatella* ordinated along the second and third principal component axes and grouped into six broad time intervals to illustrate changing morphospace occupation with time. Symbols as in Figure 5. 12.

samples. It should be noted that these samples have a small overlap with other samples in the glabella data set (Figure 5. 15), but that data set includes more specimens.

By examination of the eigenvectors (Appendix 6), it can be inferred that b10 and b!10 are the measurements having most effect on PC2. This is in agreement with the glabella data set. It can also be seen that C1 (not used in the glabella data set) makes a contribution at a lower level. Variables having large effect on PC3 are b5 and b!5. Again, this is in agreement with the glabella data set.

PCA on pygidium data set. PCs of the 4 variables making up the pygidium data set were calculated. The resulting eigenvalues and eigenvectors are given in Appendix 6 and the PC scores are given in Appendix 7. PC1 accounts for 84.5% of the total variance, PC2 accounts for 12.5%, PC3 2.2%. The specimens are plotted against the first three PCs in Figure 5. 18. As before, PC1 sorts the specimens with respect to overall size (compare Figure 5. 18 with Figure 5. 19). Notice that the KILLEY pygidia all fall in the negative region of PC1, reflecting their large overall size. The correlation coefficient relating score on PC1 to pygidial length is r=-0.944, and all eigenvector values for PC1 are closely similar. When PC1 is dropped out of the analysis, the specimens do not sort well into discrete groups on PC2 and PC3. Once again they have been grouped into time windows for clarity (Figure 5. 20). As was found for cephala, there is broad overlap between the fields occupied by the stratigraphical samples, and specimens from the KILLEY sample (and indeed all Cautleyan specimens) occupy a very broad region of morphospace encompassing the regions occupied by all the other samples.

From the eigenvector lists (Appendix 6), the variables weighted on PC2 are W and number of pleural segments, while on PC3 the number of axial segments has greatest effect.

Bivariate and univariate plots. A number of bivariate plots of the *Achatella* data have been constructed. In some cases these involve measurements excluded from the PCA data sets because of unacceptable amounts of missing data. All best-fit lines have been calculated using the reduced major axis (RMA) method of Davis (1986: 201-204), and all correlation coefficients are Pearson product-moment (r) coefficients. In general, preoccipital glabellar length (B) is used as the index of specimen size. Again, plotting symbols are as in Figure 5. 12.

Figure 5. 14 shows a length-width plot for cephala of *Achatella*. All specimens lie on the same linear trend. The growth of the cephalon is strongly anisometric, but not noticeably allometric. The slope of the RMA best-fit line is 1.96, and it passes close to

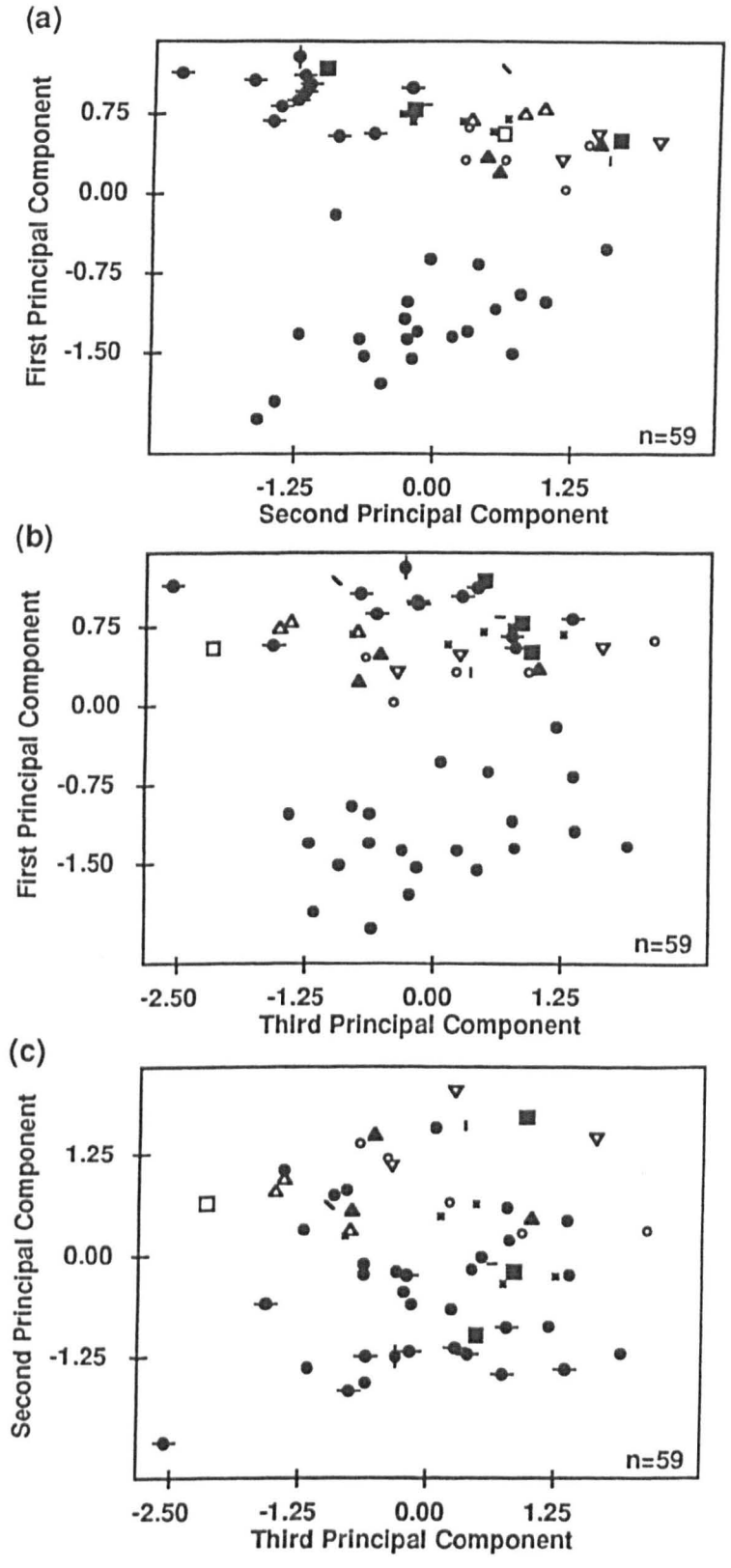

Figure 5. 18. Pygidia of *Achatella* ordinated along the first three principal component axes calculated from the pygidium measurement scheme. Symbols as in Figure 5. 12.

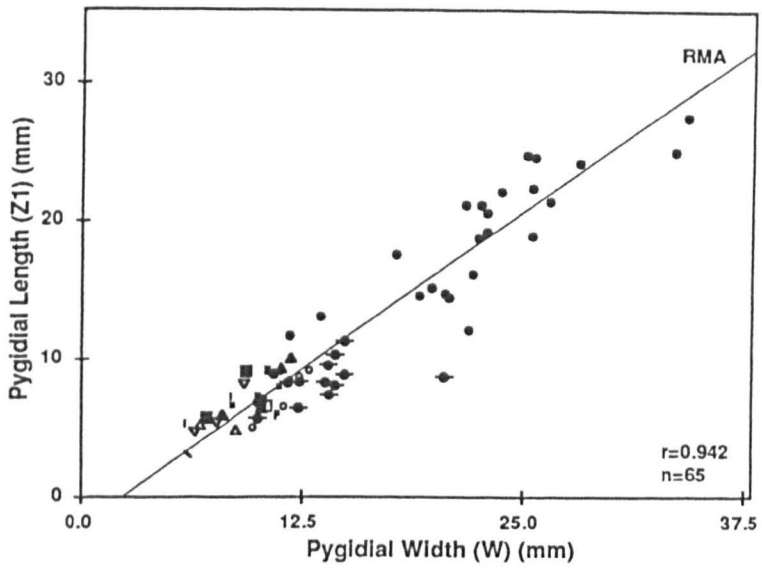

Figure 5. 19. Bivariate scatter plot of pygidial length (Z1) against pygidial width (W) for *Achatella*. The best-fit line to the data is calculated using the reduced major axis method. Symbols as in Figure 5. 12.

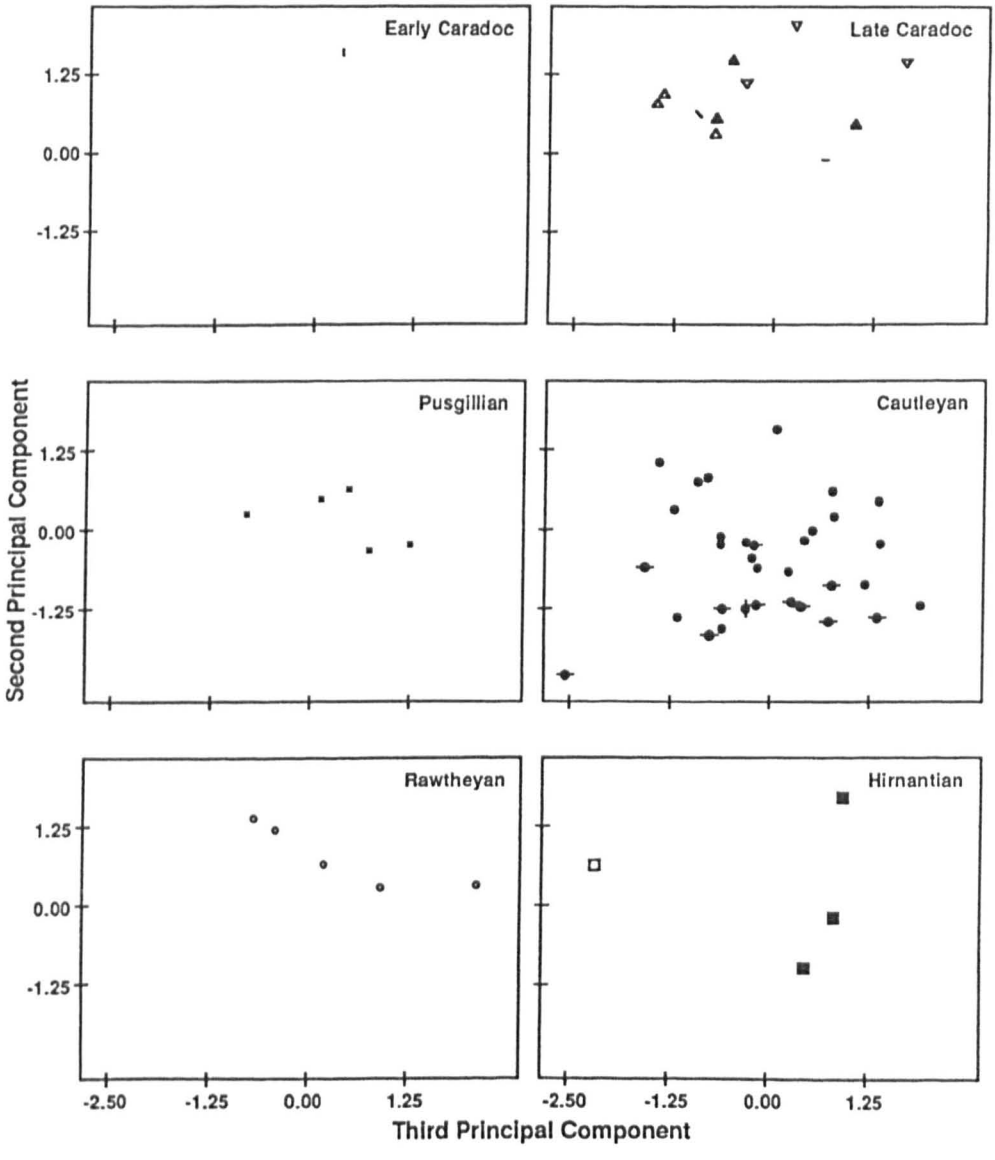

Figure 5. 20. Pygidia of *Achatella* ordinated along the second and third principal component axes and grouped into six broad time intervals to illustrate changing morphospace occupation with time. Symbols as in Figure 5. 12.

the origin. A similar plot is obtained when mid-palpebral cephalic width is replaced by maximum cephalic width: the RMA line slope becomes 2.11, and the correlation coefficient is similar, r=0.957.

In Figure 5. 21 lateral separation of the eyes on the cephalon is ordinated against preoccipital glabellar length B. The graph again shows a single linear trend, the RMA line having a slope of 1.46 and passing close to the origin. The slope of the line is less than that in Figure 5. 14, which means that the lateral separation of the eyes increases with ontogeny at a lower rate than cephalic width, so that the largest specimens of *Achatella* (e.g. those from the KILLEY sample) have relatively wider (tr.) librigenae than the smaller ones.

Figures 5. 22 and 5. 23 show the longitudinal position of the anterior and posterior-most points of the eyes ordinated against preoccipital glabellar length B. Figure 5. 22 shows two distinct linear trends. One (RMA 1 on the figure) is defined by all specimens apart from those from the KILLEY sample (44 specimens). The best-fit line has a slope of 0.57. The second (RMA 2) is defined by the KILLEY specimens alone (8 specimens). The best-fit line to this trend has a slope of 0.37. The difference is because the anterior of the eye in the KILLEY specimens is located further forwards (*i.e.* C1 has smaller magnitude) than would be predicted from the other specimens. This accounts for the variation in C1 highlighted in the PC analysis of the cephalon data set described earlier.

In fact, since the anterior of the eye as defined is seen to be always opposite or nearly opposite the distal end of the S3 furrow in *Achatella*, a close relationship between C1 and exsagittal frontal glabellar lobe length b5 is to be expected, and this is confirmed in Figure 5. 24. Virtually the same two trends are present. The best-fit line to all specimens except those from the KILLEY sample (RMA 1, 56 specimens) has slope 0.53. The line fitted to the KILLEY specimens alone (RMA 2, 11 specimens) has slope 0.37. Clearly there is a tightly constrained relationship between the location of the anterior of the eye and the length (exsag.) of the frontal lobe. A t-test was undertaken to test the statistical significance of the difference in exsagittal frontal lobe length between the KILLEY specimens and the other specimens. The specimens were grouped into two sets: set 1 contained all KILLEY specimens; set 2 contained all other *Achatella* specimens. The null hypothesis stated that the mean of the distribution of b5/B (*i.e.* exsagittal frontal lobe length ratioed against preoccipital glabellar length to correct for specimen size) for set 1 is the same as the mean of b5/B for set 2. The null hypothesis was rejected at the 95% confidence interval. This means that the exsagittal frontal lobe length in KILLEY specimens is significantly different from that for all other specimens of *Achatella*. This fact can therefore be used as a diagnostic character for the Killey Bridge Formation specimens.

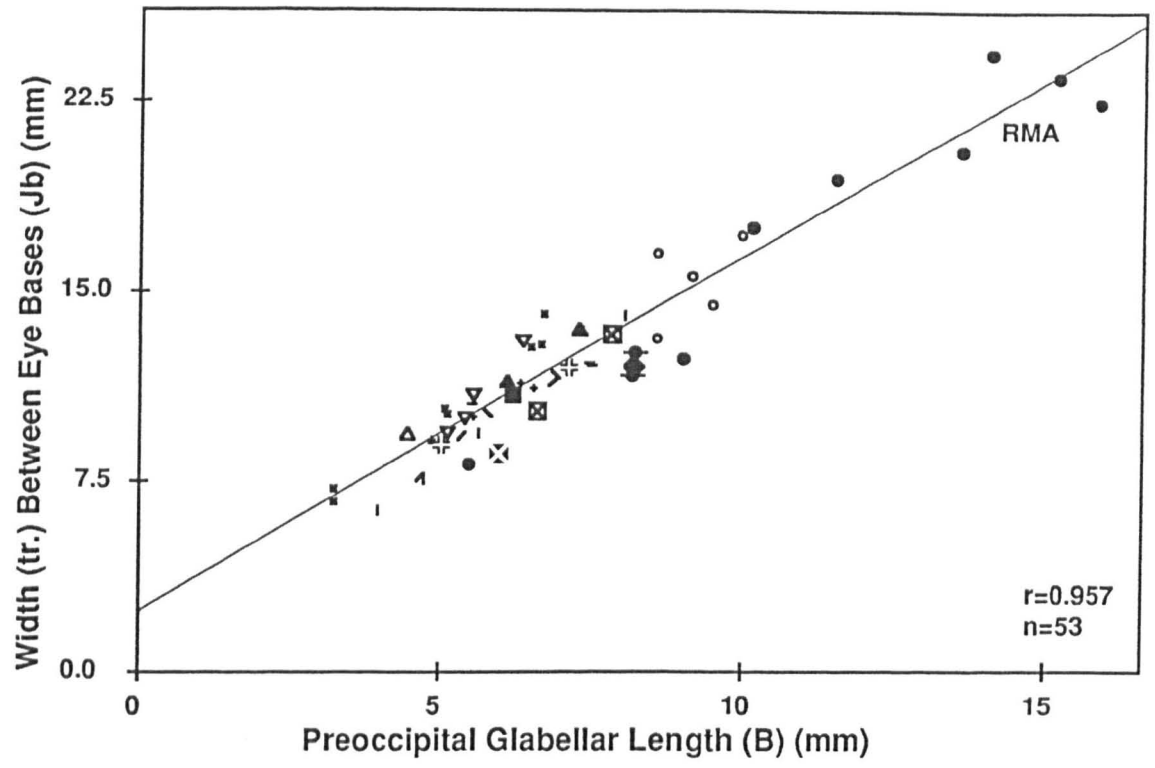

Figure 5. 21. Bivariate scatter plot of width (tr.) between eye bases (Jb) against preoccipital glabellar length (B). Best-fit line to the data calculated using the reduced major axis method. Symbols as in Figure 5. 12.

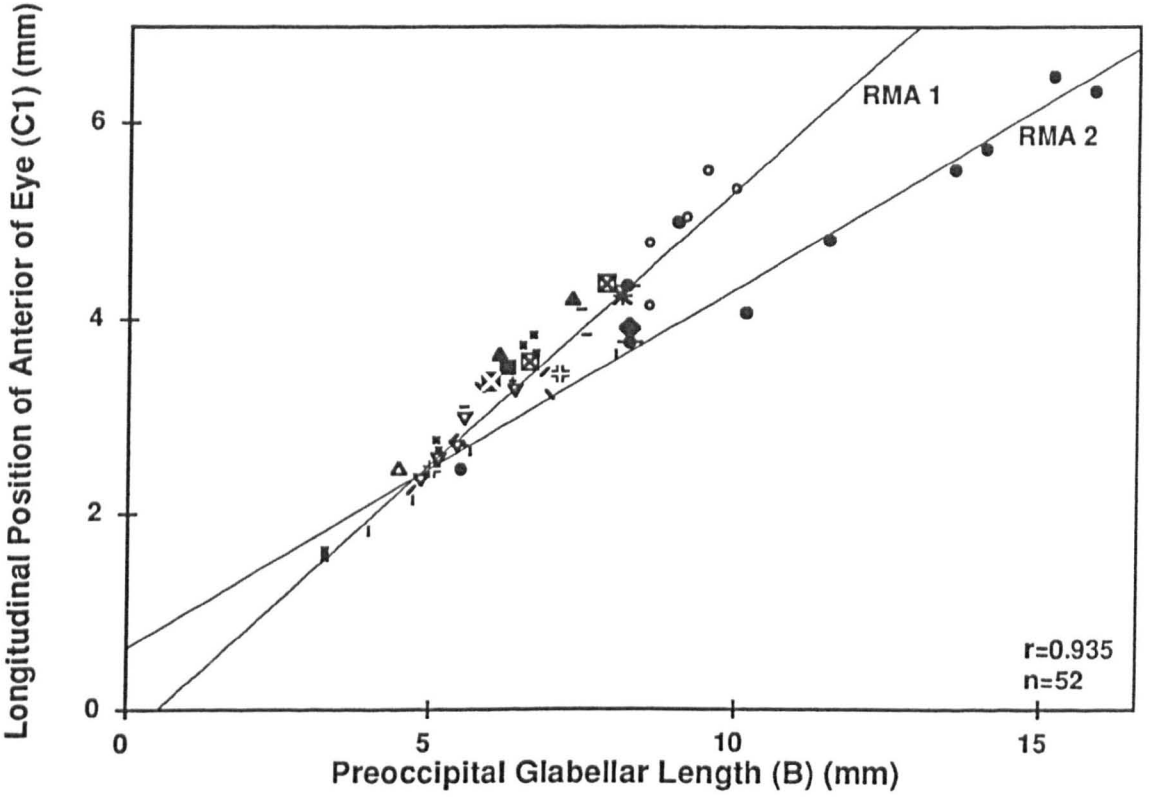

Figure 5. 22. Bivariate scatter plot of longitudinal position of anterior of eye (C1) against preoccipital glabellar length (B). Best-fit lines to the data calculated using the reduced major axis method. RMA1 fitted to all specimens except those from KILLEY. RMA2 fitted to specimens from KILLEY only. Symbols as in Figure 5. 12.

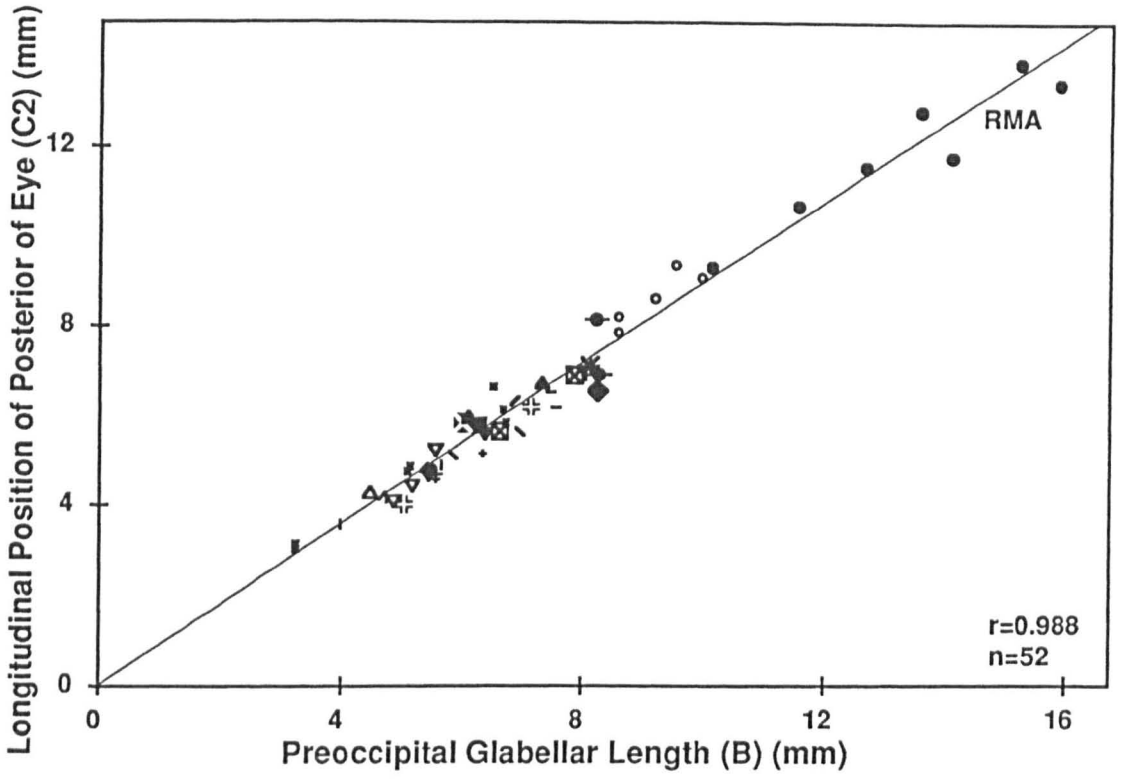

Figure 5. 23. Bivariate scatter plot of longitudinal position of posterior of eye (C2) against preoccipital glabellar length (B). Best-fit line to the data calculated using the reduced major axis method. Symbols as in Figure 5. 12.

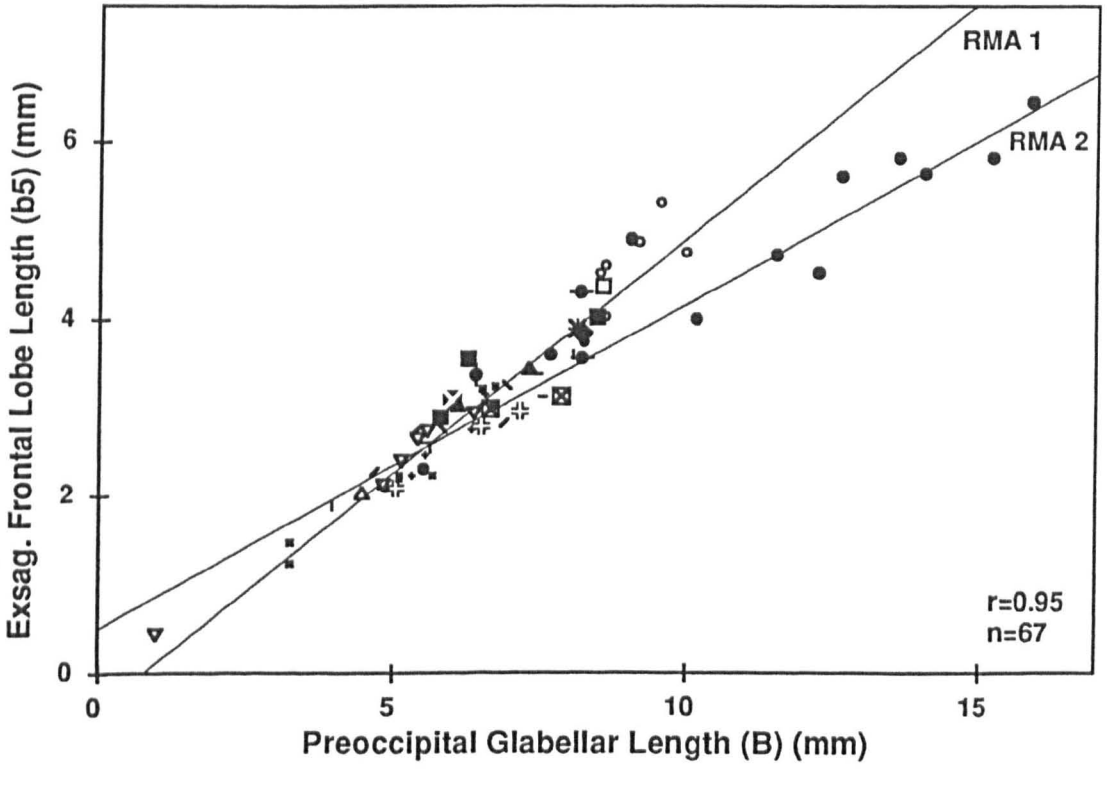

Figure 5. 24. Bivariate scatter plot of distal length of frontal lobe (b5) against preoccipital glabellar length (B). Best-fit lines to the data calculated using the reduced major axis method. RMA1 fitted to all specimens except those from KILLEY. RMA2 fitted to specimens from KILLEY only. Symbols as in Figure 5. 12.

Figure 5. 23 shows a remarkably constant relationship between C2 (longitudinal position of posterior point of eye) and glabellar length B, and hence indicates a constant location for the posterior of the eye. The trend is almost isometric: the RMA line has slope 0.9 and passes through the origin. In morphological terms this means that the posterior of the eye is always opposite or nearly opposite the mid-point of the occipital furrow.

It has therefore been shown that, while the posterior of the eye has a constant position on the cephalon, the location of the anterior shows a discrete variation, being significantly further forward in KILLEY specimens. The probable reason for this becomes apparent when the number of dorso-ventral lens files in the eye is counted. Figure 5. 5 shows a summary of the number of lens files in the eye of *Achatella*. For each specimen the number of files in the left eye was counted; where the left eye was not preserved, the right eye was used instead. Only one eye per specimen is therefore represented. Specimens belonging to all samples except KILLEY have between 18 and 27 files. Specimens belonging to the KILLEY sample have between 32 and 36 files, with a mean of 34 for 13 counted specimens. To test the statistical significance of the observed difference in file number, a t-test was undertaken. The specimens were grouped into two sets: set 1 contained all the KILLEY specimens; set 2 contained all the other *Achatella* specimens. The null hypothesis stated that the mean number of files in the eyes of specimens belonging to set 1 is the same as the mean number in set 2. The null hypothesis was rejected at the 99% confidence interval.

Figure 5. 25 shows statistical lens charts for the stratigraphical samples. The charts were constructed using the method of Campbell (1977: 44). Again, left eyes have been used where possible, the right eye being used instead for specimens in which the left was not preserved, so that each specimen is represented in the charts only once. The charts show the number of specimens which have a lens at each location on the visual surface. They were constructed by matching up the eyes of specimens from the same stratigraphical sample at the anterior end, using the harmonious matching of the anteriormost few files. In some samples (e.g. KILLEY, KILN) anomalous files are developed at the anterior of the eye as shown. Notice that KILLEY specimens, as well as having more lens files than specimens from other samples, also have more lenses in the deepest files (up to 15, compared with maximum numbers of around 12 for the other samples). There is no significant variation among the other samples (both LORRAINE and KNOCK are represented by single damaged eyes in which the topmost few lenses may be missing).

The relatively large size of the KILLEY specimens allows for larger eyes containing

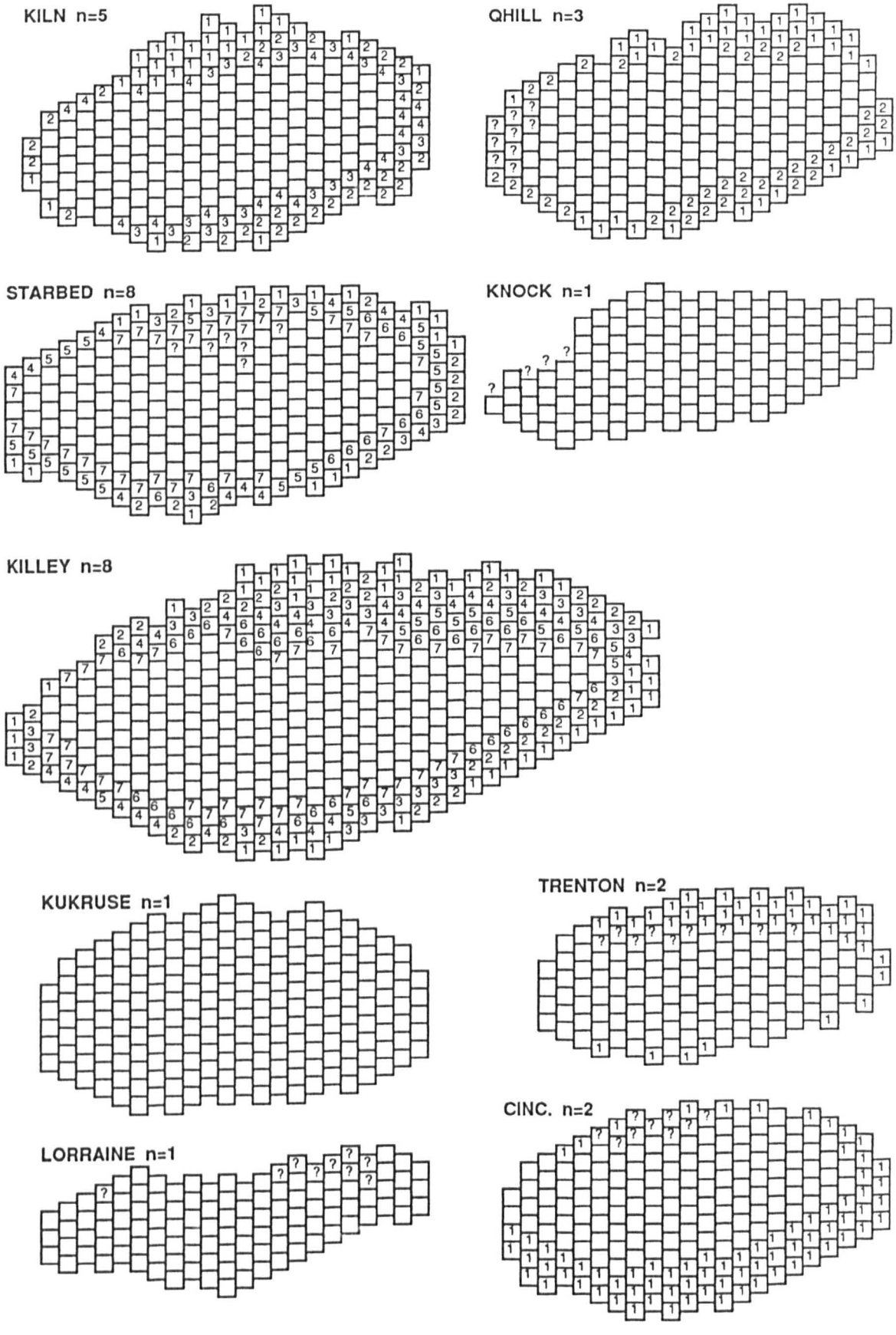

Figure 5. 25. Statistical lens charts for stratigraphical samples of *Achatella*. Charts constructed using the method of Campbell (1977). Left eye of each specimen used where sufficiently well preserved, right eye used otherwise. Anterior of eyes to the left. Numbers indicate how many specimens possess a lens at that location on the visual surface. Locations with no number indicate that all specimens possess a lens at that location.

more lenses (the diameter of the lenses themselves has not been measured, but does not vary noticeably between KILLEY and the other samples). This may have allowed for greater visual resolving power. Also, as demonstrated above, the anterior of the eye is slightly further forward in KILLEY specimens than in other specimens of the genus, and this may have increased the region of binocular overlap in front of the trilobite. McNamara (1980) suggested that increased binocular overlap may have increased hunting efficiency in predatory trilobites.

PCA (above) highlighted variation in b10 (and also in b!10, a closely related measurement). To check whether this variation is systematic, the distributions of b10 and b!10 (ratioed against preoccipital glabellar length B) have been plotted for the various stratigraphical samples (Figure 5. 26). Notice that each sample overlaps with the preceding and succeeding ones (where samples consist of more than one specimen). The large effect these measurements have on the PCA is clearly because of non-systematic variation. A probable explanation for this variation is that these two measurements commonly have small magnitudes (of the order of 0.5-2.0mm) so it may be that the minimum resolution of 0.05mm in the digitising tablet used to make the measurements is causing undue variation.

Figure 5. 27 shows the angles at which the glabellar furrows diverge from the sagittal line. All of the distributions are unimodal and approximately normal. If the stratigraphical samples are considered separately, none of them have angles which are restricted to a small part of the total range of angles. Rather they are all spread more or less uniformly throughout. This measurement cannot therefore be considered to be of taxonomic importance.

Figure 5. 4 shows variation in the ratio total cephalic length A10 / preoccipital glabellar length B. This information was the basis for the coding of character 10 in the cladistic analysis of the genus. The small number of specimens for which total cephalic length is measurable makes the drawing of inferences from this plot difficult. However, the single specimens from the ?BODA and PROSSER samples are clearly separated from the rest. Their low A10/B values reflect their lack of genal spines. KNOCK and KUKRUSE have relatively short genal spines, giving low (but not as low as ?BODA and PROSSER) mean A10/B values of less than 2.0.

Figure 5. 19 shows a length/width plot for pygidia of *Achatella*. The plot is close to isometric: the RMA line has slope 0.90 and passes close to the origin. The relatively wide scatter of the data points about the line may reflect slight flattening of some specimens. Pygidia are particularly susceptible to this. Note that all of the QHILL and STARBEDS specimens fall below the RMA line, meaning that they are relatively

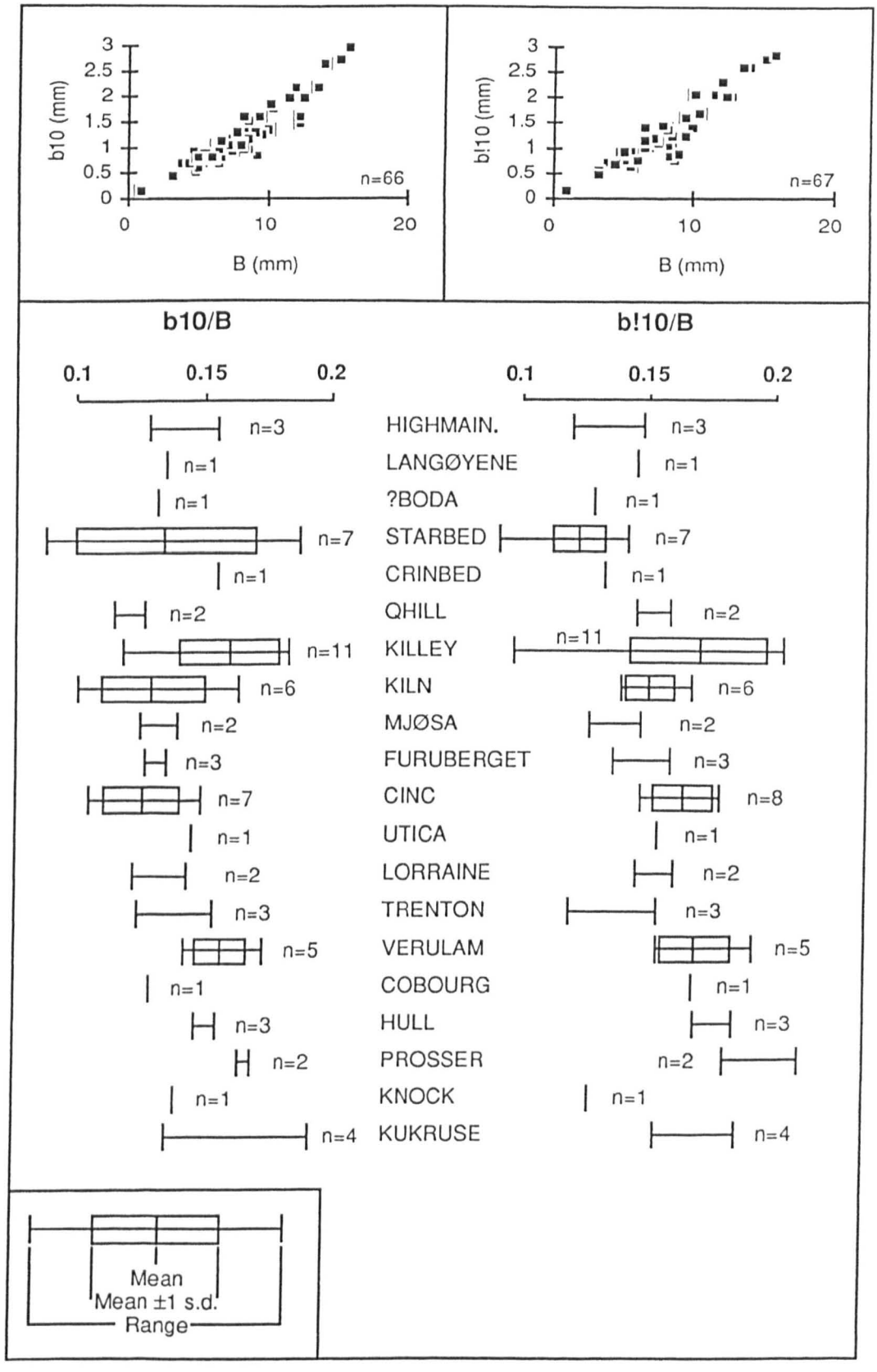

Figure 5. 26. Univariate variation in the ratios distal length of L1 (b10) / pre-occipital glabellar length (B), and proximal length of L1 (b!10) / preoccipital glabellar length (B). Total range shown for each stratigraphical sample, mean value and one standard deviation to either side of the mean shown for samples containing five or more measurable specimens. Insets show bivariate scatter plots of b10 against B, and b!10 against B.

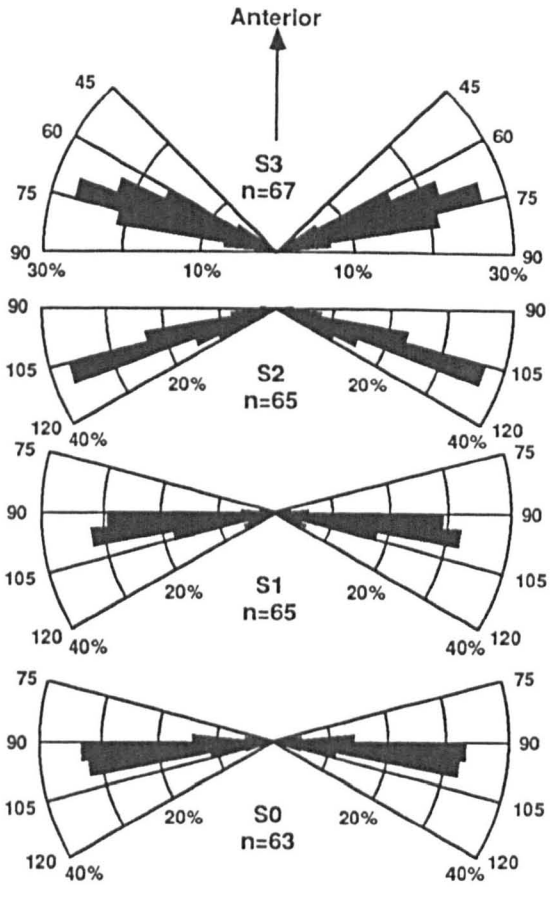

Figure 5. 27. Angles of divergence of lateral glabellar furrows from the sagittal line in *Achatella*. Angles of divergence of S3, S2, S1 and S0 shown. For each furrow of each specimen, the angle between the trace of the furrow and the sagittal line was measured in the anterior quadrant and the mean value was then obtained for corresponding left and right furrows of the specimen. It is this mean value for each left and right furrow pair which is plotted here.

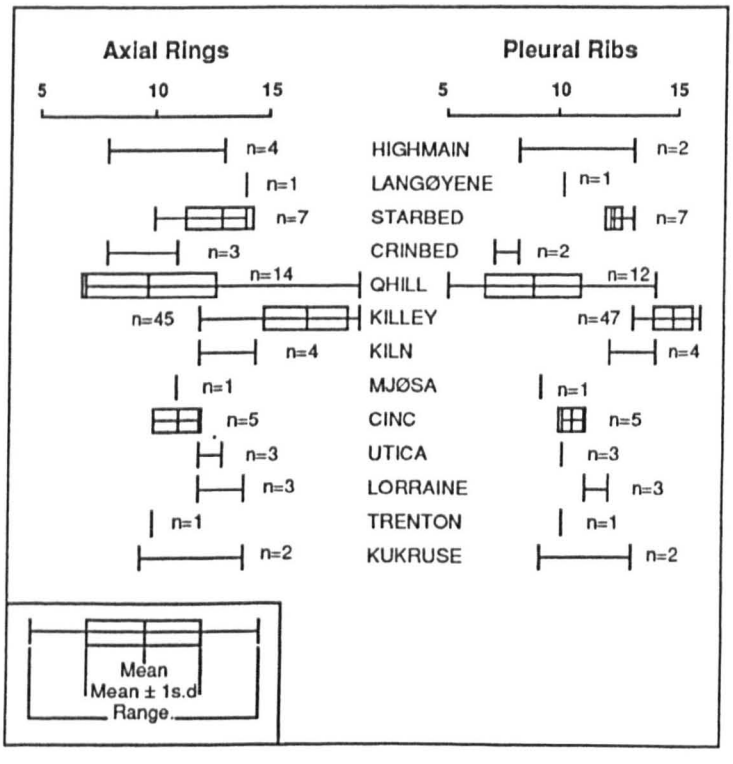

Figure 5. 28. Univariate variation in the number of axial rings and pleural ribs in *Achatella*. Total range shown for each stratigraphical sample, mean value and one standard deviation to either side of the mean shown for samples containing five or more countable specimens. Indistinct rings and ribs counted as half values.

shorter and wider than the others. A t-test was undertaken to test the statistical significance of this shape difference. The specimens were grouped into two sets: set 1 contained all pygidia belonging to the QHILL and STARBEDS samples; set 2 contained all other *Achatella* pygidia. The null hypothesis for the test stated that the mean of the ratio Z1/W for set 1 was the same as the mean of Z1/W for set 2. The null hypothesis was rejected at the 95% confidence interval, demonstrating that the shape of pygidia from the QHILL and STARBED samples is significantly different from the others.

Figure 5. 28 shows univariate plots of the numbers of axial rings and pleural ribs in the pygidia. As with other characters, there is wide overlap between the samples, so that this character on its own does not have taxonomic significance. The restricted range of both variables for KILLEY pygidia is striking in view of the large sample size. The range of values for QHILL is adversely affected by a pygidium from Glenmard Quarry which shows an anomalously high number of axial rings and pleural ribs. In general, a number of axial rings greater than 15 can be considered to be diagnostic of Killey Bridge Formation specimens. Increased pygidial width could reflect the development of more segments, which would result in a relationship between axial length and number of axial rings and pleural ribs. In fact, the correlation coefficient relating number of axial segments to axial length (Y1) for all specimens on which these two parameters were measurable (64 specimens) is r=0.733. The coefficient relating number of pleural segments to axial length (measurable for 62 specimens) is r=0.712. So, although the correlation is not very close, in general it is the larger pygidia (e.g. those from the KILLEY sample) which have most segments. When the pattern within individual stratigraphical samples is considered (for samples which have significant numbers of specimens, Figure 5. 29), lower correlations are obtained. For specimens from the KILLEY sample, the correlation between number of axial segments and axial length Y1 is only r=0.529 for 23 specimens, and the correlation for pleural segments is r=0.503, again for 23 specimens. For the specimens from the QHILL sample, the correlation between number of axial segments and Y1 is r=0.643 for 12 specimens, and the correlation for pleural segments is r=0.699 for 11 specimens. This suggests that pygidial length depends on more than just the number of segments present. The segments themselves must increase in (sag.) length at each successive moult stage.

5. 4. 3. Conclusions from Morphometrics.

Some conclusions can be drawn from the preceding discussion:

1. It has been demonstrated that there is marked shape conservatism in *Achatella* over an extended period of geological time from the early Caradoc to the Hirnantian. PCA demonstrated that the vast majority of variance exhibited by measurements describing the shape of the glabella, cephalon and pygidium

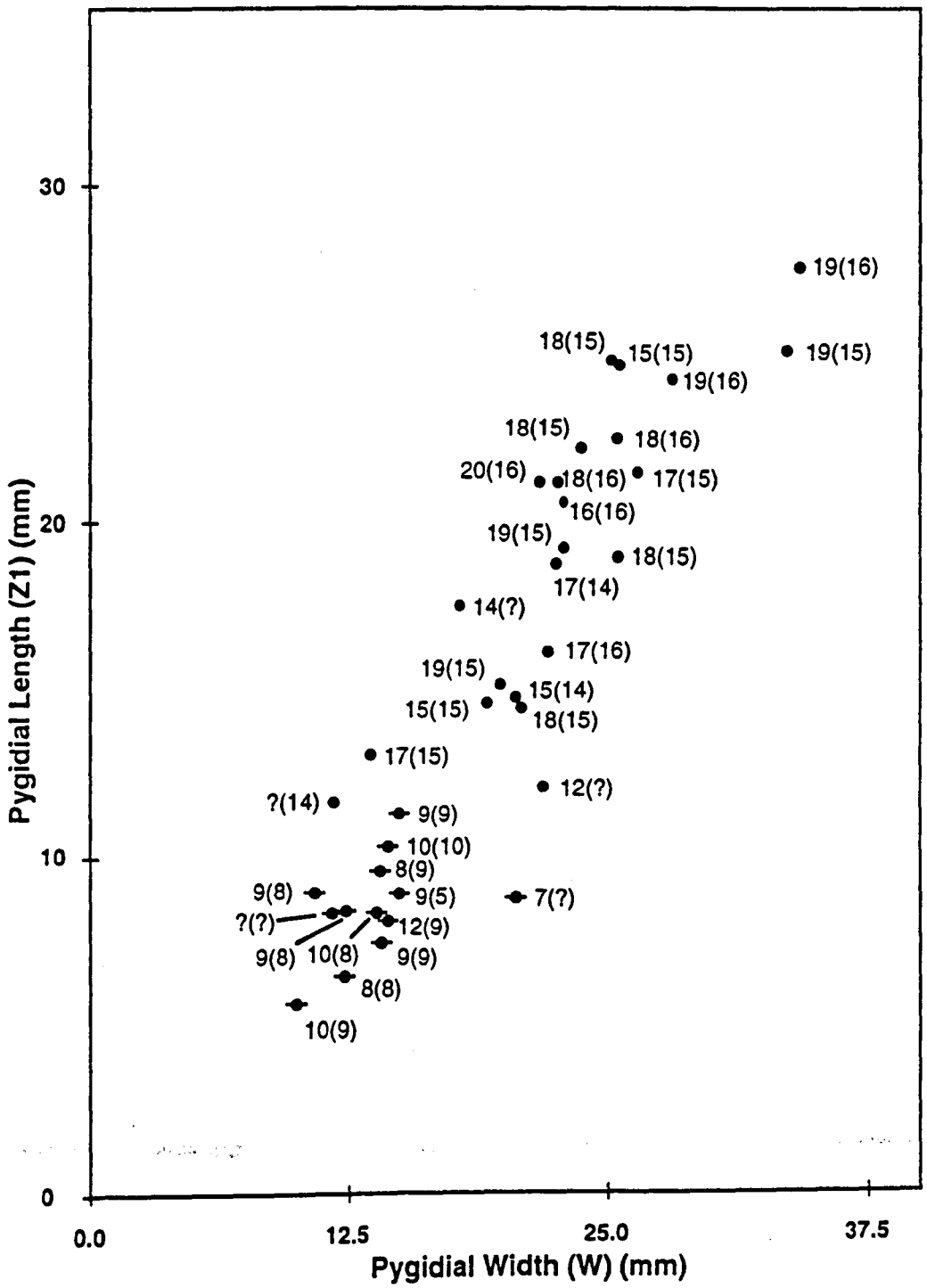

Figure 5. 29. Bivariate scatter plot of pygidial length (Z1) against pygidial width (W) for specimens from the stratigraphical samples KILLEY (circles) and QHILL (circles with bars). For each pygidium, the number of axial rings and pleural ribs (in parentheses) is given.

simply represents overall size of individual specimens (89.3% for glabellae, 90.0% for cephala, and 84.5% for pygidia). When size (represented by PC1) was dropped out of the analysis to leave just shape information, the stratigraphical samples were found to be inseparable in the resulting morphospace (Figures 5. 15, 5. 17 and 5. 20).

2. It has been demonstrated that morphometric variance in glabellae, cephala and pygidia of Cautleyan specimens (considered as a group) is relatively high (*i.e.* they occupy a broad region of morphospace) when compared with stratigraphically earlier and later specimens (Figures 5. 15, 5. 17 and 5. 20).
3. Several of the morphological variables were found to show systematic variance between the various stratigraphical samples, and this can be used to help elucidate the species-level taxonomy of the genus. Some of the variables showed discontinuities between stratigraphical samples and were therefore used in the phylogenetic analysis presented in Section 5.3. Nine species are recognised together with one form which is compared with one of the named species. The species are diagnosed using a combination of the morphometric information presented above, and the cladistic information described in Section 5.3. In stratigraphical order they are:

A. kuckersiana (Schmidt, 1881) is defined for the specimens from the KUKRUSE sample on the basis of:

(i) Possession of relatively short genal spines (Figure 5. 4). This is a synapomorphy shared with *A.* sp. A (cladistic character 10).

(ii) Preglabellar furrow which entirely circumscribes the lateral extremity of the frontal glabellar lobe (Plate 5. 1, figs. 8, 10). This is an autapomorphy for the species (cladistic character 8).

(iii) Lack of a subocular furrow (Plate 5. 1, figs. 8, 10). This is an autapomorphy for the species (cladistic character 14).

A. sp. A is defined for specimens from the KNOCK sample on the basis of:

(i) Possession of relatively short genal spines (Figure 5. 4). This is a synapomorphy shared with *A. kuckersiana* (cladistic character 10).

(ii) Relatively long postocular length (Figure 5. 6). This is an apparent reversion to the plesiomorphic state (cladistic character 15).

(iii) Central area of glabella raised above level of lateral lobes. This character state was apparently independently derived by this species and upper Ashgill species of Laurentia (cladistic character 5).

A. sp. B. This new species is defined for specimens from the FURUBERG and MJØSA samples. It is very similar to *A. kuckersiana* but may be distinguished

by:

(i) Possession of relatively long genal spines, whereas *A. kuckersiana* has short spines (Figure 5. 4) (cladistic character 10).

(ii) Anterior embayment on frontal glabellar lobe. This is the plesiomorphic state (cladistic character 4).

A. achates (Billings, 1860). Specimens from the CINC, COBOURG, HULL, VERULAM, UTICA, LORRAINE and TRENTON samples are placed together on their co-occurrence in both cephalic and pygidial morphospace (Figures 5. 15, 5. 17 and 5. 20), and on their agreement in all morphometric and most cladistic characters. The species is defined by:

(i) Long genal spines (Figure 5. 4) (cladistic character 10).

(ii) Anteriormost extremity of palpebral lobe located slightly back from the distal end of S3 lateral glabellar furrow. This is a synapomorphy shared by this species, *A. consobrina* and *A.* cf. *schmidti* (cladistic character 11).

A. sp. C. The specimens from the sample PROSSER are very similar to *A. schmidti*. *A.* sp. C is defined by:

(i) Lack of genal spines (Figure 5. 4). This synapomorphy is shared with *A. schmidti* (cladistic character 10).

(ii) Anteriormost extremity of palpebral lobe located a little behind distal extremity of S3. This character distinguishes the *A.* sp. C from *A. schmidti*. (Cladistic character 11).

A. consobrina Tripp, 1954 is defined for specimens from the KILN sample. It is indistinguishable from *A. achates* on morphometric measures, but can be distinguished on the following cladistic characters:

(i) Possessing a furrow for the posterior branch of the facial suture. This is a plesiomorphic character state (cladistic character 7).

(ii) Fixigenal sculpture of scattered small tubercles. This is a synapomorphy shared by this species, *A. achates, A. truncatocaudata, A.* cf. *truncatocaudata*, and *A. retardata* (cladistic character 9).

A. truncatocaudata Portlock, 1843 is defined for specimens from the KILLEY sample using the following characteristics:

(i) Relatively large mean size (e.g. Figures 5. 14, 5. 19).

(ii) Relatively short distal length of frontal lobe (Figure 5. 24). Mean ratio b5/B=0.42 compared with 0.47 for all other *Achatella* specimens.

(iii) Large number of lens files in the eye (Figure 5. 5). KILLEY specimens have between 32 and 36 files, compared with a range of 18-27 files for all

other *Achatella* specimens. This is an autapomorphy for the species (cladistic character 13).

(iv) Lack of a distal node on L1 lateral glabellar lobe. This is a synapomorphy shared by *A. truncatocaudata* and *A.* cf. *truncatocaudata* (cladistic character 6).

A. cf. *truncatocaudata* is defined for specimens from the sample CRINBED. It is closely similar to *A. truncatocaudata*, with which it may be conspecific. It is herein held separate on the basis of:

(i) Smaller overall size (e.g. Figure 5. 24).

(ii) Relatively longer distal length of frontal lobe (Figure 5. 24). Mean ratio b5/B=0.52, compared with 0.42 for *A. truncatocaudata.*

(iii) Inflation of the frontal lobe of the glabella. This is a synapomorphy shared by *A.* cf. *truncatocaudata* and *A. retardata* (cladistic character 3).

A. schmidti (Warburg, 1925). The single specimen from the ?BODA sample is assigned to a species of its own, defined by:

(i) Lack of genal spines (Figure 5. 4). This synapomorphy is shared with *A.* sp. C (cladistic character 10).

(ii) Anteriormost extremity of palpebral lobe opposite distal end of S3 lateral glabellar furrow (cladistic character 11).

A. retardata (Reed, 1914) is defined for specimens from the STARBED, QHILL, LANGØYENE and HIGHMAIN samples on the basis of their morphospace overlap in both cephalic and pygidial measurements (Figures 5. 15, 5. 17 and 5. 20), and on their close agreement in all morphometric and cladistic characters. The species is defined by:

(i) Inflation of the frontal lobe of the glabella. This is a synapomorphy shared by this species and *A.* cf. *truncatocaudata* (cladistic character 3).

(ii) Lack of anterior embayment to frontal lobe. This character was possibly independently derived by this species and the lower Caradoc species *A. kuckersiana* and *A.* sp. A (cladistic character 4).

(iii) Central area of glabella raised above the level of the lateral lobes (cladistic character 5).

5. 5. Systematic Palaeontology.

Family Pterygometopidae Reed, 1905
Subfamily Pterygometopinae Reed, 1905
Genus *Achatella* Delo, 1935

Emended Generic Diagnosis.
Pterygometopinae with glabella widest across frontal lobe (extending across the facial sutures) and tapering strongly rearwards. Length (exsag.) of lateral glabellar lobes: frontal lobe>L3>L2≥L1 (>Occipital ring). Low cephalic convexity, elevated occipital ring. Eyes remote from glabella with palpebral lobes raised up above level of glabella.

Type Species.
Dalmanites achates Billings, 1860 from the Cobourg Fm. (Shermanian-Edenian) of Ottawa, Ontario (see Ludvigsen and Chatterton 1982 for illustration of the holotype).

Included Species.
A. achates (Billings, 1860); *A. consobrina* Tripp, 1954; *A. kuckersiana* (Schmidt, 1881); *A. retardata* (Reed, 1914); *A. schmidti* (Warburg, 1925); *A. truncatocaudata* (Portlock, 1843); *A.* sp. nov. A; *A.* sp. nov. B; *A.* sp. nov. C.

Temporal and Geographical Range.
Llanvirn to Ashgill. Restricted to Baltica in the Llanvirn. First appearance in Laurentia in the Kirkfieldian-Shermanian (mid-upper Caradoc) of eastern North America, and Shermanian of Girvan, Scotland. One species known from early Caradoc strata within the Iapetus suture zone between Avalonia and Laurentia (Grangegeeth terrane of eastern Ireland, Owen *et al.* 1992) but no known occurrences within Avalonia itself. Continued into Ashgill in North America, and into Hirnantian in Scotland and Norway.

Remarks.
Delo (1935) erected *Achatella* for some middle and upper Ordovician trilobites from North America and Britain although, apart from the type species, he did not explicitly assign any species. His later, more complete treatment of the genus (Delo 1940) focused exclusively on forms from the interval Kirkfieldian (middle Caradoc) to Maysvillian (middle Ashgill) of eastern North America. Subsequently, further specimens belonging to Delo's species, as well as new species, were described from eastern North America (Okulitch 1942; Sinclair 1944; Wilson 1947), and new species were described from western Scotland (Tripp 1954; Harper 1981; Owen 1986) and eastern Ireland (Harper 1952; Romano 1980; Romano and Owen 1993). Some species previously assigned to *Pterygometopus* Schmidt, 1881 were reassigned to *Achatella*

(Estonian species, Männil 1958; North American species, Ludvigsen and Chatterton 1982; western Scottish and Irish species Morris and Tripp 1986, Morris 1988).

In reviewing the Pterygometopinae, Jaanusson and Ramsköld (1993) considered *Achatella* as defined by Ludvigsen and Chatterton (1982) to be a monophyletic group, albeit one which shows extraordinary (their word) variation in certain characters: length of genal spines; location of the eyes; development of the subocular, preglabellar, and lateral glabellar furrows; shape of the pygidial pleural area (see preceding two sections herein). They erected two subgenera, and assigned to the nominate subgenus the type species *A. achates, A. bailyi* (Salter, 1864) (Tramore Limestone, Llandeilian, western Ireland), *A. nieszkowskii* (Schmidt, 1881) (Rakvere Stage, northern Estonia), *A. consobrina* Tripp, 1954 (Kiln Mudstone, upper Caradoc, Girvan district), and a new species from the Mjøsa Limestone (middle to upper Caradoc, Oslo region) included herein as *A.* sp. nov. B. They also tentatively included *A. truncatocaudata* (Portlock, 1843) from the Killey Bridge Fm. (Cautleyan, Co. Tyrone), *A. retardata* (Reed, 1914) and *A. quarrelensis* (Reed, 1930) from the Upper Drummuck Gp. (Cautleyan-Rawtheyan, Girvan district). They considered this subgenus to be characterised by possession of relatively long (tr.) glabellar furrows, S2 furrows which shallow abaxially, eyes of moderate size with their anterior end located away from the axial furrow (but note that the eyes of *A. truncatocaudata* and *A. retardata* both have their anterior ends in contact with the axial furrow, see Plate 5.3, figs. 1, 3, 8, 11 and Plate 5.4, figs. 1-3), and convex to weakly concave outer portion of the pygidial pleural region. The occurrence of this subgenus, with the species tentatively included, is in upper *gracilis* to upper *anceps* Zone strata of Baltica (northern Estonia, Oslo Region) and Laurentia (eastern North America, Ireland and western Scotland). Their second subgenus, *A. (Vironiaspis)* has as its type species *A. kuckersiana* (Schmidt, 1881) (Kukruse stage, northern Estonia), with one other species, *A. kegelensis* (Schmidt, 1881) tentatively assigned. They considered this subgenus to be characterised by possession of glabellar furrows of moderate length, S2 furrow not, or only slightly, shallowing abaxially, relatively large eyes with their anterior end in contact with the axial furrow, lack of a subocular furrow, and outer portion of the pygidial pleural region distinctly concave-outward. The occurrence of this subgenus is in *teretiusculus* to *clingani* Zone strata (Uhaku to Keila stages) of northern Estonia. It has not proved possible to examine specimens of *A. kegelensis*, which is represented only by rare and fragmentary specimens (Jaanusson and Ramsköld 1993), for this study. Since this species is only tentatively assigned to the subgenus by Jaanusson and Ramsköld, *A. (Vironiaspis)* is essentially defined for a single species in a genus which is known to display abundant variation in certain characters. It seems to this author that one could just as easily erect a subgenus to include *A. kuckersiana* and *A.* sp. nov. B on the basis of their relatively short genal spines and lack of anterior embayment on the frontal lobe.

It therefore seems more appropriate to view *A. kuckersiana* as one species in a genus which shows wide variation in "peripheral characters" and not single it out by raising it to the level of subgenus in the absence of better supporting evidence from *A. kegelensis.*

Species not explicitly considered. It has not proved possible to examine specimens of *A. kegelensis* (Schmidt, 1881) from the Keila Stage (middle Caradoc) of northern Estonia (see above). Neither has it been possible to include specimens of *A. nieszkowskii* (Schmidt, 1881) from the Rakvere Stage (upper Caradoc) of northern Estonia. The original specimens of *A. bailyi* (Salter, 1864) from the Tramore Limestone (Llandeilian) cannot now be traced and no other material unequivocally attributable to *Achatella* has been collected from the formation, although the pterygometopid *Estoniops* is very common (A. W. Owen, pers comm.). The generic assignment of Salter's species must therefore remain uncertain.

In the following section, the type species is described first, followed by a description of the other species in stratigraphical order.

Achatella achates (Billings, 1860)

Plate 5.1, figs. 1-7.

1860 *Dalmanites achates* Billings, p. 63, fig. 9.
1873 *Dalmanites carleyi* Meek, p. 170, pl. 14, figs. 2a-d.
1897 *Dalmanites achates* Billings; Clarke, p. 726, fig. 44.
1919 *Dalmanites achates* Billings; Foerste, p. 397, pl. 19, figs. 8, 18a.
1921 *Dalmanites achates* Billings; Raymond, p. 38, pl. 11, fig. 3.
1930 *Dalmanites katherina* Bradley, p. 286, pl. 30, figs. 19-28.
1935 *Achatella achates* (Billings); Delo, p. 416, figs. 38-39.
1940 *Achatella achates* (Billings); Delo, p. 110, pl. 13, figs. 19-21.
1942 *Achatella achates* (Billings); Okulitch, p. 104, pl. 1, fig. 1.
1944 *Achatella billingsi* Sinclair, p. 17, pl. 1, figs. 1-2.
1947 *Achatella achates* (Billings); Wilson, p. 60, pl. 10, fig. 16.
1947 *Pterygometopus billingsi* (Sinclair); Wilson, p. 55, pl. 10, figs. 4a-b.
1978 *Achatella achates* (Billings); Ludvigsen, pl.5, fig. 47.
1979 *Achatella achates* (Billings); Ludvigsen, fig. 47A-B.
1982 *Achatella achates* (Billings); Ludvigsen & Chatterton, p. 2183, pl. 1, figs. 1-7; Fig. 3.

Holotype.
A flattened complete individual (GSC 1784) from the Cobourg Fm., Ottawa, Ontario. Refigured by Ludvigsen and Chatterton (1982: pl. 1, fig. 1).

Occurrence.

Verulam and Cobourg formations (Shermanian-Edenian), Ontario and Québec; Trenton Group (Shermanian), New York; Lorraine Group (Edenian-Maysvillian), Tennessee; Utica Shale and Fairmount Shale (Shermanian-Maysvillian), Ohio; Kimmswick Limestone (Edenian), Missouri and Illinois.

Material.

Two complete individuals (the holotype specimen and one from the Trenton Limestone, New York), 23 other cephala and cranidia and 12 pygidia, from Verulam Fm., Ontario, Trenton Limestone, New York, Lorraine Gp., Tennessee, Utica Shale and Fairmount Shale, Ohio.

Emended Diagnosis.

Anterior embayment on frontal glabellar lobe; posterior branch of the facial suture lacking a furrow; long, slender genal spines of length approximately equal to sagittal cranidial length; anterior-most point of the palpebral lobe located slightly away from the axial furrow and slightly behind the distal extremity of the S3 lateral glabellar furrow; eye with 18-23 dorso-ventral files with up to 10 lenses each; pygidium with 10-14 axial rings and 10-12 pleural ribs.

Description.

Cephalon semicircular in outline, with a wide lateral border delimited by a sharp break in slope. Glabella narrowest (tr.) across L1, widest (tr.) across frontal lobe. Occipital ring oval, mesially vaulted to a level higher than the midline of the glabella. Width (tr.)/length (sag.) ratio about 3.2. Occipital furrow moderately impressed mesially, deeper abaxially. L1 lobes rectangular or close to rectangular, combined width (*i.e.* total tr. width of glabella across L1, measured from left axial furrow to right axial furrow) / length (exsag.) ratio about 5.0. A distal node to L1 is defined by a shallow, posteriorly-directed branch of the S1 lateral glabellar furrow (Plate 5.1, figs. 1, 3 and 5), which does not reach the occipital furrow. S1 deep, directed approximately transversely, slightly concave-forwards and extending inwards to about one third of the glabellar width. L2 lobes approximately rectangular in shape, combined width (tr.) / length (exsag.) ratio about 7.5. S2 furrow deep proximally, shallowing abaxially, innermost end about one third of the glabellar width in from the axial furrow. S2 directed abaxially rearwards at an angle of about 108° to the sagittal line (measured in the forward quadrant). L3 lobes approximately triangular. Combined width (tr.) / length (exsag.) ratio about 3.4. All lateral lobes confluent with central area of the glabella. S3 deep proximally, shallowing slightly abaxially, then deepening rapidly into deep pit where it intersects the axial furrow. S3 directed abaxially forwards at an angle

of 74° to the sagittal line. Frontal lobe oval, width (tr.) / length (sag.) ratio about 2.5. Anterior of frontal lobe bears muscle attachment pits in a shallowly impressed "V" formation (Plate 5.1, figs. 4, 5). Pronounced anteromedial embayment ("anterior embayment") in frontal lobe, commonly enhanced by slight forward projection of median part of frontal lobe between the muscle insertion pit lines (Plate 5.1, figs. 4, 5). Lateral projection of frontal lobe continues beyond facial suture to form the "transsutural wing" of Jaanusson and Ramsköld (1993), which is short (Plate 5.1, fig. 2). Preglabellar furrow moderately deep anteromesially, dying out laterally (Plate 5.1, fig. 2). Axial furrows moderately deep, shallowest adjacent to S3. Posterior border furrows deepen and widen abaxially. Anterior branch of facial suture lies in front of preglabellar furrow and cuts across lateral wings of the frontal glabellar lobe (see above), intersecting the axial furrows at the deep pit at the distal end of S3. Posterior branch of facial suture not confined in a furrow, reaches lateral border furrow opposite L1. Eyes tall, turret-like, delineated basally by deep, narrow furrow ("subocular furrow" of Jaanusson and Ramsköld 1993). Palpebral lobe steeply sloping, tightly curved with deep palpebral furrow (Plate 5.1, fig. 4). Anteriormost extremity of palpebral lobe located close to, but not in contact with, axial furrow, slightly to posterior of distal end of S3 (Plate 5.1, figs. 4, 5). Posteriormost point located opposite L2 or slightly further back. Visual surface has 18-23 dorso-ventral files of up to 10 lenses per file, in hexagonal packing (Figure 5. 5). Genal spines long and slender, posteriorly-directed, length approximately equal to sagittal cranidial length (Plate 5.1, fig. 5). Sculpture of scattered small tubercles on the glabella (Plate 5.1, figs. 1-5, 7), usually fine pits on the field of the fixigena, although specimens from the Lorraine Formation bear a coarse granulation similar to that on the glabella.

Hypostome unknown.

Thorax of 11 segments. Axial furrows moderately deep, axial width about one third total thoracic width. Pleural furrows moderately impressed, directed laterally and curving posterolaterally about half way along their length, extending almost to the margin.

Pygidium (Plate 5.1, fig. 6) triangular in outline with length/width ratio about 0.7. Margins slightly convex-outward in dorsal view. Very shallow marginal furrow, lateral surface concave-upward when pygidium is viewed from the posterior. Axis widest anteriorly, where it is about one third of maximum pygidial width, tapering uniformly rearward. Axis of 10-14 axial rings separated by deep ring furrows. Rings becoming indistinct in posterior terminal piece. Axial furrows moderately deep. Pleural regions with 10-12 pleural ribs. Interpleural furrows deep and wide, extending laterally to marginal furrow. Pleural furrows shallow though still distinct, becoming obsolete just

before reaching the marginal furrow. External surface of pygidium smooth.

Remarks.
Ludvigsen and Chatterton (1982) considered *A. katherina* (Bradley, 1930) and *A. billingsi* (Sinclair, 1944) to be junior synonyms of *A. achates*. They reserved judgement on the status of Meek's (1873) species from the Cincinnatian of Ohio, not having had access to type specimens or adequate photographs. Specimens of Meek's species have been examined in the course of this study, and due to its similarity with *A. achates* specimens, it is herein considered to be a junior synonym of the type species.

Two types of fixigenal sculpture are displayed by the specimens considered to belong to this species. Most specimens have fine pits (Plate 5.1, figs. 1-2). Those from the Lorraine Formation however (USNM43063/1, USNM43063/2) bear a coarse granulation similar to that on the glabella. This is not considered to be a preservational feature. However, since the Lorraine Fm. specimens agree with the other *A. achates* material in all other characteristics, they are herein included in that species.

In specimens belonging to some of the stratigraphical samples studied (those from the Cobourg Fm., Trenton Limestone in New York, and Verulam Fm.) the posterior extremity of the palpebral lobe is located opposite the L2 lateral glabellar lobe (Plate 5.1, fig. 4), while in the other specimens, it is opposite the anterior portion of L1. Since the specimens exhibiting this variation agree with all other specimens of *A. achates* in all other characteristics, this variation alone is not considered sufficient to warrant a new species or subspecies.

Achatella kuckersiana (Schmidt, 1881)

Plate 5.1, figs 8-14; Figure 5. 30.

1881 *Phacops (Pterygometopus) kuckersianus* Schmidt, p. 90, pl. 5, figs. 11-13; pl. 11, fig. 7; pl. 12, figs. 16-18.

1993 *Achatella (Vironiaspis) kuckersiana* (Schmidt); Jaanusson and Ramsköld, p. 766, pl. 5, figs. 2-3.

Occurrence.
Kukruse Stage (C2) of northern Estonia (basal Caradoc).

Material.
Four cephala (including one with eyes preserved) and three pygidia.

Emended Diagnosis.

No anterior embayment on the frontal glabellar lobe; posterior branch of facial suture confined in a furrow; preglabellar furrow present both anteriorly and laterally of frontal lobe; short genal spines, length equal to about half the sagittal cranidial length; anteriormost extremity of palpebral lobe in contact with axial furrow adjacent to distal end of S3 furrow; posteriormost extremity of palpebral lobe opposite L1; visual surface with 22 lens files of up to 12 lenses each; no subocular furrow present at the base of the visual surface; pygidium with 10-14 axial rings, 9-13 pleural ribs.

Remarks.

A. kuckersiana is very similar to the type species and differs in only a few characteristics. The V-shaped pattern of muscle insertion pits in the frontal glabellar lobe is faint, though still present, and there is no anterior embayment (Plate 5.1, figs. 8, 14). The preglabellar furrow is deep and continues around the lateral extremities of the frontal lobe to meet the axial furrow (Plate 5.1, fig. 10). The posterior branch of the facial suture is contained within a narrow but distinct furrow, and it meets the lateral border furrow opposite the anterior portion of the L2 lateral glabellar lobe (Plate 5.1, fig. 10).

The lack of a subocular furrow basally delineating the eye (Plate 5.1, figs. 8, 10, also Figure 5. 30; compare Plate 5.2 figs. 1-2) is unique in *Achatella* or any other pterygometopine. Jaanusson and Ramsköld (1993) used this as an important character in the diagnosis of their new subgenus *A. (Vironiaspis)*, but this subgenus is not supported herein (see remarks above).

The genal spines of this species are much shorter than those in the type species, only having a length equal to about half the sagittal cranidial length (Plate 5.1, figs. 13-14; see also Figure 5. 4). The cephalic sculpture is similar to that exhibited by most specimens of *A. achates, i.e.* small scattered tubercles on the glabella and fine pits on the fixigenae (Plate 5.1, figs. 8, 10, 13-14). The hypostome and thorax of this species are unknown. The pygidium is very similar to that of *A. achates* (Plate 5.1, figs. 9, 11-12). There are 10-14 axial rings and 9-13 pleural ribs. The lateral surfaces are noticeably concave-upwards when seen in posterior view. There is no obvious sculpture.

***Achatella* sp. nov. A**

Plate 5.2, figs. 1-2.

1952 *Achatella* sp.; Harper, pl. 5, fig. 5.

1980 ?*Achatella* cf. *truncatocaudata* (Portlock); Romano, p. 67.

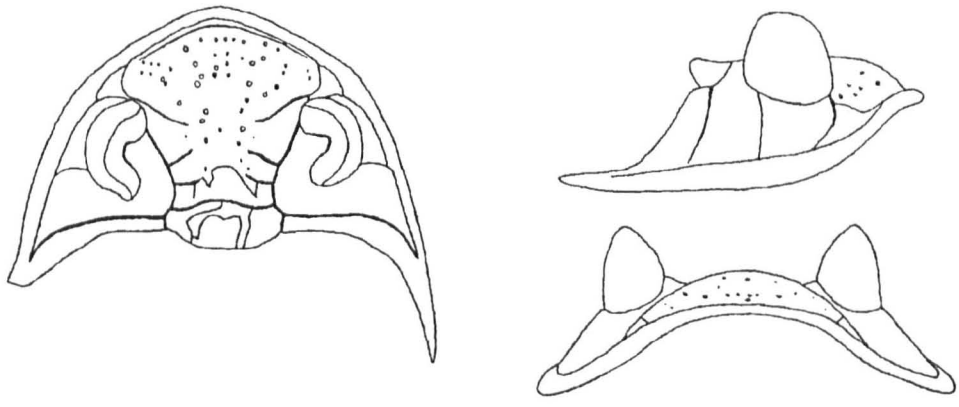

Figure 5. 30. *Achatella kuckersiana* (Schmidt, 1881). Dorsal, lateral and anterior views of cephalon. RM Ar50493. Viivikonna Fm., Kukruse Stage (*gracilis* Zone). Kukruse, northeastern Estonia. x6.

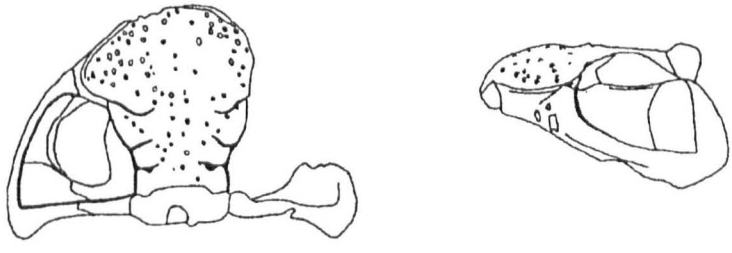

Figure 5. 31. *Achatella schmidti* (Warburg, 1925). Dorsal and lateral views of holotype cephalon. PMU D189, probably from Boda Fm. (Ashgill, post *linearis* Zone), Osmundsberget, Siljan district, Sweden. x4.

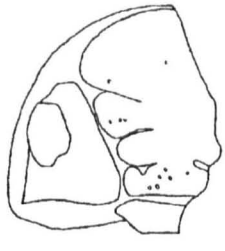

Figure 5. 32. *Achatella* sp. nov. C. Dorsal view of damaged cephalon. USNM 79028/2. Prosser Fm. (Shermanian). Duck Creek Quarry, Wisconsin, US. x4.

1993 *Achatella truncatocaudata* ? (Portlock); Romano and Owen, p. 711, text-fig. 5A-F.

Occurrence.
Knockerk House Sandstone Member of the Knockerk Formation (lower Caradoc), Grangegeeth district, eastern Ireland.

Material.
Two cephala (one very poorly preserved). Thorax, pygidium and hypostome unknown.

Diagnosis.
No anterior embayment on the frontal glabellar lobe; central body of glabella raised to a level slightly above the lateral glabellar lobes; posterior branch of facial suture confined in a furrow; genal spines short, of a length equal to about half the sagittal cranidial length; anteriormost extremity of palpebral lobe in contact with the axial furrow opposite the distal end of the S3 glabellar furrow; posteriormost extremity of palpebral lobe opposite anterior portion of L2 lateral glabellar lobe; visual surface with 23-27 dorso-ventral lens files of up to 12 lenses each.

Remarks.
In several respects, this species is closer to *A. kuckersiana* than to *A. achates* : there is no anterior embayment on the frontal glabellar lobe; the posterior branch of the facial suture is contained within a distinct furrow, meeting the lateral border furrow opposite S1; the genal spines are short (see Figure 5. 4); the anteriormost point of the palpebral lobe is adjacent to the distal end of S3 rather than behind it as in *A. achates*. Characteristics of this species which differ from both the type species and *A. kuckersiana* are the central area of the glabella which is raised to a level above the lateral lobes (Plate 5.2, fig. 2), and the unusually short (exsag.) length of the eyes, the posterior extremity of the palpebral lobe being opposite L2 (Plate 5.2, fig. 1; see also Figure 5. 6).

Romano (1980) and Romano and Owen (1993) compared this form to *Achatella truncatocaudata* (Portlock). However a number of characteristics distinguish this species from Portlock's: the lack of an anterior embayment to the frontal glabellar lobe; presence of a distal node on L1; presence of a furrow confining the posterior branch of the facial suture; relatively much shorter genal spines; relatively shorter eyes, with their anteriormost extremities located further back than those of *A. truncatocaudata* (which are unusually far forward - see below) and their posteriormost extremities located much further forwards. The limited evidence of the number of lenses in the visual surface of the Grangegeeth species (from two specimens) suggests that it has far fewer dorso-

ventral files than *A. truncatocaudata.*

Achatella sp. nov. B

Plate 5.1, fig. 15; Plate 5.2, figs. 3-7.

1910 *Pterygometopus kuckersianus* (Schmidt); Holtedahl, p. 36.
1953 *Pterygometopus kuckersianus* (Schmidt); Størmer, p. 104.
1993 *Achatella* (*Achatella*) n. sp. Jaanusson & Ramsköld, p. 765.

Occurrence.
Furuberget and Mjøsa formations (mid-upper Caradoc), Mjøsa district, Norway.

Material.
Two damaged cephala from the lower Furuberget Fm. at Furuberget, one cephalon from the upper Furuberget Fm. at Furuberget, one cephalon from the lower Mjøsa Fm. at Furuberget, and one cephalon and one pygidium from the lower Mjøsa Fm. at Bergevika.

Diagnosis.
Anterior embayment on frontal glabellar lobe; furrow for posterior branch of facial suture; long, slender genal spines of length approximately equal to sagittal cranidial length; anteriormost point of palpebral lobe in contact with axial furrow opposite S3; posteriormost point of palpebral lobe opposite L1.

Remarks.
The species is very similar to *A. kuckersiana.* It differs in possessing an anterior embayment on the frontal glabellar lobe, long genal spines (Plate 5.1, fig. 15; see also Figure 5. 4), a preglabellar furrow which is developed only anteriorly (Plate 5.2, figs. 4, 7), and a subocular furrow (Plate 5.2, figs. 3, 4).

The hypostome and thorax are unknown and only a single pygidium was available for study. It has 11 axial rings and 9 pleural ribs, and is very similar to that of *A. kuckersiana.*

Achatella consobrina Tripp, 1954

Plate 5.2, figs. 8-16.

1954 *Achatella consobrina* Tripp, p. 683, pl. 4, figs. 26-33.
1980b *Achatella consobrina* Tripp; Tripp, table 1.
1982 *Achatella consobrina* Tripp; Ludvigsen & Chatterton, p.2183.

1988 *Achatella consobrina* Tripp; Morris, p. 11.

Holotype.
External mould of cephalon (HMA 3946) from the Kiln Mudstone, Craighead Formation (approximately Marshbrookian), Girvan. Figured by Tripp (1954: pl. 4, fig. 26).

Occurrence.
Only known from the type locality and horizon.

Material.
Six cephala, a number of thoracic segments, five pygidia and two hypostomes.

Emended Diagnosis.
Frontal lobe of glabella with an anterior embayment; weakly-developed furrow for the posterior branch of the facial suture; sculpture of scattered small tubercles on the fixigenae; long slender genal spines of length approximately equal to the sagittal cranidial length; anteriormost extremity of palpebral lobe away from the axial furrow and located a little behind the distal end of S3; posteriormost extremity of the palpebral lobe located opposite L1; eye with 20-23 files of up to 12 lenses per file; pygidium with 12-14 axial rings and 11-14 pleural ribs.

Remarks.
This species is very similar to the type species. The differences are the presence of a weakly developed furrow for the posterior branch of the facial suture (Plate 5.2, figs. 14-15), and the tuberculate fixigenal sculpture (Plate 5.2, figs. 8, 14). The location and size of the eye is similar to that in the type species.

A number of hypostomes are known for *A. consobrina* (Plate 5.2, figs. 9, 13; this sclerite is unknown for the type species *A. achates*). The middle body of the hypostome is moderately convex, and the width (tr.) measured across the middle body is about 0.7 times the sagittal length. The middle body is cut laterally by middle furrows about half way along its length, which extend in for about 1/4 of the width (tr.) of the hypostome, and are posteromedially directed. These furrows define a crescentic, slightly swollen posterior region. The lateral borders are narrow, widening posterolaterally. The anterior wings are relatively large and triangular, curving backwards. The hypostome's width (tr.) measured across the anterior wings is about 1.5 times its sagittal length. The sculpture is of fine granules with scattered faint tubercles.

The thorax is very like that of the type species, as is the triangular pygidium which has

a length/width ratio of about 0.8. The faintly impressed pleural furrows have a single row of small tubercles along their anterior and posterior margins (Plate 5.2, fig. 12). A sculpture of small tubercles is also developed on the axis. In this respect this species differs from *A. achates*, which does not show pygidial sculpture.

Achatella truncatocaudata (Portlock, 1843)

Plate 5.3, figs. 1-7.

1843 *Paradoxides ? Bucephali* var.; Portlock, p. 258, pl. 1, fig. 8.
1843 *Phacops truncato-caudatus* Portlock, p. 281, pl. 2. figs. 1-6.
1864 *Phacops (Chasmops) truncato-caudatus* Portlock; Salter, p. 42, pl. 4, figs. 13, ?14, 15.
1952 *Phacops (Achatella) truncato-caudatus* Portlock; Reed, p. 121.
1980 *Achatella truncatocaudata* (Portlock); Tunnicliff, pp. 42, 48.
1988 *Achatella truncatocaudata* (Portlock); Morris, p. 11.

Lectotype.
BGS GSM 19195 selected by Morris (1988), Lower Killey Bridge Fm, Cautleyan (probably from the Little River). Pomeroy district, Co. Tyrone, N. Ireland.

Occurrence.
Only known from the type horizon.

Material.
Fourteen cephala and cranidia, one with thorax present, 53 pygidia, five hypostomes.

Emended Diagnosis.
Frontal glabellar lobe possessing an anterior embayment; central area of glabella inflated to a level higher than the lateral glabellar lobes; no distal node on L1; no furrow for posterior branch of facial suture; anteriormost extremity of palpebral lobe in contact with the axial furrow opposite distal end of S3; posteriormost extremity opposite L1; visual surface with 32-36 files of up to 15 lenses per file; frontal glabellar lobe short (exsag.) compared with other species of the genus; pygidium with 13-19 axial rings and 13-16 pleural ribs.

Remarks.
Specimens of this species are commonly larger than those of any of the other species of the genus: the mid-palpebral width of *A. truncatocaudata* can be up to 30mm, as opposed to maximum mid-palpebral widths of 20mm (more commonly around 15mm) for the other species (see figure 5. 14).

The frontal glabellar lobe in *A. truncatocaudata* is unusually short (exsag.) as demonstrated in Section 5. 4 (see Figure 5. 24); the mean ratio of distal length of frontal lobe b5 / preoccipital glabellar length B is about 0.42, compared with about 0.47 for other species of *Achatella*. Since the anterior of the palpebral lobe is opposite S3, the anterior of the eye is also unusually far forward (Figure 5. 22). The visual surface is composed of far more lenses than in any other species of *Achatella*, having 32-36 files of up to 15 lenses each (Figures 5. 5, 5. 25).

The thorax and hypostome resemble those of *A. consobrina* (Plate 5.3, fig. 2).

The pygidium differs from other *Achatella* species in its size and unusually high number of segments (Plate 5.3, figs. 4, 7; see also Figures 5. 19 and 5. 28): there are 13-19 axial rings and 13-16 pleural ribs. In other respects, the pygidium is similar to that of *A. consobrina*, having a similar length/width ratio and similar sculpture: small tubercles on the axis, and a single row of tubercles along the anterior and posterior margins of the faint pleural furrows (Plate 5.3, fig. 7).

Achatella cf. *truncatocaudata*

Plate 5.3, fig. 10.

Occurrence.

Restricted to the "Crinoid Bed" of the upper part of the Quarrel Hill Formation (upper Cautleyan, Harper 1982), Girvan district.

Material.

Two incomplete cranidia.

Remarks.

This form is represented by only two incomplete cranidia, and its status is unclear. It agrees in a number of respects with *A. truncatocaudata* : it possesses an anterior embayment, inflated glabellar central area, and lacks a distal node on L1. There is a slight inflation of the frontal glabellar lobe which is not seen in *A. truncatocaudata*, although it is possible that specimens of the latter species are slightly crushed. Other characteristics show a closer agreement with *A. consobrina* : the relatively small size; the ratio of the distal length of the frontal lobe b5 to the preoccipital glabellar length B is around 0.52; also a fragmentary specimen of an eye suggests that the visual surface has only 23 dorso-ventral lens files, compared with 32-36 for *A. truncatocaudata*.

Although this species occurs in the Crinoid Bed of the Quarrel Hill Formation, within

the stratigraphical range of *A. retardata*, the characters described above show that it is not assignable to that species. Rather, it shows a mixture of characters of *A. truncatocaudata* and *A. retardata* (see also Section 5. 3, and Figure 5. 7). The status of this species is therefore left open, with the suggestion that it is either conspecific with *A. truncatocaudata*, or an intermediate form between that species and *A. retardata*.

***Achatella retardata* (Reed, 1914)**

Plate 5.3, figs. 8-9, 11-15; Plate 5.4, figs. 1-10.

1914 *Phacops (Pterygometopus) retardatus* Reed, p. 49, pl. 8, figs. 5-7.
1930 *Phacops (Pterygometopus) quarrelensis* Reed, p. 197, pl. 10, figs. 3, 3a.
1931 *Phacops (Pterygometopus) quarrelensis* Reed; Reed, p. 24.
1943 *Phacops (Pterygometopus) retardatus* Reed; Begg, p. 60, pl. 2, fig. 10.
1981 *Achatella* sp.; Harper, p. 352, pl. 1, figs. 1-3.
1986 *Achatella retardata* (Reed); Morris & Tripp, p. 172, pl. 4, fig. 2.
1986 *Achatella* cf. *truncatocaudata* (Portlock); Owen, p. 234, fig. 2a-e.
1988 *Achatella retardata* (Reed); Morris, p. 11.
1988 *Achatella quarrelensis* (Reed); Morris, p.11.

Lectotype.

BMIn 23603 selected by Morris and Tripp (1986), from the Starfish Beds, South Threave Fm., (Rawtheyan), South Threave Farm, Girvan. Figured by Reed (1914: pl. 8, figs. 5, 5a-b). Refigured by Morris and Tripp (1986: pl. 4, fig. 2).

Occurrence.

Quarrel Hill and South Threave formations, Drummuck Group (upper Cautleyan and Rawtheyan), and High Mains Formation (Hirnantian), Girvan district; Langøyene Formation (Hirnantian), Skien-Langesund district, Norway.

Material.

Two cephala and 15 pygidia from the Quarrel Hill Fm.; seven cephala and cranidia, and eight pygidia from the Starfish Beds, South Threave Fm.; three cranidia and five pygidia from the High Mains Fm.; a single cranidium and pygidium from the Langøyene Fm.

Emended Diagnosis.

Inflated frontal glabellar lobe; no anterior embayment; central area of glabella inflated to a level greater than the lateral lobes; no furrow for posterior branch of facial suture; fixigenae with sculpture of scattered tubercles; anteriormost extremity of palpebral lobe in contact with axial furrow opposite distal end of S3; posteriormost extremity of

palpebral lobe opposite L1; eyes with 21-26 files containing up to 12 lenses per file; pygidium with 7-14 axial rings and 5-13 pleural ribs.

Remarks.

Achatella quarrelensis (Reed, 1930) from the Quarrel Hill Fm., Girvan, *A.* cf. *truncatocaudata* from the High Mains Fm. (Owen 1986), Girvan, and *Achatella* sp. from the Langøyene Fm. of the Skien-Langesund district, Norway, are here considered to be junior synonyms of *A. retardata.* There are no differences among these specimens that cannot be attributed to preservation (see also Section 5. 3, and Figure 5. 7).

A. retardata differs from *A. achates* in the following characters: the marked inflation of the frontal glabellar lobe; faint development of the muscle insertion pits on the frontal lobe; lack of an anterior embayment; inflation of the central area of the glabella (Plate 5.3, figs. 8, 14; Plate 5.4, figs. 1, 3-4, 8, 10); sculpture of small tubercles on the fixigenae reminiscent of *A. consobrina* (Plate 5.3, fig. 15); location of the anterior of the palpebral lobe opposite S3 (Plate 5.3, fig. 8; Plate 5.4, figs. 1-3).

The pygidium is triangular with a length / width ratio of about 0.66, relatively shorter and wider than other *Achatella* species (see Figure 5. 19). The axis has 7-14 axial rings and 5-13 pleural ribs. A single anomalous pygidium is known from mudstones of the Quarrel Hill Fm. at Glenmard Quarry, which has 19 axial rings and 14 pleural ribs.

Achatella schmidti (Warburg, 1925)

Plate 5.3, figs. 16-17; Figure 5. 31.

non 1894 *Pterygometopus schmidti* Clarke, p. 729, fig. 50.
1925 *Pterygometopus schmidti* Warburg, p. 396, pl. 11, figs. 27-28.
1993 *Pterygometopus schmidti* Warburg; Jaanusson and Ramsköld, p. 765, pl. 5, figs. 4a-b.

Holotype.

Damaged cephalon (PMU D189), probably from the Boda Formation at Osmundsberg, but possibly from the Kullsberg Formation at Sinksjön (see Warburg 1925). Figured by Warburg (1925: pl. 11, figs. 27-28). Refigured by Jaanusson and Ramsköld (1993: pl. 5, figs. 4a-b) and herein (Plate 5. 3, figs, 16-17).

Occurrence.

Only known from the holotype specimen.

Emended Diagnosis.

Anterior embayment present; no furrow for posterior branch of facial suture; anteriormost extremity of palpebral lobe in contact with axial furrow opposite S3; posteriormost extremity of palpebral lobe opposite L1; no genal spines.

Remarks.

This species bears a close resemblance to *A. achates*. It differs in having the anterior of the palpebral lobe opposite S3, being relatively narrower, and lacking genal spines (Plate 5.3, fig. 17). This is clearly an original feature of the animal and is not due to incomplete preservation (Plate 5.3, fig. 16). The eyes are not preserved on the single specimen known, but judging by the location of the subocular furrow and the trace of the posterior branch of the facial suture, they were probably of a comparable size to those in *A. retardata.*

This specimen is considered to belong in *Achatella* due to its close agreement in all characteristics, except its lack of genal spines, with that genus.

***Achatella* sp. nov. C**

Figure 5. 32.

Occurrence.

Restricted to the Prosser Fm. (approx. Shermanian) at Duck Creek Quarry, Wisconsin.

Material.

Two fragmentary cranidia.

Remarks.

These two cranidia (USNM79028/1, USNM79028/2) are similar to *A. schmidti* in all respects (including the lack of genal spines) except that the anteriormost extremity of the palpebral lobe is slightly behind the distal end of S3 rather than opposite it. The visual surface has 22 lens files. Because of incomplete preservation of the eyes it is not known how many lenses are in each lens file. The status of these two specimens is left open with the note that it is unlikely to be resolved unless better specimens of this form become available. They are held apart from *A. schmidti* on the basis of the geographical and stratigraphical separation.

5. 6. Conclusions.

The known stratigraphical durations and suggested phylogeny of the nine species and one form under open nomenclature of *Achatella* recognised herein are shown in Figure 5. 33. The total duration of the genus is from the Llandeilian (Uhaku Stage,

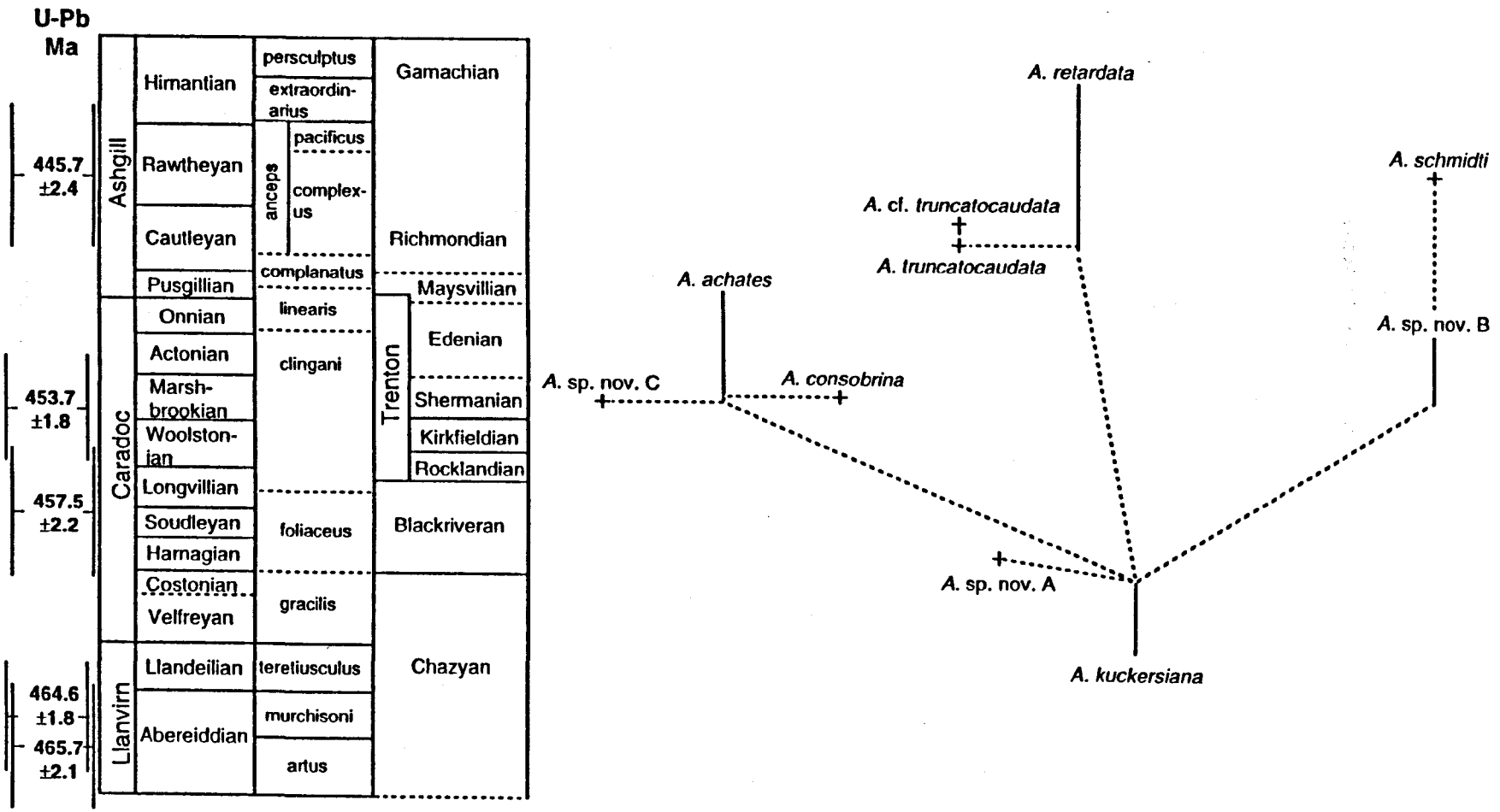

Figure 5. 33. Stratigraphical relationships, durations and suggested phylogeny of the species of *Achatella* recognised herein. Crosses indicate species known from only a single horizon. Stratigraphy and U-Pb dates as in Figure 5. 2.

teretiusculus Zone of northern Estonia; Jaanusson and Ramsköld 1993) to the Hirnantian (High Mains Fm., Girvan district; Owen 1986), a duration of approximately 22 myr. Several of the species are only known from single horizons. The longest ranging species is *A. retardata* which has a duration of approximately 6 myr, from the Quarrel Hill Fm. (Cautleyan) to the High Mains Fm. (Hirnantian), both in the Girvan district.

On Figure 5. 33, the suggested phylogenetic relationships within *Achatella* are based on the cladistic analysis presented in Section 5. 3 (see in particular the discussion of phylogenetic conclusions, pp. 82-83). The species are grouped in Figure 5. 33 according to their groupings on the cladogram (Figure 5. 9); *i.e.* early Caradoc "*kuckersiana* - type" species from Estonia and eastern Ireland (*A. kuckersiana* and *A.* sp. A), characterised by short genal spines and the lack of a mesial anterior embayment on the frontal glabellar lobe; middle and upper Caradoc "*achates* - type" species (*A. achates*, *A.* sp. C, *A. consobrina*) of Laurentia characterised by the presence of an anterior embayment on the frontal lobe, frontal and lateral glabellar lobes which are confluent with the middle area of the glabella, and anteriormost point of palpebral lobe which is set slightly behind the distal extremity of S3; middle to upper Caradoc *A.* sp. B from Norway which is very similar to the "*achates* - type" except in having the anterior of the eye opposite the distal end of S3; *A. schmidti* from the Boda Limestone which is similar to *A.* sp. B but with the genal spines secondarily lost; the Cautleyan variants *A. truncatocaudata* and *A.* cf. *truncatocaudata* which are similar to the "*achates* - type" species except in having relatively longer (exsag.) eyes with their anteriormost extremity located opposite the distal end of S3, an independent convexity to the central area of the glabella, and no distal node on L1; the Rawtheyan and Hirnantian *A. retardata*, characterised by its inflated frontal lobe lacking an anterior embayment, inflated central area of the glabella, and anteriormost point of the palpebral lobe which is opposite the distal end of S3. Each group of species on Figure 5. 33 contains species which occur geographically relatively close together, so that the horizontal distribution of species on the figure is close to a representation of the geographical relationships between the species. This is made explicit in Figure 5. 34.

The most characteristic feature of the phylogeny of the genus is its mosaic pattern of evolution, with many convergences between different species which gives rise to a poorly resolved consensus tree (see Figures 5. 9 and 5. 10). Few of the species can be diagnosed by the possession of unequivocal apomorphies; rather they are recognised on unique patterns of possession of suites of character states. This state also holds true for two other long duration, highly shape conservative genera, *Calyptaulax* Cooper, 1930 and *Acernaspis* Campbell, 1967 (see Chapters 6 and 7).

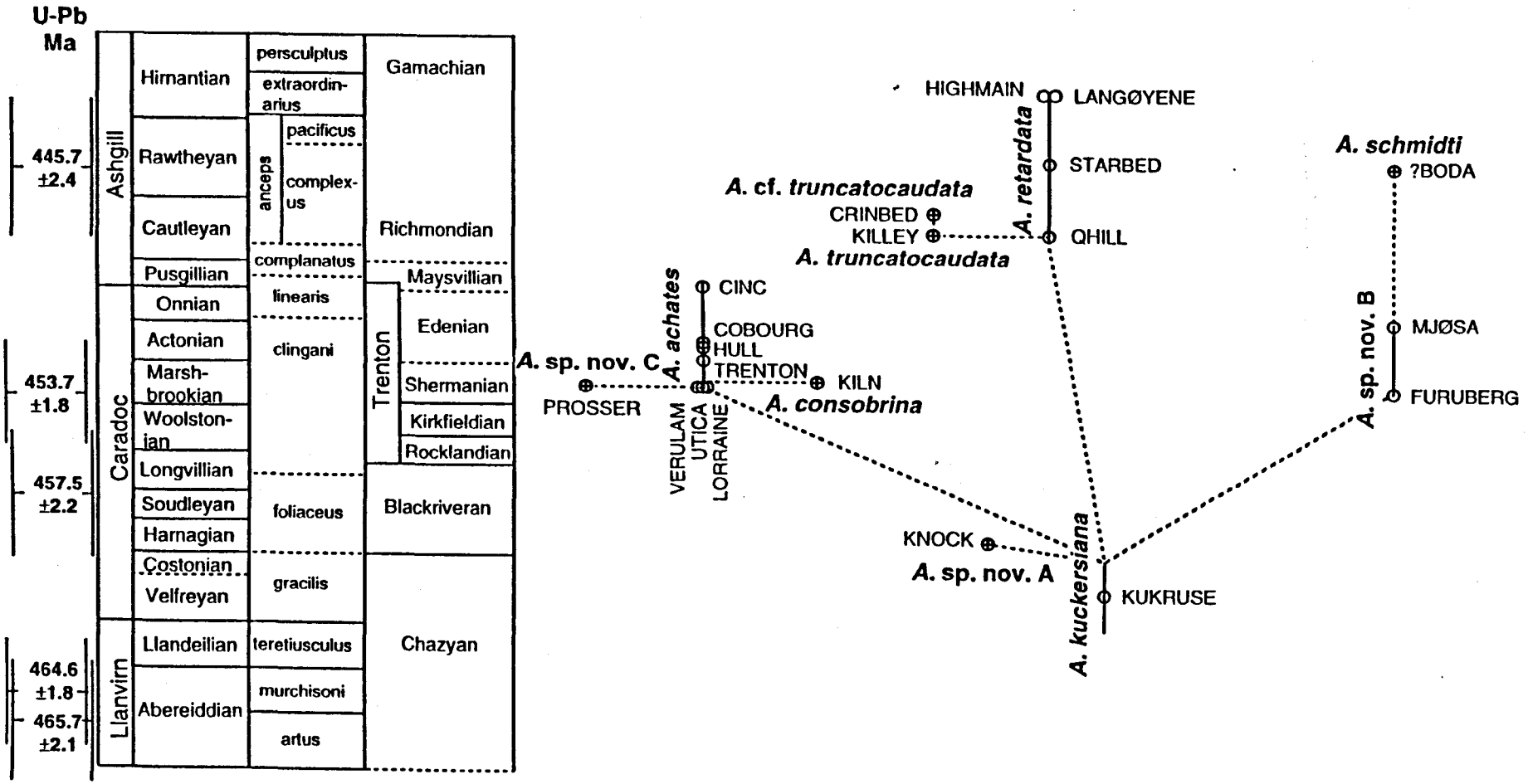

Figure 5. 34. Stratigraphical relationships, durations and suggested phylogeny of the species of *Achatella* recognised herein together with stratigraphical samples used in phylogenetic and morphometric analyses. Crosses indicate species known from only a single horizon, circles indicate stratigraphical samples. Stratigraphy and U-Pb dates as in Figure 5. 2.

Morphometric analysis of the genus has demonstrated that *Achatella* possesses a relatively stable body plan throughout its entire 22 myr duration (consider the overlapping PC fields occupied by the various stratigraphical samples in Figures 5. 15, 5. 17 and 5. 20), overlain by relatively slight variations in what might be termed "peripheral" features (e.g. relative length of genal spines, Figure 5. 4; relative length and position of the eye, Figures 5. 6, 5. 22 combined with associated variations in the number of lenses in the visual surface, Figure 5. 5). Some of these variations have previously been noted by Jaanusson and Ramsköld (1993) leading to their description of *Achatella* as a highly variable genus. It should be noted that this variability is only in the "peripheral" characters noted here; the basic body plan is constant throughout the entire duration.

An interesting link has been demonstrated between the location of the anteriormost extremity of the eye and the distal end of the S3 lateral glabellar furrow. The anterior of the eye is always either directly opposite the end of S3 or slightly behind it (cladistic character 11, Section 5. 3). In one member of the former group (*A. truncatocaudata*) in which the anterior of the eye is located relatively further forward, apparently to accommodate more lenses in the visual surface, the S3 furrow is also relatively further forward so that the anterior of the eye is still located opposite the furrow (see Figures 5. 22 and 5. 24). There is therefore a clear link between the location of these two structures. This implies that the breaking of this link to separate one group of species (*A. kuckersiana*, *A.* sp. A, *A.* sp. B, *A. truncatocaudata*, *A.* cf. *truncatocaudata*, *A. retardata* and *A. schmidti*, in which the anterior of the eye is opposite the distal end of S3) from the other group (the entirely Caradoc, Laurentian group *A. achates*, *A. consobrina* and *A.* sp. C in which the anterior of the eye is slightly behind S3) was a major evolutionary event.

The relatively larger size of *A. truncatocaudata* compared with other species of the genus is worthy of note. Such variation in size in a descendant taxon relative to the ancestor has often been ascribed to heterochrony (see for example McNamara 1978, 1981, 1982, 1983; Fortey and Rushton 1980; Edgecombe and Chatterton 1987; and Fortey and Owens 1990 on heterochrony in trilobites; McNamara 1988b, 1990 described many examples from fossil invertebrates and vertebrates). McNamara (1988a) defined two fundamental heterochronic processes: paedomorphosis, in which ancestral juvenile characters are retained in the descendant adult; and peramorphosis (in which ancestral adult characters appear in the descendant juveniles). He further subdivided paedomorphosis into three processes: neoteny (reduction in the rate of morphological development, which may affect the whole organism or only certain structures); progenesis (the precocious sexual maturation of the descendant, resulting in an adult descendant of smaller size than the ancestor); and post-displacement (delayed

onset of growth of particular morphological structures, resulting in structures in the descendant adult resembling those of the juvenile ancestor). He also subdivided peramorphosis into three processes: acceleration (increased rate of morphological development, usually operating on particular morphological structures); hypermorphosis (delayed onset of sexual maturation, resulting in a descendant adult of larger size than the ancestor); and pre-displacement (earlier onset of growth of structures, resulting in structures which are morphologically more "advanced" than those of the ancestor). Progenesis results in a descendant adult of smaller size than the ancestor, and therefore can be excluded as the process of derivation of *A. truncatocaudata.* In the absence of ontogenetic material for *Achatella* it is not possible to choose definitively between the other processes in this case. However, *A. truncatocaudata* displays similar general proportions to the smaller *Achatella* species with the exception that ontogenetic development of the eye appears to have continued relatively longer, resulting in its relatively greater exsag. length and number of lenses, and the linked shortening of the frontal glabellar lobe (see above). This is consistent with a derivation through hypermorphosis from a smaller *Achatella* species, probably *A. retardata* (see Figure 5. 9).

As well as interspecific variation in "peripheral" characters, *Achatella* displays high intraspecific variation in certain measurable characters, *viz.* postocular length (F) (Figure 5. 6), length of L1 (Figure 5. 26) and (especially) pygidial segmentation (Figure 5. 28; compare counts of pygidial ribs in Ordovician trilobites of the Builth inlier given by Sheldon 1987, which exhibit much lower within-sample variability). This again may be important in the long duration and lack of morphological change of the genus, and this is a theme which will be developed in subsequent chapters.

Explanation of Plates for Chapter Five

Plate 5. 1

Achatella achates (Billings, 1860)

1 & 2. Dorsal and oblique anterolateral views of damaged cephalon, internal mould. ROM 49475, Verulam Fm. (Shermanian), Trenton Gp. McCarthy Bros. Quarry, 1.5 miles northwest of Gamebridge, Ontario, Canada. Both x3. Original of Ludvigsen and Chatterton (1982: pl. 1, fig. 4, erroneously identified as ROM 35371).

3. Dorsal view of cranidium, internal mould. ROM 49473, horizon and locality as for fig. 1. x4.

4. Dorsal view of cephalon, internal mould. ROM 18747/1, Trenton Gp. (Kirkfieldian or Shermanian). Hull, Québec, Canada. x3. Original of Ludvigsen and Chatterton (1982: pl. 1, fig. 3).

5. Dorsal view of damaged cephalon, internal mould. ROM 49474, horizon and locality as for fig. 1. x4.

6. Dorsal view of pygidium, internal mould. BM It7174, possibly from Kimmswick Limestone (Rocklandian-Edenian). Locality unknown. x4.

7. Dorsal view of cranidium, internal mould. ROM 18747/3, horizon and locality as for fig. 4. x4.

Achatella kuckersiana (Schmidt, 1881)

8 & 10. Dorsal and oblique anterolateral views of damaged cephalon, internal mould. RM Ar34691, Kukruse Stage C2 (lowermost Caradoc). Estonia, exact locality unknown. Fig. 8 x4, fig. 10 x3.

9, 11 & 12. Dorsal, lateral and oblique posterolateral views of partially exfoliated pygidium. RM Ar34692, horizon as for fig. 8. Estonia, exact locality unknown. All x4.

13 & 14. Oblique anterolateral and dorsal views of damaged cephalon, internal mould. PMO1984, horizon as for fig. 8. Estonia, exact locality unknown. Fig. 13 x2, fig. 14 x4.

Achatella sp. nov. B

15 Dorsal view of cephalon, internal mould. PMO 56672; Mjøsa Fm (upper Caradoc-?basal Ashgill). Furuberget, Nes-Hamar, Mjøsa district, Norway. x2.

Plate 5. 2

Achatella sp. nov. A

1 & 2. Dorsal and oblique lateral views of cephalon, internal mould. GSI F00880, basal Knockerk House Sandstones Mbr. (lowermost Caradoc), Knockerk Fm., Grangegeeth Gp. Small quarry to east of road, 436m north of Grangegeeth crossroads, Co. Louth, Ireland. Both x3. Original of Harper (1952: pl. 5, fig. 5); also Romano and Owen (1993: text-fig. 5 A, F).

Achatella sp. nov. B

3. Dorsal view of damaged cephalon, internal mould. PMO 37678, upper Furuberget Fm. (Marshbrookian-Actonian). Furuberget, Nes-Hamar, Mjøsa district, Norway. x3.
4. Dorsal view of partially exposed cephalon, internal mould. PMO 21991, upper Furuberget Fm. (Marshbrookian-Actonian). Nes-Hamar (exact locality unknown), Mjøsa district, Norway. x3.
5 & 7. Dorsal and lateral views of cephalon, internal mould. PMO 131629, lower Mjøsa Fm. (Marshbrookian-Actonian). Bergvika, Mjøsa district, Norway. Both x3.
6. Dorsal view of partially exposed cephalon, internal mould. PMO 37679, horizon and locality as fig. 4. x4.

Achatella consobrina Tripp, 1954

8. Dorsal view of cephalon, latex cast. BM In52648, Kiln Mudstone, Craighead Fm. (approximately Marshbrookian). Craighead Quarry, Girvan district, Scotland. x4.
9. Ventral view of hypostome, internal mould. BM In52647, locality and horizon as for fig. 8. x5.
10 & 12. Lateral and dorsal views of pygidium, internal mould. GLAHM A5170, locality and horizon as for fig. 8. Both x5.
11 & 16. Anterior and dorsal views of cephalon, internal mould. GLAHM A5167, locality and horizon as for fig. 8. Both x4.
13. Ventral view of hypostome, internal mould. GLAHM A5168, locality and horizon as for fig. 8. x4.
14 & 15. Dorsal and lateral views of cephalon, internal mould. GLAHM A3792, locality and horizon as for fig. 8. Fig. 14 x3, fig. 15 x4. Original of Tripp (1954: pl. 4, fig. 27).

Plate 5. 3

Achatella truncatocaudata (Portlock, 1843)

1, 5 & 6. Dorsal, oblique lateral and anterior views of partial cephalon, internal mould. GLAHM A64, Killey Bridge Fm. (lower Cautleyan). Desertcreat, Pomeroy district, Co. Tyrone, Ireland. All x1.5.

2. Ventral view of hypostome, internal mould. BM It15632, Killey Bridge Fm. (lower Cautleyan). Pomeroy district, exact locality unknown, Co. Tyrone, Ireland. x2.

3. Dorsal view of cephalon, internal mould. UM K1630, horizon and locality as fig. 1. x1.5.

4. Dorsal view of pygidium, internal mould. TCD 7821, Killey Bridge Fm. (lower Cautleyan). Pomeroy district, exact locality unknown, Co. Tyrone, Ireland. x2.

7. Dorsal view of pygidium, internal mould. BM I1375, Killey Bridge Fm. (lower Cautleyan). Pomeroy district, exact locality unknown, Co. Tyrone, Ireland. x2.

Achatella retardata (Reed, 1914)

8 & 9. Dorsal and lateral views of cephalon, internal mould. GLAHM A10818, Quarrel Hill Fm. (upper Cautleyan), Lower Drummuck Gp. East brow of Quarrel Hill, Girvan district, Scotland. Both x4.

11 & 14. Dorsal & oblique anterolateral views of partially exposed cephalon, internal mould. GLAHM A952/3, locality and horizon as for fig. 8. Fig. 11 x4, fig. 14 x3.

12. Dorsal view of pygidium, internal mould. GLAHM A1057, locality and horizon as for fig. 8. x2.5.

13. Dorsal view of partially exfoliated pygidium. GLAHM A953, locality and horizon as for fig. 8. x2.

15. Latex cast of right librigena and visual surface. GLAHM A952/4, locality and horizon as for fig. 8. x4.

Achatella cf. *truncatocaudata*

10. Dorsal view of partial cranidium, internal mould. GLAHM A10835/5, Quarrel Hill Crinoid Bed, upper Quarrel Hill Fm. (upper Cautleyan), Lower Drummuck Gp. East brow of Quarrel Hill (locality Q13 of Harper 1982), Girvan district, Scotland. x5.

***Achatella schmidti* (Warburg, 1925)**

16 & 17. Lateral and dorsal views of partially exposed cephalon, internal mould. PMU D.189, probably from Boda Limstone (Ashgill). ?Osmundsberget, Siljan district, Sweden. Both x4. Original of Warburg (1925: pl. 11, figs. 27-28); also Jaanusson and Ramsköld (1993: pl. 5, fig. 4).

Plate 5. 4

***Achatella retardata* (Reed, 1914)**

1. Dorsal view of complete individual, internal mould. GLAHM A4132, Starfish Bed No. 2 of Begg (1946), South Threave Fm., Upper Drummuck Gp. (Rawtheyan). Lady Burn, Girvan district, Scotland. x1.5.

2 & 4. Dorsal and oblique anterolateral views of latex cast of complete individual. BM In41172, Starfish Beds (exact bed unknown), South Threave Fm., Upper Drummuck Gp. (Rawtheyan). Lady Burn, Girvan district, Scotland. Fig. 2 x2, fig. 4 x1.5.

3. Dorsal view of latex cast of partially exposed cephalon. BM In23605, Starfish Beds (exact bed unknown), South Threave Fm., Upper Drummuck Gp. (Rawtheyan). Lady Burn, Girvan district, Scotland. x3.

5. Dorsal view of partially exposed pygidium, internal mould. A. W. Owen collection, High Mains Fm. (Hirnantian). High Mains Farm, Girvan district, Scotland. x5.

6, 7 & 9. Posterior, dorsal and lateral views of pygidium, internal mould. PMO 80488, Langøyene Fm. (Hirnantian). Lilleklostret, Skien-Langesund district, Norway. All x4.

8. Dorsal view of cranidium, internal mould. GLAHM A16155, locality and horizon as for fig. 5. x4. Original of Harper (1982: pl. 1, fig. 2); also Owen (1986: fig. 2a).

10. Dorsal view of cranidium, internal mould. PMO 80486, locality and horizon as for fig. 6. x4.

PLATE 5.1

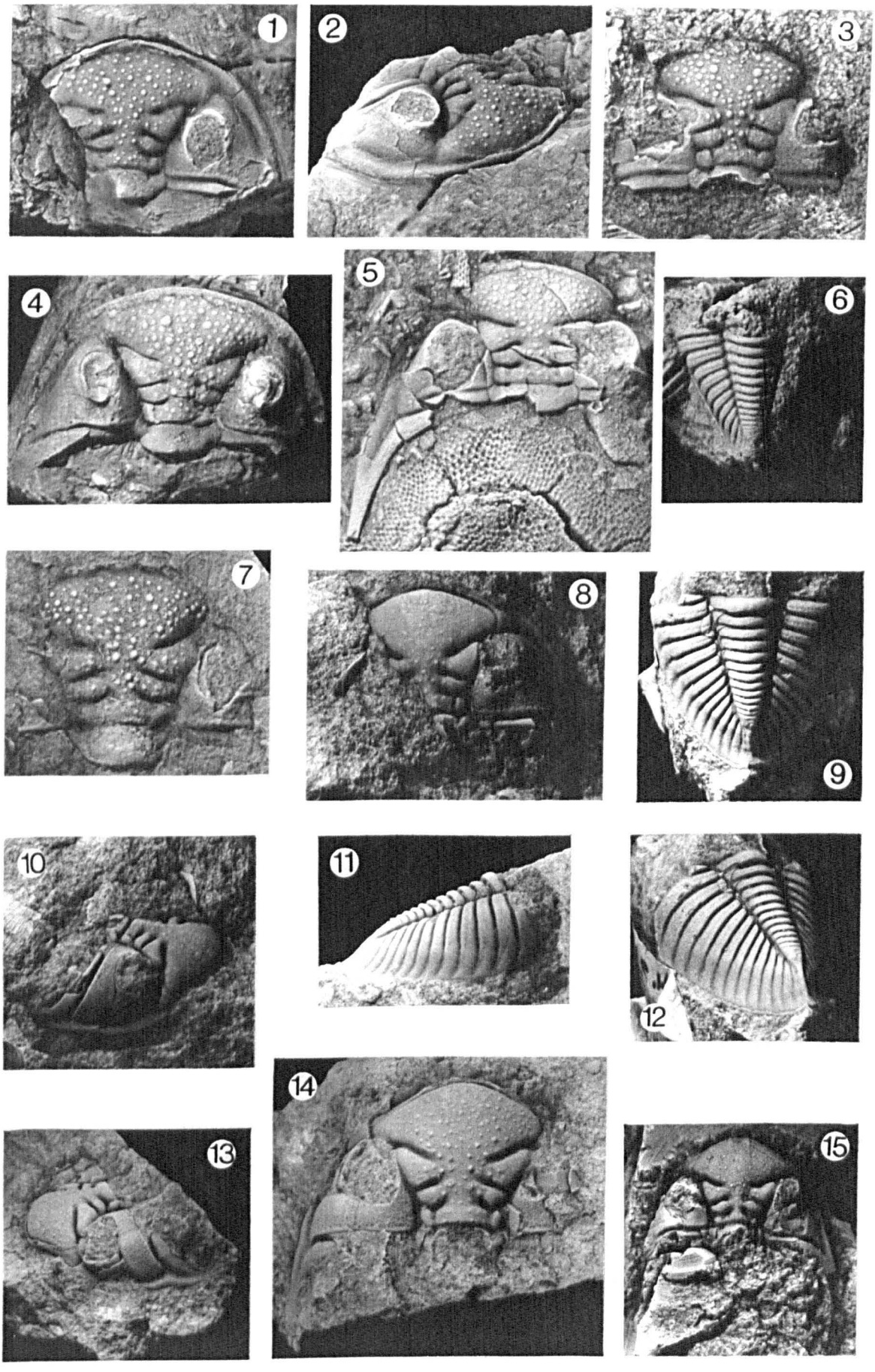

PLATE 5.2

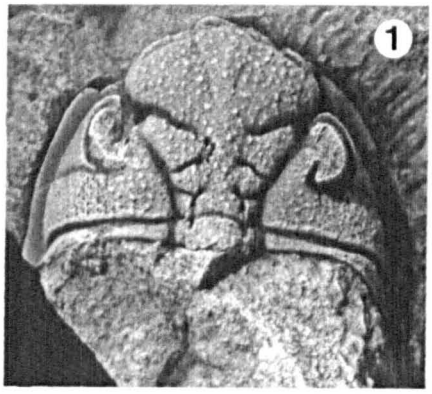
1

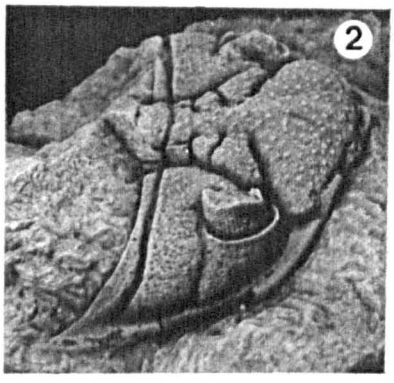
2


3

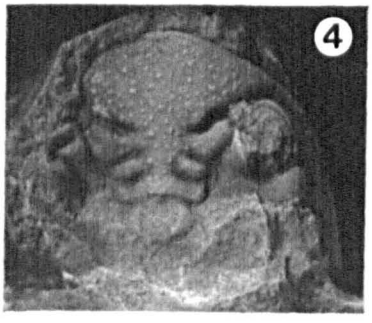
4

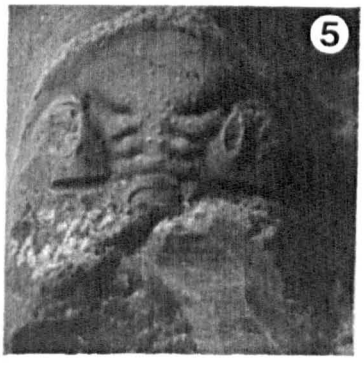
5

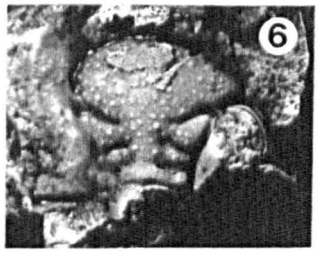
6

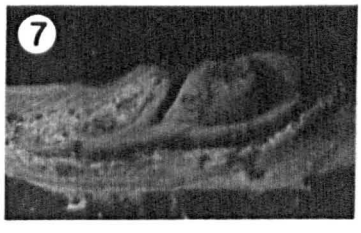
7

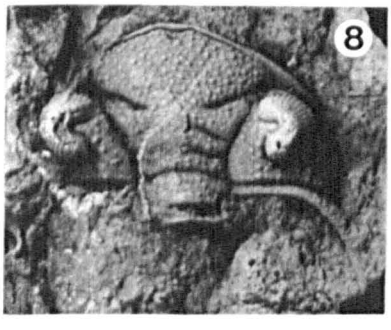
8

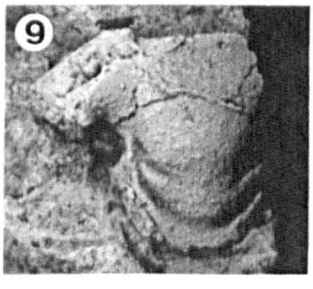
9

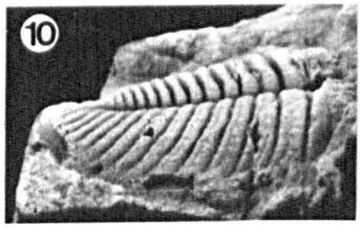
10

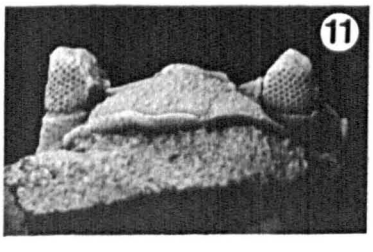
11

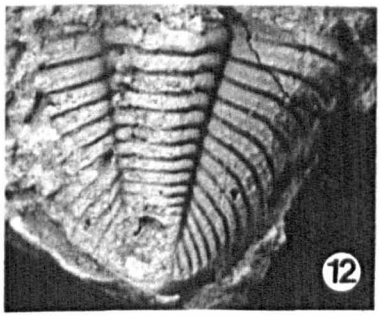
12

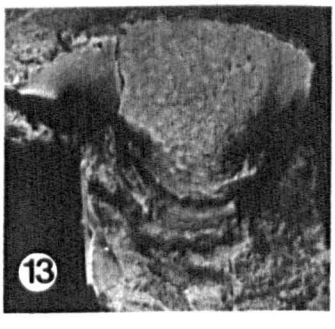
13

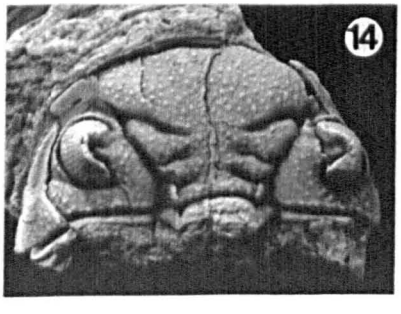
14

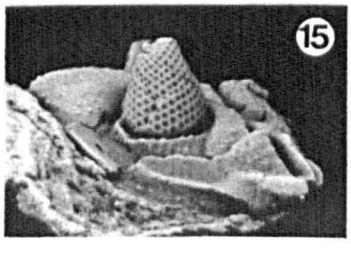
15

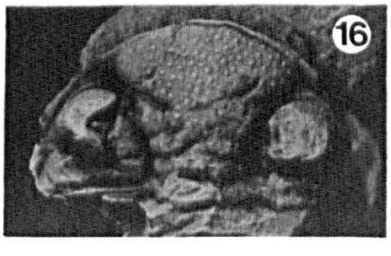
16

PLATE 5.3

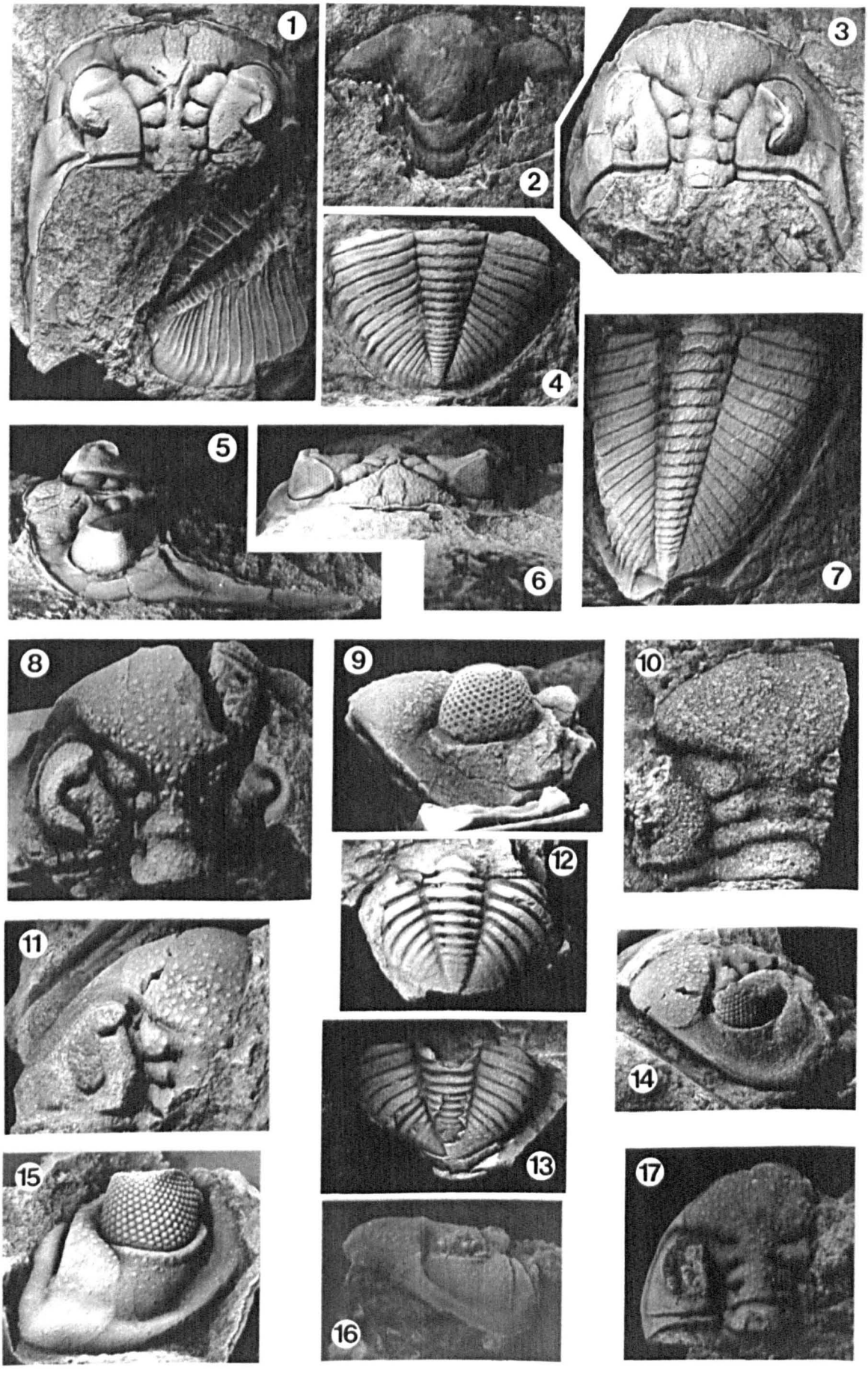

PLATE 5.4

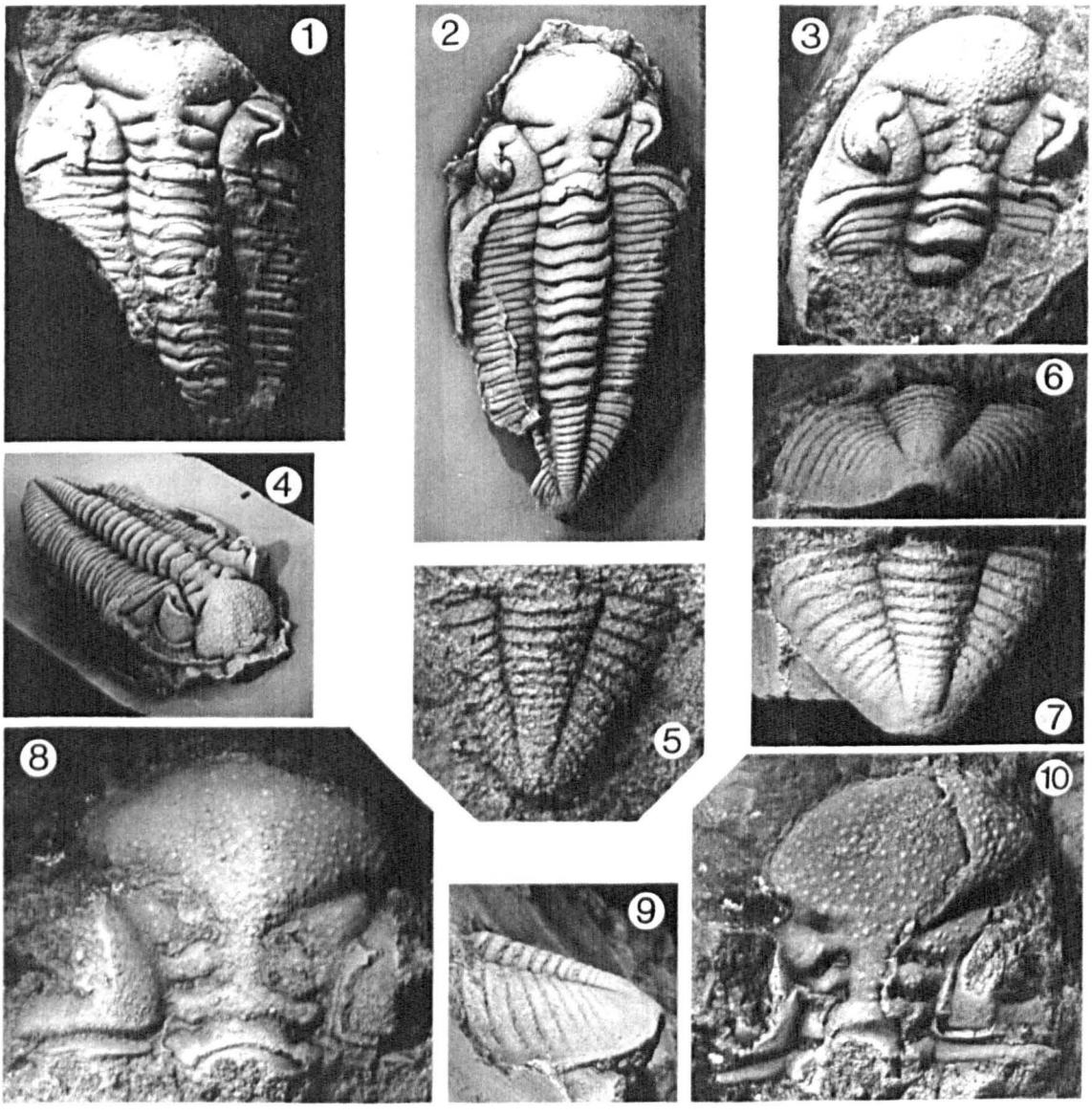

CHAPTER SIX

A PHYLOGENETIC AND MORPHOMETRIC ANALYSIS OF *CALYPTAULAX* COOPER, 1930.

6. 1. Introduction.

Calyptaulax (Suborder Phacopina, Family Pterygometopidae, Subfamily Eomonorachinae) is known from strata of Llanvirn to Ashgill (upper Rawtheyan) age. *Calyptaulax* as recognised herein comprises species previously assigned to two genera: *Calyptaulax* Cooper, 1930 and *Calliops* Delo, 1935. Historically, the many occurrences of specimens belonging to these two very similar taxa from the middle Ordovician of North America and Scotland have usually been assigned to *Calliops*, while species from England, Wales and Scandinavia have tended to be referred to *Calyptaulax*, the notable exception being Struve *in* Moore (1959) who considered the two taxa to be subgenera of *Calyptaulax*. However since 1965 a number of workers have synonymised these two genera. It will be demonstrated herein that *Calyptaulax* thus defined can in fact be considered to consist of two species groups, defined as subgenera herein. These subgenera are defined as *Calyptaulax (Calyptaulax)* and *Calyptaulax (Calliops)* (see Section 6. 6 for full discussion).

Calyptaulax was probably derived from *Pterygometopus* in the Llanvirn of Baltica (McNamara, 1980; Ludvigsen and Chatterton 1982). It made its first appearance in Laurentia shortly thereafter (as *Calyptaulax (Calliops)*) in the Llanvirn Table Head Fm. of Newfoundland (Whittington 1965). In only slightly younger strata of the Girvan district, western Scotland, species assignable to both subgenera, *Calyptaulax (Calyptaulax)* and *Calyptaulax (Calliops)* co-occur (Confinis Fm., late Abereiddian, Ingham and Owen in prep.). However, during the Llandeilian and Caradoc it was *C. (Calliops)* which became extremely widespread throughout Laurentia, with recorded occurrences in middle Ordovician strata of NW Canada (eg: Chatterton and Ludvigsen 1976), Utah and Nevada (eg: Ross 1967; Ross and Shaw 1972), Oklahoma (eg: Shaw 1974), the Southern Appalachians (eg: Cooper 1953), New York State and Ontario (eg: Shaw 1968; Titus and Cameron 1976), Newfoundland (eg: Shaw and Fortey 1977), Northern Ireland (eg: Clarkson and Tripp 1981), western Scotland (eg: Tripp 1954, 1980a, b), and the Southern Uplands (eg: Clarkson *et al.* 1992). *C. (Calliops)* reached its acme in the middle Caradoc, and was entirely restricted to Laurentia and the Laurentian margins. The latest occurrence of the subgenus is in the Richmondian of Iowa. Specimens from all of the above occurrences are very similar, which has lead workers to employ one or other of the following alternative strategies: (i) describing large numbers of species most of which are virtually indistinguishable (eg: Delo 1940; Cooper 1953); (ii) considering most of the occurrences to fall within the boundaries of a small number of species which show considerable intraspecific variability (eg: Shaw 1968, 1974; Chatterton and Ludvigsen 1976).

C. (Calyptaulax) played a subordinate role to *C. (Calliops)* throughout the Llandeilian and most of the Caradoc. It made its first appearence in strata of the Oslo Region

(Baltica) in the early Caradoc (Arnestad Fm.) and appeared in Avalonia a little later, in the Actonian. All occurrences of *Calyptaulax* in Avalonia and in Baltica from the upper Caradoc onwards are attributable to *C. (Calyptaulax).* The subgenus also colonized the Laurentian margins after the extinction of *C. (Calliops)* in the Richmondian.

Calyptaulax was chosen for study because of its long generic duration and its shape-conservative nature: both subgenera consist of a set of very similar species, particularly *Calyptaulax (Calliops).* It was also of interest to discover whether phylogenetic and morphometric analysis could detect a genuine distinction between species previously assigned to the two genera *Calyptaulax* and *Calliops* (as mentioned above, this did turn out to be possible). Specimens of *Calyptaulax* from 40 stratigraphically and geographically separate samples were subjected to phylogenetic and morphometric analysis. The samples are listed and described in Section 6. 2. The phylogenetic analysis is presented in Section 6. 3. This analysis results in a phylogenetic framework for *Calyptaulax*, and also highlights the complex pattern of mosaic evolution involving many convergences in the genus. The phylogenetic analysis included consideration of characters not amenable to morphometric analysis. A morphometric analysis of *Calyptaulax* is presented in Section 6. 4., which assesses the degree of shape conservatism and intraspecific variability in the genus. Section 6. 5 presents a systematic revision of *Calyptaulax.* Effort has been made to relate rare and poorly-known species which were not available for cladistic and morphometric analysis to the phylogenetic scheme. Section 6. 6 presents conclusions on the systematics of *Calyptaulax* and its implications for stasis.

6. 2. Material.

The specimens studied here were taken from 40 stratigraphically and geographically separate samples which taken together cover the entire stratigraphical and geographical extent of the genus. The 40 samples are listed below. Locality names and numbers (in square brackets) refer to the locality list in Appendix 3. Names in curly brackets give the species to which the specimens are currently assigned (*i.e.* the name assigned in the most recent relevant literature). Note that "material" below refers to specimens complete enough and undistorted enough for morphometrics and does not include disassociated visual surfaces which are included in Figures 6. 3 and 6. 27.

Girvan District.

1. CONFINIS A: specimens from Kirkdominae Hill, Girvan [loc. 1]. Confinis Fm., upper Abereiddian (Ingham 1978; Ingham and Owen in prep.). {*Calyptaulax foederatus* Tripp, 1962}. Material: 3 cranidia, 4 pygidia.
2. CONFINIS B: specimens from Bougang Quarry [loc. 4], Minuntion [loc. 2] and a single specimen from Auchlewan Burn [loc. 3], Girvan. Horizon as for CONFINIS A. {*Calyptaulax marginatus* (Tripp, 1962)}. Material: 8 cephala (2

from Minuntion, 6 from Bougang) and 18 pygidia (11 from Minuntion, 6 from Bougang and 1 from Auchlewan Burn).

3. STINCHAR: specimens from Auchlewan Quarry [loc. 5] and Minuntion Quarry [loc. 6], Girvan. Upper Stinchar Limestone Fm., Llandeilian (Ingham 1978; Ingham and Owen in prep.). {*Calyptaulax georgei* Tripp, 1967}. Material: 2 cranidia (both from Auchlewan Quarry) and 6 pygidia (3 from Auchlewan Quarry, 3 from Minuntion Quarry).
4. DOULARG: single cranidium from the "Separation Sandstone Bed" exposed in an excavation in Plantation Burn, Girvan [loc. 7]. Doularg Fm., lower Caradoc (Ingham and Tripp 1991). {*Calyptaulax* sp.}.
5. DOWHILL: specimens from Dow Hill, Girvan [loc. 8]. "Infra-Kilranny Greywackes", lower *peltifer* subzone, lower Caradoc (Ingham 1978; Tripp 1980a; Ingham and Owen in prep.). {*Calyptaulax brongniartii* (Portlock, 1843)}. Material: 4 cephala and 17 pygidia.
6. BALCLATCHIE A: specimens from mudstones exposed at Penwhapple Bridge, Girvan [loc. 9]. Upper Balclatchie Mudstones, upper *peltifer* subzone, middle Caradoc (Tripp 1980a; Ingham and Owen in prep.). {*Calyptaulax brongniartii* (Portlock, 1843); *Phacops (Calliops) jukesi* var. *vicina* Reed, 1945}. Material: 5 cephala and 28 pygidia.
7. BALCLATCHIE B: locality and horizon as for BALCLATCHIE A. {*Calyptaulax hunteri* (Reed, 1914)}. Material: 4 cranidia and 2 pygidia.
8. ARDMILLAN: specimens from Ardmillan, Girvan [loc. 10]. Lower Ardwell Farm Fm., *foliaceus* zone, middle Caradoc (Ingham 1978; Ingham and Owen in prep.). {*Calyptaulax brongniartii* (Portlock, 1843)}. Material: 30 cephala, 24 pygidia.
9. PINMERY: specimens from Pinmery, Girvan [loc. 11]. Middle Ardwell Farm Fm., middle-upper Caradoc (Tripp 1980a). {*Calyptaulax hunteri* (Reed, 1914)}. Material: 1 cranidium and 2 pygidia.
10. KILN: specimens from exposure of the Kiln Mudstone at Craighead Quarry, Girvan [loc. 12]. Craighead Fm., *clingani* zone, middle-upper Caradoc (Tripp 1980b; Ingham and Owen in prep.). {*Calyptaulax brongniartii* (Portlock, 1843)}. Material: 4 cephala and 2 pygidia.
11. STARFISH: specimens from the "Starfish Beds", Lady Burn, Girvan [loc. 15]. Lower South Threave Fm., Upper Drummuck Gp. Upper Rawtheyan, upper *anceps* zone (Ingham 1978; Harper 1982). {*Calyptaulax asteroideus* (Reed, 1914)}. Material: 7 cephala and 10 pygidia.

Southern Uplands.

12. KIRKCOLM: specimens from Duntercleuch [loc. 30] and Kilbucho [loc. 31], Southern Uplands. Kirkcolm Fm., middle Caradoc, upper *peltifer* - lower *clingani* zones (Owen and Clarkson 1992). {*Calyptaulax brongniartii* (Portlock, 1843)}. Material: 3 cephala (1 from Kilbucho and 2 from Duntercleuch).

Co. Tyrone.

13. BARDAHESSIAGH: specimens from the south slopes of Craigbardahessiagh, Pomeroy Inlier, Co. Tyrone [loc. 48]. Lower Bardahessiagh Fm., middle Caradoc (Mitchell 1977; Ingham pers. comm.). {*Calyptaulax brongniartii* (Portlock, 1843)}. Material: 8 cephala and 5 pygidia.

North and Central England.

14. ACTON: specimens from the "Old Quarry", Quarry Field, Gretton, Shrops. [loc. 41]. Decalcified sandstones, middle third of Acton Scott Fm., upper Caradoc (Dean 1961). {*Calyptaulax actonensis* Dean, 1961}. Material: 1 cranidium and 2 pygidia.
15. DUFTON (ONN): specimens from loc. A12 of Dean 1962, Pus Gill, Cross Fell [loc. 39]. Dufton Shale Fm., Onnian Stage, Caradoc Series (Dean 1962). {*Calyptaulax planiformis* Dean, 1962}. Material: 1 cephalon, 1 pygidium.
16. DUFTON (PUS): specimens from loc. B25 of Dean 1962, Swindale Beck, Cross Fell [loc. 40]. Dufton Shale Fm., Pusgillian Stage, Ashgill Series (Dean 1962). {*Calyptaulax planiformis* Dean, 1962}. Material: 1 cephalon, 2 pygidia.
17. APPLETHWAITE: specimens from Garburn Nook [loc. 35], Till's Hole [loc. 36], Stumfell Howe [loc. 37] and Torver Beck [loc. 38], English Lake District. Upper Applethwaite Mbr. of the Kirkley Bank Fm., Cautleyan Stage, Ashgill Series (McNamara 1979; Kneller *et al.* 1994). {*Calyptaulax planiformis* Dean, 1962}. Material: 2 cephala (both from Garburn Nook), 12 pygidia (2 from Till's Hole, 1 from Stumfell Howe, 8 from Garburn Nook, 1 from Torver Beck).

Wales.

18. SHOLESHOOK: specimens from Sholeshook Farm [loc. 42], Prendergast Place [loc. 43], Haverfordwest, and Mylet Farm [loc. 44], Carmarthenshire. Middle-upper Sholeshook Limestone Fm., Cautleyan and lowest Rawtheyan stages, Ashgill Series (Price 1980). {*Calyptaulax planiformis* Dean, 1962}. Material: 3 cephala (2 from Sholeshook Farm and 1 from Prendergast Place), 4 pygidia (3 from Sholeshook Farm and 1 from Mylet Farm).
19. RHIWLAS: specimens from Rhiwlas, Bala (exact locality unknown). Rhiwlas Limestone, Rawtheyan Stage, Ashgill Series (Whittington 1962; Williams *et al.* 1972). {*Calyptaulax* aff. *norvegicus* Størmer, 1945}. Material: 2 cephala.
20. DDOLHIR: specimens from "Cynmyd Forest", Corwen district, Berwyn Hills (exact locality unknown). Ddolhir Fm., Rawtheyan Stage, Ashgill Series (Williams *et al.* 1972). {*Calyptaulax* sp.}. Material: 5 cephala and 7 pygidia.

Oslo Region.

21. SOLVANG: specimens from Kalvøya [loc. 53], South Kuholmen [loc. 54], and East Raudskjer [loc. 55] Asker. Solvang Fm., *clingani* zone, upper Caradoc (Owen *et al.* 1990). {*Calyptaulax* aff. *norvegicus* Størmer, 1945}. Material: 4

cephala (1 from Kalvøya, 3 from E. Raudskjer), 2 pygidia (1 from E. Raudskjer, 1 from S. Kuholmen).

22. VENSTØP: specimens from Frognøya, Ringerike [loc. 56]. Venstøp Fm., Pusgillian Stage, Ashgill Series (Owen *et al.* 1990). {*Calyptaulax norvegicus* Størmer, 1945}. Material: 1 cephalon and 3 pygidia.
23. GAGNUM: specimens from Rokotjern, Gran [loc. 63] and Grina [loc. 63] Hadeland. Gagnum Mbr. of the Lunner Fm., uppermost Caradoc-lowest Ashgill (Owen *et al.* 1990). {*Calyptaulax norvegicus* Størmer, 1945}. Material: 1 cephalon, 1 pygidium.
24. SØRBAKKEN: single cephalon from NW Frognøya, Ringerike [loc. 58]. Lower Sørbakken Fm., Cautleyan Stage, Ashgill Series (Owen *et al.* 1990). Also specimens from laterally equivalent strata at Borøya, Asker [loc. 59] (Skjerholmen Fm., Ashgill), Lindøy, Asker [loc. 60], and Terneholmen, Asker [loc. 61] (both Grimsøya Fm., Ashgill) (Owen *et al.* 1990). {*Calyptaulax norvegicus* Størmer, 1945}. Material: 1 cephalon (from NW Frogøya), 4 pygidia (2 from Borøya, 1 from Lindøy, 1 from Terneholmen).
25. KJØRRVEN: specimens from Lunner Station [loc. 64] and Ringen [loc. 65], Hadeland. Kjørrven Fm., Rawtheyan Stage, Ashgill Series (Owen *et al.* 1990). {*Calyptaulax norvegicus* Størmer, 1945}. Material: 2 cephala, 1 pygidium.
26. HUSBERGØYA: single cephalon from N. Langøyene, Oslo [loc. 57]. Husbergøya Fm., upper Rawtheyan Stage, Ashgill Series (Owen *et al.* 1990). {*Calyptaulax norvegicus* Størmer, 1945}.

North America.

27. CROWNPOINT: specimens from exposures at Sloop Bay [loc. 91] and Pebble Beach [loc. 92], Valcour Island, N.Y. Middle Crown Point Fm., middle to late Chazyan (Shaw 1968). {*Calyptaulax annulata* (Raymond, 1905)}. Material: 2 holaspide cranidia and 14 holaspide pygidia. Also ontogenetic material: 6 meraspide cranidia and 1 meraspide pygidium. Ontogenetic material, holaspide cranidia and 7 of the holaspide pygidia digitised from illustrations of Shaw (1968, plates 11-12).
28. ESBATAOTTINE: specimens from sections exposed on Esbataottine Mt. and Sunblood Mt., District of Mackenzie, Northwest Territories, Canada (horizons A110, A115, A125, P1485 and P1512 of Chatterton and Ludvigsen 1976; Chatterton 1980) [loc. 102]. Lower Esbataottine Fm., upper Chazyan (Chatterton and Ludvigsen 1976). {*Calyptaulax callirachis* Cooper, 1930). Material: 3 holaspide cranidia and 3 holaspide pygidia. Also ontogenetic material: 5 meraspide cranidia, 7 meraspide pygidia and 3 protaspides. Specimens digitised from illustrations of Chatterton and Ludvigsen (1976, plate 16) and Chatterton (1980, plate 16).

29. DUCK: specimens from Duck Creek Quarry, Green Bay, Wis. [loc. 98]. Prosser Fm., Trenton Gp. (approx. Shermanian) (Ross *et al.* 1982). {*Calyptaulax callicephala* (Hall, 1847)}. Material: 28 cephala, 25 pygidia.
30. CANNON: specimens from "near Cannon Falls, Minn." Exact locality unknown. Lower Prosser Fm., Trenton Gp. (approx. Shermanian) (Ross *et al.* 1982). {*Calyptaulax callicephala* (Hall, 1847)}. Material: 4 cephala.
31. TRENTON: specimens from Trenton Falls [loc. 93], and from Pattersonville, Middleville and Amsterdam, N.Y. (exact localities unknown). Trenton Limestone, lower Denley Limestone of Ross *et al.* (1982) (approx. Denmark Fm. of Kay 1943). Shermanian-Edenian. {*Calyptaulax callicephala* (Hall, 1847)}. 6 cephala and 11 pygidia.
32. ELKADER: specimens from quarry at Elkader, Iowa [loc. 99]. Topmost Prosser Fm. (*Catazyga uphami* bed), Shermanian (Ross *et al.* 1982). {*Calyptaulax callicephala* (Hall, 1847)}. Material: 4 cephala and 9 pygidia.
33. ATHENS: specimens from quarry 1 mile south of Otes, Tenn. (exact locality unknown). Upper Athens Fm., upper Whiterock (Ross *et al.* 1982). {*Calyptaulax annulata* (Raymond, 1905)}. Material: 2 cranidia and 6 pygidia.
34. VERULAM: specimens from McCarthy Bros. Quarry [loc. 94], Lakefield Quarry [loc. 95] and Canada Cement Co. Quarry [loc. 96], Ontario. Verulam Fm., Shermanian (Barnes *et al.* 1981). {*Calyptaulax callicephala* (Hall, 1847)}. Material: 5 cephala and 2 pygidia.
35. BELLEVILLE: specimens from Belleville, Ontario, exact locality unknown. Trenton Gp. (?Verulam Fm.), Shermanian (Barnes *et al.* 1981). {*Calyptaulax callicephala* (Hall, 1847)}. Material: 2 cephala.
36. LINDSAY: single cephalon from Little Current, Gt. Cloche Island, Ontario [loc. 97]. Lindsay Fm., Edenian (Barnes *et al.* 1981). {*Calyptaulax callicephala* (Hall, 1847)}.
37. FAIRMOUNT: single cephalon from "Fairmount, Cincinnati, Ohio". Exact locality unknown. Maysvillian (Ross *et al.* 1982). {*Calyptaulax* sp.}.
38. MAQUOKETA: specimens from Maquoketa Creek, Clermont, Iowa [loc. 100]. Maquoketa Gp., Maysvillian (Ross *et al.* 1982). {*Calyptaulax larrabei* (Slocum, 1913)}. Material: 5 cephala and 9 pygidia.
39. FT. ATKINSON: specimens from section 1 mile NW of Ft. Atkinson, Iowa [loc. 101]. Maquoketa Gp., Bed E, Richmondian (Ross *et al.* 1982). {*Calyptaulax fredericki* (Slocum, 1913)}. Material: 4 cephala and 7 pygidia.
40. MATAPEDIA: specimens from Grande Coupe [loc. 88], South Cove [loc. 89] and Priest's Road [loc. 90], Percé area, Gaspé Peninsula, Québec. Matapédia Gp., Rawtheyan (Lespérance 1988). {*Calyptaulax glabella* Cooper, 1930}. Material: 8 cephala and 3 pygidia.

A summary of the stratigraphical and geographical locations of the samples is shown in Figure 6. 1.

Table 6. 1. summarises the lithologies and suggested environments of deposition of the units from which the samples were taken. *Calyptaulax* is present in strata representing a spectrum of depths of deposition, from shallow water clastics to basin slope shales. *Calyptaulax* can be associated with trilobite assemblages assignable to Fortey's (1975) shallow water illaenid-cheirurid, slightly deeper nileid, and still deeper olenid associations. The occurrence of *Calyptaulax* in such a spectrum of biofacies is well illustrated in the Barr Gp., Girvan district (Tripp 1993).

6.3. Phylogenetic Analysis.

Phylogenetic analysis was undertaken on the holaspide specimens of *Calyptaulax* in order to construct an evolutionary framework for the genus, and to study the changing patterns of character states with time. A two-stage process was adopted. In the first instance, the 40 stratigraphical samples were used as the operational taxonomic units (OTUs) in an attempt to define a set of species. The species thus recognised then became the OTUs for the second cladistic analysis.

Choice of ancestral taxon. As described in Chapter 5, *Pterygometopus* Schmidt, 1881 is considered to be ancestral to all other pterygometopids (Ludvigsen and Chatterton 1982). Therefore the genotype specimen of *Pterygometopus*, an enrolled complete individual of *P. sclerops* (Dalman, 1827) from the Arenig Expansus Limestone of Västanå, Östergotland, Sweden, redescribed and illustrated by Whittington (1950, pp. 538-540; plate 68 figs. 17-20 and plate 69 figs. 1-4) has been used to define ancestral states and character polarities.

6.3.1. Characters Used.

This analysis is based upon characters of the cephalon and pygidium. The thorax and hypostome have not been used since they are (a) not available for a number of the stratigraphical samples and (b) indistinguishable among the samples for which they are known. Figure 6. 2 shows the locations on the exoskeleton of the characters used.

The analysis focuses on members of a single genus so that there has been no problem with the recognition of homologous characters in the different OTUs. The only character for which there is a note of caution is character 9, which uses the probable homology of pygidial "rib" furrows in *Calyptaulax* with pygidial pleural furrows in the ancestral taxon *P. sclerops*, although the coding of this character is in fact not invalidated if the rib furrows turn out to be homologous with the interpleural furrows of *P. sclerops* (see list of characters below).

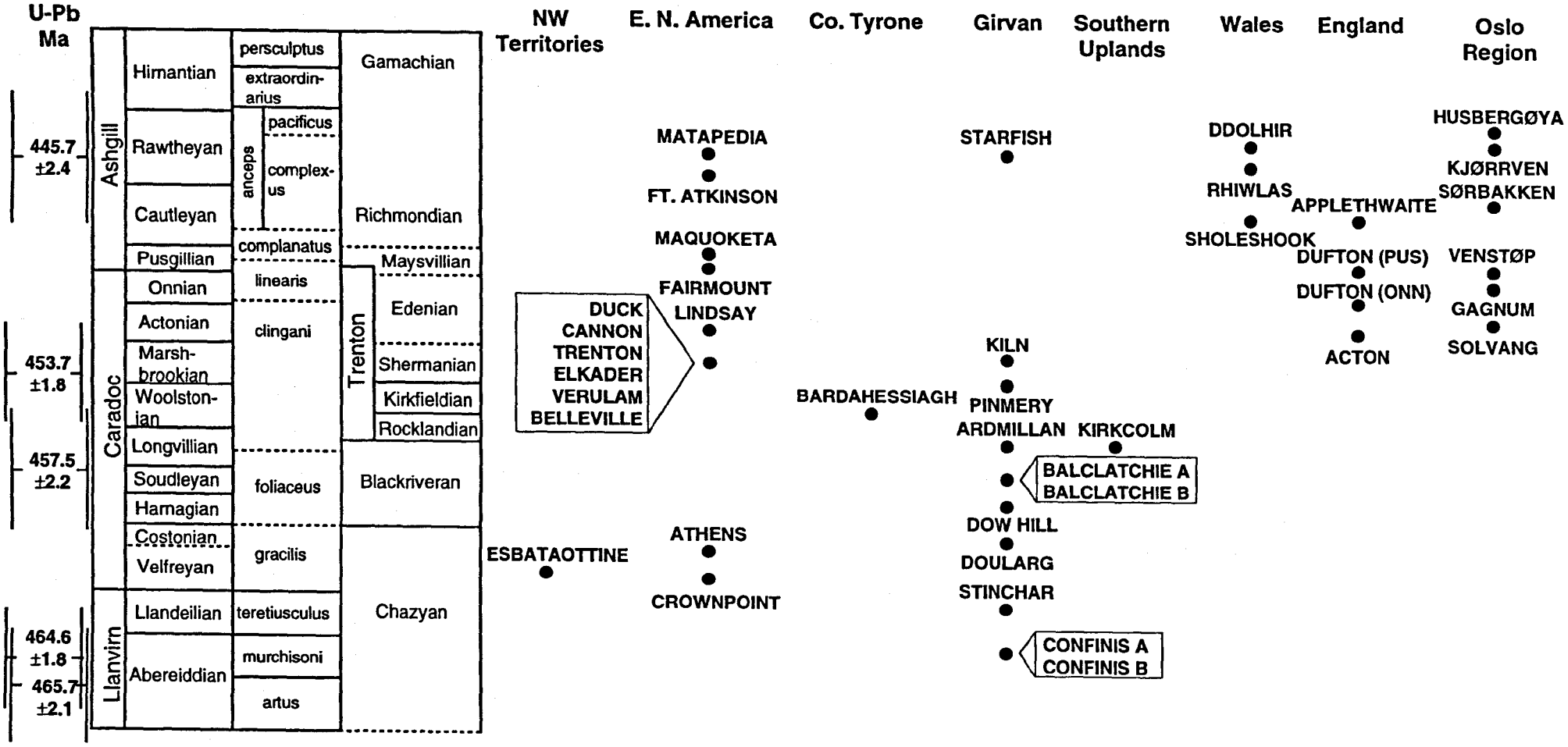

Figure 6. 1. Summary of the stratigraphical and geographical locations of the samples of *Calyptaulax* used. Stratigraphy based on Fortey *et al.* (in press) and Ross *et al.* (1982). Stratigraphical locations of samples based on references in the text. U-Pb dates are those of Tucker *et al.* (1990).

Table 6. 1. Summary of the lithologies, faunas and postulated depositional environments of the rocks associated with the stratigraphical samples of *Calyptaulax*. NB: "slope" refers to the basin slope (not continental slope) and probably represents maximum water depth of about 200m or less.

Stratigraphical Sample	Unit and Age	Lithology	Fauna	Environment of Deposition	References
CONFINIS A	Confinis Fm., Girvan (late Abereiddian).	Fine grained calc. sst.	Rich allochthonous shelly fauna. Trilobites of Fortey's (1975) illaenid-cheirurid assoc.	Shallow water deposition, probably locally derived.	Williams (1962); Tripp (1962, 1993).
CONFINIS B	As above.	As above.	As above.	As above.	As above.
STINCHAR	Stinchar Lst. Fm. (upper part), Girvan (Llandeilian).	Platy and decalc. lsts.	Rich shelly fauna. Trilobites of Fortey's (1975) illaenid-cheirurid assoc.	Shallow shelf.	Williams (1962); Tripp (1967, 1993).
DOULARG	"Separation Sst. Bed", Doularg Fm., Girvan (lower Caradoc).	15 cm thickness of bedded calc. silty mudst.	Sparse autochthonous shelly fauna.	Relatively shallow shelf deposition, slightly deeper than upper Stinchar Lst.	Ingham and; Tripp (1991).
DOWHILL	"Infra-Kilranny Greywackes", Girvan (lower Caradoc).	Dark slates, siltstones and mudsts.	Rich shelly faunas.	Distal turbidites.	Williams (1962); Tripp (1980a).
BALCLATCHIE A	Upper Balclatchie Gp., Girvan (middle Caradoc).	Dark green and grey mudsts. with local conglomerate horizons.	Shelly fauna dominated by raphiophorid and remopleuridid trilobites and inarticulate brachiopods.	Euxinic lower slope conditions.	Williams (1962); Tripp (1980a).

Table 6. 1. Continued.

Stratigraphical Sample	Unit and Age	Lithology	Fauna	Environment of Deposition	References
BALCLATCHIE B	As above.	As above.	As above.	As above.	As above.
ARDMILLAN	Lower Ardwell Farm Fm., Girvan (middle Caradoc).	Laminated green-grey siltstones and mudsts. with local conglomerate horizons.	Graptolites throughout. Stratigraphically localised and highly abundant allochthonous shelly faunas.	Distal turbidites.	Ingham (1978); Tripp (1980a).
PINMERY	Middle Ardwell Farm Fm., Girvan (middle Caradoc).	As above.	As above.	As above.	As above.
KILN	Kiln Mudstone, Craighead Inlier (middle Caradoc).	Locally developed mudst. tongue within complex of clastics and lsts.	Rich allochthonous shelly fauna.	Brief transgression within shallow water carb. succession.	Williams (1962); Tripp (1954, 1980b)
STARFISH	Lady Burn Starfish Beds, upper South Threave Fm., Craighead Inlier (upper Rawtheyan).	Calc. green-grey ssts.	Abundant and diverse allochthonous shelly faunas representing mixture of shelf and upper slope assocs.	Rapid downslope movement and burial, relatively shallow provenance.	Ingham (1978); Harper (1982).

Table 6. 1. Continued.

Stratigraphical Sample	Unit and Age	Lithology	Fauna	Environment of Deposition	References
KIRKCOLM	Kirkcolm Fm., Southern Uplands (middle Caradoc).	Stratigraphically localised conglomerates within turbidites.	Rich and abundant allochthonous shallow water shelly faunas.	Mass flows derived from shallow shelf area.	Clarkson *et al.* (1992); Owen & Clarkson (1992)
BARDA-HESSIAGH	Bardahessiagh Fm. (lower), Pomeroy Inlier (middle Caradoc).	Fine grained grey micaceous ssts. with rare coarse conglomerates.	Diverse brachiopod dominated shelly fauna.	Upper slope.	Mitchell (1977).
ACTON	Acton Scott Fm., south Shropshire (Actonian).	Calc. siltstones and ssts.	Rich and abundant shelly faunas.	Several facies represented, predominantly shallow water deposition.	Dean (1960-63); Hurst (1979a, b).
DUFTON (ONN)	Dufton Shale Fm., Cross Fell Inlier (Onnian).	Dark grey shales and mudsts. with occasional nodular lsts.	Stratigraphically localised shelly faunas.	Upper slope.	Ingham & McNamara (1978).
DUFTON (PUS)	As above.	As above.	As above.	As above.	As above.
APPLE-THWAITE	Applethwaite Mbr. (upper), Kirkley Bank Fm. (Cautleyan).	Blue-grey calc. mudsts. with argillaceous and nodular lsts.	Diverse autochthonous trilobite assoc. dominated by calymenids.	Relatively deep water shelf deposition away from direct influence of fluviatile input.	McNamara & Fordham (1981); Kneller *et al.* (1994).

Table 6. 1. Continued.

Stratigraphical Sample	Unit and Age	Lithology	Fauna	Environment of Deposition	References
SHOLESHOOK	Sholeshook Lst. Fm., S. Wales (Cautleyan-lowest Rawtheyan).	Variable succession of calc. mudsts., ssts. and siltstones.	Rich and diverse autochthonous shelly faunas. Mixed shelf edge and slope trilobite assoc.	Upper to middle slope deposition.	Price (1973, 1980).
RHIWLAS	Rhiwlas Lst., Moelfryn Mudsts., Bala (Rawtheyan).	1.5 to 3 m thick muddy, impersistent lst. mbr.	Rich and diverse trilobite fauna. Mixed shelf edge and slope trilobite assoc.	Upper to middle slope deposition.	Bassett *et al.* (1966); Whittington (1968).
DDOLHIR	Ddolhir Fm., Berwyn Hills (Rawtheyan).	Mudsts. and lsts.	Rich shelly fauna. Trilobite fauna similar to that of Rhiwlas Lst.	Probably upper to middle slope deposition.	Whittington (1968).
SOLVANG	Solvang Fm., Oslo Region (upper Caradoc).	Nodular and bedded lsts. and calc. shales.	Abundant and diverse autochthonous shelly faunas.	Relatively deep water shelf deposition.	Owen *et al.* (1990).
VENSTØP	Venstøp Fm., Oslo Region (Pusgillian).	Dark locally graptolitic shales with occasional lsts.	High abundance, low diversity autochthonous shelly faunas: *Tretaspis*, *Flexacalymene* ; inarticulate brachiopods.	Deposition in low energy conditions, lower slope.	Owen *et al.* (1990).

Table 6. 1. Continued.

Stratigraphical Sample	Unit and Age	Lithology	Fauna	Environment of Deposition	References
GAGNUM	Gagnum Mbr., Lunner Fm., Oslo Region (upper Caradoc-lower Ashgill).	Dark calc. shales with abundant nodular lsts.	Diverse autochthonous shelly fauna. Trilobites dominated by *Tretaspis*.	Upper slope deposition.	Owen *et al.* (1990).
SØRBAKKEN	Sørbakken Fm., Oslo Region (Cautleyan).	Nodular and bedded lsts. and thin calc. shales.	Diverse autochthonous shelly fauna.	Upper slope deposition.	Owen *et al.* (1990).
KJØRRVEN	Kjørrven Fm., Oslo Region (Rawtheyan).	Interbedded dark grey lsts., calc. siltstones and shales.	Highly diverse autochthonous shelly fauna.	Upper slope deposition.	Owen *et al.* (1990).
HUSBERG-ØYA	Husbergøya Fm., Oslo Region (upper Rawtheyan).	Shales with calc. ssts.	Sparse but relatively diverse. Trilobites belonging to *Tretaspis* assoc.	Deep water distal shelf deposition.	Owen *et al.* (1990).
CROWNPOINT	Crown Point Fm. (middle), Valcour Island (middle to upper Chazyan).	Fine grained blue-grey silty lsts. with thin dolomites.	Rich and diverse shelly faunas, especially within stromatoporoid supported carbonate mounds.	Shallow water carbonate shelf edge.	Shaw (1968); Shaw & Fortey (1977).
ESBATAOTT-INE	Esbataottine Fm. (lower), District of Mackenzie (upper Chazyan).	Grey-buff thinly bedded lsts.	Rich and diverse shelly fauna; 4 trilobite biofacies recognised.	Shallow water (sublittoral) deposition in quiet carbonate shelf environment.	Chatterton & Ludvigsen (1976).

Table 6. 1. Continued.

Stratigraphical Sample	Unit and Age	Lithology	Fauna	Environment of Deposition	References
ATHENS	"Athens Shale" (upper), Tennessee (upper Whiterock).	Dark grey to black platy shales.	Moderately diverse graptolite fauna; sparse shelly fauna.	Lower slope depositional environment.	Shaw & Fortey (1977).
DUCK	Prosser Fm., Trenton Gp., Wisconsin (Shermanian).	Pale grey bioclastic limestones.	Rich and diverse autochthonous shelly faunas.	Relatively deep water offshore shelf environment.	Ross et al. (1982); Bunker *et al.* (1988).
CANNON	Prosser Fm., Trenton Gp., Minnesota (Shermanian).	As above.	As above.	As above.	As above.
ELKADER	Prosser Fm., Trenton Gp., Iowa (Shermanian).	As above.	As above.	As above.	As above.
TRENTON	Trenton Lst., Trenton Gp., N.Y. (Shermanian-Edenian).	Dark grey fossiliferous silty bioclastic limestones.	Low diversity autochthonous shelly fauna: trilobites of Fortey's (1975) illaenid-cheirurid association.	Relatively deep water outer shelf deposition.	Titus & Cameron (1976); Shaw & Fortey (1977).
VERULAM	Verulam Fm., Trenton Gp., South Ontario (Shermanian).	Thinly bedded calcarenites and calcareous shales.	Rich and diverse autochthonous shelly fauna. Trilobites of Fortey's (1975) illaenid-cheirurid assoc.	Middle shelf depositional environment, relatively deep water.	Titus & Cameron (1976); Barnes *et al.* (1981).

Table 6. 1. Continued.

Stratigraphical Sample	Unit and Age	Lithology	Fauna	Environment of Deposition	References
BELLEVILLE	?Verulam Fm., Trenton Gp., Ontario (Shermanian).	As above.	As above.	As above.	As above.
LINDSAY	Lindsay Fm., Trenton Gp., Ontario (Edenian).	Dark grey fossiliferous silty bioclastic limestones.	Low diversity autochthonous shelly fauna: trilobites of Fortey's (1975) illaenid-cheirurid association.	Relatively deep water offshore shelf environment.	Titus & Cameron (1976); Barnes *et al.* (1981).
FAIRMOUNT	Maysvillian, Cincinnati Region.	Grey or green-grey silty shales and impersistent biomicrosparitic lsts.	Allochthonous assemblages of shelly fragments	Lower slope.	Twenhofel (1954); Scotford (1965).
MAQUOKETA	Maquoketa Gp., Iowa (Maysvillian).	Brown organic-rich shales with interbedded lsts. and phosphorites.	Abundant and diverse allochthonous shelly faunas.	Upper slope deposition.	Bunker *et al.* (1988).
FT.ATKINSON	Maquoketa Gp., Iowa (Richmondian).	Organic-rich shales with interbedded lsts; lower carb. content than MAQUOKETA.	As above.	As above.	Bunker *et al.* (1988).
MATAPEDIA	Matapédia Gp., Gaspé Peninsula, Québec (Rawtheyan).	Bedded calcilutites and shales with rare calcarenites.	Abundant and diverse autochthonous shelly faunas.	Relatively deep water outer shelf environment.	Cooper (1930); Lespérance (1988).

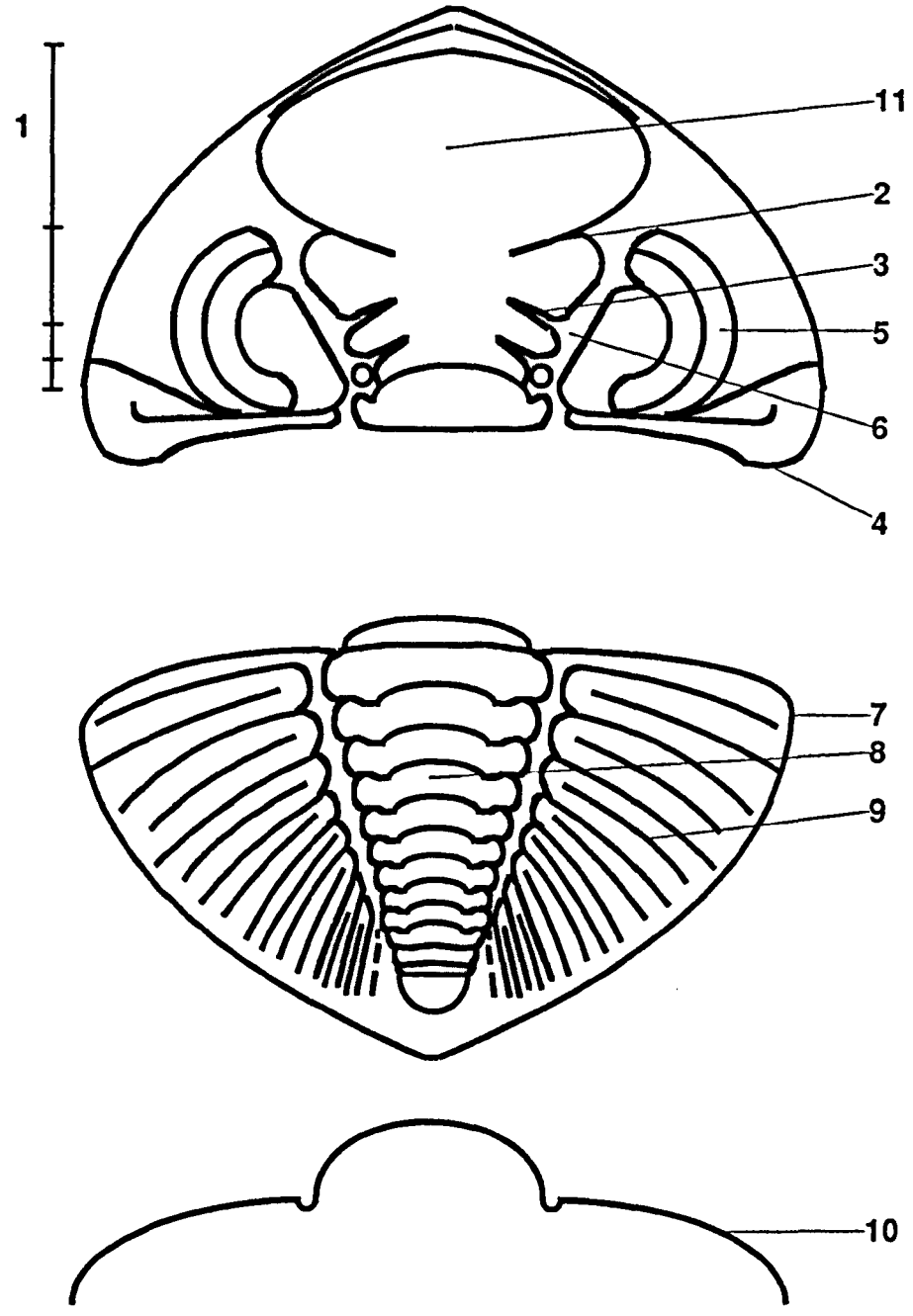

Figure 6. 2. Location of the characters used in phylogenetic analysis of *Calyptaulax* on the cephalon and pygidium.

All characters used are on the exterior of the exoskeleton. Most characters can be coded equally well from internal moulds or from counterparts. Glabellar sculpture (character 11) was coded only from counterparts or testate specimens. Character states which could not be determined were coded as "missing".

All characters are defined as undirected and unordered so as to simplify the analysis and avoid making too many assumptions. All characters are polarised from 0 to 1 (to 2 to 3 where applicable) where 0 is the ancestral state exhibited by *P. sclerops*.

List of characters.

1. Relative lengths of glabellar lobes.

There is variation in the relative lengths (sag. and exsag.) of the glabellar lobes in *Calyptaulax*. In some specimens, the frontal lobe is much longer than L3, which itself is longer than L2 and L1 (which are of approximately equal length). In others however (particularly Ashgill forms) the frontal lobe is approximately equal in length to L3, or may even be slightly shorter. Again, L2 and L1 are of approximately equal length in these forms. In specimens from the samples BALCLATCHIE A and PINMERY, L2 is unusually short (Plate 6. 2, figs. 6-10).

Ancestor comparison. In *P. sclerops*, the frontal lobe is longer (sag. and exsag.) than L3, which itself is of roughly equal length to L2 and L1.

States. 0: frontal lobe longer than L3, with L3, L2 and L1 of approximately equal lengths; 1: frontal lobe longer than L3, which itself is longer than L2, L2 and L1 of approximately equal lengths; 2: frontal lobe of approximately equal length with L3, L2 and L1 of approximately equal, shorter length; 3: frontal lobe equal in length or slightly longer than L3, L2 much shorter than both L3 and L1.

2. Shape of S3 lateral glabellar furrow.

In many specimens, S3 is straight or very slightly sigmoidal (see for example Plate 6. 4). It is not possible to separate these two character states because of the transitional nature of the relationship between them. Some stratigraphical samples contain individuals exhibiting both straight and sigmoidal furrows. However, many other specimens possess S3 furrows which are markedly concave-forwards (for example Plate 6. 1, figs. 1-4, 8-9, 12, 15-17) and these are separable from the above-mentioned state.

Ancestor comparison. The S3 furrow in *P. sclerops* is markedly convex-forwards.

States. 0: S3 convex-forwards; 1: S3 straight or slightly sigmoidal; 2: S3 concave-forwards.

3. Shape of S2 lateral glabellar furrow.

In many specimens, S2 is straight, while in some, principally the Ashgill forms, it is markedly hooked (convex-forwards). Compare, for example, Plate 6. 2, figs. 1-3 with Plate 6. 2, figs. 14, 16.

Ancestor comparison. In *P. sclerops* S2 is approximately straight.

States. 0: S2 straight; 1: S2 hooked.

4. Nature of the genal angles.

There is some variation in the shape of the genal angles. In many specimens of *Calyptaulax* from the Caradoc of North America the genal angles, while being rounded, are slightly produced posteriorly (see for example Plate 6. 3, figs. 8-9, 12, 15). In all other specimens examined as part of this study, the genal angles are rounded and not produced posteriorly (for example, Plate 6. 4, figs. 1, 4-5, 10). Calyptaulax meraspides possess genal spines, but these are generally lost by the time the holaspide stage is attained (see Section 6. 4. 4.; also Figure 6. 29). Occasionally, vestigial genal spines are retained in early holaspide stages (see for example Figure 6. 31, and discussion of variation in this feature in specimens from Duck Creek Quarry in Section 6. 6). The specimen with a fragmentary cephalon possessing genal spines described and figured as *Calliops troosti* (Safford and Vogdes, 1889) by Cooper (1953, pp 39-40; pl. 14 fig. 7) is here considered not to be a member of this genus and probably belongs in *Eomonorachus* (compare illustrations of *Eomonorachus intermedius* in Ludvigsen and Chatterton 1982: plate 1, figs. 8-9; plate 2, figs. 4-15; plate 3, fig. 1; text-fig. 5).

Ancestor comparison. P. sclerops possesses rounded genal angles, not produced posteriorly.

States. 0: genal angles not produced posteriorly; 1: genal angles slightly produced posteriorly.

5. Number of dorso-ventral lens files.

There is a striking discontinuity in the mean number of dorso-ventral lens files in the visual surface of specimens from each stratigraphical sample (Figure 6. 3), so that the samples can be divided into two groups, one containing samples with mean numbers of files less than or equal to 25, the other with mean numbers of files greater than or equal to 28. These two groups do show a slight overlap in total range of numbers of lens files (the group containing all samples with means less than or equal to 25 has total range 20 - 27; the group containing all samples with means greater than or equal to 28 has total range 26 - 38).

Ancestor comparison. The visual surface of *P. sclerops* has 23 - 27 files of lenses (Whittington 1950).

States. 0: mean number of lens files 25 or less; 1: mean number of lens files 28 or more.

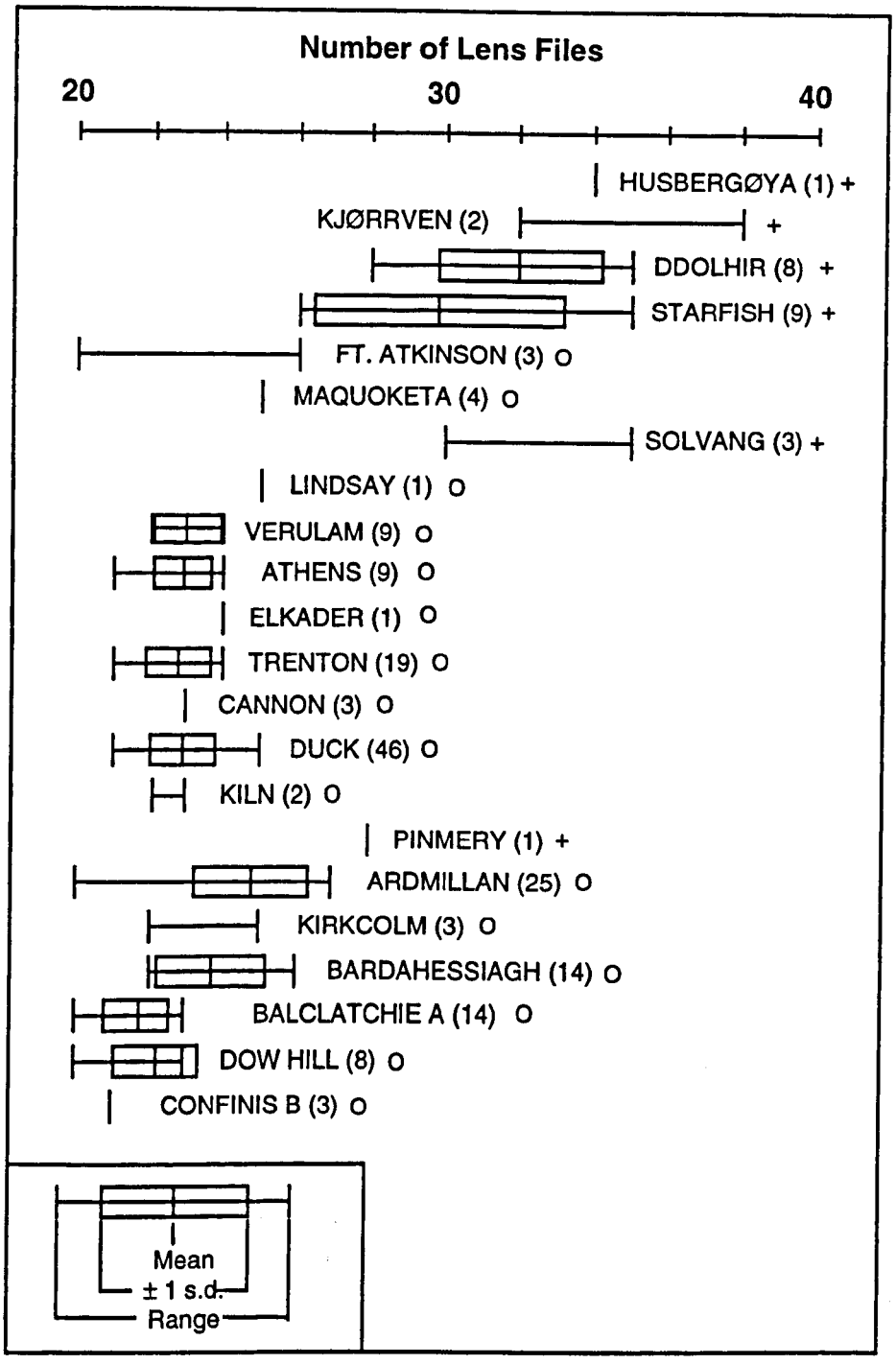

Figure 6. 3. Univariate variation in the number of dorso-ventral lens files in the visual surface of *Calyptaulax*. Left eye used if sufficiently well preserved, right eye used otherwise. Each specimen is therefore represented only once in the figure. Range of values shown for each stratigraphical sample. Number of measurable specimens in each sample given in parentheses. Mean value and one standard deviation to either side of the mean shown for samples containing five or more specimens. Samples assigned to *C. (Calliops)* on the basis of phylogenetic analysis identified by a circle; samples assigned to *C. (Calyptaulax)* identified by a cross (see Section 6. 3. 3).

6. Depth of axial furrows.

There is a clear variation in the relative depths of cephalic axial furrows among the stratigraphical samples, with specimens belonging to some samples possessing relatively deep axial furrows (for example Plate 6. 4, figs. 1, 4, 7, 10-13, 15, 17, 19), and specimens belonging to other samples possessing relatively shallow axial furrows (for example Plate 6. 1, figs. 1-5, 7-10, 12, 15).

Ancestor comparison. The axial furrows of *P. sclerops* are relatively deep.

States. 0: deep axial furrows; 1: shallow axial furrows.

7. Shape of the pygidium.

Pygidia of *Calyptaulax* can be broadly divided into three categories on their overall shape as seen in dorsal view (Figure 6. 4).

Ancestor comparison. The pygidium of *P. sclerops* is triangular with outwardly-convex lateral margins.

States. 0: triangular with lateral margins outwardly convex; 1: triangular with straight lateral margins; 2: triangular with lateral margins sinuous, meeting at a pronounced point posteriorly.

8. Shape of pygidial axial rings.

There is variation in the shape of the individual rings making up the axis of the pygidium as seen in dorsal view (Figure 6. 4).

Ancestor comparison. The axial rings of *P. sclerops* are approximately oval in outline.

States. 0: axial rings oval; 1: axial rings markedly scalloped (Figure 6. 4).

9. Nature of the pygidial rib furrows.

A certain amount of confusion exists surrounding the correct definition of pleural and interpleural furrows on the pygidium of *Calyptaulax*. Ludvigsen and Chatterton (1982, p. 2192) and Whittington (1962, p. 13) use the term "pleural furrow" in reference to the furrows which extend from the axial furrow across the inner part of the pleural field. Cooper (1930) used the same term in reference to the furrows which extend from about half-way across the pleural field nearly to the margin of the pygidium. In order to avoid confusion it has been decided to follow Clarkson and Tripp (1982) and refer to the furrows which traverse the outer portion of the pleural field and do not reach the axial furrow as "rib furrows", and those that extend outward from the axial furrow across the inner portion of the pleural field as "inter-rib furrows", the unit thus delineated by two succeeding inter-rib furrows being termed a "pygidial rib" (Figure 6. 4). In fact it is here considered that the pygidial rib furrows of *Calyptaulax* are homologous with the pygidial pleural furrows of other trilobites. Compare for example Plate 6. 1, fig. 14 with Plate 5. 2, fig. 12 which shows a pygidium of *Achatella*. The pleural field of both consists of an anterior articulating facet succeeded by pleurae which become progressively more

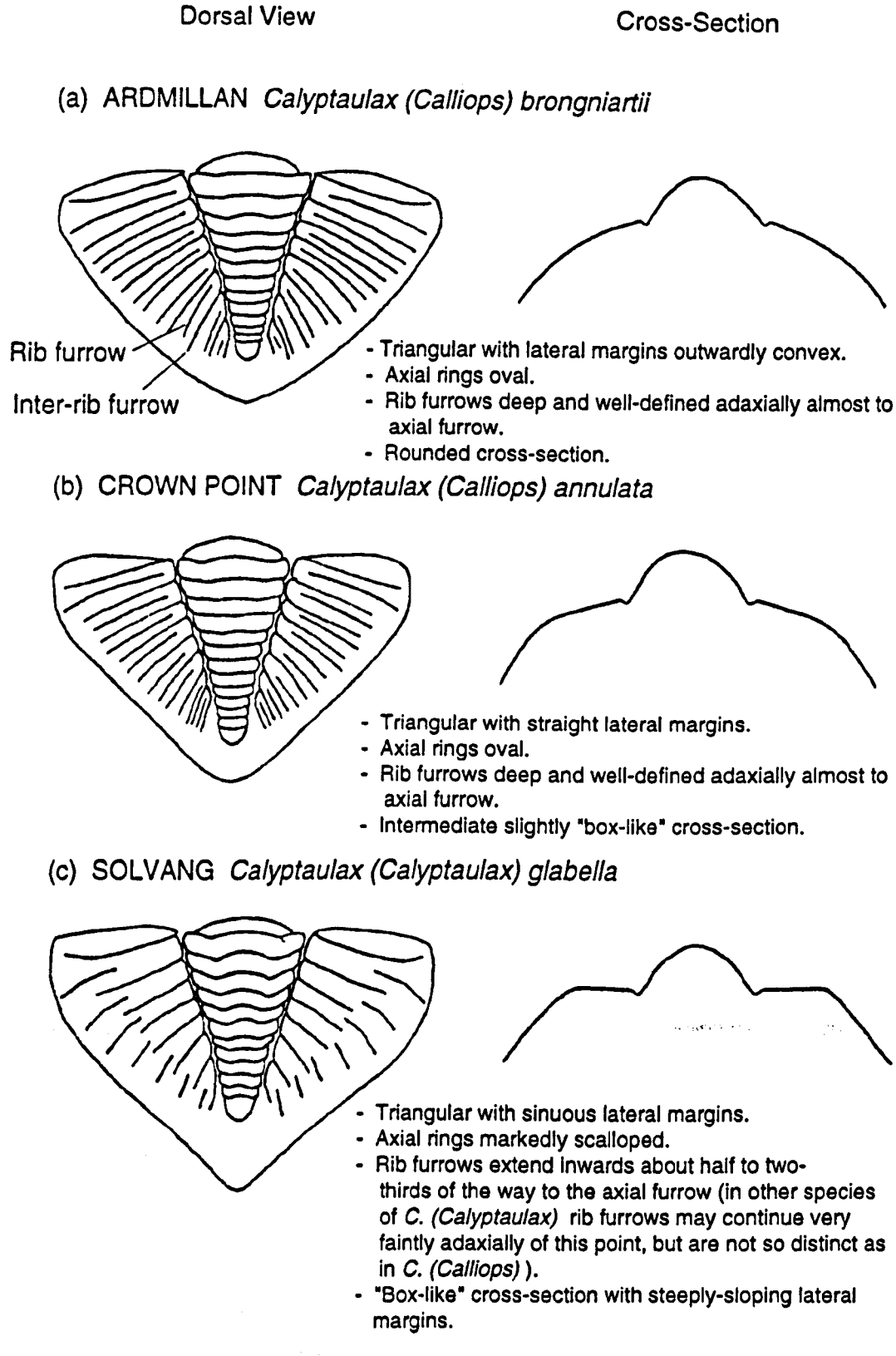

Figure 6. 4. Pygidia belonging to three selected stratigraphical samples of *Calyptaulax*, illustrating variation in shape of the pygidium as seen in dorsal view (cladistic character 7), shape of the pygidial axial rings (character 8), nature of the pygidial rib furrows (character 9) and shape of the pygidium as seen in cross-section (character 10).

indistinct posteriorly. Only the anteriormost three or four ribs (= pleurae) of *Calyptaulax* are confluent with axial rings. It can be seen that the rib furrows and inter-rib furrows of *Calyptaulax* are homologous with the pleural furrows and interpleural furrows respectively of other trilobites.

The coding for cladistic analysis of this character is based upon the variation in the nature of development of these rib furrows.
Ancestor comparison. As described above, it is considered that the rib furrows of *Calyptaulax* are homologous with the pleural furrows of other trilobites. In *P. sclerops* the pleural furrows are deep and well-defined adaxially as far as the axial furrow. (In fact if the rib furrows of *Calyptaulax* turn out to be homologous with the interpleural furrows of *P. sclerops* instead of the pleural furrows, this will make no difference to the coding of this character since the interpleural furrows of *P. sclerops* also extend in as far as the axial furrow).
States: 0: rib furrows deep and well-defined adaxially nearly as far as the axial furrow; 1: rib furrows deep and well-defined distally, much shallower or obsolete proximally.

10. Shape of the pygidium in cross-section.
There is variation in the cross-sectional shape of the pygidium (Figure 6. 4).
Ancestor comparison. The pygidium of *P. sclerops* has a somewhat rounded cross-section.
States. 0: rounded cross-section; 1: intermediate, slightly "box-like" cross-section; 2: very "box-like" cross-section with steeply-sloping lateral areas.

11. Nature of the glabellar sculpture.
There is variation in the nature of the glabellar sculpture. Many specimens of *Calyptaulax* possess small, densely-packed tubercles which are scattered over the entire surface of the glabella (see for example Plate 6. 4, figs. 1-4, 9-10, 15, 17). Some specimens from the Caradoc of North America however possess slightly coarser tubercles, again densely-packed over the whole glabella (Plate 6. 3, figs. 7-10, 12, 15).

The glabellar sculpture of many Caradoc specimens is visible on both the internal cast and the external mould (compare for example Plate 6. 4, fig. 17, an internal mould, with Plate 6. 4, fig. 4, a latex cast made from the corresponding counterpart). This does not however appear to be the case for some of the Caradoc and Ashgill forms. In these specimens, the internal mould may show a faint trace of small densely-packed tubercles (for example Plate 6. 2, fig. 16), or may show only an oval pattern of small tubercles on the frontal lobe (Plate 6. 3, fig. 17). Plate 6. 1, fig. 2, which is a testate specimen, demonstrates that while the internal mould (part of which is visible through a missing piece of the test) may be smooth (except for the oval pattern of small tubercles on the

frontal lobe), the external surface of the test may be tuberculate. For this reason, glabellar sculpture has been coded for all samples from counterparts or testate specimens. Also for this reason, Cooper's (1930) separation of two species, *Calyptaulax glabella and C. compressa*, from the Rawtheyan of Percé, Québec, chiefly on the criterion that one possesses a sculpture of small tubercles while the other is smooth, is here considered invalid.

Ancestor comparison. The glabella of *P. sclerops* is covered with "small, closely spaced tubercles" (Whittington 1950).

States. 0: small, closely spaced tubercles; 1: slightly larger tubercles, still densely packed; 2: larger, densely packed tubercles.

6.3.2. Results.

The matrix of character states for the stratigraphical samples of *Calyptaulax* is shown in Table 6. 2. It is to be expected that the phylogenetic analysis will find a large number of equally parsimonious trees since a number of the OTUs (= stratigraphical samples) are identical in their codings (see for example DOW HILL, BALCLATCHIE B, ARDMILLAN, KILN, BARDAHESSIAGH and probably KIRKCOLM as well when one allows for missing data) and a lot of trees will result simply from rearranging these identical OTUs. Also, it was accepted *a priori* that there is a lot of "noise" in the data matrix due to the presence of characters of low burden, especially that subset of it which pertains to North American middle-to-late Caradoc samples.

Phylogenetic analysis was performed using the PAUP computer program version 3.1 run on an Apple Macintosh IIsi. Because of the size of the data matrix (41 OTUs, including *P. sclerops*) it was not feasible to run a search using the branch and bound algorithm. Instead a heuristic search was undertaken using the "simple" addition sequence and tree bisection-reconnection (TBR) branch swapping. The PAUP nexus file is given in Appendix 4. A limit was set so that the analysis would not retain more than 1000 most parsimonious trees, and this limit was hit during the search. This means that there are at least 1000 equally parsimonious trees for this matrix, for the reasons described above. The minimum tree length is 22 steps. The strict consensus tree is shown in Figure 6. 5, and has a consistency index (Rohlf's CI(1)) of 0.115. This low index is due to (a) noise in the matrix, discussed above, and (b) the sheer number of OTUs in the analysis: consistency index is negatively correlated with the number of OTUs included in an analysis (Klasser *et al.* 1991).

The tree can be separated into two halves:

(i) A clade of 20 OTUs defined by two synapomorphies at node 2 (character 9, state 1; character 10, state 2). This clade subdivides into two groups: firstly a Llanvirn to middle Caradoc group containing the samples CONFINIS A, STINCHAR and

Table 6. 2. Character states for cladistic analysis of *Calyptaulax* stratigraphical samples. See Section 6. 2 for explanation of the samples.

Sample	1	2	3	4	5	6	7	8	9	10	11
P. SCLEROPS	0	0	0	0	0	0	0	0	0	0	0
CONFINIS A	1	2	0	0	?	0	0	1	1	2	1
CONFINIS B	1	1	0	0	0	0	1	0	0	0	0
STINCHAR	1	2	0	0	0	0	0	1	1	2	1
DOULARG	1	2	0	?	?	0	?	?	?	?	1
DOW HILL	1	1	0	0	0	0	0	0	0	0	1
BALCLATCHIE A	1	1	0	0	0	0	0	0	0	0	1
BALCLATCHIE B	3	2	0	?	?	0	2	1	1	2	1
KIRKCOLM	1	1	0	0	0	0	?	?	0	0	1
ARDMILLAN	1	1	0	0	0	0	0	0	0	0	1
PINMERY	3	2	0	?	?	0	2	1	1	2	1
KILN	1	1	0	0	0	0	0	0	0	0	1
STARFISH	1	1	0	0	1	1	2	1	1	2	?
BARDAHESSIAGH	1	1	0	0	0	0	0	0	0	0	1
CROWN POINT	1	1	0	0	0	0	1	0	0	1	1
ESBATAOTTINE	1	1	0	1	0	0	2	1	0	1	2
DUCK	1	1	0	1	0	0	0	0	0	0	2
CANNON	1	1	0	1	0	0	?	?	?	?	2
TRENTON	1	1	0	1	0	0	0	0	0	0	2
ELKADER	1	1	0	1	0	0	0	0	0	0	2
ATHENS	1	1	0	?	0	0	2	1	0	1	2
VERULAM	1	1	0	1	0	0	0	0	0	0	2
BELLEVILLE	1	1	0	1	?	0	?	?	?	?	2
LINDSAY	1	1	0	1	0	0	?	?	?	?	2
FAIRMOUNT	1	1	0	1	?	0	?	?	?	?	2
MAQUOKETA	1	1	0	1	0	0	0	0	0	0	1
FT. ATKINSON	1	1	0	1	0	0	0	0	0	0	1
MATAPEDIA	2	2	0	0	?	1	2	1	1	2	1
ACTON	2	2	1	0	?	1	2	1	1	2	1
DUFTON (ONN)	2	2	0	?	?	1	?	1	1	2	?
DUFTON (PUS)	2	2	1	?	?	1	2	1	1	2	1
APPLETHWAITE	2	2	1	?	?	1	2	1	1	2	?
SHOLESHOOK	2	2	0	?	?	1	2	1	1	2	?
RHIWLAS	2	2	0	?	?	1	2	1	1	2	?
DDOLHIR	2	2	0	0	1	1	2	1	1	2	1
SOLVANG	2	2	0	0	1	1	2	1	1	2	1
VENSTØP	2	2	0	0	?	1	2	1	1	2	1
GAGNUM	2	2	0	0	?	1	2	1	1	2	?
SØRBAKKEN	2	2	0	0	?	1	2	1	1	2	?
KJØRRVEN	2	2	0	0	1	1	2	1	1	2	?
HUSBERGØYA	2	2	0	0	1	1	?	?	?	?	?

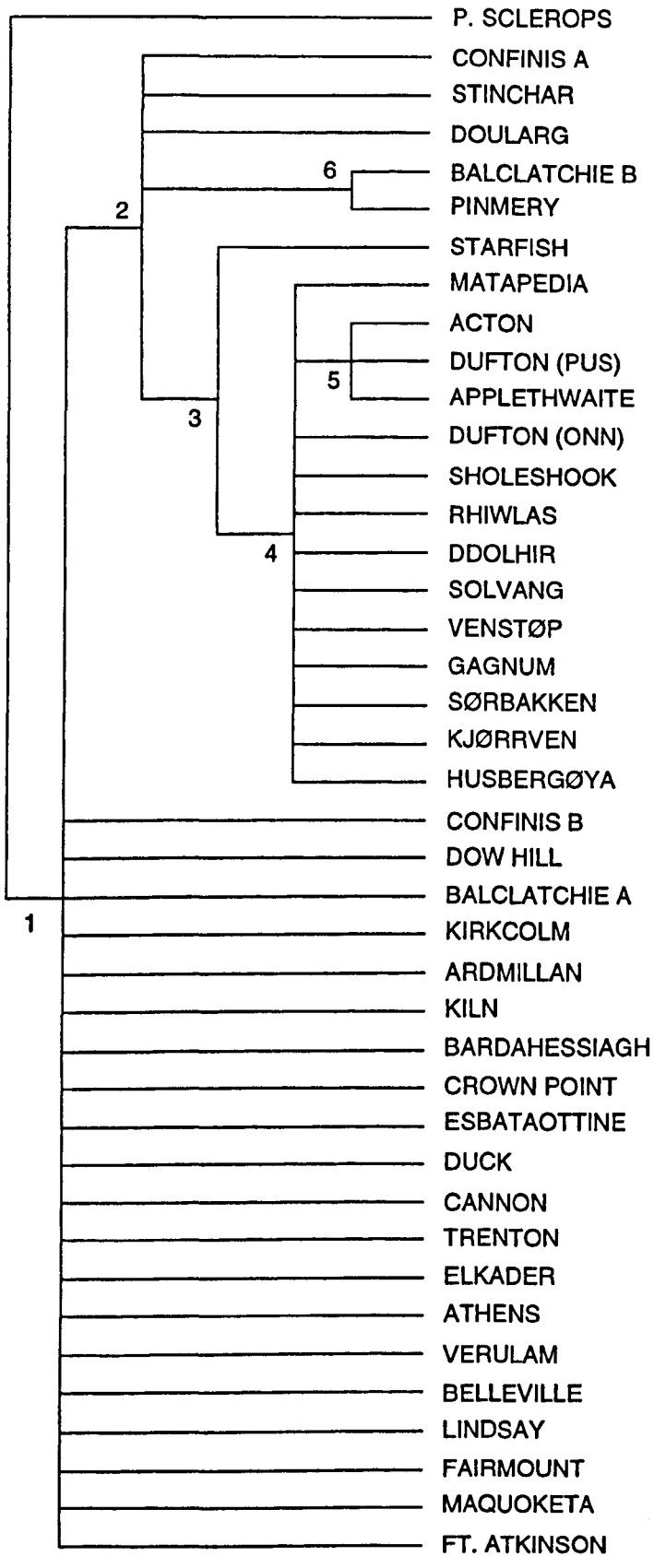

Figure 6. 5. Strict consensus tree for stratigraphical samples of *Calyptaulax* based on 1000 trees. Length 22 steps, consistency index 0.115.

DOULARG which are identical (allowing for missing data) as well as BALCLATCHIE A and PINMERY which are joined by a synapomorphy at node 6 (character 1, state 3); and secondly a clade defined by two synapomorphies at node 3 (character 5, state 1; character 6, state 1), containing upper Caradoc and Ashgill samples (STARFISH - HUSBERGØYA clade). A further synapomorphy at node 4 (character 1, state 2) defines a clade which consists of two groups of samples: one. defined by the synapomorphy at node 5 (character 3, state 1) consists of the upper Caradoc Avalonian samples ACTON, DUFTON (PUS) and APPLETHWAITE; the other group consists of Ashgill samples from Avalonia, Laurentia and Baltica as well as the upper Caradoc samples DUFTON (ONN) and SOLVANG.

(ii) An unresolved group consisting mainly of Caradoc samples from Laurentia with the addition of MAQUOKETA and FT. ATKINSON from the Ashgill, also in Laurentia. Although there is only one synapomorphy to define a subclade within this half of the cladogram, a number of groupings can be identified based on shared possession of character complexes. The early to middle Caradoc samples DOW HILL, BALCLATCHIE A, KIRKCOLM, ARDMILLAN, KILN, BARDAHESSIAGH and ATHENS are identical in their character codings (allowing for missing data in KIRKCOLM). Similarly the Shermanian (approximately late middle Caradoc) samples DUCK, TRENTON, ELKADER and VERULAM are identical in their codings while the approximately contemporaneous samples CANNON, BELLEVILLE and LINDSAY and the Maysvillian FAIRMOUNT are also probably members of this species when allowance is made for missing pygidial characters. CROWN POINT and ESBATAOTTINE are joined by a synapomorphy (character 10) although they each share other characters in common with other samples. MAQUOKETA and FT. ATKINSON are identical in their character codings, and are very similar to the DUCK - FAIRMOUNT group, differing only in the nature of the glabellar sculpture (character 11) which they share with the DOW HILL - ATHENS group.

The overall impression that is given by the cladogram in Figure 6. 5 is that *Calyptaulax* can be separated into two broad groups of samples on the basis of pygidial characters (characters 9 and 10). One group (upper half of the tree, group (i) above) is made up of samples representing the entire duration and geographical extent of the genus, and subdivides into a set of subclades which can be regarded as representing species. The other group (lower half of the tree, group (ii) above) consists of Laurentian samples from the middle - to - upper Caradoc and Ashgill, and is unresolved because of a complex pattern of states expressed by characters which are clearly of low burden. See Figure 6. 6 for traces of the character states through the consensus tree.

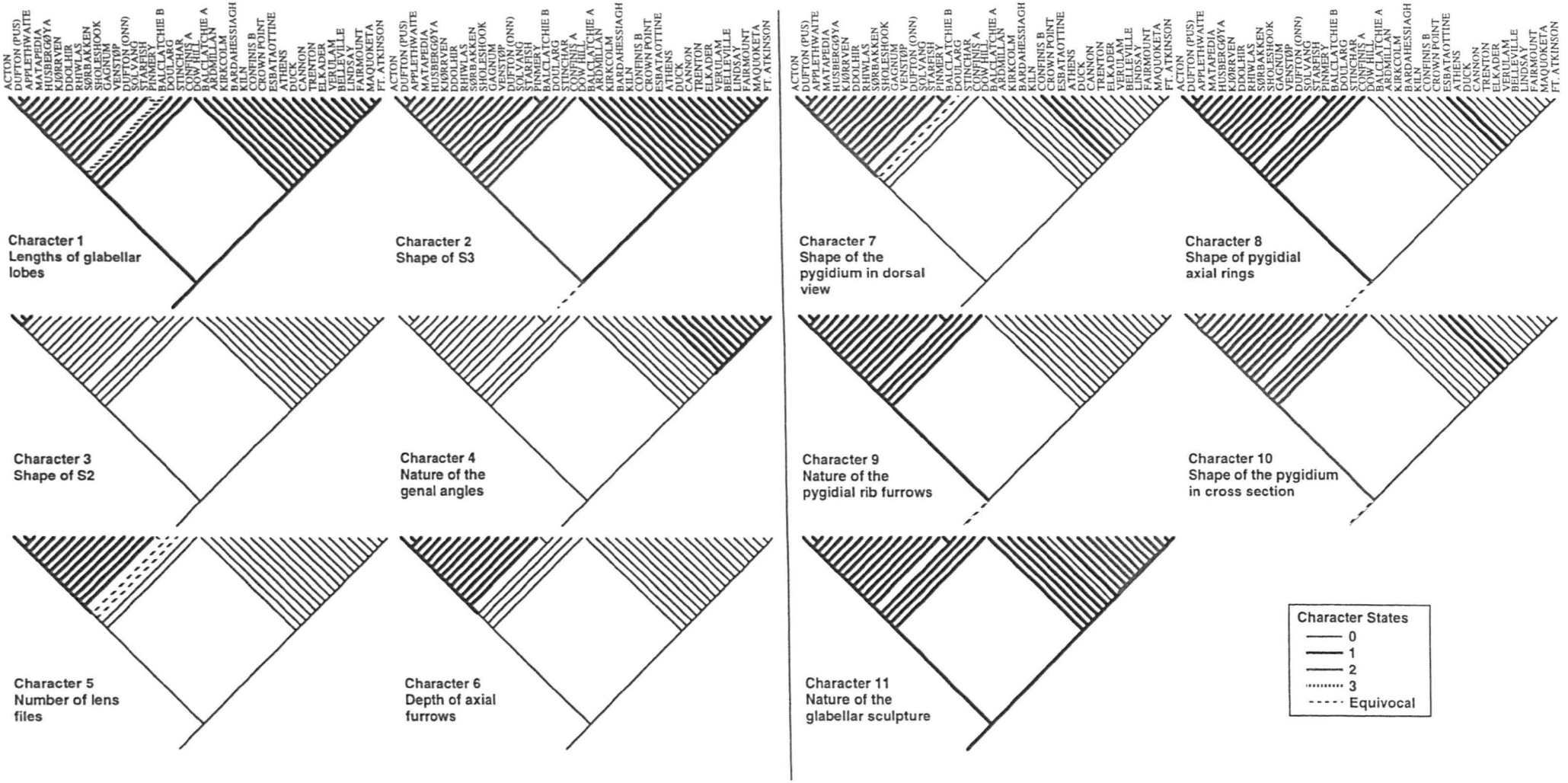

Figure 6. 6. Character state traces through the strict consensus tree for stratigraphical samples of *Calyptaulax*.

The second step of the phylogenetic analysis was to group stratigraphical samples together into presumed species and subject these species to cladistic analysis. The assignment of samples to species has been done on the basis of the following:

1. The clustering exhibited by the sample-based cladogram (Figure 6. 5).
2. Shared identity of combinations of character states in the input data matrix (allowing for missing data).
3. Stratigraphical and geographical affinity.

The samples are assigned to species as follows:

1. *P. sclerops* (Dalman, 1827). The genotype specimen figured by Whittington (1950).
2. C. *foederatus* Tripp, 1962 = CONFINIS A, STINCHAR, DOULARG.
3. *C. marginatus* Tripp, 1962 = CONFINIS B.
4. *C. annulata* Raymond, 1905 = CROWN POINT.
5. *C. callirachis* Cooper, 1953 = ESBATAOTTINE, ATHENS.
6. *C. brongniartii* (Portlock, 1843) = DOW HILL, BALCLATCHIE A, KIRKCOLM, ARDMILLAN, KILN, BARDAHESSIAGH.
7. *C. hunteri* (Reed, 1914) = BALCLATCHIE B, PINMERY.
8. *C. callicephala* (Hall, 1847) = DUCK, CANNON, TRENTON, ELKADER, VERULAM, BELLEVILLE, LINDSAY, FAIRMOUNT.
9. *C. actonensis* Dean, 1961 = ACTON, DUFTON (PUS), APPLETHWAITE.
10. *C. glabella* Cooper, 1930 = MATAPEDIA, DUFTON (ONN), SHOLESHOOK, RHIWLAS, DDOLHIR, SOLVANG, VENSTØP, GAGNUM, SØRBAKKEN, KJØRRVEN, HUSBERGØYA.
11. *C. larrabeei* (Slocum, 1913) = MAQUOKETA, FT. ATKINSON.
12. *C. asteroideus* (Reed, 1914) = STARFISH.

The input data matrix is shown in Table 6. 3. The characters are the same as those used in the sample-based cladistics above. As before, all characters are treated as unordered and undirected, and are polarised from 0 to 1 (to 2 to 3 where applicable) where 0 is the ancestral state as expressed in *P. sclerops*. Because of the smaller number of OTUs in this matrix and the smaller amount of missing data it was possible to perform a search using the branch and bound algorithm. The PAUP nexus file is given in Appendix 4.

Eighteen most parsimonious trees were found, of length 22 steps. The strict consensus tree has a consistency index (Rohlf's CI(1)) of 0.309 and is shown in Figure 6. 7. The character states are traced through the consensus tree in Figure 6. 8. It can be seen that the bipartite structure of the sample-based cladogram is retained:

Table 6. 3. Character states for cladistic analysis of *Calyptaulax* species.

Species	1	2	3	4	5	6	7	8	9	10	11
P. sclerops	0	0	0	0	0	0	0	0	0	0	0
C. foederatus	1	2	0	0	0	0	0	1	1	2	1
C. hunteri	3	2	0	?	?	0	2	1	1	2	1
C. asteroideus	1	1	0	0	1	1	2	1	1	2	?
C. glabella	2	2	0	0	1	1	2	1	1	2	1
C. actonensis	2	2	1	0	?	1	2	1	1	2	1
C. marginatus	1	1	0	0	0	0	1	0	0	0	0
C. annulata	1	1	0	0	0	0	1	0	0	1	1
C. callirachis	1	1	0	1	0	0	2	1	0	1	2
C. brongniartii	1	1	0	0	0	0	0	0	0	0	1
C. callicephala	1	1	0	1	0	0	0	0	0	0	2
C. larrabeei	1	1	0	1	0	0	0	0	0	0	1

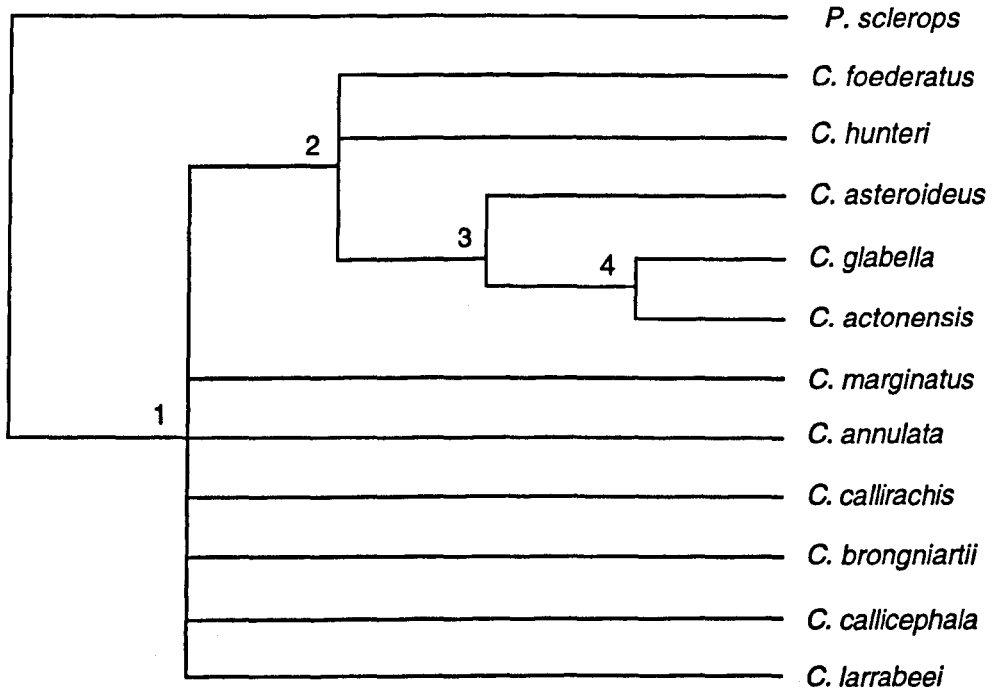

Figure 6. 7. Strict consensus tree for species of *Calyptaulax* based on 18 trees. Length 22 steps, consistency index 0.309.

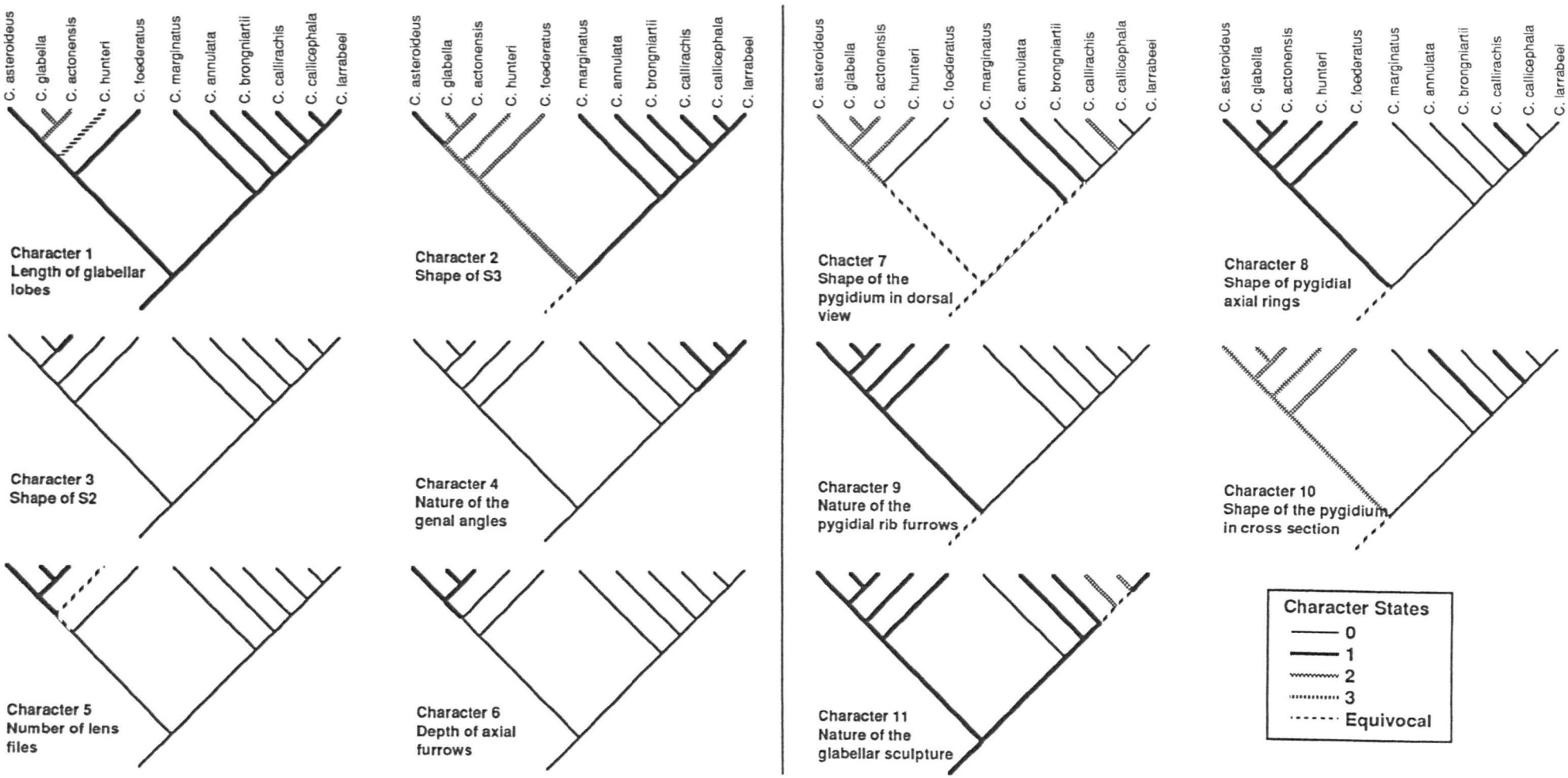

Figure 6. 8. Character state traces through the strict consensus tree for species of *Calyptaulax*.

(i) A relatively well-resolved upper group is defined by two synapomorphies (character 9, state 1; character 10, state 2) with subclades defined at node 3 (1 synapomorphy: character 6, state 1) and at node 4 (1 synapomorphy: character 1, state 2).

(ii) An unresolved group in which no unequivocal synapomorphies are revealed. Species in this group are defined on the basis of character combinations rather than synapomorphies.

6.3.3. Conclusions from Phylogenetic Analysis.

The following conclusions can be drawn from this exercise:

1. The genus *Calyptaulax* consists of two species groups, separable on the basis of pygidial characters (cladistic character 9: nature of the pygidial "rib" furrows; cladistic character 10: shape of the pygidium seen in cross-section). One group, here defined as subgenus *Calyptaulax (Calyptaulax)* (Cooper, 1930) contains five species: *C. foederatus*, *C. hunteri*, *C. asteroideus*, *C. glabella* and *C. actonensis*, and may be defined as the group in which character 9 takes the value 1 (rib furrows well-defined distally, much shallower or obsolete proximally) and character 10 takes the value 2 (pygidium very "box-like" in cross-section). The other group, here defined as subgenus *Calyptaulax (Calliops)* (Delo, 1935) contains six species: *C. marginatus*, *C. annulata*, *C. callirachis*, *C. brongniartii*, *C. callicephala* and *C. larrabeei*, and in this group character 9 takes the value 0 (rib furrows well defined adaxially nearly as far as the axial furrow) and character 10 may take either the value 0 or 1 (pygidium rounded in cross-section, or only slightly "box-like"). The diagnoses of these two subgenera do not equate to the diagnoses of the old genera *Calyptaulax* Cooper and *Calliops* Delo.
2. *C. (Calyptaulax)* is relatively well resolved on the cladogram with subclades which occur in correct stratigraphical order (Figure 6. 7).
3. *C. (Calliops)* is unresolved on the cladogram. Some of the species can only be recognised on character combinations, rather than by autapomorphies. The unresolved nature of this clade is due to mosaic evolution involving convergences in characters of low burden.

6. 4. Morphometric Analysis.

Detailed morphometrics have been undertaken on the exoskeleton of *Calyptaulax*, selected from the 40 stratigraphical samples. The analysis has similar aims to that carried out on *Achatella* (Chapter 5), *i.e.* to determine whether the genus really is morphologically stable throughout its duration, to determine the boundaries of this stability both in terms of temporal variation and intrapopulational variation on a time plane, and to study characters showing high variability to determine whether this variability is systematic or non-systematic, reversible or non-reversible. Further, to

determine whether morphometric analysis can discriminate between the putative subgenera *C. (Calyptaulax)* (Cooper, 1930) and *C. (Calliops)* (Delo, 1935) erected on the basis of phylogenetic analysis (Section 6. 3).

Since ontogenetic material is available for this genus, it is also possible to study how the form of the animal changes with growth, and investigate the possibility of a heterochronic relationship between *C. (Calyptaulax)* and *C. (Calliops)* (see Section 6. 4. 4.).

A set of measurements has been defined which together describe the shape of the cephalon and pygidium. Thoraxes and hypostomes have not been used as they are not available in sufficient numbers for most species and stratigraphical samples. Principal component analysis (PCA) has been used to analyse the data, with uni- and bivariate methods employed to study certain key variables in more detail (see Chapter 4 for discussion of PCA).

In all, detailed morphometrics has been done on 180 holaspide cephala and cranidia, 246 holaspide pygidia, 11 meraspide cranidia, 8 meraspide pygidia, and 3 protaspides. Also, 279 visual surfaces, representing 191 individual animals, have been studied in detail.

6. 4. 1. Measurements Used.

Measurements were made on internal moulds of the exoskeleton using a single orientation method as described in Chapter 4. The horizontal plane for orientation of the specimens was defined as for *Achatella* (Chapter 5), *i.e.* with the chord of the palpebral surface horizontal for cephala and cranidia, and the ventral margin of the border horizontal for pygidia (Shaw 1957: 194; Temple 1975: 463). Measurements whose defining end points are in furrows were measured to the deepest point of the furrow. Where a bilaterally symmetrical structure was missing on one side of the specimen but present on the other, the original symmetry was used to derive the full transverse measurement.

Figure 6. 9 shows the complete set of measurements made on cephala and pygidia of *Calyptaulax*. Measurements are based on those of Shaw (1957), Temple (1975) and Ramsköld (1988), and are fully defined in Table 6. 4.

The morphometric data on *Calyptaulax* are organised into two data sets for PCA as follows:

1. *Cranidium data set.* This consists of all specimens for which the following set of measurements was available:

b5 (left and right)	b!5 (left and right)
b32 (left and right)	b!32 (left and right)

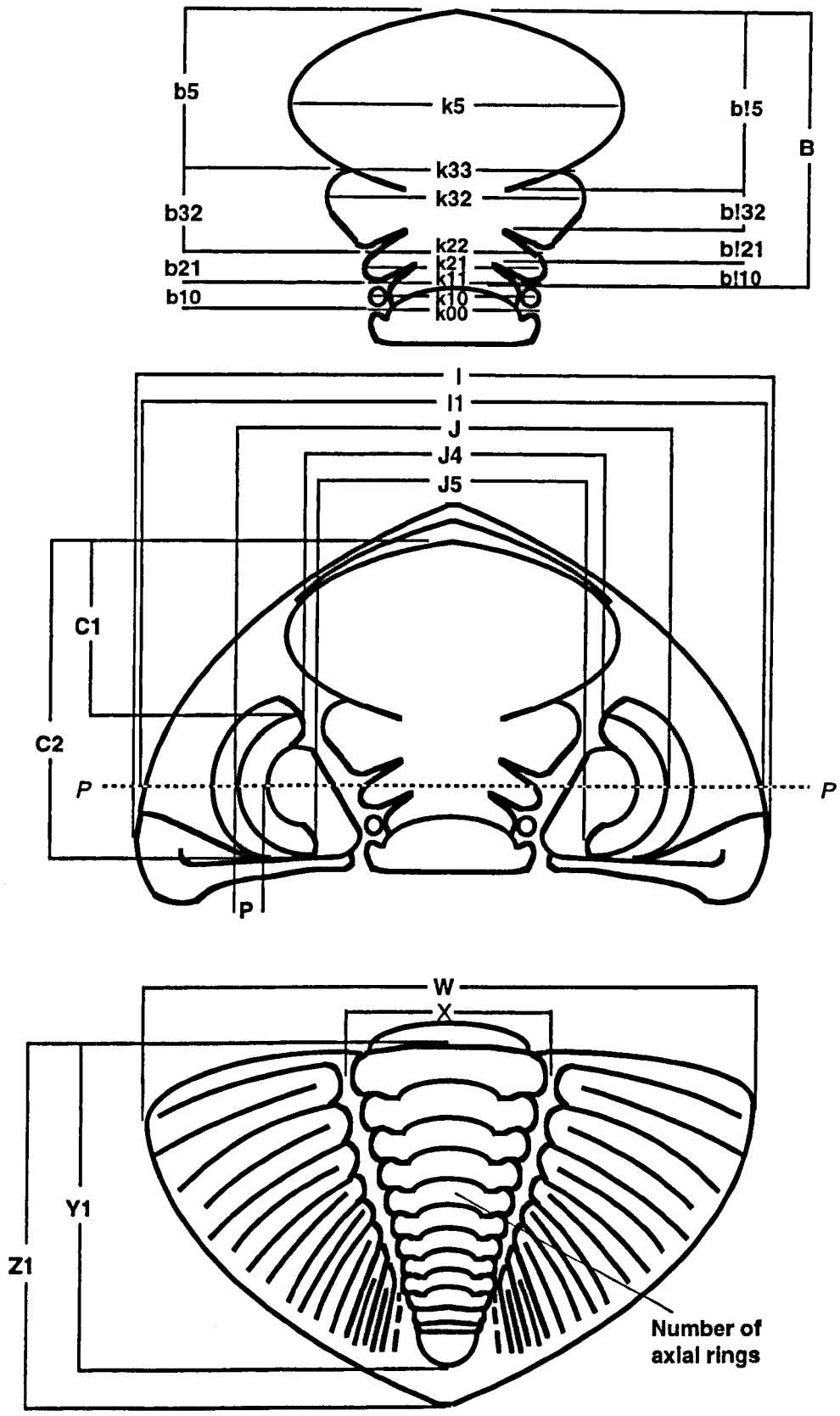

Figure 6. 9. Measurements made on cephala and pygidia of *Calyptaulax*. All measurements made on internal moulds with the specimen orientated in dorsal view (see text). Measurements used in principal components analysis (PCA) in bold type. The dotted line *PP* is the line which bisects the lengths (exsag.) of the left and right palpebral lobes. See Table 6. 4 for formal definitions of the measurements.

Table 6. 4. Definitions of measurements made on the exoskeleton of *Calyptaulax*. For each measurement, an abbreviated name (in bold), a formal name (in italics), and a full definition are given. See Figure 6. 9 for illustrative diagram.

CEPHALA

B: *Preoccipital glabellar length.* Sag. length of glabella as measured from the anteriormost extremity of the frontal lobe to the deepest point in the occipital furrow.

I: *Maximum cephalic width.* Width (tr.) of cephalon as measured across the widest point.

I1: *Mid. palpebral cephalic width.* Width (tr.) of cephalon as measured along a line which bisects the lengths (exsag.) of the left and right palpebral lobes.

J: *Palpebral cranidial width.* Width (tr.) of cranidium from outer edge of left palpebral lobe to outer edge of right palpebral lobe as measured along the line which bisects the lengths (exsag.) of the left and right palpebral lobes. All palpebral lobes are approximately symmetrical about this line.

J4: *Pre-palpebral cranidial width.* Width (tr.) of cranidium from anteriormost point of left palpebral lobe to anteriormost point of right palpebral lobe.

J5: *Post-palpebral cranidial width.* Width (tr.) of cranidium from posteriormost point of left palpebral lobe to posteriormost point of right palpebral lobe.

b5: *Distal length of frontal lobe.* Length (exsag.) of frontal lobe as measured from a point opposite the anteriormost extremity of the frontal lobe to the distal extremity of S3. Left and right side.

b32: *Distal length of L3.* Length (exsag.) of L3 as measured from the distal extremity of S3 to a point opposite the distal extremity of S2. Left and right side.

b21: *Distal length of L2.* Length (exsag.) of L2 as measured from the distal extremity of S2 to a point opposite the distal extremity of S1. Left and right side.

b10: *Distal length of L1.* Length (exsag.) of L1 as measured from the distal extremity of S1 to a point opposite the distal extremity of S0. Left and right side.

b!5: *Proximal length of frontal lobe.* Length (exsag.) of frontal lobe as measured from a point opposite the anteriormost extremity of the frontal lobe to the proximal extremity of S3. Left and right side.

b!32: *Proximal length of L3.* Length (exsag.) of L3 as measured from the proximal extremity of S3 to a point opposite the proximal extremity of S2. Left and right side.

b!21: *Proximal length of L2.* Length (exsag.) of L2 as measured from the proximal extremity of S2 to a point opposite the proximal extremity of S1. Left and right side.

b!10: *Proximal length of L1.* Length (exsag.) of L1 as measured from the proximal extremity of S1 to the deepest point of S0 on the sagittal line. Left and right side.

Table 6. 4. Continued.

k5: *Width (tr.) of frontal lobe.* Maximum width (tr.) of frontal lobe as measured from left branch of facial suture to corresponding point on right branch.

k32: *Width (tr.) of glabella across L3.* Width (tr.) of glabella across widest point of L3 lobes (*i.e.* just to posterior of distal end of S3 furrows), measured from deepest point in left axial furrow to corresponding point in right axial furrow.

k21: *Width (tr.) of glabella across L2.* Width (tr.) of glabella across widest point of L2 lobes measured from deepest point in left axial furrow to corresponding point in right axial furrow.

k10: *Width (tr.) of glabella across L1.* Width (tr.) of glabella across widest point of L1 lobes measured from deepest point in left axial furrow to corresponding point in right axial furrow.

k33: *Width (tr.) of glabella across S3.* The transverse measurement from the point of intersection of the left hand S3 furrow with the left axial furrow, to the corresponding point on the right hand side.

k22: *Width (tr.) of glabella across S2.* The transverse measurement from the point of intersection of the left hand S2 furrow with the left axial furrow, to the corresponding point on the right hand side.

k11: *Width (tr.) of glabella across S1.* The transverse measurement from the point of intersection of the left hand S1 furrow with the left axial furrow, to the corresponding point on the right hand side.

k00: *Width (tr.) of glabella across S0.* The transverse measurement from the point of intersection of the left branch of the occipital furrow with the left axial furrow, to the corresponding point on the right hand side.

C1: *Longitudinal position of anterior of eye.* Exsag. distance from a point opposite the anteriormost extremity of the frontal lobe to the anteriormost extremity of the palpebral lobe as seen in dorsal view. Left and right side.

C2: *Longitudinal position of posterior of eye.* Exsag. distance from a point opposite the anteriormost extremity of the frontal lobe to the posteriormost extremity of the palpebral lobe as seen in dorsal view. Left and right side.

P: *Width (tr.) of palpebral lobe.* Transverse width of the palpebral lobe from the outer edge to the deepest point in the palpebral furrow, measured along the line which bisects the lengths (exsag.) of the left and right palpebral lobes. Left and right side.

PYGIDIA

W: *Pygidial width.* Width (tr.) of pygidium measured across the widest point.

Z1: *Pygidial length.* Length (sag.) of pygidium measured from the deepest point in the articulating furrow to the posteriormost extremity of the pygidium.

Table 6. 4. Continued.

Y1:	*Length of pygidial axis.* Length (sag.) of pygidial axis measured from the deepest point in the articulating furrow to the posteriormost extremity of the axis.
X:	*Width of pygidial axis.* Width (tr.) of pygidial axis measured across the widest point, from the deepest point in the left axial furrow to the corresponding point in the right axial furrow.
	Number of axial rings. Number of distinct rings making up the pygidial axis, excluding the articulating facet at the anterior of the pygidium.

b21 (left and right)	b!21 (left and right)
b10 (left and right)	b!10 (left and right)
k5	k33
k32	k22
k21	k11
k10	k00
B	C1 (left and right)
J	C2 (left and right)
J4	P (left and right)
J5	

These measurements almost completely describe the form of the cranidium. All of the above measurements were obtainable for 153 specimens.

2. *Pygidium data set.* This set consists of all pygidia for which the following measurements were obtainable:

W	Z1
Y1	Number of axial rings

These measurements were obtainable for 192 specimens.

In the following plots, the various stratigraphical samples are represented by coloured symbols. Figure 6. 10 explains the symbols used. Results of the analysis of morphometrics on holaspide material will be described first, followed by a consideration of the ontogenetic material.

6. 4. 2. Results.

PCA on cranidium data set. Principal components (PCs) of the 34 measurements used were calculated. The resulting eigenvalues and eigenvectors are given in Appendix 6 and the PC scores are given in Appendix 7. PC1 summarises 85.8% of the total variance in the data set, PC2 3.3%, PC3 2.3%. The 153 specimens are ordinated on the first three PC axes in Figure 6. 11.

As discussed in Chapter 4, PC1 sorts the specimens with respect to size. This can be confirmed by comparing Figure 6. 11 (a) with Figure 6. 12, which is a bivariate plot of width (tr.) of frontal lobe (k5) against preoccipital glabellar length (B). Also, on inspection of the values in eigenvector 1 (Appendix 6), it is seen that all measurements have an approximately equal contribution in the calculation of PC1, further evidence that this PC represents specimen size. The Pearson correlation coefficient relating score on PC1 to B for the 153 cranidia is r = -0.991. As one would expect, the ontogenetic

Figure 6. 10. Symbols used to distinguish stratigraphical samples in morphometric plots of *Calyptaulax*. Stratigraphical samples formally defined in the text. See Section 6. 2. for stratigraphy.

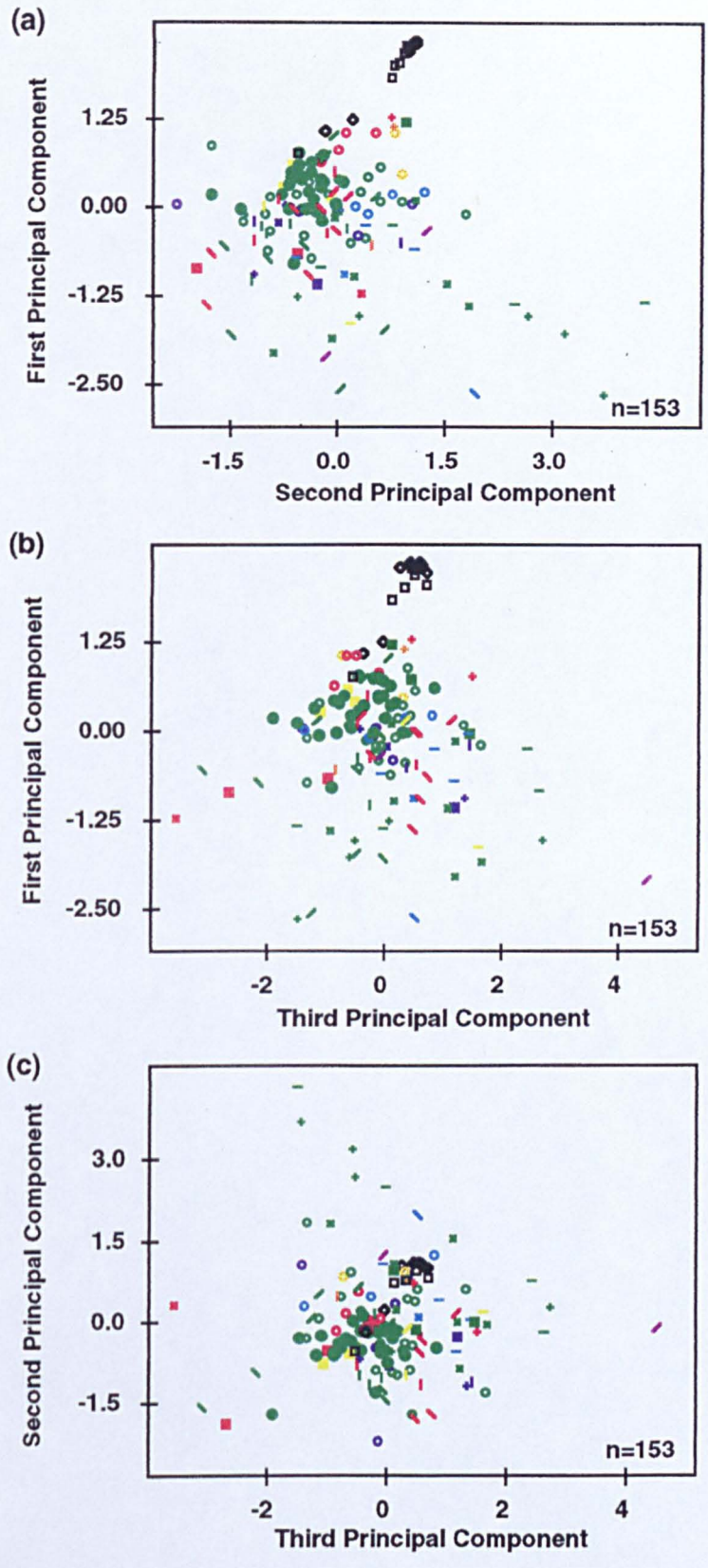

Figure 6. 11. Cranidia of *Calyptaulax* ordinated along the first three principal component axes calculated from the cranidium measurement scheme. Symbols as in Figure 6. 10.

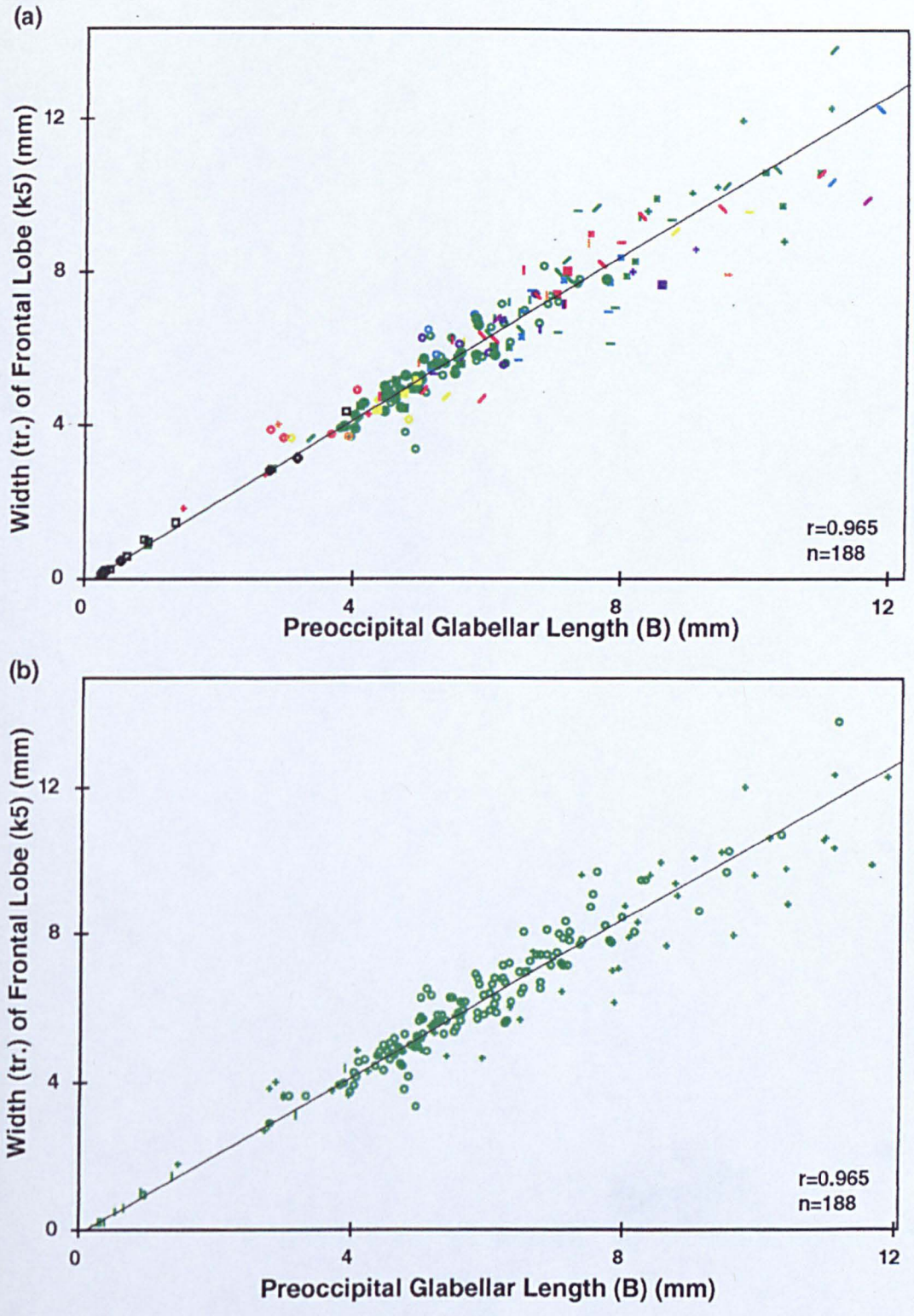

Figure 6. 12. Bivariate scatter plot of width (tr.) of frontal lobe (k5) against preoccipital glabellar length (B) for *Calyptaulax*. (a) stratigraphical samples, symbols as in Figure 6. 10; (b) subgenera, symbols used: specimens assigned to *C. (Calliops)* (circles); specimens assigned to *C. (Calyptaulax)* (crosses); meraspide specimens (vertical bars); protaspide specimens (horizontal bars).

material from the CROWN POINT and ESBATAOTTINE samples plots at the extreme end of the PC1 scale (note that positive values of PC1 represent small size, negative values large size). Ontogenetic material will be discussed more fully later.

Figure 6. 11 (c) shows the cranidia ordinated on PC2 and PC3, to summarise the majority of size-independent (*i.e.* shape) variation in the data (see Chapter 4 for explanation of how PCA does this). The stratigraphical samples are not separated on the plot. Three of the specimens plot in aberrant locations:

- A specimen from the sample BELLEVILLE (red x, left of plot). This is a slightly damaged, although not obviously distorted, specimen;
- A specimen from the sample APPLETHWAITE (Purple /, right of plot). This specimen is slightly distorted, but was included due to the small number of measurable specimens available for this sample;
- A specimen from the sample DDOLHIR (green -, top of plot). This is a slightly flattened specimen.

Figure 6. 13 is a reproduction of Figure 6. 11, but here specimens assigned to the subgenera *C. (Calyptaulax)* and *C. (Calliops)* on the basis of phylogenetic analysis (see Section 6. 3), and also the ontogenetic material, are distinguished by different plotting symbols. In 6. 13 (a) it can be seen that both subgenera occupy the whole range of overall size variation. *C. (Calyptaulax)* appears to be more concentrated in the upper size range (negative values of PC1) while *C. (Calliops)* tends to concentrate in the middle and lower range. On Figure 6. 13 (c), which shows size-independent variation, *C. (Calliops)* specimens tend to lie in the centre of the plot with outliers in the left-hand and lower areas. *C. (Calyptaulax)* occupies the right-hand side and upper regions.

The changing pattern of morphospace occupation is revealed in Figure 6. 14. Here, the stratigraphical samples are grouped into four broad time windows (this is merely a convenient way of grouping the samples; there is no implication that samples plotted in the same time window are precisely contemporaneous). The upper half of the diagram highlights the stratigraphical samples. In general morphospace occupation in the Llanvirn and lower Caradoc is relatively restricted. One holaspide specimen from the sample CROWN POINT plots away from the rest (red dot, lower left of Llanvirn plot, Figure 6.14 (a)). There is no real change in morphospace occupied (both in terms of area filled and locus of centre of occupation) until the Ashgill. At this time, the apparent centre of occupation is shifted right and upwards relative to earlier times, and the area occupied is greatly increased. The stratigraphical samples themselves still overlap greatly. Specimens from MAQUOKETA (green \) are well grouped together and appear to some extent separable from the rest (see below).

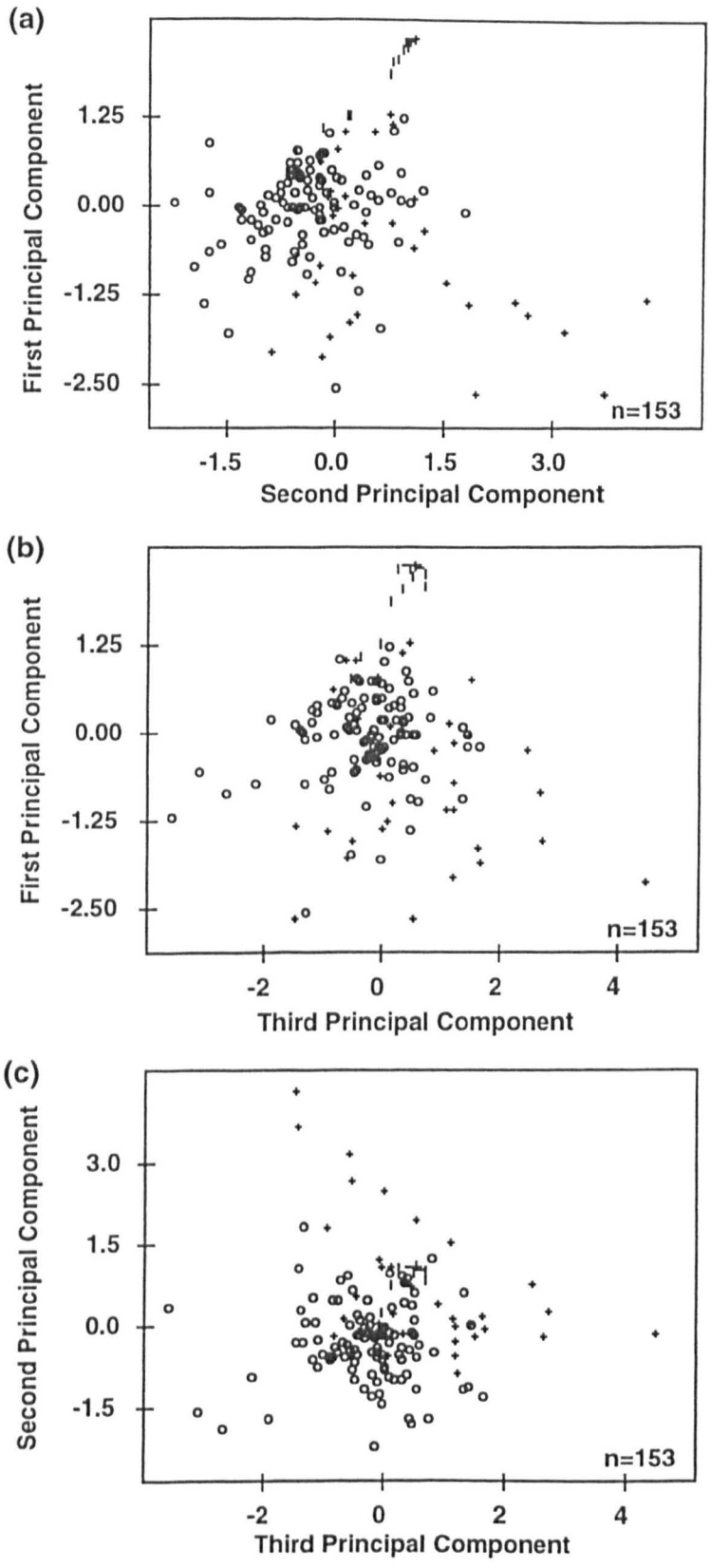

Figure 6. 13. Cranidia of *Calyptaulax* ordinated along the first three principal component axes calculated from the cranidium measurement scheme. Symbols: specimens assigned to*C. (Calliops)* (circles); specimens assigned to *C. (Calyptaulax)* (crosses); meraspide specimens (vertical bars); protaspide specimens (horizontal bars).

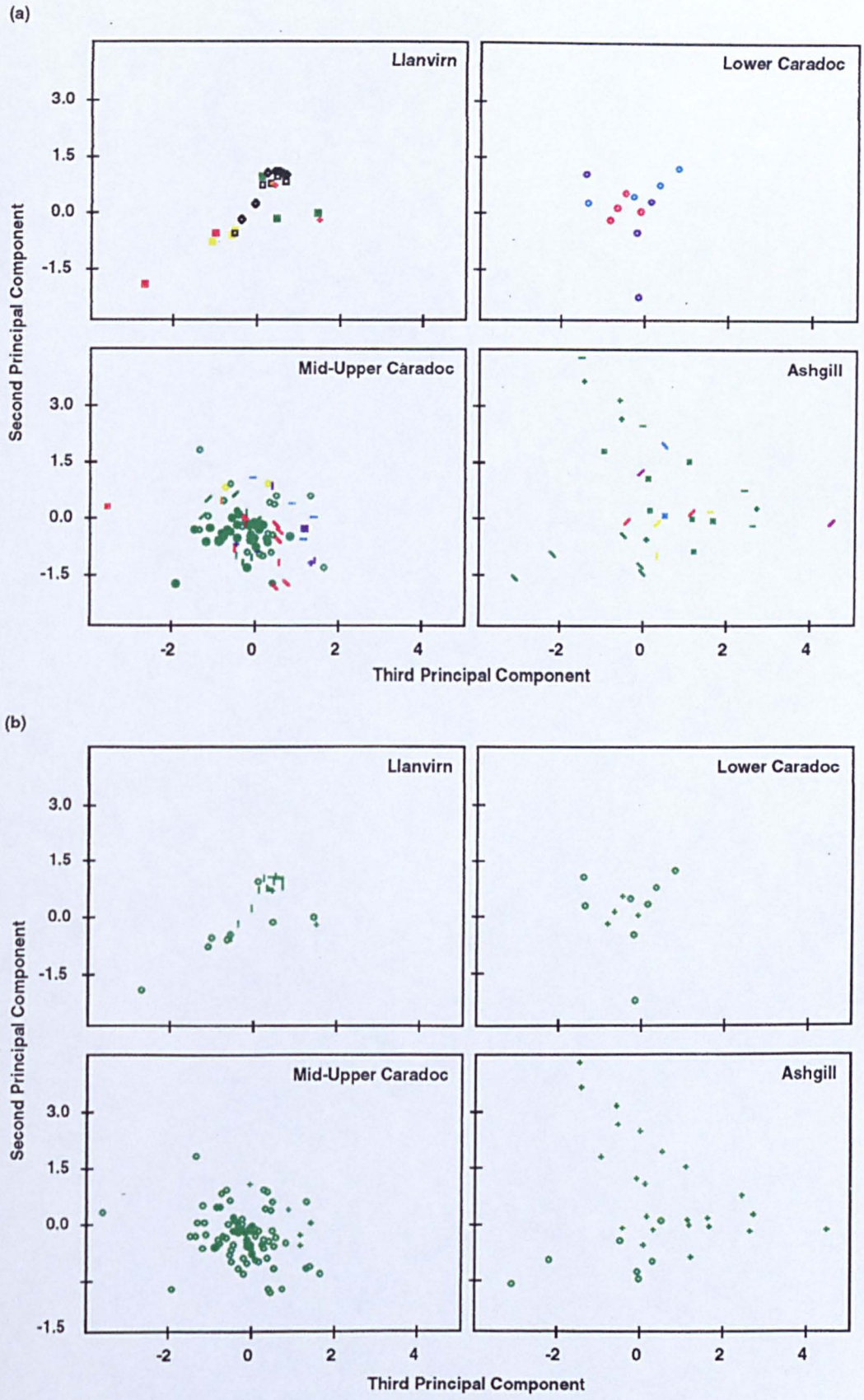

Figure 6. 14. Cranidia of *Calyptaulax* ordinated along the second and third principal component axes and grouped into four broad time intervals to illustrate changing morphospace occupation with time. (a) stratigraphical samples (see Figure 6. 10 for explanation of symbols); (b) subgenera, symbols used: specimens assigned to *C. (Calliops)* (circles); specimens assigned to *C. (Calyptaulax)* (crosses); meraspide specimens (vertical bars); protaspide specimens (horizontal bars).

Figure 6. 14 (b) indicates a divergence of *C. (Calyptaulax)* from *C. (Calliops)* with time. In the Llanvirn and lower Caradoc, the two subgenera occupy the same region of the morphospace. In the middle-upper Caradoc interval, the large number of *C. (Calliops)* specimens (all of which are from the Laurentian province) cluster about the central region of the plot, while the smaller number of *C. (Calyptaulax)* specimens (belonging to the Avalonian and Baltic provinces) are displaced slightly to the right. In the Ashgill, *C. (Calliops)* (rare) remains in the central and lower left portion of the plot (these include the MAQUOKETA specimens mentioned above), while *C. (Calyptaulax)* occupies the right-hand and uppermost regions, with a central area of overlap (as previously noted the specimens at the right hand and uppermost extremities of the plot are slightly damaged). The increase in morphospace occupied by the Ashgill specimens is clearly due to a greater spread of *C. (Calyptaulax)* specimens compared with *C. (Calliops).* This could be due to greater morphological variation in the former subgenus compared with the latter, or to slight distortion in the specimens of *C. (Calyptaulax)* (although effort was made to exclude obviously distorted specimens from the analysis).

On inspection of the second and third eigenvectors (Appendix 6) it is seen that the measurement most heavily weighted in the calculation of PC2 is b!10 (proximal length of L1), while that most heavily weighted in PC3 is P (palpebral lobe width). Thus there appears in the first instance to be some evidence to suggest that *C. (Calliops)* can be separated from *C. (Calyptaulax)* on the basis of these measurements. These variables will be investigated in more detail below.

PCA on pygidium data set. The eigenvalues and eigenvectors calculated for the four measurements made on pygidia are given in Appendix 6 and the PC scores are in Appendix 7. PC1 accounts for 73.7% of the total variance in the data set, PC2 for 22.1%, PC3 for 3.4%. The specimens are ordinated on the first three PCs in Figure 6. 15.

As was seen for cranidia, PC1 sorts the specimens with respect to overall size (compare Figure 6. 16, a bivariate plot of pygidial length (Z1) against pygidial width (W)). The correlation coefficient relating score on PC1 to Z1 for the 192 pygidia is r = 0.971. The plot of PC2 against PC3 (Figure 6. 15 (c)) does not separate the stratigraphical samples - there is a high degree of overlap between them. Notice that the STARFISH pygidia (green +) group quite tightly at the lower left of the plot.

Figure 6. 17 reproduces Figure 6. 15 with specimens assignable to *C. (Calyptaulax)* and *C. (Calliops)* highlighted. In Figure 6. 17 (a) it can be seen that although the largest pygidia belong to *C. (Calyptaulax)* and the smallest to *C. (Calliops)*, specimens of both occupy almost the whole range of size variation (PC1). Considering plot (c), *C.*

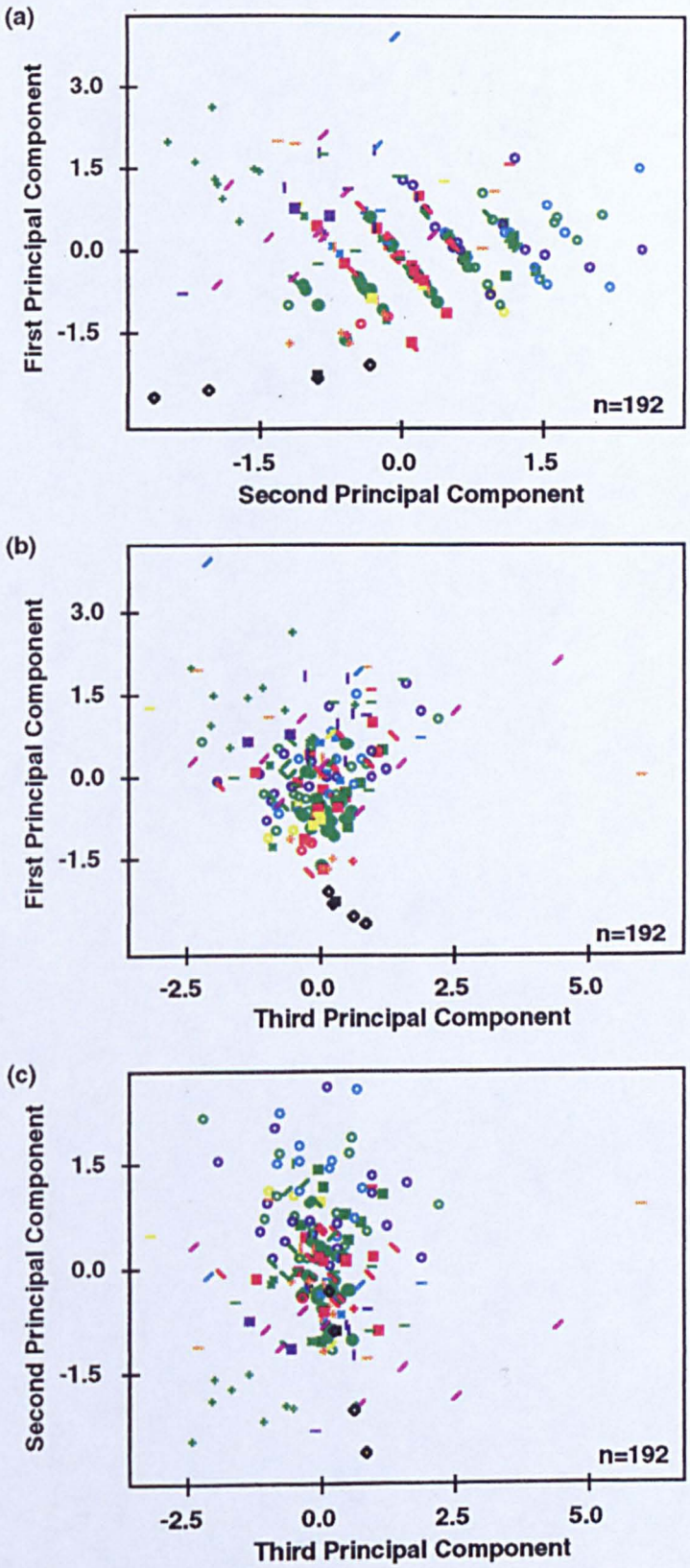

Figure 6. 15. Pygidia of *Calyptaulax* ordinated along the first three principal component axes calculated from the pygidium measurement scheme. Symbols as in Figure 6. 10.

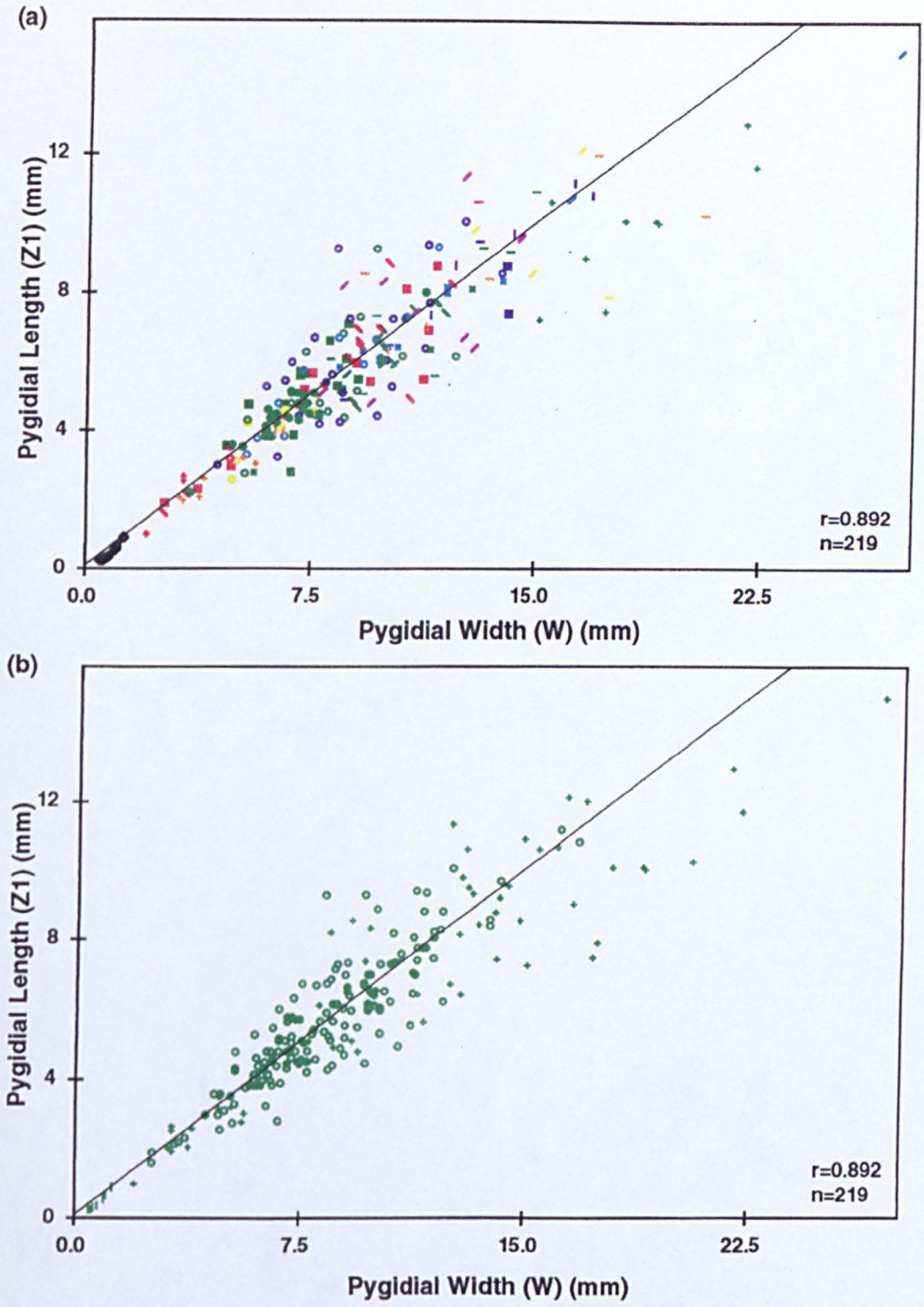

Figure 6. 16. Bivariate scatter plot of pygidial length (Z1) against pygidial width (W) for *Calyptaulax* (a) stratigraphical samples, symbols as in Figure 6. 10; (b) subgenera, symbols used: specimens assigned to *C. (Calliops)* (circles); specimens assigned to *C. (Calyptaulax)* (crosses); meraspide specimens (vertical bars); protaspide specimens (horizontal bars).

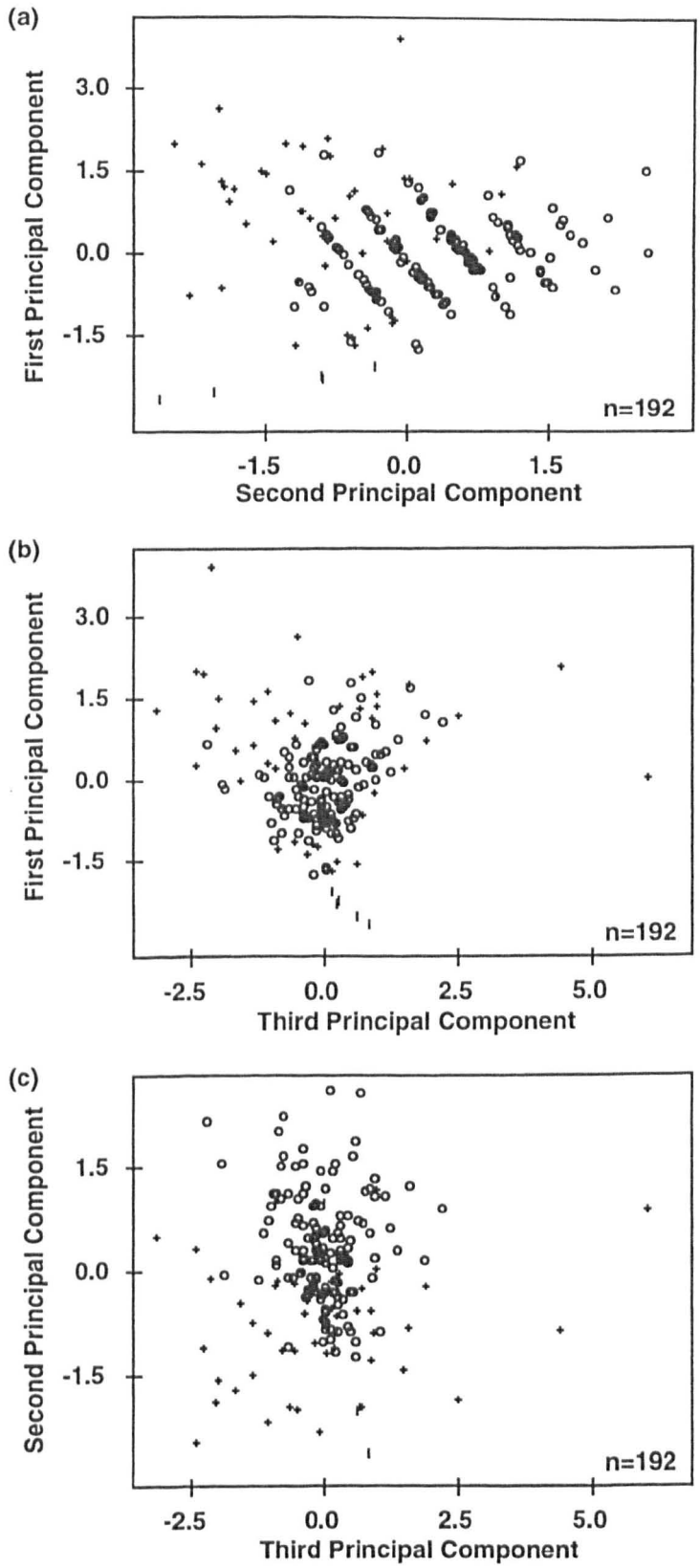

Figure 6. 17. Pygidia of *Calyptaulax* ordinated along the first three principal component axes calculated from the pygidium measurement scheme. Symbols: specimens assigned to *C. (Calliops)* (circles); specimens assigned to *C. (Calyptaulax)* (crosses); meraspide specimens (vertical bars); protaspide specimens (horizontal bars).

(Calliops) plots at high values on PC2 while *C. (Calyptaulax)* occupies the lower region with a large zone of overlap in the midrange. Both subgenera occupy the whole range of variation on PC3. From Appendix 6 it is found that the number of axial rings has greatest weighting in the calculation of PC2 (larger numbers of axial rings giving higher scores on PC2), while pygidial width W has greatest weighting on PC3 (greater width giving lower scores on PC3). Again, these variables are discussed in more detail below.

Figure 6. 18 shows the pygidia grouped into four time windows as was done for cranidia. A similar area of morphospace is filled throughout the Llanvirn to late Caradoc interval, with a slight increase in area in the Ashgill. The centre of morphospace occupation shifts upwards (towards higher scores on PC2) from the Llanvirn to the Caradoc, then back down in the mid-upper Caradoc and Ashgill, apparently reflecting changes in numbers of axial rings (the variable most heavily weighted on the PC2 axis).

From figure 6. 18 (b) it can be seen that *C. (Calliops)* specimens always group relatively tightly in morphospace - the increase in occupied area in the Ashgill is due to *C. (Calyptaulax)* specimens. As was noted for cranidia this could reflect actual morphological variability in *C. (Calyptaulax)*, or quality of preservation.

Univariate and bivariate plots. A number of bivariate plots of the *Calyptaulax* data have been constructed.

Figure 6. 12 is a bivariate scatter plot of width (tr.) of frontal lobe (k5) against preoccipital glabellar length (B). All of the specimens fall on the same linear trend, which is close to isometric: a reduced major axis (RMA) line fitted to the data has slope 1.06 and ordinate intercept -0.06. Two meraspide cranidia from the ESBATAOTTINE sample have unusually large size, B = 2.76mm and B = 3.17mm. These two specimens are definitely meraspides as they possess short genal spines (see Chatterton 1980, plate 16, figs. 17 and 23). This suggests that achievement of the holaspide stage may have been slightly delayed in ontogeny in these stratigraphically early North American forms relative to later forms, allowing a larger meraspide. Figure 6. 12 (a) does not reveal any systematic difference which can be used to separate any of the stratigraphical samples. Figure 6. 12 (b) does not reveal any morphometric difference between the two subgenera *C. (Calyptaulax)* and *C. (Calliops).*

Figure 6. 19 is a bivariate plot of palpebral cranidial width (J) against preoccipital glabellar length (B). As for the graph of k5 against B, the specimens plot on a single linear trend. The slope of the RMA best-fit line is 1.52, with ordinate intercept at 0.30. Thus J increases with ontogeny at a greater rate than glabellar width k5, *i.e.* the eyes become situated progressively further away from the glabella during ontogeny. Figure

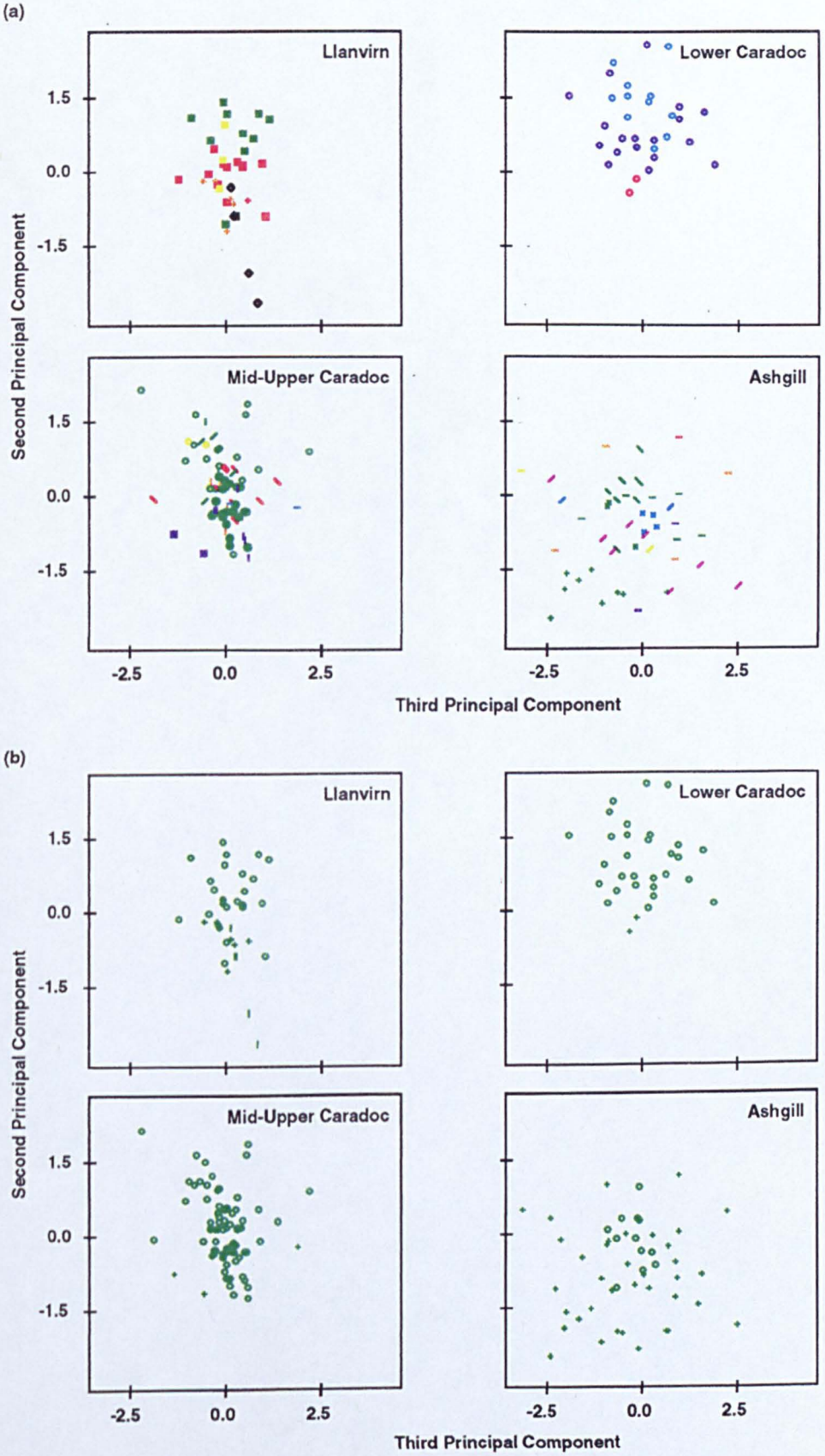

Figure 6. 18. Pygidia of *Calyptaulax* ordinated along the second and third principal component axes and grouped into four broad time intervals to illustrate changing morphospace occupation with time. (a) stratigraphical samples (see Figure 6. 10 for explanation of symbols); (b) subgenera, symbols used: specimens assigned to *C. (Calliops)* (circles); specimens assigned to *C. (Calyptaulax)* (crosses); meraspide specimens (vertical bars); protaspide specimens (horizontal bars).

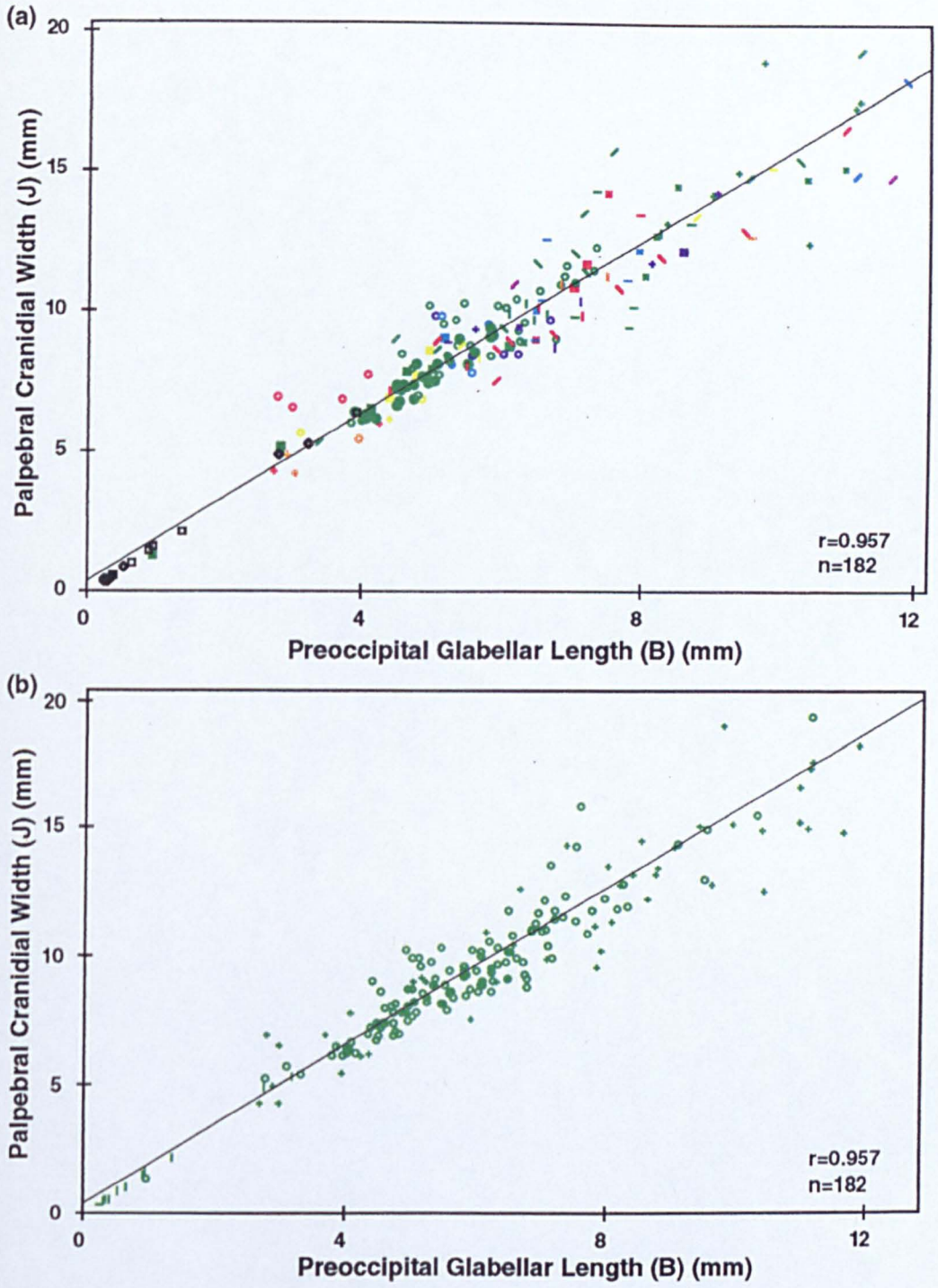

Figure 6. 19. Bivariate scatter plot of palpebral cranidial width (J) against preoccipital glabellar length (B) for *Calyptaulax*. (a) stratigraphical samples, symbols as in Figure 6. 10; (b) subgenera, symbols used: specimens assigned to *C. (Calliops)* (circles); specimens assigned to *C. (Calyptaulax)* (crosses); meraspide specimens (vertical bars); protaspide specimens (horizontal bars).

6. 19 (b) does not show any systematic variation between *C. (Calyptaulax)* and *C. (Calliops)* in terms of these measurements. Figure 6. 20 shows mid-palpebral cephalic width (I1) ordinated against preoccipital glabellar length (B). The slope of an RMA line fitted to this plot is 1.91, slightly steeper than that for J against B, with ordinate intercept at -0.23. So it can be seen that I1 increases with ontogeny at a still greater rate than J, *i.e.* with ontogeny, the relative widths of the librigenae increase. Again, no systematic difference between *C. (Calyptaulax)* and *C. (Calliops)* is revealed (Figure 6. 20 (b)).

Figure 6. 21 is a plot of distal length of the frontal lobe (b5) against B. The plot is anisometric, the RMA line fitted to the data having slope 0.46, ordinate intercept 0.04. It can be seen from Figure 6. 21 (b) that most specimens assigned to *C. (Calyptaulax)* on the basis of phylogenetic analysis have relatively lower values of b5 (*i.e.* relatively shorter frontal lobe) than those assigned to *C. (Calliops).* Exceptions to this are specimens belonging to the stratigraphically early *C. (Calyptaulax)* samples CONFINIS A, STINCHAR, DOULARG, BALCLATCHIE B and PINMERY. These samples were assigned to *C. (Calyptaulax)* in the phylogenetic analysis because of the nature of their pygidia (see Section 6. 3). However, in terms of the relative length of their frontal lobe they follow the *C. (Calliops)* trend.

In order to test whether the difference in frontal lobe length between *C. (Calyptaulax)* and *C. (Calliops)* is significant, a t-test was undertaken. The cranidium data set was divided into two subsets: subset 1 contained all specimens assigned to *C. (Calyptaulax)* on the basis of phylogenetic analysis; subset 2 contained all specimens assigned to *C. (Calliops).* The null hypothesis for the test was that the mean of the distribution of the ratio b5/B for subset 1 was the same as the mean for subset 2. A pooled estimate of population variance was used. The t-test rejected the null hypothesis at the 95% confidence interval. This means that b5 is significantly greater in *C. (Calliops)* than *C. (Calyptaulax).*

Figure 6. 22 shows that many specimens assigned to *C. (Calyptaulax),* as well as having relatively smaller b5 than *C. (Calliops),* also have relatively greater distal length of L3 (b32) (exceptions again are: CONFINIS A, STINCHAR, DOULARG, BALCLATCHIE B and PINMERY which have relative length of L3 similar to *C. (Calliops)*). This means that the distal extremity of S3 is located relatively further back in *C. (Calliops)* than in *C. (Calyptaulax).* The proximal extremity of S3 is constant in its location in both *C. (Calyptaulax)* and *C. (Calliops),* so the angle at which S3 diverges from the sagittal line must be more acute in the former subgenus than in the latter.

The angles at which the lateral glabellar furrows diverge from the sagittal line are summarised in Figure 6. 23. Within *C. (Calliops)* and *C. (Calyptaulax),* there is overlap

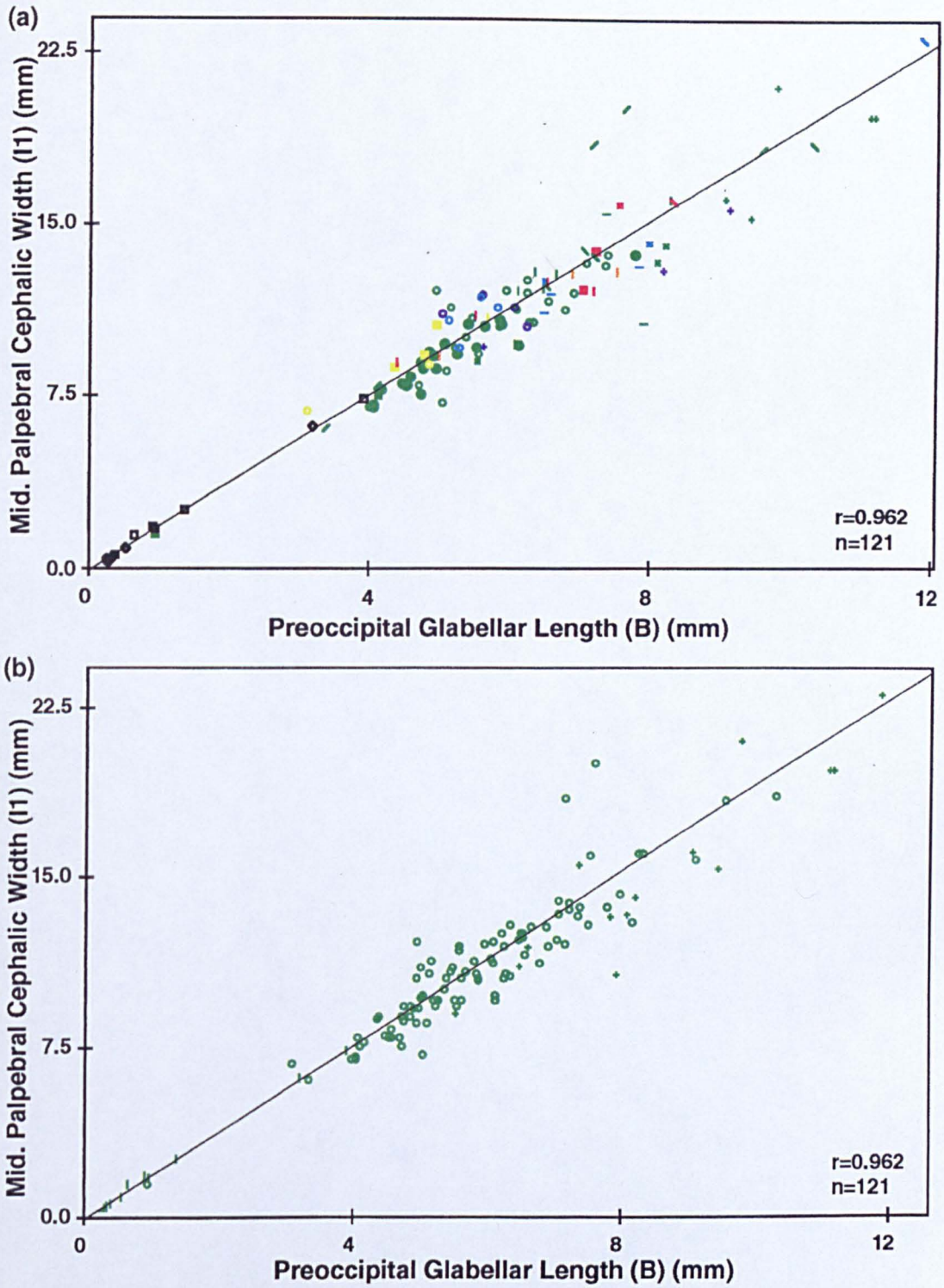

Figure 6. 20. Bivariate scatter plot of mid-palpebral cephalic width (I1) against preoccipital glabellar length (B) for *Calyptaulax*. (a) stratigraphical samples, symbols as in Figure 6. 10; (b) subgenera, symbols used: specimens assigned to *C. (Calliops)* (circles); specimens assigned to *C. (Calyptaulax)* (crosses); meraspide specimens (vertical bars); protaspide specimens (horizontal bars).

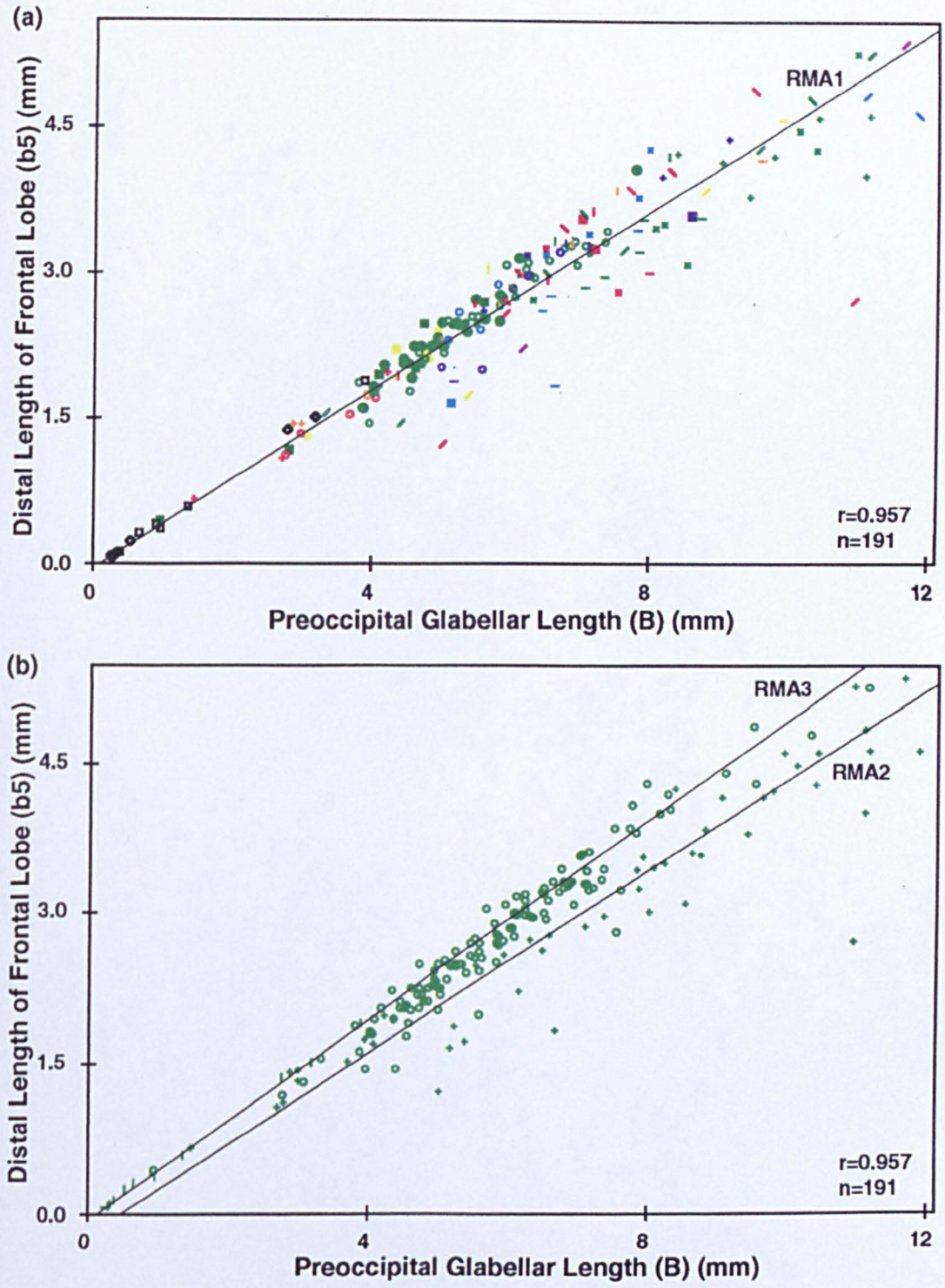

Figure 6. 21. Bivariate scatter plot of distal length of frontal lobe (b5) against preoccipital glabellar length (B) for *Calyptaulax*. (a) stratigraphical samples, symbols as in Figure 6. 10 ; (b) subgenera, symbols used: specimens assigned to *C. (Calliops)* (circles); specimens assigned to *C. (Calyptaulax)* (crosses); meraspide specimens (vertical bars); protaspide specimens (horizontal bars). RMA1 is a reduced major axis line fitted to all specimens. RMA2 is fitted to all specimens assigned to *C. (Calyptaulax)* on the basis of phylogenetic analysis, RMA3 is fitted to all specimens assigned to *C. (Calliops)*.

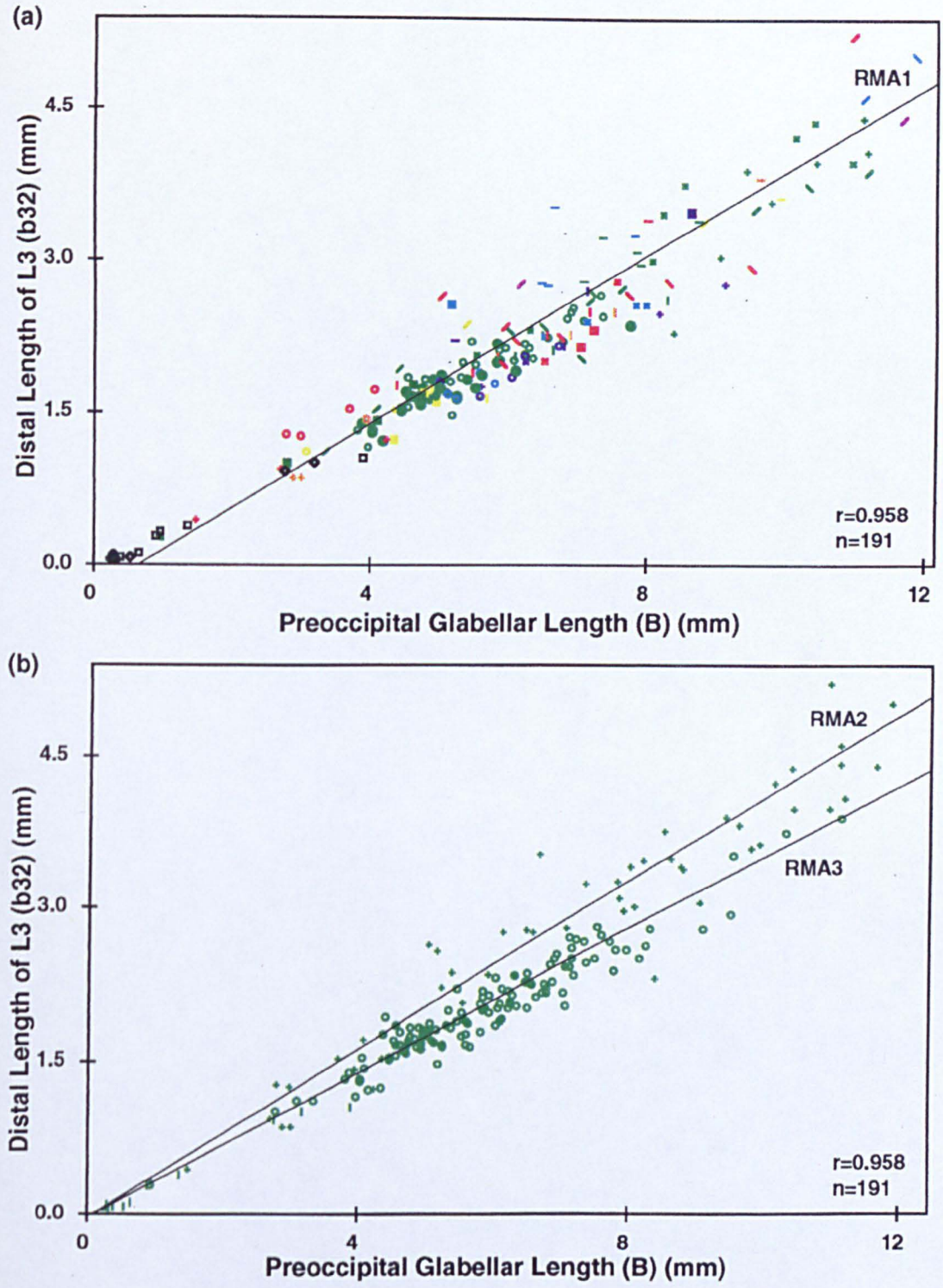

Figure 6. 22. Bivariate scatter plot of distal length of L3 (b32) against preoccipital glabellar length (B) for *Calyptaulax*. (a) stratigraphical samples, symbols as in Figure 6. 10; (b) subgenera, symbols used: specimens assigned to *C. (Calliops)* (circles); specimens assigned to *C. (Calyptaulax)* (crosses); meraspide specimens (vertical bars); protaspide specimens (horizontal bars). RMA1 is a reduced major axis line fitted to all specimens. RMA2 is fitted to all specimens assigned to *C. (Calyptaulax)* on the basis of phylogenetic analysis, RMA3 is fitted to all specimens assigned to *C. (Calliops)*.

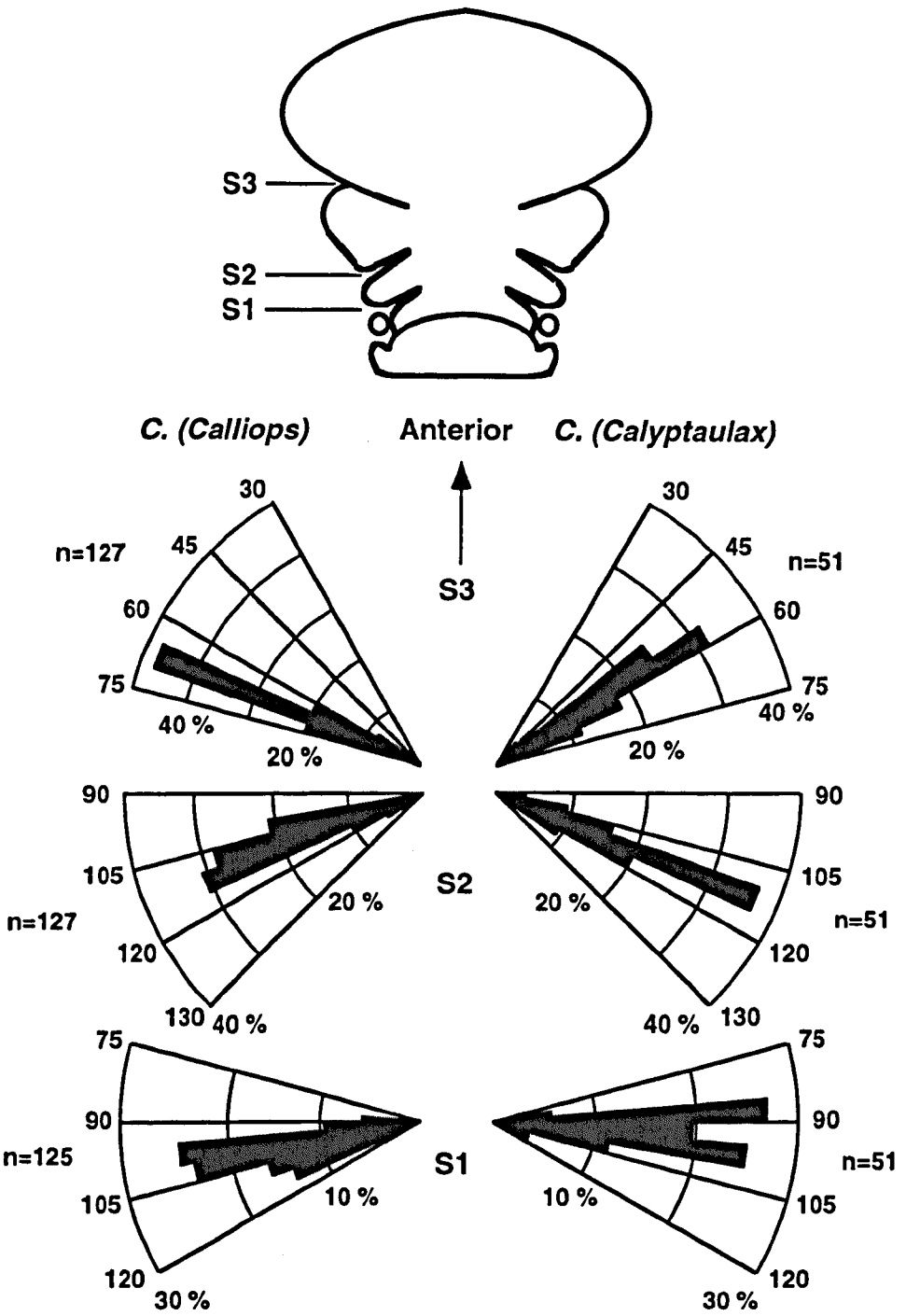

Figure 6. 23. Angles of divergence of lateral glabellar furrows from the sagittal line in *Calyptaulax*. Specimens assigned to *C. (Calliops)* on the basis of phylogenetic analysis shown on the left hand side, specimens assigned to *C. (Calyptaulax)* on the right hand side. Angles of divergence of S3, S2 and S1 furrows shown. For each furrow of each specimen, the angle between the trace of the furrow and the sagittal line was measured in the anterior quadrant. Furrows on both the left and right hand sides of the specimen were used. The angles of corresponding left and right furrows were then averaged to obtain the mean value plotted here.

between the distributions of angles for the various stratigraphical samples, so that none of the samples are separable from the others. But the two subgenera are distinguishable from each other, primarily on the basis of the angle of divergence of S3. Almost all of the angles of divergence of S3 measured for *C. (Calliops)* lie between 60° and 75°, the most frequent class interval being 65°-69.9°. The majority of angles for *C. (Calyptaulax)* lie between 50° and 70°, the most frequent class interval being 55°-59.9°. The region of overlap between the two subgenera in the range 60°-70° occurs because the specimens from the samples CONFINIS A, STINCHAR, DOULARG, BALCLATCHIE B and PINMERY, while belonging to the subgenus *C. (Calyptaulax)* have glabellar proportions like those of *C. (Calliops)* (see above). The distribution of angles of divergence of S2 is similar for both subgenera. The most frequent class interval in both cases is 110°-114.9°. There is a slight difference in the distribution of angles of divergence of S1 for the two subgenera. In *C. (Calliops)* the distribution is approximately normal, while that for *C. (Calyptaulax)* is bimodal. The total range of values for each subgenus is similar (80°-115°). t-tests were used to test the significance of the differences between the two subgenera. For each test, the null hypothesis was that the mean of the distribution of angles of divergence for all specimens assigned to *C. (Calliops)* on the basis of phylogenetic analysis was the same as the mean of the distribution for *C. (Calyptaulax).* A pooled estimate of population variance was used in each case. The null hypothesis of similarity was rejected at the 95% confidence interval for the comparison of angles of divergence of both S3 and S1, *i.e.* the mean values of these angles are significantly different between the two subgenera. The t-test comparing S2 between the two subgenera failed to reject the null hypothesis of similarity at the 95% confidence interval.

PCA on the cranidium data set revealed high variability in the measurements b!10 (=proximal length of L1) and P (=width of palpebral lobe). The distributions of these variables is shown in Figure 6. 24. Figure 6. 24 (a) shows univariate variation in the ratio proximal length of L1 (b!10) / preoccipital glabellar length (B) (when considering univariate variation, a ratio of the variable under consideration against some other variable is always used in order to correct for specimen size). The figure shows that there is no clear pattern to the distribution of values. The ranges exhibited by all of the stratigraphical samples overlap, and there is no difference between the distributions of values for specimens assigned to *C. (Calliops)* and *C. (Calyptaulax).* Thus relative length of L1 is not usable taxonomically either to diagnose samples, or to separate the two subgenera. The high range of values exhibited by specimens from ARDMILLAN is due to three specimens with extreme values (two unusually low, one unusually high). The other 27 specimens from this sample all lie in the range b!10/B = 0.075 to 0.18, hence the much more restricted standard deviation. The high range of values exhibited by BALCLATCHIE A is due to one specimen which has an unusually high ratio; the other 3

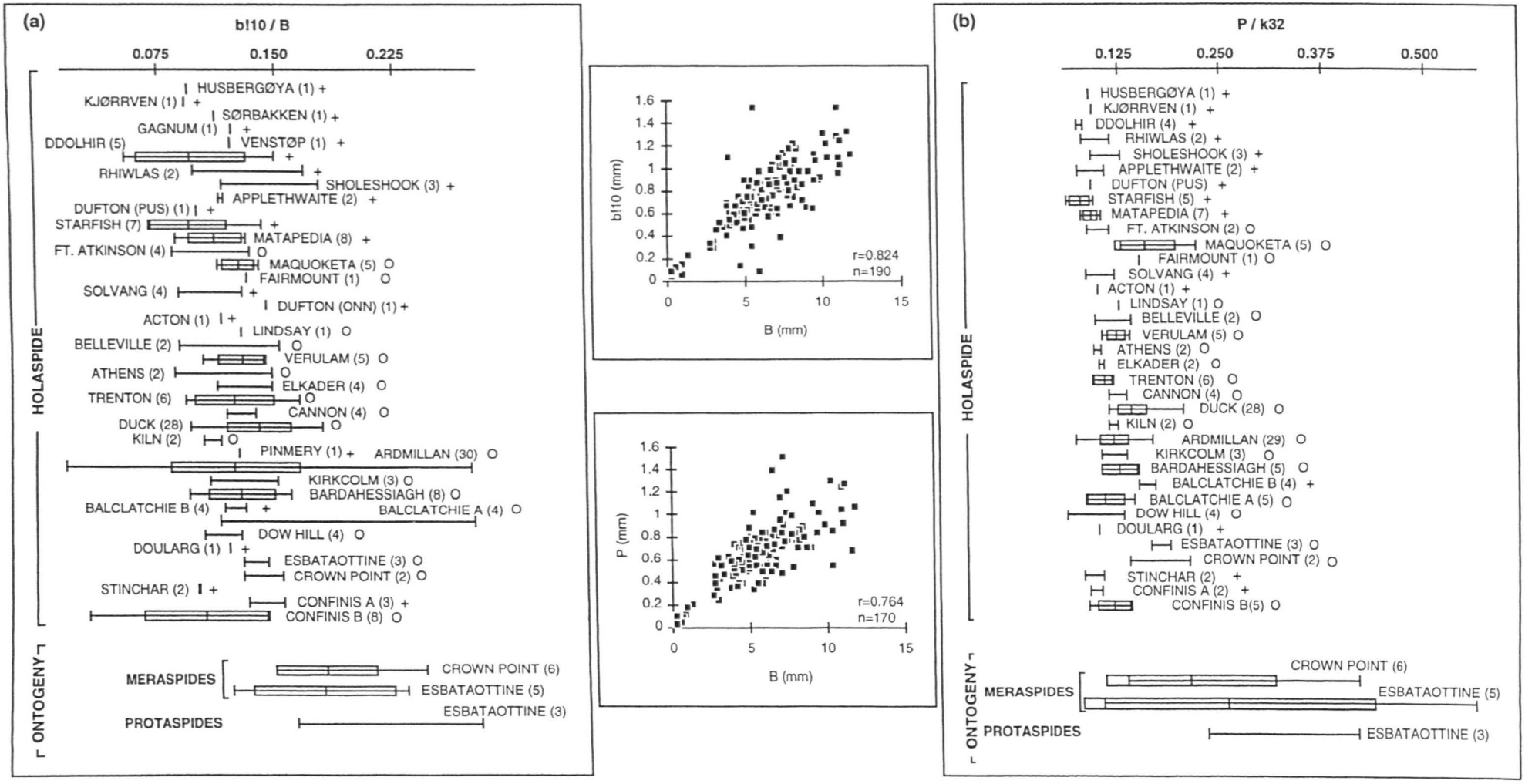

Figure 6. 24. Univariate variation in the measurements most heavily weighted on the second and third principal components calculated for the cranidium data set. (a) ratio of proximal length of L1 (b!10) / preoccipital glabellar length (B); (b) ratio of width of palpebral lobe (P) / preoccipital glabellar length (B). Total range of values and number of measurable specimens shown for each stratigraphical sample, mean value and one standard deviation to either side of the mean shown for samples containing five or more measurable specimens. Samples assigned to *C. (Calliops)* on the basis of phylogenetic analysis identified by a circle; those assigned to *C. (Calyptaulax)* identified by a cross. Insets show bivariate plots of b!10 against B, and P against B.

specimens in the sample all lie close to b!10/B = 0.12. Clearly b!10 is a measurement which shows high variance.

Figure 6. 24 (b) shows univariate variation in the ratio of width (tr.) of palpebral lobe (P) / width (tr.) of glabella across L3 (k32). As for b!10, the figure shows a great deal of overlap between stratigraphical samples so that they cannot be separated. There is also no definite discontinuity in P/k32 to separate samples assigned to *C. (Calliops)* from those assigned to *C. (Calyptaulax)*, although in general the former have slightly higher values of P/k32 than the latter. A t-test performed using the null hypothesis that the mean of the distribution of values of P/k32 for *C. (Calyptaulax)* is the same as the mean for *C. (Calliops)* did reject the null hypothesis at the 95% confidence interval, but the lack of a distinct discontinuity makes this ratio unusable as a taxonomic tool. Notice the wide spread in values exhibited by the ontogenetic material. It appears that this is the cause of much of the variation which PCA detected, and it may be due to the effect of allometry in this ratio. Ontogenetic material is discussed more fully below.

Eyes. Figure 6. 25 shows a plot of longitudinal position of anterior of eye (C1) against preoccipital glabellar length (B). Two specimens plot in anomalous locations: one from the sample DDOLHIR is a slightly distorted specimen; the other, from the sample SHOLESHOOK, is poorly preserved and was only included in the analysis because of the paucity of measurable specimens from that stratigraphical unit. All the other specimens lie close to the same trend, the RMA best-fit line having slope 0.48 and ordinate intercept -0.19. This trend is virtually identical to that exhibited by the plot of distal length of frontal lobe (b5) against B. This is to be expected, since the anterior of the palpebral lobe is always located opposite the distal extremity of S3 in *Calyptaulax*. There is also a similar distribution of specimens assignable to *C. (Calliops)* versus those assignable to *C. (Calyptaulax)* (the RMA line fitted to *C. (Calliops)* has slope 0.52, ordinate intercept -0.31; the line fitted to *C. (Calyptaulax)* has slope 0.49, ordinate intercept -0.50). The difference in the ratio of distal length of frontal lobe (b5) / B for *C. (Calliops)* and *C. (Calyptaulax)* was found to be statistically significant at the 95% confidence interval (see earlier). Because of the close relationship between b5 and C1 described above, it is to be expected that the ratio C1/B will also show a significant difference between the two subgenera, and indeed this is found to be the case. A t-test with null hypothesis that the mean of C1/B for all specimens assigned to *C. (Calliops)* on the basis of phylogenetic analysis is the same as the mean of this ratio for all specimens assigned to *C. (Calyptaulax)*, using a pooled estimate of population variance, rejected the null hypothesis at the 95% confidence interval, *i.e.* C1/B is significantly lower in *C. (Calyptaulax)* than in *C. (Calliops)*. Figure 6. 26 shows longitudinal position of posterior of eye (C2) plotted against B, and exhibits a very well-constrained single trend which is close to isometric (slope 1.05, ordinate intercept -0.06 for the RMA

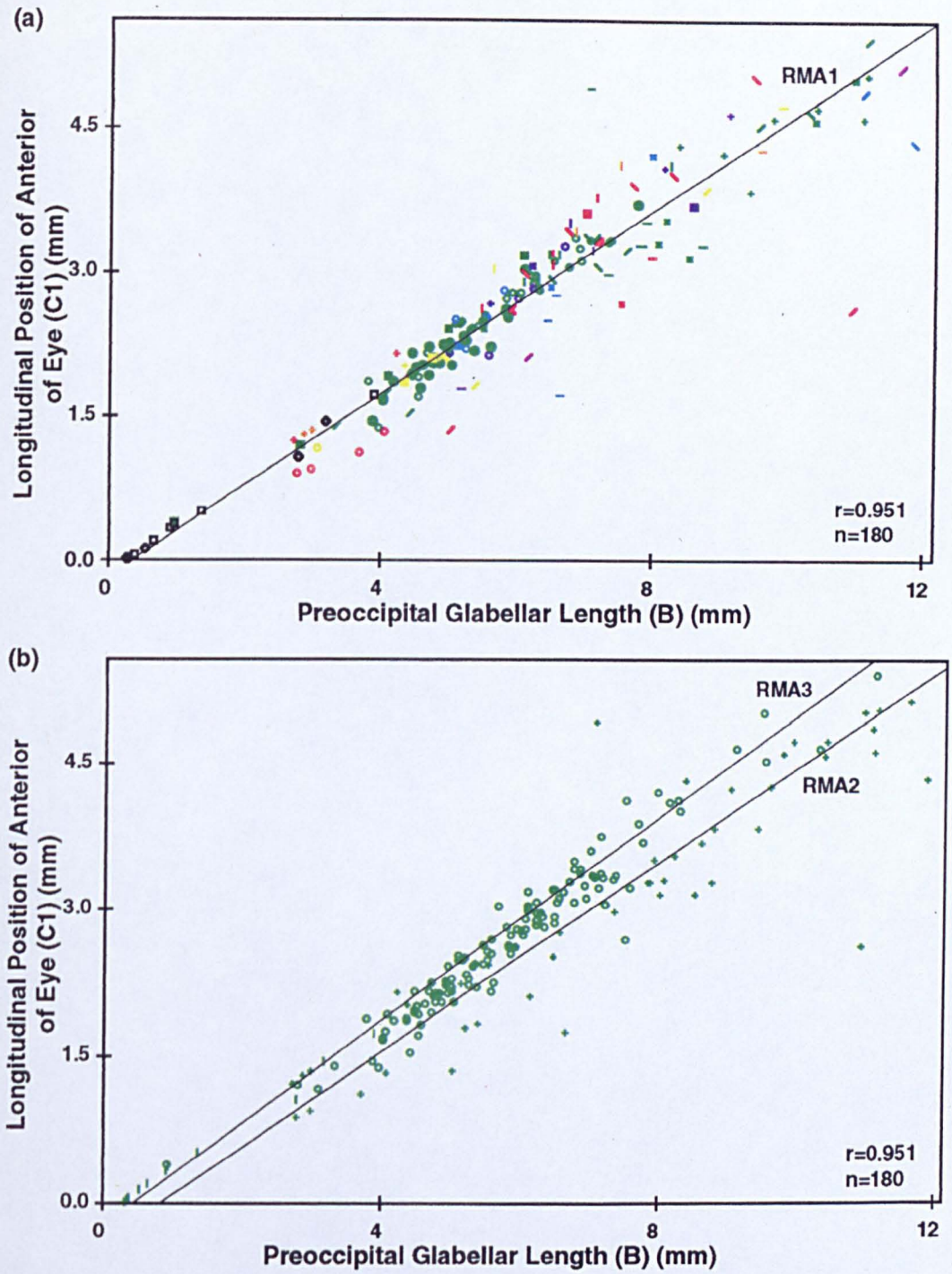

Figure 6. 25. Bivariate scatter plot of longitudinal position of anterior of eye (C1) against preoccipital glabellar length (B) for *Calyptaulax*. (a) stratigraphical samples, symbols as in Figure 6. 10; (b) subgenera, symbols used: specimens assigned to *C. (Calliops)* (circles); specimens assigned to *C. (Calyptaulax)* (crosses); meraspide specimens (vertical bars); protaspide specimens (horizontal bars). RMA1 is a reduced major axis line fitted to all specimens. RMA2 is fitted to all specimens assigned to *C. (Calyptaulax)* on the basis of phylogenetic analysis, RMA3 is fitted to all specimens assigned to *C. (Calliops)*.

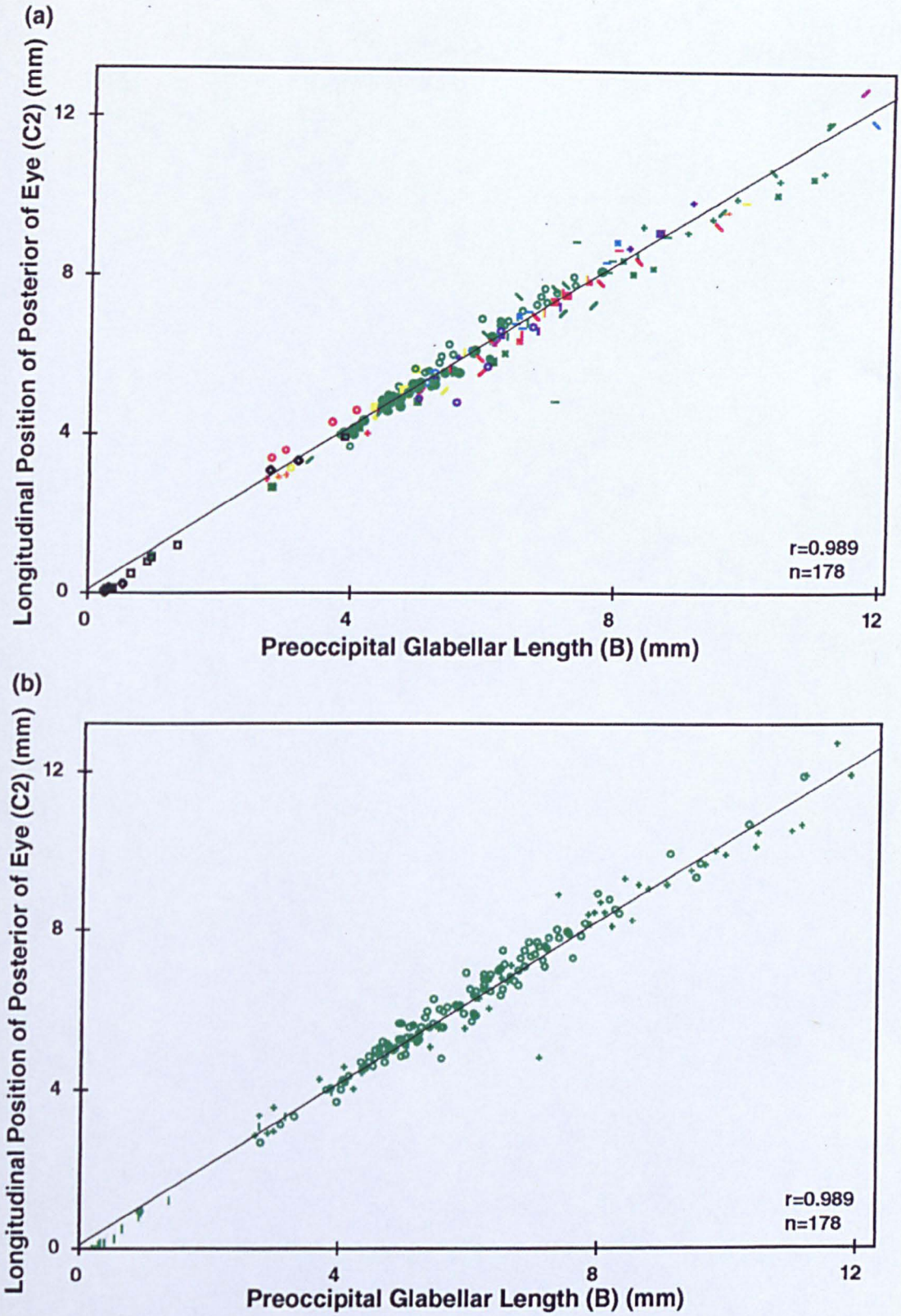

Figure 6. 26. Bivariate scatter plot of longitudinal position of posterior of eye (C2) against preoccipital glabellar length (B) for *Calyptaulax*. (a) stratigraphical samples, symbols as in Figure 6. 10; (b) subgenera, symbols used: specimens assigned to *C. (Calliops)* (circles); specimens assigned to *C. (Calyptaulax)* (crosses); meraspide specimens (vertical bars); protaspide specimens (horizontal bars).

best-fit line) *i.e.* the posteriormost extremity of the palpebral lobe is always very close to being opposite the middle point of the occipital furrow (the point to which B is measured). Since the position of the posteriormost extremity of the palpebral lobe is relatively constant in all specimens and the anteriormost extremity is significantly further forward in *C. (Calyptaulax)* than in *C. (Calliops)*, the eye of *C. (Calyptaulax)* must be significantly longer (exsag.) than the eye of *C. (Calliops)*.

Figure 6. 3 shows a summary of counts made of the number of dorso-ventral lens files in the visual surface of *Calyptaulax*. For each specimen, the left eye was counted if it was preserved sufficiently well. If there was no adequate left eye present, the right eye was used instead. Thus each specimen is represented only once in the figure. There is overlap in the ranges of all of the samples assigned to *C. (Calliops)*, the ranges lying between 20 and 27 files with all the means in the region 22-25. None of the *C. (Calliops)* samples is separable from the others on this character. There is also overlap between the samples assigned to *C. (Calyptaulax)*, all of the ranges lying between 26 and 38, all of the means in the region 28-35. Samples of *C. (Calyptaulax)* are therefore also not separable on this character alone. However *C. (Calliops)* is separable from *C. (Calyptaulax)*. Except in the case of the STARFISH sample, the total ranges of observed values for *C. (Calliops)* and *C. (Calyptaulax)* do not overlap, and the ranges of means of samples assigned to *C. (Calliops)* and *C. (Calyptaulax)* do not overlap at all. A t-test has been undertaken to test the significance of this difference. The null hypothesis stated that the mean number of lens files in all eyes assigned to *C. (Calliops)* is the same as the mean in all eyes assigned to *C. (Calyptaulax)*. A pooled estimate of population variance was used. The null hypothesis was rejected at the 95% confidence interval, *i.e.* the number of lens files is significantly different in the two subgenera.

To test the significance of the overlap in the ranges of values between members of the STARFISH sample and samples assigned to *C. (Calliops)*, three further t-tests were carried out:

(i) A comparison between all eyes belonging to the STARFISH sample and all eyes assigned to *C. (Calliops)*. The null hypothesis that there was no difference between the mean number of files for STARFISH and the mean number for all samples assigned to *C. (Calliops)* was rejected at the 95% confidence interval.

(ii) A comparison between all eyes belonging to the STARFISH sample and all eyes from the sample ARDMILLAN (that member of *C. (Calliops)* with which STARFISH shows the greatest overlap in terms of number of lens files). The null hypothesis that there was no difference between the mean number of files for STARFISH and the mean number for ARDMILLAN was rejected at the 95% confidence interval.

(iii) A comparison between all eyes belonging to STARFISH and all available eyes belonging to the other samples assigned to *C. (Calyptaulax)* on the basis of phylogenetic analysis (*i.e.* HUSBERGØYA, KJØRRVEN, DDOLHIR, SOLVANG, and PINMERY). The t-test failed to reject the null hypothesis that the mean number of lens files for STARFISH was the same as the mean number for all other members of *C. (Calyptaulax).* This means that there is no statistically significant (at least at the 95% confidence interval) difference between the numbers of files in specimens from the STARFISH sample and the number in specimens from the other samples assigned to *C. (Calyptaulax).*

So it is clear that the STARFISH sample is closer to the other members of *C. (Calyptaulax)* on this character than it is to *C. (Calliops).*

Figure 6. 27 shows lens charts compiled for each stratigraphical sample. The charts were compiled using the method of Campbell (1977) as modified by Clarkson and Tripp (1982). In Figure 6. 27 (a) the charts for specimens from the samples DOW HILL, BALCLATCHIE A, ARDMILLAN and BARDAHESSIAGH were compiled independently of those shown by Clarkson and Tripp (1982: fig. 6) but show close agreement with them. The relatively deeper eye of the ARDMILLAN population as compared with the other morphologically very similar middle Caradoc samples noted by Clarkson and Tripp is confirmed here. The visual structure of all middle Caradoc samples from North America (DUCK, CANNON, TRENTON, VERULAM, and LINDSAY) are very similar to each other. In Figure 6. 27 (b) the difference in number of lens files and depth of the eye between the single useable specimen from sample PINMERY and the other samples assigned to *C. (Calyptaulax)* is immediately apparent. The lens structure of the PINMERY sample bears a close resemblance to those assigned to *C. (Calliops)* (Figure 6. 27 (a)) which are approximately contemporaneous. However, on the criteria used in Section 6. 3, specimens from the sample (and the identical specimens from the sample BALCLATCHIE B) definitely fit within *C. (Calyptaulax)* rather than *C. (Calliops)* (the two subgenera are defined on pygidial morphology, Section 6. 3).

Pygidia. Figure 6. 16 is a bivariate plot of pygidial length (Z1) against pygidial width (W). There is a wide spread of data points about the line of trend. An RMA best-fit line fitted to the data has slope 0.63 and ordinate intercept 0.27. PCA on the pygidium data set detected high variation in W (on PC3, see earlier in this section), which is reflected in this plot. It is probable that the wide spread of the data points is due to flattening of some of the pygidia. There is no obvious systematic distinction between stratigraphical samples, or between the two subgenera *C. (Calliops)* and *C. (Calyptaulax)* (Figure 6. 16 (b)). Figure 6. 28 shows univariate variation in the number of pygidial axial rings

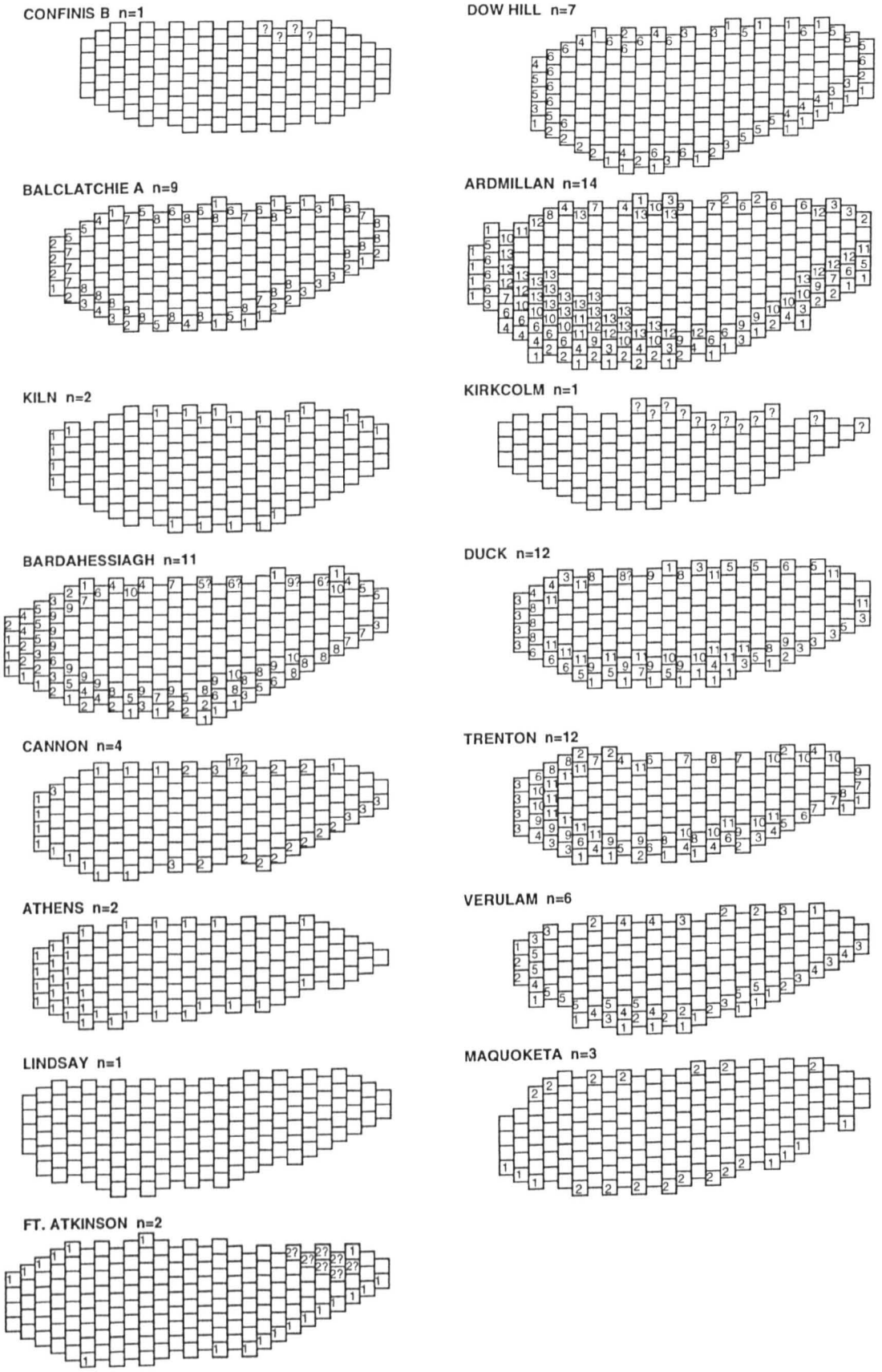

Figure 6. 27 (a). Statistical lens charts for stratigraphical samples of *Calyptaulax* assigned to *C. (Calliops)* on the basis of phylogenetic analysis (Section 6. 3). Charts constructed using the method of Campbell (1977) as modified by Clarkson and Tripp (1982). Left eye of each specimen used where sufficiently well preserved, right eye used otherwise. Anterior of eyes to the left. Numbers indicate how many specimens possess a lens at that location. Locations with no number indicate that all specimens possess a lens at that location.

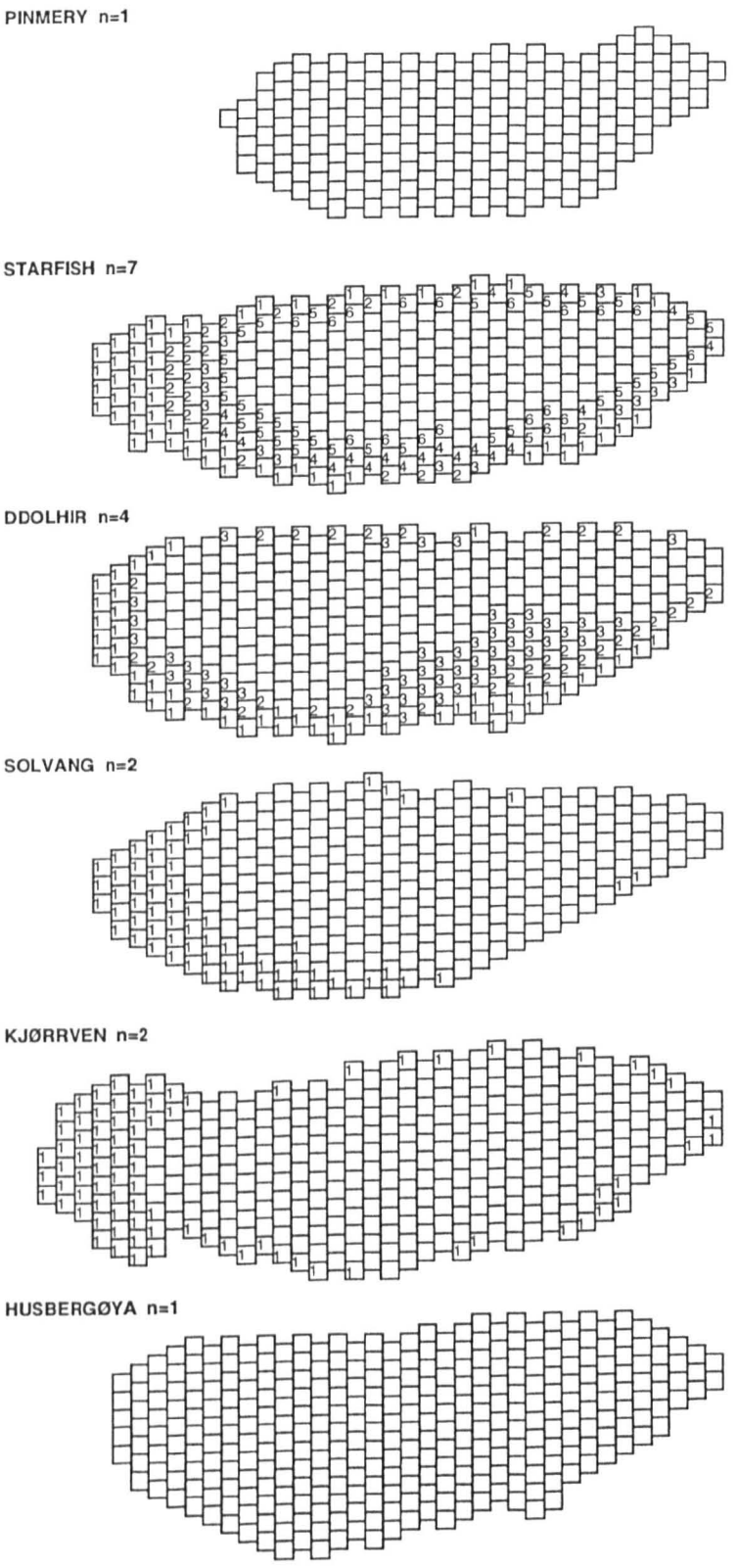

Figure 6. 27 (b). Statistical lens charts for stratigraphical samples of *Calyptaulax* assigned to *C. (Calyptaulax)* on the basis of phylogenetic analysis (Section 6. 3). Charts constructed as in Figure 6. 27 (a). Anterior of eyes to the left.

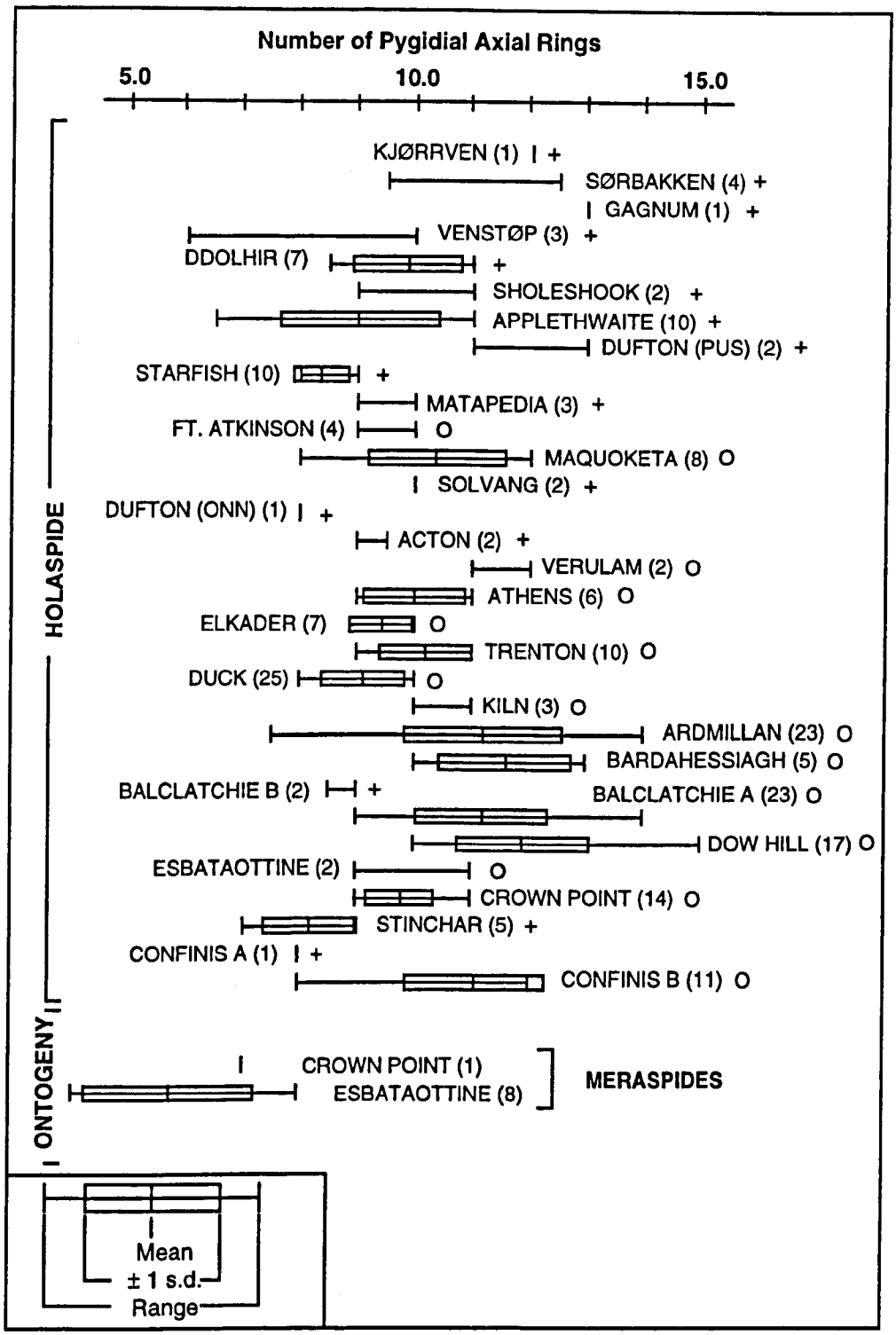

Figure 6. 28. Univariate variation in number of pygidial axial rings in *Calyptaulax*. Range of values shown for each stratigraphical sample. Number of measurable specimens in the sample given in parentheses. Mean value and one standard deviation to either side of the mean shown for samples containing five or more specimens. Samples assigned to *C. (Calliops)* on the basis of phylogenetic analysis identified by a circle; samples assigned to *C. (Calyptaulax)* identified by a cross. Unclear rings counted as half values.

in *Calyptaulax*. There is overlap between all of the stratigraphical samples, and *C. (Calliops)* cannot be differentiated from *C. (Calyptaulax)* on this character.

6. 4. 3. Conclusions from Morphometrics on Holaspides.

The above consideration of holaspide specimens can be briefly summarised:

(i) PCA was used to investigate morphospace occupation by cranidia and pygidia, and for both it was found that morphospace occupation increases in the Ashgill, coincident with the increased abundance of *C. (Calyptaulax)* over *C. (Calliops)* (see Figures 6. 14 and 6. 18).

(ii) It did not prove possible to separate out any of the stratigraphical samples of *Calyptaulax* on the PCA plots, either of cranidia or of pygidia.

(iii) In PCA on the cranidium measurements, a degree of divergence with time is seen between samples assigned to *C. (Calliops)* and *C. (Calyptaulax)*, with stratigraphically earlier representatives of the two subgenera (Llanvirn - lower Caradoc) occupying the same region of morphospace, stratigraphically later ones (middle Caradoc - Ashgill) becoming more separated (Figure 6. 14).

(iv) When the variables most heavily weighted by the PCA calculation were considered, it was found that they were highly variable (see for example Figure 6. 24) but that the variation was not systematic and could not therefore account for the morphospace divergence between the two subgenera.

(v) However systematic variation was discovered in measurements showing less overall variation (distal length of frontal lobe (b5), distal length of L3 (b32), longitudinal position of anterior of eye (C1), and angle of divergence of S3) which describe the relative proportions of the glabellar lobes and the related length (exsag.) of the eye. It was found that stratigraphically later representatives of *C. (Calyptaulax)* (middle Caradoc - Ashgill) have a relatively shorter frontal lobe and relatively longer L3, combined with a relatively longer eye containing more dorso-ventral lens files, than stratigraphically earlier (Llanvirn - lower Caradoc) ones, which exhibit proportions more like those of *C. (Calliops)*. This change is coincident with the morphospace divergence seen in Figure 6. 14, and it is therefore concluded that it is this change in glabellar proportions and related eye length which is the cause of that morphospace divergence.

(vi) The two subgenera were not separable on any of the measurements made on the pygidia.

6. 4. 4. Ontogeny of *Calyptaulax*.

A number of protaspide and meraspide specimens of *Calyptaulax* are known. Shaw (1968) illustrated a nearly complete developmental series of *C. annulata* (= *C. (Calliops) annulata* as defined herein) from the Crown Point Fm. (middle - upper Chazyan) at Pebble Beach, Valcour Island, N.Y. (=the stratigraphical sample CROWN POINT

herein). Shaw described and figured three protaspides (Shaw 1968: pl. 12, figs. 33, 35, 36), a complete degree eight meraspide (*ibid.*: pl. 12, figs. 19-20), four meraspide cranidia (*ibid.*: pl. 12, figs. 18, 29, 30, 32) and two meraspide pygidia (*ibid.*: pl. 12, figs. 24, 34). Chatterton (1980) described and illustrated ontogenetic material of *C. callirachis* (= *C. (Calliops) callirachis* as defined herein) from the lower Esbataottine Fm. (late Chazyan) of the Mackenzie Mtns., Northwest Territories (= the stratigraphical sample ESBATAOTTINE herein). His developmental series included seven protaspides (Chatterton 1980: pl. 16, figs. 1-3, 8-10, 19), one complete enrolled meraspide (*ibid.*: pl. 16, fig. 21), eight meraspide cephala and cranidia (*ibid.*: pl. 16, figs. 4, 11, 12, 15, 17, 18, 20, 23) and nine meraspide pygidia (*ibid.*: pl. 16, figs. 5-7, 13-14, 16, 22, 26, 32). Chatterton compared his material with that of Shaw (1968), concluding that the two sets of specimens were similar. He also noted that one of his protaspide specimens was smaller and more bulbous than any of Shaw's, presumably representing a stage ontogenetically earlier than any previously known, and adapted for a pelagic mode of life (Chatterton 1980, p. 51). The morphology of the protaspide and meraspide stages is shown in Figure 6. 29.

For the present study, measurements have been obtained by digitising selected illustrations of the ontogenetic material taken from Shaw (1968) and Chatterton (1980) where it was considered that the specimens had been figured in true dorsal orientation, using the method described in Chapter 4. Of the changes with ontogeny highlighted by Shaw and Chatterton, those amenable to morphometric consideration are:

Width of the glabella. Both Shaw (1968) and Chatterton (1980) noted that ontogenetically later specimens have relatively slightly wider glabellae than ontogenetically earlier ones. This is borne out by Figures 6. 30 (a) (relative width of frontal lobe) and 6. 30 (b) (relative width of glabella across L3). Both plots show an allometric relationship in protaspides and ontogenetically early meraspides (those for which B ≤ about 1mm), markedly so in 6. 30 (b). The growth relationship appears to become more constant for specimens for which B > 1mm. The frontal lobe expands slightly more rapidly than the remaining portion of the glabella (a reduced major axis line fitted to Figure 6. 30 (a) has slope 1.11; one fitted to 6. 30 (b) has slope 1.01). For specimens in which B > 1mm (*i.e.* the post-allometric part of the two graphs) the reduced major axis (RMA) line has slope 1.12 for the graph of k5 against B (comparable with the slope of 1.06 for holaspide specimens, see Figure 6. 12) and 1.00 for the graph of k32 against B.

Size increase. Figure 6. 30 (c) also exhibits a markedly allometric relationship for specimens with B ≤ about 1mm, becoming more stable in larger specimens. The slope of an RMA line fitted to all of these specimens is 2.02, indicating that the total width of the

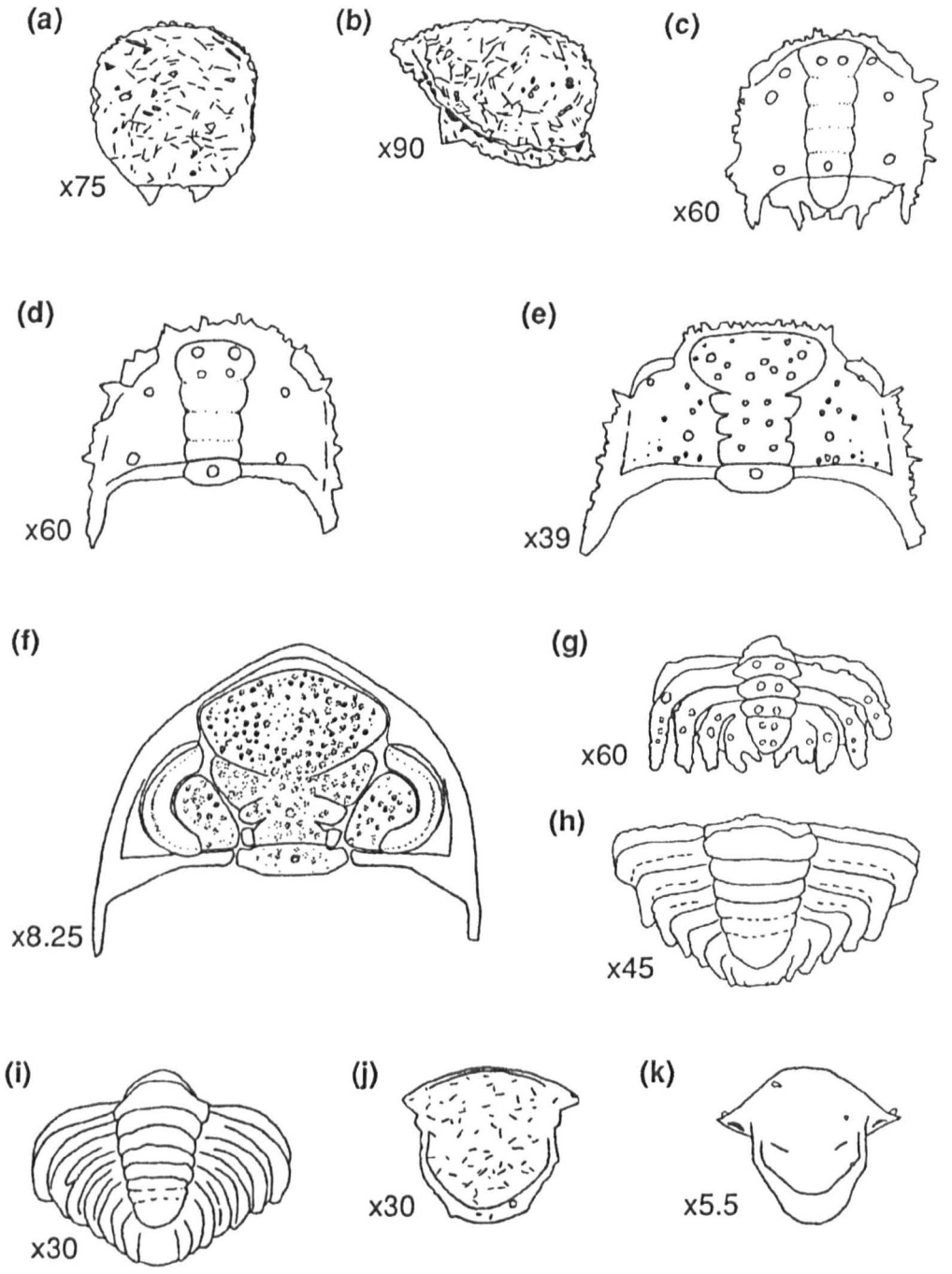

Figure 6. 29. Ontogeny of *Calyptaulax (Calliops) callirachis* Cooper, 1953, from the lower Esbataottine Fm. (middle Ordovician), Mackenzie Mountains, Canada. (a) dorsal view of small protaspide, UA2850; (b) lateral view of same, UA2851; (c) dorsal view of metaprotaspide, UA2844; (d) dorsal view of small meraspide cranidium, UA2846; (e) dorsal view of meraspide cranidium, UA2857; (f) dorsal view of meraspide cephalon, UA1416; (g) dorsal view of small meraspide pygidium, UA2849; (h) dorsal view of meraspide pygidium, UA2864; (i) posterodorsal view of meraspide pygidium, UA2866; (j) ventral view of small hypostome, UA2863; (k) ventral view of hypostome, UA1421. All redrawn from Chatterton (1980) plate 16.

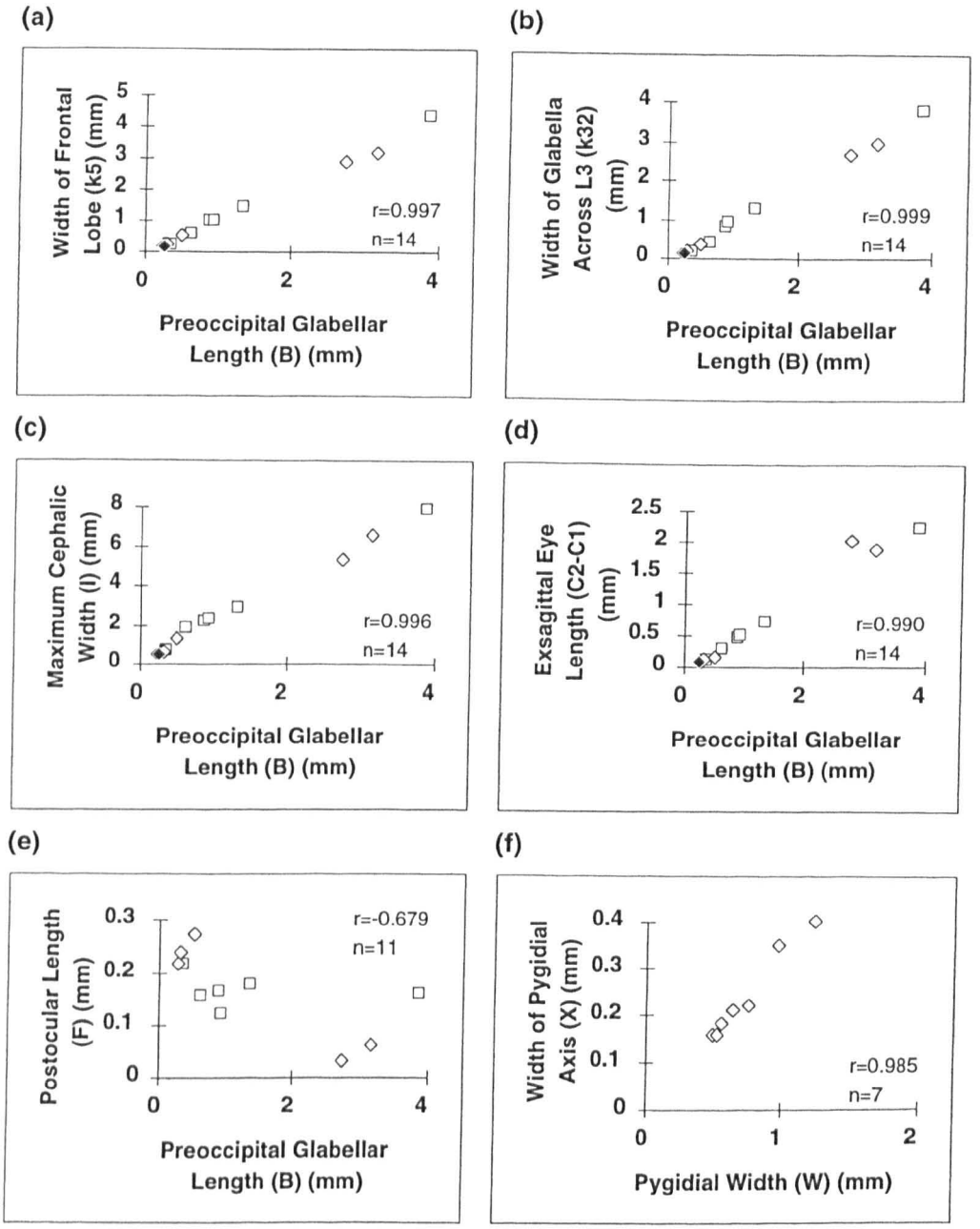

Figure 6. 30. Bivariate plots on ontogenetic material of *Calyptaulax*. (a) width of frontal lobe (k5) against preoccipital glabellar length (B); (b) width of glabella across L3 (k32) against preoccipital glabellar length (B); (c) maximum cephalic width (I) against preoccipital glabellar length (B); (d) exsaggital eye length (C2-C1) against preoccipital glabellar length (B); (e) postocular length (F) against preoccipital glabellar length (B); (f) width of pygidial axis (X) against pygidial width (W). Plotting symbols as in Figure 6. 10.

cephalon increases at a greater rate than that of the glabella, as was found for holaspide specimens (see previous section).

Length of the eyes. Shaw (1968) reported that the eyes of meraspide specimens are relatively slightly longer than those of protaspides (see Figure 6. 29). Figure 6. 30 (d) shows that, once again, there is an allometric relationship in the smallest (protaspide and early meraspide) specimens, the growth relationship becoming more stable for specimens with B < 1mm.

Position of the posterior of the eye. The dramatic shortening of the postocular length with ontogeny is clear in Shaw's (1968) and Chatterton's (1980) illustrations (see Figure 6. 29 herein). The relationship between postocular length and specimen size is shown in Figure 6. 30 (e). Shaw (1968) noted that the posterior extremity of the eye remains separated from the posterior border furrow until the individual has achieved a sagittal length of nearly 3mm, and this is supported by plot 6. 30 (e) (note that B is preoccipital glabellar length, slightly shorter than total sagittal length). It is interesting to note that the rate of decrease in F appears to be less in meraspides from the Crown Point Fm. (open squares) than in those from the lower Esbataottine Fm. (open diamonds). However, this impression is mainly due to a single Crown Point Fm. meraspide which plots at an unusually high value of F (far right of plot). Re-examination of Shaw's (1968) illustrations does not reveal that this specimen is obviously distorted or damaged in any way; clearly this measurement can show significant variation.

Width of the pygidial axis. Chatterton (1980) considered that the pygidial axis becomes relatively narrower with ontogeny, particularly in the late meraspide and early holaspide stages. Figure 6. 30 (f) does not appear to support this suggestion. An RMA line fitted to these specimens has slope 0.35.

Shaw (1968) and Chatterton (1980) also discussed ontogenetic changes in a number of other characters not directly amenable to morphometrics:

Spinosity of the cephalic border. Protaspides possess spinose margins (Chatterton 1980: pl. 16, figs. 1-3; Figure 6. 29 (c) herein) and these spines are retained in the earliest meraspide stages (Shaw 1968: pl. 12, figs. 29-30, 37-38; Chatterton 1980: pl. 16, figs. 4, 11, 15; Figure 6. 29 (d)-(e) herein). These spines are lost in later meraspide stages (Chatterton 1980: pl. 16, figs. 17-18, 20, 23; Figure 6. 29 (f) herein).

Occipital ring tubercle. Protaspides and ontogenetically early meraspides possess a mesial tubercle on the occipital ring (Chatterton 1980: pl. 16, figs. 1-4, 11, 15; Figure 6. 29 (c)-(e) herein). By the later meraspide stages, this tubercle is no more than a

slightly larger granule among others (Chatterton 1980: pl. 16, figs. 17, 23; Figure 6. 29 (f) herein), and is entirely absent in holaspides (Shaw 1968, pl. 12, fig. 7; Chatterton 1980: pl. 16, fig. 27; Plates 6. 1 - 6. 4 herein).

Fixigenal spines. Fixigenal spines are present throughout the protaspide and meraspide stages, and also appear to be retained in ontogenetically early holaspide stages (Shaw 1968: pl. 12, figs. 18-20, 29-30, 36-37; Chatterton 1980: pl. 16, figs. 1-4, 11-12, 15, 17-18, 23; Figure 6. 29 (a)-(f) herein). Shaw (1968) noted that the fixigenal spines are lost when the individual attains a sagittal length of about 3mm.

Spinosity of the pygidium. Both Shaw (1968) and Chatterton (1980) noted that small meraspide pygidia (of sagittal length less than about 1mm, Shaw 1968) have their pleurae produced laterally into spines (Chatterton 1980: pl. 16, figs. 5-7, 12-14, 16; Figure 6. 29 (g) herein). During subsequent ontogeny, these marginal spines are reduced (Shaw 1968: pl. 12, figs. 24, 34; Chatterton 1980: pl. 16, figs. 22, 26, 32; Figure 6. 29 (h)-(i) herein) and finally lost, and the pleural and interpleural furrows (= inter-rib and rib furrows as used herein) retreat from the pygidial margin (Chatterton 1980).

Lateral glabellar furrows. These furrows become relatively longer and more deeply impressed as the glabella expands during ontogeny (Shaw 1968: pl. 12, figs. 18, 20, 29-30, 35-38; Chatterton 1980: pl. 16, figs. 1-4, 11, 15, 17-18, 23, 27; Figure 6. 29 (c)-(f) herein).

Changes to the hypostome. The relative proportions and sculpture of the hypostome change during ontogeny. The holaspide hypostome is relatively more elongate mesially than the meraspide hypostome, with better developed anterior wings and a longer (sag. and exsag.) posterior border. The meraspide hypostome is somewhat spinose around its margins, and this spinosity is lost in the holaspide (Chatterton 1980: pl. 16, figs. 24-25, 28; Figure 6. 29 (j)-(k) herein).

Sculpture. In both *C. (Calliops) callirachis* and *C. (Calliops) annulata* the protaspide and early meraspide stages (both cephala and pygidia) are highly spinose (Shaw 1968: pl. 12, figs. 35-38; Chatterton 1980: pl. 16, figs. 1-7, 11-14; Figure 6. 29 (a)-(d), (g) herein). During later meraspide stages this spinosity is reduced and a sculpture of tubercles develops on the glabella and palpebral fields, with fine granules elsewhere on the cephalon (Shaw 1968: pl. 12, figs. 18, 29-30; Chatterton 1980: pl. 16, figs. 15, 17-18, 23; Figure 6. 29 (e)-(f) herein). The pygidium becomes granulate with tubercles present on the axis (in *C. (Calliops) callirachis* and *C. (Calliops) annulata*) (Shaw 1968: pl. 12, figs. 8-11, 24, 26; Chatterton 1980: pl. 16, fig. 31).

Fusion of the facial suture. Chatterton (1980) noted that the facial suture, while being functional in earlier meraspide stages (Chatterton 1980: pl. 16, figs. 15, 17; Figure 6. 29 (e) herein), becomes fused later, probably during the early-to-middle holaspide period.

6.5. Systematic Palaeontology.

Family Pterygometopidae Reed, 1905
Subfamily Eomonorachinae Pillet, 1954
Genus *Calyptaulax* Cooper, 1930

Emended Generic Diagnosis.

Eomonorachinae with palpebral lobes at the same height as the palpebral areas (= that part of the cheek bounded laterally by the palpebral furrow and the axial furrow and merging posteriorly with the postocular area, Chlupáč 1977) and also level with or slightly lower than the top of the glabella; posteriormost extremity of the palpebral lobe close to the posterior border furrow. Cephalic doublure with deep lateral vincular furrow. Pygidium arched with pointed posterior apex. Pygidial axis subdivided in some species into a short anterior sector of three or four rings and a longer, more gently tapering posterior sector with between four and 11 rings. Pleural field crossed by between five and nine pairs of deep inter-rib furrows (=pleural furrows as used by Ludvigsen and Chatterton 1982) extending out about 3/4 of the way to the margin, and shallower rib furrows (=interpleural furrows as used by Ludvigsen and Chatterton 1982) which extend almost to the lateral margin.

Type Species.

Calyptaulax glabella Cooper, 1930 from the Matapédia Gp. (Ashgill), Percé area, Gaspé Peninsula, Québec.

Remarks.

Many species have been ascribed to this genus, some of them known only from rare and fragmentary specimens. Many of these species have already been recognised as being very closely similar or conspecific (see for example Shaw 1968, Chatterton and Ludvigsen 1976). It is no understatement to say that revising the taxonomy of this genus is a complex undertaking.

Cooper (1930) erected *Calyptaulax* for two forms from the Ashgill Matapédia Gp. of the Gaspé Peninsula, Québec. He described the chief generic character as the reduction of the "second glabellar furrow" (=S2) to a faint impression which does not reach the axial furrow. Indeed the name *Calyptaulax* comes from the Greek meaning "hidden furrow". However, he noted that while S2 is thus reduced on the external surface, on internal

moulds it is clearer, and extends to the axial furrow. The utility of this feature alone as a diagnostic character was therefore already called into some doubt.

Delo (1935) erected the genus *Calliops*, taking as his type species *Phacops callicephalus* Hall, 1847 from the Trenton Group of New York State. He stated that *Calliops* differs from *Calyptaulax* in having smaller "second lateral lobes" (=L3) and a "second lateral furrow" (=S2) which reaches the axial furrow. *Calypataulax* and *Calliops* were thus originally defined as separate genera distinguishable on the basis of a cranidial character.

This distinction was maintained by other workers throughout the interval 1935 - 1965. B. N. Cooper (1953), in describing 13 species of *Calliops* and one of *Calyptaulax* from the lower Champlainian of the Appalachians, described *Calyptaulax* as: "Phacopidae resembling *Calliops* but with obsolescence of second lateral furrows distally and consequent merger of the first and second lateral lobes. Pygidium and thorax much as in *Calliops*." Tripp (1954; 1962; 1967) distinguished the two genera, as apparently did Dean (1962), judging by the diagnosis which the latter gave for *Calyptaulax*. The one important pre-1965 exception to this practice of separating *Calyptaulax* and *Calliops* was that of Struve in Moore (1959) who considered the two taxa to be subgenera of *Calyptaulax*, although he continued to differentiate them on the basis of the cranidial character described above.

Whittington (1965) synonymised the two genera because of the uncertain utility of the S2 furrow as a diagnostic character, as described above. He also felt that the uncertain provenance of Hall's (1847) types of *P. callicephalus*, and the fact that the type specimens are now untraceable, also meant that *Calliops* was invalid as a genus. Ross (1967) followed Whittington in synonymising the two genera, as did Shaw (1968), who illustrated a specimen of *Calyptaulax larrabeei* (Slocum, 1913) from the Maquoketa Fm. at Clermont, Iowa, on which the S2 furrow shows the *Calliops* condition (*i.e.* it reaches the axial furrow) on the left hand side, and the *Calyptaulax* condition on the right hand side (Shaw 1968, plate 12 fig. 6). He noted that DeMott (1963) had described similar variation in ptergometopids from Iowa and Wisconsin. He further noted that no fewer than 31 species of *Calyptaulax* (as redefined to include *Calliops* Delo) had been described by this time, separable by only minor differences. He concluded that the high number of species was an artefact, and that there was in fact a rather small number of highly variable species present in widely separated geographical and stratigraphical localities.

Ross (1972), Shaw (1974), Chatterton and Ludvigsen (1976), and Ludvigsen and Chatterton (1982) continued to consider *Calyptaulax* and *Calliops* co generic, as well as agreeing that the majority of described forms of *Calyptaulax*, at least in North America,

were members of a small number of highly variable species. Therefore, although *Calliops* and *Calyptaulax* were erected as separate genera and were usually considered as such until the middle 1960s, it was recognised that the main character used to distinguish them (the nature of the S2 furrow) is of doubtful utility, and they have generally been considered synonymous since 1965.

Phylogenetic analysis carried out herein suggests that *Calyptaulax* can be separated into two distinct sets of species (see Section 6.3), but the distinction, rather than resting on the cranidial character historically used to separate *Calyptaulax* and *Calliops*, rests entirely on pygidial characters, namely the shape of the pygidium in cross-section and the nature of the rib furrows. These two species groups show close similarity to each other in most respects and are clearly closely related. For this reason, two subgenera are recognised: *Calyptaulax (Calyptaulax)* (diagnosis emended from the original generic diagnosis), and *Calyptaulax (Calliops)* (diagnosis emended from the original generic diagnosis).

Calyptaulax (Calyptaulax) Cooper, 1930

Subgeneric Diagnosis.
Subgenus of *Calyptaulax* in which the pygidial rib furrows are deep and well-defined distally, remaining so to a point about 30% to 50% of the way in towards the axial furrow, and are much shallower or obsolete proximally, and the pygidium, as seen from the posterior, appears "box-like" in cross-section with steeply-sloping lateral margins (Figure 6. 4).

Type Species.
Calyptaulax glabella Cooper, 1930, from the Matapédia Gp. (Ashgill) of the Percé area, Gaspé Peninsula, Québec.

Included Species.
Calyptaulax (Calyptaulax) actonensis Dean, 1961; *Calyptaulax (Calyptaulax) asteroideus* (Reed, 1914); *Calyptaulax (Calyptaulax) foederatus* Tripp, 1962; *Calyptaulax (Calyptaulax) glabella* Cooper, 1930; *Calyptaulax (Calyptaulax) hunteri* (Reed, 1914).

Temporal and Geographical Range.
Total stratigraphical range Llanvirn to upper Rawtheyan. Restricted to Laurentia (North America and western Scotland) during the interval Llanvirn to early Caradoc. The subgenus spread to Avalonia and Baltica in the early Caradoc and was widespread throughout the remaining part of the Caradoc and the early and mid. Ashgill. The latest occurrence is in the Husbergøya Fm. (upper Rawtheyan), Oslo district, Norway.

In the following section the type species is described first, followed by the other species in stratigraphical order.

Calyptaulax (Calyptaulax) glabella Cooper, 1930
Plate 6. 1, figs. 1-15.

1930 *Calyptaulax glabella* Cooper, p. 388, pl. 5, figs. 9-11.
1930 *Calyptaulax compressa* Cooper, p. 389, pl. 5, figs. 7-8.
1940 *Calyptaulax glabella* Cooper; Delo, p. 102, pl. 12, figs. 13-15.
1944 *Calyptaulax glabella* Cooper; Shimer and Schrock, pl. 273, figs. 24-26.
1945 *Calyptaulax norvegicus* Størmer, p. 417, pl. 4, figs. 2-3.
1945 *Calyptaulax* sp. Størmer, p. 418, pl. 4, fig. 10.
1962 *Calyptaulax* aff. *norvegicus* Størmer; Whittington, p. 12, pl. 2, figs. 17-18, and synonymy therein.
1980 *Calyptaulax* aff. *norvegicus* Størmer; Owen and Bruton, p. 33, pl. 9, figs. 16-22; pl. 10, figs. 1-4.
1980 *Calyptaulax planiformis* Dean; Price, p. 870, pl. 112, figs. 14-15, but *not* synonymy therein.
1981 *Calyptaulax norvegicus* Størmer; Owen, p. 62, pl. 14, fig. 20; pl. 15, figs. 1-6, 8, 9, 14, and synonymy therein.
1982 *Calyptaulax glabella* Cooper; Ludvigsen and Chatterton, p. 2191, pl. 4, figs. 1-10; Fig. 6.

Lectotype.
By designation of Delo (1940), an incomplete cranidium (YPM12918) from the Matapédia Gp. (Ashgill), Grande Coupe, near Percé, Gaspé Peninsula, Québec. Figured by Delo (1940: pl. 12, fig. 13). Refigured by Ludvigsen and Chatterton (1982: pl. 4, figs. 1-3) and herein (Plate 6. 1, fig. 1).

Occurrence.
As well as the type horizon, the species as rediagnosed is also known from: Rhiwlas Limestone (Rawtheyan), Bala district, and Ddolhir Fm. (Rawtheyan), Corwen district, Wales; lower Duftom Shales (Onnian), Cross Fell, England; Solvang Fm. (upper Caradoc), Asker, Venstøp Fm. (Pusgillian) and Sørbakken Fm. (Cautleyan), Ringerike, Gagnum Mbr. of the Lunner Fm. (late Caradoc - early Ashgill) and Kjørrven Fm. (Rawtheyan), Hadeland, Husbergøya Fm. (upper Rawtheyan), Oslo district, Norway. Rather poorly preserved material from the Sholeshook Limestone Fm. (Cautleyan and lowermost Rawtheyan), Haverfordwest is also tentatively assigned to this species.

Material Studied.

Eight cephala and three pygidia from the Matapédia Gp.; three cephala and four pygidia from the Sholeshook Limestone Fm.; two cephala from the Rhiwlas Limestone; five cephala and seven pygidia from the Ddolhir Fm.; a single cephalon and pygidium from the Onnian part of the Dufton Shale Fm.; four cephala and two pygidia from the Solvang Fm.; a single cephalon and three pygidia from the Venstøp Fm.; a single cephalon and four pygidia from the Sørbakken Fm.; a single cephalon and pygidium from the Gagnum Mbr.; two cephala and a pygidium from the Kjørrven Fm.; a single cephalon from the Husbergøya Fm.

Emended Diagnosis.

Distal length of L3 similar to distal length of frontal lobe, L2 and L1 of about equal, much shorter distal length (see table 6.4 for definition of distal length); S3 markedly concave-forward; S2 directed posterolaterally, straight or only very slightly curved (convex-forward); relatively shallow cephalic axial furrows; sculpture of small tubercles scattered over the whole of the glabella and palpebral area; pygidial axial rings markedly scalloped in their posterior margins; pygidium "box-like" in cross-section; pygidial sculpture of fine granules; rib and inter-rib furrows shallow.

Description.

Cephalon sub-semicircular with a subangular anterior extremity and lateral margins subparallel. Width (tr.) / length (sag.) ratio of cephalon between 1.2 and 1.6 (mean 1.45) for six specimens on which these measurements can be made) in the holaspide. Border narrow anteriorly, widening laterally, marked off laterally by a shallow lateral border furrow. Genal angles rounded, not produced posteriorly. Posterior border furrow deep and narrow proximally becoming shallower distally until it meets the lateral border furrow. Occipital ring sub-oval, height not greater than the glabella. Width (tr.) / length (sag.) ratio of occipital ring variable between 2.6 and 3.9 (mean value 3.32 for 17 specimens in which the occipital ring appears undamaged). Faint node at middle of occipital ring. Occipital furrow shallow and narrow mesially, deepening distally. Glabella narrowest across L1 (slightly narrower than the occipital ring), widest across L3 or frontal lobe. L1 approximately rhomboid, outer margins slightly divergent. Rhomboid distal node delimited by a posterior-directed branch of the S1 furrow which intersects the occipital furrow. Distal node to L1 depressed. Ratio of width of glabella across L1 (=k10, see Table 6. 4) / distal length of L1 (=b10) variable, making the distal node appear quite small in some populations (eg: specimens from the Matapédia Gp., k10/b10 ratio between 5.4 and 7.6, mean value 6.3), relatively larger in other populations (eg: specimens from the Rhiwlas Limestone, k10/b10 ratio between 3.5 and 4.2, mean value 3.9). S1 extends adaxially 30% of glabellar width (tr.). Directed posterolaterally proximally, turning sharply at the mid-point to be directed slightly anterolaterally distally.

Deepest at the mid-point, from where the posteriorly-directed branch which delimits the distal node to L1 originates. L2 with divergent lateral margins, ratio of width of glabella across L2 (=k21) / distal length of L2 (=b21) highly variable between 5.4 and 16.2 (mean value 8.8, 29 specimens; NB: this ratio is probably heavily affected by the lateral extent of S2 which varies between testate and non-testate specimens, see below). S2 shallow on external surface of the test, straight or only very slightly curved (convex-forwards), directed posterolaterally at about 25° to the sagittal line, not reaching the axial furrow abaxially. On internal moulds, S2 more deeply impressed, becoming virtually obsolete distally, just reaching the axial furrow. L3 triangular, ratio of width of glabella across L3 (=k32) / distal length of L3 (=b32) between 2.1 and 3.1 (mean value 2.5, 29 specimens). L2 and L3 lobes confluent with the middle area of the glabella. S3 shallow proximally and deepening distally, anterolaterally directed at about 58° to the sagittal line and slightly concave-forwards. More deeply impressed on the internal mould than on the external surface of the test. Frontal lobe approximately rhombohedral in shape, width (tr.) approximately equal to width of glabella across L3; ratio of width of frontal lobe (=k5) / distal length of frontal lobe (=b5) between 1.8 and 4.1 (mean value 2.6, 29 specimens). Anterior of frontal lobe subangular with a faint furrow subparallel to the facial suture at its anteriormost extremity. Anterior branch of facial suture situated to the anterior of the frontal lobe and marked by a faint preglabellar furrow which circumscribes the lateral extremities of the frontal lobe and meets the axial furrow at the point where the latter is intersected by the distal end of S3. Axial furrows diverge at an approximately constant rate, and are shallowest adjacent to L3, slightly deeper anterior to and posterior to this. Posterior branch of the facial suture not confined in a furrow and meets the lateral margin opposite S1.

Palpebral lobes strongly curved, anteriormost point opposite distal end of S3, posteriormost point usually very close to posterior border furrow. Eye with 28 to 38 dorso-ventral lens files with up to 13 lenses in a file. Top of eye lower than the level of the glabella. Sculpture of small tubercles scattered over the glabella and palpebral areas, clearly visible on external surfaces, also visible on some internal moulds. Oval pattern of tubercles visible on the frontal lobe of some internal moulds.

Hypostome only known for specimens from the Solvang Fm. (Owen and Bruton 1980: p. 33, pl. 10, fig. 4). Oval with parallel margins, subangular at the posterior end. Width (tr.) across middle body equal to about 2/3 of the sagittal length. Middle body convex, with well-defined lateral furrows which widen around the posterior extremity of the middle body. Wide (tr.) anterior wings.

Thorax of 11 segments. Thoracic axis equal to about 30% of total thoracic width (tr.). Axial rings approximately oval, slightly scalloped, with distal nodes delimited by a break

in slope laterally. Pleurae gently widening (exsag.) and steeply sloping (almost vertical) distally, with rounded distal extremities. Shallow pleural furrows directed obliquely across each pleura from the anteromesial extremity (in contact with the axial furrow) to the posterolateral tip. Axial furrows shallow. Axis and pleurae smooth.

Pygidium triangular with sinuous lateral margins meeting at a slightly produced posterior point. The ratio of maximum width (tr.) / length (sag.) is between 1.2 and 2.2 (mean value 1.6, 24 specimens; NB: this ratio is heavily affected by postmortem distortion of the pygidia). Lateral margins steeply sloping giving a rather "box-like" cross-sectional shape to the pygidium when it is viewed from the posterior. Maximum width of pygidial axis (=X) equal to between 21% and 41% of maximum pygidial width (=W) (mean value 32%, 17 specimens). Between six and 13 axial segments, becoming less distinct posteriorly. Posterior margin of each axial ring (which in turn defines the anterior margin of the next ring) markedly scalloped, with non-functional remanent half-rings visible between the anteriormost two-or-three rings. Ring furrows shallowly impressed mesially, becoming more deeply impressed abaxially. Anterior portion of axis tapers relativey rapidly, posterior portion tapers less rapidly, almost parallel-sided. Axial furrows shallow, becoming indistinct around the posterior extremity of the axis. Length of pygidial axis (=Y1) equal to between 59% and 100% of total pygidial length (=Z1) (mean 81%, 22 specimens). Pleural fields composed of an anterior articulating facet and between five and seven pleural "ribs" (see Figure 6. 4). Inter-rib furrows sinuous and extend from the axial furrow abaxially to about 10% of total pygidial width (tr.) in from the margin. Anteriormost inter-rib furrows moderately impressed, others less impressed. Rib furrows present on outer portion of pleural field, alternating with the inter-rib furrows and extending from close to the margin adaxially to about 17% of pygidial width (tr.) in from the margin. Anteriormost rib furrow moderately impressed, others very weakly impressed. Surface of pygidium finely granular on axis and pleural fields.

Remarks.

Cooper (1930) described two species of *Calyptaulax* from the Matapédia Gp. of Percé: *C. glabella* and *C. compressa*, noting that they co-occur at one locality (South Cove, F8 of Cooper 1930). Cooper quoted the differences in *C. compressa* as being: coarse ornamentation, difference in outline of the glabella and frontal lobe, more deeply impressed first lateral furrows (=S3), deeper occipital furrow, less marked trace of second lateral furrow (=S2). It is here considered that the sculpture is preserved only on external surfaces and not internal moulds, and its presence in some specimens and not in others is a preservational artefact. Differences in the development of S3, S2 and the occipital furrow are similarly attributable to the nature of preservation. Glabellar shape does not show any more variation between the specimens than is commonly seen within

other species of *Calyptaulax*. *C. compressa* is therefore here considered a synonym of *C. glabella*.

Størmer (1945) erected *Calyptaulax norvegicus* for specimens from the Gagnum Mbr. of the Lunner Fm., Hadeland, Norway. He noted that the cephalon of this species is very like that of *C. glabella* from the Matapédia Gp., differing only in having slightly larger third glabellar lobe (=L1). Størmer further noted that the pygidium differs in possessing a slightly wider marginal band. Whittington (1962) described *Calyptaulax* aff. *norvegicus* from the Rhiwlas Limestone at Rhiwlas in the Bala area and considered both the cranidium and the pygidium to be very similar to Størmer's (1945) Gagnum Mbr. specimens. Owen and Bruton (1980) described specimens from the upper Caradoc Solvang Fm. of the Asker district, Norway, which they also referred to *Calyptaulax* aff. *norvegicus*, stating that they differ from the Gagnum Mbr. specimens in having broader palpebral lobes which are more strongly curved and possibly more lens files on the visual surface. This difference in palpebral lobe width is barely detectable morphometrically, as is any variation in curvature of the lobes. Known material of this species from the Gagnum Mbr. does not have eye lenses preserved, and Størmer (1945) did not quote a number of lens files for it. Owen (1981) noted that *C. norvegicus* from the Ashgill of the Oslo Region resembles Matapédia Gp. specimens very closely, differing in possessing slightly larger L1 and having the axial furrows a little more strongly divergent along L1 and L2. In fact, length of L1 shows a continuous range of variation in *C. (C.) glabella* (see description above). Ludvigsen and Chatterton (1982) noted that all quoted differences separating *C. norvegicus* from *C. glabella* are minor and the two are probably conspecific. This synonymy is formalised herein.

A cranidium and pygidium from the lower part of the Dufton Shale Fm. (Onnian) are herein included in *C. (C.) glabella* (rather than in *C. (C.) actonensis*, see below), on the basis of the straight or nearly straight S2 furrow on the cranidium (see phylogenetic analysis, Section 6. 3). The relatively long (sag.) L1 in this cranidium is not quite as long as that of Størmer's (1945) Gagnum Shale specimens. Similarly, specimens from the Sholeshook Limestone Fm. (Cautleyan and lowest Rawtheyan) described by Price (1980) as *Calyptaulax planiformis* are here included in *C. (C.) glabella* for the same reason.

Owen (1981) noted that a pygidium assigned to *Homalops* cf. *altumii* Remelé, from the Slandrom Limestone (topmost Caradoc, lowest Ashgill) at Fjäcka, Västergötland, illustrated by Jaanusson (1953) closely resembles that of *C. norvegicus* (herein synonymised with *C. (C.) glabella*), as does one from erratic boulders of Östseekalk (upper Ordovician) illustrated and assigned to *Homalops altumii* by Wiman (1908: pl. 8, fig. 10). Struve in Moore (1959) considered that Remelé's species and Jaanusson's

specimen constituted a new but unnamed subgenus of *Calyptaulax*. Specimens of *H. altumi* have not been available for study, and in the absence of detailed information on the cephalon its status is unclear. It may well be conspecific with *C. (C.) glabella.*

Calyptaulax (Calyptaulax) foederatus Tripp, 1962
Plate 6. 1, figs. 16-19; Plate 6. 2, figs. 1-5.

1962 *Calyptaulax foederatus* Tripp, p. 29, pl. 4, figs. 20-25.
1967 *Calyptaulax georgei* Tripp, p. 77, pl. 6, figs. 3-9.
1988 *Calyptaulax foederatus* Tripp; Morris, p. 46.
1991 *Calyptaulax* sp.; Ingham and Tripp, Fig. 15 (h).

Holotype.
By original designation of Tripp (1962), an incomplete cranidium (HM A5352) from the Confinis Fm. (Llanvirn), Girvan district, Scotland. Figured by Tripp (1962: pl. 4, fig. 20). Refigured herein (Plate 6. 2, fig. 1).

Occurrence.
As well as the type horizon the species is also known from the upper Stinchar Limestone Fm. (Llandeilian) and the Separation Sandstone Mbr. of the Doularg Fm. (earliest Caradoc).

Material Studied.
Three cephala and four pygidia from the Confinis Fm.; two cranidia and six pygidia from the upper Stinchar Limestone Fm.; a single cranidium from the Separation Sandstone Mbr.

Emended Diagnosis.
Frontal lobe of greater distal length than L3, L2 and L1 of approximately equal, shorter distal length; S3 concave-forwards; S2 approximately straight; cephalic axial furrows relatively deep; pygidium triangular, with convex-out lateral margins giving an outline which is close to parabolic; sculpture of closely-packed tubercles on the glabella and palpebral areas and also on the pygidial axis and pleurae of some specimens.

Remarks.
This species differs from *C. (Calyptaulax) glabella* in the following respects: its relatively small overall size (preoccipital glabellar length of 4.35mm for the largest specimen, compared with 11.8mm for *C. (C.) glabella*); having the frontal lobe of greater length (sag.) than L3; possession of relatively deep cephalic axial furrows; pygidial rib furrows and inter-rib furrows which are somewhat deeper than those of *C.*

(C.) glabella. Tripp (1962) noted that *C. foederatus* possesses "typical *Calyptaulax* characters" but also observed that S2 may be obsolete distally or may reach the axial furrow (compare Plate 6. 2, fig. 1 with Plate 6. 2, fig. 2). Tripp (1967) described *Calyptaulax georgei* from the upper Stinchar Limestone Fm. of the Girvan district, Scotland, stating its differences from *C. foederatus* to be:

(i) Greater width of the glabella. In the small number of specimens suitable for measurement, the Stinchar Limestone Fm. specimens do have slightly greater mean width / length ratios for each subdivision of the glabella, but the overlap in total ranges of values and the small number of undistorted, measurable specimens means that there is no diagnostic difference:

	Range	Mean	No. specimens	
Doularg Fm.	2.43	/	1	Frontal lobe
Stinchar Fm.	2.53 - 2.82	2.68	2	(k5/b5)
Cofinis Fm.	2.19 - 2.73	2.47	3	
Doularg Fm.	2.61	/	1	L3 lobes
Stinchar Fm.	3.48 - 3.93	3.71	2	(k32/b32)
Cofinis Fm.	2.86 - 3.88	3.35	3	
Doularg Fm.	7.68	/	1	L2 lobes
Stinchar Fm.	7.11 - 10.04	8.58	2	(k21/b21)
Cofinis Fm.	6.08 - 10.00	8.14	3	
Doularg Fm.	3.82	/	1	L1 lobes
Stinchar Fm.	5.33 - 6.00	5.67	2	(k10/b10)
Cofinis Fm.	4.00 - 5.88	4.84	3	

(Specimen from the Doularg Fm. included in anticipation of discussion of it below).

(ii) Lack of an embayment to the anterior margin. This is probably a preservational artefact. A few specimens from the Confinis Fm. appear to possess a medial embayment of the frontal lobe (eg: Plate 6. 2, fig. 2), but this is not seen in all specimens and may be due to slight crushing.

(iii) Shorter anterior and posterior lateral lobes. The relative distal lengths of the subdivisions of the glabella (expressed as a ratio of the total glabellar length) do not show any significant systematic difference between the Stinchar Limestone Fm. and Confinis Fm. material:

	Range	Mean	No. specimens	
Doularg Fm.	0.45	/	1	Frontal lobe
Stinchar Fm.	0.49 - 0.50	0.50	2	(b5/B)
Confinis Fm.	0.41 - 0.47	0.45	3	
Doularg Fm.	0.35	/	1	L3 lobes
Stinchar Fm.	0.29 - 0.30	0.30	2	(b32/B)
Confinis Fm.	0.29 - 0.36	0.32	3	
Doularg Fm.	0.07	/	1	L2 lobes
Stinchar Fm.	0.08 - 0.10	0.09	2	(b21/B)
Confinis Fm.	0.06 - 0.12	0.10	3	
Doularg Fm.	0.14	/	1	L1 lobes
Stinchar Fm.	0.10 - 0.14	0.12	2	(b10/B)
Confinis Fm.	0.13 - 0.14	0.13	3	

(iv) Broader palpebral lobes. There is no detectable difference in the relative widths of the palpebral lobes (expressed as a ratio of the palpebral cranidial width) of the Stinchar Limestone Fm. and Confinis Fm. specimens.

	Range	Mean	No. specimens	
Doularg Fm.	0.06	/	1	Width of
Stinchar Fm.	0.06 - 0.07	0.07	2	Palp. lobes
Confinis Fm.	0.06 - 0.07	0.07	2	(P/J)

It is therefore herein considered that *C. georgei* is a synonym of *C. foederatus* (in agreement with Shaw 1974).

Ingham and Tripp (1991) figured a cranidium from the Separation Sandstone bed of the Doularg Fm. as *Calyptaulax* sp (Plate 6.1, fig. 16 herein). Because of its close similarity with the Confinis Fm. and Stinchar Limestone Fm. material in both cladistic and morphometric characters (see tables above) this specimen is herein considered to be conspecific with them.

Calyptaulax (Calyptaulax) hunteri (Reed, 1914)
Plate 6. 2, figs. 6-10.

1914 *Phacops (Pterygometopus) hunteri* Reed, p. 52, pl. 8, figs. 8-9.

1931 *Phacops (Calyptaulax) hunteri* Reed; Reed, p. 24.

1986 *Calyptaulax hunteri* (Reed); Morris and Tripp, p. 172, pl. 4, fig. 3.
1988 *Calyptaulax hunteri* (Reed); Morris, p. 47.

Lectotype.
Selected by Morris and Tripp (1986), a cranidium with 7 thoracic segments attached (BM In23612) from the Upper Balclatchie Gp. (*peltifer* subzone, lower-middle Caradoc) at Balclatchie, Girvan district, Scotland. Figured by Reed (1914: pl. 8, fig. 8). Refigured by Morris and Tripp (1986: pl. 4, fig. 3) and herein (Plate 6. 2, fig. 9).

Occurrence.
As well as the type locality and horizon, also known from the middle Ardwell Farm Fm. (*wilsoni* subzone, middle Caradoc).

Material Studied.
Four cranidia and two pygidia from the Upper Balclatchie Gp; one cranidium and two pygidia from the middle Ardwell Farm Fm.

Emended Diagnosis.
Frontal lobe of approximately equal distal length to L3, L2 very much shorter than L3 and L1; L2 also very much narrower (tr.) than the other lateral lobes, pinched out distally by near convergence of L3 and L1; S3 concave forwards; S2 approximately straight; cephalic axial furrows relatively deep; pygidium triangular with sinuous lateral margins; sculpture of densely-packed tubercles scattered over whole glabella and palpebral area; V-shaped pair of furrows on anterior of frontal lobe; furrow, or succession of tiny pits, along palpebral lobe, just to the outside of the mid-line.

Remarks.
C. (Calyptaulax) hunteri differs from the type species of the subgenus in its very short (sag.) and narrow (tr.) L2 (relative length about 50% that of the type species, relative width about 75%), and in the pronounced V-shaped furrow pair on the frontal lobe (Plate 6. 2, figs. 6-7, 9). Both of these characters are diagnostic of the species. Reed (1914) noted that the cephalon of this species resembles that of *C. brongniartii* in many characters. However, the pygidium is clearly of *C. (Calyptaulax)* type in that it is "box-like" in cross-section with rib furrows which only extend adaxially about half way across the pleural field (Plate 6. 2, fig. 8) and this reveals the true affinity of the species.

Calyptaulax (Calyptaulax) actonensis Dean, 1961
Plate 6. 2, figs. 11-17.

1961 *Calyptaulax actonensis* Dean, p. 328, pl. 50, figs. 11, 13-14; pl. 51, figs. 1-2.

1962 *Calyptaulax planiformis* Dean, p. 98, pl. 13, figs. 1-5.
non 1980 *Calyptaulax planiformis* Dean; Price, p. 870, pl. 112, figs. 14-15.
1988 *Calyptaulax actonensis* Dean; Morris, p. 46.

Holotype.
By original designation of Dean (1961), a pygidium from the middle Acton Scott Fm. at Quarry Field, Gretton (upper Caradoc) (BM In49771). Figured by Dean (1961: pl. 50, figs. 11, 14). Refigured herein (Plate 6. 2, fig. 13).

Occurrence.
Acton Scott Fm. (Dean 1961), South Shropshire; upper Dufton Shale Fm. (Pusgillian), Cross Fell; Applethwaite Mbr. of Kirkley Bank Fm. (Cautleyan), English Lake District.

Material Studied.
One cranidium and two pygidia from the Acton Scott Fm.; one cranidium and two pygidia from the upper Dufton Shale Fm.; two cranidia and 12 pygidia from the Applethwaite Mbr.

Emended Diagnosis.
Distal length of frontal lobe approximately equal to that of L3; L2 and L1 of approximately equal, shorter distal length. S3 concave forwards; S2 markedly hooked, convex forwards; cephalic axial furrows relatively shallow; pygidium with sinuous lateral margins, meeting at a posterior point; pygidial axial rings scalloped; sculpture of small tubercles scattered over the glabella and palpebral area; pygidium finely granular.

Remarks.
Dean (1961) described the cranidium of his new species as being "typical of the genus" and very difficult to distinguish from *C. norvegicus* from the Ashgill of the Oslo Region (herein synonymised with *C. glabella*). *C. (C.) actonensis* is here separated from *C. (C.) glabella* on the basis of its hooked S2 furrow (Plate 6. 2, figs. 14, 16). Dean (1961) considered the pygidium of *C. actonensis* to taper more uniformly than that of *C. glabella*, but this is not supported by material studied here (compare Plate 6. 2, figs. 12-13, 15, 17 with Plate 6. 1, figs. 11, 13-14). Dean (1962) stated that another species, *Calyptaulax planiformis* from the Dufton Shale Fm. of Cross Fell, can be distinguished from *C. actonensis* on pygidial characters, *C. actonensis* having:

(i) Shorter pygidium. The difference in the ratio of pygidial width (=W) / pygidial length (=Z1) between specimens from the type localities of Dean's *C. actonensis* and *C. planiformis* (within the middle Acton Scott Fm., Shrops. and the Pusgillian part of the Dufton Shale Fm., Cross Fell respectively) is very small

indeed, particularly when one considers that the relative dimensions of pygidia are highly susceptible to post-mortem distortion.

	Range	Mean	No. specimens	
Acton Scott Fm.	1.60 - 1.90	1.75	2	Width/length
Dufton Shale Fm.	1.49 - 1.80	1.64	4	(W/Z1)
Applethwaite Mbr.	0.91 - 2.02	1.46	10	

(Pygidia from the Applethwaite Mbr. (Cautleyan, English Lake District) included in anticipation of discussion of them below).

(ii) Shorter axis with fewer axial rings. There is a small difference in the length of the pygidial axis (=Y1) expressed as a ratio of the total pygidial length (=Z1) between the specimens from the type localities of *C. actonensis* and *C. planiformis*, but this alone is not considered sufficient to warrant separation as species. There is no significant difference in the number of axial rings.

	Range	Mean	No. specimens	
Acton Scott Fm.	0.72 - 0.83	0.78	2	Relative axial
Dufton Shale Fm.	0.75 - 0.93	0.84	5	length
Applethwaite Mbr.	0.68 - 0.88	0.77	11	(Y1/Z1)

	Range	Mean	No. specimens	
Acton Scott Fm.	9	9	2	Number of
Dufton Shale Fm.	7 - 13	10.3	5	axial rings
Applethwaite Mbr.	6 - 11	9	10	

(iii) More strongly defined pleural furrows. There is no obvious difference in the depth of the pleural furrows between the two groups of specimens (compare Plate 6. 2 fig. 13, from the middle Acton Scott Fm. with Plate 6. 2 fig. 17 from the Pusgillian part of the Dufton Shale Fm.).

(iv) Better-developed terminal spine. The terminal spine does not appear to be better developed in one set of specimens than in the other (again, compare Plate 6. 2 fig. 13 with fig. 17).

C. planiformis is thus considered to be synonymous with *C. actonensis*. Specimens from the Applethwaite Mbr., Kirkley Bank Fm. (Cautleyan) of the English Lake District are also included in this species, on the basis of phylogenetic analysis (they share the characteristic hooked S2 of *C. (C.) actonensis*; see Section 6. 3 and Figure 6. 5) and close morphometric similarity (Section 6. 4). It can be seen from the above tables that

pygidia from the Applethwaite Mbr. are closely similar to pygidia from the type locality in all parameters.

Price (1980) assigned specimens from the Sholeshook Limestone Fm. (Cautleyan and lowest Rawtheyan) to *C. planiformis* Dean. However, on the basis of phylogenetic analysis, these specimens are herein reassigned to *C. (C.) glabella* (see Section 6. 3 and earlier in this section).

Calyptaulax (Calyptaulax) asteroideus (Reed, 1914)
Plate 6. 3, figs. 1-6.

1914 *Phacops (Dalmanitina?) asteroideus* Reed, p. 53, pl. 8, figs. 10-11.
1931 *Phacops (Calyptaulax) asteroideus* Reed; Reed, p. 24.
1986 *Calyptaulax asteroideus* (Reed); Morris and Tripp, p. 172, pl. 4, fig. 4.
1988 *Calyptaulax asteroideus* (Reed); Morris, p. 46.

Lectotype.
Selected by Morris and Tripp (1986), a pygidium (BM In23622) from the Ladyburn Starfish Beds, South Threave Fm. (Rawtheyan), Girvan district, Scotland. Figured by Reed (1914: pl. 8, fig. 10). Refigured by Morris and Tripp (1986: pl. 4, fig. 4).

Occurrence.
Only known from the type locality and horizon.

Material Studied.
Seven cephala and ten pygidia.

Emended Diagnosis.
Distal length of frontal lobe greater than that of L3, which itself is longer than L2; L2 and L1 of approximately equal distal length; S3 slightly sigmoidal; S2 approximately straight; shallow cephalic axial furrows.

Remarks.
This species differs from the type species in the relative lengths of the glabellar lobes, in that the distal length of the frontal lobe is greater than the distal length of L3 in *C. (C.) asteroideus*, while in *C. (C.) glabella* the frontal lobe and L3 are of similar distal length. This characteristic suggests that this species is more closely allied to *C. (C.) foederatus* and *C. (C.) hunteri* than the other members of this subgenus (see phylogenetic tree, Figure 6. 7). Owen (1981) noted that *C. asteroideus* differs from *C. norvegicus* Størmer (herein synonymised with *C. glabella*) in having the facial suture meeting the

axial furrow a short distance behind the anteriormost point of L3, while in *C. norvegicus* the axial furrow, facial suture and S3 all meet at a single point. This is confirmed herein.

Calyptaulax (Calliops) Delo, 1935

Subgeneric Diagnosis.
Distal length of frontal glabellar lobe always greater than that of L3; cephalic axial furrows deep; pygidial rib furrows deep and well-defined for their whole length adaxially almost to the axial furrow; pygidium, seen in dorsal view, has lateral margins which are convex outward or straight and, seen in posterior view, has either a rounded cross-section or may be slightly "box-like"; pygidial axial rings usually oval.

Type Species.
Phacops callicephalus Hall, 1847 from the Trenton Gp. near Middleville, New York.

Included Species.
Calyptaulax (Calliops) angusta Cooper, 1953; *Calyptaulax (Calliops) annulata* (Raymond, 1905); *Calyptaulax (Calliops) brevipostica* Cooper 1953; *Calyptaulax (Calliops) brongniartii* (Portlock, 1843); *Calyptaulax (Calliops) callicephala* (Hall, 1847); *Calyptaulax (Calliops) callirachis* (Cooper, 1953); *Calyptaulax (Calliops) holstonensis* (Raymond, 1925); *Calyptaulax (Calliops) larrabeei* (Slocum, 1913); *Calyptaulax (Calliops) marginatus* (Tripp, 1962).

Temporal and Geographical Range.
Total stratigraphical range lower Llanvirn to lower Ashgill. Earliest appearance in the lower Table Head Gp. (Whittington 1965) of Newfoundland. The subgenus is entirely restricted to Laurentia and the Laurentian margins (North America, Pomeroy district of Northern Ireland, Girvan district and Southern Uplands of Scotland). The subgenus was most widely distributed in the middle Caradoc. Rare in the Ashgill. Latest occurrence is in the Maquoketa Gp. (Richmondian) near Ft. Atkinson, Iowa.

The type species is described first, followed by the other species in stratigraphical order.

Calyptaulax (Calliops) callicephala (Hall, 1847)
Plate 6. 3, figs. 7-12, 15; Figure 6. 31.

1847 *Phacops callicephalus* Hall, p. 247, pl. 65, figs. 3a-i.
1935 *Calliops callicephalus* (Hall); Delo, p. 417, Figs. 42-43.
1940 *Calliops antecavatus* Ulrich and Delo; Delo, p. 92, pl. 11, figs. 13-14.
1940 *Calliops brevis* Ulrich and Delo; Delo, p. 93, pl. 11, figs. 9-11.

1940 *Calliops callicephalus* (Hall); Delo, p. 94, pl. 11, figs. 1-4.
1940 *Calliops leithi* Delo, p. 97, pl. 12, figs. 1-3.
1940 *Calliops plattevillensis* Ulrich and Delo; Delo, p. 98, pl. 12, figs. 4-5.
1940 *Calliops schmidti* (Clarke); Delo, p. 99, pl. 12, figs. 6-7, and synonymy therein.
1953 *Calliops callicephala* (Hall); Cooper, p. 33, pl. 16, fig. 12.

Type Specimens.
Hall's (1847) type specimens cannot be traced. It is known that they were from the Trenton Gp. near Middleville, Herkimer Co., New York, although the exact horizon is uncertain (Whittington 1965). Both Delo (1940) and Cooper (1953) based their descriptions on material collected from Trenton Falls, New York.

Occurrence.
Trenton Gp. Prosser Fm. (approx. Shermanian) of Wisconsin, Iowa and Minnesota; Trenton Limestone (Shermanian - Edenian) of New York; Verulam Fm. (Shermanian) and Lindsay Fm. (Edenian) of Ontario; Fairmount Shale (Maysvillian) of Ohio.

Material Studied.
Twenty eight cephala and 25 pygidia from the Prosser Fm. at Duck Creek Quarry, Wisconsin; four cephala and nine pygidia from the topmost Prosser Fm. (*catazyga uphami* bed) at the quarry at Elkader, Iowa; four cephala from the lower Prosser Fm. "near Cannon Falls" (exact locality unknown), Minnesota; six cephala and 11 pygidia from the Trenton Limestone, Trenton Falls, New York; five cephala and two pygidia from the Verulam Fm., Ontario; two cephala from the Trenton Gp. (probably Verulam Fm.) at Belleville, Ontario; one cephalon from the Lindsay Fm., Gt. Cloche Island, Ontario; one cephalon from the Fairmount Shale (Maysvillian) of Cincinnati, Ohio (exact locality unknown).

Emended Diagnosis.
S3 straight or slightly sigmoidal; genal angles slightly produced posteriorly; axial furrows curved convex-outward; visual surface with 21 to 25 dorso-ventral lens files; pygidium triangular with lateral margins convex outward, rounded in cross-section; sculpture of relatively large tubercles densely packed on the glabella and palpebral areas.

Description.
Cephalon sub-semicircular with rounded anterior extremity. Width (tr.) / length (sag.) ratio of cephalon between 1.3 and 1.7 (mean 1.6 for 27 specimens). Border narrow anteriorly, widening laterally, marked off by moderately deep lateral border furrow. Genal angles rounded and slightly produced posteriorly. Posterior border furrow deep and narrow proximally, shallowing and widening distally until it meets the lateral border

furrow. Occipital ring sub-oval in outline, height not greater than the rest of the glabella. Ratio of width (tr.) / lenth (sag.) of occipital ring between 2.5 and 3.9 (mean 3.2 for 35 specimens in which this structure is undamaged). Occipital furrow narrow and shallow mesially, deepening abaxially. Small posteriorly-directed branch of the occipital furrow delimits, but does not entirely cut off, a distal node on the occipital ring. Glabella narrowest (tr.) across L1 (slightly narrower than the occipital ring), widest across frontal lobe. L1 approximately rhomboidal, outer margins sub-parallel. Small depressed distal node delimited by a shallow posteriorly-directed branch of S1 furrow which intersects the occipital furrow. Ratio of width of glabella across L1 (=k10, see Table 6. 4) / distal length of L1 (=b10) variable between 4.4 and 9.9 (mean 6.3, 46 specimens). Proximal portion of S1 directed posterolaterally, turning sharply at the mid-point to be directed anterolaterally. S1 deepest at the mid-point, from where the posteriorly-directed branch originates to delimit the distal node. L2 approximately oval, ratio of width of glabella across L2 (=k21) / distal length of L2 (=b21) between 5.2 and 11.6 (mean 7.5, 50 specimens). S2 shallow proximally, deepening markedly abaxially, straight or very slightly curved, directed abaxially rearwards at about 20° to the sagittal line and reaching the axial furrow. L3 triangular, ratio of width of glabella across L3 (=k32) / distal length of L3 (=b32) between 2.6 and 3.4 (mean 2.9, 50 specimens). L2 and L3 lobes confluent with the middle area of the glabella. S3 shallow proximally, deepening distally; either straight or slightly sigmoidal, directed anterolaterally at about 70° to the sagittal line. Frontal lobe approximately oval, ratio of width of frontal lobe (=k5) / distal length of frontal lobe (=b5) between 1.9 and 3.2 (mean 2.3, 48 specimens). Frontal lobe rounded anteriorly with a faint pit. Anterior branch of facial suture lies in a faint furrow a little to anterior of preglabellar furrow. Faint suture traceable around the lateral extremity of the frontal lobe to meet the axial furrow where it is intersected by S3. Axial furrows convex-outward adjacent to L2 and L3, shallowest adjacent to L3, deeper elsewhere. Posterior branch of facial suture not confined in a furrow and meets the lateral margin opposite S1.

Palpebral lobes strongly curved, anteriormost point close to the distal end of S3, posteriormost point very close to the posterior border furrow, distance from axial furrow equal to about 9% of maximum cephalic width. Eye with between 21 and 25 dorso-ventral lens files with up to eight lenses in the highest files. Top of eye approximately level with the top of the glabella. Sculpture of relatively large tubercles densely distributed over the glabella, palpebral areas and fixigenae. Smaller, more scattered tubercles on the cephalic margin.

Moderately impressed vincular furrow on the lateral part of the doublure. Furrow simple in form, not possessing notches. Hypostome unknown.

Thorax of 11 segments. Axis about 30% of total thoracic width. Axial segments slightly scalloped. Pleurae widening (exsag.) distally with rounded distal extremities which are steeply inclined (almost vertical). Deeply impressed pleural furrows directed obliquely across each pleura from the anteromesial corner (in contact with the axial furrow) to become hidden beneath the distal portion of the preceeding pleura abaxially. Deeply impressed axial furrows. Tuberculation similar to that on the glabella scattered over the thoracic axis, pleurae finely granular.

Pygidium triangular with lateral margins convex-outward as seen in dorsal view. Ratio of pygidial width (=W) / pygidial length (=Z1) is between 1.1 and 2.2 (mean 1.5, 41 specimens; NB: this ratio can be heavily affected by post-mortem distortion of the pygidia). Rounded outline in cross-section. Width of pygidial axis (=X) / total pygidial width (=W) between 0.27 and 0.39 (mean 0.34, 45 specimens). Between eight and 12 axial rings which become less distinct posteriorly. Posterior of anteriormost five or six rings slightly scalloped with non-functional remanent half-rings visible between the anterior three-to-five rings. Ring furrows shallowly impressed mesially, deeper abaxially. Anterior portion of the axis tapers strongly, posterior portion much less so, close to parallel-sided. Axial furrows deeply impressed, remaining distinct around the posterior extremity of the axis. Length of pygidial axis occupies between 77% and 90% of the total pygidial length. Pleural fields composed of an anterior articulating facet and between five and eight pleural "ribs" (see Figure 6. 4). Inter-rib furrows sinuous, anterior furrows deeply impressed, posterior ones moderately impressed; furrows extend from the axial furrow abaxially almost to the margin. Rib furrows alternate with inter-rib furrows; extend adaxially from near the margin to close to the axial furrow. Anteriormost rib furrows deeply impressed, others moderately impressed. Axis of pygidium tuberculate, tubercles of slightly smaller size than those on the glabella; pleural fields finely granular.

Remarks.

Delo (1940) described and illustrated several species from North America which, as he noted, are very similar to *C. callicephala* : *Calliops leithi* Delo, 1940 from the Long Point Gp. (Blackriveran and lowermost Rocklandian) of the St. George Peninsula, Newfoundland (specimens not available for detailed study); *Calliops plattevillensis* Ulrich and Delo, 1940 from the Platteville Fm. (Blackriveran) of Minnesota and Illinois (specimens not available for detailed study); *Calliops antecavatus* Ulrich and Delo, 1940 from the Middle Kimmswick Fm. (approx. Shermanian) of Missouri (specimens not available for detailed study); *Calliops brevis* Ulrich and Delo, 1940 from the Prosser Fm. (Shermanian), Minnesota (represented by stratigraphical sample CANNON herein); *Calliops schmidti* (Clarke, 1894) from the Galena Gp. (Prosser Fm.) of the upper Mississippi Valley (represented by stratigraphical sample DUCK herein). Delo (1940)

considered each of these species to differ from *C. callicephala* in minor details of cephalic or pygidial proportions, or in possessing slightly less pronounced sculpture on the glabella or pygidium. The differences appear from Delo's illustrations to be small, and all probably fall within the range of variation of the type *C. callicephala* (certainly the ranges of variation of CANNON and DUCK are comparable with that of the Trenton Falls specimens as represented by the stratigraphical sample TRENTON, Figures 6. 14, 6. 18). These species are therefore all considered synonymous with *C. (Calliops) callicephala.*

One further interesting variation is seen in specimens assigned to *Calliops schmidti* by Delo (1940) (represented by the stratigraphical sample DUCK herein). Delo stated that the cephala of these specimens are indistinguishable from *C. callicephala* except that they possess short, sharp genal spines. In fact, only a few of the smaller specimens from the Prosser Fm. at Duck Creek Quarry examined as part of this study (stratigraphical sample DUCK) possess such spines (and can therefore presumably be assigned to Clarke's *Calliops schmidti*). The majority of the specimens have rounded genal angles, slightly produced posteriorly, and are indistinguishable from the type *C. (Calliops) callicephala.* Figure 6. 31 shows the range of variation in the genal angles of the Duck Creek specimens. In view of the close similarity between all of the Duck Creek specimens in all features except the nature of the genal angle, it is herein considered that the presence of such residual genal spines in a few individuals represents the slightly prolonged retention of these spines later in ontogeny (or could possibly represent sexual dimorphism) rather than the presence of two distinct species at this locality. All specimens are, so far as can be ascertained, holaspides. This is in agreement with Chatterton's (1980) assertion that the genal spines present in juveniles of *Calyptaulax* are lost during the holaspide period. The occurrence of residual genal spines in a few holaspide individuals is known in other species of *Calyptaulax (Calliops)* : compare Chatterton and Ludvigsen (1976: pl. 16, fig. 1), which shows a holaspide of *C. (Calliops) callirachis* with rounded genal angles, with Chatterton and Ludvigsen (1976: pl. 16, fig. 5) which shows an individual with residual nodes on its genal angles (see also Figure 6. 33 herein).

Delo (1940: p. 102, pl. 13, figs. 1-2) also discussed *Calyptaulax eboraceous* (Clarke, 1894) from the Trenton Limestone (Shermanian - Edenian), New York (specimens not available for detailed study), which is contemporaneous with the type material of *C. callicephala.* Delo stated that this species differs from other species of *Calyptaulax* in possessing short (exsag.) eyes with their posterior extremities some way from the posterior border furrow, short, stout genal spines and a rather blunt pygidium. Delo noted that the species is superficially similar to *Eomonorachus intermedius* (Walcott, 1877), differing in its possession of smaller eyes, shorter pygidium, shorter genal spines, and S2 furrow which does not reach the axial furrow (this being the reason for

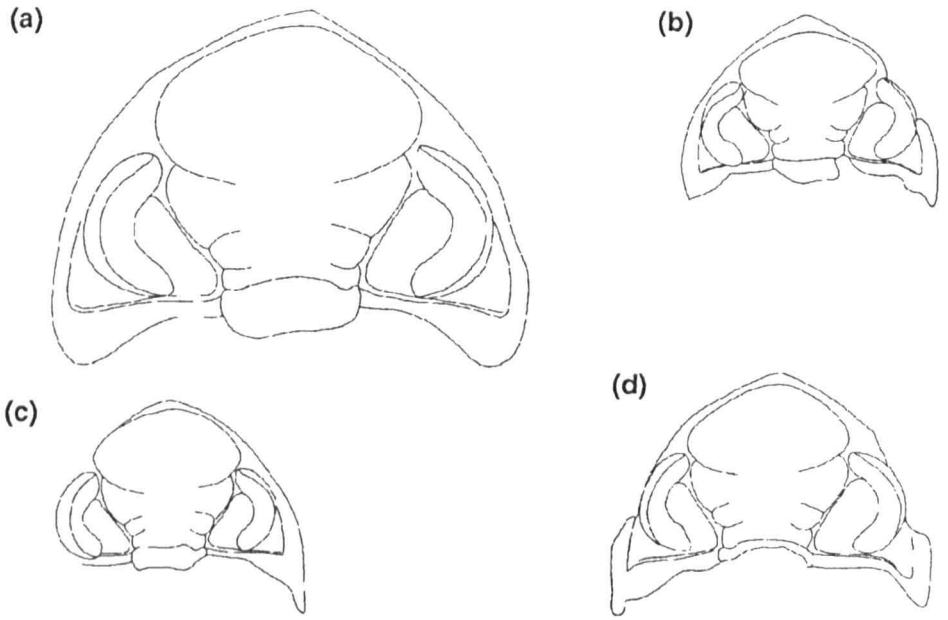

Figure 6. 31. Line drawings of selected cephala of *Calyptaulax (Calliops) callicephala* (Hall, 1847) from the Prosser Fm. (approx. Shermanian) at Duck Creek Quarry, Wisconsin, showing the range of variation in the nature of the genal angles. (a) usual condition, genal angles rounded and slightly produced posteriorly; one of a set of specimens catalogued as USNM 79001; (b), (c) and (d) smaller cephala showing genal spines in varying degrees of reduction; all from a set of specimens catalogued as USNM 79000. Redrawn from photographs taken by the author. All x5.

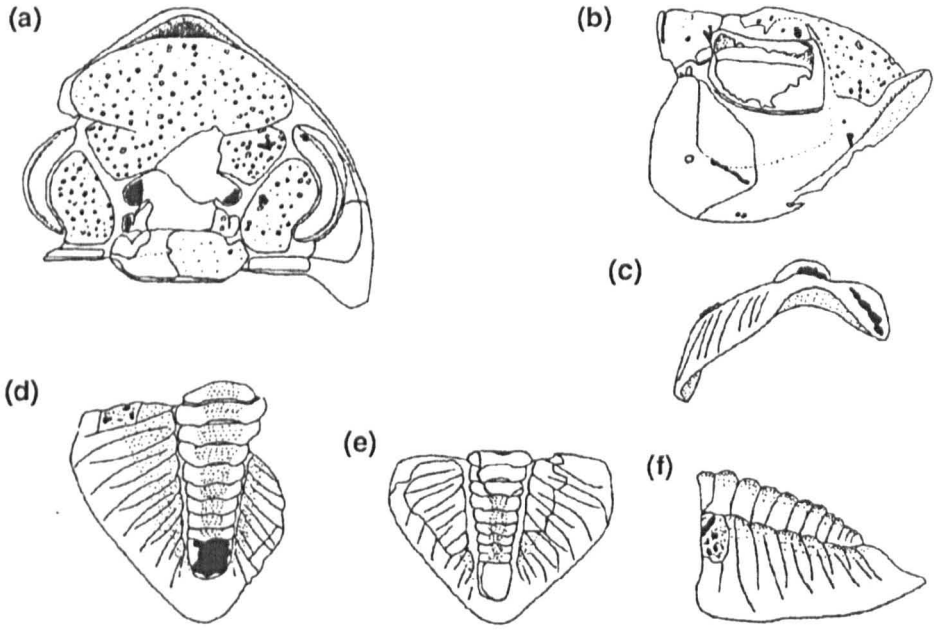

Figure 6. 32. *Calyptaulax (Calliops) annulata* from the middle Crown Point Fm. (Chazyan), Valcour Island, New York. (a) and (b) dorsal and lateral views of silicified cephalon, NYSM 12368, x4.5; (c), (d) and (f) posterior, dorsal and lateral views of silicified pygidium, NYSM 12372, x6; (e) dorsal view of internal mould of pygidium, NYSM 12373, x3. All redrawn from Shaw (1968: pls. 11 and 12).

placing this species within *Calyptaulax*). It is difficult to resolve the status of this material on the basis of Delo's figures. It may be a member of *Calptaulax (Calliops)* (the pygidium appears from Delo's photographs to be of the *Calliops* -type, with rib furrows which extend adaxially nearly to the axial furrows and rounded cross-sectional shape), or it may alternatively be a member of *Eomonorachus* Delo, 1935.

Calyptaulax (Calliops) marginatus (Tripp, 1962)
Plate 6. 3, figs. 13-14, 16-18.

1962 *Calliops marginatus* Tripp, p. 28, pl. 4, figs. 10-17.
1988 *Calyptaulax marginatus* (Tripp); Morris, p. 47.

Holotype.
By original designation of Tripp (1962), a cranidium (HM A5237) from the Confinis Fm. (late Llanvirn) at Bougang Quarry, Girvan district, Scotland.

Occurrence.
Only known from the type horizon.

Material Studied.
Eight cephala and 19 pygidia.

Emended Diagnosis.
S3 sigmoidal; genal angles not produced posteriorly; 21 lens files on the visual surface with seven lenses in the highest files; triangular pygidium with straight lateral margins, rounded in cross-section; pygidial rib furrows effaced, not visible on internal moulds; sculpture of fine granules scattered over the whole surface.

Remarks.
The relatively small size of individuals of this species, the finely granular sculpture and the poor development of the pygidial rib furrows distinguish this species from other members of the subgenus. Tripp (1962) considered *C. marginatus* to be closely allied to *C. hunteri* because they share the characteristic of a flattened anterior border clearly marked off from the frontal lobe (but note that all members of *C. (Calliops)* as defined herein show this feature) and also both have reduced L2 lobes (L2 in *C. (Calliops) marginatus* is relatively slightly shorter (sag.) than that in other members of *C. (Calliops)*, but not so much so as in *C. (Calyptaulax) hunteri*). However, cladistic analysis of the genus (Section 6.3) does not suggest a close relationship between the two species, chiefly because of their different pygidia: the pygidium of *C. (Calliops) marginatus* has straight lateral margins and a rounded posterior margin while that of *C.*

(Calyptaulax) hunteri has sinuous lateral margins which meet at a pronounced posterior point; the pygidium of *C. (Calliops) marginatus* is rounded in cross-section while that of *C. (Calyptaulax) hunteri* is "box-like" (Figure 6. 4); the rib furrows in *C. (Calliops) marginatus* are effaced while those in *C. (Calyptaulax) hunteri* are deep and extend adaxially about half way across the pleural field; the pygidial axis in *C. (Calliops) marginatus* is clearly subdivided into an anterior, rapidly tapering section, and a posterior parallel-sided section which extends almost to the posterior extremity of the pygidium, whereas the axis in *C. (Calyptaulax) hunteri* is more uniformly tapering and does not reach the posterior margin (compare Plate 6. 2, figs. 8, 10 with Plate 6. 3, figs. 13-14, 18). On the cephalon, *C. (Calliops) marginatus* has much finer sculpture, narrower palpebral lobes, and lacks the distinctive V-shaped furrow pair on the anterior of the frontal lobe exhibited by *C. (Calyptaulax) hunteri* (compare Plate 6. 2, figs. 6-7, 9 with Plate 6. 3, figs. 16-17).

Calyptaulax (Calliops) annulata (Raymond, 1905)
Figure 6. 32.

1905 *Pterygometopus annulatus* Raymond, p. 376, pl. 14, figs. 24-25.
1925 *Pterygometopus gracilens* Raymond, p. 162, pl. 10, fig. 18.
1940 *Calliops annulatus* (Raymond); Delo, p. 92, pl. 11, figs. 5-8.
1953 *Calliops annulata* (Raymond); Cooper, p. 33.
1968 *Calyptaulax annulata* (Raymond); Shaw, p. 84, pl. 11, figs. 39-45; pl. 12, figs. 7-38.
1974 *Calyptaulax annulata* (Raymond); Shaw, p. 40, pl. 10, figs. 14-15, 18-25; pl. 11, figs. 10, 13-21.

Holotype.
The holotype specimen is lost, but it is known that it came from the Chazy Gp. at Sloop Bay, Valcour Island, New York (Delo 1940).

Occurrence.
Day Point, Crown Point and Valcour fms. of the Chazy Gp., New York. Also Lenoir Fm., Virginia (Shaw 1968).

Material Studied.
Two holaspide cranidia and 14 pygidia from the Crown Point Fm., Chazy Gp.

Emended Diagnosis.
S3 slightly sigmoidal; genal angles not produced posteriorly; pygidium triangular with straight lateral margins, slightly "box-like" in cross-section; pygidial axial rings oval or

slightly scalloped; sculpture of densely packed tubercles on the glabella and palpebral areas.

Remarks.

C. (Calliops) annulata differs from *C. (Calyptaulax) callicephala* in having genal angles which are not posteriorly produced and straight rather than convex-out lateral margins to the pygidium. These features suggest a closer relationship to *C. (C.) marginatus* than to *C. (C.) callicephala.* The difference in the nature of the pygidial margins described above is the probable reason for Shaw's (1968) suggestion that *C. callicephala* differs from *C. annulata* in having a slightly broader (tr.) pygidium with a more evenly semicircular posterior margin. Shaw (1968) considered *Calliops gracilens* (Raymond, 1925) (also described and illustrated by Delo 1940: p. 96, pl. 11, fig. 26; Cooper 1953: p. 34, pl. 15, figs. 4-7, 15) from the lower Lenoir Limestone, Tennesee (not included in morphometrics herein) to be conspecific with *C. annulata* and this is also considered to be the case herein. Shaw (1974) considered *C. strasburgensis* (Ulrich and Delo, 1940) (also described and illustrated by Delo 1940: p. 99, pl. 12, figs. 8-10; Cooper 1953, p. 37, pl. 17, figs. 1-15) from the lower Edinburg Fm., Virginia also to be conspecific with *C. annulata.* However, on the basis of Cooper's (1953) figures this Edinburg Fm. material appears to agree more closely with *C. (Calliops) brongniartii* (see below) particularly in the shape of the pygidium which has convex-out lateral margins as seen in dorsal view as opposed to the straight lateral margins of *C. (C.) annulata.*

Calyptaulax (Calliops) callirachis (Cooper, 1953)
Figure 6. 33.

1953 *Calliops callirachis* Cooper, p. 39, pl. 18, figs. 1-6, 8-14.
1953 *Calliops loxorachis* Cooper, p. 37, pl. 16, figs. 7-11, 14.
1975 *Calyptaulax* sp. 1 Ludvigsen, pl. 4, figs. 27-29.
1976 *Calyptaulax callirachis* (Cooper); Chatterton and Ludvigsen, p. 77, pl. 16, figs. 1-35; pl. 22, figs. 2-4.

Holotype.

By original designation of Cooper (1953), a silicified cephalon with thorax (USNM116535a) from the lower Edinburg Fm. (Blackriveran) (*Echinosphaerites* beds), near Strasburg Junction, Shenandoah Co., Virginia. Figured by Cooper (1953: pl. 18, figs. 13-14).

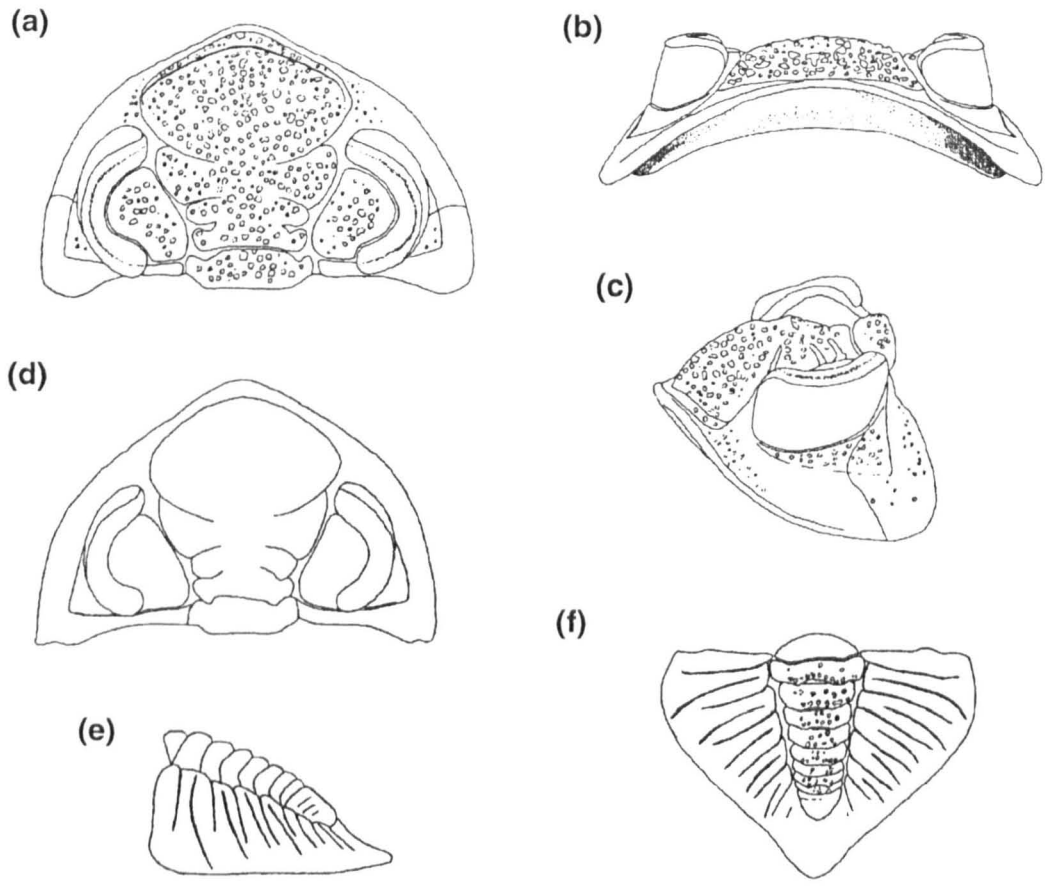

Figure 6. 33. *Calyptaulax (Calliops) callirachis* Cooper, 1953, lower Esbataottine Fm. (late Chazyan), Mackenzie Mountains, Canada. (a), (b) and (c) dorsal, anterior and oblique anterolateral views of silicified cephalon, UA 1412, x 5.5; (d) line drawing of dorsal view of silicified cephalon showing variation in the nature of the genal angles; compare the slightly produced nodes with the rounded genal angles of (a); UA 1413, x 5.5; (e) and (f) lateral and dorsal views of silicified pygidium, UA 1418, x 8.25. All redrawn from Chatterton and Ludvigsen (1976: plate 16).

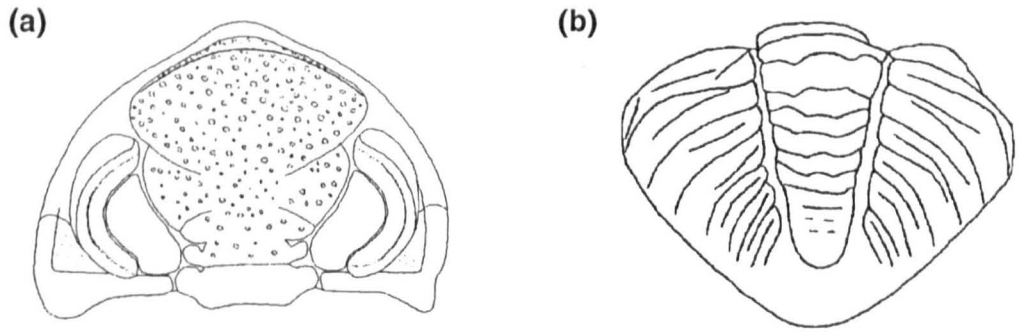

Figure 6. 34. *Calyptaulax (Calliops) larrabeei* (Slocum, 1913), Maquoketa Gp. (Maysvillian), Maquoketa Creek, Clermont, Iowa. (a) dorsal view of cephalon, MCZ 5105, x 4; (b) dorsal view of pygidium, Walker Mus. 28043, x 4. (a) redrawn from photograph taken by the author, (b) redrawn from Delo (1940: plate 11, fig. 21).

Occurrence.

As well as the type horizon, known from the Athens black shale (upper Chazyan) near Otes, Tennessee; also from the lower Esbataottine Fm. (late Chazyan), District of Mackenzie, North Western Territories.

Material Studied.

Two cephala and six pygidia from the upper Athens Shale, Tennesee; three holaspide cranidia and three holaspide pygidia from the lower Esbataottine Fm., District of Mackenzie, North Western Territories.

Emended Diagnosis.

S3 straight or slightly sigmoidal; S2 straight or slightly curved; genal angles slightly produced posteriorly; pygidium triangular with sinuous lateral margins which meet at a pronounced point posteriorly; pygidial axial rings markedly scalloped; pygidial rib furrows extend inwards almost as far as the axial furrow; pygidium moderately "box-like" when seen from the posterior; sculpture of relatively large, densely-packed tubercles.

Remarks.

C. (C.) callirachis differs from *C. (C.) callicephala* in the shape of the pygidium as seen in both dorsal and posterior view (the pygidium of the former species has sinuous lateral margins and is somewhat "box-like" in cross-section, while the pygidium of the latter species has convex-out lateral margins and is more rounded in cross-section) and in the shape of the axial rings (scalloped in *C. (C.) callirachis*, oval in *C. (C.) callicephala*). In these respects, the pygidium of *C. (C.) callirachis* seems to be intermediate between the *C. (Calyptaulax)* type and the typical *C. (Calliops)* type. In the phylogenetic analysis of *Calyptaulax* (Section 6. 3) *C. (C.) callirachis* plotted within the poorly-resolved *C. (Calliops)* portion of the cladogram (Figure 6. 7).

Chatterton and Ludvigsen (1976) considered *C. loxorachis* (Cooper, 1953) to be conspecific with *C. callirachis*, and this is also considered to be the case herein. Chatterton and Ludvigsen considered this species and *C. annulata* (as redefined by Shaw 1974 to include *C. strasburgensis* (Ulrich and Delo) - synonymy not supported herein) to account for the majority of *Calliops* material known from North America. Chatterton and Ludvigsen distinguished *C. callirachis* and *C. annulata* on the basis of the following characteristics:

(i) Shape of the cephalon. Chatterton and Ludvigsen (1976) stated that the cephalon of *C. callirachis* is more semicircular in shape than that of *C. annulata*, which tends towards the sub-triangular. It may be that the slightly posteriorly produced genal angles of *C. callirachis*, as compared with the rounded angles of *C.*

annulata, give this impression. It should be noted that apparent cephalic shape is strongly influenced by any damage to the cephalic margins and genal angles.

(ii) Shape of the pygidium. Chatterton and Ludvigsen (1976) stated that *C. callirachis* has a triangular pygidium with straight lateral margins, while that of *C. annulata* has outwardly bowed sides. However, Chatterton and Ludvigsen's own illustrations of *C. callirachis* from the lower Esbataottine Fm. (1976: pl. 16) show pygidia with sinuous lateral margins, while illustrations of pygidia assigned to *C. annulata* (not including specimens originally designated *C. strasburgensis* (Ulrich and Delo)) shown by Delo (1940: pl. 11, figs. 7-8), and Shaw (1968: pl. 12, figs. 8, 10-11, 13-14 and 16) clearly show straight margins.

(iii) Sculpture. Chatterton and Ludvigsen (1976) stated that *C. callirachis* possesses a coarse tubercular sculpture, while that of *C. annulata* is relatively finer. This distinction is confirmed herein.

It is therefore considered here that *C. (C.) callirachis* differs from *C. (C.) annulata* in the following characteristics: possession of genal angles which are slightly produced posteriorly; possession of a pygidium with sinuous lateral margins as opposed to the straight margins of *C. (C.) annulata* ; possession of a cephalic sculpture of relatively large tubercles as opposed to the slightly finer sculpture of *C. (C.) annulata.*

Calyptaulax (Calliops) brongniartii (Portlock, 1843)
Plate 6. 4, figs. 1-19.

1843 *Phacops Brongniartii* Portlock, p. 282, pl. 2, figs. 8a-d; pl. 3, fig. 8d.
1843 *Phacops Dalmanni* Portlock, p. 282, pl. 2, figs. 7a-c; ?pl. 3, fig. 7d.
1843 *Phacops Murchisoni* Portlock; p. 283, pl. 2, figs. 9a-b; pl. 3, figs. 9c-d.
1864 *Phacops (Acaste) Brongniarti* Portlock; Salter, p. 34, pl. 1, figs. 21-26.
1906 *Phacops (Pterygometopus) brongniartii* Portlock; Reed, p. 154, pl. 19, figs. 17-18.
1940 *Calliops strasburgensis* Ulrich and Delo, p. 99, pl. 12, figs. 8-10.
1945 *Phacops (Calliops) jukesi* var. *vicina* Reed, p. 314, pl. 4, fig. 6.
1953 *Calliops strasburgensis* Ulrich and Delo; Cooper, p. 37, pl. 17, figs. 1-15.
1954 *Calliops brongniartii* (Portlock); Tripp, p. 685, pl. 4, figs. 34-38.
1980 *Calyptaulax brongniartii* (Portlock); Tripp, p. 149.
1982 *Calyptaulax brongniartii* (Portlock); Clarkson and Tripp, p. 287, figs. 1-5.
1992 *Calyptaulax brongniartii* (Portlock); Owen and Clarkson, p. 15, fig. 4 N-P, R-S.

Lectotype.
Selected by Clarkson and Tripp (1982), a complete individual (BGS GSM13983) from the Bardahessiagh Fm., South of Craigbardahessiagh, Pomeroy district, Co. Tyrone,

Northern Ireland. Figured by Portlock (1843: pl. 2, figs. 8a; pl. 3, fig. 8d), Salter (1864: pl. 1, fig. 22) and Clarkson and Tripp (1982: fig. 3a).

Occurrence.
As well as the type locality and horizon, also known from the lower-middle to upper Caradoc of the Girvan district, Scotland (Infra-Kilranny Greywackes, Upper Balclatchie Gp., lower Ardwell Farm Fm., Kiln Mudstone of the Craighead Fm.), lower-middle Caradoc of the Southern Uplands (Kirkcolm Fm.). Material from the Edinburg Fm. (equivalent to lower-middle Caradoc), Virginia is also assigned to this species.

Material Studied.
Eight cephala and five pygidia from the type locality; four cephala and 17 pygidia from the Infra-Kilranny Greywackes at Dow Hill, Girvan; five cephala and 28 pygidia from the Upper Balclatchie Gp., Balclatchie, Girvan; 30 cephala and 24 pygidia from the lower Ardwell Farm Fm. at Ardmillan, Girvan; four cephala and two pygidia from the Kiln Mudstone, Craighead Fm., Craighead Quarry, Girvan; a cephalon from the Kirkcolm Fm. at Kilbucho and two others from the same horizon at Duntercleuch, both in the Southern Uplands.

Emended Diagnosis.
S3 furrow straight or slightly sigmoidal; S2 straight; genal angles rounded, not produced posteriorly; triangular pygidium with margins convex outward, rounded in cross-section; axial rings oval; sculpture of densely packed tubercles, not as large as those of *C. (C.) callicephala.*

Remarks.
C. (C.) brongniartii differs from *C. (C.) callicephala* in having genal angles which are not produced posteriorly, less coarse glabellar tuberculation, and axial furrows which are not so convex-out as seen in dorsal view. In other characteristics, the two species are very similar.

Salter (1853) synonymised Portlock's (1843) *Phacops Dalmanni* and *P. Murchisoni* with his *P. Brongniartii.* All are from the type horizon. Clarkson and Tripp (1982) synonymised Reed's (1945) *Phacops (Calliops) jukesi* var *vicina* from the Upper Balclatchie Fm. of Balcletchie, Girvan, with this species.

Clarkson and Tripp (1982) discussed geographical variation within *C. (C.) brongniartii,* largely affecting the structure of the eye. They considered other characteristics which showed variation between different populations (glabellar tuberculation and convexity of the exoskeleton) to be of limited utility, because of overlap between states exhibited by

different populations and preservational effects (especially important in exoskeletal convexity). They used lens charts to demonstrate that specimens from Dow Hill and Craighbardahessiagh possess eyes of similar depth with a similar number of lenses per dorso-ventral file, while those from Ardmillan have deeper eyes with more lenses per file (see Clarkson and Tripp 1982 figure 6; see also Figure 6. 27 (a) herein which was compiled independently). Clarkson and Tripp suggested that depth of eye probably correlates with cephalic convexity, a more convex cephalon being able to accommodate a deeper eye.

Clarkson and Tripp (1982) further noted that *C. brongniartii* is very similar to *C. strasburgensis* (Ulrich and Delo, 1940) (not included in the morphometric study herein) from the Edinburg Fm., Virginia. They considered *C. brongniartii* to differ in the following respects:

(i) Possessing more lenses in the eye.

(ii) Having a more depressed L1 lobe. The degree of depression in L1 in *C. strasburgensis* is difficult to assess from published illustrations, but there may be a slight populational variation (eg: Delo 1940, pl. 12, figs. 8-10; Cooper 1953, pl. 17).

(iii) Having L3 and L2 lobes which are not as tuberculate as the rest of the glabella. Published illustrations do show a slightly greater density of tuberculation on the L3 and L2 lobes of *C. strasburgensis* as compared with *C. (C.) brongniartii.*

(iv) Having a less strongly medially embayed doublure.

It is here considered that the differences between *C. (C.) brongniartii* and *C. strasburgensis* are relatively minor and possibly attributable to populational variances. *C. strasburgensis* is therefore tentatively considered to be a synonym of *C. (C.) brongniartii* (and not a synonym of *C. (C.) annulata* as was considered to be the case by Shaw 1974, see earlier in this section).

Calyptaulax (Calliops) larrabeei (Slocum, 1913)
Figure 6. 34.

1913 *Pterygometopus larrabeei* Slocum, p. 81, pl. 18, figs. 6-8.
1913 *Pterygometopus fredricki* Slocum, p. 79, pl. 18, figs. 1-5.
1940 *Calliops larrabeei* (Slocum); Delo, p. 97, pl. 11, figs. 20-21.
1940 *Calliops fredricki* (Slocum); Delo, p. 96, pl. 11, figs. 22-25.
1940 *Calliops tuberculatus* Delo, p. 100, pl. 12, figs. 11-12.

Holotype.

An almost complete individual (Field Mus. No. P11256) from the lower Maquoketa Gp. at Clermont, Iowa. Figured by Slocum (1913: pl. 18, fig. 6).

Occurrence.

As well as the type locality, also known from the type horizon at Elgin and Bloomfield, Iowa. Also from the Maquoketa Gp. (Richmondian) near Ft. Atkinson, Iowa.

Material Studied.

Five cephala and nine pygidia from the lower Maquoketa Gp. at Maquoketa Creek, Clermont, Iowa. Four cephala and seven pygidia from the Ft. Atkinson section near Ft. Atkinson, Iowa.

Emended Diagnosis.

S3 straight or slightly sigmoidal; S2 straight; genal angles slightly produced posteriorly; pygidium triangular with outwardly-convex lateral margins; pygidium rounded in cross-section; glabellar sculpture of scattered tubercles, not as coarse as those of the type species of the subgenus.

Remarks.

Slocum (1913) stated that his *Phacops larrabeei* differed from *Phacops callicephala* in the following characteristics:

(i) Having a relatively longer cephalon. The morphometric data do not support this. The ratio of maximum cephalic width (=I) / sagittal cephalic length (=A1) for specimens from the type horizon of *C. (C.) larrabeei* is very similar to the ratio for all specimens assigned to *C. (Calliops) callicephala*:

	Range	Mean	No. specimens	
C. (C.) larrabeei	1.56 - 1.70	1.61	4	Width / length of
C. (C.) callicephala	1.26 - 1.72	1.56	27	cephalon (I/A1)

(ii) Having a less anteriorly inflated glabella. This is confirmed here.

(iii) Having more axial rings in the pygidium. There is in fact no clear difference in the numbers of axial rings between pygidia assigned to *C. (C.) larrabeei* and pygidia assigned to *C. (C.) callicephala* (see Figure 6. 28):

	Range	Mean	No. specimens	
C. (C.) larrabeei	8 - 12	10.38	8	Number of axial
C. (C.) callicephala	8 - 12	9.52	44	rings.

(iv) Having tuberculation which is restricted to the glabella, with the palpebral areas, occipital ring and cheeks being punctate. This is confirmed here.

Slocum (1913) also erected another species, *P. fredricki*, for specimens from the Maquoketa Gp. near Ft. Atkinson, Iowa (Richmondian), distinguishing it from *P. larrabeei* on the basis of the following:

(i) Possession of a lower eye with fewer lenses in the lens files. Visual surfaces studied as part of this study do not show any difference in relative height or number of lenses between these two groups of specimens (see Figures 6. 3 and 6. 27 (a)).

(ii) Greater anterior inflation of the glabella. This difference was confirmed by Delo (1940), but has not been seen in any of the specimens examined as part of this study.

(iii) Shorter pygidium with fewer axial rings. The ratio of pygidial width (=W) / pygidial length (=Z1) is in fact not significantly different between the two groups of specimens, and neither is the number of axial rings:

	Range	Mean	No. specimens	
C. (C.) larrabeei	1.43 - 1.94	1.62	9	Width / length of
P. fredericki	1.44 - 1.65	1.52	7	pygidium (W/Z1)

	Range	Mean	No. specimens	
C. (C.) larrabeei	8 - 12	10.38	8	Number of axial
P. fredericki	9 - 10	9.5	4	rings.

Delo (1940) also considered this distinction to be invalid.

Delo (1940) considered *P. fredricki* to have a relatively wider cephalon than *P. larrabeei.* The small amount of morphometric data indicates that the Ft. Atkinson specimens can indeed have a very slightly wider cephalon, but the difference is negligible. The ratio of maximum cephalic width (=I) / sagittal cephalic length (=A1) for the two sets of specimens is virtually identical:

	Range	Mean	No. specimens	
C. (C.) larrabeei	1.56 - 1.70	1.61	4	Width / length of
P. fredericki	1.61 - 1.74	1.68	2	cephalon (I/A1)

P. fredricki is therefore here considered a synonym of *C. (C.) larrabeei.*

Delo (1940) described and illustrated pygidia from the Fernvale Fm. (Maysvillian), Arkansas, for which he erected *Calliops tuberculatus* Delo. These pygidia are very broadly rounded in outline as seen in dorsal view, which general proportions which look similar to those of the approximately contemporaneous *C. (C.) larrabeei.* They also have a similar number of axial rings (*viz* eight). They differ from *C. (C.) larrabeei* in being tuberculate (pygidia of *C. (C.) larrabeei* are smooth). In the absence of cephala it is difficult to resolve the status of these specimens. It is here considered that they may be a variation of *C. (C.) larrabeei.*

Other species not included in the morphometrics.

To complete the systematic treatment of the genus, a number of other species, not included in the morphometric study due to unavailability of material, are briefly considered here in stratigraphical order.

Calyptaulax (Calliops) angusta Cooper, 1953

1953 *Calliops angusta* Cooper, p. 35, pl. 14, figs. 1-6.
1965 *Calyptaulax incepta* Whittington, p. 428, pl. 67, figs. 1-4, 6.

Holotype.
By original designation of Cooper (1953), an incomplete testate cephalon (USNM 78976a) from the upper Lenoir Limestone (middle Chazy), about 1/4 mile SE of Friendsville, Tennessee.

Occurrence.
Known from several localities in the upper Lenoir Limestone of Tennessee and Virginia. Also known from the Little Oak Limestone (topmost Chazyan, Ross *et al.* 1982) of Alabama and the Rockdell Fm. (Blackriveran, Ross *et al.* 1982) of Virginia (Cooper 1953). Also lower Table Head Fm., middle Whiterockian (Llanvirn, Barnes *et al.* 1981) of Newfoundland.

Remarks.
This species appears from Cooper's (1953) illustrations to be quite distinctive in its glabellar structure: L1 and L2 are relatively long (sag. and exsag.) for the genus, almost of equal length to L3; the lateral glabellar lobes are relatively short (tr.) giving a wide middle area to the glabella; frontal lobe somewhat lozenge-shaped. Cooper also noted that the tuberculation of the cephalic margins and indistinct nature of the posterior extremity of the pygidial axis are distinctive. Cooper stated that the thorax has only eight segments, but this may be based on an incomplete thorax. The thorax which he figured

(Cooper 1953: pl. 14, fig. 5) is definitely incomplete. This species is here considered to belong in subgenus *Calyptaulax (Calliops)* because its pygidium shows the typical *C. (Calliops)* structure (rib furrows which extend adaxially almost to the axial furrows, rounded cross-section).

Calyptaulax incepta, described and illustrated by Whittington (1965) from the lower Table Head Fm. (Whiterock), Port au Port Peninsula, Newfoundland is very similar to *C. (C.) angusta* (as Whittington noted), and different in its glabellar proportions from any other species of *Calyptaulax*. It is herein considered a synonym of *C. (C.) angusta*.

Calyptaulax (Calliops) holstonensis (Raymond, 1925)

1925 *Pterygometopus holstonensis* Raymond, p. 161, pl. 10, figs. 9-11.
1940 *Calliops declivis* Ulrich and Delo; Delo, p. 95, pl. 11, figs. 15-19.
1940 *Calyptaulax? holstonensis* (Raymond); Delo, p. 103, pl. 13, figs. 3-4.
1953 *Calliops declivis* Ulrich and Delo; Cooper, p. 35, pl. 15, figs. 1-3, 8-12.
1953 *Calyptaulax holstonensis* (Raymond); Cooper, p. 41, pl. 15, figs. 13-14, 16-18.

Holotype.
By original designation of Raymond (1925), a damaged cranidium (MCZ 1644) from the Holston Limestone (topmost Chazyan - lowermost Blackriveran, Ross *et al.* 1982) at Hoge Farm, Bland County, Virginia.

Occurrence.
As well as the type horizon, also known from the Effna Limestone (late Chazyan - early Blackriveran, Ross *et al.* 1982), Virginia; the upper Lenoir Limestone (middle Chazy) Tennessee; the Botetourt Limestone Mbr. of the Edinburg Fm. (Blackriveran, Ross *et al.* 1982), Virginia; the "Holston Marble" (late Chazyan - early Blackriveran, Ross *et al.* 1982), Tennessee; granular limestone just below Athens Shale (Chazyan, Ross *et al.* 1982), Alabama; Little Oak Limestone (late Chazyan, Ross *et al.* 1982), Alabama.

Remarks.
As was noted by both Delo (1940) and Cooper (1953), the quadrangular shape of the glabella of this species is distinctive, as is the short (sag. and exsag.) L2. Delo (1940) and Cooper (1953) both placed this species within *Calyptaulax* as opposed to *Calliops* because the S2 furrow does not reach the axial furrow. However, the pygidium is clearly of *Calyptaulax (Calliops)* -type as defined herein (rib furrows extending adaxially almost to the axial furrow, rounded cross-section, also convex-out lateral margins as seen in dorsal view) and this species is therefore placed in that subgenus. *Calliops declivis* from

the upper Lenoir Limestone of Tennessee resembles *C. (C.) holstonensis* closely, and is here considered to be synonymous with that species.

The short L2 of this species calls to mind *C. (Calyptaulax) hunteri* and *C. (Calliops) marginatus* from the Girvan succession. The latter is approximately contemporaneous with this Appalachian material (the former is a middle Caradoc species). Also Delo's (1940) and Cooper's (1953) illustrations of the pygidia of the Appalachian material show that it is assignable to *C. (Calliops)* rather than *C. (Calyptaulax)* (see above). This species is therefore probably most closely related to *C. (C.) marginatus*. Differences from *C. (C.) marginatus* are: coarser sculpture on the glabella and palpebral areas; relatively wider palpebral lobes; pygidium with lateral margins which are convex-out as seen in dorsal view (although because of the preservation of the material illustrated by Delo and Cooper, this is not absolutely unequivocal), rather than straight as in *C. (C.) marginatus*.

Calyptaulax (Calliops) cornwalli Ross, 1967

1967 *Calyptaulax cornwalli* Ross, p. D29, pl. 8, figs. 28-33.

Holotype.
By original designation of Ross (1967), a testate cephalon from the upper part of the Pogonip Gp. (middle Ordovician, Ross 1967), near Joshua Hollow, Bare Mountain Quadrangle, Nevada.

Occurrence.
Restricted to the type locality and horizon.

Remarks.
Ross (1967) noted the close resemblance between this species and *Calliops strasburgensis* (herein synonymised with *C. (Calliops) brongniartii*). From Ross's illustrations it can be seen that this is the case, the Nevada specimens showing especially close similarity with specimens of *C. (C.) brongniartii* from the Kiln Mudstone in the Girvan succession. However, a significant difference is that the anterior face of the frontal lobe slopes much more steeply in the Nevada specimens than it does in the Scottish specimens. Ross described the pygidium of the Nevada material as possessing eight axial rings, and this is less than is present in the pygidium of any British *C. (C.) brongniartii* specimens (Figure 6. 28). The pygidium is otherwise very similar to that of *C. (C.) brongniartii*. However these specimens are stratigraphically much older than the British *C. (C.) brongniartii* (and *C. strasburgensis*). Because of this and the differences described above, this species is maintained herein.

Calyptaulax (sensu lato) armatus Ulrich and Delo, 1940

1940 *Calliops armatus* Ulrich and Delo; Delo, p. 93, pl. 11, fig. 12.

Holotype.
By original designation of Ulrich and Delo in Delo (1940), a testate cephalon (USNM 89988) from the Bromide Fm. (Blackriveran), Hickory Creek, Criner Hills, Oklahoma.

Occurrence.
Only known from the type locality and horizon.

Remarks.
Delo (1940) noted that this species is unique in its possession of unusually wide lateral cephalic borders and short, stout genal spines. Delo stated that the thorax and pygidium of this species are both unknown. In the absence of a pygidium, this species cannot be assigned to a subgenus.

Calyptaulax (Calliops) brevipostica Cooper, 1953

1953 *Calliops brevipostica* Cooper, p. 38, pl. 18, fig. 7.

Holotype.
By original designation of Cooper (1953), a silicified pygidium (USNM 116536) from the Edinburg Fm. (upper Blackriveran) at Willow Grove, Virginia.

Occurrence.
As well as the type locality and horizon, also known from the Effna Limestone (late Chazyan - early Blackriveran, Ross *et al.* 1982), Virginia (Cooper 1953).

Remarks.
This species is only known from its unusual pygidium, which resembles a meraspide pygidium of *Calyptaulax*, but of unusually large size (the holotype is of 6mm axial length, Cooper 1953). The pygidium has very rounded lateral and posterior margins as seen in dorsal view and is strongly tuberculate. It may just be an unusually large meraspide pygidium (possibly of *C. (Calliops) brongniartii* which also occurs in the Edinburg Fm., see above). However, Cooper (1953) gave two localities from which this species has been collected, indicating that at least two specimens are known. In the absence of cephala, the status of this species is unclear.

6. 6. Conclusions.

The known stratigraphical durations and suggested phylogeny of the 16 species of *Calyptaulax* recognised herein (including those not included in the morphometrics) are shown in Figure 6. 35. McNamara (1980) considered it likely that the genus originated in the early Llanvirn of Estonia, from *Pterygometopus*. The latest occurrence is in the topmost Rawtheyan of the Oslo Region (Husbergøya Fm., Owen 1981). The total range of the genus is therefore about 25myr on the basis of Tucker's U-Pb dating of the Ordovician. A few species are known only from single horizons. The longest ranging species is *C. (Calyptaulax) glabella* which has a duration of approximately 8myr, from the Solvang Fm. (upper Caradoc) to the Husbergøya Fm. (topmost Rawtheyan), Oslo Region.

Two stratigraphical samples were found to comprise two separate species: CONFINIS (Confinis Fm., Girvan district, upper Abereiddian) yielded *Calyptaulax (Calyptaulax) foederatus* Tripp, 1962 (designated CONFINIS A; see p. 153 for diagnosis of species) and *C. (Calliops) marginatus* (Tripp, 1962) (designated CONFINIS B; see p. 165 for diagnosis of species); BALCLATCHIE (Upper Balclatchie Mudstones, Girvan district, middle Caradoc) yielded *Calyptaulax (Calliops) brongniartii* (Portlock, 1843) (designated BALCLATCHIE A, see p. 169 for diagnosis of species) and *C. (Calyptaulax) hunteri* (Reed, 1914) (designated BALCLATCHIE B, see p. 155 for diagnosis of species). It is thus interesting to note that where two species co-occur, there is one from either subgenus (as diagnosed herein). It could be argued that these represent two cases of sexual dimorphism, but this is discounted since *C. (Calyptaulax) foederatus*, *C. (Calyptaulax) hunteri* and *C. (Calliops) brongniartii* all occur independently elsewhere.

The horizontal scale on Figure 6. 35 is a notional scale of morphology. The entirely Laurentian subgenus *C. (Calliops)* (left side of diagram) exhibits approximate net morphological stasis throughout its history (indicated by the narrow horizontal distribution of species; deliberately no species have been placed directly vertically above one another as this would give a spurious impression that the species were identical). The Laurentian, Baltic and Avalonian subgenus *C. (Calyptaulax)* (right side of diagram) exhibits net morphological change throughout its history, indicated by the positioning of successive species further towards the right. This net change affects body size, relative length (exsag.) of the eye, number of lens files, degree of effacement of the cephalic furrows (see Section 6. 3).

The relationship between the phylogenetics of *Calyptaulax* and the geographical distribution of the species is shown in Figure 6. 36.

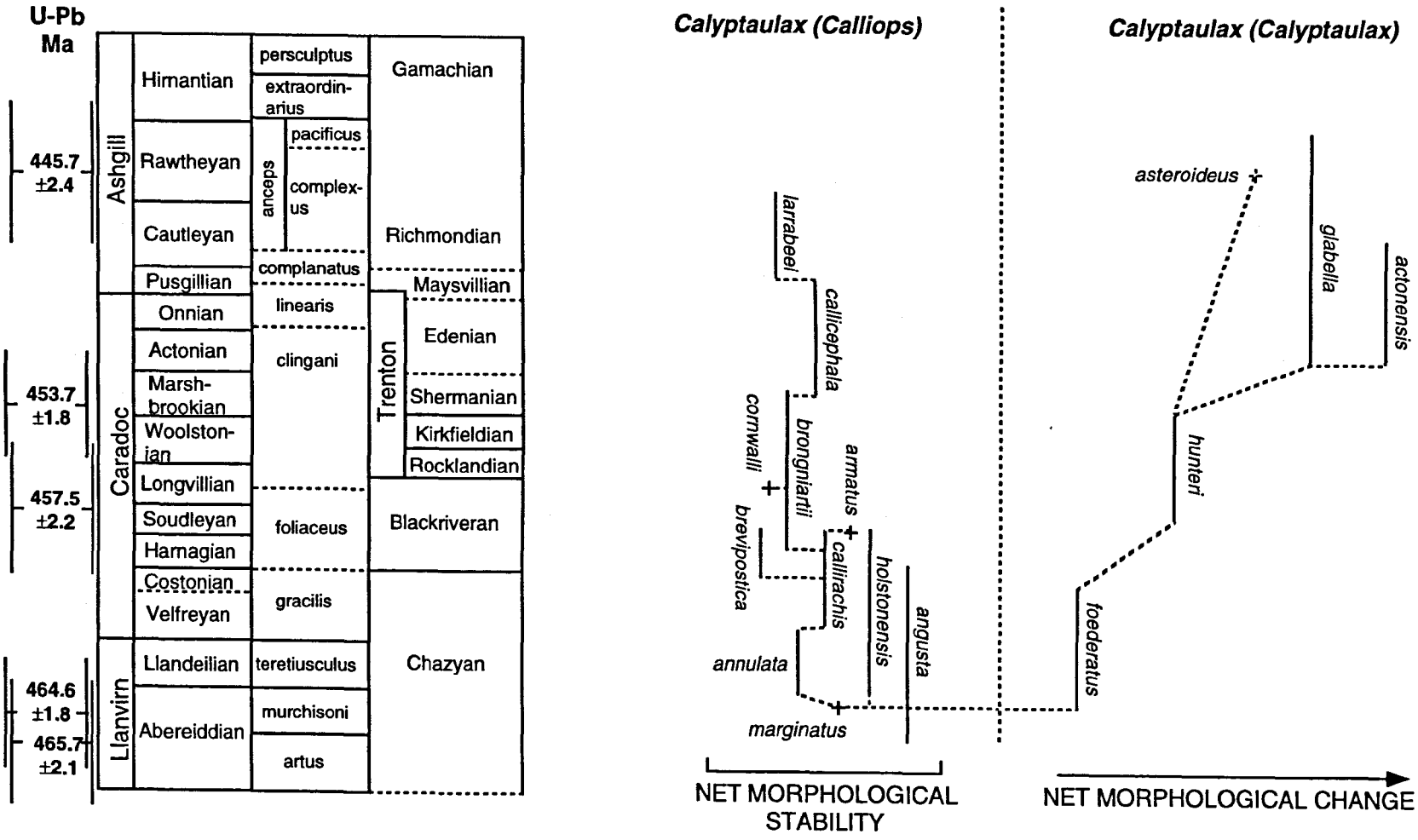

Figure 6. 35. Stratigraphical relationships, durations and suggested phylogeny of the species of *Calyptaulax* recognised herein. Crosses indicate species known from only a single horizon. Stratigraphy and U-Pb dates as in Figure 6. 1. "Net morphological change" in *C. (Calyptaulax)* is a broad trend towards larger body size, relatively larger eyes with greater number of lens files, more effaced cephalic furrows.

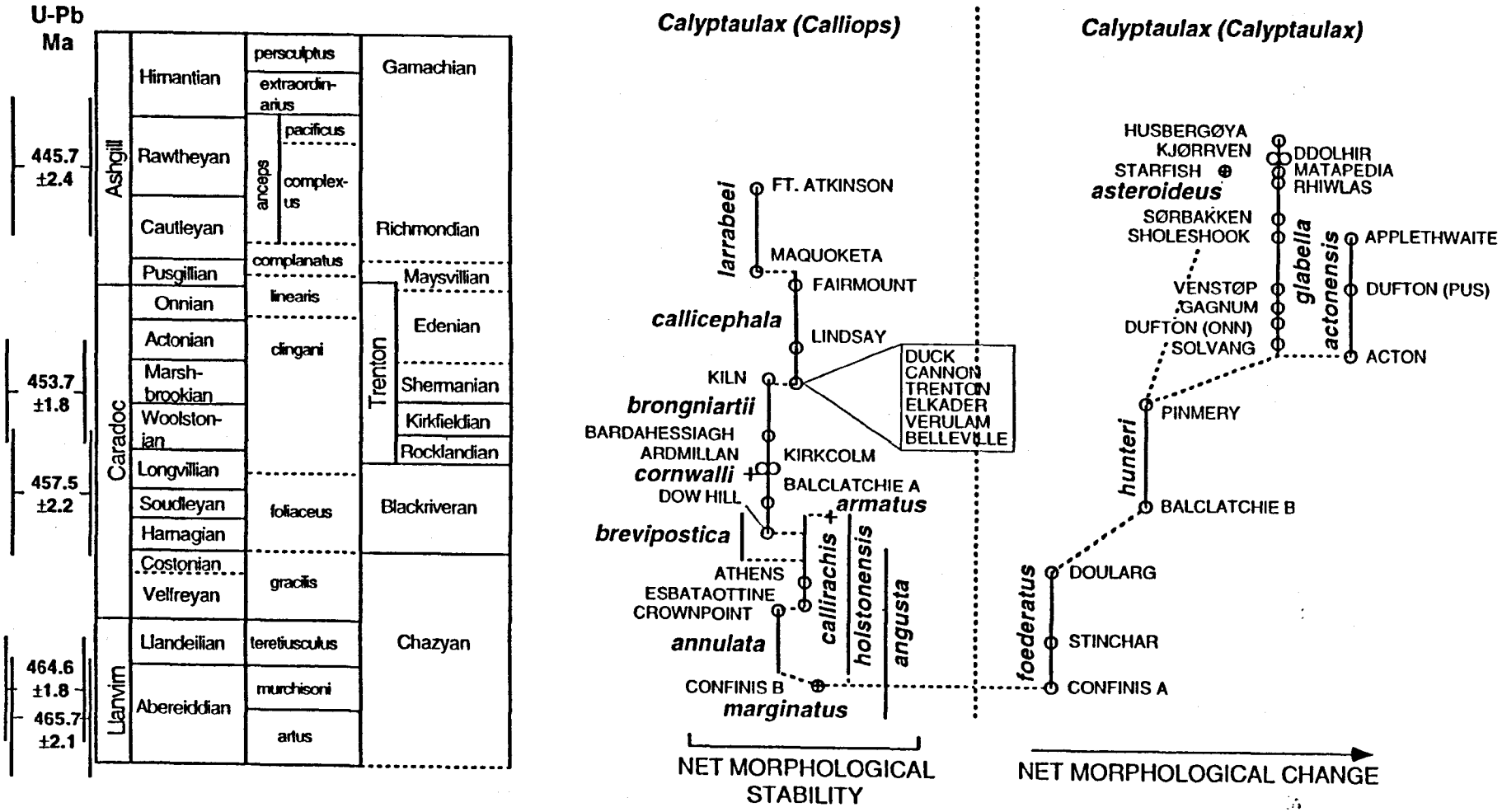

Figure 6. 36. Stratigraphical relationships, durations and suggested phylogeny of the species of *Calyptaulax* recognised herein together with stratigraphical samples used in phylogenetic and morphometric analyses. Crosses indicate species known from only a single horizon, circles indicate stratigraphical samples. Stratigraphy and U-Pb dates as in Figure 6. 1. "Net morphological change" in *C. (Calyptaulax)* is a broad trend towards larger body size, relatively larger eyes with greater number of lens files, more effaced cephalic furrows.

Phylogenetic analysis (Section 6. 3) demonstrated that *Calyptaulax* can be subdivided into two subgenera, defined as *Calyptaulax (Calyptaulax)* Cooper, 1930 (type species *Calyptaulax glabella* Cooper, 1930), and *Calyptaulax (Calliops)* Delo, 1935 (type species *Phacops callicephala* Hall, 1847). These two subgenera are defined on the basis of their pygidial morphology (and therefore have different definitions from the previous concepts of the genera *Calyptaulax* Cooper and *Calliops* Delo). *Calyptaulax (Calyptaulax)* is recognised on the possession of a pygidium which is "box-like" in cross-section, with rib-furrows which are well-defined distally, becoming much shallower or obsolete proximally. *Calyptaulax (Calliops)* is recognised on the possession of a pygidium which is more rounded in cross-section, with rib-furrows which are deep and well-defined across the entire pleural field almost as far as the axial furrow (Figure 6. 4).

The earliest definitive occurrence of *C. (Calyptaulax)* is in the Confinis Fm. (Llanvirn), Girvan district, and the latest occurrence is that within the Husbergøya Fm. mentioned above. The total range of the subgenus is therefore about 20myr. Throughout the lower half of this range the subgenus is subordinate in abundance and specific diversity to *C. (Calliops)*, but it becomes more prominent in the upper Caradoc and Ashgill in Avalonia and Baltica. *C. (Calliops)* has its earliest definitive occurrence in the Table Head Fm. (Llanvirn) of Newfoundland (Whittington 1965), and latest occurrence in the Maquoketa Gp. (Richmondian), Iowa (Slocum 1913). The total range of the subgenus is also about 20myr. This subgenus was entirely restricted to Laurentia and the Laurentian margins, and reached its acme in the middle Caradoc.

As well as the split into two subgenera, the phylogeny of *Calyptaulax* is characterised by complex mosaic evolution with many convergences between different species which gives rise to a poorly-resolved consensus tree (Figures 6. 5 - 6. 8). Species are recognisable on the basis of suites of character states rather than on unequivocal apomorphies. A similar condition was discovered for another long-duration, shape-conservative genus, *Achatella* in Chapter 5.

Morphometric analysis has demonstrated that *Calyptaulax* possesses a highly stable body plan throughout its 25myr history (consider the overlapping PC-fields occupied by the stratigraphical samples, Figures 6. 14, 6. 18) although individual measurements can show high variability within samples (eg: b!10, Figure 6. 24; relative length of the pygidial axis, noted in *C. (Calyptaulax) actonensis*). *C. (Calyptaulax)* shows greater within-subgenus variability than *C. (Calliops)* (manifested as greater area of PC-field occupation, Figure 6. 14).

A gradual divergence in morphospace occupation between the two subgenera is seen in the interval middle Caradoc - to - Ashgill (Figure 6. 24), and it has been demonstrated that this coincides with a slight but systematic shortening (sag, and exsag.) of the frontal glabellar lobe and a complementary lengthening of L3 in *C. (Calyptaulax)* during this interval (Figures 6. 21, 6. 22). This change is accompanied by an increase in the acuteness with which S3 diverges from the sagittal line (Figure 6. 23) and an anteriorwards advance in the location of the anteriormost extremity of the eye (Figure 6. 25) so that it remains opposite the distal end of S3. The eye also carries more dorso-ventral lens files in the stratigraphically later species of *C. (Calyptaulax)* (Figures 6. 3, 6. 27 (b)). This close link between the location of the front of the eye and the distal end of S3 has previously been noted in *Achatella* (Chapter 5), and it may be a general constraint on pterygometopid morphology.

Explanation of Plates for Chapter Six

Plate 6. 1

Calyptaulax (Calyptaulax) glabella Cooper, 1930

1. Dorsal view of cranidium, internal mould. Lectotype specimen YPM 12918. Matapédia Gp. (Rawtheyan Stage, Ashgill Series). Grande Coup, about 1 mile N of Percé, Gaspé Peninsula, Québec. x3.
2. Dorsal view of testate cranidium. Paralectotype specimen YPM 30466. Matapédia Gp. Near School on Priest's Road, 2.5 miles NW of Percé, Gaspé Peninsula, Québec. x4.
3. Dorsal view of cranidium, internal mould, partially testate. BM It7159. Matapédia Gp. South Cove, Gaspé Peninsula, Québec. x3.

4, 5 & 6. Dorsal, oblique anterolateral and lateral views of cephalon, internal mould. BM It20637. Solvang Fm., (*clingani* Zone, upper Caradoc Series) 2m below base of overlying Venstøp Fm. Kalvøya, Asker district, Oslo Region. x3.

7. Oblique lateral view of complete individual, internal mould. BM It15845. Ddolhir Fm. (Rawtheyan Stage, Ashgill Series). Forest track in Cynmyd Forest, Corwen district, Berwyn Hills, North Wales. x1.5.
8. Dorsal view of cranidium, internal mould. SM A77847. Middle to upper Sholeshook Limestone Fm. (Cautleyan or lowermost Rawtheyan Stage, Ashgill Series). Prendergast Place, Haverfordwest, Pembrokeshire, South Wales. x4.
9. Dorsal view of cephalon, internal mould. PMO 100374. Solvang Fm., 8m below base of overlying Venstøp Fm. East Raudskjaer, Asker district, Oslo Region. x4. Original of Owen and Bruton (1980: pl. 9, figs. 16-18).
10. Oblique anterolateral view of complete individual, internal mould. PMO 20408. Husbergøya Fm. (upper Rawtheyan Stage, Ashgill Series). N. Langøyene, Oslo district. x4. Original of Owen (1981: pl. 14, fig. 20).

11 & 14. Dorsal view of latex cast of pygidium, and dorsal view of internal mould of same. GLAHM A11863. Gagnum Mbr, Lunner Fm. (latest Caradoc - early Ashgill). Gamme Hill, Hadeland, Oslo Region. Both x6.

12. Dorsal view of cranidium, internal mould. BM In54961. Rhiwlas Limestone (Rawtheyan Stage, Ashgill Series). Rhiwlas, Bala, N. Wales. x4. Original of Whittington (1962: pl. 12, fig. 18).
13. Dorsal view of pygidium, internal mould. PMO 100630. Skjaerholmen Fm. (Cautleyan Stage, Ashgill Series). Borøya, Asker district, Oslo Region. x3.5. Original of Owen (1981: pl. 15, fig. 5).
15. Dorsal view of cranidium, internal mould. BM In54960. Locality and horizon as for fig. 12. x3. Original of Whittington (1962: pl. 12, fig. 17).

***Calyptaulax (Calyptaulax) foederatus* Tripp, 1962**

16. Dorsal view of damaged cranidium, internal mould. GLAHM A9173. Separation Sandstone Bed, Doularg Fm. (*gracilis* Zone, lower Caradoc Series). Plantation Burn, Girvan district. x8.
17. Dorsal view of cranidium, internal mould. GLAHM A6946. Upper Stinchar Limestone Fm. (Llandeilian Stage, upper Llanvirn Series). Auchlewan Quarry, Girvan district. x10. Original of Tripp (1967: pl. 6, fig. 4).
18. Dorsal view of damaged pygidium, internal mould. GLAHM A5354. Confinis Fm. (late Llanvirn Series). Kirkdominae, Girvan district. x8. Original of Tripp (1962: pl. 4, fig. 24).
19. Dorsal view of pygidium, internal mould. Paratype specimen GLAHM A5355. Locality and horizon as for fig. 18. x10. Original of Tripp (1962: pl. 4, fig. 25).

Plate 6. 2

***Calyptaulax (Calyptaulax) foederatus* Tripp, 1962**

1. Dorsal view of cranidium, internal mould. Holotype specimen GLAHM A5352. Confinis Fm. (late Llanvirn Series). Kirkdominae, Girvan district. x12. Original of Tripp (1962: pl. 4, fig. 20).
2. Dorsal view of cranidium, internal mould. GLAHM A5333. Locality and horizon as for fig. 1. x7. Original of Tripp (1962: pl. 4, fig. 21).
3. Dorsal view of immature cranidium. BM In58134. Locality and horizon as for fig. 1. x14.
4. Dorsal view of pygidium, internal mould. GLAHM A6951. Upper Stinchar Limestone Fm. (Llandeilian Stage, upper Llanvirn Series). Auchlewan Quarry, Girvan district. x8. Original of Tripp (1967: pl. 6, fig. 9).
5. Dorsal view of pygidium, internal mould. GLAHM A6950. Locality and horizon as for fig. 4. x12. Original of Tripp (1967: pl. 6, fig. 8).

***Calyptaulax (Calyptaulax) hunteri* (Reed, 1914)**

6. Dorsal view of cranidium, internal mould. BM In40471. Upper Balclatchie Mudstones (upper *peltifer* Subzone, lower-middle Caradoc Series). Penwhapple Bridge (also known as Balclatchie), Girvan district. x5.
7. Dorsal view of glabella, internal mould. GLAHM A19675. Middle Ardwell Farm Fm. (*wilsoni* Subzone, middle Caradoc Series). Pinmery, Girvan district. x8.
8. Dorsal view of pygidium, internal mould. BM In23614. Locality and horizon as for fig. 6. x8.

9. Dorsal view of cranidium and seven thoracic segments, internal mould. Lectotype specimen BM In23612. Locality and horizon as for fig. 6. x6. Original of Reed (1914: pl. 8, fig. 8) and Morris and Tripp (1986: pl. 4, fig. 3).
10. Dorsal view of damaged pygidium, internal mould. GLAHM A19675. Locality and horizon as for fig. 7. x16.

***Calyptaulax (Calyptaulax) actonensis* Dean, 1961**

11. Dorsal view of slightly damaged cranidium, internal mould. SM A98742. Upper Applethwaite Mbr., Kirkley Bank Fm. (Cautleyan Stage, Ashgill Series). Garburn Nook, Troutbeck, English Lake District. x4.
12. Dorsal view of pygidium, internal mould. BM In56278. Upper Dufton Shale Fm. (Pusgillian Stage, Ashgill Series). Locality B25 of Dean (1962), Swindale Beck, Cross Fell, N. England. x3.
13. Dorsal view of pygidium, internal mould. Holotype specimen BM In49771. Middle Acton Scott Fm. (Actonian Stage, upper Caradoc Series). Quarry Field, Gretton, Shropshire. x3. Original of Dean (1961: pl. 50, figs. 11, 14).
14. Dorsal view of damaged cranidium, internal mould. BM In49903. Dufton Shale Fm. (Onnian Stage, Ashgill Series). Locality A5 of Dean (1962), Pus Gill, Cross Fell, N. England. x3. Original of Dean (1962: pl. 13, fig. 3).
15. Dorsal view of pygidium, internal mould. BM In56276. Locality and horizon as for fig. 12. x2.
16. Dorsal view of cranidium, internal mould. Paratype specimen BM In49318. Locality and horizon as for fig. 13. Original of Dean (1961: pl. 51, fig. 1).
17. Dorsal view of incomplete pygidium, internal mould. BM In49907. Locality and horizon as for fig. 12. x3. Original of Dean (1962: pl. 13, fig. 5).

Plate 6. 3

***Calyptaulax (Calyptaulax) asteroideus* (Reed, 1914)**

1, 3 & 5. Dorsal, lateral and oblique anterolateral views of complete individual, internal mould. GLAHM A3613. Lady Burn Starfish Beds, lower South Threave Fm., Upper Drummuck Gp. (upper *anceps* Zone, Rawtheyan Stage, Ashgill Series). Lady Burn, Girvan district. Fig. 1 x2, figs. 3 and 5 x1.5.
2. Dorsal view of damaged cephalon with three thoracic segments, internal mould. GLAHM A1059. Locality and horizon as for fig. 1. x2.
4. Dorsal view of pygidium, internal mould. GLAHM A5691/3. Locality and horizon as for fig. 1. x3.
6. Oblique dorsal view of complete individual, internal mould. GLAHM A3614. Locality and horizon as for fig. 1. x4.

***Calyptaulax (Calliops) callicephala* (Hall, 1847)**

7. Dorsal view of incomplete cephalon, internal mould. ROM 49476. Verulam Fm. (Shermanian). McCarthy Bros. Quarry, 1.5 miles NW of Gamebridge, Ontario. x4.
8. Dorsal view of complete individual, internal mould. ROM 35167. Locality and horizon as for fig. 7. x3.
9, 12 & 15. Lateral, dorsal and oblique posterolateral view of cephalon, internal mould. ROM 49477. Locality and horizon as for fig. 7. All x3.
10. Dorsal view of cranidium, internal mould. ROM 36191. Lindsay Fm. (Edenian). 2.2 miles E. of Little Current, Great Cloche Island, Manitoulin, Ontario. x4.
11. Ventral view of median and right half of cephalic doublure, internal mould. ROM 35166. Locality and horizon as for fig. 7. x4.

***Calyptaulax (Calliops) marginatus* (Tripp, 1962)**

13. Dorsal view of pygidium, internal mould. BM In58148. Confinis Fm. (late Llanvirn Series). Bougang Quarry, Girvan district. x8.
14. Dorsal view of pygidium, internal mould. BM In58146. Locality and horizon as for fig. 13. x8.
16. Dorsal view of incomplete cephalon, internal mould. BM In58142. Locality and horizon as for fig. 13. x5.
17. Dorsal view of incomplete cranidium. Holotype specimen GLAHM A5237. Locality and horizon as for fig. 13. x5. Original of Tripp (1962: pl. 4, fig. 10).
18. Dorsal view of testate pygidium with abnormally developed furrows on the left pleural field. GLAHM A5238. Locality and horizon as for fig. 13. x4. Original of Tripp (1962: pl. 4, fig. 16).

Plate 6. 4

***Calyptaulax (Calliops) brongniartii* (Portlock, 1843)**

1, 2 & 3. Dorsal, anterior and lateral views of cephalon with two disarticulated thoracic segments, internal mould. BM In40780. Lower Ardwell Farm Fm. (middle Caradoc Series). Ardmillan, Girvan district. All x3.
4 & 5. Oblique anterolateral and lateral views of latex cast of cephalon. GLAHM 101155c. Locality and horizon as for fig. 1. x4.
6. Ventral view of latex cast of cephalic doublure. GLAHM 101154b. Locality and horizon as for fig. 1. x4.

7 & 11. Dorsal and oblique anterolateral views of cephalon, internal mould. TCD 7634. Lower Bardahessiagh Fm. (middle Caradoc Series). South slope of Craigbardahessiagh, Pomeroy district, Co. Tyrone. Both x2.5.

8. Dorsal view of complete individual, internal mould. TCD 7757. Locality and horizon as for fig. 7. x2.

9. Dorsal view of incomplete cephalon, internal mould. GLAHM 101165. Locality and horizon as for fig. 1. x5.

10. Dorsal view of incomplete cephalon, internal mould. BM In47564. "Infra-Kilranny Greywackes" (lower Caradoc Series). Dow Hill, Girvan district. x4.

12. Dorsal view of cephalon, internal mould. BGS collection. Kirkcolm Fm. (lower to middle Caradoc Series). Duntercleuch Burn, Southern Uplands. x3.

13. Dorsal view of cephalon, internal mould. GLAHM A3950. Kiln Mudstone, Craighead Fm. (upper middle Caradoc Series). Craighead Quarry, Girvan district. x5. Original of Tripp (1954: pl. 4, figs. 34 a-c).

14. Dorsal view of latex cast of pygidium. GLAHM A3954. Locality and horizon as for fig. 13. x4.

15. Dorsal view of incomplete cephalon, internal mould. BM In40276. Upper Balclatchie Mudstones (upper *peltifer* Subzone, lower-middle Caradoc Series). Penwhapple Bridge, Girvan district. x4.

16 & 17. Lateral and dorsal views of damaged cephalon, internal mould. GLAHM 101155a. Locality and horizon as for fig. 1. Note that this is the internal mould corresponding to the external from which the latex cast shown in figs. 4 and 5 was made. x4.

18. Dorsal view of pygidium, internal mould. Lapworth Museum unregistered specimen. Locality and horizon as for fig. 10. x4.

19. Dorsal view of slightly distorted cephalon, internal mould. BGS collection. Kirkcolm Fm. (lower to middle Caradoc Series). Kilbucho, Southern Uplands. x3.

PLATE 6.1

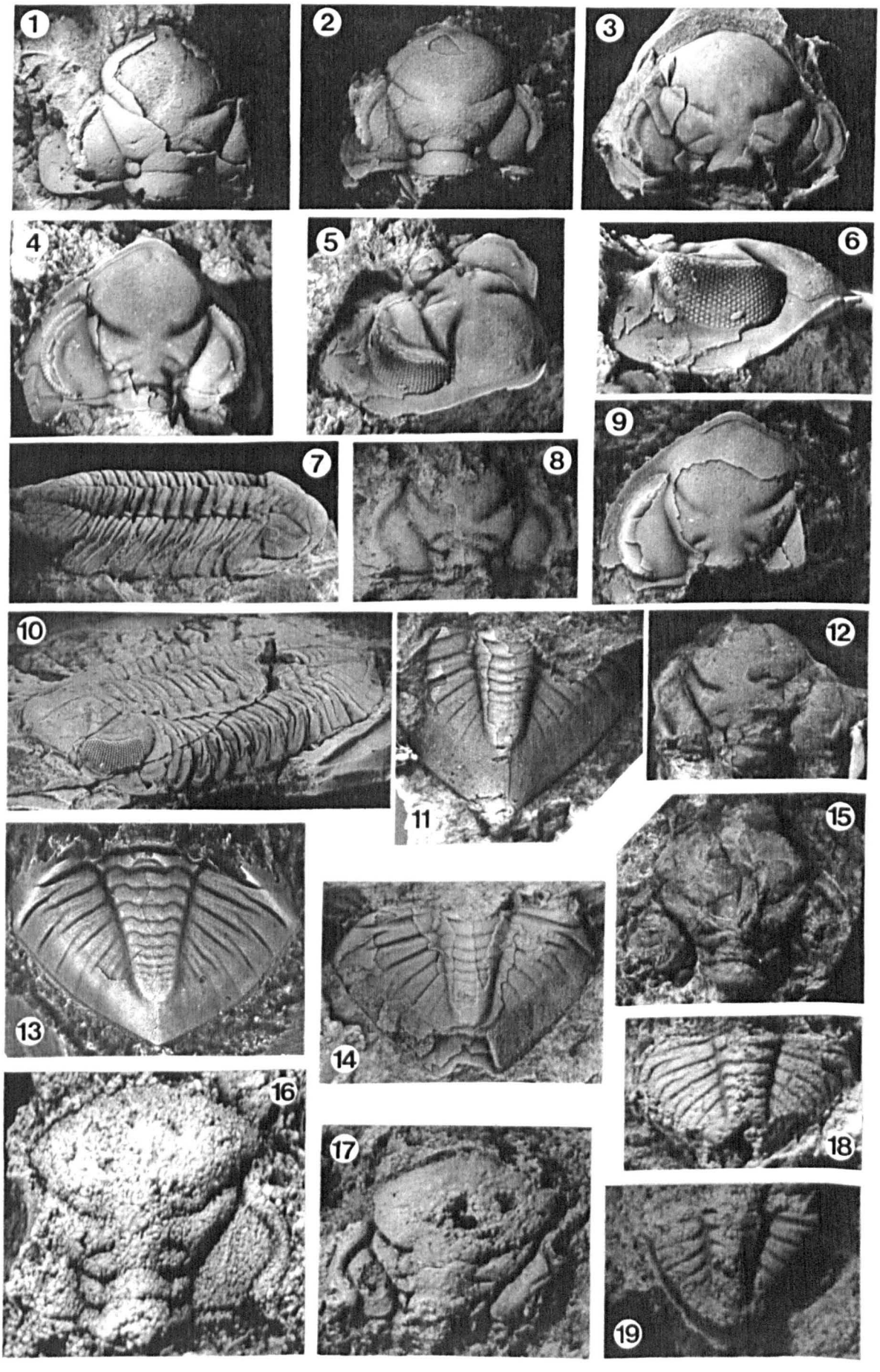

PLATE 6.2

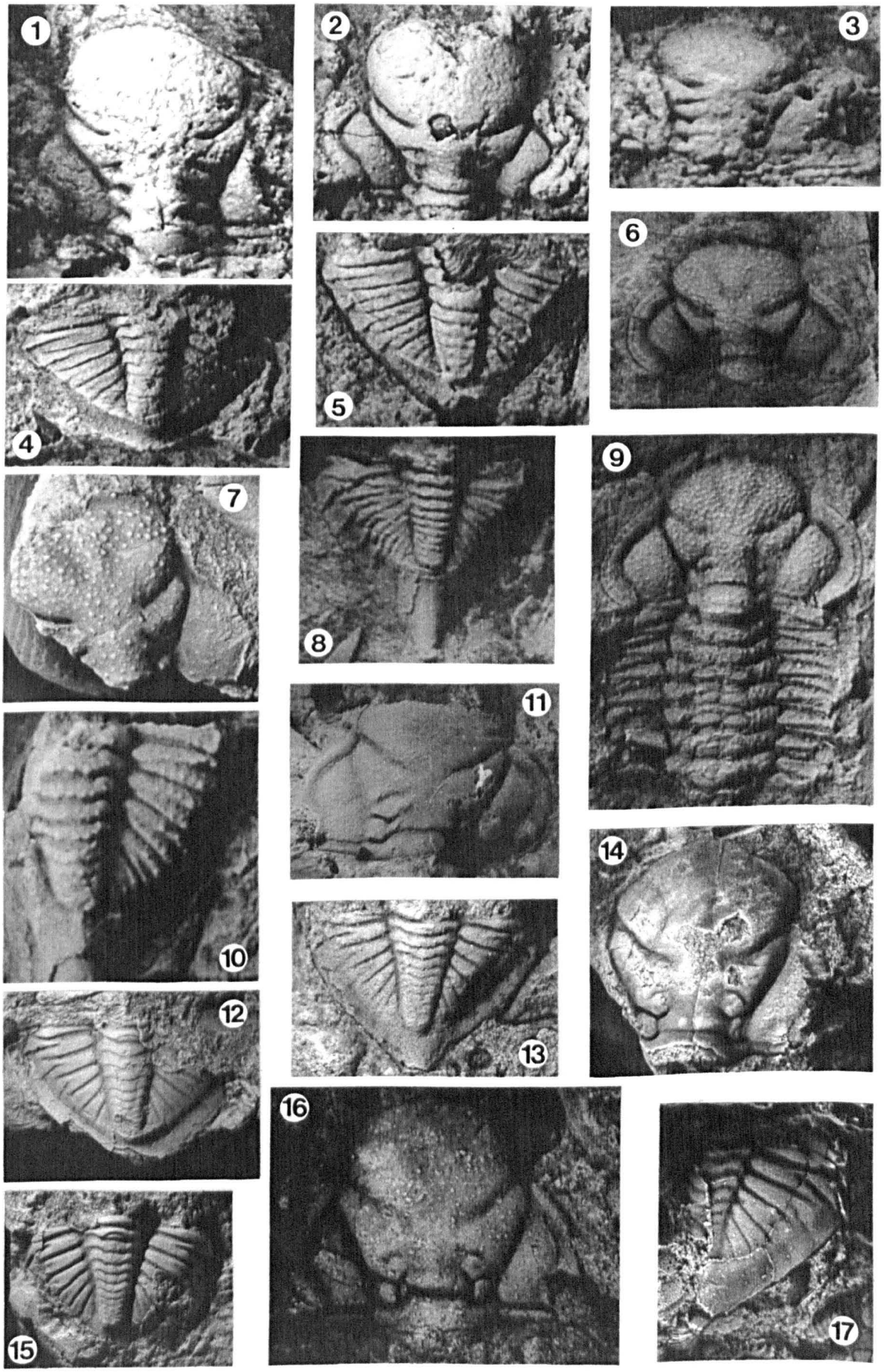

PLATE 6.3

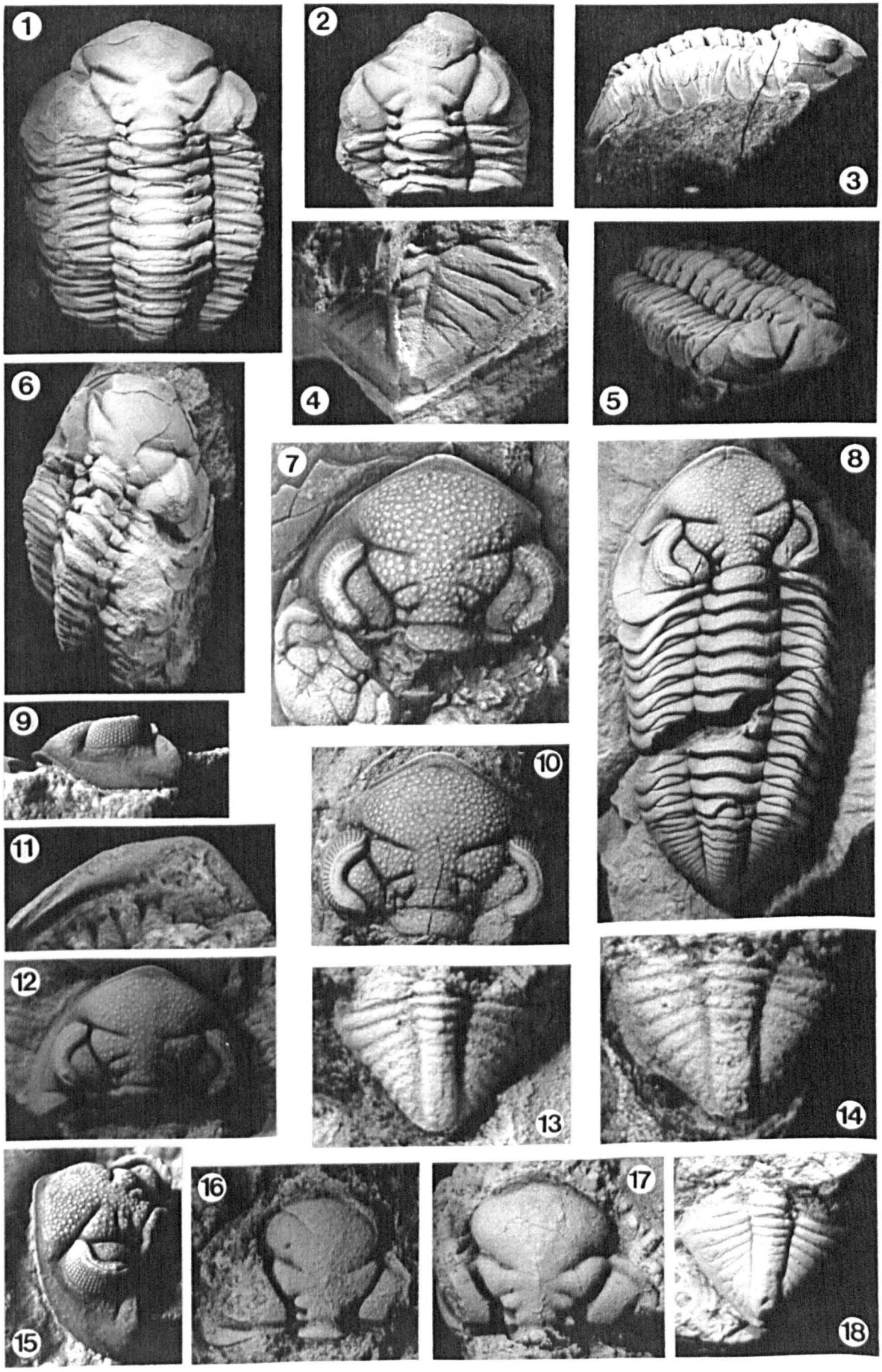

PLATE 6.4

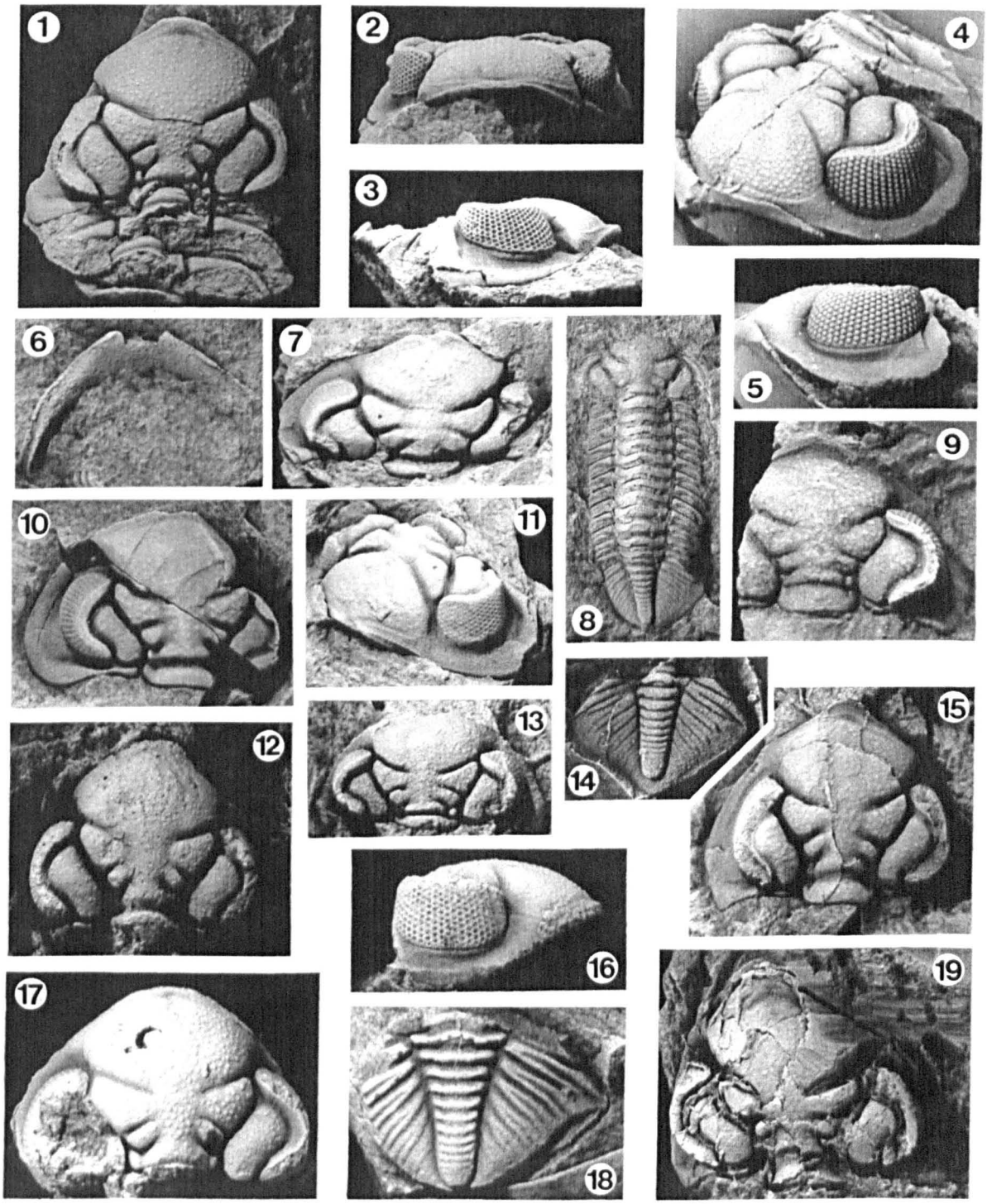

CHAPTER SEVEN

A PHYLOGENETIC AND MORPHOMETRIC ANALYSIS OF *ACERNASPIS* CAMPBELL, 1967.

7. 1. Introduction.

Acernaspis Campbell, 1967 (Suborder Phacopina, Family Phacopidae, Subfamily Phacopinae) is known from rocks of lower Llandovery to Wenlock (Sheinwoodian) age, and its occurrences are widespread throughout the world, the genus being represented within the British Isles, Scandinavia, northern Europe and North America. The total duration of the genus is some 13 myr (Harland *et al.* 1989: figure 1.7). *Acernaspis* first appeared in the early Llandovery (Rhuddanian) of northern Estonia and the Oslo Region. It rapidly became widespread, and was distributed worldwide by the middle Llandovery (Ramsköld and Werdelin 1991). *Acernaspis* continued to be widespread throughout the late Llandovery. The last appearance of the genus is in the Wenlock Series (Sheinwoodian Stage) Högklint Fm., Gotland, and this is the only known Wenlock *Acernaspis* species.

Campbell (1967, 1977) considered the Phacopina to be divisible into a main "trunk" stock within which he identified a number of paraphyletic taxa which he considered to grade into each other in a continuum of form, and a number of genera which branched off from this main stock but which became extinct without leaving descendant genera. Campbell (1967, 1977) considered *Acernaspis* to be the earliest member of this main "trunk" stock (Figure 7. 1).

Ananaspis Campbell, 1967 is a Wenlock-Ludlow genus. The genus was widely distributed within a palaeolatitude of 30 - 40° (Ramsköld and Werdelin 1991). The earliest occurrences are in the upper Mottled Mudstone of the lower Nantglyn Flags Gp., Clwyd, North Wales, the Much Wenlock Limestone Fm. of the Welsh Borderlands, and the Mulde Fm. of Gotland (all Homerian Stage, Wenlock Series, Cocks *et al.* 1992). The Gotland species is *A. amelangorum* Ramsköld, 1985, which Ramsköld (1985) assigned to *Ananaspis*, although Ramsköld and Werdelin (1991) later considered it *incertae sedis.* The Much Wenlock species is *Ananaspis stokesii* (Milne Edwards, 1840) which Ramsköld and Werdelin (1991) also considered *incertae sedis.* The Welsh material was described as *Ananaspis* aff. *fecunda* (Barrande, 1846) by Rushton *in* Warren *et al.* (1984). The latest occurrence of *Ananaspis* is in the upper Kopanina Fm., Bohemia (Ludlow, Cocks *et al.* 1992) and the Pagegiai Fm., Latvia (Kuressaare Stage, upper Ludlow, Cocks *et al.* 1992).

Campbell (1967, 1977) recognised that *Ananaspis* was probably derived from *Acernaspis* (Figure 7. 1). Ramsköld (1988) argued that *Ananaspis* was derived through the heterochronic process of neoteny from *Acernaspis*, in a process which was already occurring in later species of *Acernaspis* and which therefore tends to blur the distinction between the two genera.

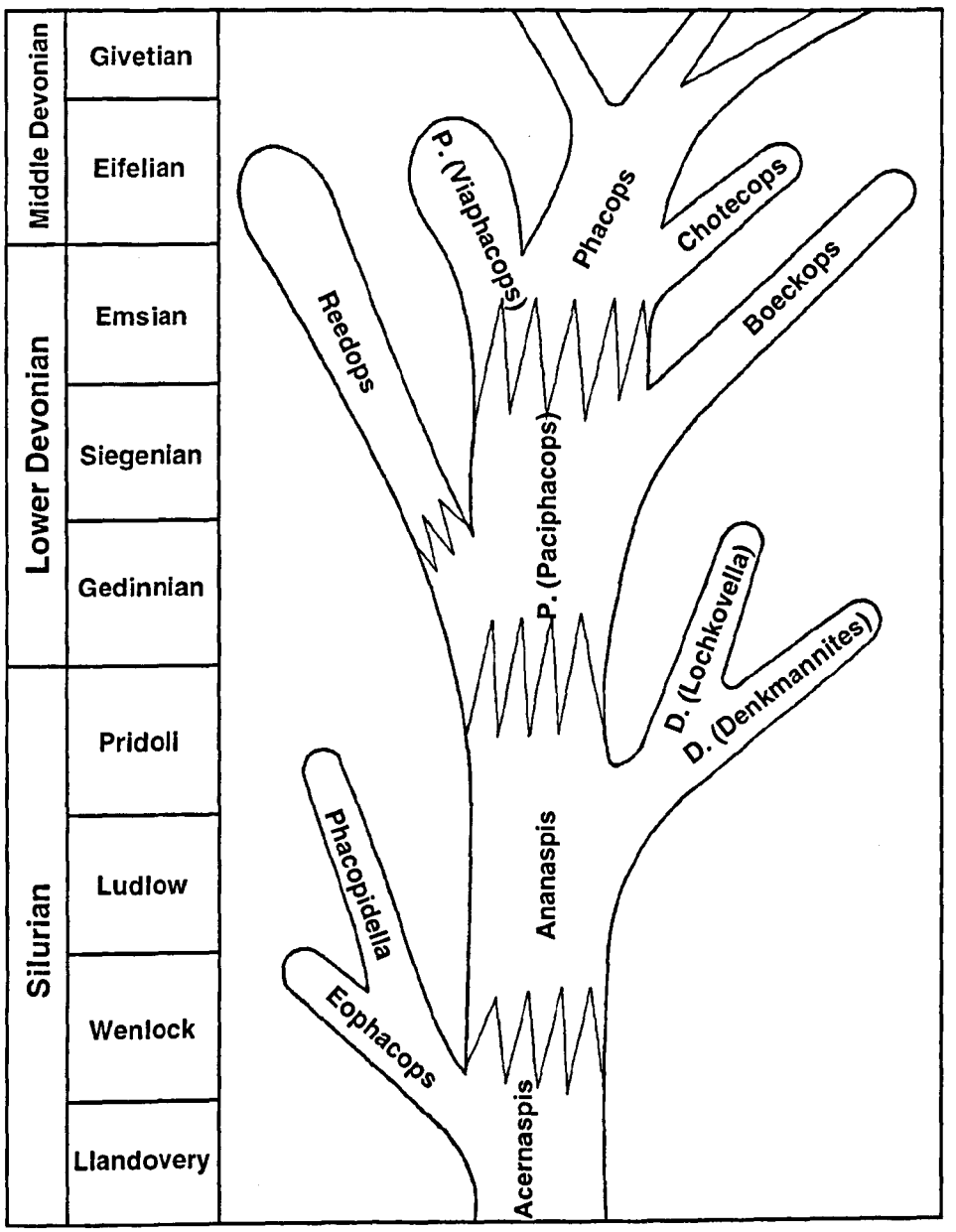

Figure 7. 1. Phylogeny within the Phacopinae as proposed by Campbell (1977). Redrawn with slight modification from Campbell (1977).

The extremely close similarity between all described species of *Acernaspis* makes this genus an ideal candidate for study as an example of stasis. The transition to *Ananaspis* also makes it possible to study the postulated heterochronic derivation of one genus from another. In this chapter, Section 7. 2 describes the results of a phylogenetic analysis carried out on the phacopid trilobites by Ramsköld and Werdelin (1991), and discusses their results with reference to *Acernaspis* and *Ananaspis*. Section 7. 3 describes 20 stratigraphically and geographically separate samples from which specimens of *Acernaspis* were studied, as well as five samples from which specimens of *Ananaspis* were studied. In Section 7. 4 a detailed morphometric analysis of *Acernaspis* is presented, based on the 20 stratigraphical samples. Specimens of *Ananaspis* from its five samples are also included in an attempt to assess the claim for neotenic derivation of *Ananaspis* from *Acernaspis*. Section 7. 5 presents a systematic revision of *Acernaspis*. The systematic palaeontology of the species of *Ananaspis* which were included in the morphometric analysis is also considered. Section 7. 6 summarises the conclusions drawn in the preceding sections.

7. 2. Phylogenetic Analysis.

Ramsköld and Werdelin (1991) undertook a cladistic analysis of all known Silurian Phacopinae, including *Acernaspis* and *Ananaspis*, as well as selected Devonian species (those assigned to *Paciphacops*, some *Viaphacops* and *Phacops*). In most cases the species were coded for the analysis from published illustrations. Their matrix consisted of 48 terminal taxa (including the hypothetical ancestor) and 32 characters (24 from the cephalon, 1 from the thorax, 7 from the pygidium; see Ramsköld and Werdelin 1991 for list of characters used). Ramsköld and Werdelin defined all characters except five as ordered, the remaining five characters being defined as unordered (see Swofford 1990 for definitions of character types). They ran a heuristic search on the matrix, using tree bisection-reconnection branch swapping on the PAUP computer program running on an Apple Macintosh II computer.

Ramsköld and Werdelin found 108 equally parsimonious trees of length 301 steps and consistency index 0.291. However this set consisted of two mutually exclusive groups of trees (*i.e.* no single heuristic search could find more than one of these two groups). The consensus tree for both groups consists of an *Acernaspis* clade and another clade containing the remaining taxa except *Podowrinella* Clarkson, Eldredge and Henry, 1977 which was the outgroup (Figure 7. 2). The topology of the *Acernaspis* clade changes between the two groups, and Ramsköld and Werdelin interpreted this as indicating that there are two quite different possible resolutions within this clade. The topology of the remaining part of the tree is the same in both groups.

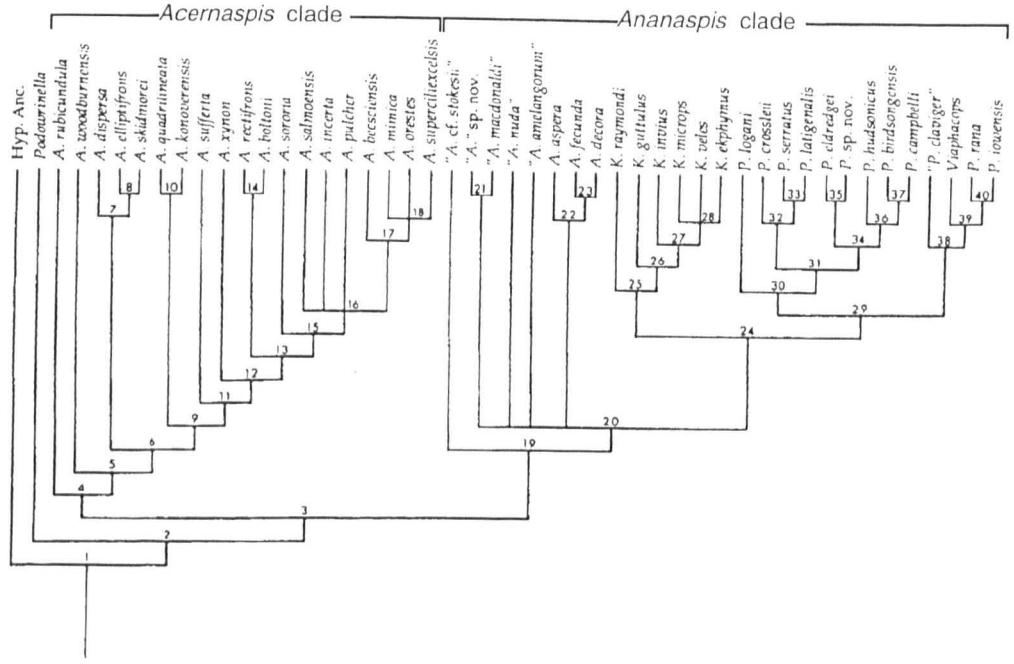

(a)

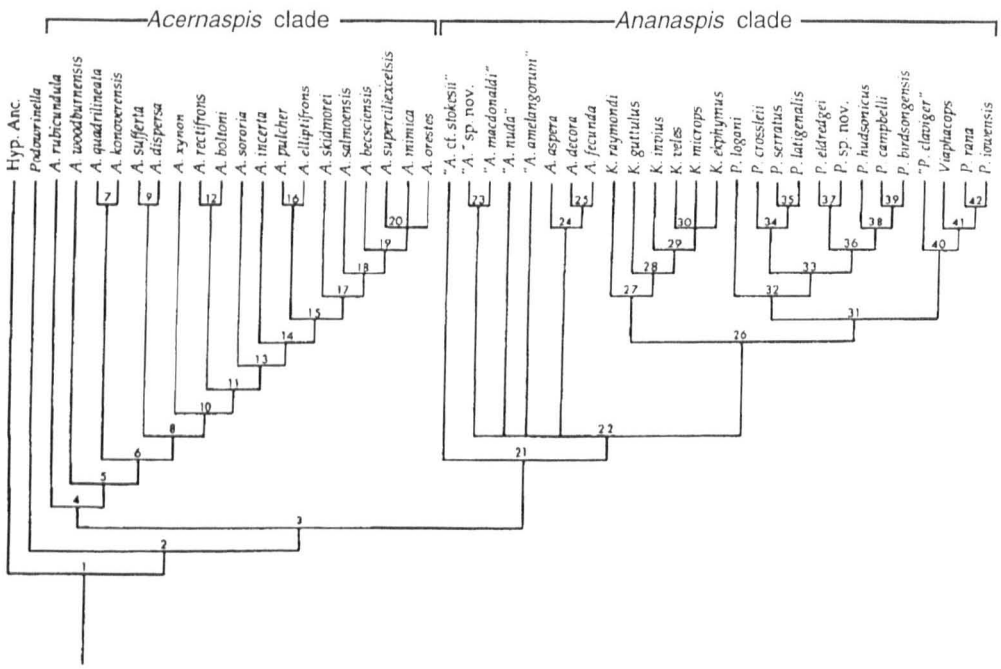

(b)

Figure 7. 2. Ramsköld and Werdelin's (1991) consensus trees for their cladistic analysis of phacopid trilobites. A heuristic search discovered two mutually exclusive groups of trees: (a) based on 36 trees of length 301 steps and consistency index 0.291; (b) based on 72 trees of length 301 steps and consistency index 0.291. The topology of the "*Acernaspis* clade" is different for each group, while the "*Ananaspis* clade" remains stable.

Ramsköld and Werdelin separated the *Acernaspis* clade from the rest of the taxa (which they called collectively the "*Ananaspis* clade") and analysed the two clades separately. Analysis of the *Ananaspis* clade gave 32 most parsimonious trees of length 208 steps, CI=0.386, and a consensus tree whose topology was essentially the same as that of the "*Ananaspis* half" of the original cladogram (that shown in Figure 7. 2). Analysis of the *Acernaspis* clade resulted in 248 most parsimonious trees of length 98 steps, CI=0.495. However, this set of 248 trees was itself discovered to consist of a number of mutually exclusive subgroups, which taken together gave an unresolved consensus tree (Figure 7. 3 (a)). Ramsköld and Werdelin therefore removed *Acernaspis rubicundula* Ramsköld, 1985 (Högklint Fm., Wenlock, Gotland) from the analysis, justifying this decision on the basis of its "very odd morphology" (Ramsköld and Werdelin 1991: 50), its position on the original cladogram as sister taxon to all other species of *Acernaspis* (Figure 7. 2), and its variable position in the 248 *Acernaspis* clade trees. Analysis of the new matrix gave three most parsimonious trees of length 88 steps and CI=0.512, the consensus tree for which is shown in Figure 7. 3 (b). This tree is almost fully resolved, and its topology matches that of the *Acernaspis* clade in the consensus tree for one of the versions of the original cladogram (Figure 7. 2 (b)).

Ramsköld and Werdelin (1991) drew some phylogenetic conclusions from their analysis. Those that pertain to *Acernaspis* and *Ananaspis* can be briefly summarised:

1. Ramsköld and Werdelin considered *Acernaspis* to be monophyletic. They did not recognise the subgenera *A. (Eskaspis)* Clarkson *et al.*, 1977, or *A. (Murphycops)* Lespérance and Letendre, 1981. These subgenera had both previously been diagnosed on the basis of their vincular morphology, *A. (Eskaspis)* having a pair of shallow subfrontal depressions and deep lateral vincular furrows on the ventral surface of the doublure (Clarkson *et al.* 1977), *A. (Murphycops)* having the anterior part of the vincular furrow entirely absent from the medial third of the doublure (Lespérance and Letendre 1981). Both these subgenera were thus differentiated from the nominate subgenus in which the anteromedial part of the vincular furrow is deep and continuous (Clarkson *et al.* 1977) (see Section 7. 5 for a fuller discussion). Ramsköld and Werdelin (1991) found that the species originally assigned to these subgenera (*i.e. A. (A.) elliptifrons* (Esmark, 1833), *A. (A.) orestes* (Billings, 1860), *A. (A.) primaeva* (Clarke, 1908), *A. (A.) boltoni* Lespérance and Letendre, 1982, *A. (A.) salmoensis* Lespérance, 1988, *A. (E.) sufferta* (Lamont, 1947), *A. (E.) woodburnensis* (Clarkson *et al.* 1977), *A. (E.) becsciensis* Lespérance and Letendre, 1982, *A. (E.) gaspensis* Lespérance and Letendre, 1982, *A. (E.) mimica* Lespérance and Letendre, 1982, and *A. (M.) skidmorei* (Lespérance, 1968) were distributed more or less randomly throughout the cladogram (Figure 7. 2). The characters used to diagnose the subgenera (*i.e.* the vincular structure,

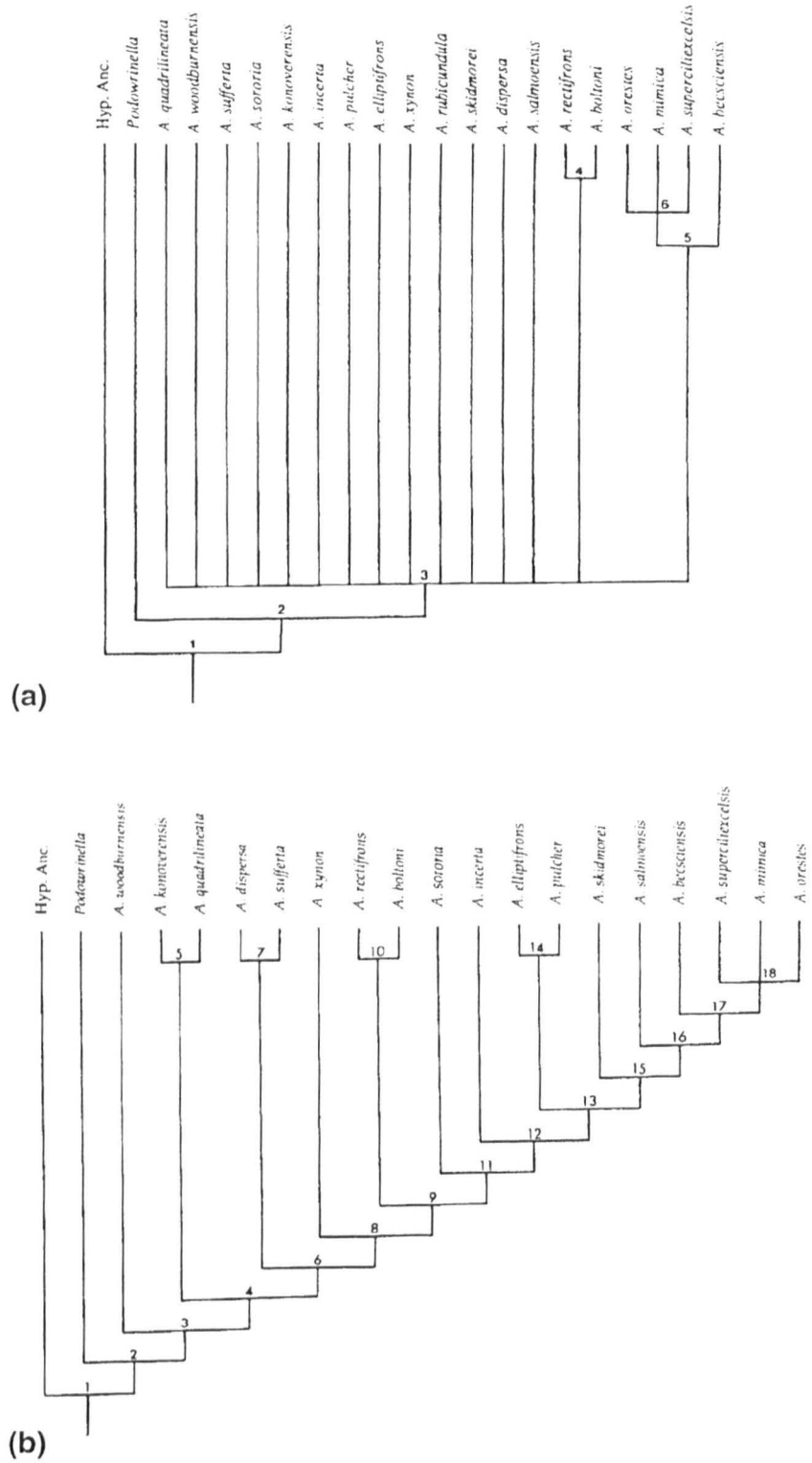

Figure 7. 3. Ramsköld and Werdelin's (1991) consensus trees for their analysis of the *Acernaspis* clade. (a) consensus tree for the *Acernaspis* clade based on 248 trees of length 98 steps and consistency index 0.495. (b) consensus tree for the *Acernaspis* clade excluding *A. rubicundula*, based on three trees of length 88 steps and consistency index 0.512.

represented in Ramsköld and Werdelin's character matrix by their characters 24 (nature of the medial part of the vincular furrow) and 25 (nature of the lateral vincular notches)) displayed no regular pattern within the cladogram. Therefore Ramsköld and Werdelin synonymised the subgenera. In view of Ramsköld and Werdelin's results, and further evidence cited below (see Section 7. 5), it is here agreed that the subgenera are synonymous.

2. Ramsköld and Werdelin considered *Ananaspis* as defined by previous authors to be paraphyletic or polyphyletic. They therefore reassigned *A. guttulus* Campbell, 1967, *A. ekphymus* Jones *et al.*, 1986, and *A.* sp. Holloway, 1980 to *Kainops* Ramsköld and Werdelin, 1991. They considered *A. amelangorum* Ramsköld, 1985 and *Phacops stokesii* Milne Edwards, 1840 (referred by many authors to *Ananaspis*, for example Campbell 1967, Chlupá č, 1977) *incertae sedis*. *Ananaspis* as redefined by Ramsköld and Werdelin includes five species: *A. aspera* (Hawle and Corda, 1847); *A. calvescens* Chlupá č, 1972; *A. decora* Männil, 1987; *A. fecunda* (Barrande, 1846); and *A. orientalis* (Maksimova, 1968). *A. calvescens* and *A. orientalis* were not coded for cladistics by Ramsköld and Werdelin and therefore do not appear on the cladograms in Figure 7. 2. Such a definition restricts the genus to the Ludlow Series. As stated in Section 7. 1, Ramsköld and Werdelin (1991) considered the species from the Wenlock Mulde Fm. of Gotland *incertae sedis* ; their phylogenetic analysis did not include the material from the Wenlock upper Mottled Mudstone illustrated by Rushton *in* Warren *et al.* (1984).

Morphometric work undertaken during the course of this study on specimens of *A. amelangorum* and *P. stokesii* (see Section 7. 4) had already been started when Ramsköld and Werdelin's (1991) results became available. Although Ramsköld and Werdelin considered these two species *incertae sedis*, it was decided that there was nothing to be lost by retaining representatives of them in the morphometric analysis to see how they compared with species of *Acernaspis* and *Ananaspis*, especially since a number of workers have referred *P. stokesii* to *Ananaspis* as mentioned above.

The unresolved nature of the *Acernaspis* clade and the low consistency index (before removal of *A. rubicundula*, Figure 7. 3) are of particular interest. Ramsköld and Werdelin noted a large number of convergences within their data, both within the *Acernaspis* and *Ananaspis* clades and between them (see their tables 2 and 3 which give synapomorphy schemes for the cladograms shown in Figure 7. 2 (a) and (b) and note the occurrences of within- and between-clade convergences). This is in accord with the cladistic results obtained in the present study for *Achatella* (Section 5. 3) and *Calyptaulax* (Section 6. 3) in which convergences between species were found to play

an important role. This may be an important factor in the maintenance of morphological stasis.

7. 3. Material.

Specimens of *Acernaspis* belonging to 20 stratigraphically and geographically separate samples have been studied in detail. These samples cover the entire stratigraphical duration of the genus. In addition, specimens assigned to *Ananaspis* belonging to five samples have been included in the morphometric analysis for comparison with *Acernaspis*, specifically to address the question of the possible neotenic derivation of *Ananaspis* from *Acernaspis*. The samples used for both genera are listed below. Locality names and numbers refer to the locality list in Appendix 3. Names in curly brackets give the species to which the specimens are currently assigned (*i.e.* the name assigned in the most recent relevant literature). "Material" refers to the number of specimens complete enough for morphometrics and does not include disassociated visual surfaces which are included in Figures 7. 18 and 7. 19.

Acernaspis

Girvan District

1. MULLOCH. Specimens from small cuttings along the road which skirts the southern slope of Kirk Hill, Craighead Inlier, Girvan district [locs. 17 to 23; listed in Howells 1982 as her locs. 1 to 7]. Mulloch Hill Fm., Llandovery Series, Rhuddanian Stage, *atavus* Zone (Howells 1982; Cocks *et al.* 1992). {*A.* cf *elliptifrons* (Esmark, 1833)}. Material: three cephala and 18 pygidia.
2. ROUGH NEUK. Specimens from Rough Neuk Quarry, Ladywell Wood, Girvan district [loc. 24]. Mulloch Hill Fm., Llandovery Series, Rhuddanian Stage, low *cyphus* Zone (Howells 1982). {*A.* cf *elliptifrons* (Esmark, 1833)}. Material: eight pygidia.
3. WOODLAND A. Specimens from Woodland Point, Girvan foreshore [loc. 25], listed by Howells (1982) as Woodland Fm, *cyphus* Zone. {*A. superciliexcelsis* Howells, 1982}. Material: four holaspide cephala, six holaspide pygidia. Also one meraspide cranidium.
4. WOODLAND B. Locality and horizon as for WOODLAND A. {*A. xynon* Howells, 1982}. Material: seven cephala, four pygidia.
5. NEWLANDS. Specimens from Newlands Farm, Craighead Inlier, Girvan district [loc. 26]. Newlands Fm., Llandovery Series, Aeronian Stage, lower *gregarius* Zone (Cocks *et al.* 1992). {*A. superciliexcelsis* Howells, 1982}. Material: 25 holaspide cephala, 30 holaspide pygidia. Also one meraspide cranidium.
6. CAMREGAN. Specimens from Camregan Wood Quarry, Girvan district [loc. 27]. Lower Camregan Grits, Llandovery Series, Aeronian Stage, *sedgwickii* Zone (Cocks *et al.* 1992). {*A.* sp. A of Howells 1982}. Material: four cephala, seven pygidia.

7. WOOD BURN. Specimens from Bargany Pond Burn [loc. 28], and Penkill [loc. 29], Girvan district. Wood Burn Fm., Llandovery Series, topmost Aeronian - basal Telychian stages, *sedgwickii* - *turriculatus* zones (Cocks *et al.* 1992). {*A. woodburnensis* Clarkson, Eldredge and Henry, 1977}. Material: five cephala, 13 pygidia.

Pentland Hills

8. RESERVOIR. A single complete specimen from Deerhope Burn [loc. 32]. Upper Reservoir Fm., Llandovery Series, Telychian Stage (Howells 1982). {*A.* sp. B of Howells 1982}.
9. DEERHOPE. Single cephalon from the Coral Bed, Deerhope Burn [loc. 33]. Deerhope Fm., Llandovery Series, Telychian Stage (Clarkson, Eldredge and Henry, 1977). {*A. sufferta* (Lamont, 1947)}.
10. WETHER LAW. Specimens from Wether Law Linn [loc. 34]. Wether Law Linn Fm., "Lower Mbr." of Robertson (1989), Llandovery Series, topmost Telychian Stage (Howells 1982; Cocks *et al.* 1992). {*A. sufferta* (Lamont, 1947)}. Material: 10 cephala, 15 pygidia.

Galway

11. KILBRIDE. Specimens from Glenglosh [loc. 50]. Middle Kilbride Fm., *crispus* or *griestoniensis* zones, Llandovery Series, Telychian Stage (Doyle 1989; Cocks *et al.* 1992). {*A.* sp. B of Doyle 1989}. Material: two cranidia.

Oslo Region

12. SOLVIK A. Specimens from Skytterveien, Asker [loc. 67], Spirodden, Asker [loc. 68], Malmøya, Oslo [loc. 69] and Malmøykalven, Oslo [loc. 70]. Solvik Fm., lower Llandovery Series, etages 6b and 6c (Rhuddanian to Aeronian stages) (Helbert 1985; Cocks *et al.* 1992). {*A. elliptifrons* (Esmark, 1833)}. Material: 25 holaspide cephala and cranidia, 30 holaspide pygidia. Also three meraspide cranidia from Spirodden (described by Lespérance and Letendre (1982) as *A. norvegiensis*).
13. SOLVIK B. Specimens from Sjursøya, Oslo district [loc. 71]. Solvik Fm., lower Llandovery Series, Rhuddanian Stage, etage 6a (Helbert 1985). {*A. phyxis* Helbert, 1985 nomen nudum}. Material: two cephala, five pygidia.
14. RYTTERÅKER. Specimens from Ulvøya [loc. 72] and Bjerkøya [loc. 73], Oslo district. Rytteråker Fm., Llandovery Series, upper Aeronian Stage, etage 7a, *convolutus* or *sedgwickii* zones (Helbert 1985; Cocks *et al.* 1992). {*A.* sp. C of Helbert 1985)}. Material: a single cephalon and two pygidia.
15. VIK. Specimens from Garntangen [loc. 74], near Vik [loc. 75] and Storøya [loc. 76], Ringerike. Vik Fm., upper Llandovery Series, Telychian Stage, etage 7c (Worsley *et al.* 1983; Helbert 1985). {*A. labronios* Helbert, 1985 nomen nudum}. Material: three cephala, three pygidia.

Gotland

16. VISBY A. Specimens from area of Visby, Gotland, localities at Norderstrand [loc. 77] and Kronviken [loc. 78]. Lower Visby Fm., Llandovery Series, topmost Telychian Stage (Ramsköld 1985; Cocks *et al.* 1992). {*A. quadrilineata* (Angelin, 1851)}. Material: 17 cephala, 38 pygidia.
17. VISBY B. Specimens from area of Visby, Gotland, localities at Norderstrand [loc. 77], Kronviken [loc. 78], and Rönnklint [loc. 79]. Horizon as for VISBY A. {*A. sororia* Ramsköld, 1985}. Material: three cephala, five pygidia.
18. HÖGKLINT. Specimens from Vattenfallsprofilen [loc. 80], Ireviken [loc. 81], Kopparsvik 3 [loc. 82], Visby area, Gotland. Högklint Fm., Wenlock Series, Sheinwoodian Stage (Ramsköld 1985; Cocks *et al.* 1992). {*A. rubicundula* Ramsköld 1985}. Material: eight holaspide cephala, seven holaspide pygidia. Also two meraspide cranidia.

Östergötland

19. MOTALA. Specimens from Gustavsvik (exact locality unknown), Östergötland. Motala Fm., middle Llandovery Series (Ramsköld and Werdelin 1991). Material: two holaspide cephala, six holaspide pygidia. Also three meraspide cranidia and three meraspide pygidia.

Anticosti Island

20. JUPITER. Specimens from Jupiter Cliff, Anticosti Island, Quebec [loc. 87]. Jupiter Fm., Llandovery Series, Telychian Stage (Helbert *et al.* 1982; Cocks *et al.* 1992). {*A. orestes* (Billings, 1860)}. Material: two cephala and a single pygidium.

Ananaspis

England

21. DUDLEY. Specimens from the Dudley area, exact localities unknown. Much Wenlock Limestone Fm., Wenlock Series, Homerian Stage (Cocks *et al.* 1992). {*A. stokesii* (Milne Edwards, 1840)}. Material: nine cephala, six pygidia.

Wales

22. UCHAF. Specimens from Plas Uchaf, Llanrwst, Clwyd [loc. 45]. Upper Mottled Mudstone, lower Nantglyn Flags Gp., Wenlock Series, Homerian Stage (Warren *et al.* 1984; Cocks *et al.* 1992). {*A.* aff. *fecunda* (Barrande, 1846)}. Material: two cephala.

Gotland

23. MULDE. Specimens from Sudervik 1, Gotland [loc. 83]. Mulde Fm. (undifferentiated), Wenlock Series, Homerian Stage (Ramsköld 1985; Cocks *et al.* 1992). {*A. amelangorum* Ramsköld, 1985}. Material: three cephala, four pygidia.

Bohemia

24. KOS-KOL-LOC. Specimens from Kosov [loc. 84], Kolednik [loc. 85] and Lockhov [loc. 86] quarries. Kopanina Fm. (upper part), Ludlow Series (Chlupáč 1984). {*A. fecunda* (Barrande, 1846)}. Material: 22 cephala, 23 pygidia.

The spatial and geographical location of the samples is summarised in Figure 7. 4. Table 7. 1 is a summary of the lithologies and postulated depositional environments of the rocks from which the samples were obtained. It is notable that virtually all of the *in situ* occurrences are in the shelf environment, although there is a range of shelf sites represented (e.g. shallow inner shelf of MULLOCH, to relatively deep water outer shelf of WOOD BURN). There are two exceptions to this shelf occurrence. The sample DEERHOPE is from the "Coral Bed", Deerhope Fm., N. Esk Inlier, which Robertson (1989) considered to have been deposited in somewhat deeper water, with an *in situ* fauna (see Chapter 3). The sample UCHAF is from the Upper Mottled Mudstone at Plas Uchaf in Clwyd, and occurs in sediments which Warren *et al.* (1984) considered to represent a deep water, low oxygen environment (Chapter 3).

7. 4. Morphometrics.

Detailed morphometrics have been done on the cephalon and pygidium of *Acernaspis* and *Ananaspis*, with the aim of assessing the boundaries of morphological stasis in the lineage and also assessing Ramsköld's (1988) claim for neotenic derivation of *Ananaspis* from *Acernaspis*.

As for *Achatella* (Chapter 5) and *Calyptaulax* (Chapter 6), principal component analysis has been used to test the hypothesis of stasis in the lineage, and to highlight those measurable characters which show most variation. Univariate and bivariate techniques have been used to study selected characters in more detail. In all, the analysis is based on 185 cephala (135 *Acernaspis* and 50 *Ananaspis*) and 249 pygidia (202 *Acernaspis*, 47 *Ananaspis*). In addition, visual surfaces belonging to 183 individual animals have been studied in detail.

7. 4. 1. Measurements Used.

All measurements were made on internal moulds of the exoskeleton, or on silicified specimens, using a single orientation method utilising photography and the digitising tablet for cephala, and the moving stage microscope for pygidia, as described in Chapter 4. The horizontal plane for measurement of cephala was defined as in Shaw (1957: 194) and Temple (1975: 463) *i.e.* with the chord of the palpebral surface horizontal. The horizontal plane for pygidia was also defined as in Shaw (1957: 194) and Temple (1975: 463) *i.e.* with the ventral margin of the pygidial border horizontal.

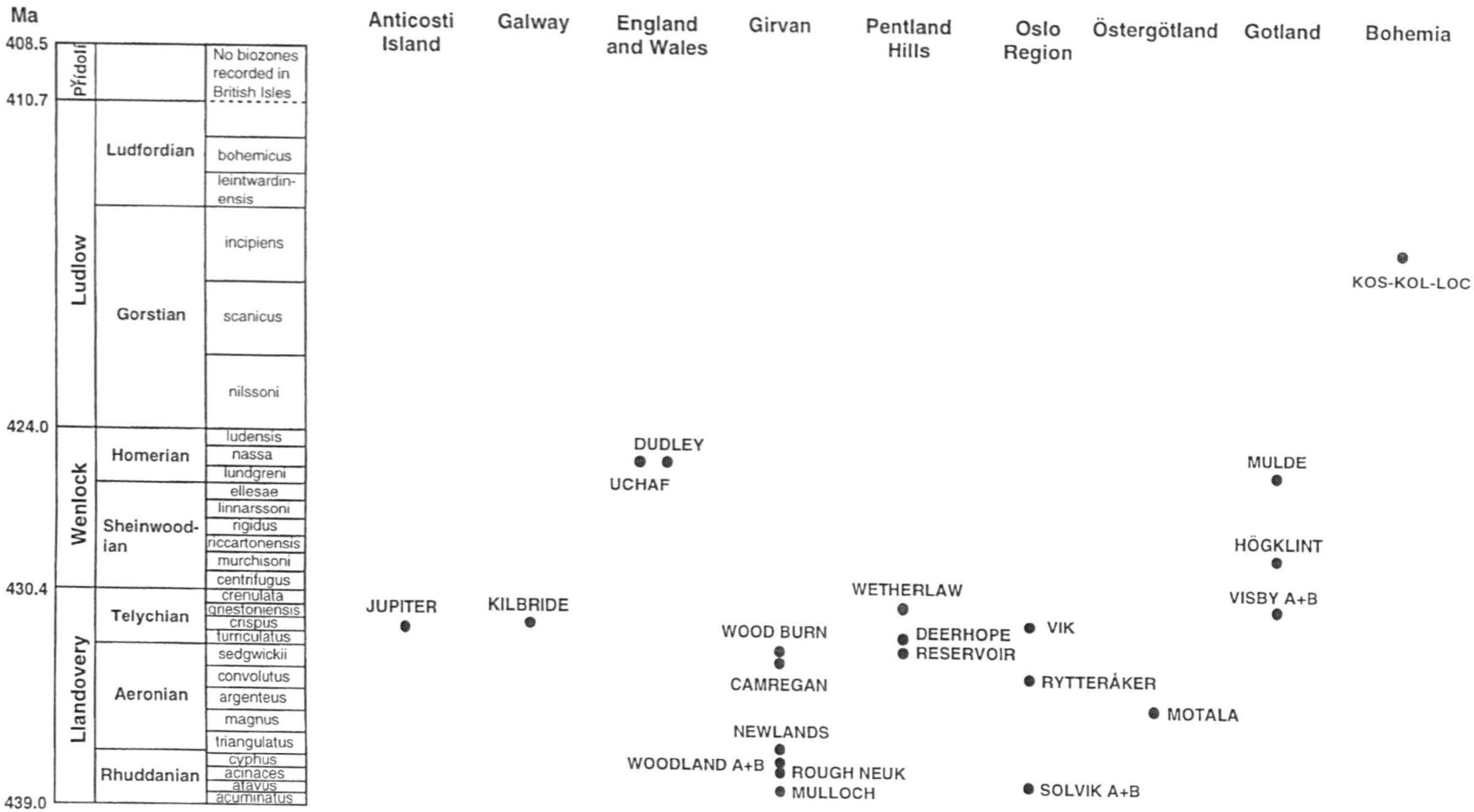

Figure 7. 4. Summary of the stratigraphical and geographical locations of the samples of *Acernaspis* and *Ananaspis* used. Stratigraphy based on Cocks *et al.* (1992). Chronostratigraphy is that of Harland *et al.* (1989). Stratigraphical location of the samples based on references in the text.

Table 7. 1. Summary of the lithologies, faunas and postulated depositional environments of the rocks associated with the stratigraphical samples of *Acernaspis* and *Ananaspis*.

Stratigraphical Sample	Unit and Age	Lithology	Fauna	Environment of Deposition	References
MULLOCH	Mulloch Hill Fm., Craighead Inlier, Girvan (Rhuddanian, *atavus* Zone).	Interbedded shales, siltstones and ssts.	Abundant and diverse shelly fauna. Brachiopods of high diversity *Cryptothyrella* assoc.	Relatively shallow water inner shelf deposition.	Cocks & Toghill (1973); Howells (1982).
ROUGH NEUK	As above.	As above.	As above.	As above.	As above.
WOODLAND A	Woodland Fm., Girvan (Rhuddanian, *cyphus* Zone).	Massive and bedded purple and grey flaggy siltstones and shales.	Rich and diverse shelly faunas. Brachiopods of *Stricklandia* and *Clorinda* assocs., highest levels graptolitic.	Relatively deep water, outer shelf deposition.	Cocks & Toghill (1973); Howells (1982).
WOODLAND B	As above.	As above.	As above.	As above.	As above.
NEWLANDS	Newlands Fm., Craighead Inlier, Girvan (Aeronian, *gregarius* Zone).	Buff weathering bedded calc. siltstones and ssts.	Extremely abundant and diverse shelly fauna, partly *in situ*. Brachiopods of *Stricklandia* and *Clorinda* assocs.	Relatively deep water, outer shelf deposition, probably as result of turbidity currents.	Cocks & Toghill (1973); Howells (1982).
CAMREGAN	Lower Camregan Grits, Girvan (Aeronian, *sedgwickii* Zone).	Fine-medium grained red-brown thinly bedded ssts; sole marks.	Allochthonous shelly fauna with brachiopods of *Eocoelia* assoc.	Relatively shallow water high energy inner shelf deposition.	Cocks & Toghill (1973); Howells (1982).

Table 7. 1. Continued.

Stratigraphical Sample	Unit and Age	Lithology	Fauna	Environment of Deposition	References
WOOD BURN	Wood Burn Fm., Girvan (topmost Aeronian-basal Telychian).	Hard grey and blue-grey siltstones and, ssts. and shales.	Shelly fauna with brachiopods of *Pentamerus* and *Clorinda* assocs.	Relatively deep water outer shelf deposition	Cocks & Toghill (1973); Howells (1982).
RESERVOIR	Reservoir Fm. (upper), N. Esk Inlier (basal Telychian).	Interbedded red, green and brown mudsts., ssts. and shales; sole marks.	Stratigraphically confined allochthonous faunas in upper part: eurypterid and starfish beds. Fossils rare otherwise.	Turbidites deposited at mid fan fringe, outer fan or basin plain.	Mykura & Smith (1962); Tipper (1976); Robertson (1989).
DEERHOPE	Deerhope Coral Bed, Deerhope Fm., N. Esk Inlier (lower Telychian).	Red and grey laminated mudsts., siltstones and shales.	Abundant and well preserved *in situ* benthic fauna preserved at the base of a mudst. band.	Deep water ?upper slope deposition on fringes of inner submarine fan.	Mykura & Smith (1962); Tipper (1976); Robertson (1989).
WETHER LAW	Wether Law Linn Fm. (Lower Mbr. of Robertson 1989) N. Esk Inlier (upper Telychian).	Calc. mudsts., siltstones and fine ssts.	Very abundant and diverse shelly fauna, largely *in situ.*	Shallow water sublittoral environment.	Mykura & Smith (1962); Tipper (1976); Robertson (1989).
KILBRIDE	Kilbride Fm. (middle), Glenglosh, Co. Galway (Telychian).	Ssts., pebbly ssts. and siltstones displaying a variety of facies; fining up.	Fossiliferous at some levels, allochthonous shelly faunas; brachiopods of *Clorinda* assoc. in topmost levels.	Shallow marine high energy, deepening from tidal lagoon (base) to near wave base (top).	Piper (1972); Doyle (1989).

Table 7. 1. Continued.

Stratigraphical Sample	Unit and Age	Lithology	Fauna	Environment of Deposition	References
SOLVIK A	Solvik Fm., Oslo Region (lower Llandovery).	Dark grey shales with thin siltstone and lst. interbeds.	Abundant shelly faunas, partly *in situ*.	Relatively deep water deposition in quiet muddy conditions, shallowing slightly towards the top.	Worsley *et al.* (1983).
SOLVIK B	As above (Rhuddanian).	As above.	As above.	As above.	As above.
RYTTERÅKER	Rytteråker Fm., Oslo Region (upper Aeronian-lower Telychian).	Thickly bedded biosparites with some calc. nodules.	Very abundant pentamerid brachiopods.	Shallow and extensive carbonate shelf.	Worsley *et al.* (1983).
VIK	Vik Fm., Oslo Region (Telychian).	Red and green-grey shales with some marls and nodular lsts.	Abundant and diverse shelly fauna from middle part of formation, sparser in lower and upper parts.	Slightly shallower than underlying Rytteråker but with shallower marl banks developed in middle part.	Worsley *et al.* (1983).
VISBY A	Visby Fm. (lower), Gotland (topmost Telychian).	Alternating thin bedded blue-grey marls and pale marly lsts.	Abundant and diverse *in situ* shelly faunas: *Stricklandia* locally very abundant.	Extensive platform at moderate depth.	Manten (1971); Bassett & Cocks (1974).
VISBY B	As above.	As above.	As above.	As above.	As above.
HÖGKLINT	Högklint Fm., Gotland (Sheinwoodian).	Finely crystalline lsts, with stromatoporoid-supported carb. mounds.	Highly abundant and diverse shelly present in both carb. mounds and host sediments.	Slightly shallower depth than Lower Visby Fm.	Manten (1971); Bassett & Cocks (1974).

Table 7. 1. Continued.

Stratigraphical Sample	Unit and Age	Lithology	Fauna	Environment of Deposition	References
JUPITER	Jupiter Fm., Anticosti Island (Telychian).	Interbedded argillaceous brown and grey lsts. and shales. Carb. mounds developed locally.	Rich allochthonous shelly fauna in both carbonate mounds and host sediments.	Deposition at moderate depth on extensive carbonate platform.	Bolton (1971); Lespérance & Letendre (1981, 1982).
DUDLEY	Much Wenlock Lst. Fm., Welsh Borderlands (Homerian).	Pale coloured, pure bioclastic lsts. with well developed carb. mounds.	Extremely abundant and diverse shelly faunas in carb. mounds and host sediments.	Deposition in relatively shallow water on broad carbonate platform.	Bassett (1974); Thomas (1978-1981).
UCHAF.	Upper Mottled Mudst., Clwyd (Homerian).	Massive mottled calc. silty mudsts.	Autochthonous shelly fauna and graptolitic fauna, both rich but of low diversity.	Relatively deep water, low oxygen environment, possibly a restricted basin.	Warren *et al.* (1984).
MULDE	Mulde Fm., Gotland (Homerian).	Interbedded blue-grey marls and marly lsts.	Rich and diverse autochthonous shelly faunas.	Extensive platform at moderate depth.	Manten (1971); Bassett & Cocks (1974).
KOS-KOL-LOC	Kopanina Fm., Barrandian region (Ludlow).	Carbonate facies of the Kopanina Fm., dense nodular or tabular lsts. and crinoidal lsts.	Abundant and diverse autochthonous shelly fauna.	Shallow water deposition as shoals around the margins of volcanic islands.	Svoboda (1966); Chlupáč (1984).

Measurements whose defining end points are in furrows were made to the deepest points in the furrows, thus allowing direct comparison between internal moulds and silicified specimens. Where a bilaterally symmetrical structure was missing on one side of the specimen but present on the other, the original symmetry was used to derive the full transverse measurement.

The full set of measurements made on cephala and pygidia of *Acernaspis* and *Ananaspis* is shown in Figure 7. 5. The measurement scheme is based upon those of Shaw (1957), Temple (1975) and Ramsköld (1988), and the measurements are formally defined in Table 7. 2.

7. 4. 2. Results.

The morphometric data on *Acernaspis* and *Ananaspis* are listed in Appendix 5. The specimens are organised into three data sets as follows:

1. *Cephalon data set.* This consists of all specimens for which the following set of measurements was obtainable:

B	J
J4	J5
P (left and right)	b21 (left and right)
b!21 (left and right)	b10 (left and right)
b!10 (left and right)	k22
k!22	k11
k!11	k00
K2	K1
K	k10
C1 (left and right)	C2 (left and right)
F (left and right)	

All of the above measurements were obtainable for 113 specimens.

2. *Glabellar furrow data set.* This set consists of all specimens for which the following set of measurements was obtainable:

b5 (left and right)	b!5 (left and right)
b6 (left and right)	b!6 (left and right)
b32 (left and right)	b!32 (left and right)
b21 (left and right)	b!21 (left and right)
b10 (left and right)	b!10 (left and right)
k33	k!33
k34	k!34
k22	k!22

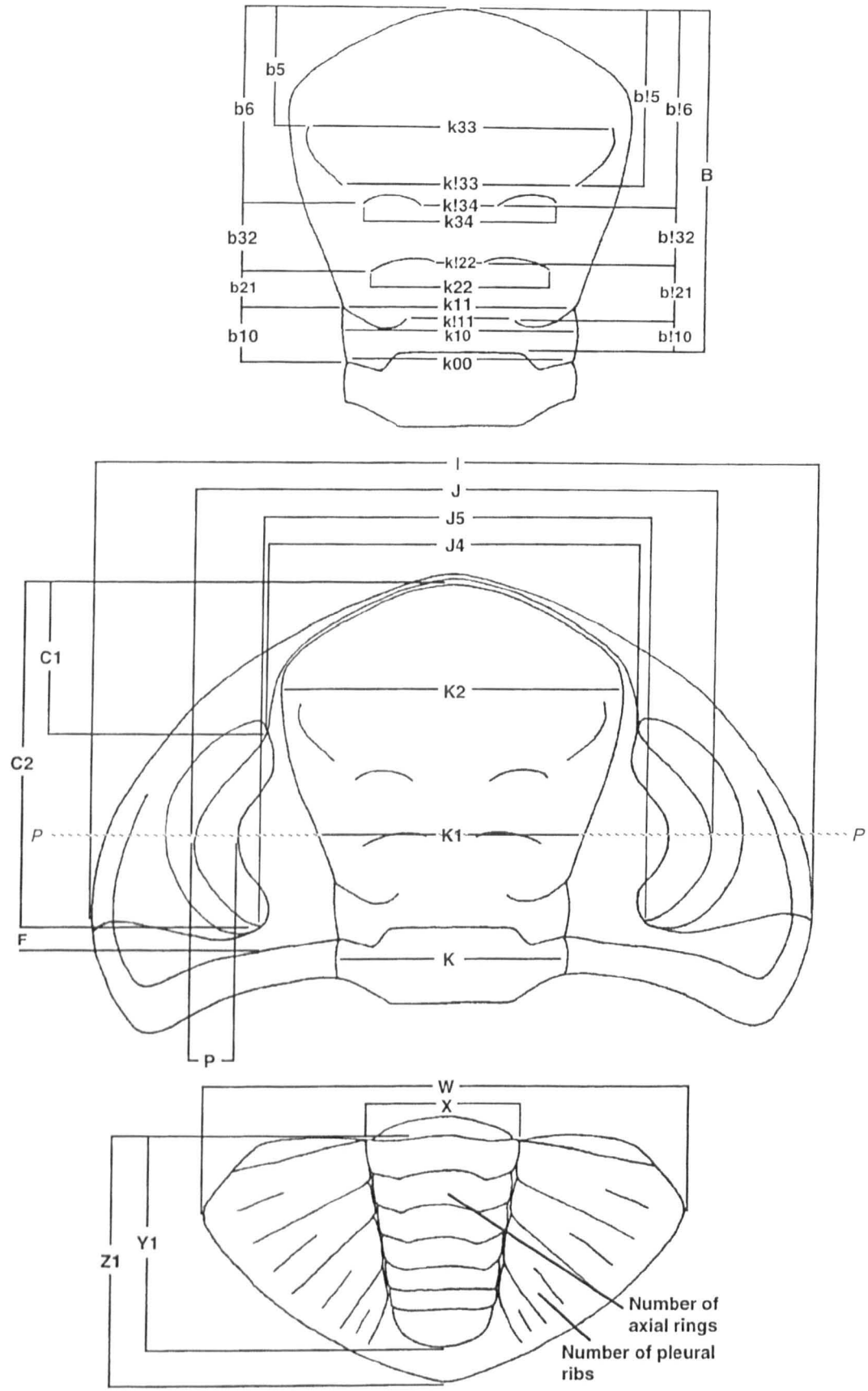

Figure 7. 5. Measurements made on glabellae, cephala and pygidia of *Acernaspis* and *Ananaspis*. All measurements made on internal moulds or silicified specimens with the specimen orientated in dorsal view (see text). Measurements used in principal components analysis (PCA) in bold type. The dotted line *PP* is the line which bisects the lengths (exsag.) of the left and right palpebral lobes. See Table 7. 2. for formal definitions of the measurements.

Table 7. 2. Definitions of measurements made on the exoskeleton of *Acernaspis* and *Ananaspis*. For each measurement an abbreviated name (in bold), a formal name (in italics), and a full definition are given. See Figure 7. 5 for illustrative diagram.

CEPHALA

B: *Preoccipital glabellar length.* Sag. length of glabella as measured from the anteriormost extremity of the frontal lobe to the deepest point in the occipital furrow.

I: *Maximum cephalic width.* Width (tr.) of cephalon as measured across the widest point.

J: *Palpebral cranidial width.* Width (tr.) of cranidium from outer edge of left palpebral lobe to outer edge of right palpebral lobe as measured along the line which bisects the lengths (exsag.) of the left and right palpebral lobes. All palpebral lobes are approximately symmetrical about this line.

J4: *Pre-palpebral cranidial width.* Width (tr.) of cranidium from anteriormost point of left palpebral lobe to anteriormost point of right palpebral lobe.

J5: *Post-palpebral cranidial width.* Width (tr.) of cranidium from posteriormost point of left palpebral lobe to posteriormost point of right palpebral lobe.

K2: *Maximum glabellar width.* Maximum width (tr.) of the glabella as measured from the left axial furrow to the corresponding point in the right axial furrow.

K1: *Median glabellar width.* Width (tr.) of glabella as measured along the line which bisects the lengths (exsag.) of the left and right palpebral lobes, from the left axial furrow to the corresponding point in the right axial furrow.

K: *Width of occipital ring.* Maximum width (tr.) of the occipital ring as measured from the left axial furrow to the corresponding point in the right axial furrow.

b5: *Longitudinal position of distal extremity of distal branch of S3.* Exsag. length measured from a point level with the anteriormost extremity of the glabella to the distal extremity of the distal branch of S3.

b!5: *Longitudinal position of proximal extremity of distal branch of S3.* Exsag. length measured from a point level with the anteriormost extremity of the glabella to the proximal extremity of the distal branch of S3.

b6: *Longitudinal position of distal extremity of proximal branch of S3.* Exsag. length measured from a point level with the anteriormost extremity of the glabella to the distal extremity of the proximal branch of S3.

b!6: *Longitudinal position of proximal extremity of proximal branch of S3.* Exsag. length measured from a point level with the anteriormost extremity of the glabella to the proximal extremity of the proximal branch of S3.

b32: *Distal length of L3.* Length (exsag.) of L3 as measured from a point level with the distal extremity of the proximal branch of S3 to a point level with the distal extremity of S2.

Table 7. 2. Continued.

b!32: *Proximal length of L3.* Length (exsag.) of L3 as measured from a point level with the proximal extremity of the proximal branch of S3 to a point level with the proximal extremity of S2.

b21: *Distal length of L2.* Length (exsag.) of L2 as measured from the distal extremity of S2 to a point opposite the distal extremity of S1. Left and right side.

b!21: *Proximal length of L2.* Length (exsag.) of L2 as measured from the proximal extremity of S2 to a point opposite the proximal extremity of S1. Left and right side.

b10: *Distal length of L1.* Length (exsag.) of L1 as measured from the distal extremity of S1 to a point opposite the distal extremity of S0. Left and right side.

b!10: *Proximal length of L1.* Length (exsag.) of L1 as measured from the proximal extremity of S1 to the deepest point of S0 on the sagittal line. Left and right side.

k33: *Width between distal ends of distal branches of S3.* The transverse measurement from the distal extremity of the distal branch of the left hand S3 furrow to the corresponding distal extremity of the distal branch of the right hand S3 furrow.

k!33: *Width between proximal ends of distal branches of S3.* The transverse measurement from the proximal extremity of the distal branch of the left hand S3 furrow to the corresponding proximal extremity of the distal branch of the right hand S3 furrow.

k34: *Width between distal ends of proximal branch of S3.* The transverse measurement from the distal extremity of the proximal branch of the left hand S3 furrow to the corresponding distal extremity of the proximal branch of the right hand S3 furrow.

k!34: *Width between proximal ends of proximal branch of S3.* The transverse measurement from the proximal extremity of the proximal branch of the left hand S3 furrow to the corresponding proximal extremity of the proximal branch of the right hand S3 furrow.

k22: *Width between distal ends of S2.* The transverse measurement from the distal extremity of the left hand S2 furrow to the corresponding distal extremity of the right hand S2 furrow.

k!22: *Width between proximal ends of S2.* The transverse measurement from the proximal extremity of the left hand S2 furrow to the corresponding proximal extremity of the right hand S2 furrow.

k11: *Width of glabella across S1.* The transverse measurement from the point of intersection of the left hand S1 furrow with the left axial furrow, to the corresponding point on the right hand side.

Table 7. 2. Continued.

k!11: *Width between proximal ends of S1.* The transverse measurement from the proximal extremity of the left hand S1 furrow to the corresponding proximal extremity of the right hand S1 furrow.

k10: *Width of glabella across L1.* Width (tr.) of glabella across widest point of L1 lobes measured from deepest point in left axial furrow to corresponding point in right axial furrow.

k00: *Width of glabella across S0.* The transverse measurement from the point of intersection of the left branch of the occipital furrow with the left axial furrow, to the corresponding point on the right hand side.

C1: *Longitudinal position of anterior of eye.* Exsag. distance from a point opposite the anteriormost extremity of the frontal lobe to the anteriormost extremity of the palpebral lobe as seen in dorsal view. Left and right side.

C2: *Longitudinal position of posterior of eye.* Exsag. distance from a point opposite the anteriormost extremity of the frontal lobe to the posteriormost extremity of the palpebral lobe as seen in dorsal view. Left and right side.

F: *Postocular length.* Exsag. distance from the posteriormost extremity of the palpebral lobe as seen in dorsal view to the deepest point in the posterior border furrow. Left and right side.

P: *Width of palpebral lobe.* Transverse width of the palpebral lobe from the outer edge to the deepest point in the palpebral furrow, measured along the line which bisects the lengths (exsag.) of the left and right palpebral lobes. Left and right side.

PYGIDIA

W: *Pygidial width.* Width (tr.) of pygidium measured across the widest point.

X: *Width of pygidial axis.* Width (tr.) of pygidial axis measured across the widest point, from the deepest point in the left axial furrow to the corresponding point in the right axial furrow.

Z1: *Pygidial length.* Length (sag.) of pygidium measured from the deepest point in the articulating furrow to the posteriormost extremity of the pygidium.

Y1: *Length of pygidial axis.* Length (sag.) of pygidial axis measured from the deepest point in the articulating furrow to the posteriormost extremity of the axis.

Number of axial rings. Number of distinct rings making up the pygidial axis, excluding the articulating facet at the anterior of the pygidium.

Number of pleural ribs. Number of pleural ribs making up the pleural region of the pygidium, excluding the articulating facet at the anterior of the pleural field.

The reason why this set has been separated from the cephalon data set is because of the often poor preservation of the glabellar furrows, especially in specimens of *Acernaspis* from the Girvan district, which are commonly rather abraded internal moulds, which means that the measurements b5, b!5, b6, b!6, b32, b!32, k33, k!33, k34 and k!34 are often not obtainable for a large number of specimens. Thus the inclusion of these measurements in the cephalon data set would seriously reduce the number of specimens which could be included in the PCA. The above measurements were obtainable for 108 specimens.

3. *Pygidium data set.* This set consists of all specimens for which the following measurements were obtainable:

W	X
Z1	Y1
Number of axial rings	Number of pleural ribs

The above measurements were obtainable for 166 specimens.

In the plots which follow, the stratigraphical samples are represented by different symbols. Figure 7. 6 lists the symbols used. Morphometric results on holaspide specimens will be described first, followed by a consideration of the ontogenetic material which is from the samples WOODLAND A, NEWLANDS, SOLVIK A, HÖGKLINT, and MOTALA.

PCA on cephalon data set. Principal components (PCs) were calculated for the 29 measurements used in the cephalon data set. The eigenvalues and eigenvectors are given in Appendix 6. The PC scores are given in Appendix 7. PC1 summarises 86.8% of the total variance in the data set, PC2 4.3%, PC3 2.4%. The specimens are shown ordinated along the first three PCs in Figure 7. 7.

PC1 sorts the specimens according to size (see Chapter 4). This can be confirmed by comparing the distribution of data points in Figure 7. 8 (a length against width plot for the specimens under consideration) with that in Figure 7. 7 (a). It is clear that the vast majority of variation in the data, 86.8%, represents nothing more than overall size variation. When PC1 is dropped out of the analysis, the resulting size-independent plot of PC2 against PC3, which accounts for 6.7% of the total variance in the data, shows significant overlap between samples (Figure 7. 7(c)). The distribution of samples in the PC-space is clearer in Figure 7. 9, in which the samples are grouped into five broad time intervals. Note that specimens belonging to the sample SOLVIK A have been placed in the "Rhuddanian" window for convenience, although in fact the sample is

Symbol	Stratigraphical Horizon	Sample Name
▬	Mulloch Hill Fm.	MULLOCH
▩	Mulloch Hill Fm.	ROUGH NEUK
⊠	Woodland Fm.	WOODLAND A
⊠	Woodland Fm.	WOODLAND B
▲	Newlands Fm.	NEWLANDS
◆	Lower Camregan Grits	CAMREGAN
■	Wood Burn Fm.	WOODBURN
□	Upper Reservoir Fm.	RESERVOIR
⊞	Deerhope Fm.	DEERHOPE
●	Wether Law Linn Fm.	WETHER LAW
◈	Middle Kilbride Fm.	KILBRIDE
○	Solvik Fm.	SOLVIK A
+	Solvik Fm.	SOLVIK B
△	Rytteråker Fm.	RYTTERÅKER
◇	Vik Fm.	VIK
□	Lower Visby Fm.	VISBY A
▣	Lower Visby Fm.	VISBY B
×	Högklint Fm.	HÖGKLINT
✳	Motala Fm.	MOTALA
⩓	Jupiter Fm.	JUPITER
◇	Much Wenlock Fm.	DUDLEY
△	Upper Mottled Mudst.	UCHAF
⨯	Mulde Fm.	MULDE
✳	Kopanina Fm.	KOS-KOL-LOC

Juvenile Specimens

▪	Woodland Fm.	WOODLAND A juvenile
▴	Newlands Fm.	NEWLANDS juvenile
•	Solvik Fm.	SOLVIK A juvenile
⬩	Högklint Fm.	HÖGKLINT juvenile
-	Motala Fm.	MOTALA

Figure 7. 6. Symbols used to represent the different stratigraphical samples of *Acernaspis* and *Ananaspis* on the morphometric plots.

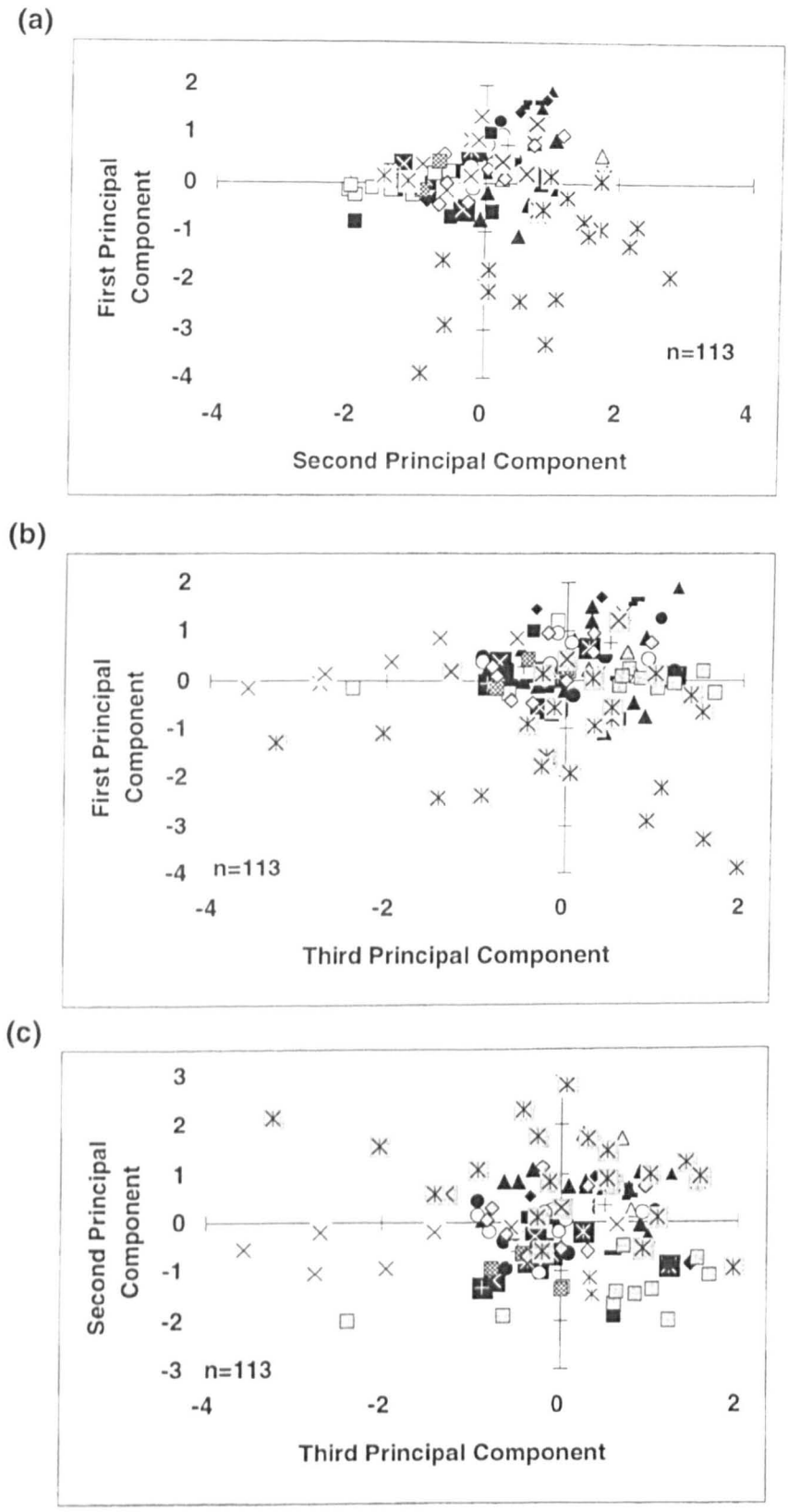

Figure 7. 7. Cephala of *Acernaspis* and *Ananaspis* ordinated along the first three principal component axes calculated from the cephalon measurement scheme. Symbols as in Figure 7. 6.

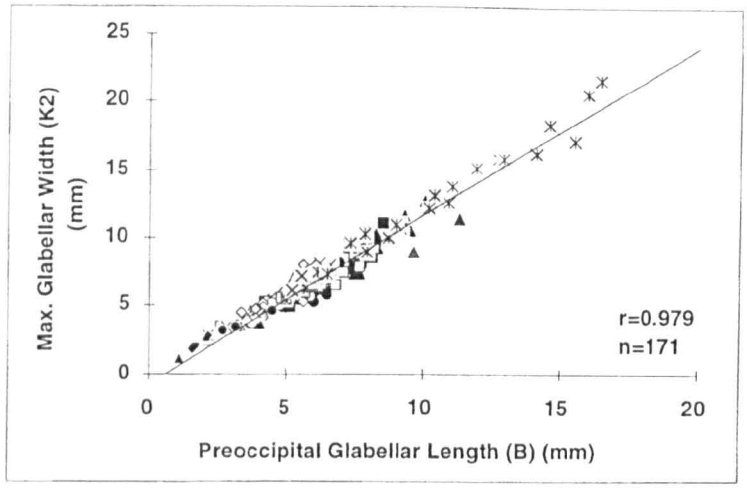

Figure 7. 8. Bivariate scatter plot of maximum width (tr.) of glabella (K2) against preoccipital glabellar length (B). Best-fit line to the data calculated using the reduced major axis method. Symbols as in Figure 7. 6.

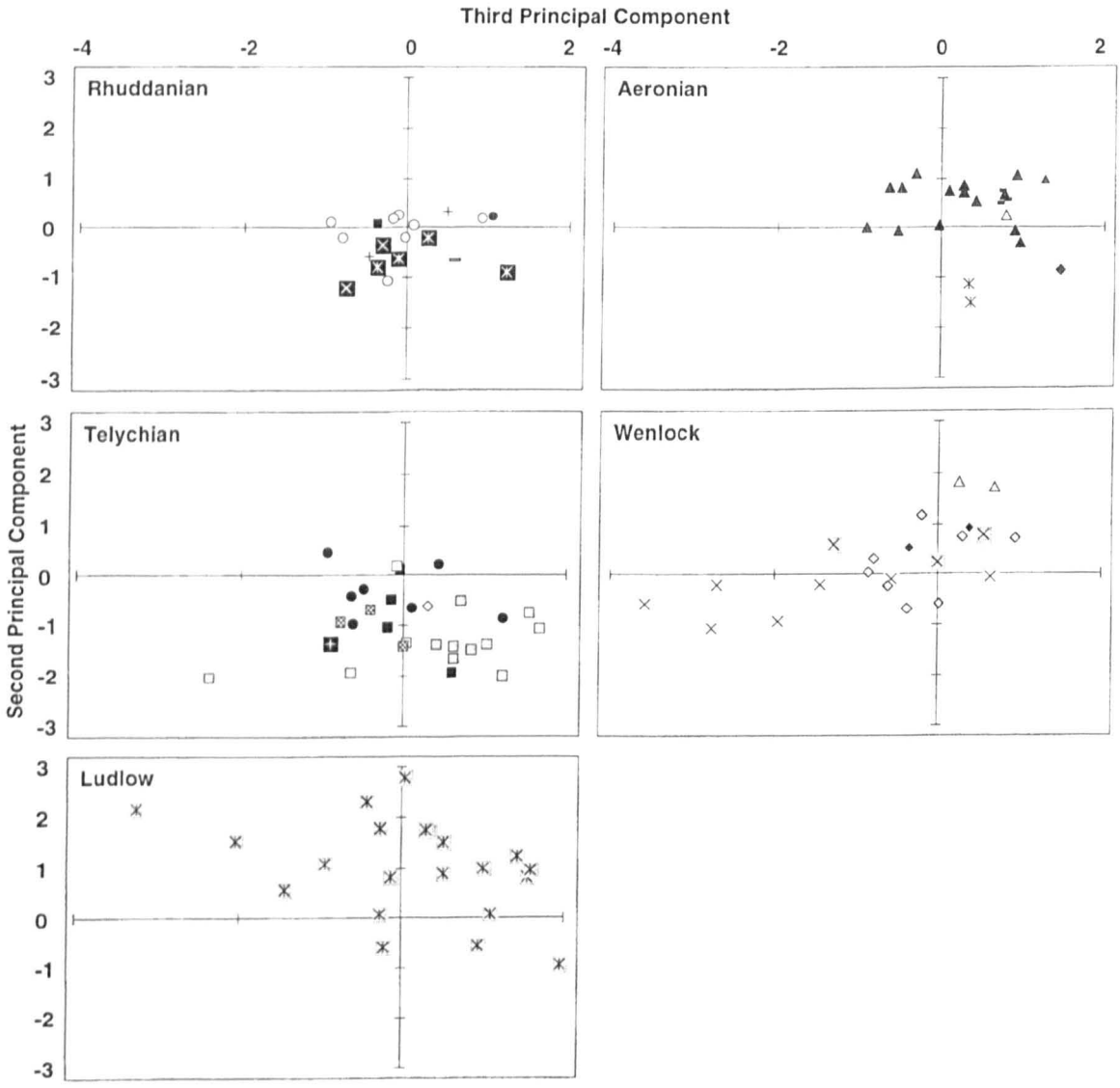

Figure 7. 9. Cephala of *Acernaspis* and *Ananaspis* ordinated along the second and third principal component axes and grouped into five broad time intervals to illustrate changing morphospace occupation with time. Symbols as in Figure 7. 6. n=113.

dated only as "lower Llandovery". Specimens belonging to the sample WOOD BURN are placed in the "Telychian" window, although the sample is actually dated as topmost Aeronian - basal Telychian (see Section 7.3). On inspection of the eigenvector lists (Appendix 6) it is seen that PC2 is most heavily weighted on proximal length of L1 (b!10), and that postocular length (F) is also heavily weighted. PC3 is most heavily weighted on width of palpebral lobe (P). Variation in the variables F and P is illustrated in Figure 7. 10. (NB: The variable most heavily weighted on PC2, b!10, is not shown on Figure 7. 10 since, as will be seen shortly, that variable is also most heavily weighted on PC2 in the PCA on the glabella data set, so, in order to avoid repetition, variation in b!10 is illustrated at that time instead, see Figure 7. 12).

It can be seen from Figure 7. 9 that Rhuddanian specimens group relatively tightly about the origin of the PC space, and specimens belonging to SOLVIK A and SOLVIK B are in close proximity with each other, as are WOODLAND A and WOODLAND B. Aeronian specimens also cluster (a little less tightly) about the origin. On the whole, NEWLANDS, CAMREGAN and RYTTERÅKER more or less coincide with PC region occupied by SOLVIK A and B and WOODLAND A and B in the Rhuddanian, although with a little more variance (*i.e.* greater spread of data points). In the Telychian, the centre of occupation is shifted relatively "southward" (*i.e.* toward lower scores on PC2). WOOD BURN coincides with VISBY B. VISBY A lies relatively further to the right, indicating higher scores on PC3. In the Wenlock, HÖGKLINT is the only sample assigned to *Acernaspis* (UCHAF is considered to belong to *Ananaspis* (Warren *et al.* 1984) while specimens belonging to both MULDE and DUDLEY are considered to be of uncertain status; see Section 7.2). Of particular note is the unusual location in the PC space occupied by HÖGKLINT, with low scores on PC2 and PC3. These specimens occupy a region of the morphospace which does not coincide with any other samples of *Acernaspis.* UCHAF specimens exhibit relatively high scores on PC2. The samples DUDLEY and MULDE more or less coincide (with HÖGKLINT juveniles). In the Ludlow, the specimens of sample KOS-KOL-LOC (assigned to *Ananaspis* by Ramsköld and Werdelin 1991; see also Section 7. 2 herein) are widely scattered in the PC space, although mainly in the upper half of the plot (PC2≥0).

PCA on glabella data set. In order to test whether there is any systematic variation in the location of the furrows on the glabella of *Acernaspis* and *Ananaspis*, the set of measurements describing the location of the furrows was subjected to PCA. Figure 7. 11 shows the specimens ordinated along the second and third PCs (*i.e.* overall size information, summarised by PC1, is not included) and grouped into five time intervals as was done for the cephalon data set, Figure 7. 9. Plots of PC1 against PC2 and PC1 against PC3 have been omitted. PC1 accounts for 87.2% of total variance, PC2 for 4.0%, PC3 for 2.0%. The eigenvalues and eigenvectors are given in Appendix 6, and

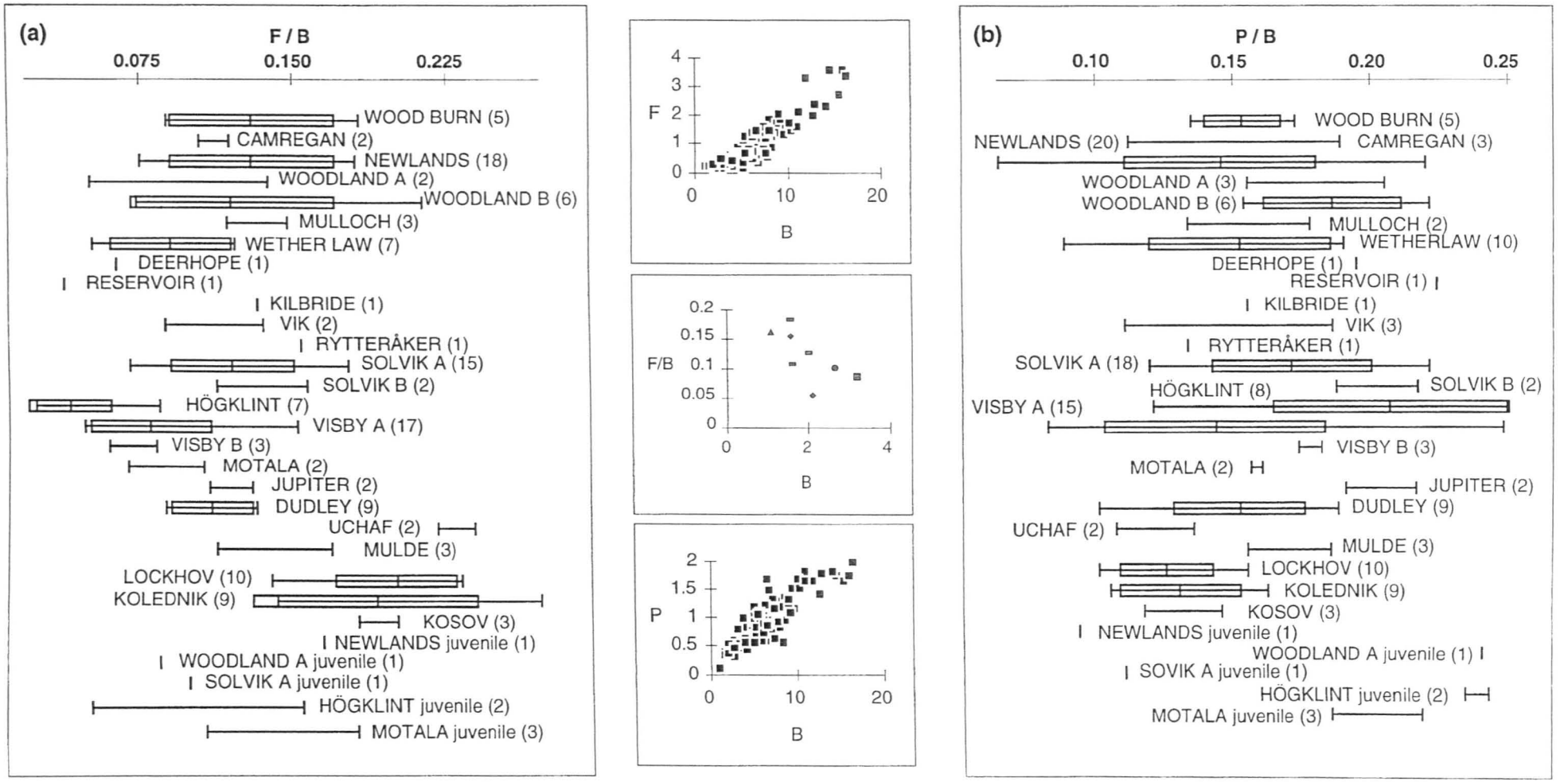

Figure 7. 10. Univariate variation in two measurements heavily weighted on the second and third principal components calculated from the cephalon data set. (a) ratio of postocular length (F) / preoccipital glabellar length (B); (b) ratio of width of palpebral lobe (P) / preoccipital glabellar length (B). Total range and number of measurable specimens shown for each stratigraphical sample, mean value and one standard deviation to either side of the mean shown for samples containing five or more measurable specimens. Insets show bivariate plots of F against B, the ratio F/B against B for juvenile specimens (symbols as in Figure 7. 6.), and P against B. The three localities which make up the KOS-KOL-LOC sample are shown individually.

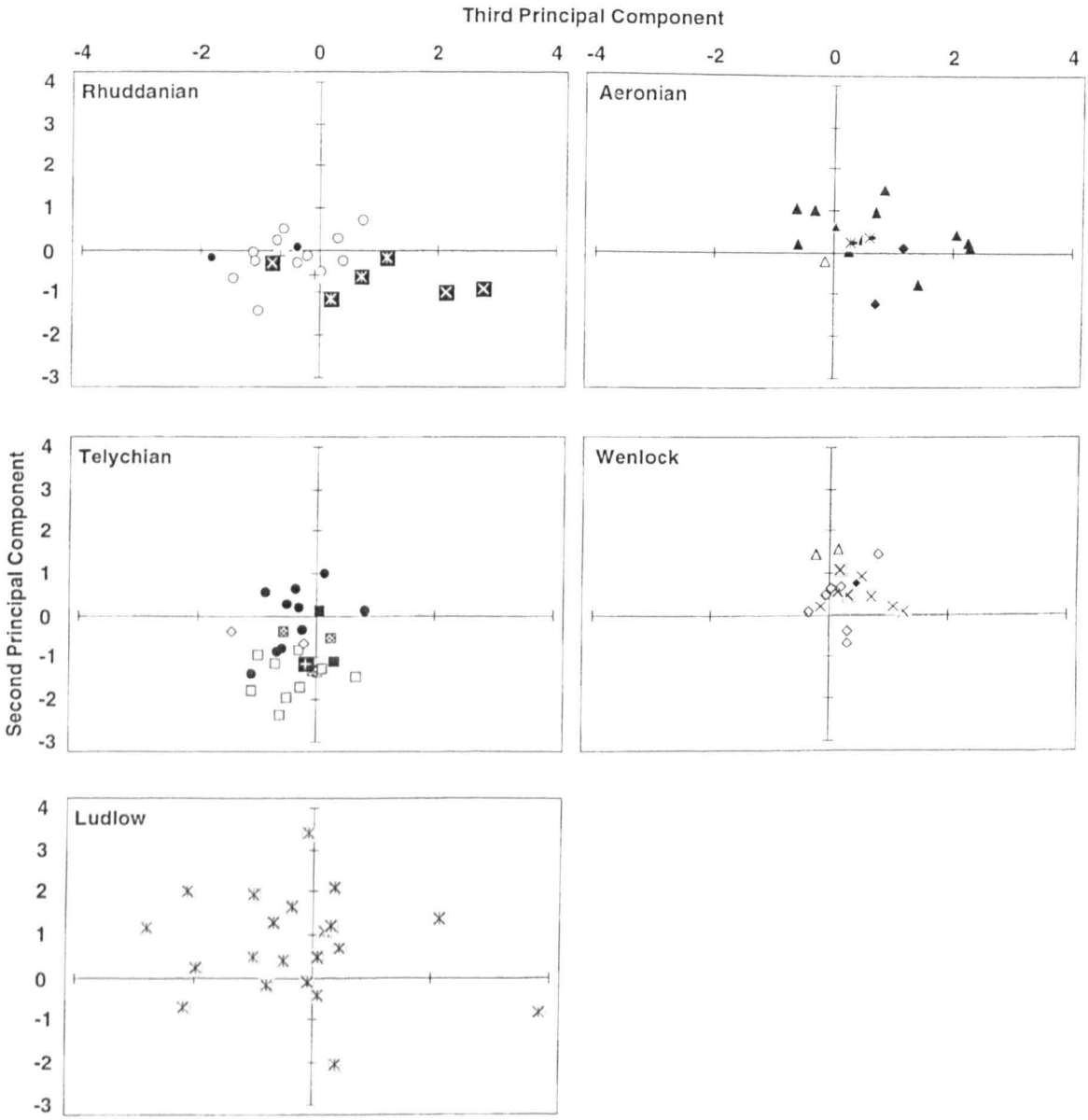

Figure 7. 11. Locations of glabellar furrows of *Acernaspis* and *Ananaspis* ordinated along the second and third principal component axes and grouped into five broad time intervals. Symbols as in Figure 7. 6. n=108.

the PC scores are given in Appendix 7. From the eigenvector list, it is seen that PC2 is most heavily weighted on proximal length of L1 (b!10; this variable was also most heavily weighted on PC2 in PCA on the cephalon data set, see above). PC3 is most heavily weighted on distal length of L1 (b10). Variation in these variables is illustrated in Figure 7. 12. Perhaps the most obvious feature shown by the PC plot in Figure 7. 11 is that, as was found for measurements describing the cephalon as a whole, specimens from the Ludlow (all of which are assigned to *Ananaspis*) exhibit much greater variance than earlier (mainly *Acernaspis*) specimens. Looking in more detail, it is noticeable that VISBY A (Telychian) occupies a reasonably well-constrained region with low PC2 scores. Specimens of VISBY B overlap with the "northernmost" (highest PC2 scores) part of the range of VISBY A.

PCA on the pygidium data set. PCs were calculated for the six measurements used in the pygidium data set. The associated eigenvalues and eigenvectors are given in Appendix 6, and the PC scores are given in Appendix 7. PC1 summarises 70.8% of total variance in the data set and, as for earlier examples, sorts the specimens with respect to size. PC2 summarises 16.3% of total variance, PC3 9.7%. On inspection of the eigenvectors, it is found that PC2 is most heavily weighted on the number of axial rings, while PC3 is most heavily weighted on the number of pleural ribs. The distribution of these variables is shown in Figure 7. 13.

The specimens are grouped into the same five time intervals used for cephala and ordinated along the second and third PCs in Figure 7. 14. Rhuddanian, Aeronian, Telychian and Wenlock samples all cluster about the origin, with a lot of variation evident in the wide scatter of data points. Ludlow samples are shifted relatively westward, reflecting their relatively higher numbers of pleural segments (Figure 7. 13(b)).

Eyes. Figures 7. 15 to 7. 17 show bivariate scatter plots which detail the position on the cephalon and exsaggital length of the eye. Figure 7. 15 indicates that the location of the anterior extremity of the eye is relatively uniform in specimens belonging to all samples. Figure 7. 16 suggests that the posterior extremity of the eye is relatively further forward in some specimens than in others, notably in the samples NEWLANDS, KOS-KOL-LOC, and UCHAF. This means that the eye is relatively shorter in these samples than in the others (Figure 7. 17). If the samples are separated into two groups such that one group contains the samples NEWLANDS, KOS-KOL-LOC and UCHAF, and the other group contains all of the other samples, and a reduced major axis line is fitted to each group, it is seen that there are two clear trends: the RMA line fitted to the NEWLANDS group has slope 0.34 and intercept 0.24; the RMA line fitted to the group of remaining samples has slope 0.55 and intercept -0.22 (Figure 7. 17). A t-test rejected

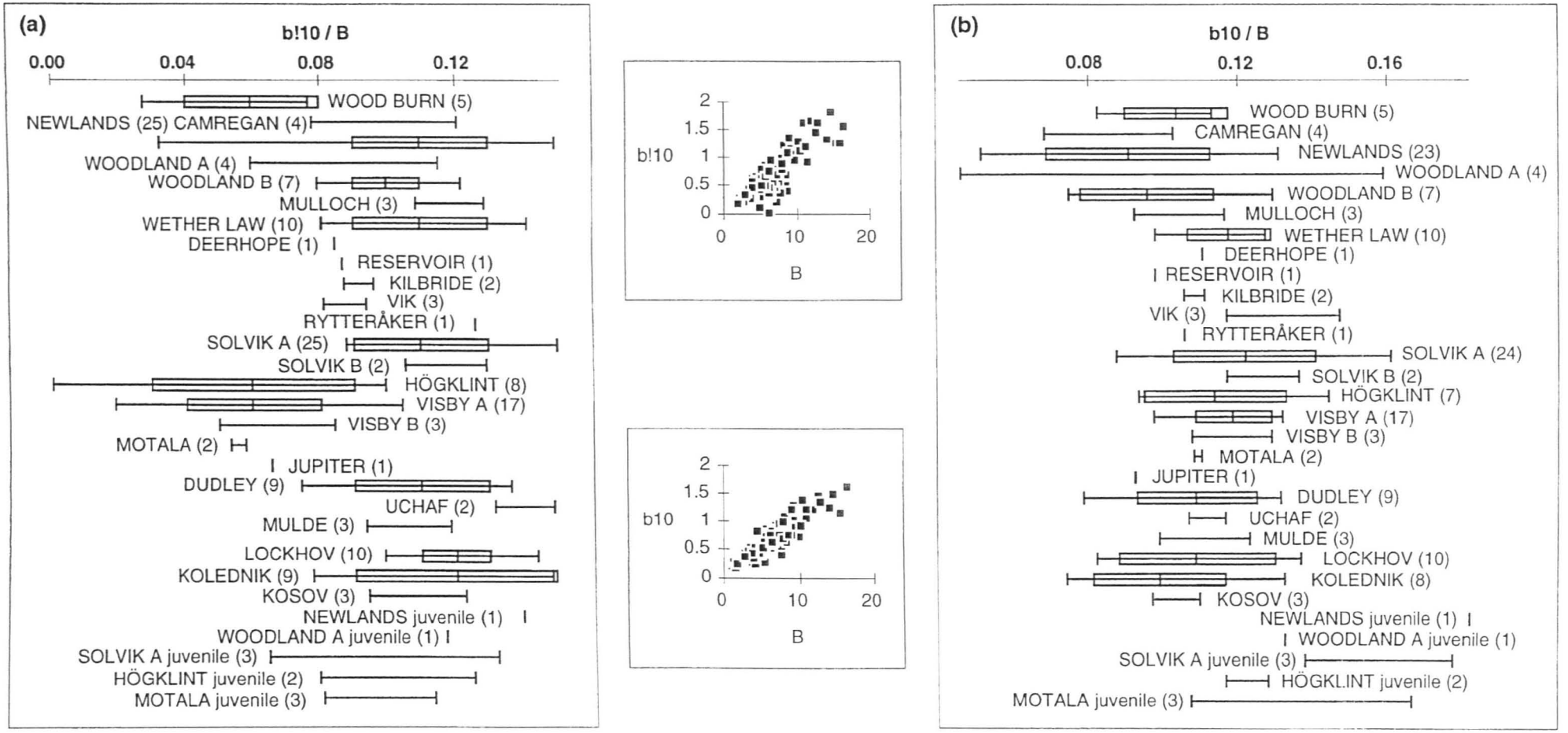

Figure 7. 12. Univariate variation in the measurements most heavily weighted on the second and third principal components calculated for the glabella data set. (a) ratio of proximal length of L1 (b!10) / preoccipital glabellar length (B); (b) ratio of distal length of L1 (b10) / preoccipital glabellar length (B). Total range and number of measurable specimens shown for each stratigraphical sample, mean value and one standard deviation to either side of the mean shown for samples containing five or more measurable specimens. Insets show bivariate plots of b!10 against B and b10 against B. The three localities which make up the KOS-KOL-LOC sample are shown individually.

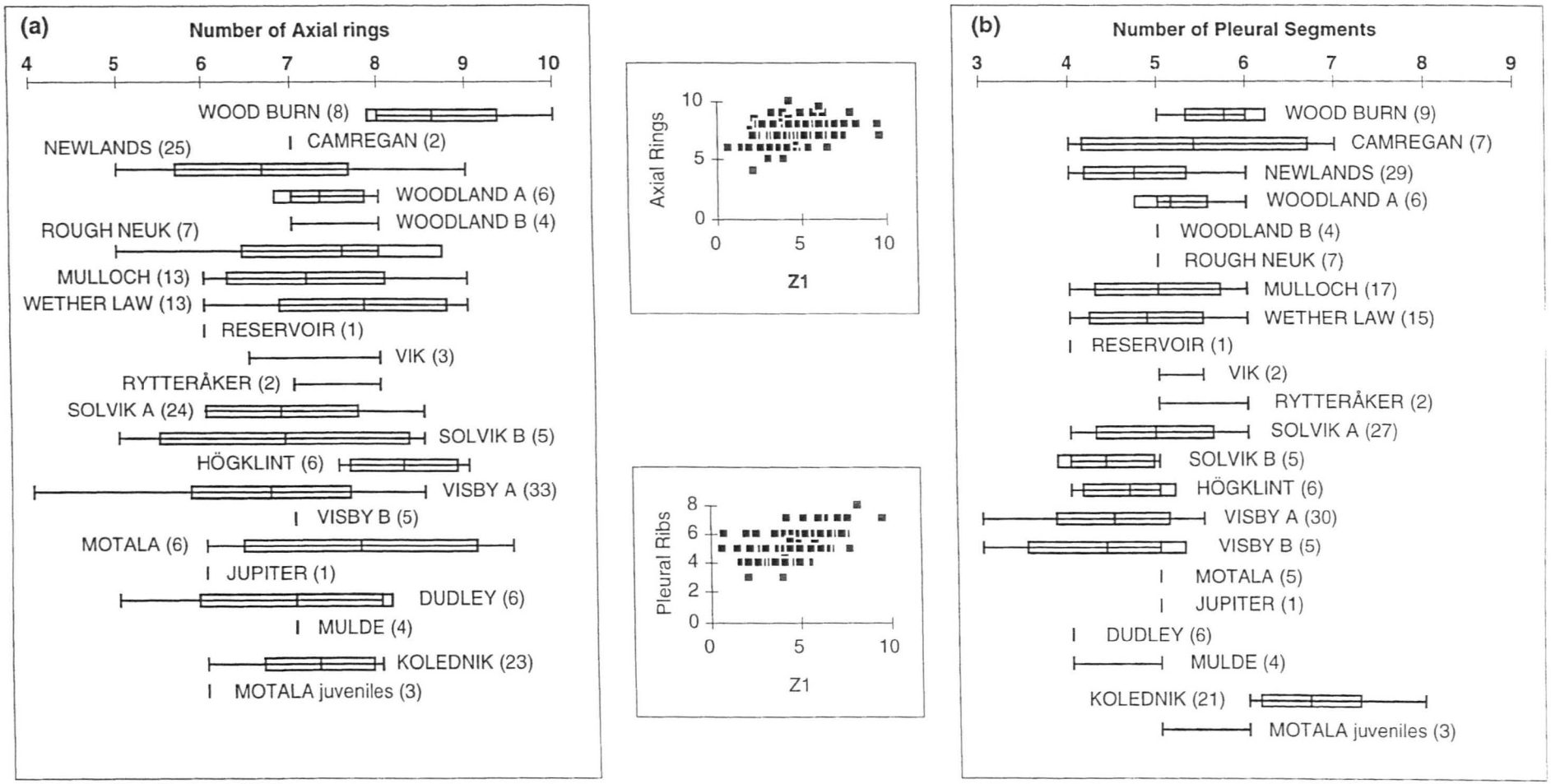

Figure 7. 13. Variation in (a) number of axial rings and (b) pleural ribs in pygidia of *Acernaspis* and *Ananaspis*. Total range and number of measurable specimens shown for each stratigraphical sample, mean value and one standard deviation to either side of the mean shown for samples containing five or more measurable specimens. Insets show bivariate plots of the number of axial rings against pygidial length (Z1) and the number of pleural ribs against pygidial length (Z1). Indistinct axial rings counted as half values. All KOS-KOL-LOC pygidia are from the Kolednik locality.

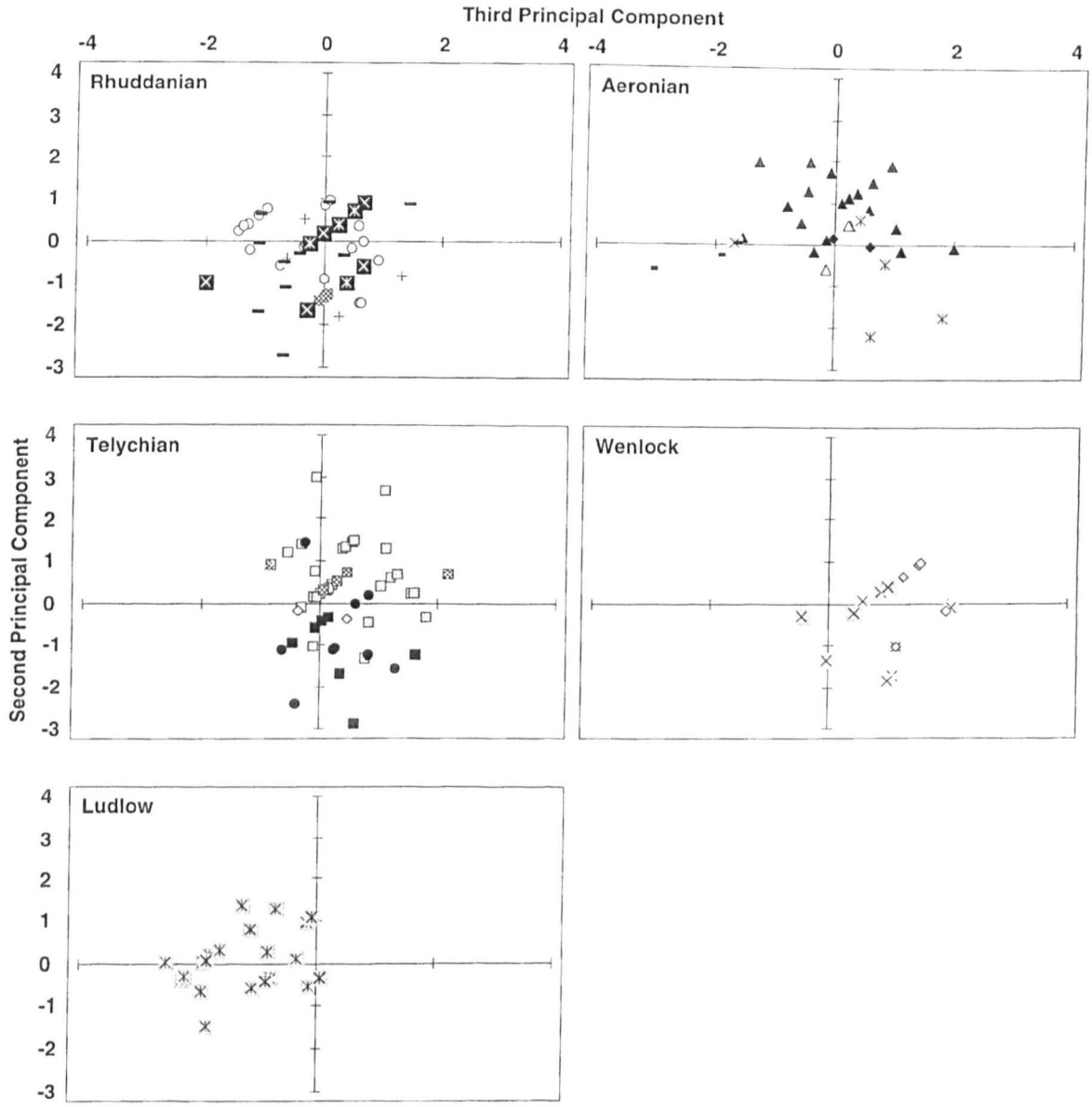

Figure 7. 14. Pygidia of *Acernaspis* and *Ananaspis* ordinated along the second and third principal component axes and grouped into five broad time intervals to illustrate changing morphospace occupation with time. Symbols as in Figure 7. 6. n=166.

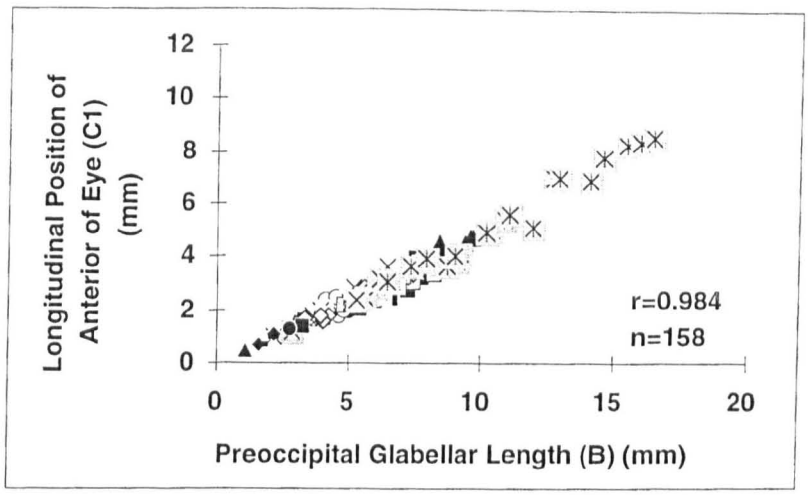

Figure 7. 15. Bivariate scatter plot of longitudinal position of anterior of eye (C1) against preoccipital glabellar length (B). Symbols as in Figure 7. 6.

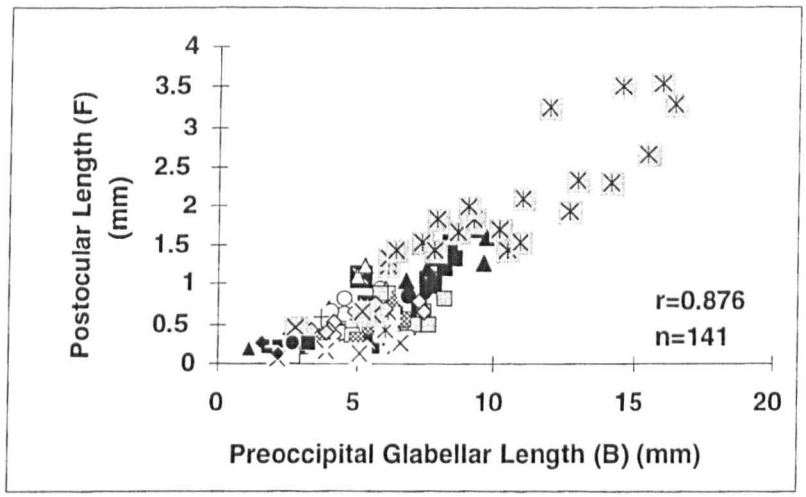

Figure 7. 16. Bivariate scatter plot of postocular length (F) against preoccipital glabellar length (B). Symbols as in Figure 7. 6.

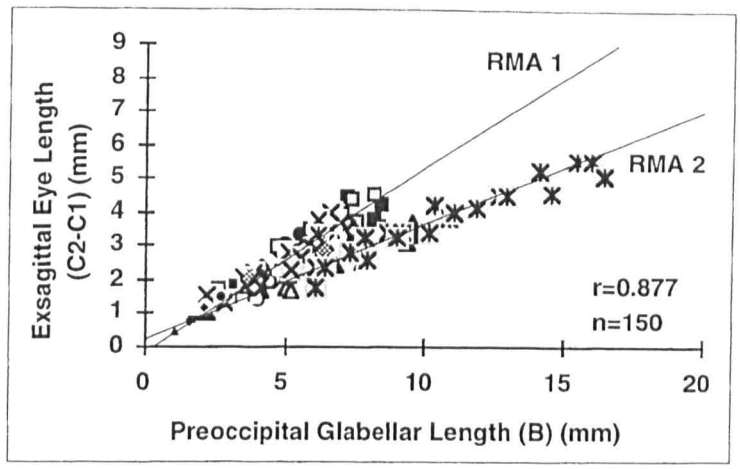

Figure 7. 17. Bivariate scatter plot of exsaggital length of eye (C2-C1) against preoccipital glabellar length (B). Best-fit lines to the data calculated using the reduced major axis method. RMA 2 fitted to specimens from the samples NEWLANDS, KOS-KOL-LOC and UCHAF. RMA 1 fitted to all other specimens. Symbols are as in Figure 7. 6.

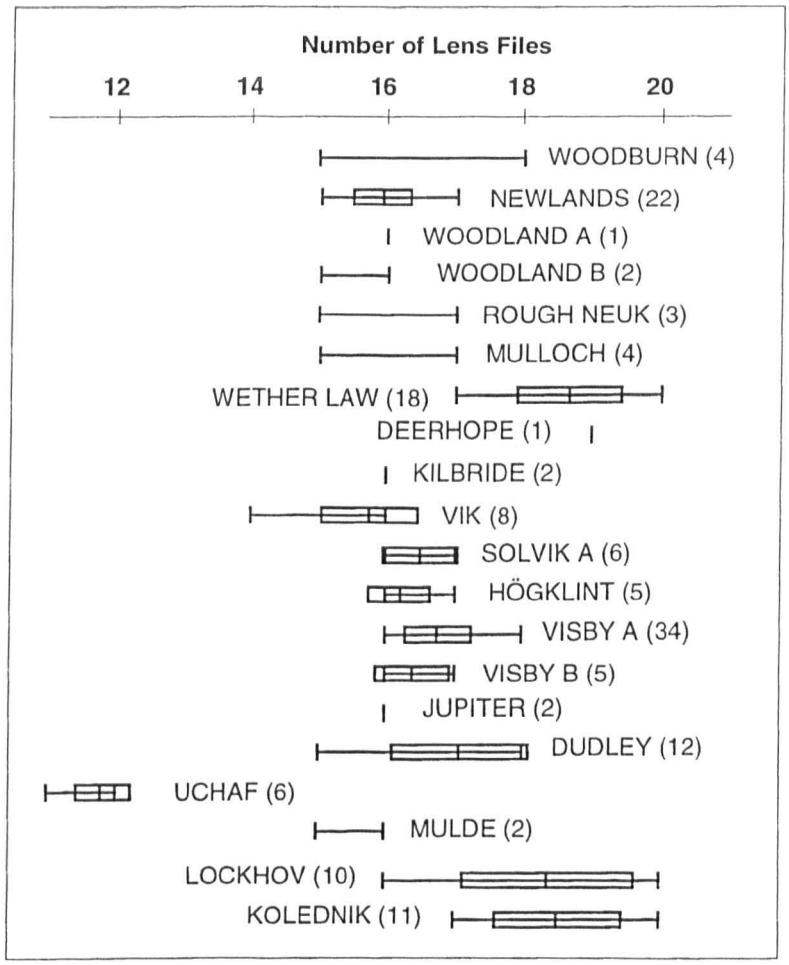

Figure 7. 18. Variation in the number of dorso-ventral lens files in the visual surface. Total range of values and number of countable specimens shown for each stratigraphical sample, mean value and one standard deviation to either side of the mean shown for samples containing five or more countable specimens. Localities which make up the KOS-KOL-LOC sample are shown individually.

the null hypothesis that mean eye length (C2-C1) for samples in the NEWLANDS group is the same as the mean for samples in the group of remaining samples at the 95% confidence interval.

However, if one considers the number of lens files in the visual surface (Figure 7. 18) there is no obvious relationship between exsag. eye length and number of lens files (this is therefore a different situation to that found with *Achatella* (Chapter 5) and *Calyptaulax* (Chapter 6) where it was found that species possessing relatively longer eyes also had more lenses in the visual surface). The diameter of the lenses has not been measured. However, on inspection of the visual surfaces of specimens belonging to the samples NEWLANDS, UCHAF, and KOS-KOL-LOC, it can be seen that the lenses are relatively small with clear regions of sclera between neighbouring lenses (see for example Plate 7. 1, fig. 15). This is a different condition to that shown by specimens belonging to other samples, in which the lenses appear generally slightly bigger and are in contact with their neighbours (see for example Plate 7. 2, figs. 9, 11; see also illustrations of the visual surface of *A. superciliexcelsis* (represented herein by sample NEWLANDS) in Howells 1982: pl. 11, figs. 3b, 4). One obvious feature of Figure 7. 18 is that all specimens belonging to UCHAF have relatively fewer lens files (11 or 12) than other samples. These Welsh specimens are also rather small (maximum glabellar length 5.3mm), but all known specimens are of similar size and, despite their small size, of similar proportions to the much larger specimens belonging to KOS-KOL-LOC (cf. their overlapping PC occupation fields, Figure 7. 9), so there is no reason to suppose that they are not adult specimens.

Figure 7. 19 shows statistical lens charts for the samples, compiled after the method of Campbell (1977) as modified by Clarkson and Tripp (1982). It can be seen from Figure 7. 19 that visual surfaces of *Acernaspis* fall broadly into two classes: slightly "smaller" (*i.e.* shorter and lower) visual surfaces with maximum number of lens files in the range 16-18 and maximum number of lenses in a file in the range 5-7 (stratigraphical samples MULLOCH, ROUGH NEUK, WOODLAND A, WOODLAND B, NEWLANDS, KILBRIDE, VIK, VISBY B, and HÖGKLINT), and slightly "larger" (*i.e.* longer and deeper) visual surfaces with maximum number of lens files in the range 17-20 and maximum number of lenses in a file in the range 8-9 (stratigraphical samples WOOD BURN, DEERHOPE, WETHER LAW, SOLVIK A, and VISBY A). The samples DUDLEY, UCHAF, MULDE and KOS-KOL-LOC show a range of variation in visual structure. Specimens belonging to UCHAF have very small eyes (up to 12 lens files, maximum of five lenses in a file). The eye of MULDE is comparable with the "smaller type" of *Acernaspis* eye noted above. The DUDLEY eye resembles the "larger type" *Acernaspis* eye described

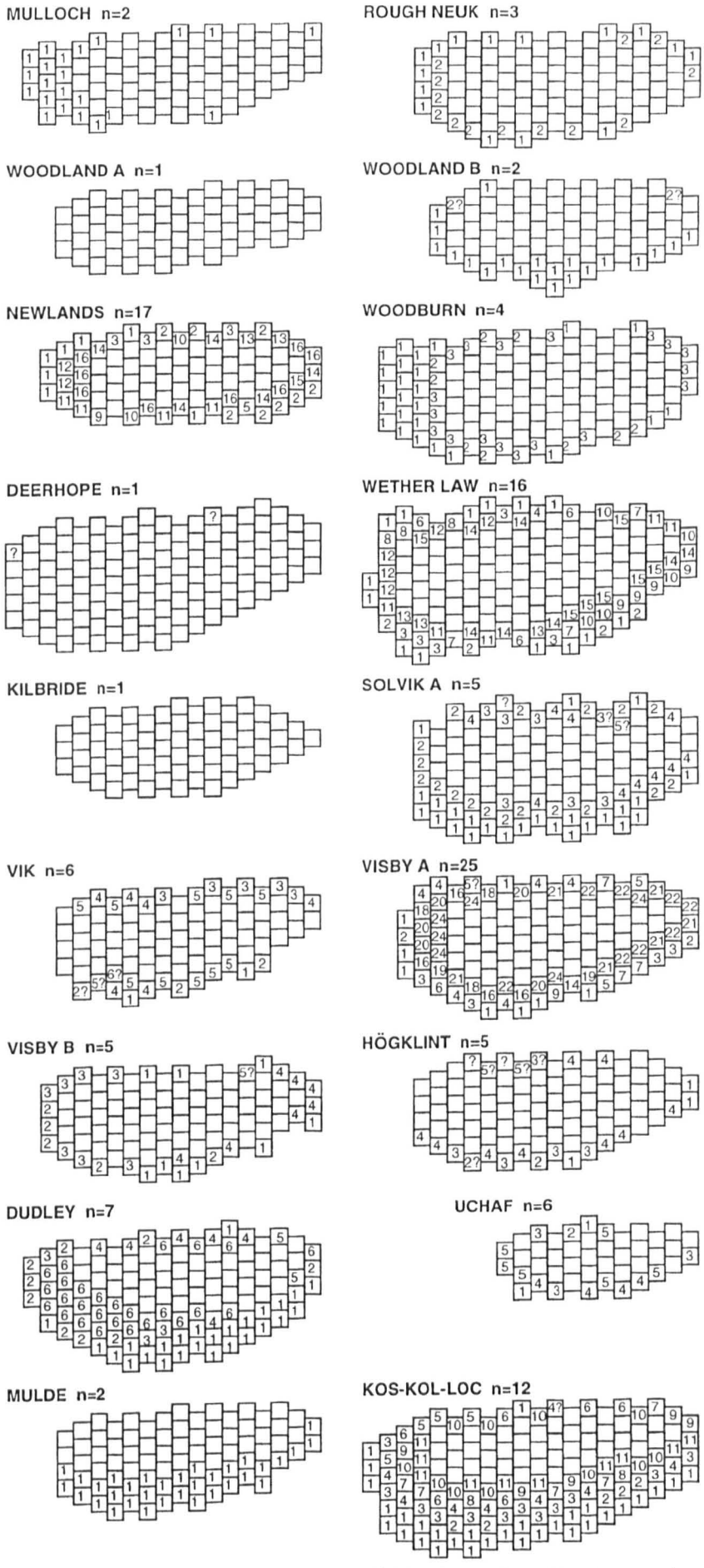

Figure 7. 19. Statistical lens charts for stratigraphical samples assigned to *Acernaspis* and *Ananaspis* (see Section 7. 2). Charts constructed using the method of Campbell (1977) as modified by Clarkson and Tripp (1982). Left eye of each specimen used where sufficiently well preserved, right eye used otherwise. Anterior of eyes to the left. Numbers indicate how many specimens possess a lens at that location on the visual surface. Locations with no number indicate that all specimens possess a lens at that location.

above. KOS-KOL-LOC has many more lenses in the visual surface than any *Acernaspis* specimen.

In their cladistic analysis of phacopines, Ramsköld and Werdelin (1991) considered several other measurable characteristics which show variation both within *Acernaspis* and between *Acernaspis* and *Ananaspis*. These were: relative glabellar width (tr.) across the widest point (their character 1; represented by the ratio K2/J herein); relative width (tr.) of the occipital ring (their character 3; represented by the ratio K/J herein); relative length of L2 and L3 lobes (their character 6; represented by the ratio b32/b21 herein); relative width of pygidial axis (their character 26; represented by the ratio X/W herein). Variation in these characters is shown in Figures 7. 20 to 7. 23. Any slight flattening of the cephalon has the effect of splaying out its lateral margins so that the measurement I is slightly altered, and this may account for some of the wide variation in the ratios K2/I and K/I in some samples, notably NEWLANDS and SOLVIK A. The cladistic codings used by Ramsköld and Werdelin (1991) do not take the actual variation in these measurements adequately into account, and this seems to be a serious limitation on the quality of their results.

On the basis of the morphometrics carried out in this study and the phylogenetic analysis of Ramsköld and Werdelin (1991), the stratigraphical samples are assigned to species as follows (in stratigraphical order):

Acernaspis :

A. elliptifrons (Esmark, 1833). Includes SOLVIK A, SOLVIK B, MULLOCH, ROUGH NEUK. This species is defined on the basis of:

(i) Intercalating ring confluent with the glabella or raised slightly above it (Plate 7. 1, figs. 2-3, 5, 8).

(ii) Relatively large eye (Figure 7. 17) with 16-18 lens files (Figure 7. 18, 7. 19 (a)).

(iii) Vincular furrow shallow and continuous anteriorly (Ramsköld and Werdelin 1991: cladistic character 24) with seven well defined lateral vincular notches (Ramsköld and Werdelin 1991: character 25; Plate 7. 1, fig. 4).

Contrary to Helbert (1985), specimens from the Solvik Fm. at Sjursøya, Oslo district (stratigraphical sample SOLVIK B) are considered conspecific with those from elsewhere in the Solvik Fm. (sample SOLVIK A). They show no morphometric difference (Figures 7. 9 - 7. 14).

A. superciliexcelsis Howells, 1982. NEWLANDS, WOODLAND A. This species is defined on the basis of:

(i) High glabellar convexity (Plate 7. 1, figs. 12, 14-15).

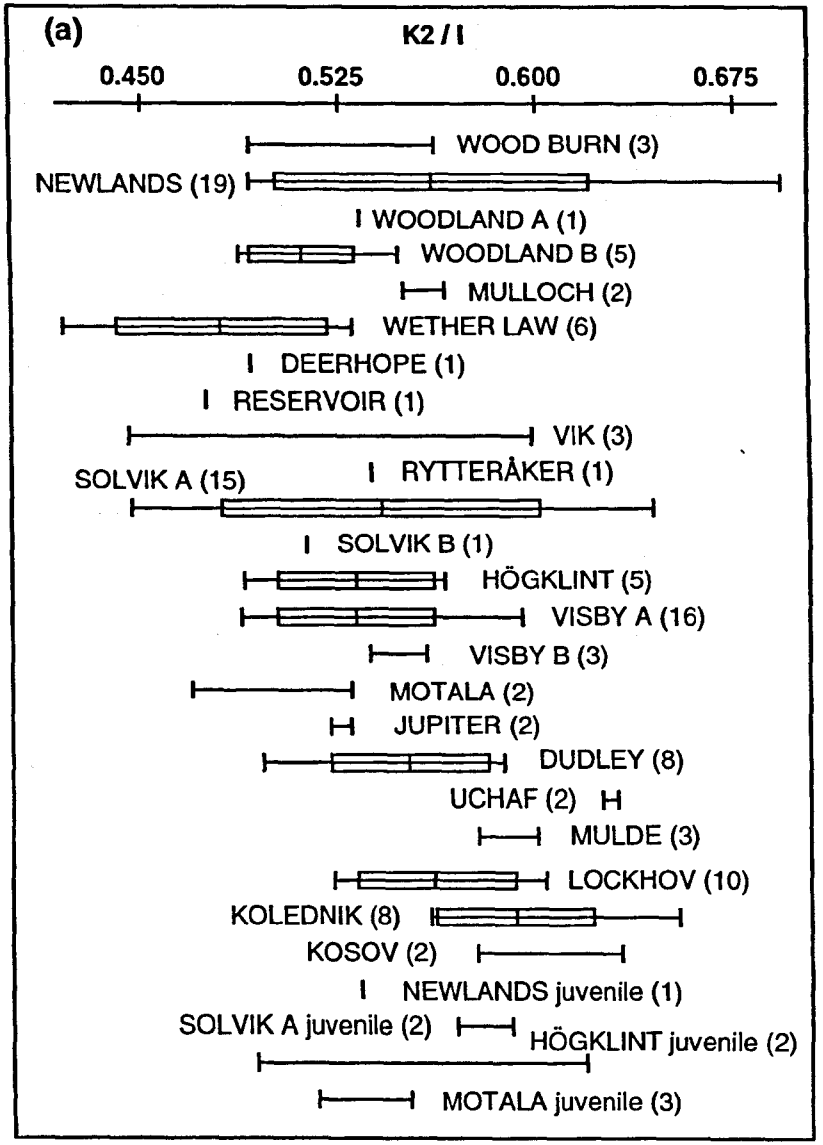

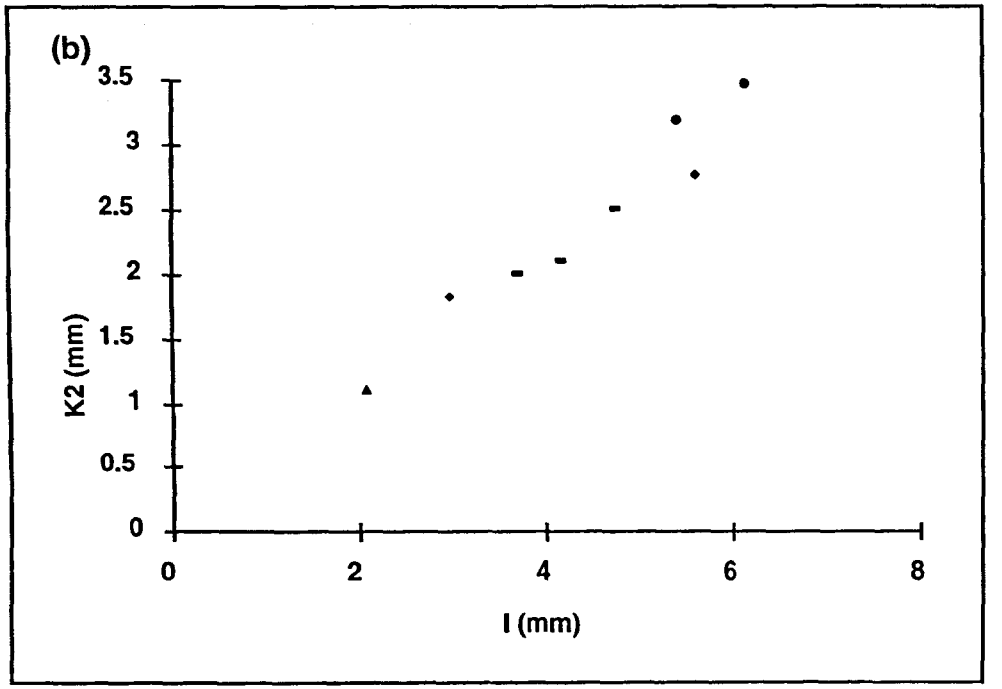

Figure 7. 20. Variation in relative maximum width of the glabella. (a) univariate variation in the ratio of maximum glabellar width (K2) / maximum cephalic width (I). Total range of values and number of measurable specimens shown for each stratigraphical sample, mean value and one standard deviation to either side of the mean shown for samples containing five or more measurable specimens. (b) bivariate scatter plot of K2 against I for ontogenetic (juvenile) specimens. Symbols as in Figure 7. 6.

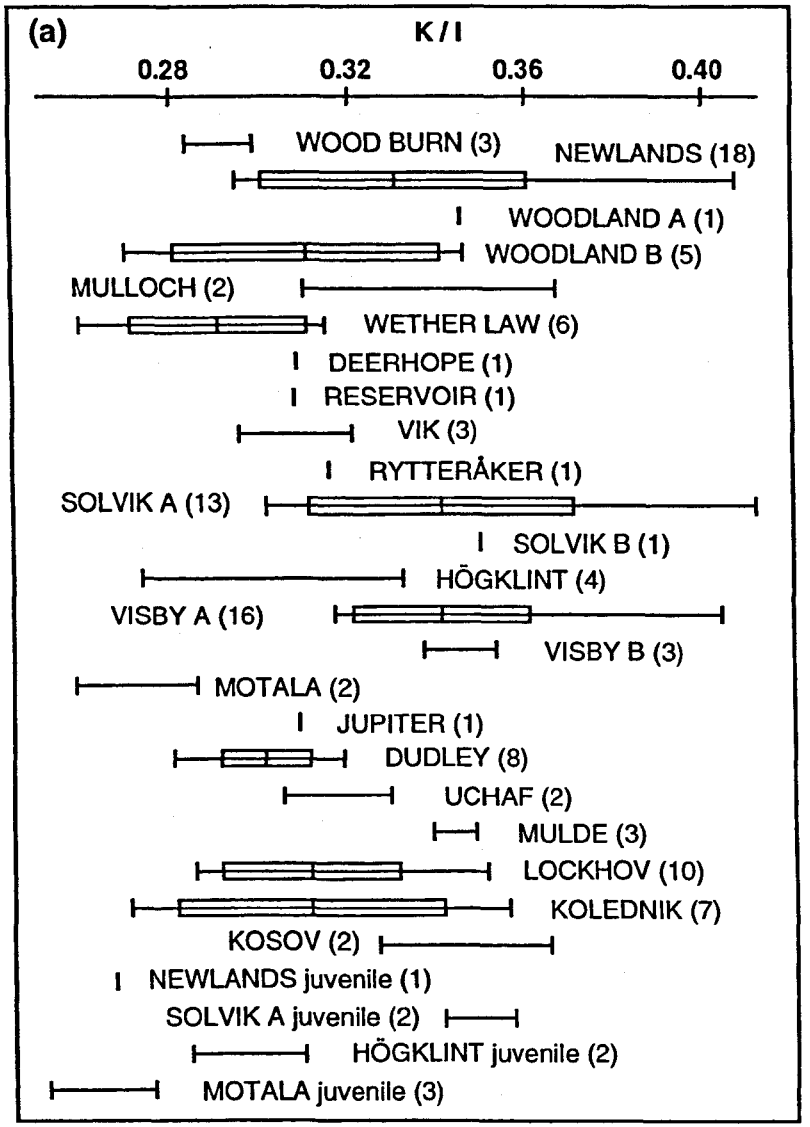

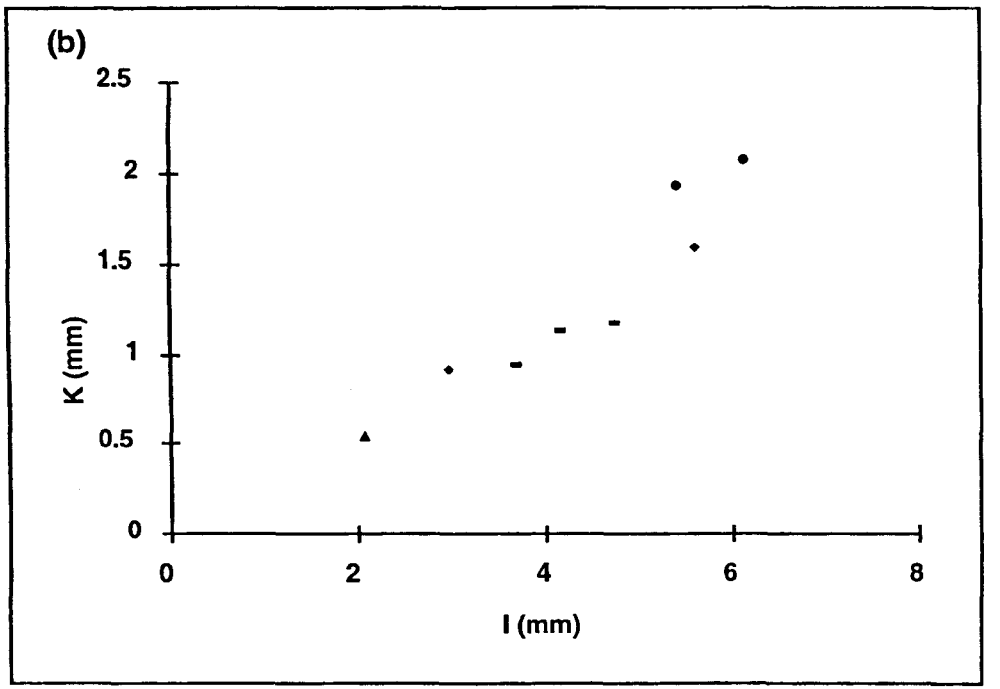

Figure 7. 21. Variation in relative maximum width of the occipital ring. (a) univariate variation in the ratio of width of occipital ring (K) / maximum cephalic width (I). Total range of values shown for each stratigraphical sample, mean and one standard deviation to either side of the mean shown for samples containing five or more measurable specimens. (b) bivariate scatter plot of K against I for ontogenetic (juvenile) specimens. Symbols as in Figure 7. 6.

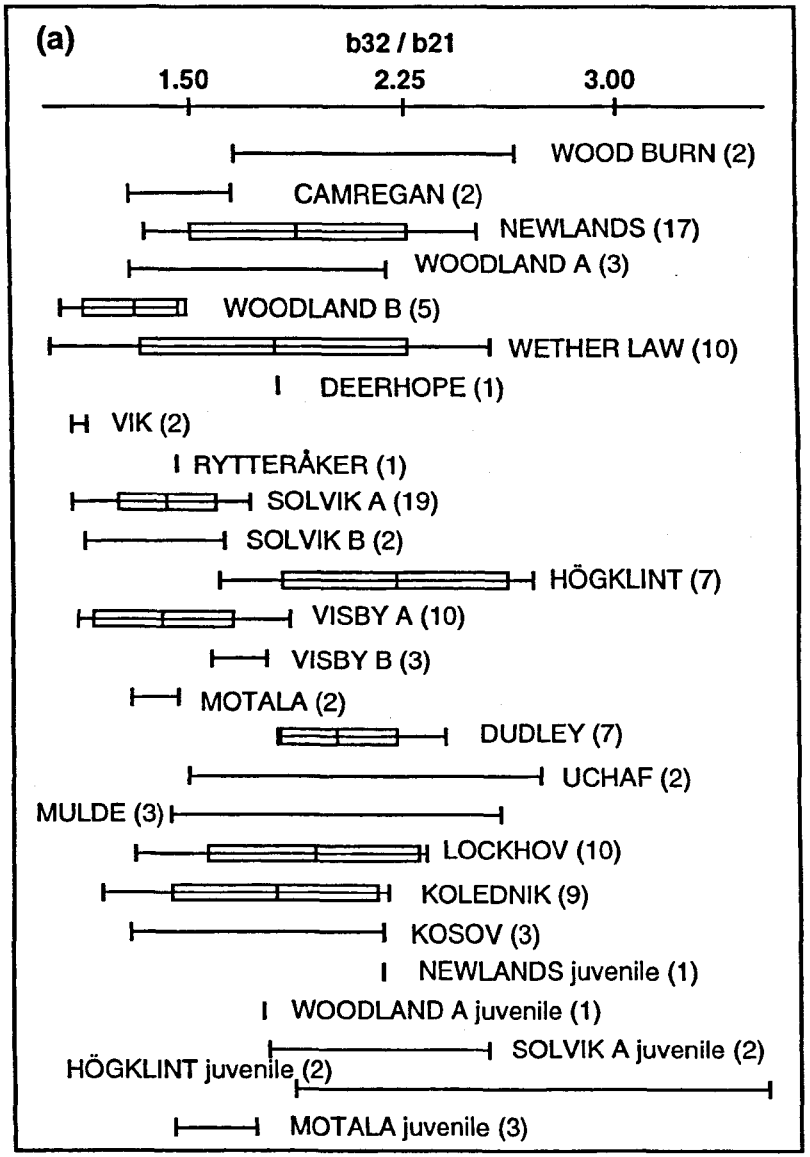

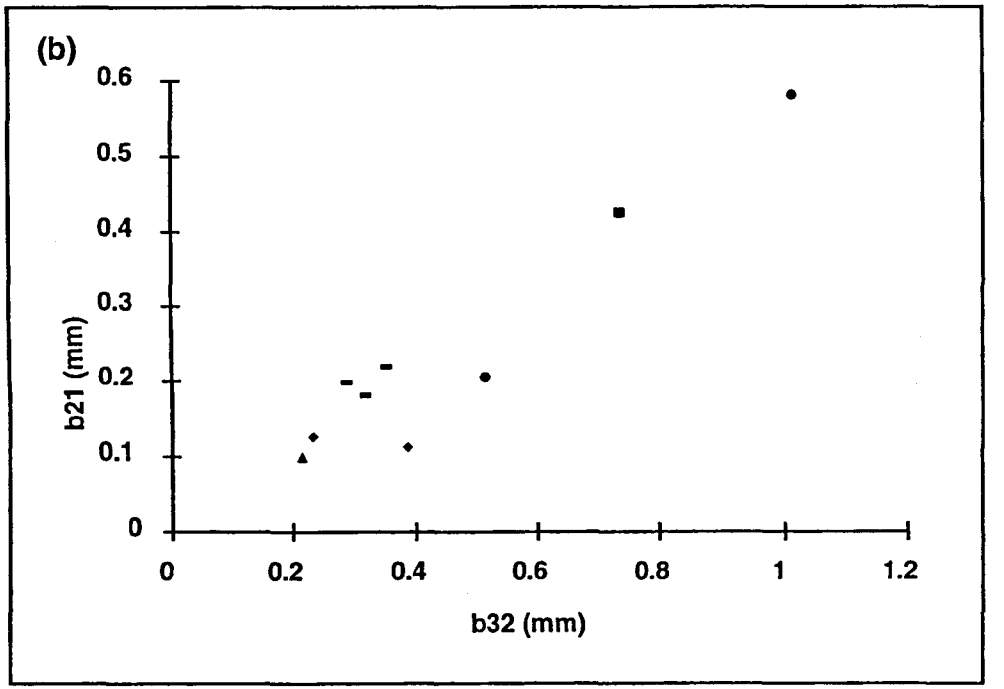

Figure 7. 22. Variation in the relative lengths of the L3 and L2 glabellar lobes. (a) univariate variation in the ratio of distal length of L3 (b32) / distal length of L2 (b21). Total range of values shown for each stratigraphical sample, mean and one standard deviation to either side of the mean shown for samples containing five or more measurable specimens. (b) bivariate scatter plot of b32 against b21 for ontogenetic (juvenile) specimens. Symbols as in Figure 7. 6.

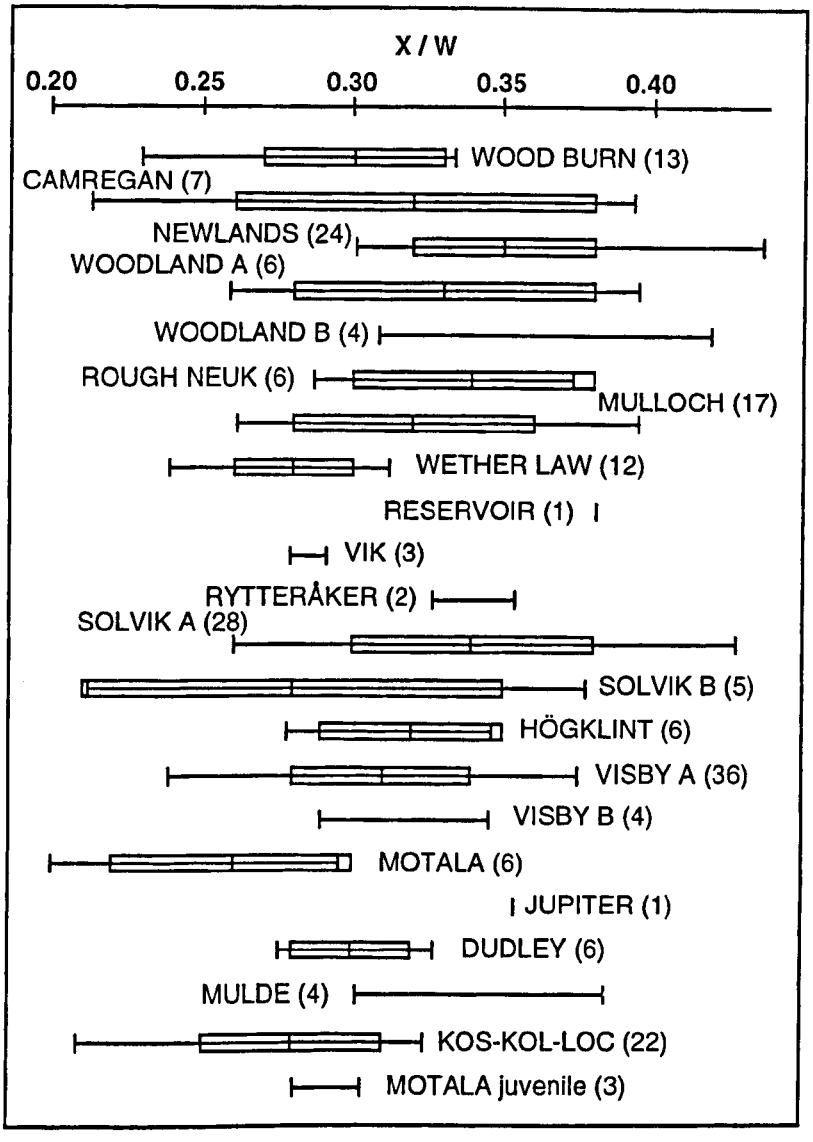

Figure 7. 23. Univariate variation in the ratio width of pygidial axis (X) / pygidial width (W). Total range of values and number of measurable specimens shown for each stratigraphical sample, mean and one standard deviation to either side of the mean shown for samples containing five or more measurable specimens.

(ii) Very deeply impressed S1 furrows (Plate 7. 1, figs. 11-12, 14-15).
(iii) Intercalating ring markedly depressed below the level of the glabella.
(iv) Relatively short (exsag.) eye (Figure 7. 17) with 15-17 lens files.
(v) Palpebral lobe approximately level with the palpebral area.
(vi) Anterior of vincular furrow continuous and shallow (Ramsköld and Werdelin 1991: cladistic character 24), lateral part deeper with nine well defined vincular notches (Ramsköld and Werdelin 1991: character 25; Plate 7. 1, fig. 17).

A. xynon Howells, 1982. WOODLAND B. Morphometrically similar to WOODLAND A and NEWLANDS, but distinguished by:
(i) Small genal spines on the genal angles (Ramsköld and Werdelin 1991: cladistic character 16; Plate 7. 1, fig. 20; Plate 7. 2, fig. 2).
(ii) Intercalating ring confluent with the glabella (Plate 7. 1, figs. 19-20; Plate 7. 2, figs. 1-2).
(iii) Maximum glabellar width slightly lower than that of *A. superciliexcelsis* (Figure 7. 20).
(iv) Pygidial axis terminates some way from the posterior pygidial margin, whereas in *A. superciliexcelsis* the axis extends posteriorly almost to the posterior margin.

A. sp. nov. A. CAMREGAN, MOTALA. Due to quality of preservation, many measurements are not obtainable for the Lower Camregan Grits specimens. Specimens from the approximately contemporaneous sample MOTALA are here considered conspecific with CAMREGAN. They are morphometrically very similar (Figure 7. 7 - 7. 23) and agree with the CAMREGAN material in all the characteristics listed below. The species is distinguished by the following characteristics:
(i) Low glabellar convexity (Plate 7. 2, figs. 3, 5).
(ii) Slightly depressed intercalating ring (Plate 7. 2, fig. 3).
(iii) Transverse proximal branch of S3, close to parallel with S2.
(iv) Virtually straight axial furrows.
(v) Depressed L1.

A. sp. nov. B. VIK, RYTTERÅKER. This material was described by Helbert (1985). The species is distinguished by the following:
(i) Eye with 14-16 lens files (less than *A. sufferta*) with up to seven lenses in a file (Figure 7. 19 (a)).
(ii) Poorly impressed glabellar furrows (Plate 7. 2, fig. 10).
(iii) Palpebral area on a similar level to the palpebral lobe (Plate 7. 2, fig. 9).
(iv) Vincular structure consisting anteriorly of a pair of subfrontal depressions; laterally nine well-defined vincular notches.

A. orestes (Billings, 1860). JUPITER. The type species of the genus (as designated by Campbell 1967). It is characterised by:

(i) Palpebral area approximately level with the palpebral lobes (Ramsköld and Werdelin 1991, character 13; Figure 7. 27).

(ii) Small, circular L1 lobes which are deeply depressed below the level of the intercalating ring (Plate 7. 1, fig. 1).

(iii) Possession of a pair of deep incisions on the anterior face of the occipital ring (Plate 7. 1, fig. 1; Figure 7. 27).

(iv) Anterior part of vincular furrow deep and continuous, lateral part with well defined vincular pits.

(v) Intercalating ring small, subtriangular, transversely vaulted (Ramsköld and Werdelin 1991, character 4).

A. woodburnensis Clarkson, Eldredge and Henry, 1977. WOODLAND. Morphometrically similar to *A. sufferta* (Figures 7. 9, 7. 11, 7. 14 - 7. 17, 7. 20 - 7. 23). Differs from that species in the following:

(i) Straight axial furrows (Plate 7. 2, figs. 7, 13).

(ii) Relatively high number of axial rings (eight to ten; Figure 7. 13).

(iii) Lower mean number of lens files than *A. sufferta* (15-18 files, whereas *A. sufferta* has 17-20; Figure 7. 18).

(iv) Relatively narrow occipital ring (a character shared with *A. sufferta*, Figure 7. 21; Ramsköld and Werdelin 1991 character 3).

A. sufferta Lamont, 1947. WETHERLAW, RESERVOIR, DEERHOPE. Morphometrically similar to *A. woodburnensis* and *A.* sp. nov. B (Figures 7. 9, 7. 11, 7. 14). *A. sufferta* is distinguished by the following:

(i) Eye with 17-20 lens files, up to eight lenses per file (Figure 7. 18, 7. 19 (a)).

(ii) Anterior portion of vincular furrow consisting of a pair of subfrontal depressions to either side of the midline. This character is shared with *A. woodburnensis*. However, *A. sufferta* has no shallow furrow connecting these depressions with the lateral part of the vincular furrow.

(iii) Convex-outward axial furrows as seen in dorsal view. This distinguishes this species from *A. woodburnensis* (Plate 7. 2, figs. 8, 12, 14, 16)

(iv) Relatively narrow glabella (Figure 7. 20).

(v) Posterior extremities of palpebral lobes approximately same distance apart as the anterior extremities. This distinguishes this species from *A. woodburnensis* in which the anterior of the eyes are closer together than the posterior.

(vi) Shares the characteristic of having a relatively narrow occipital ring with *A. woodburnensis* (Figure 7. 21).

A. sp. nov. C. KILBRIDE. Due to poor preservation of these specimens, few measurements could be obtained for this material. This species is very similar in appearence to *A.* sp. nov. A. It differs from that species in the following:

(i) Intercalating ring not depressed below the level of the glabella (Plate 7. 2, fig. 18).

These specimens are therefore tentatively held as a separate species from *A.* sp. nov. A.

A. quadrilineata (Angelin, 1851). VISBY A. This species is characterised by:

(i) Shallow furrows on the cephalon and pygidium. The cephalic axial furrows are especially shallow adjacent to L1 (Plate 7. 2, figs. 21-22; Plate 7. 3, fig. 1).

(ii) Anterior branch of vincular furrow consisting of a wide, shallow continuous furrow; lateral parts with well-defined vincular notches (Ramsköld and Werdelin 1991, characters 24 and 25).

A. sororia (Ramsköld, 1985). VISBY B. This species is morphometrically similar to *A. quadrilineata* (Figures 7. 9 - 7. 23). It is distinguished from that species on the basis of the following:

(i) Sculpture of dense granules (Plate 7. 3, figs. 2-3). The surface of *A. quadrilineata* is smooth in most specimens, or has scattered, low granules in a few specimens.

(ii) Axial and posterior border furrows deeply impressed; palpebral furrows moderately impressed.

(iii) Genal angles have small nodes (Plate 7. 3, fig. 3).

(iv) Occipital ring more strongly incised anteriorly.

A. rubicundula (Ramsköld, 1985). HÖGKLINT. This species is characterised by the following:

(i) Short postocular area (Figure 7. 10 (a)).

(ii) High ratio of distal length of L3 / distal length of L2 (=b32/b21), comparable with that of species of *Ananaspis* (Figure 7. 22).

(iii) Tuberculate glabella (Plate 7. 3, fig. 4).

Ananaspis:

A. sp. nov. A. UCHAF. These specimens were compared with *A. fecunda* by Rushton *in* Warren *et al.* (1984), and morphometrically they are very similar to that species (Figures 7. 9 - 7. 17, 7. 20 - 7. 22). They are distinguished on the basis of the following:

(i) Relatively small size (Figure 7. 8).

(ii) Possession of only 11 or 12 lens files in the eye, with up to four lenses in the deepest files (as opposed to 16 - 20 files of up to eight lenses per file in the type species).

(iii) Less steeply sloping anterior face of the glabella.

(iv) Maximum width of the glabella is at the point at which the posterior branch of the facial suture meets the lateral border furrow, rather than just behind this point as in the type species (Plate 7. 3, fig. 12).

Ananaspis amelangorum Ramsköld, 1985. MULDE. This species is distinguished by:

(i) Possession of a narrow anterior border; the anterior face of the glabella rises much less steeply than in the type species of the genus.

(ii) Lesser glabellar convexity than the type species.

(iii) Maximum cephalic width is at the point at which the posterior branch of the facial suture meets the lateral cephalic border, rather than just behind this point as in the type species.

(iv) Possession of only moderately coarse glabellar tuberculation.

(v) Anterior branch of the vincular furrow is a continuous furrow, rather than a bevel on the anterior of the vincular surface of the doublure as in the type species.

(vi) The pygidial axis is relatively wider than that of other species of the genus (Figure 7. 23).

(vii) Eye with 15 or 16 lens files with up to six lenses per file, as opposed to 16 to 20 files with up to eight lenses per file in the type species (Figures 6. 18, 6. 19 (b)),

Ananaspis stokesii (Milne Edwards, 1840). DUDLEY. This species is morphometrically similar to *A. amelangorum* (Figures 7. 9 - 7. 18, 7. 20). It is distinguished by:

(i) Low cephalic convexity (less than that of *A. amelangorum* ; Plate 7. 3, fig. 16).

(ii) Possession of only moderate tuberculation on the glabella and palpebral areas (Plate 7. 3, figs. 9, 13, 15).

(iii) Postocular area short for the genus (Figure 7. 10(a)).

(iv) Anterior part of vincular furrow is a bevel on the anterior of the doublure (Plate 7. 3, fig. 17).

Ananaspis fecunda (Barrande, 1846). KOL-KOS-LOC. This is the type species of the genus, as designated by Campbell (1967). It is distinguished by the following characteristics:

(i) Strongly inflated glabella with its anterior face standing vertically over the anterior cephalic margin (Plate 7. 3, fig. 10).

(ii) Possession of coarse tuberculation on the glabella and palpebral areas (Plate 7. 3, figs. 6-8).

(iii) Anterior part of vincular furrow forming a bevel on the anterior of the ventral surface of the cephalic doublure; lateral part with only weakly developed vincular pits.

(iv) Eye with 16 to 20 lens files of up to eight lenses in a file (Figures 7. 18, 7. 19 (b)).

These are the species of *Acernaspis* and *Ananaspis* recognised for the stratigraphical samples morphometrically studied herein. A number of species identified by Ramsköld and Werdelin (1991) (chiefly those from Estonia and Anticosti Island) could not be included due to unavailability of well preserved material.

7. 4. 3. Ontogeny and the Relationship between *Acernaspis* and *Ananaspis*.

Ramsköld (1988) and Ramsköld and Werdelin (1991) highlighted ontogentic variation in a number of characters in *Acernaspis*, and Ramsköld (1988) suggested a neotenic derivation of *Ananaspis* from *Acernaspis* on the basis of this variation. Both these two studies included consideration of species of *Ananaspis* not available for direct study herein. Figure 7. 24 shows ontogenetic material of *Acernaspis*. The characters considered by Ramsköld (1988) which are amenable to morphometric analysis are the following:

Shape of the occipital ring. (Character A of Ramsköld 1988; cladistic character 3 of Ramsköld and Werdelin 1991; represented by the ratio K/I herein; Figure 7. 21). Ramsköld (1988) noted an increase in relative width of the occipital ring with ontogeny in *Acernaspis*, which is borne out in Figure 7. 21. However he detected no clear distinction in this character between *Acernaspis* and *Ananaspis*, and this is also clear from the data studied herein. While holaspides of some species of *Ananaspis* resemble juvenile *Acernaspis* in this character, others do not.

Length of L2 relative to L3. (Character C of Ramsköld 1988; character 6 of Ramsköld and Werdelin 1991; represented by the ratio b32/b21 herein; Figure 7. 22). Ramsköld (1988) noted a relative increase in the length of L2 with ontogeny in *Acernaspis*. The relative length of L2 against L3 in *Ananaspis* was described by him as variable, but holaspides of *Ananaspis* in general possess slightly shorter L2 than holaspides of *Acernaspis*. This is confirmed in Figure 7. 22. This character therefore shows similarity between *Acernaspis* juveniles and holaspides of most species of *Ananaspis*. The ratio of b32/b21 in HÖGKLINT, for which Ramsköld (1985) erected *Acernaspis rubicundula*, and which was maintained within *Acernaspis* by Ramsköld and Werdelin (1991) in spite of its "very odd morphology" (Ramsköld and Werdelin 1991: 50), is

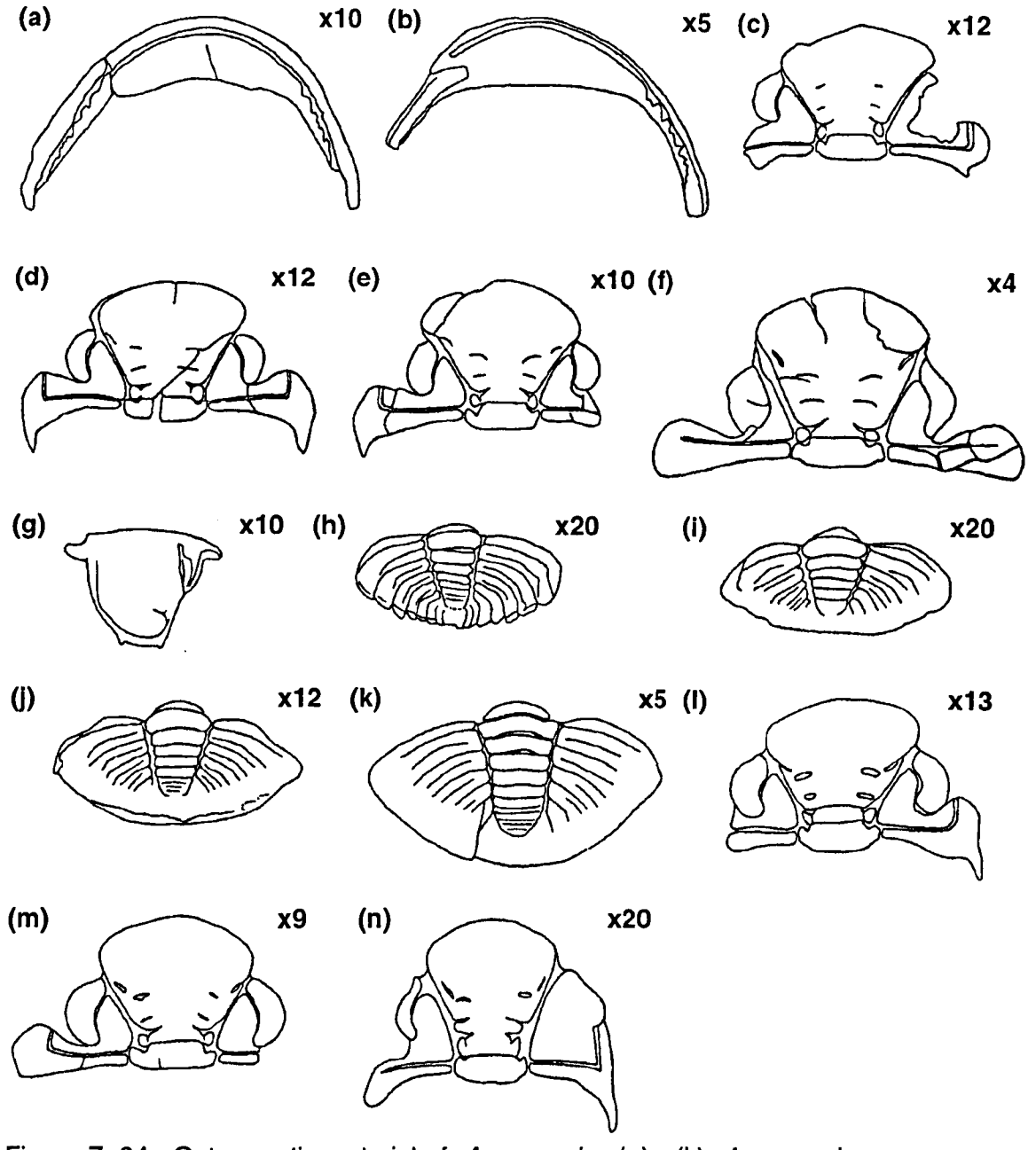

Figure 7. 24. Ontogenetic material of *Acernaspis*. (a) - (k) *Acernaspis* sp. nov. A (=*A.* "*dispersa* " of Ramsköld 1988) (middle Llandovery), Gustavsvik, Motala, Östergötland. (a) ventral view of cephalic doublure of juvenile, RM Ar53607; (b) same, adult, RM Ar53608; (c) dorsal view of juvenile cranidium, RM Ar53609; (d) same, RM Ar53610; (e) same, RM Ar53611; (f) dorsal view of adult cranidium, RM Ar 53612; (g) ventral view of juvenile hypostome, RM Ar53613; (h) dorsal view of juvenile pygidium, RM Ar53614; (i) same, RM Ar53615; (j) same, RM Ar53616; (k) dorsal view of adult pygidium, RM Ar53617. (l) - (m) *Acernaspis rubicundula* Ramsköld, 1985, Högklint Fm. (Sheinwoodian Stage, Wenlock Series), Visby district, Gotland. (l) dorsal view of juvenile cranidium, RM Ar53618; (m) same, SGU Type 5200. (n) *Acernaspis superciliexcelsis* Howells, 1982, Newlands Fm. (Aeronian Stage, Llandovery Series), Newlands Farm, Girvan district, Scotland. Dorsal view of juvenile cranidium, HM A10308. All redrawn from Ramsköld (1988: figure 1).

comparable with *Ananaspis* specimens. (Note that relative length of L2 and L3 is quantified in this study using measurements made parallel to the sagittal line (see Figure 7. 5), and is therefore not directly comparable with the method used by Ramsköld 1988 and Ramsköld and Werdelin 1991 who measured the lengths of these lobes normal to the direction of S2). Therefore, in this glabellar proportion, and in its tubercular glabellar sculpture (see above), *A. rubicundula* resembles *Ananaspis* rather than *Acernaspis*. However, this species exhibits other characteristics diagnostic of *Acernaspis* (see below): only moderate convexity of the glabella; distal branch of S3 straight or convex-outward in the holaspide (this furrow is concave-outward in holaspides of *Ananaspis*, see below); lack of a lateral border furrow. In view of these features and the phylogenetic conclusions of Ramsköld and Werdelin (1991) this species is maintained within *Acernaspis* herein. However, it appears to be morphologically intermediate between other species of *Acernaspis* and *Ananaspis*.

Length of the postocular area. (Character F of Ramsköld 1988; character 11 of Ramsköld and Werdelin 1991; represented by the ratio F/B herein; Figure 7. 10). Ramsköld (1988) noted a marked decrease in the length of the postocular area with ontogeny in *Acernaspis*. He also noted a high degree of variation in this measurement in *Ananaspis*, so that on its own this measurement does not distinguish between the two genera. PCA on the cephalon data set (above) highlighted this variation, which is illustrated in Figure 7. 10 (a). The ontogenetic trend described by Ramsköld (1988) is also borne out by Figure 7. 10. While holaspides of some species of *Ananaspis* resemble juvenile *Acernaspis*, others do not.

Ramsköld (1988) also described ontogenetic variation in several other characters not directly amenable to morphometric analysis. Briefly, these were:

Shape of the intercalating ring. (Character B of Ramsköld 1988; character 4 of Ramsköld and Werdelin 1991). The intercalating ring is higher and longer (sag. and exsag.) in juveniles of *Acernaspis* than in adults (Figure 7. 24). The form of the intercalating ring in *Ananaspis* cannot be used to distinguish that genus from *Acernaspis* (Ramsköld 1988). Therefore, it cannot be stated that juveniles of *Acernaspis* resemble holaspides of *Ananaspis* in this character.

Depth of S2 and the proximal part of S3. (Character D of Ramsköld 1988; not used by Ramsköld and Werdelin 1991). These furrows are deeper in juveniles of *Acernaspis* than in adults. They are also moderately deep or deep in adults of all species of *Ananaspis* (Ramsköld 1988) (Plate 7. 3, figs. 5-8, 11-13). Therefore, juvenile *Acernaspis* resemble holaspide *Ananaspis* in this character.

Lateral extension of S2. (Character E of Ramsköld 1988; not used by Ramsköld and Werdelin 1991). S2 tends to extend further abaxially (closer to the axial furrow) in *Acernaspis* juveniles than in adults (Figure 7. 24). This character cannot be used to distinguish *Ananaspis* from *Acernaspis* (Ramsköld 1988). It cannot therefore be stated that juveniles of *Acernaspis* resemble holaspides of *Ananaspis* in this character.

Depth of the palpebral furrow. (Character G of Ramsköld 1988; character 15 of Ramsköld and Werdelin 1991). The palpebral furrow is deep in juvenile specimens, shallower in adults. The furrow is also deep in most species of *Ananaspis* (Ramsköld 1988) (Plate 7. 3, figs. 6-9, 11-15). Juvenile *Acernaspis* therefore resemble holaspides of most species of *Ananaspis* in this character.

Nature of the lateral border furrow. (Character H of Ramsköld 1988; character 12 of Ramsköld and Werdelin 1991). Juvenile *Acernaspis* specimens possess a deep lateral border furrow, while adult specimens have only a faint furrow or no furrow at all (Figure 7. 24). Species of *Ananaspis* usually possess a deep lateral border furrow (Ramsköld 1988) (Plate 7. 3, figs. 5, 7, 9-16). Juvenile *Acernaspis* therefore resemble holaspides of most species of *Ananaspis* in this character.

Length (exsag.) of fixed cheek between the facial suture and the posterior border furrow. (Character I of Ramsköld 1988; not used by Ramsköld and Werdelin 1991). Ramsköld (1988) noted that this measurement is closely dependent on the course of the posterior branch of the facial suture, which itself is largely dependent on the position of the eye. This character can therefore be expected to show a pattern resembling that of "length of postocular area" above. Ramsköld (1988) described a decrease in this measurement during ontogeny in *Acernaspis*. He further noted that *Ananaspis* species exhibit wide variation in this character, from values comparable with *Acernaspis* juveniles to values comparable with *Acernaspis* adults. Therefore, while holaspides of some species of *Ananaspis* resemble juvenile *Acernaspis* in this character, others do not.

Shape of the genal angle. (Character J of Ramsköld 1988; character 16 of Ramsköld and Werdelin 1991). Ramsköld (1988) observed that *Acernaspis*, in common with many other trilobites, possesses genal spines in the juvenile stage which are gradually reduced and finally lost during ontogeny (Figure 7. 24), an exception being holaspide specimens of *A. xynon* Howells, 1982 (stratigraphical sample WOODLAND B herein) which possess short genal spines (Plate 7. 1, fig. 20; Plate 7. 2, fig. 2). This character cannot be used to distinguish *Ananaspis* from *Acernaspis*, since no species of *Ananaspis* has genal spines in the holaspide stage. It cannot therefore be stated that juvenile *Acernaspis* resemble holaspides of *Ananaspis* in this character.

Tuberculation. (Character K of Ramsköld 1988; character 8 of Ramsköld and Werdelin 1991). Ramsköld (1988) noted that juvenile specimens of *Acernaspis* are tuberculate on the glabella, while holaspides usually lack tuberculation, an exception being *A. rubicundula* Ramsköld, 1988 (stratigraphical sample HÖGKLINT herein) which retains glabellar tuberculation in the adult (see above and Plate 7. 3, fig. 4). Species of *Ananaspis* possess moderate or strong tuberculation in the holaspide (Plate 7. 3, figs. 5-9, 11, 13, 15). Juvenile *Acernaspis* therefore resemble holaspides of all species of *Ananaspis* in this character.

Presence of an occipital node. (Character L of Ramsköld 1988; character 9 of Ramsköld and Werdelin 1991). Ramsköld (1988) stated that a central tubercle on the occipital ring is present in *Acernaspis* juveniles, but usually lost in adults. Again, *A. rubicundula* is an exception, possessing a faint node in the adult (Plate 7. 3, fig. 4). *Ananaspis* species may possess a strong node, a faint node, or may lack a node altogether. Holaspides of some species of *Ananaspis* therefore resemble juvenile *Acernaspis*, while others do not.

Curvature of the distal branch of S3. A further difference between holaspides of *Acernaspis* and *Ananaspis* is evident, but was not noted by Ramsköld (1988) or Ramsköld and Werdelin (1991). The distal branch of S3 is either straight or curved convex-outward in *Acernaspis* holaspides, while it is invariably curved concave-outwards in *Ananaspis* holaspides (Plate 7. 3, figs. 5-13, 16). Limited evidence in Ramsköld (1988: figure 1) suggests that the distal branch of S3 in juvenile *Acernaspis* tends to be concave-outward (Figure 7. 24). Juvenile *Acernaspis* therefore resemble holaspides of all species of *Ananaspis* in this character.

Of the 13 characters which show ontogenetic variation listed above, six show similarity between juvenile *Acernaspis* and holaspides of most species of *Ananaspis*. With the exception of the character dealing with length of L2 relative to L3, all characters which show such similarity relate to cephalic sculpture and nature (depth and curvature) of cephalic furrows.

Ramsköld (1988) created a matrix showing the number of characters shared by each of his 13 species of *Ananaspis* (some of which were later reassigned to other genera by Ramsköld and Werdelin 1991, but which are still envisaged as forming part of the same general lineage; see Section 7. 2) with a generalised *Acernaspis* juvenile. His matrix (Ramsköld 1988: table 1) showed an increase in the number of shared states (NSS) between *Ananaspis* and juvenile *Acernaspis* for each successively stratigraphically later species of *Ananaspis*. Ramsköld interpreted this as indicating progressive neoteny

with time (*i.e.* stratigraphically later *Ananaspis* species have more in common with juvenile *Acernaspis* than do stratigraphically earlier ones). As mentioned above, Ramsköld's (1988) NSS analysis included a number of *Ananaspis* species subsequently reassigned to other genera. Also, he did not include the specimens from the upper Mottled Mudstone (Homerian Stage) of North Wales. Further, it is unclear what sample sizes Ramsköld's (1988) quoted cephalic proportions for *Ananaspis* holaspides are based on. In order to take advantage of the more complete morphometric data available herein, to elucidate the position of the upper Mottled Mudstone species in the *Acernaspis* - *Ananaspis* morphological series, and to highlight the much closer similarity of *Acernaspis* juveniles to *Ananaspis* holaspides than to *Acernaspis* holaspides, an NSS analysis has been done for all species of *Acernaspis* and *Ananaspis* morphometrically studied herein, using the method of Ramsköld (1988). Each species of *Acernaspis* and *Ananaspis* has been compared with a generalised *Acernaspis* juvenile, using the following eight ontogenetically varying characters:

1. Length of L2 relative to L3: coded simply as "short" or "long" (juvenile *Acernaspis* "short", Ramsköld 1988). Coded with reference to Figure 7. 22.
2. Depth of S2 and proximal part of S3: coded as "deep" or "shallow" (juvenile *Acernaspis* "deep", Ramsköld 1988).
3. Length of the postocular area: coded as "short" or "long" (juvenile *Acernaspis* "long", Ramsköld 1988). Coded with reference to Figure 7. 10.
4. Depth of palpebral furrow: coded as "deep" or "shallow" (juvenile *Acernaspis* "deep", Ramsköld 1988).
5. Depth of lateral border furrow: coded as "deep" or "shallow" (juvenile *Acernaspis* "deep", Ramsköld 1988).
6. Length of fixed cheek between facial suture and posterior border furrow: coded as "long" or "short" (juvenile *Acernaspis* "long", Ramsköld 1988).
7. Tuberculation: coded as "tubercled" or "not tubercled" (juvenile *Acernaspis* "tubercled", Ramsköld 1988).
8. Presence of occipital node: coded as "present" or "absent" (juvenile *Acernaspis* "present", Ramsköld 1988).

The other ontogenetically-varying characters (shape of the occipital ring, shape of the intercalating ring, lateral extent of S2, and shape of the genal angle) were omitted by Ramsköld from his NSS analysis as they did not show any distinction between *Acernaspis* and *Ananaspis*, and they have been omitted here also.

The number of character states shared by each species with the generalised *Acernaspis* juvenile is shown in Table 7. 3. Some of the character states are necessarily rather arbitrary, and this fact, combined with the availability of more comprehensive morphometric data herein, leads to the slight discrepancy between NSS calculated

Table 7. 3. Number of character states shared between holaspides of morphometrically analysed species of *Acernaspis* and *Ananaspis* and a generalised *Acernaspis* juvenile. The eight characters used are listed in the text, and are after Ramsköld (1988). NSS = number of shared states. Generalised *Acernaspis* juvenile characterised as described in the text. Species are listed in approximate stratigraphical order.

Species	Age	NSS
Ananaspis fecunda	Ludlow	8
Ananaspis stokesii	Wenlock, Homerian	4
Ananaspis amelangorum	Wenlock, Homerian	5
Ananaspis sp. nov. A	Wenlock, Homerian	6
Acernaspis rubicundula	Wenlock, Sheinwoodian	3
Acernaspis sororia	Llandovery, Telychian	0
Acernaspis quadrilineata	Llandovery, Telychian	0
Acernaspis sp. nov. C	Llandovery, Telychian	0
Acernaspis orestes	Llandovery, Telychian	0
Acernaspis sufferta	Llandovery, Telychian	0
Acernaspis woodburnensis	Llandovery, Aeronian - Telychian	0
Acernaspis sp. nov. B	Llandovery, Aeronian - Telychian	0
Acernaspis sp. nov. A	Llandovery, Aeronian	0
Acernaspis superciliexcelsis	Llandovery, Aeronian	1
Acernaspis xynon	Llandovery, Aeronian	1
Acernaspis elliptifrons	Llandovery, Rhuddanian - Aeronian	1
Acernaspis juvenile	Llandovery	

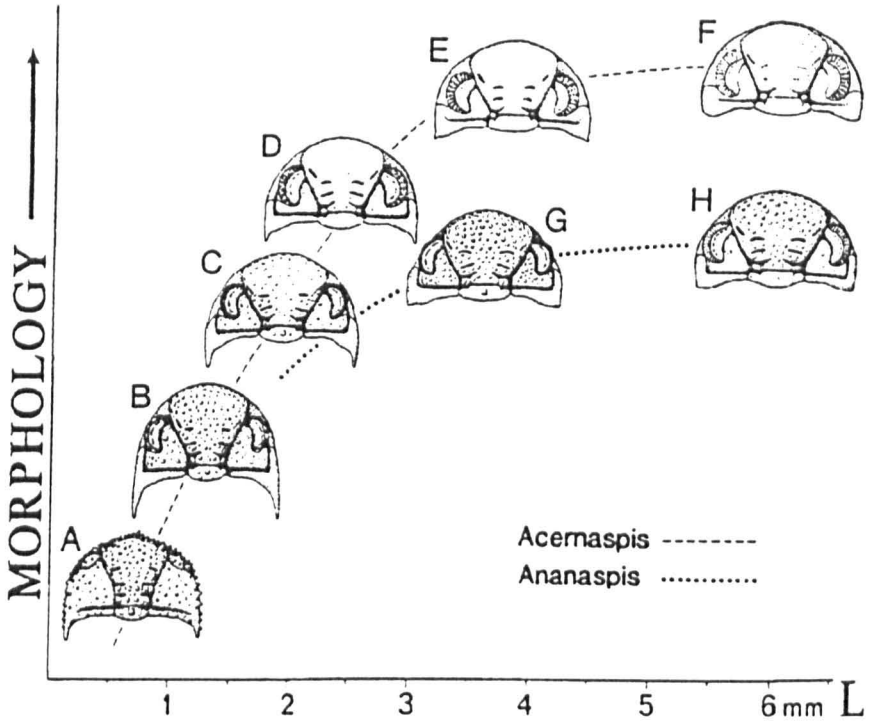

Figure 7. 25. Schematic ontogenetic trajectories for *Acernaspis* (dashed line) and *Ananaspis* (dotted line) to show neotenic derivation of *Ananaspis* from *Acernaspis* as envisaged by Ramsköld (1988). Reconstructions drawn to same actual size, but each with its sagittal length (L) in the correct position relative to the ordinate axis. Reconstruction of ontogenetically early meraspide (A) based on *Phacops spedeni* Chatterton, 1971, on assumption that all phacopids were relatively similar at early meraspide stages. Reconstructions B-F based on ontogenetic material of *Acernaspis* figured by Ramsköld (1988: figure 1; see also Figure 7. 24 herein). This material includes *Acernaspis* "*dispersa*" of Ramsköld (1988), *A. elliptifrons*, *A. rubicundula*, and *A. superciliexcelsis*, although Ramsköld (1988) does not make it clear which reconstructions are based upon which species. Reconstructions G-H based on *Ananaspis amelangorum* figured by Ramsköld (1985: plate 4). From Ramsköld (1988).

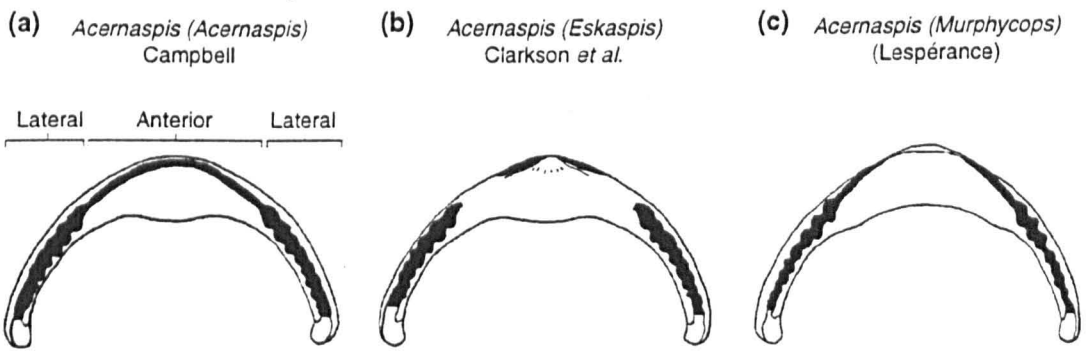

Figure 7. 26. Schematic reconstructions of the cephalic doublure of three species of *Acernaspis*, to illustrate the subspecies concepts of Clarkson *et al.* (1977) and Lespérance and Letendre (1981). (a) *Acernaspis orestes*; (b) *Acernaspis sufferta*; (c) *Acernaspis skidmorei*. Furrows indicated by black shading. Modified from Lespérance (1991: figure 4) with reference to Clarkson *et al.* (1977) and Lespérance and Letendre (1981).

herein and that quoted by Ramsköld (1988: table 1) for *A. stokesii* and *A. amelangorum*. It is clear from Table 7. 3 that holaspides of all species of *Ananaspis* studied herein are much more similar to the *Acernaspis* juvenile than are *Acernaspis* holaspides. The intermediate morphological position of *A. rubicundula* is also evident. However, within the *Ananaspis* species, there is no simple pattern whereby stratigraphically later species are more like *Acernaspis* juveniles than stratigraphically earlier ones, as was claimed by Ramsköld (1988). On the basis of Table 7. 3, it is concluded that *Ananaspis* is derived by a process of neoteny from earlier *Acernaspis* species. However, it does not appear that successively later species (at least those studied herein) are successively more neotenic with respect to *Acernaspis*.

7. 5. Systematic Palaeontology.

Family Pacopidae Hawle and Corda, 1847
Subfamily Phacopinae Hawle and Corda, 1847
Genus Acernaspis Campbell, 1967

Emended Generic Diagnosis.

Phacopinae with glabella moderately convex, expanding forward, not overhanging the anterior cephalic margin. S1 deeply impressed, inner end directed strongly forward. S2 and S3 moderately impressed, S2 not reaching axial furrow. Distal branch of 3S may be curved convex-outward or may be straight in the holaspide, and reaches almost to the axial furrow. Axial furrow deep and straight or slightly convex-out. Lateral border furrow not present or very shallow in the holaspide. Cephalon widest at the point at which the posterior branch of the facial suture meets the lateral cephalic margin.

Type Species.

Phacops orestes Billings, 1860, from the Jupiter Fm. (topmost Aeronian and Telychian, Cocks *et al.* 1992), Anticosti Island, Gaspé, Québec.

Included Species.

A. becsciensis Lespérance and Letendre, 1982; *A. boltoni* Lespérance and Letendre, 1982; *A. elliptifrons* (Esmark, 1833); *A. gaspensis* Lespérance and Letendre, 1982; *A. mimica* Lespérance and Letendre, 1982; *A. orestes* (Billings, 1860); *A. quadrilineata* (Angelin, 1851); *A. rubicundula* Ramsköld, 1985; *A. salmoensis* Lespérance, 1988; *A. skidmorei* (Lespérance, 1968); *A. sororia* Ramsköld, 1985; *A. sufferta* (Lamont, 1947); *A. superciliexcelsis* Howells, 1982; *A. woodburnensis* Clarkson *et al.* 1977; *A. xynon* Howells, 1982; *A.* sp. nov. A; *A.* sp. nov. B; *A.* sp. nov. C.

Temporal and Geographical Range.

Acernaspis first appears in early Llandovery (Rhuddanian) strata of the Oslo Region (Solvik Fm.) and approximately contemporaneous strata of northern Estonia (Juuru Stage, Rhuddanian, Ramsköld and Werdelin 1991). Shortly thereafter the genus appears in middle-to-upper Rhuddanian strata of the Girvan district (Mulloch Hill Fm.) and Québec (Becscie Fm.). The genus has a worldwide distribution by middle Llandovery times except for areas south of approximate palaeolatitude 30°S (Ramsköld and Werdelin 1991: figure 8). *Acernaspis* continues to be widespread throughout the upper Llandovery. Only one Wenlock species, *A. rubicundula* Ramsköld, 1985 from the Högklint Fm. (Sheinwoodian, Cocks *et al.* 1992) of Gotland, is known.

Remarks.

In his review of the systematics and phylogeny of the Phacopinae, Campbell (1967) erected the genus *Acernaspis* for some species of trilobites from Llandovery strata of Québec, the Oslo Region, Estonia, the British Isles, and New South Wales, as well as for three species from Siberia which Maksimova (1962) had previously assigned to *Eophacops* Delo, 1935. Campbell (1967, 1977) used a number of morphological characters to subdivide the Phacopinae, and concluded that the subfamily consisted of two main groups of species: (i) a group of species which could each be diagnosed by the possession of a distinctive character state which was derived from an earlier species, but which subsequently became extinct without giving rise to any subsequent morphologies; (ii) a "trunk" stock within which Cambell (1967, 1977) identified a number of "horizontal" groups (*i.e.* paraphyletic taxa which graded into each other in a continuum of form, Ramsköld and Werdelin 1991), each of which was defined on the basis of the stage which that taxon had reached in a number of complex character trends. Campbell (1967, 1977) considered *Acernaspis* to be the earliest member this second broad group (see Figure 7. 1).

Clarkson *et al.* (1977) erected a new subgenus, *A. (Eskaspis)*, distinguished from the nominate subgenus on the basis of ventral cephalic morphology. *Acernaspis* possesses a vincular structure on the ventral surface of the doublure, which may be considered to consist of two parts: anterior and lateral (Figure 7. 26). The lateral part in holaspides of all species of *Acernaspis* consists of about nine vincular notches which receive the tips of the pygidial pleurae during enrollment. *A. (Acernaspis)* was considered by Clarkson *et al.* (1977) to be characterised by the possession of a deep and continuous anterior vincular furrow situated on the anterior of the doublure (Figure 7. 26 (a)); *A. (Eskaspis)* was on the other hand characterised by the lack of such a continuous anterior vincular furrow, having instead a pair of shallow subfrontal depressions meeting at the midline (Figure 7. 26 (b)). Clarkson *et al.* made *A. sufferta* (Lamont, 1947) the type species of their new subgenus, and also assigned *A. woodburnensis* Clarkson, Eldredge and

Henry, 1977 to the subgenus, although they noted that in possessing a shallow vincular furrow between the subfrontal depressions and the lateral vincular notches, *A. woodburnensis* was in fact somewhat intermediate between the states exhibited by *A. (Eskaspis) sufferta* and species belonging to their *A. (Acernaspis).* They considered *A. (Eskaspis)* to be a localised late Llandovery derivative of *A. (Acernaspis)* confined to the Scottish area. Lespérance and Letendre (1981), in their description of phacopids from the Llandovery of Anticosti Island and the Gaspé peninsula of Québec, agreed with Clarkson *et al.* (1977) in subdividing *Acernaspis* into subgenera, and erected a third, *A. (Murphycops)* (in the process demoting *Murphycops* Lespérance, 1968 from genus to subgenus) for species from the Llandovery of Québec in which the anterior vincular furrow was absent from the anterior third of the doublure (Figure 7. 26 (c)). Lespérance and Letendre (1981) took *M. skidmorei* Lespérance, 1968 as the type species of their new subgenus.

Howells (1982) however, in her review of Scottish Silurian trilobites, noted that morphologically very similar vincular structures occur in species of *Acernaspis* which are dorsally quite dissimilar, thus suggesting that homeomorphy has played an important part in the development of these structures. On this basis she considered the three subgenera, *A. (Acernaspis), A. (Eskaspis)* and *A. (Murphycops),* which were based entirely on vincular morphology, to be synonymous. Ramsköld (1985) followed Howells (1982) in considering the subgenera invalid, for similar reasons. Lespérance (1991) made a detailed study of vincular morphology in the Phacopidae, and identified no less than 12 configurations of anterior and lateral vincular furrows, six of which are represented in *Acernaspis* (Lespérance 1991: figure 4). He noted that in Devonian phacopids, very different vincular morphologies are seen in specimens considered to belong in subspecies of the same species (on the basis of their dorsal morphology). This observation seems to the present writer to support the reasoning of Howells (1982) and Ramsköld (1985) in abandoning the three subgenera *A. (Acernaspis), A. (Eskaspis)* and *A. (Murphycops).*

In their phylogentic analysis of the members of the phacopidae, Ramsköld and Werdelin (1991) discovered that species assigned to the three subgenera did not group together in their cladograms, but rather were distributed randomly throughout. Further, they noted that the characters used in the diagnoses of *A. (Acernaspis), A. (Eskaspis)* and *A. (Murphycops)* (cladistic characters 24 and 25, Ramsköld and Werdelin 1991) also displayed no regular pattern in the cladograms (see Section 7. 2 herein). In view of this they considered the three subgenera to be synonymous, a view supported herein.

Species not explicitly considered. Due to unavailability of specimens, it did not prove possible to include the following species in the systematic treatment: *A. arctica*

(Poulsen, 1934); *A. estonica* Männil, 1970a; *A. glaber* (Marr and Nicholson, 1888); *A. henanensis* Zhang and Meng, 1986; *A. incerta* Männil, 1970a; *A. khatangensis* (Weber, 1951); *A. konoverensis* Männil, 1970b; *A. marklandensis* (McLearn, 1918); *A. nanus* (Maksimova, 1962); *A. newfoundlandensis* (Shrock and Twenhofel, 1939); *A. pulchella* (Foerste, 1887); *A. pulcher* (Maksimova, 1962); *A. rectifrons* Männil, 1970a; *A. semicircularis* Männil, 1970a; *A. sulcata* Männil, 1970.

In the following systematic treatment, the type species, *A. orestes*, is described first, and then the other species on which morphometrics have been undertaken are considered in stratigraphical order. Following this, there is a brief consideration of other species which were not available for morphometric study, again in stratigraphical order.

Acernaspis orestes (Billings, 1860)
Plate 7. 1, fig. 1; Figure 7. 27.

1860 *Phacops orestes* Billings, p. 64, fig. 10.
1928 *Phacops (Portlockia) orestes* (Billings); Twenhofel, p. 335, pl. 50, figs. 11-12.
1940 *Phacops orestes* Billings; Delo, p. 21, pl. 1, figs. 22-25.
1967 *Acernaspis orestes* (Billings); Campbell, pl. 12, figs. 1-4, 19; pl. 13, fig. 7.
1972 *Acernaspis orestes* (Billings); Bolton, pl. 8, fig. 18.
1981 *Acernaspis (Acernaspis) orestes* (Billings); Bolton, pl. 6, figs. 17-18.
1981 *Acernaspis (Acernaspis) orestes* (Billings); Lespérance and Letendre, p. 199, pl. 1, figs. 2-6 (non pl. 1, fig. 1).
1982 *Acernaspis (Acernaspis) orestes* (Billings); Lespérance and Letendre, p. 330, pl. 1, figs. 6-9.
1991 *Acernaspis (Acernaspis) orestes* (Billings); Lespérance, p. 290, figs. 4. 2, 6. 16, 6. 17.

Lectotype.
GSC 2472 selected by Lespérance (1991). A complete enrolled individual from the Jupiter Fm. (Llandovery Series, Telychian Stage, Cocks *et al.* 1992), probably from the south-central shore of Anticosti Island (Lespérance 1991). Figured by Twenhofel (1928: pl. 50, fig. 12). Refigured by Lespérance and Letendre (1981: pl. 1, figs. 2-3; 1982: pl. 1, fig. 6).

Occurrence.
Becscie (Rhuddanian Stage) and Jupiter (Telychian Stage) formations, Anticosti Island, Québec (Lespérance and Letendre 1982; Lespérance 1991).

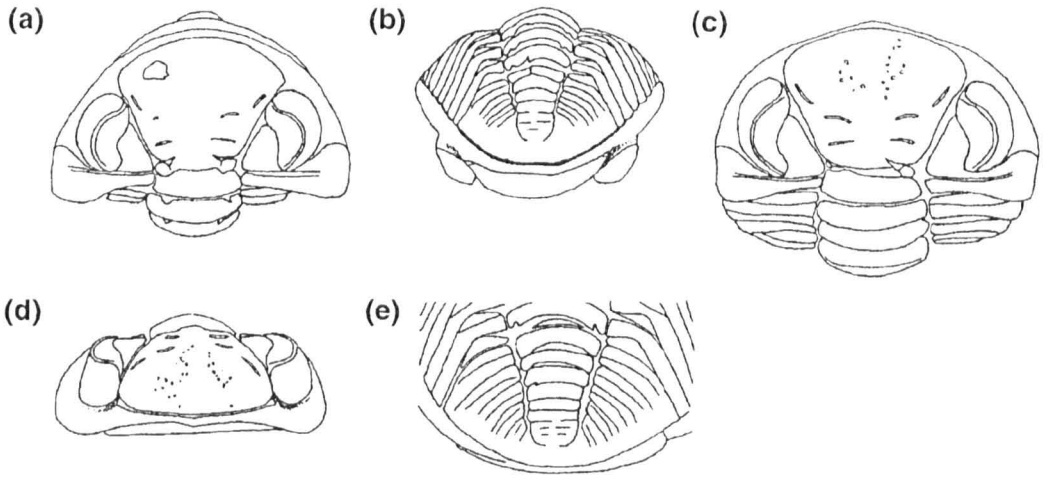

Figure 7. 27. *Acernaspis orestes* (Billings, 1860), Jupiter Fm. (Telychian Stage, Llandovery Series), Anticosti Island, Québec. (a) and (b) cephalon and pygidium of complete enrolled individual, GSC 2472, (a) x3.5, (b) x3. (c) and (d) dorsal and anterior views of cephalon of complete enrolled individual, GSC 29690, (c) x3, (d) x2.6. (e) dorsal view of pygidium of complete enrolled individual, GSC 67083, x3.6. (a) and (c) redrawn from Lespérance and Letendre (1981: plate 1); (b), (d) and (e) redrawn from Lespérance and Letendre (1982: plate 1).

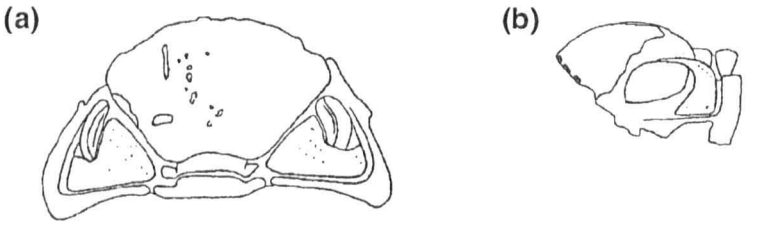

Figure 7. 28. *Ananaspis* sp. nov. A, upper Mottled Mudstone, lower Nantglyn Flags Gp. (Homerian Stage, Wenlock Series), roadside NE of Plas Uchaf near Llanrwst, Denbighshire, North Wales. (a) dorsal view of cephalon, BGS Dt7727; (b) lateral view of same. Both x4.5. Redrawn from Warren *et al.* (1984: plate 9).

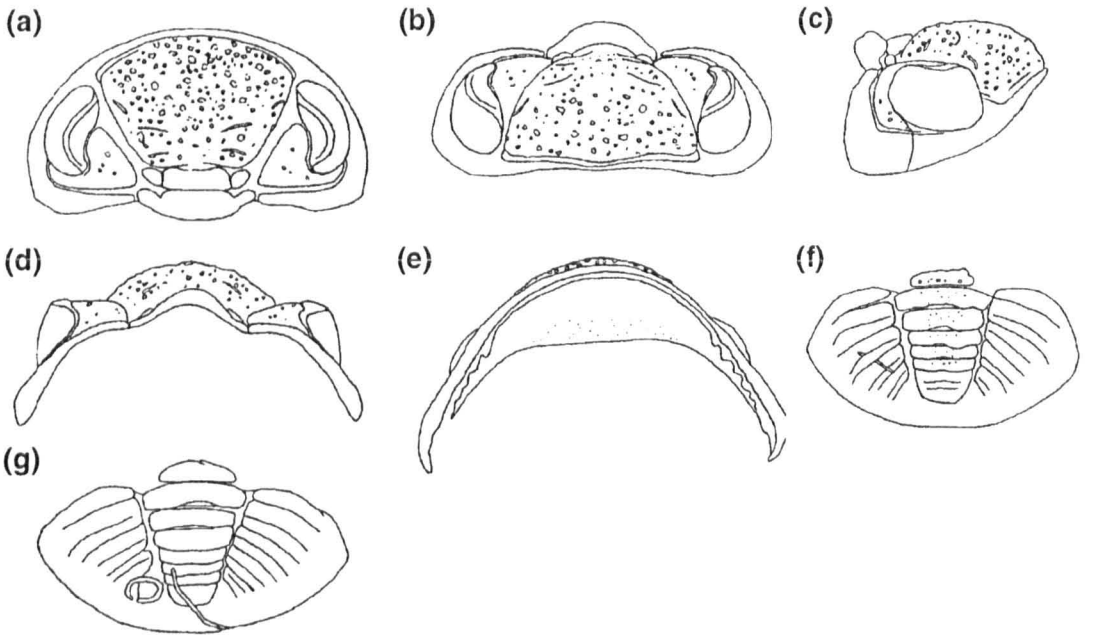

Figure 7. 29. *Ananaspis amelangorum* Ramsköld, 1985, Mulde Fm. (Homerian Stage, Wenlock Series), Sudervik 1, Gotland. (a) - (d) dorsal, dorso-anterior, lateral and posterior views of holotype cephalon, RM Ar52869, all x4. (e) ventral view of cephalic doublure, RM Ar52871, x4. (f) dorsal view of pygidium, RM Ar52874, x6. (g) dorsal view of pygidium, RM Ar52873, x6. All redrawn from Ramsköld (1985: plate 4).

Material.

Two cephala, one with thorax attached, and a single pygidium from the Jupiter Fm.

Emended Diagnosis.

Species of *Acernaspis* with palpebral areas approximately level with the palpebral lobes; intercalating ring small and triangular; L1 small, circular, and deeply depressed below the level of the intercalating ring; rounded genal angles may have small nodes; deep incisions on anterior face of occipital ring; anterior branch of vincular furrow deep and continuous, well incised pits laterally; interring furrows of pygidial axis shallow or absent mesially; pleural furrows deep, interpleural furrows shallow.

Description.

Cephalon approximately sub-semicircular, smoothly rounded anteriorly, tendency to approximately straight anterolateral margins. Cephalon widest at the point at which the posterior branch of the facial suture meets the lateral margin. Width (tr.) of cephalon about 1.8 times its length in the holaspide. Anterior border very narrow. No lateral border furrow either anterior to or posterior to the point at which the posterior branch of the facial suture meets the lateral margin. Genal angles rounded, sometimes with a small node. Posterior border furrow deep proximally, shallowing distally and becomming obsolete a little way in from the lateral margin. Occipital ring slightly narrower anteriorly than posteriorly, raised to a similar height as the preoccipital portion of the glabella. Occipital ring about 30% maximum cephalic width in the holaspide (this measurement undergoes marked allometry during early ontogeny, Figure 7. 21). Occipital ring with a pair of incisions in its anterior face, about 10% of the way in from either side, which cut about half way through (exsag.) the ring. Occipital furrow narrow and moderately deep mesially, becoming deeper distally. Glabella narrowest across L1 (slightly narrower than the maximum width of the occipital ring) and expanding forwards to a point of maximum width near its anterior margin, the maximum width being equal to about 52% of maximum cephalic width in the holaspide (this measurement also undergoes marked allometry in early meraspide stages). L1 small, approximately circular, and depressed to a level below the intercalating ring, and separated from the latter by a shallow posteriorly-directed branch of S1. S1 furrows deep distally, shallowing and becoming directed obliquely forward proximally, so that the small intercalating ring has a triangular appearance. S2 moderately impressed on the external surface (shallowly impressed on the internal mould) and directed posterolaterally at an angle of about 80° to the sagittal line, not reaching the axial furrow. S3 subdivided into proximal and distal branches. Proximal branch slightly curved convex-forward and directed slightly anterolaterally so as to make an angle of about 82° with the sagittal line; distal branch more strongly impressed, subparallel with the axial furrow and slightly curved convex-outward.

Furrow does not quite extend to the axial furrow. Anterior margin of glabella rounded, anterior face sloping steeply down to the anterior cephalic border. Oval pattern of auxillary muscle insertion scars on the anterior of the frontal lobe. Anterior branch of facial suture continuous around the anterior of the glabella, and cuts across the lateral extremities of the frontal lobe. Axial furrows deep along their whole length, diverging forwards and very slightly curved convex-outward. Posterior branch of facial suture not confined in a furrow, directed anterolaterally across the cheek and curving backward distally to cut the lateral margin at the point at which the cephalic width is a maximum (opposite L2).

Palpebral lobe strongly curved and approximately level with the palpebral area, slightly lower than the glabella. Anterior of eye adjacent to the anterior extremity of the distal branch of S3; posterior of the eye opposite L1, a short distance from the posterior border furrow. Posterior extremities of palpebral lobes slightly further apart than anterior extremities. Palpebral furrow moderately impressed. Visual surface with 16 to 18 lens files containing between four and seven lenses inclusive in the highest rows (Lespérance and Letendre 1981).

Ventral surface of cephalic doublure with deep anterior part of vincular furrow which is continuous around the anterior of the doublure. Lateral part of the vincular furrow with nine well developed pits separated by walls. Hypostome unknown.

Thorax of eleven segments. Axis about 30% of total thoracic width, not narrowing significantly rearwards. Anterior axial rings with incisions in their anterior faces (cf. occipital ring above), these incisions becoming less well defined in posterior rings. Pleurae widening (exsag.) and steeply sloping (close to vertical) distally, with rounded distal extremities. Narrow, deeply impressed pleural furrows directed obliquely across each pleura from just behind its anteromesial extremity (in contact with the axial furrow) and becoming hidden beneath the posterior of the preceding pleura distally. Axial furrows moderately deep. Thoracic rings and pleurae finely granulated.

Pygidium subtriangular in dorsal view with rounded posterior margin. Ratio of maximum width (tr.) / length (sag.) about 2.5. Maximum width of axis about 35% of maximum width of pygidium. Anterior portion of pygidial axis (*i.e.* the anteriormost three axial rings) narrowing markedly rearwards. Posterior portion of axis narrowing rearwards more gradually. Six to ten axial rings (Lespérance and Letendre 1982). Anteriormost inter-ring furrows well defined, shallow mesially, deeper distally. Posterior inter-ring furrows shallower, with the posteriormost three or four furrows not reaching the axial furrows and being discontinuous across the sagittal line. Length of axis equal to about 80% of total pygidial length. Axial furrows moderately impressed

and still quite distinct around the rounded posterior end of the axis. Pleural fields composed of an anterior articulating facet and five pleurae. Anteriormost interpleural furrows deep and narrow, posterior ones shallower. Interpleural furrows extend from the axial furrow abaxially almost to the margin. Pleural furrows shallower, anterior ones more deeply impressed than posterior ones. Pleural furrows extend from close to the axial furrow abaxially almost to the margin. Pygidium finely granular over its entire surface.

Remarks.
The condition of having the palpebral area approximately level with the palpebral lobe is rare in *Acernaspis* ; *A. orestes* shares this state only with *A. superciliexcelsis* Howells, 1982 (Plate 7. 1, figs. 11-12, 14-15, 18) and *A. mimica* Lespérance and Letendre, 1982 (see below).

A number of species of *Acernaspis* are known from the Llandovery strata of Anticosti Island and the Gaspé Peninsula (*A. becsciensis* Lespérance and Letendre, 1982; *A. boltoni* Lespérance and Letendre, 1982; *A. gaspensis* Lespérance and Letendre, 1982; *A. mimica* Lespérance and Letendre, 1982; *A. salmoensis* Lespérance, 1988; and *A. skidmorei* (Lespérance, 1968), some of which co-occur with *A. orestes*. Most are very similar to the type species in dorsal appearance (although all except *A. mimica* have the palpebral area lower than the palpebral lobe, Ramsköld and Werdelin 1991). However, they exhibit varying vincular structures, and it is felt herein that this warrants the mainenance of these forms as separate species (see treatment of these species below).

Acernaspis elliptifrons (Esmark, 1833)
Plate 7. 1, figs. 2-8, 10.

1833 *Trilobites elliptifrons* Esmark, p. 269, pl. 7, figs. 6-7.
1859 *Trilobites (Proetus?) elliptifrons* Esmark; Murchison, p. 370.
1940 *Phacops elliptifrons* (Esmark); Størmer, p. 122, text-fig. 2, figs. 6-7; pl. 1, figs. 2-4.
1967 *Acernaspis (Acernaspis) elliptifrons* (Esmark); Campbell, p. 32, pl. 12, fig. 5.
1972 *Phacops (Acernaspis)* cf. *elliptifrons* (Esmark); Shrank, p. 49, pl. 14, fig. 8; pl. 15, figs. 1-2.
1981 *Acernaspis (Acernaspis) primaeva* (Clarke); Lespérance and Letendre, p. 200, pl. 2, figs. 1-3; pl. 3, figs. 7-8 (and synonymy therein).
1981 *Acernaspis* (subgenus?) n. sp. Lespérance and Letendre, p. 203, pl. 3, figs. 9-13.
1982 *Acernaspis* cf. *A. elliptifrons* (Esmark); Howells, p. 44, pl. 11, figs. 18-23, 25-26.

1982 *Acernaspis* (subgenus?) *norvegiensis* Lespérance and Letendre, p. 335, pl. 1, figs. 17-18; pl. 2, figs. 17-20.

Neotype.

PMO 20966, selected by Størmer (1940). An enrolled individual from the Solvik Fm. (Rhuddanian-Aeronian, Cocks *et al.* 1992) at Malmøykalven, Oslo district, Norway. Figured by Størmer (1940: pl. 1, figs. 2-4).

Occurrence.

Solvik and Sælabonn formations (Rhuddanian Stage, *acuminatus* Zone to Aeronian Stage, *convolutus* Zone, Cocks *et al.* 1992), Oslo, Asker and Ringerike districts, Norway; Mulloch Hill Fm. (Rhuddanian Stage, *atavus* to *cyphus* Zones, Cocks *et al.* 1992), Girvan district, Scotland; also tentatively included are specimens from the White Head Fm. (lower Llandovery), Percé area, Québec.

Material.

Thirty cephala and cranidia, including three juvenile specimens, and 35 pygidia from the Solvik Fm., Oslo and Asker districts, Oslo Region, Norway; three cranidia and 26 pygidia from the Mulloch Hill Fm., Girvan district.

Emended Diagnosis.

Acernaspis with glabella subrounded anteriorly; S1 deeply impressed, S2 and proximal part of S3 moderately impressed, distal part of S3 deeply impressed; intercalating ring approximately confluent with the glabella or raised slightly above it; eye relatively long (exsag.) with moderately impressed palpebral furrow; visual surface with 16 to 17 (rarely 18) dorso-vetral lens files usually containing up to six lenses each (rarely up to eight); vincular furrow continuous around anterior of cephalic doublure, anterior part shallow; lateral part of vincular furrow with seven or eight vincular notches which almost converge one with the next; pygidium highly convex with between five and nine axial rings.

Remarks.

A. elliptifrons differs from *A. orestes* in the following respects: the shape of the intercalating ring, which in *A. elliptifrons* is larger and more transverse; possession of slightly larger L1 lobes (Figure 7. 12); having the palpebral lobes raised above the palpebral area (they are on the same level in *A. orestes*); possession of a more deeply impressed palpebral furrow (although in their cladistic analysis of the phacopines Ramsköld and Werdelin 1991 do not code the character which describes this feature differently for the two species); wide and relatively shallow anterior part of the vincular

furrow (Plate 7. 1, fig. 4); interpleural furrows on the pygidium which are slightly shallower than those in *A. orestes* (Plate 7. 1, fig. 6).

Howells (1982) referred material from the Mulloch Hill Fm. (Rhuddanian) of the Girvan district to *A.* cf. *A. elliptifrons*, noting in particular the similar glabellar outline and shape of the L1 lobes (Plate 7. 1, fig. 10). Howells stated that the Girvan form has relatively longer (exsag.) eyes than the Norwegian material, although morphometrics herein do not reveal a major difference between the two sets of specimens (Figure 7. 17). This Girvan material is therefore here considered conspecific with *A. elliptifrons.*

Specimens of *A. primaeva* (Clarke, 1908) from the White Head Fm. (lower Llandovery) of Québec illustrated by Lespérance and Letendre (1981) bear a close resemblance to *A. elliptifrons.* The anterior of the glabella of the Québec form is slightly more rounded than the Norwegian form. Also the distal extremities of the posterior border furrow (near the genal angles) are flexed forwards in the Québec specimens. This region is not well preserved in any Norwegian *A. elliptifrons* specimens, so it is not known if they show the same characteristic. There is close similarity between *A. primaeva* and *A. elliptifrons* in all other characters, so they are tentatively considered conspecific herein.

Lespérance and Letendre (1981, 1982) described and illustrated material from the Solvik Fm. (lower Llandovery) at Spirodden, Asker district, Norway, for which they erected *A.* (subgenus?) *norvegiensis* Lespérance and Letendre, 1982 (see Plate 7. 1, fig. 7). The specimens are all small (glabellar length of the cranidia all less than or equal to 4.5mm). The cranidia are densely granulated, with short genal spines and glabellae which expand markedly forwards. Ramsköld (1988) considered these specimens to be juveniles of *A. elliptifrons* which is the only adult *Acernaspis* species occurring at the locality (and which is abundant there). This is also considered to be the case herein and *A. norvegiensis* is therefore synonymised with *A. elliptifrons.*

Helbert (1985) erected a new species, *A. phyxis*, for specimens from the Solvik Fm. at Sjursøya, Oslo district. He considered this species to differ from *A. elliptifrons* in the following: lower cephalic convexity; possessing a visual surface with 15 or 16 dorso-ventral lens files, as opposed to a quoted count for *A. elliptifrons* of 18 (in fact all specimens of *A. elliptifrons* studied herein have 16 or 17 lens files; see Figures 7. 18 and 7. 19 (a) on which *A. elliptifrons* is represented by the stratigraphical sample SOLVIK A); possession of glabellar auxillary muscle impressions which form a single area on the anterior of the glabella rather than an oval pattern as seen in all other *Acernaspis* specimens (this impression may be the result of a wide spread in the

location of the muscle impressions, so that the left and right "branches" appear to merge into one another); possession of eight (as opposed to a quoted count of seven for *A. elliptifrons*) axial rings in the pygidium (in fact the numbers of axial rings in specimens studied herein show no significant difference between specimens from Sjursøya and specimens from other localities in the Solvik Fm., although the Sjursøya specimens do show a very wide spread in observed values; see Figure 7. 13 on which Helbert's *A. physis* is represented by the stratigraphical sample SOLVIK B, specimens from elsewhere in the Solvik Fm. are represented by SOLVIK A). In view of the close morphometric similarity between the Sjursøya specimens and those from elsewhere in the Solvik Fm. (Figures 7. 7 to 7. 17, 7. 20 to 7. 23), *A. physis* is herein considered conspecific with *A. elliptifrons*.

Acernaspis superciliexcelsis Howells, 1982
Plate 7. 1, figs. 9, 11-15, 17-18; Figure 7. 24.

1906 *Phacops (Phacopidella) elegans* (Sars and Boeck); Reed, p. 154, pl. 19, figs. 21-23.
1943 *Phacops elliptifrons* (Esmark); Begg, p. 60, pl. 2, fig. 9.
1951 *Phacops (Phacops) elliptifrons* (Esmark); Begg, p. 368, pl. 1, figs. 6-12.
1965 *Phacops elliptifrons* (Esmark); Lamont, p. 40.
1977 *Acernaspis (Acernaspis) elliptifrons* (Esmark); Clarkson et al., p. 124.
1982 *Acernaspis superciliexcelsis* Howells, p. 40, pl. 10, figs. 17-24; pl. 11, figs. 1-11, 13; text-figs. 7-8.
1988 *Acernaspis superciliexcelsis* Howells; Morris, p. 11.
1991 *Acernaspis superciliexcelsis* Howells; Ramsköld and Werdelin, p. 63, 74.

Holotype.
BM In23571 by original designation of Howells (1982). A complete individual from the Newlands Fm. (Aeronian Stage, lower *gregarius* Zone, Cocks *et al.* 1992), Newlands Farm, Girvan district. Figured by Howells (1982: pl. 10, fig. 18).

Occurrence.
Newlands Fm. (Aeronian Stage, lower *gregarius* Zone) and Woodland Fm. (Rhuddanian Stage, *cyphus* Zone, Cocks *et al.* 1992), Girvan district.

Material.
Twenty-six cephala and cranidia, including one juvenile specimen, and 30 pygidia from the Newlands Fm. at Newlands Farm, Girvan district; five cephala, including one juvenile specimen, and six pygidia from the Woodland Fm. at Woodland Point, Girvan district.

Emended Diagnosis.

Acernaspis with very convex glabella, intercalating ring markedly depressed below the level of the glabella; S1 very deeply impressed, almost reaching the sagittal line; S2 and S3 deeply impressed, particularly on the external surface; eye with 16 (rarely 15 or 17) dorso-ventral lens files of up to five (rarely six) lenses per file; palpebral areas on a similar level with the palpebral lobes; anterior part of the vincular furrow continuous and shallow; lateral part deeper with nine well defined notches.

Remarks.

A. superciliexcelsis is very similar to the type species *A. orestes*, sharing with it the characteristic, unusual in *Acernaspis*, of having the palpebral area approximately level with the palpebral lobe (Plate 7. 1, figs. 12, 14-15, 18). *A. superciliexcelsis* differs from the type species in the following respects: its depressed intercalating ring; the greater convexity of the glabella; the rather weak incisions on the anterior of the occipital ring (those in *A. orestes* are much stronger, extending nearly half way through the occipital ring, Plate 7. 1, fig. 1). Howells (1982) considered *A. superciliexcelsis* to have relatively longer (tr.) glabellar furrows than the type species, but these dimensions have not been quantifiable for the material of *A. orestes* available.

Acernaspis xynon Howells, 1982
Plate 7. 1, figs. 16, 19-20; Plate 7. 2, figs. 1-2.

1899 *Phacops (Acaste) Downingae* (Murch); Peach and Horne, p. 542.
1906 *Phacops (Phacopidella) elegans* (Sars and Boeck); Reed, p. 154, pl. 19, fig. 20.
1906 *Phacops (Phacopidella) downingae* (Murchison); Reed, p. 156.
1982 *Acernaspis xynon* Howells, p. 43, pl. 11, figs. 12, 14-17; text-fig. 9.
1988 *Acernaspis xynon* Howells; Morris, p. 11.
1991 *Acernaspis xynon* Howells; Ramsköld and Werdelin, p. 63, 74.

Holotype.

BM In44521 by original designation of Howells (1982). A cranidium from the Woodland Fm. (Rhuddanian Stage, *cyphus* Zone, Cocks *et al.* 1992) at Woodland Point, Girvan district. Figured by Howells (1982: pl. 11, figs. 12 a-b).

Occurrence.

As well as the type locality, the species is also known from a small exposure on Kirk Hill in the Mulloch Hill Fm. (Rhuddanian Stage, *cyphus* Zone), Girvan district (Howells 1982).

Material.
Seven cranidia and four pygidia, all from the type locality.

Emended Diagnosis.
Acernaspis with glabellar furrows deeply impressed; small triangular intercalating ring confluent with the glabella; visual surface with 16 lens files containing up to six lenses per file; small genal spine present in all specimens; anterior part of vincular furrow continuous and moderately impressed, lateral part slightly deeper with nine well defined vincular notches; pygidial axis terminates some way from the posterior margin.

Remarks.
A. xynon differs from the type species in the following respects: its palpebral area is lower than the palpebral lobes; the anterior part of the vincular furrow is wider and shallower than that in *A. orestes* (Plate 7. 1, fig. 16); possession of short genal spines in adult specimens, which is unique in the genus (Plate 7. 1, fig. 20; Plate 7. 2, fig. 2). *A. xynon* co-occurs with *A. superciliexcelsis* at the Woodland Point locality, but differs from that species in the following: its relatively lower maximum glabellar width (see Figure 7. 20 in which *A. xynon* is represented by the stratigraphical sample WOODLAND B; *A. superciliexcelsis* from Woodland Point is represented by WOODLAND A, *A. superciliexcelsis* from Newlands Farm is represented by NEWLANDS); the intercalating ring which is confluent with the glabella, not depressed to a lower level (Plate 7. 1, figs. 19-20; Plate 7. 2, figs. 1-2); greater length (sag. and exsag.) of L2 relative to L3 (giving a lower ratio of b32/b21, Figure 7. 22); the presence of small genal spines; deeper anterior incisions on the occipital ring; pygidial axis terminating further from the posterior margin.

Howells (1982) noted that the co-occurrence of two species at the Woodland Point locality might have indicated dimorphism were it not for the fact that both species occur separately elsewhere (*A. xynon* in the Mulloch Hill Fm., Kirk Hill; *A. superciliexcelsis* in the Newlands Fm., Newlands Farm).

Acernaspis sp. nov. A
Plate 7. 2, figs. 3-6; Figure 7. 24.

1982 *Acernaspis* sp. A Howells, p. 45, pl. 12, figs. 6-12, 15.
1988 *Acernaspis dispersa* Ramsköld and Bassett; Ramsköld, p. 309, figures 1 A-K, 3 B.
1991 *Acernaspis dispersa* Ramsköld and Bassett; Ramsköld and Werdelin, p. 63, 71.

Occurrence.

Lower Camregan Grits, Llandovery Series, Girvan district (*sedgwickii* Zone, Aeronian Stage, Cocks *et al.* 1992). Also Motala Fm., middle Llandovery, Östergötland.

Material.

Four cranidia and seven pygidia.

Remarks.

Howells (1982) noted that these specimens differ from *A. superciliexcelsis* in the following respects: lesser inflation of the glabella; more angular anterior margin (in fact there is some variation in this character, Plate 7. 2, figs. 3, 5); intercalating ring which is almost (but not quite) confluent with the glabella; S1 not extending so far adaxially as in *A. superciliexcelsis* ; proximal branch of S3 close to parallel with S2 (in *A. superciliexcelsis* the proximal branch of S3 is markedly convex-forward, Plate 7. 1, figs. 12, 14-15, 18); poorly developed vincular notches (Plate 7. 2, fig. 4; this could be a preservational feature as the Camregan Grits specimens are preserved in a friable coarse sandstone). Howells (1982) also noted the close similarity between this Camregan Grits material and *A. elliptifrons* (as used herein) from the Mulloch Hill Fm. of the Girvan district (=*A.* cf. *elliptifrons* as used by Howells 1982), listing the differences as being the slightly depressed nature of the intercalating ring in the Camregan Grits specimens, the less well incised distal branch of S3 (this could be a preservational feature), and deeper vincular furrow. All known specimens of *A.* sp. A are poorly preserved so that morphometric data could only be obtained for a few individuals. The PCA plots of locations of glabellar furrows (Figure 7. 11) and pygidial measurements (Figure 7. 14) seem to indicate a close morphometric similarity between these specimens and *A. elliptifrons*, and indeed there is no significant difference between *A.* sp. A (represented by stratigraphical sample CAMREGAN) and *A. elliptifrons* (represented by stratigraphical samples SOLVIK A and SOLVIK B) in any of the ratios quoted herein (Figures 7. 10, 7. 12, 7. 13, 7. 22). This species is clearly very similar to *A. elliptifrons*, but in view of the (slight) differences listed above and the stratigraphical separation, it is herein considered to be a separate species.

Ramsköld (1988) and Ramsköld and Werdelin (1991) referred to (but did not describe) some specimens which they termed "*A. dispersa* ", from the middle Llandovery Motala Fm. of Östergötland, Sweden. This form shows close similarity to *A.* sp. nov. A, particularly in the straight axial furrows (reminiscent of *A. woodburnensis*, see below), the size and degree of depression of L1, and the location and orientation of the glabellar furrows (compare Figure 7. 24 (f) with Plate 7. 2, fig. 5). The specimens assigned to *A. dispersa* by Ramsköld (1988) and those from the Lower Camregan Grits also agree

closely in all morphometric characters (Figures 7. 7 to 7. 23). *A. "dispersa "* is therefore considered conspecific with *A.* sp. nov. A.

***Acernaspis* sp. nov. B**
Plate 7. 2, figs. 9-10.

Occurrences.
Braksøya Fm. (topmost Telychian to lower Sheinwoodian stages, "8c", Worsley *et al.* 1983), Vik Fm. (Telychian Stage, "7c") and Rytteråker (upper Aeronian Stage, "7a") formations, Oslo and Ringerike districts, Oslo Region.

Material.
Four cephala and cranidia, five pygidia.

Remarks.
Helbert (1985) erected a species which he called *A. labronios* for specimens from the Braksøya Fm., Ringerike district, Oslo Region. It is herein considered that material studied from the Rytteråker and Vik formations of the Oslo and Ringerike districts is identical with Helbert's species. Helbert (1985) quoted the diagnostic characters of this species as being the following: intercalating ring of low convexity (*i.e.* depressed below the level of the glabella); possession of large eyes with 15 or 16 lens files and a maximum of six lenses per file; pygidial axis with eight rings. The material studied herein does indeed have an intercalating ring which is slightly lower than the glabella (Plate 7. 2, fig. 9); the visual surface has between 14 and 16 lens files inclusive (Figures 7. 18 and 7. 19 (a), stratigraphical sample VIK; visual surfaces not available from the Rytteråker Fm.); the pygidial axis has between six and eight rings inclusive (Figure 7. 13, samples VIK and RYTTERÅKER). Helbert (1985) noted that the specimens are very similar in dorsal appearance to *A. sufferta* from the Telychian of Scotland, and this is clearly the case (cf. Plate 7. 2, figs. 8, 11-12, 14-17). The Norwegian species differs from *A. sufferta* in the following characteristics: *A. sufferta* has more lenses in its eye (17 to 20 lens files compared with 14 to 16 for the Norwegian species, Figure 7. 18; up to eight lenses in the highest files in *A. sufferta* whereas the Norwegian species has between five and seven inclusive, Figure 7. 19 (a)). *A. sufferta* has slightly more rounded genal angles; *A. sufferta* has slightly deeper impressed S2 and S3 furrows (although quality of preservation may affect this feature); the palpebral area of *A. sufferta* is below the palpebral lobe, whereas these two structures are on a similar level in the Norwegian species. The vincular structures of both species are very similar, but the subfrontal depressions in *A. sufferta* are better defined (Helbert 1985).

This species is herein defined as *A.* sp. nov. B, and is considered to be a separate species from, but closely related to, the stratigraphically slightly older *A. sufferta.*

Acernaspis woodburnensis Clarkson, Eldredge and Henry, 1977
Plate 7. 2, figs. 7, 13.

1899 *Phacops stokesi* (Milne-Edwards); Peach and Horne, p. 538.
1906 *Phacops elegans* Sars and Boeck; Reed, p. 155.
1977 *Acernaspis (Eskaspis) woodburnensis* Clarkson *et al.*, p. 132, pl. 19, figs. 9, 11-13.
1982 *Acernaspis woodburnensis* Clarkson *et al.*; Howells, p. 44, pl. 11, fig. 24; pl. 12, figs. 1-3.
1988 *Acernaspis woodburnensis* Clarkson *et al.*; Morris, p. 11.
1991 *Acernaspis woodburnensis* Clarkson *et al.*; Ramsköld and Werdelin, p. 63, 74.

Holotype.
BGS GSE 5777 by original designation of Clarkson *et al.* (1977). Complete individual from the Wood Burn Fm. (topmost Aeronian, Cocks *et al.* 1992), Bargany Pond Burn, Girvan district. Figured by Clarkson *et al.* (1977: pl. 19, figs. 9, 11). Refigured by Howells (1982: pl. 11, fig. 24).

Occurrence.
Only known from the type horizon.

Material.
Five cephala and 13 pygidia, all from the type locality.

Emended Diagnosis.
Acernaspis with straight axial furrows; relatively long (exsag.) eyes with 15 to 18 lens files containing up to eight lenses per file; ventral surface of doublure with two shallow subfrontal depressions closely adjoining the sagittal line and a shallow furrow connecting them to the lateral parts of the vincular furrow which contains nine well defined vincular notches.

Remarks.
This species differs from the type species in the following characters: possession of weak raised rims along S2 and S3 (Plate 7. 2, fig. 7); palpebral areas lower than the palpebral lobes; relatively narrower maximum width of the pygidial axis (Figure 7. 23); weaker pleural and interpleural furrows on the pygidium. The dorsal surface of *A.*

woodburnensis is very similar to *A. sufferta* (Lamont), but the two species may be distinguished on the basis of their respective vincular morphologies (see below).

Acernaspis sufferta (Lamont, 1947)
Plate 7. 2, figs. 8, 11-12, 14-17, 20.

1861 *Phacops Stokesii* Milne-Edwards; Howell and Geikie, p. 134.
1865 *Phacops Stokesii* Milne-Edwards; Haswell, p. 37, pl. 4, figs. 6-7.
1867 *Phacops Stokesii* Milne-Edwards; Henderson, p. 22.
1869 *Phacops Stokesii* Milne-Edwards; Brown and Henderson, p. 31.
1899 *Phacops stokesii* (Milne-Edwards); Peach and Horne, p. 597.
1947 *Eophacops* cf. *elliptifrons* var. *glaber* (Marr and Nicholson); Lamont, p. 290.
1947 *Eophacops sufferta* Lamont, p. 6, pl. 1, figs. 21-22.
1962 *Phacops* aff. *stokesii* (Milne-Edwards); Mykura and Smith, p. 138.
1975 *Acernaspis* sp.; Tipper, p. 297.
1977 *Acernaspis (Eskaspis) sufferta* (Lamont); Clarkson et al., p. 125, pl. 18, figs. 1-9; pl. 19, figs. 1-7.
1982 *Acernaspis sufferta* (Lamont); Howells, p. 43, pl. 12, figs. 4-5.
1988 *Acernaspis sufferta* (Lamont); Morris, p. 10.
1991 *Acernaspis sufferta* (Lamont); Ramsköld and Werdelin, p. 63, 74.

Neotype.
BGS GSE 1035, selected by Clarkson *et al.* (1977). An almost complete individual from the Wether Law Linn Fm. (upper Telychian, Cocks *et al.* 1992), Wether Law Linn, Pentland Hills. Figured by Clarkson *et al.* (1977: pl. 18, fig. 1).

Occurrence.
Deerhope (lower Telychian) and Wether Law Linn (upper Telychian) formations, Pentland Hills. Poorly preserved material from the upper Reservoir Fm. (upper Aeronian) may also be conspecific (Clarkson *et al.* 1977).

Material.
Ten cephala and 15 pygidia from the Wether Law Linn Fm., one cephalon from the Deerhope Fm., and one cephalon and one pygidium tentatively assigned to this species from the upper Reservoir Fm.

Emended Diagnosis.
Acernaspis possessing relatively large eyes with 17 to 20 lens files containing up to 8 lenses per file; axial furrows slightly convex-outward as seen in dorsal view; no anterior

part to the vincular furrow, rather there are two subfrontal depressions on either side of the mid-line; lateral part of vincular furrow with nine well developed notches.

Remarks.

In its dorsal appearence, *A. sufferta* is very similar to *A. woodburnensis*. It differs in the following characters: the convex-out axial furrows (those of *A. woodburnensis* are straight, Plate 7. 2, figs. 7, 13); relatively narrower glabella (Figure 7. 20; the glabella of *A. sufferta*, represented by the stratigraphical sample WETHERLAW is unusually narrow for the genus; *A. woodburnensis* is represented by the sample WOOD BURN); the posteriormost extremities of the palpebral lobes in *A. sufferta* are approximately the same distance apart as the anterior extremities, whereas the posterior extremities in *A. woodburnensis* are noticeably further apart than the anterior extremities; *A. sufferta* has a slightly longer L2 lobe relative to L3 than *A. woodburnensis*, giving a slightly lower ratio of b32/b21 (Figure 7. 22); *A. sufferta* does not possess raised rims along S2 and S3; the pygidial pleural and interpleural furrows are shallower in *A. sufferta*. The two species are perhaps more easily distinguished on the basis of their vincular morphology: both possess a pair of shallow depressions in the doublure to either side of the mid-line; however *A. woodburnensis* has a shallow furrow connecting these depressions to the lateral part of the vincular structure, whereas *A. sufferta* lacks such a connective furrow (Figure 7. 26).

Acernaspis sp. nov. C
Plate 7. 2, fig. 18.

Occurrence.

Middle Kilbride Fm. (*crispus* and *griestoniensis* zones, Telychian Stage, Cocks *et al.* 1992), Glenglosh, Co. Galway.

Material.

Two poorly preserved cranidia.

Remarks.

These two cranidia are very similar to the Camregan Grits specimens (*A.* sp. nov. A). Again, due to poor preservation, few measurements could be obtained from these specimens, but those that could agree closely with the Camregan Grits material (Figures 7. 10, 7. 15, 7. 16, 7. 17). The Kilbride specimens differ slightly in having the intercalating ring not at all depressed below the level of the glabella, and possibly in having the anterior of the eye slightly further forward. These specimens are therefore tentatively held as a separate species.

***Acernaspis quadrilineata* (Angelin, 1851)**
Plate 7. 2, figs. 21-22; Plate 7. 3, fig. 1.

1851 *Phacops 4-lineata* Angelin, p. 12, pl. 9, figs. 5, 5a-b, ?5c.
1985 *Acernaspis quadrilineata* (Angelin); Ramsköld, p. 5, pl. 1, figs. 1-2, 4.
1991 *Acernaspis quadrilineata* (Angelin); Ramsköld and Werdelin, p. 63, 73.

Neotype.
RM Ar49777, selected by Ramsköld (1985). A complete enrolled individual from the lower Visby Fm. (upper Telychian, Cocks *et al.* 1992), Norderstrand, Visby district, Gotland, Sweden. Figured by Ramsköld (1985: pl. 1, figs. 1a-f).

Occurrence.
Only known from the type horizon.

Material.
Seventeen cephala and 38 pygidia from various localities within the Visby district, Gotland.

Emended Diagnosis.
Acernaspis with large, subrectangular L1; axial furrows very shallow, especially adjacent to L1; surface smooth, or with very small, low granules; eye with 16 to 18 lens files with between five and seven (eight in one specimen) lenses in the highest files; pygidial pleural and interpleural furrows not deeply impressed (however note that all known specimens are more or less abraded by wave action, Ramsköld 1985); anterior branch of vincular furrow wide, shallow and continuous, lateral part with well incised notches.

Remarks.
A. quadrilineata differs from *A. orestes* in the following features: much larger, more rectangular L1 (Plate 7. 2, figs. 21-22); having the palpebral area lower than the palpebral lobe; possession of very shallow axial furrows; much fainter palpebral furrow (in fact, all cephalic furrows in *A. quadrilineata* are poorly impressed); possession of rather weak anterior incisions on the occipital ring (those in *A. orestes* are much more deeply incised); possession of a wide, shallow anterior part to the vincular furrow (the anterior vincular furrow in the type species is rather deeper); weakly impressed pygidial pleural and interpleural furrows.

Acernaspis sororia Ramsköld, 1985
Plate 7. 3, figs. 2-3.

1972 *Phacops (Acernaspis) quadrilineata* Angelin; Schrank, p. 48, pl. 14, figs. 6-7.
1985 *Acernaspis sororia* Ramsköld, p. 13, pl. 1, figs. 3, 5-7; pl. 3, figs. 1-3.
1991 *Acernaspis sororia* Ramsköld; Ramsköld and Werdelin, p. 63, 74.

Holotype.
RM Ar49775 by original designation of Ramsköld (1985). Complete enrolled individual from the lower Visby Fm. (upper Telychian, Cocks *et al.* 1992), Norderstrand, Visby district, Gotland. Figured by Ramsköld (1985: pl. 1, fig. 3; pl. 3, figs. 1a-f).

Occurrence.
Only known from the type horizon.

Material.
Three cephala and five pygidia from various localities in the Visby district.

Emended Diagnosis.
Acernaspis with sculpture of very fine granulation over the entire surface; deeply impressed axial furrows; eye with 16 or 17 lens files, five or six lenses in the highest files; small L1 lobes; vincular structure consisting of a wide, shallow anterior furrow, lateral part with nine deep notches.

Remarks.
A. sororia co-occurs with the far more abundent *A. quadrilineata* in the lower Visby Fm. of Gotland. *A. sororia* differs from *A. quadrilineata* in the following characteristics: far more deeply impressed furrows on the cephalon, notably the axial and palpebral furrows; possession of slightly more angular genal angles which have a small node on them; much deeper incisions on the anterior face of the occipital ring (Plate 7. 3, figs. 2-3).

Acernaspis rubicundula Ramsköld, 1985
Plate 7. 2, figs. 19, 23; Plate 7. 3, fig. 4.

1979 *Acernaspis* sp. a; Owens *in* Jaanusson *et al.*, p. 118.
1979 *Acernaspis* sp. b; Owens *in* Jaanusson *et al.*, p. 118.
1985 *Acernaspis rubicundula* Ramsköld, p. 8, pl. 2, figs. 1-11; pl. 3, fig. 4; figure 2.
1991 *Acernaspis rubicundula* Ramsköld; Ramsköld and Werdelin, p. 63, 74.

Holotype.

SGU Type 5199 by original designation of Ramsköld (1985). Cranidium from the Högklint Fm., unit b (Sheinwoodian Stage, Cocks *et al.* 1992) at Vattenfallsprofilen 1, Visby district, Gotland. Figured by Ramsköld (1985: pl. 2, fig. 10).

Occurrence.

Restricted to the Högklint Fm., units b and c.

Material.

Eight cephala and cranidia, seven pygidia from various locations within the Visby district.

Emended Diagnosis.

Acernaspis with a distinctly tuberculate glabella; very short (exsag.) L2; posteriormost extremity of the palpebral lobe in contact with the posterior border furrow; straight axial furrows; eyes with 16 or 17 lens files with six or seven lenses in the highest files; vincular structure consisting of a wide, shallow furrow anteriorly with deep well defined notches laterally.

Remarks.

In many ways, *A. rubicundula* is not unlike *A. sororia* in appearance. It differs from that species in the following respects: possession of a relatively narrower occipital ring (Figure 7. 21); having L2 relatively much shorter (Figure 7. 22 shows that L2 in *A. rubicundula* (represented by the stratigraphical sample HÖGKLINT) is very much shorter with respect to L3 than it is in *A. sororia* (represented by VISBY B); the relative length of L2 and L3 are comparable with values for samples assigned to *Ananaspis*); possession of a much more tuberculate glabella than *A. sororia* (Plate 7. 3, fig. 4); possession of slightly raised rims along S2 and S3; the relatively very short postocular area which is characteristic of the species (Figure 7. 10); possession of more rounded genal angles which do not have a node; greater number of axial rings in the pygidium (between seven and nine inclusive for *A. rubicundula* compared with only seven for *A. sororia*, Figure 7. 13; *A. sororia* represented by the sample VISBY B).

Other Species Not Included in the Morphometric Study.

Brief mention is made here of a number of other known species of *Acernaspis*, specimens of which were not available for inclusion in the morphometric study.

Acernaspis becsciensis Lespérance and Letendre, 1982

1981 *Acernaspis (Murphycops)* n. sp. A. Lespérance and Letendre, p. 202, pl. 3, figs. 3-6.

1982 *Acernaspis (Eskaspis) becsciensis* Lespérance and Letendre, p. 334, pl. 2, figs. 1-6.

1991 *Acernaspis becsciensis* Lespérance and Letendre; Ramsköld and Werdelin, p. 63, 71.

Holotype.

GSC 67146 by original designation of Lespérance and Letendre (1982). An incomplete cephalon from the middle Becscie Fm. (Rhuddanian Stage, Cocks *et al.* 1992), Anticosti Island, Québec. Figured by Lespérance and Letendre (1981: pl. 3, figs. 3-4; 1982: pl. 2, figs. 1-3).

Occurrence.

Becscie Fm. (Rhuddanian Stage), Anticosti Island, where it co-occurs with *A. orestes* (Lespérance and Letendre 1982).

Remarks.

Ramsköld and Werdelin (1991) considered *A. becsciensis* to differ from *A. orestes* in the following characters: slightly larger, more transverse intercalating ring; possession of a palpebral area which is lower than the palpebral lobe; slightly less well defined anterior incisions on the occipital ring. The first and third of the differences listed above are difficult to substantiate on the basis of Lesérance and Letendre's (1981, 1982) illustrations of the species, but the second (palpebral area) character is clearly discernible. Also it is apparent from Lesérance and Letendre's description and photographs that the vincular structure in *A. becsciensis* is somewhat different from that in *A. orestes* : the anterior part of the vincular furrow forms a bevel on the anterior of the doublure in *A. becsciensis* which meets a boss located on the sagittal line, while in *A. orestes* this furrow is entirely on the vincular surface of the doublure and there is no medial boss. Because of these differences it is herein considered that *A. becsciensis* is a separate species from *A. orestes.*

Acernaspis boltoni Lespérance and Letendre, 1982

1981 *Acernaspis (Acernaspis)* n. sp. A Lespérance and Letendre, p. 201, pl. 1, figs. 7-12.

1982 *Acernaspis (Acernaspis) boltoni* Lespérance and Letendre, p. 332, pl. 1, figs. 10-15.

1991 *Acernaspis boltoni* Lespérance and Letendre; Ramsköld and Werdelin, p. 62, 71.

Holotype.
GSC 17091 by original designation of Lespérance and Letendre (1982). A complete enrolled individual from the basal Jupiter Fm. (topmost Aeronian - lowest Telychian, Cocks *et al.* 1992) of Anticosti Island, Québec. Figured by Lespérance and Letendre (1981: pl. 1, figs. 7-10; 1982: pl. 1, figs. 10-13).

Occurrence.
Becscie, Gun River and Jupiter formations (Rhuddanian - Telychian, Cocks *et al.* 1992), Anticosti Island, Québec.

Remarks.
This unusual species differs from *A. orestes* in the following characteristics: possession of extremely wide (tr.) cheeks which make up about 2/3 of the area of the cephalon in dorsal view (Lespérance and Letendre 1981); L1 of relatively larger size; palpebral area at a lower level than the palpebral lobe; more incised palpebral furrows; possession of genal angles which are slightly more drawn out and angular than those of *A. orestes*. Ramsköld and Werdelin (1991) noted the occurrence of weak raised rims along the S2 and S3 furrows of this species, although they are difficult to make out in Lespérance and Letendre's (1981, 1982) photographs. The unusually wide cephalon makes this species unmistakable.

Acernaspis salmoensis Lespérance, 1988

1981 *Acernaspis* sp. Lespérance and Letendre, p. 197.
1982 *Acernaspis* sp. Lespérance and Letendre, p. 329.
1985 *Acernaspis (Acernaspis)* n. sp. Lespérance, p. 845.
1988 *Acernaspis (Acernaspis) salmoensis* Lespérance, p. 372, figs. 16-19.
1991 *Acernaspis salmoensis* Lespérance; Ramsköld and Werdelin, p. 63, 74.

Holotype.
GSC 69146 by original designation of Lespérance (1988). A cephalic doublure from the basal Becscie Fm. (Rhuddanian), Anticosti Island. Figured by Lespérance and Letendre (1982: pl. 1, fig. 16). Refigured by Lespérance (1988: fig. 18).

Occurrence.
Becscie Fm. (Rhuddanian), Anticosti Island, Québec.

Remarks.

This species is very similar in all dorsal characteristics to *A. becsciencis*, with which it co-occurs. It differs in its vincular structure: whereas *A. becsciensis* possesses a bevel on the anterior of the ventral surface of the doublure (see earlier), *A. salmoensis* has a shallow, continuous anterior branch to the vincular furrow. The lateral portion of the vincular furrow is very distinctive in *A. salmoensis*, consisting of nine vincular notches with well defined separating walls between them.

Acernaspis skidmorei (Lespérance, 1968)

1968 *Murphycops skidmorei* Lespérance, p. 819, text-fig. 2; pl. 106, figs. 4-7.

1969 *Murphycops skidmorei* Lespérance *in* : Ayrton *et al.*, p. 478.

1981 *Acernaspis (Murphycops) skidmorei* (Lespérance); Lespérance and Letendre, p. 201, pl. 3, figs. 1-2.

1991 *Acernaspis skidmorei* (Lespérance); Ramsköld and Werdelin, p. 63, 74.

Holotype.

GSC 21905 by original designation of Lespérance (1968). A cephalon, figured by Lespérance (1968: pl. 106, figs. 4-7).

Occurrence.

White Head Fm. (lower Llandovery), Percé area, Québec.

Remarks.

In dorsal appearance, *A. skidmorei* differs from *A. orestes* in the following characteristics: it has slightly larger L1; relatively longer postocular area (in their cladistic analysis Ramsköld and Werdelin 1991 coded the postocular length of this species as being greater than the length (exsag.) of the postocular border directly behind the eye, while they coded the postocular length of *A. orestes* as shorter than the length (exsag.) of the postocular border directly behind the eye); the palpebral area of *A. skidmorei* is lower than the palpebral lobe; the pleural and interpleural furrows of the pygidium are less incised in *A. skidmorei*. On the ventral surface, *A. skidmorei* is characterised by the absence of the anteromesial third of the vincular furrow (in *A. orestes* the anterior portion of the vincular furrow is continuous around the anterior of the doublure).

Acernaspis mimica Lespérance and Letendre, 1982

1981 *Acernaspis (Eskaspis)* n. sp. B Lespérance and Letendre, p. 202, pl. 2, figs. 4-9.

1982 *Acernaspis (Eskaspis) mimica* Lespérance and Letendre, p. 335, pl. 2, figs. 11-16.

1991 *Acernaspis mimica* Lespérance and Letendre; Ramsköld and Werdelin, p. 63, 73.

Holotype.

GSC 67142 by original designation of Lespérance and Letendre (1982). An enrolled individual with a damaged pygidium from the upper Gun River Fm. (Aeronian, Cocks *et al.* 1992), Anticosti Island, Québec. Figured by Lespérance and Letendre (1981: pl. 2, figs. 4-6; 1982: pl. 2, figs. 11-12).

Occurrence.

Gun River (Aeronian) and Jupiter (Telychian) formations, Anticosti Island (Lespérance and Letendre 1982).

Remarks.

This species is very similar to *A. orestes* in its dorsal appearance. Its primary difference from that species is in its vincular structure: anteriorly this consists of a pair of shallow, almost triangular depressions, lacking a medial boss between them. The lateral portions of the vincular furrows bear deeply incised vincular notches, with the proximal vincular wall being more deeply scalloped than the distal vincular wall. Lespérance and Letendre (1981) noted that the pygidial ribs are somewhat flat-topped in this species, with only the anteriormost rib bearing a (weak) pleural furrow, whereas all ribs are furrowed in *A. orestes*.

Acernaspis gaspensis Lespérance and Letendre, 1982

1981 *Acernaspis (Eskaspis)* n. sp. A Lespérance and Letendre, p. 202, pl. 2, figs. 10-12.

1982 *Acernaspis (Eskaspis) gaspensis* Lespérance and Letendre, p. 334, pl. 1, fig. 20, pl. 2, figs. 7-10.

1991 *Acernaspis gaspensis* Lespérance and Letendre; Ramsköld and Werdelin, p. 63, 72.

Holotype.

GSC 67144 by monotypy (Lespérance and Letendre 1982). A complete enrolled individual from the Llandovery part of the Matapédia Gp., Gaspé, Québec. Figured by Lespérance and Letendre (1981: pl. 2, figs. 10-12; 1982: pl. 1, fig. 20; pl. 2, figs. 7-10).

Occurrence.
Only known from the type locality and horizon.

Remarks.
This single, damaged specimen is notable for its unusually short (exsag.) eye, only equal to about 1/3 of the cephalic length though still with at least 17 dorso-ventral lens files (Lespérance and Letendre 1982). From the illustrations given by Lespérance and Letendre (1981, 1982) it can be seen that the specimen has small L1, very like that of *A. orestes*, axial, posterior border and palpebral furrows slightly shallower than those of *A. orestes*, very rounded genal angles not at all produced posteriorly, and a smooth pygidium. The vincular structure consists mesially of an inflated central boss with shallow depressions to either side of it (Lespérance and Letendre 1982). The relative size and location of the eye are reminiscent of *A. superciliexcelsis*, but the intercalating ring of this specimen is not depressed below the level of the glabella as it is in the Girvan species. *A. gaspensis* is here held as a separate species, with the qualification that it may represent only an unusual individual of *A. orestes*.

Genus *Ananaspis* Campbell, 1967

Emended Generic Diagnosis.
Phacopinae with aproximately semicircular cephalon; convex glabella expanding strongly forwards, anterior face of glabella rising steeply from, or overhanging, the anterior cephalic border; S1 deeply incised, inner end directed strongly forwards; S2 and S3 moderately to deeply impressed; S2 not reaching the axial furrow; proximal branch of S3 curved convex-forward, distal branch curved concave outward (*i.e.* with the opposite sense to *Acernaspis*) and reaching almost to the axial furrow; Axial, posterior border, lateral border and palpebral furrows strongly impressed; axial furrows straight; glabella and palpebral areas tuberculate.

Type Species.
Phacops fecundus communis Barrande, 1852, from the Kopanina Fm. (Ludlow, Cocks *et al.* 1992), Bohemia.

Included Species.
A. amelangorum Ramsköld, 1985; *A. fecunda* (Barrande, 1846); *A. stokesii* (Milne Edwards, 1840); *A.* sp. nov. A.

Temporal and Geographical Range.
Ananaspis first appears in the Wenlock Series (Homerian Stage) of North Wales (upper Mottled Mudstone, lower Nantglyn Flags Gp., Denbigh-Conway district; Rushton *in*

Warren *et al.* 1984). Shortly thereafter the genus appears in Homerian strata of Gotland and the Welsh Borders. In the Ludlow, *Ananaspis* is widely distributed in Baltica, Kazakhstan and Gondwana, between palaeolatitudes of 0° and about 40°S (Ramsköld and Werdelin 1991: figure 8). The latest appearances are in upper Ludlow (Ludfordian Stage) strata of Bohemia (Kopanina Fm.) and Latvia (Pagegiai Fm.) (Ramsköld and Werdelin 1991).

Remarks.

A complete review of all known species of *Ananaspis* is beyond the scope of this study and has not been undertaken here. Rather, the transition from *Acernaspis* to *Ananaspis* has been studied in order to assess the postulated for neotenic derivation of the latter genus from the former. Ramsköld (1985) viewed the morphological series *Acernaspis sororia - Acernaspis rubicundula - Phacops stokesii - Ananaspis amelangorum* (described in that work as *Ananaspis amelangi*) as representing a gradual transition from typical *Acernaspis* to typical *Ananaspis*. However, Ramsköld (1985) advocated the retention of *Acernaspis* and *Ananaspis* as separate genera since synonymising them would result in a genus including an inconveniently large number of species and encompassing a range of variation much greater than that exhibited by other phacopid genera. Ramsköld and Werdelin (1991) excluded both *P. stokesii* and *A. amelangorum* from *Ananaspis*, considering the resolution of their cladograms too low to permit assignment of these two species (see Section 7. 2) which did not fit easily within *Ananaspis* as then conceived. Ramsköld and Werdelin's (1991) cladograms (Figure 7.2) do still however support the hypothesis that these two species lie in an intermediate morphological (and phylogenetic) position between *Acernaspis* and *Ananaspis*. *Ananaspis* Campbell has therefore been redefined to include these two species (and also *A.* aff. *fecundus* from the Nantglyn Flags Gp.) since they are part of the *Acernaspis - Ananaspis* lineage and should be included in one or other of these two genera.

Species not explicitly considered. Because of unavailability of specimens it did not prove possible to include the following species in the systematic section: *A. aspera* (Hawle and Corda, 1847); *A. calvescens* Chlupáč, 1972; *A. decora* Männil, 1987; *A. orientalis* (Maksimova, 1968).

The type species will be described first, and then the other species included in the morphometric analysis will be considered in stratigraphical order.

Ananaspis fecunda (Barrande, 1846)
Plate 7. 3, figs. 5-8, 10.

1846 *Phacops fecundus* Barrande, p. 46.

1852 *Phacops fecundus* var. *communis* Barrande, p. 514, pl. 21, figs. 1-9.

Lectotype.
NMP 783/66 from the Kopanina Fm. (Ludlow Series), Kolednik, near Beroun, Czech Republic.

Occurrence.
Unit E, Kopanina Fm. (Ludlow Series), Barrandian Basin.

Material.
Twenty-two cephala (ten from Lockhov, nine from Kolednik and three from Kosov) and 23 pygidia (all from Kolednik).

Emended Diagnosis.
Glabella strongly inflated, anterior face standing vertically over the anterior cephalic border; glabella and palpebral areas coasely tuberculate; anterior part of vincular furrow is a bevel on the anterior of the doublure; lateral part with only weak vincular notches; pleural and interpleural furrows on the pygidium deep, interpleural furrows wide; eye with 16 to 20 lens files of up to six (rarely eight) lenses per file; postocular length equal to about 20% of preoccipital glabellar length.

Description.
Cephalon approximately semicircular. Maximum width of cephalon slightly to the posterior of the point at which the posterior branch of the facial suturemeets the lateral cephalic margin. Width (tr.) of cephalon about 1.8 times its length in the holaspide. No anterior border. Lateral border furrow wide and deep, anteriormost extremity below the anterior of the eye. Posterior border furrow also wide and deep for its whole length until it meets the posterior extremity of the lateral border furrow. Genal angles rounded. Occipital ring not raised as high as the glabella (Plate 7. 3, fig. 10). Maximum width of the occipital ring between 27% and 36% of the maximum cephalic width in the holaspide (mean 32% for 19 specimens; this measurement undergoes marked allometry during ontogeny in *Acernaspis* (Figure 7. 21) and probably does so in *Ananaspis* too, but no ontogenetic material of the latter genus is known, Ramsköld 1985). Occipital ring has a pair of deep incisions anteriorly, about 10% of the way in from either side, which cut about half way through (exsag.) the ring (Plate 7. 3, figs. 7-8). Lateral extremities of occipital ring rounded. Occipital furrow wide and deep along its whole length. Glabella narrowest across L1 (slightly narrower than the maximum width across the occipital ring). Glabella expands strongly forwards to a point of maximum width just behind its anterior margin: this maximum width equal to between 52% and 65% of the maximum cephalic width in the holaspide (mean 58% for 20

specimens; again, this measurement undergoes marked allometry during ontogeny, Figure 7. 20). L1 small, approximately circular, and depressed to a level below the intercalating ring; set off from the intercalating ring by a wide, deep, posteriorly-directed branch of S1. S1 deep distally, shallower and directed obliquely forward proximally, giving the intercalating ring a triangular appearance in dorsal view. S2 moderately impressed proximally, a little more deeply impressed distally, directed posterolaterally at an angle of about 80° to the sagittal line. S2 does not reach the axial furrow. S3 subdivided into a moderately impressed proximal branch and a slightly more deeply impressed distal branch. Proximal branch directed transversely and markedly curved convex-forward. Distal branch sub-parallel with the axial furrow and slightly curved concave-outward (*i.e.* curved in the opposite sense to that shown by the holaspide of any species of *Acernaspis*). Distal branch of S3 does not quite extend into the axial furrow. Anterior margin of glabella rounded in dorsal view, and standing vertically above the anterior cephalic margin in lateral view (Plate 7. 3, fig. 10). No auxillary muscle insertion impressions visible on the anterior of the glabella. Anterior branch of facial suture continuous around the anterior of the glabella, and cuts across the lateral extremities of the frontal lobe. Axial furrows deep, wide and straight along their whole length, diverging forwards. Posterior branch of facial suture not confined in a furrow, directed anterolaterally across the cheek and turning strongly backwards near to the lateral cephalic margin, to meet the lateral margin opposite the mid-point of L2. Sculpture of large tubercles densely distributed over the glabella and palpebral areas. Also fine granulation superimposed on the tuberculation. Cheeks and borders granular but not tuberculate.

Palpebral lobes curved, approximately level with the palpebral area, and markedly lower than the maximum height of the glabella (Plate 7. 3, fig. 10). Anterior of eye opposite the anteriormost extremity of the distal branch of S3; posterior of eye opposite or slightly behind the distal extremity of S2. Postocular length equal to between 14% and 27 % of the preoccipital glabellar length (mean 20% for 22 specimens). Posterior extremities of palpebral lobes slightly further apart (tr.) than anterior extremities. Palpebral furrows deeply impressed. Visual surface with between 16 and 20 dorso-ventral lens files, with up to six (rarely seven or eight) lenses in the deepest files (Figures 7. 18, 7. 19 (b)).

On the ventral surface, the anterior part of the vincular furrow forms a bevel on the anterior face of the doublure; the lateral part of the vincular furrow has approximately eight notches. No hypostomes were available for detailed study. However, this sclerite of *A. fecunda* has been illustrated by Barrande (1852) and described by Campbell (1967). Anterior border of hypostome straight and transverse. Middle body convex and tapering backwards, width of middle body across widest point equal to about 0.75

times its sagittal length. Lateral borders narrow (tr.). Posterior border short (sag., exsag.) and angular posteriorly, with three small spines. Anterior wings relatively small, triangular and curving backwards distally. Width of hypostome measured across the anterior wings about 1.4 times its sagittal length. Granular sculpture.

Thorax unknown.

Pygidium sub-semicircular in dorsal view. Ratio of maximum width (tr.) / length (sag.) between 188% and 302% (mean 228% for 22 specimens; this ratio probably heavily affected by post-mortem distortion). Maximum width of pygidial axis between 21% and 32% of maximum pygidial width (mean 28% for 22 specimens, Figure 7. 23). Axis tapers more-or-less uniformly rearwards, with six to eight axial rings (Figure 7. 13). Terminal piece very small. All interring furrows well defined, anteriormost ones deep and wide for their whole length, posterior ones narrower and shallower, especially so mesially. Length of axis equal to between 80% and 98% of total length of the pygidium (mean 91%, 23 specimens). Axial furrows wide and deep, remaining distinct around the rounded posterior extremity of the axis. Pleural fields with an anterior articulating facet and between six and eight pleural ribs. Interpleural furrows wide and deep, extending from the axial furrow abaxially almost to the lateral margin. Pleural furrows shallower, though still distinct, anterior four or so more deeply impressed than the remaining posterior ones. Pleural furrows extend from the axial furrow abaxially almost to the lateral margin. Axis finely granular. Pleural fields smooth.

Ananaspis sp. nov. A
Plate 7. 3, figs. 11-12; Figure 7. 28.

1984 *Ananaspis* aff. *communis* (Barrande); Rushton *in* Warren *et al.*, p. 75, pl. 9, figs. 31-32.

Occurrence.
Upper Mottled Mudstone, lower Nantglyn Flags Gp. (Homerian Stage, Wenlock Series, Cocks *et al.* 1992), Plas Uchaf, Clwyd, north Wales.

Material.
Two complete cephala, and a third which is too distorted for morphometrics.

Emended Diagnosis.
Eye much deeper anteriorly than posteriorly, with 11 or 12 dorso-ventral lens files consisting of up to four lenses in the deepest files. Vincular structure unknown.

Remarks.

These specimens were compared with *A. fecunda* from the Kopanina Fm. by Rushton *in* Warren *et al.* (1984), and they are clearly very similar (Plate 7. 3, figs. 5-8, 10). The Welsh specimens are close to the material from Kolednik, Kosov and Lockhov in all morphometric characteristics (Figures 7. 7 to 7. 17). They differ from *A. fecunda* in having far fewer lenses in the visual surface (11 or 12 files of up to 4 lenses per file, as opposed to 16 to 20 files of up to 8 lenses in a file for the Bohemian species, Figures 7. 18, 7. 19 (b)), and in having the anterior face of the glabella sloping less steeply (compare Warren *et al.* 1984: pl. 9, fig. 32 which shows a lateral view of the upper Mottled Mudstone species with Plate 7. 3, fig. 10 herein which shows a lateral view of *A. fecunda*). Also the maximum width of the cephalon in the Welsh species occurs at the point at which the posterior branch of the facial suture meets the lateral border, rather than just behind this point as in *A. fecunda*. The sculpture is poorly preserved, but appears to consist of coarse, densely scattered tubercules over the glablella and palpebral surfaces (Plate 7. 3, fig. 11). In view of these differences, and the stratigraphical separation of these specimens from *A. fecunda*, a new species is erected for this material.

Ananaspis amelangorum Ramsköld, 1985
Figure 7. 29.

1985 *Ananaspis amelangi* Ramsköld, p. 18, pl. 4, figs. 1-6, 8-9.

1991 *Ananaspis amelangorum* Ramsköld; Ramsköld and Werdelin, p. 61, 70.

Holotype.

RM Ar52869 by original designation of Ramsköld (1985). A cephalon from the Mulde Fm. (middle Homerian Stage, Wenlock Series, Cocks *et al.* 1992) at Sudervik 1, Eksta parish, Gotland.

Occurrence.

Only known from the type locality and horizon.

Emended Diagnosis.

Moderately coarse glabellar tuberculation; anterior portion of vincular furrow continuous and deep (not a bevel as in *A. fecunda*); lateral part of vincular furrow with about six deep, well defined notches; pygidium with seven axial rings; pygidial axis relatively wider than other species of the genus; interpleural furrows deep and thin; pleural furrows moderately deep; eye with 15 or 16 files consisting of up to six lenses per file.

Remarks.

This species differs from *A. fecunda* in the following characteristics: possession of a narrow anterior border, from which the anterior facet of the glablella rises less steeply than that in the type species; lesser glabellar convexity (Figure 7. 29); widest point of the cephalon is where the facial suture meets the lateral cephalic margin, rather than behind this point; the glabellar tuberculation is less coarse; the anterior part of the vincular furrow is continuous and deep, rather than a bevel; the lateral part of the vincular furrow has well defined notches; the pygidial axis is relatively wider (Figure 7. 23); the interring furrows on the pygidium are narrower and shallower, especially mesially, than those of the type species; the eye has 15 or 16 files of up to six lenses per file, as opposed to 16 to 20 files of up to 8 lenses in the type species; the rounded genal angles can have tiny nodes on them (Figure 7. 29). The first three characteristics above recall the nearly contemporaneous *A.* sp. A (see above), with which this species may be closely allied.

Ananaspis stokesii (Milne Edwards, 1840)
Plate 7. 3, figs. 9, 13-17.

1839 *Calymene macrophthalma* Brongniart; Murchison, p. 655, pl. 14, fig. 2.
1840 *Calymene Stokesii* Milne Edwards, p. 324.
1864 *Phacops (Phacops) Stokesii* Milne Edwards; Salter, p. 21, pl. 2, figs. 1-6.
1967 *Ananaspis stokesii* (Milne-Edwards); Campbell, p. 32.
1977 *Ananaspis stokesii* (Milne-Edwards); Chlupáč, p.77.
1988 *Ananaspis stokesii* (Milne Edwards); Morris, p. 18.

Syntypes.

The whereabouts of the syntypes are unknown. Milne Edwards cited material from the Wenlock of Coalbrookdale and Dudley, England, as well as material from unknown horizons in Bohemia and the US (Morris 1988).

Occurrence.

Wenlock Series (Sheinwoodian and Homerian Stages, *riccartonensis* - *ludensis* zones, Thomas *et al.* 1984), Coalbrookdale and Much Wenlock formations, Welsh Borderlands.

Material.

Nine cephala and six pygidia, all from the Much Wenlock Fm. (upper Homerian, Cocks *et al.* 1992), Dudley.

Emended Diagnosis.

Cephalon of low convexity for the genus, occipital ring forming the highest point; eye with 15-18 lens files consisting of up to six (rarely seven or eight) lenses per file; postocular area short for the genus; sculpture of medium-sized tubercles on the glabella and palpebral areas; anterior part of vincular furrow is a bevel on the antero-ventral surface of the doublure; lateral part of vincular furrow with well defined notches; pygidium with five to eight axial rings.

Remarks.

This species differs from the type species of the genus in the following characteristics: the glabella is much less inflated (even less so than *A. amelangorum*, see above), giving *A. stokesii* a profile more like that of *Acernaspis* (Plate 7. 3, fig. 16); the cephalic sculpture consists of smaller tubercles in the English species; the postocular area is shorter (Figure 7. 10); the palpebral furrow is shallower (Plate 7. 3, figs. 9, 13-15); the lateral part of the vincular furrow has better-defined vincular notches (Plate 7. 3, fig. 17); the pygidial pleural and interpleural furrows are poorly developed (Plate 7. 3, figs. 14-15). The low convexity of this species is a shared characteristic with *Acernaspis*, and illustrates the necessarily somewhat transitional nature of the boundary between *Acernaspis* and *Ananaspis*. Although Ramsköld and Werdelin (1991) considered *A. stokesii incertae sedis*, it is herein placed within *Ananaspis* because of its concave-outward distal branch of S3, deeply impressed lateral border furrow, straight axial furrows, and coarse cephalic tuberculation, all of which are features of *Ananaspis* as diagnosed above.

7. 6. Conclusions.

The known stratigraphical durations and suggested phylogeny of the 18 species of *Acernaspis* (including those not used in the morphometrics) and four species of *Ananaspis* recognised herein are shown in Figure 7. 30. The earliest occurrences of *Acernaspis* are in the lower Llandovery of the Oslo Region and in approximately contemporaneous strata of northern Estonia (Ramsköld and Werdelin 1991). The latest occurrence is in Wenlock (Sheinwoodian Stage) strata of Gotland (Ramsköld 1985). The total range of the genus is therefore about 11 myr. A few species are known only from single horizons. The longest ranging species is *A. orestes* which has a duration of approximately 7 myr from the Becscie Fm. to the Jupiter Fm., Anticosti Island, Québec. *Ananaspis* has its earliest occurrence in the Wenlock (Homerian Stage) of North Wales. The latest occurrence is in upper Ludlow strata of Bohemia. The total duration of this genus is therefore about 15 myr. The longest duration species is probably *A. fecunda* which exists throughout the middle part of the Kopanina Fm. (Ludlow Series) of Bohemia, although detailed chronostratigraphical data is unavailable.

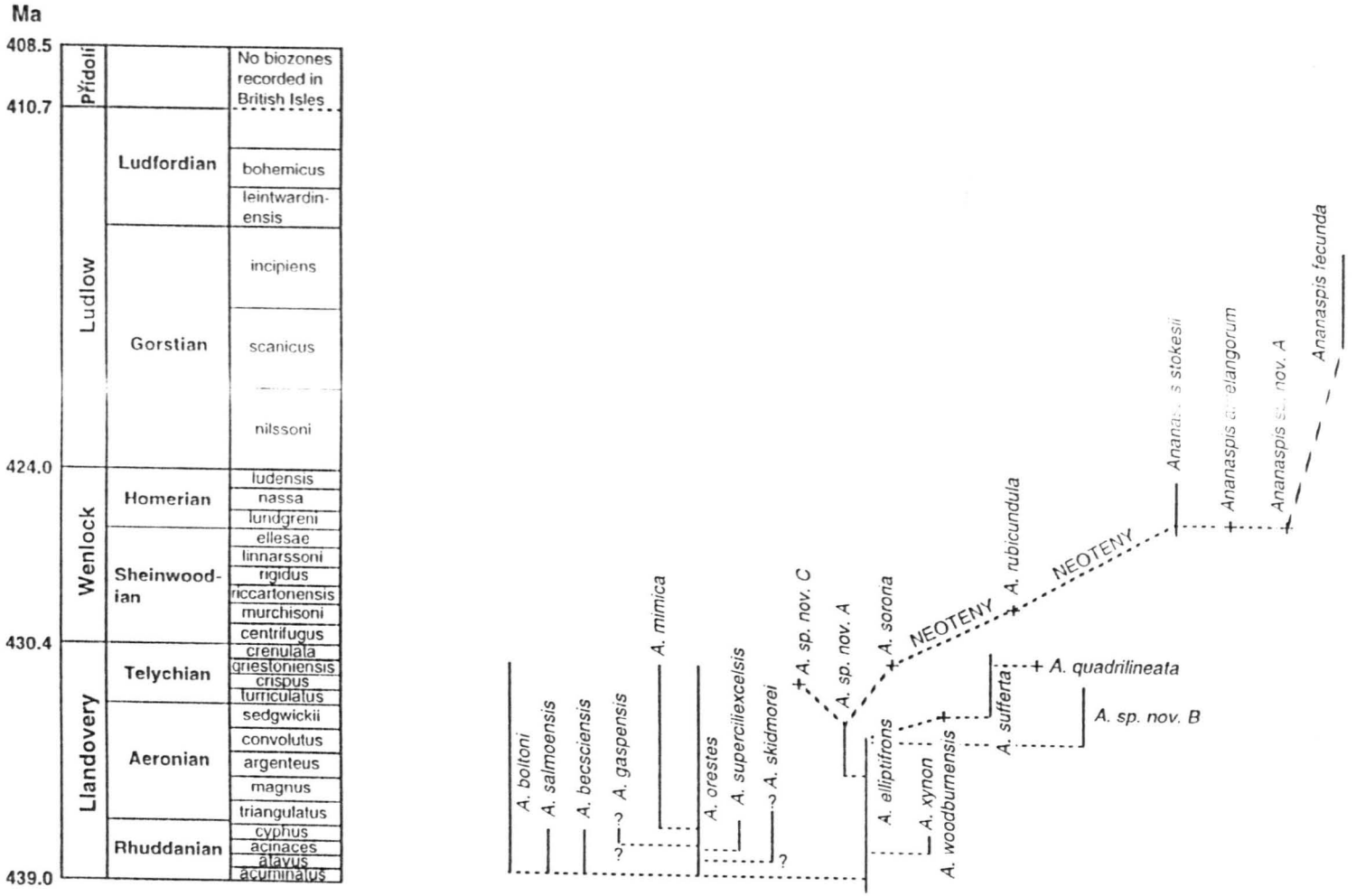

Figure 7. 30. Stratigraphical relationships, durations and suggested phylogeny of the species of *Acernaspis* ("*A.*") and *Ananaspis* recognised herein. Crosses indicate species known from only a single horizon. Chronostratigraphy as in Figure 7. 4. The phylogenetic relationships are based on the phylogenetic trees shown in Figures 7. 2 and 7. 3 (b). Neotenic steps are shown between *A. sororia* and *A. rubicundula*, and between *A. rubicundula* and *Ananaspis stokesii*, but continuing progressive neoteny throughout the history of *Ananaspis* is not envisaged.

Two stratigraphical samples were found to comprise two separate species: WOODLAND (Woodland Fm., Girvan district, upper Rhuddanian) yielded *Acernaspis superciliexcelsis* Howells, 1982 (designated WOODLAND A, see p. 217 for diagnosis) and *Acernaspis xynon* Howells, 1982 (designated WOODLAND B, see p. 218 for diagnosis); VISBY (Lower Visby Fm., topmost Telychian, Gotland) yielded *Acernaspis quadrilineata* (Angelin, 1851) (designated VISBY A,. see p. 225 for diagnosis) and *Acernaspis sororia* Ramsköld, 1985 (designated VISBY B, see p. 226 for diagnosis). A suggestion by Helbert (1985) that two separate species of *Acernaspis* can be diagnosed within the Rhuddanian - Aeronian Solvik Fm. of the Oslo Region (*A. elliptifrons* (Esmark, 1833), treated herein as stratigraphical sample SOLVIK A, and *A. phyxis* of Helbert 1985, treated herein as SOLVIK B) has been discounted herein.

The phylogenetic relationships shown on Figure 7. 30 are based on those shown on the cladograms in Figures 7. 2 and 7. 3(b). Insofar as species which occur geographically close together tend to be grouped together by the cladistic results, then the horizontal distribution of species in Figure 7. 30 is close to a representation of the geographical relationships between the species. This is made explicit in Figure 7. 31.

Phylogenetic analysis of the phacopid trilobites carried out by Ramsköld and Werdelin (1991; see Section 7. 2 herein) has demonstrated that convergent evolution has played an important role in the phlogeny of *Acernaspis*, resulting in a poorly-resolved consensus tree with low consistency index for this clade (Figure 7. 3). The species of *Acernaspis* are only recognisable on possession of suites of character states rather than on unequivocal unique apomorphies. This recalls the situation that was found for *Achatella* (Chapter 5) and *Calyptaulax* (Chapter 6).

Morphometrics demonstrates that the body plan of the *Acernaspis* - *Ananaspis* lineage is relatively stable (consider the overlapping PC fields occupied by the various stratigraphical samples, Figures 7. 9, 7. 11 and 7. 14). Some individual measurements were found to exhibit high variation, for example: postocular length (F); distal length of L2 (b21); proximal length of L2 (b!21); and proximal length of L1 (b!10) (Figures 7. 10, 7. 12). Only one unequivocal morphometric difference was detected between *Acernaspis* and *Ananaspis*, this being the relative lengths (exsag.) of L2 and L3. *Ananaspis* is characterised by a relatively short L2 and longer L3; L2 in *Acernaspis* is generally longer relative to L3 (Figure 7. 22). It was shown that *Acernaspis rubicundula* from the Sheinwoodian Stage of Gotland is an exception to this, as it exhibits a ratio of length of L3 to length of L2 similar to that shown by *Ananaspis* (Figure 7. 22). Ramsköld (1985) had previously considered this species intermediate between true *Acernaspis* and *Ananaspis* on the basis of its tuberculate cephalic

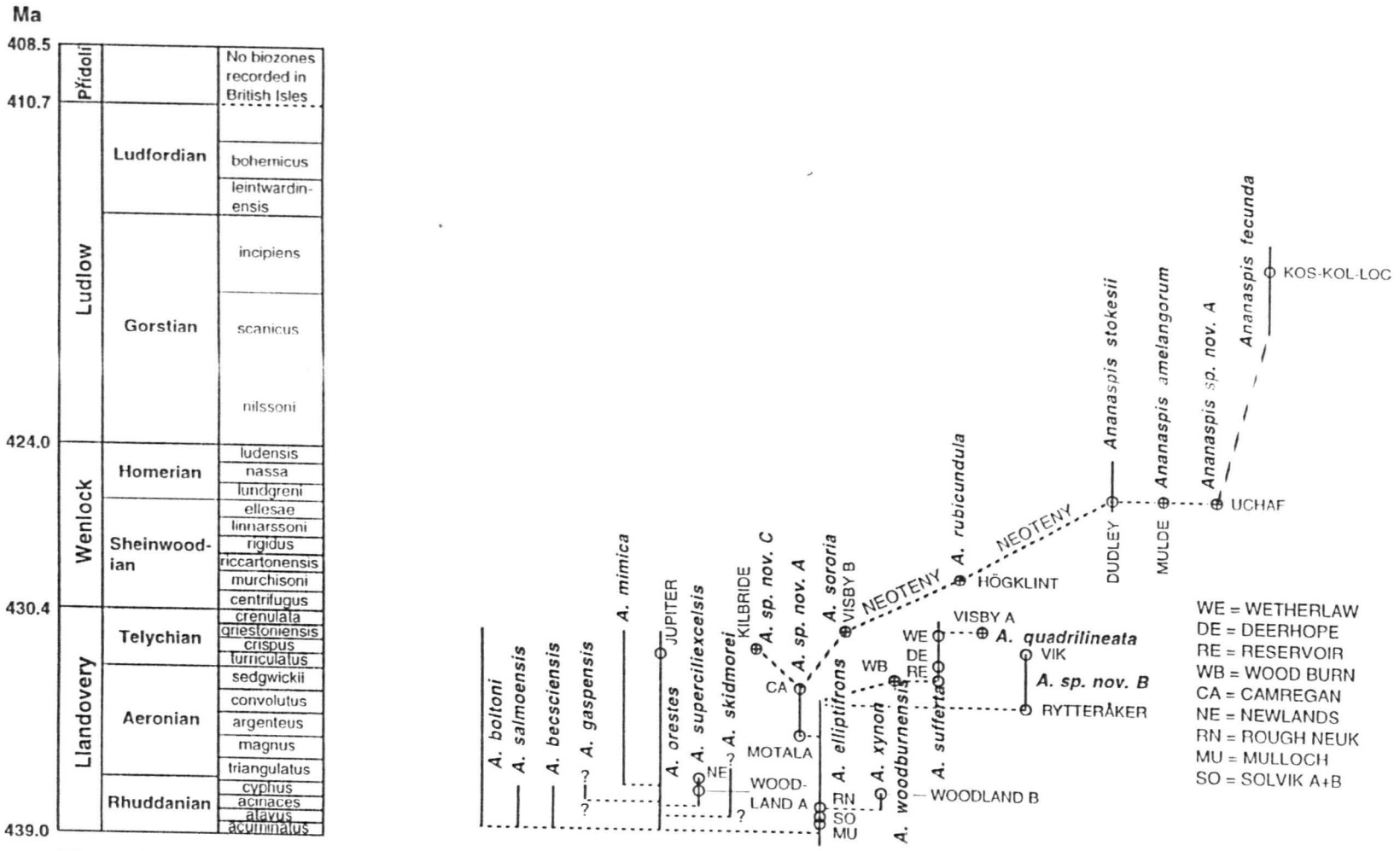

Figure 7. 31. Stratigraphical relationships, durations and suggested phylogeny of the species of *Acernaspis* ("*A.*") and *Ananaspis* recognised herein together with stratigraphical samples used in morphometric analyses. Crosses indicate species known from only a single horizon, circles indicate stratigraphical samples. Chronostratigraphy as in Figure 7. 4. The phylogenetic relationships are based on the phylogenetic trees shown in Figures 7. 2 and 7. 3 (b).

sculpture and its glabellar proportions (although Ramsköld did not quantify these proportions).

By demonstrating the similarity between holaspides of *Ananaspis* and juveniles of *Acernaspis*, it has been shown that the heterochronic process of neoteny is a plausible mechanism for the derivation of *Ananaspis* from *Acernaspis* (Table 7. 3). However, from the small sample of *Ananaspis* species studied herein, it does not appear that successively stratigraphically later species of *Ananaspis* are progressively more similar to the juvenile of *Acernaspis* as was claimed by Ramsköld (1988). Although it is true that the stratigraphically latest *Ananaspis* studied herein (*A. fecunda*) is the most similar to the *Acernaspis* juvenile, the next most similar is the earliest *Ananaspis* species, *A.* sp. A (which, has has been noted in Section 7. 5, is very similar to *A. fecunda*).

On the ventral surface of the doublure of *Acernaspis*, great variation in vincular structure is apparent. Species which are very similar in their dorsal appearance may have radically different enrolment structures. For example, in the Llandovery of Anticosti Island, species which co-existed show a range of vincular structures. Ramsköld and Werdelin (1991) demonstrated that vincular structure does not vary in a systematic way in *Acernaspis*, but rather that closely related species could have very different enrolment structures. Clearly these differing structures were evolved very rapidly by the genus, since several types of vincular structure already existed in the lower Llandovery species of Anticosti Island.

Stasis therefore appears to be maintained in *Acernaspis* through abundant convergence affecting the exoskeleton in a disassociated mosaic way. This is particularly evident in the ranges of vincular morphologies evolved, but also affected many elements of the dorsal morphology.

The phylogenetic trees of Ramsköld and Werdelin (1991) (Figure 7. 2) suggest that the taxonomic separation of *Ananaspis* from *Acernaspis* is a genuine reflection of evolutionary reality. The neotenic step from the *Acernaspis* clade to the *Ananaspis* clade seems to represent a breakdown in stasis in the former genus, and a discrete shift to a recognisably different phenotype. All *Acernaspis* species are very similar to one another; all *Ananaspis* species (at least those studied herein) are fairly similar to one another, but they are recognisably different from *Acernaspis* species. It is therefore considered that the two genera are valid.

The species treated here as being members of *Ananaspis* do not define a monophyletic clade in the cladistic results of Ramsköld and Werdelin (1991) (Figures 7. 2, 7. 3).

However, as was noted in section 7. 4. 2., their codings of some characters (e.g. their characters 1, 3, 6 and 26) did not take account of the full range of variation in these measurements. Repeating the cladistic analysis using a more adequate method of coding this morphometric data might yield different results.

Explanation of Plates for Chapter Seven

Plate 7. 1

Acernaspis orestes (Billings, 1860)

1. Dorsal view of cephalon and anterior eight thoracic segments of partially enrolled individual, internal mould. YPM 24885, Jupiter Fm. (Telychian Stage, Llandovery Series). Near mouth of Iron River, Anticosti Island, Québec. x5.

Acernaspis elliptifrons (Esmark, 1833)

2. Dorsal view of slightly damaged cephalon, internal mould. PMO 41744, Solvik Fm. (lower Llandovery Series). Malmøya, Oslo district, Oslo Region. x5.
3. Dorsal view of damaged cephalon, internal mould. PMO 112745, Solvik Fm. (lower Llandovery Series). Spirodden, Asker district, Oslo Region. x4.
4. Ventral view of cephalic doublure, internal mould. PMO 110871, Solvik Fm. (lower Llandovery Series). Skytterveien, Asker district, Oslo Region. x4.
5. Dorsal view of glabella, internal mould. PMO 112162, horizon and locality as for fig. 4. x6.
6. Dorsal view of damaged pygidium, internal mould. PMO 106508, horizon and locality as for fig. 3. x10. Paratype of *A.* (subgenus?) *norvegiensis* Lespérance and Letendre, 1982. Original of Lespérance and Letendre (1981: pl. 3, fig. 9; 1982: pl. 1, fig. 18).
7. Dorsal view of damaged cranidium, internal mould. PMO 106511, horizon and locality as for fig. 3. x8. Paratype of *A.* (subgenus?) *norvegiensis* Lespérance and Letendre, 1982. Original of Lespérance and Letendre (1981: pl. 3, fig. 13; 1982: pl. 2, figs. 18-19).
8. Dorsal view of damaged cranidium, internal mould. PMO 110889, horizon and locality as for fig. 4. x4.
10. Dorsal view of complete individual, internal mould. BM In23570, Mulloch Hill Fm. (Rhuddanian Stage, Llandovery Series). "Craigens Quarry", S side of Craigens Hill, Craighead Inlier, Girvan district, Scotland. x2. Original of Howells (1982: pl. 11, fig. 19).

Acernaspis superciliexcelsis Howells, 1982

9. Dorsal view of partial testate cranidium. BM In43239, Newlands Fm. (Aeronian Stage, Llandovery Series, lower *gregarius* Zone). Sandstone ridge on E bank of stream 150m E of Newlands Farm, Craighead Inlier, Girvan district, Scotland. x4.

11. Dorsal view of complete individual, internal mould. Paratype specimen, BM In23574, horizon and locality as for fig. 9. x4. Original of Howells (1982: pl. 10, fig. 24).
12. Dorsal view of complete individual, internal mould. Holotype specimen, BM In23571, horizon and locality as for fig. 9. x2. Latex cast of counterpart figured by Howells (1982: pl. 10, fig. 18).
13. Dorsal view of pygidium, internal mould. NMW 79.2G.219, horizon and locality as for fig. 9. x6.
14. Dorsal view of cephalon, internal mould. GLAHM A20881, horizon and locality as for fig. 9. x3.
15. Dorsal view of cephalon, internal mould. Paratype specimen, GLAHM A17358, horizon and locality as for fig. 9. x4. Original of Howells (1982: pl. 11, figs. 3a-b).
17. Ventral view of latex cast of cephalic doublure. NMW 79.2G.212, horizon and locality as for fig. 9. x3.
18. Dorsal view of incomplete individual, internal mould. Paratype specimen, BM In23579, Woodland Fm. (Rhuddanian Stage, Llandovery Series, *cyphus* Zone). Woodland Point, 430m W of Woodland Farm. x3. Original of Howells (1982: pl. 11, fig. 13).

***Acernaspis xynon* Howells, 1982**

16. Ventral view of partial cephalic doublure, internal mould. Paratype specimen, GLAHM A17361, horizon and locality as for fig. 18. x4. Original of Howells (1982: pl. 11, fig. 15.
19. Dorsal view of cranidium, internal mould. Paratype specimen, BM In44479, horizon and locality as for fig. 18. x4. Original of Howells (1982: pl. 11, fig. 17).
20. Dorsal view of cranidium, internal mould. GLAHM A20936, horizon and locality as for fig. 18. x5.

Plate 7. 2

***Acernaspis xynon* Howells, 1982**

1. Dorsal view of partially testate cranidium. BM In47894, Woodland Fm. (Rhuddanian Stage, Llandovery Series, *cyphus* Zone). Woodland Point, 430m W of Woodland Farm. x5.
2. Dorsal view of cranidium, internal mould. BM In44454, horizon and locality as for fig. 1. x6.

***Acernaspis* sp. nov. A**

3. Dorsal view of cranidium, internal mould. GLAHM A20868, Lower Camregan Grits (Aeronian Stage, Llandovery Series, *sedgwickii* Zone). Camregan Wood Quarry, S side of Camregan Hill, about 800m SW of Penkill Castle. x8.
4. Ventral view of cephalic doublure, internal mould. GLAHM A17369, horizon and locality as for fig. 3. x4. Original of Howells (1982: pl. 12, fig. 10).
5. Dorsal view of incomplete cranidium, internal mould. BM It14242, horizon as for fig. 3. Small quarry on S side of Craigfin Hill. x4. Latex cast of counterpart figured by Howells (1982: pl. 12, fig. 8).
6. Ventral view of cephalic doublure, internal mould. RM Ar53607, Motala Fm. (middle Llandovery Series). Gustavsvik, Motala district, Östergötland. x5. Original of Ramsköld (1988: fig. 1A).

***Acernaspis woodburnensis* Clarkson, Eldredge and Henry, 1977**

7. Dorsal view of complete individual, internal mould. Holotype specimen BGS GSE5777, Wood Burn Fm. (Llandovery Series, topmost Aeronian - basal Telychian stages, *sedgwickii* - *turriculatus* zones). "Bargany Pond Burn", exposures in sides of tributary of Lauchlan Burn 1000m SW of summit of Maxwellston Hill. x1.5. Original of Clarkson *et al.* (1977: pl. 19, fig. 11); also Howells (1982: pl. 11, fig. 24).
13. Dorsal view of partially exfoliated complete individual. Paratype specimen, BGS GSE5780, horizon and locality as for fig. 7. x1.5. Original of Clarkson *et al.* (1977: pl. 19, figs. 12-13); also Howells (1982: pl. 12, figs. 1a-b).

***Acernaspis sufferta* (Lamont, 1947)**

8. Dorsal view of slightly damaged complete individual, internal mould. RSM 1885.26.82C, Wether Law Linn Fm. (Llandovery Series, topmost Telychian Stage). Exposure in S bank of Wether Law Linn, North Esk Inlier, Pentland Hills, Scotland. x2.

11 & 15. Lateral and oblique anterolateral views of cephalon, internal mould. RSM 1876.42.5, horizon and locality as for fig. 8. Fig. 11 x4, fig. 15 x3.

12. Dorsal view of cephalon, internal mould. RSM 1984.8.79, Deerhope Coral Bed, Deerhope Fm. (Llandovery Series, Telychian Stage, *griestoniensis* Zone). S bank of Deerhope Burn, North Esk Inlier, Pentland Hills, Scotland. x3.

14 & 17. Dorsal and oblique lateral views of complete individual, internal mould. RSM 1982.43.2, upper Llandovery Series, North Esk Inlier, exact locality unknown, Pentland Hills, Scotland. Both x3.

16. Dorsal view of complete individual, internal mould with recrystallised surface. RSM 1978.61.534, upper Reservoir Fm. (Llandovery Series, Telychian Stage). Exposure in Deerhope Burn, 20m below the Coral Bed, North Esk Inlier, Pentland Hills, Scotland. x4. Original of Clarkson and Howells (1981: pl. 81, fig. 6).
20. Dorsal view of pygidium, internal mould. Uncatalogued RSM specimen, horizon and locality as for fig. 8. x4.

***Acernaspis* sp. nov. B**

9 & 10. Lateral and dorsal views of cephalon, internal mould. PMO 100552, Vik Fm. (Llandovery Series, Telychian Stage). Garntangen, Ringerike district, Oslo Region. Both x4.

***Acernaspis* sp. nov. C**

18. Dorsal view of cranidium, internal mould. JMM TR62, Middle Kilbride Fm. (Llandovery Series, Telychian Stage, *crispus* or *griestoniensis* zones). Glenglosh, Co. Galway, Ireland. x8.

***Acernaspis rubicundula* Ramsköld, 1985**

19. Ventral view of silicified cephalic doublure. Paratype specimen, RM Ar52907, Högklint Fm, unit b (Wenlock Series, Sheinwoodian Stage). Kopparsvik 3, Visby district, Gotland. x3. Original of Ramsköld (1985: pl. 2, fig. 3).
23. Dorsal view of silicified cephalon. Paratype specimen, RM Ar53034, horizon as for fig. 19. Ireviken 3, Visby district, Gotland. x4. Original of Ramsköld (1985: pl. 2, figs. 4a-c).

***Acernaspis quadrilineata* (Angelin, 1851)**

21. Dorsal view of complete enrolled individual, silicifed. RM Ar31373, lower Visby Fm. (Llandovery Series, topmost Telychian Stage). Visby district, exact locality unknown, Gotland. x3.
22. Dorsal view of complete enrolled individual, silicifed. RM Ar31377, horizon as for fig. 21. Visby district, exact locality unknown, Gotland. x3. Original of Ramsköld (1985: pl. 1, figs. 2a-b).

Plate 7. 3

Acernaspis quadrilineata (Angelin, 1851)

1. Dorsal view of complete enrolled individual, silicified. RM Ar31381, lower Visby Fm. (Llandovery Series, topmost Telychian Stage). Visby district, exact locality unknown, Gotland. x3.

Acernaspis sororia Ramsköld, 1985

2. Dorsal view of complete enrolled individual, silicified. Paratype specimen, RM Ar31388, horizon as for fig. 1. Kronviken, Visby district, Gotland. x4. Original of Ramsköld (1985: pl. 1, fig. 3; pl. 3, figs. 2a-c).
3. Dorsal view of slightly damaged silicified cephalon. Paratype specimen, RM Ar53010, horizon as for fig. 1. Rönnklint 1, Visby district, Gotland. x4. Original of Ramsköld (1985: pl. 3, figs. 3a-c).

Acernaspis rubicundula Ramsköld, 1985

4. Dorsal view of complete enrolled individual, silicified. RM Ar53619, Högklint Fm, unit b (Wenlock Series, Sheinwoodian Stage). Kopparsvik 3, Visby district, Gotland. x5.

Ananaspis fecunda (Barrande, 1846)

5, 7 & 10. Oblique anterolateral, dorsal and lateral views of cephalon, internal mould. RSM 1982.48.74, middle Kopanina Fm. (Ludlow Series). Kosov Quarry, Bohemia. All x2.

6. Dorsal view of cephalon, internal mould. RSM 1982.48.75, horizon and locality as for fig. 5. x2.
8. Dorsal view of incomplete cephalon, internal mould. RSM 1982.48.72, horizon and locality as for fig. 5. x2.

Ananaspis stokesii (Milne Edwards, 1840)

9. Dorsal view of complete individual, internal mould. BM In59329, Much Wenlock Limestone Fm. (Wenlock Series, Homerian Stage). Dudley, exact locality unknown, English West Midlands. x3.
13. Dorsal view of complete partially enrolled individual, internal mould. JMM E0062, horizon as for fig. 9. Dudley, exact locality unknown, English West Midlands. x3.

14. Dorsal view of complete individual, internal mould. BM I1519, horizon as for fig. 9. Dudley, exact locality unknown, English West Midlands. x2.

15. Dorsal view of complete individual, internal mould. BM I7953, horizon as for fig. 9. Dudley, exact locality unknown, English West Midlands. x3.

16 & 17. Lateral view of cephalon and ventral view of cephalic doublure, internal mould. BM In59043, horizon as for fig. 9. Dudley, exact locality unknown, English West Midlands. Both x3.

***Ananaspis* sp. nov. A**

11. Dorsal view of cephalon, internal mould. BGS Ru3229, upper Mottled Mudstone Fm., lower Nantglyn Flags Gp. (Wenlock Series, Homerian Stage, *ludensis* Zone). Plas Uchaf, near Llanrwst, Denbighshire, North Wales. x4.

12. Dorsal view of cephalon, internal mould. BGS Ru4094, horizon and locality as for fig. 11. x4.

PLATE 7.1

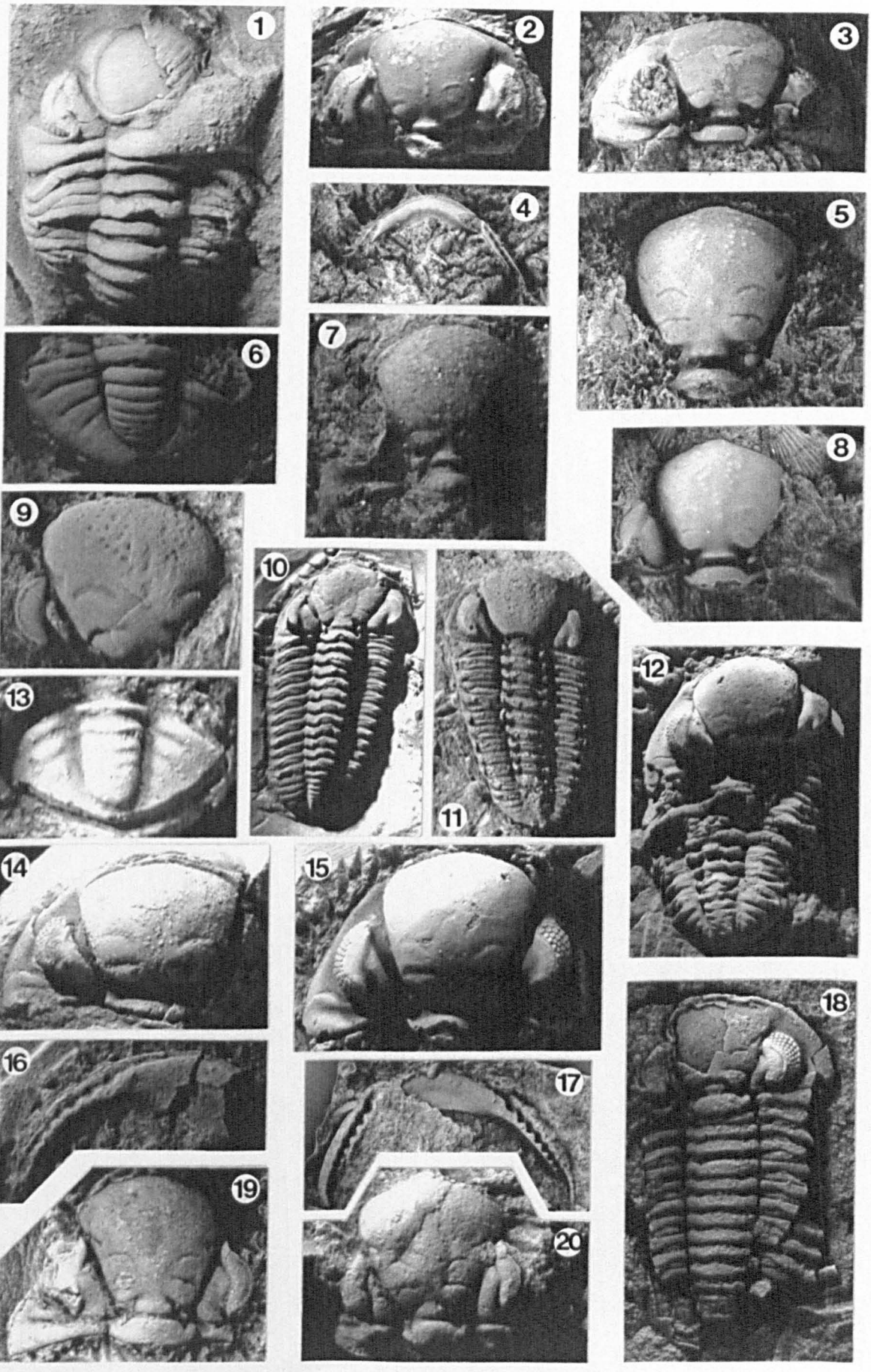

PLATE 7.2

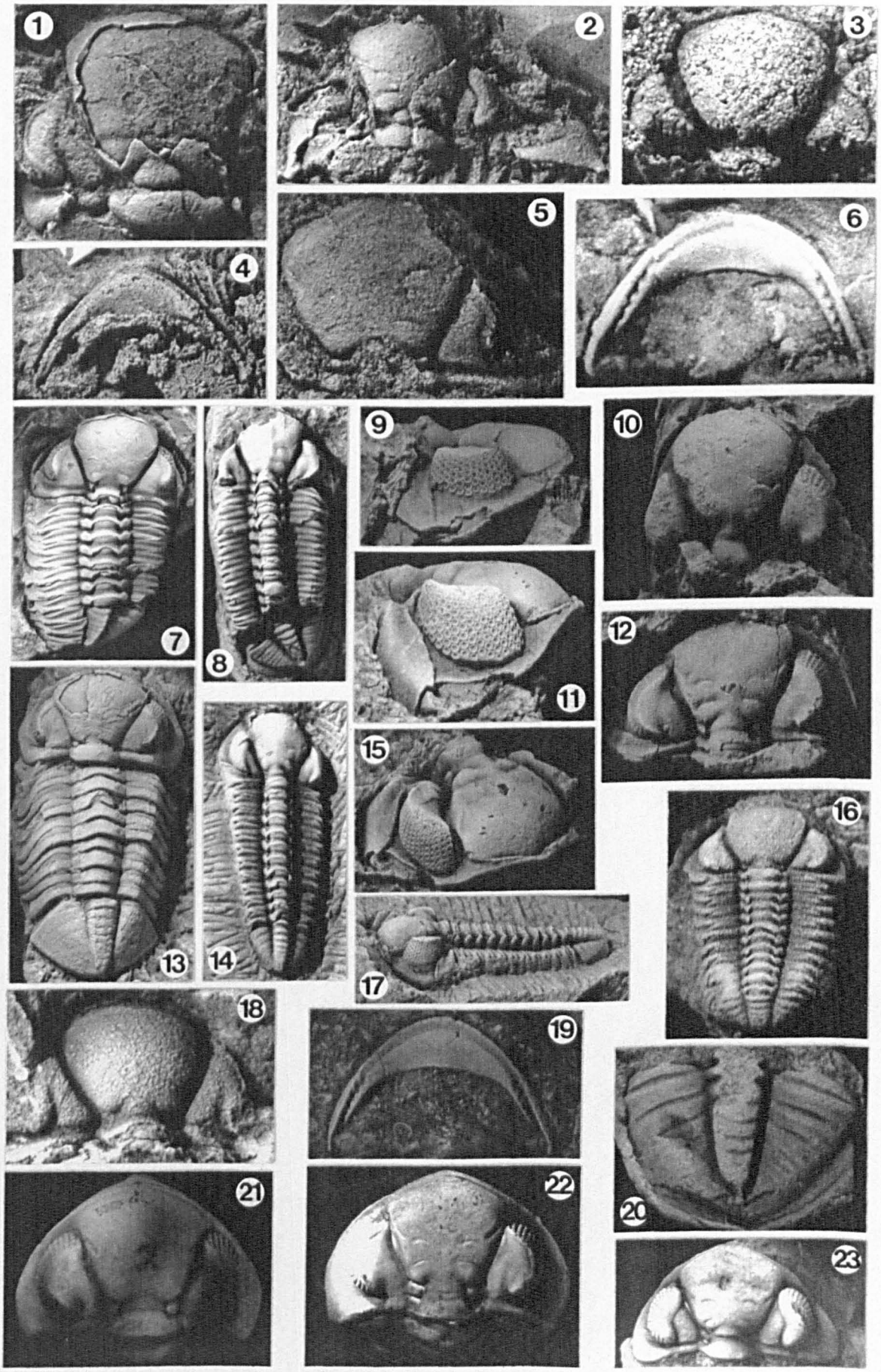

PLATE 7.3

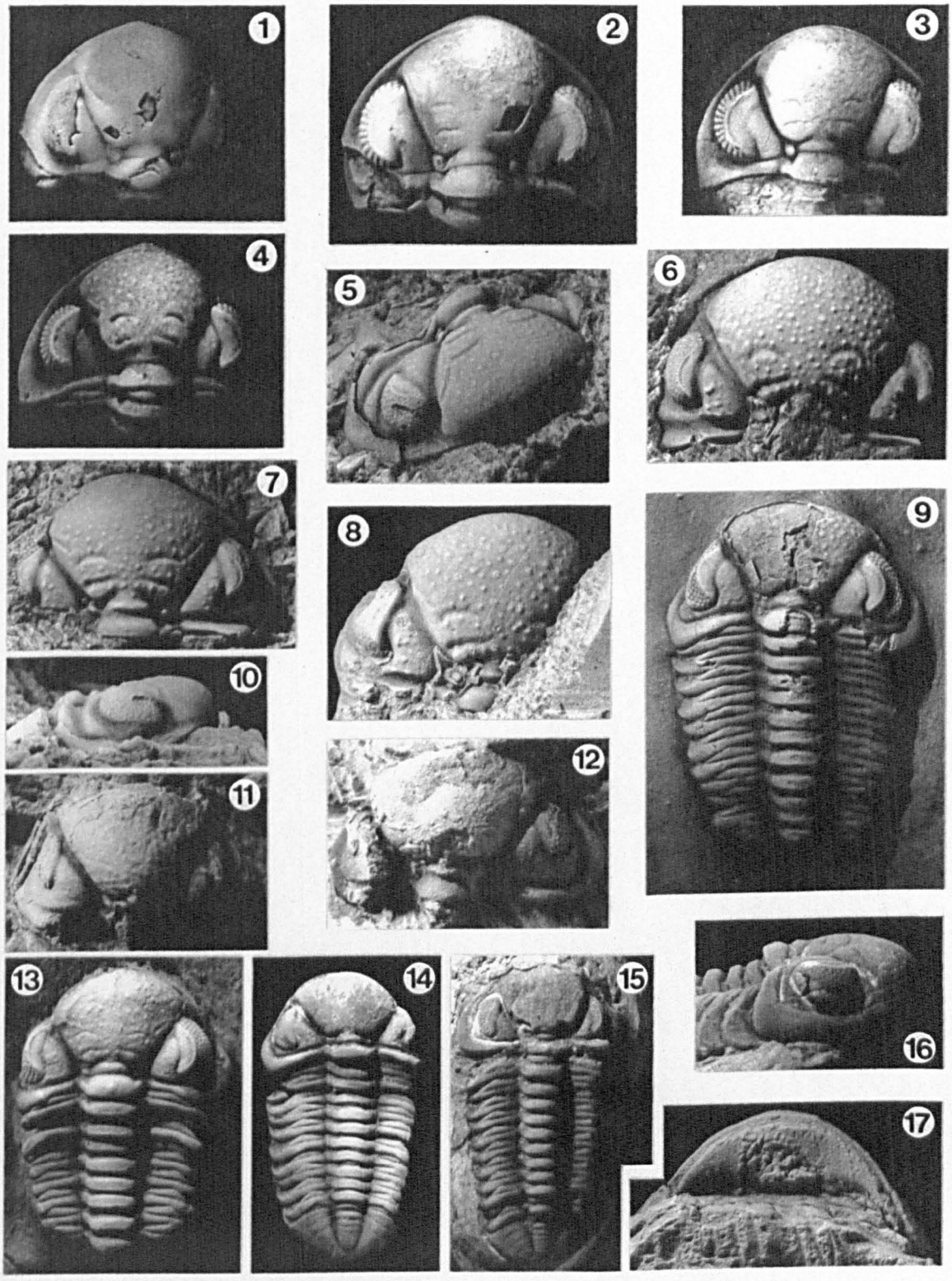

CHAPTER EIGHT

CONCLUSIONS.

8. 1. Primary Conclusions.

The following is a summary of primary conclusions drawn in this study:

1. A study of the chronostratigraphical ranges of trilobite species and genera in Cambrian to Carboniferous strata of England, Scotland and Wales reveals the following:

(i) Histograms of calibrated chronostratigraphical ranges of species and genera are usually highly positively skewed (Figures 2. 1 to 2. 3). There is often a clear discontinuity between the longest duration taxa on the histograms and the rest (*i.e.* the longest duration taxa do not appear just to form the tail end of a continuous spectrum of ranges) suggesting that they are in some qualitative way different from the others in terms of their survivorship.

(ii) Mean generic durations increase from the Cambrian to the Ordovician (from about 4.4 to about 10.9 myr.), then remain approximately constant for the Ordovician and Silurian (at between 10 and 11 myr.). Devonian genera have low mean duration (about 4.2 myr.). Carboniferous genera have much greater mean duration (about 14.8 myr.). The most durable genera from each stratigraphical system are: *Olenellus* Billings (Cambrian); *Proetus* Steininger (Ordovician); *Cornuproetus* Richter and Richter (Silurian); *Typhloproetus* Richter (Devonian); *Archegonus* Burmeister, *Brachymetopus* McCoy and *Eocyphinium* Reed (Carboniferous).

Mean specific durations are approximately constant for the Cambrian and Ordovician (at just over 2 myr.), and are slightly higher for both Silurian and Devonian species (about 3.5 myr.). Carboniferous species have high mean durations (about 5.7 myr.). The most durable species from each stratigraphical system are: *Callavia callavei* (Lapworth) (Cambrian); *Atractopyge petiolulata* Tripp (Ordovician, but note that this species is in need of taxonomic revision; more than one species may be represented). *Dalmanites myops* (König) (Silurian); *Scutellum flabelliferum* (Goldfuss) (Devonian); *Carbonocoryphe colei* (McCoy) and *Namuropyge discors* (McCoy).

(iii) Survivorship plots for all species and genera of trilobites from Palaeozoic strata of England, Scotland and Wales approximate to straight lines (Figure 2. 1) until the number of taxa has fallen to about 1% of the initial number. The longest duration 1% or so fall markedly to the right of this line on both the genus and species plots, suggesting that these longest duration taxa have lower probabilities of extinction in a given time interval than the shorter duration taxa.

(iv) The longest duration Cambrian genera (those whose durations exceed the 90% quantile value for the Cambrian system) tend to include relatively small numbers of long-duration species. Therefore, species stasis appears to play an important role in these long ranging Cambrian genera. There is no clear pattern for the longest duration (>90% quantile) Ordovician genera. Some consist of large numbers of species (suggesting relatively rapid turnover), while others consist of small numbers of species (suggesting species stasis). The Silurian longest duration (>90% quantile) genera resemble other Silurian genera in terms of the number and duration of their included species. There are not enough Devonian genera to draw any conclusion. The longest duration (>90% quantile) Carboniferous genera consist of relatively high numbers of relatively long duration species.

There is therefore no clear answer to the question of whether the longest duration genera are characterised by stasis in their included species (recognised as small numbers of long duration species) or rapid turnover in species (recognised as large numbers of short duration species).

(v) A number of calibrated range charts have been constructed, which show the durations in absolute terms of species (Figures 2. 4 - 2. 8) and genera (Figures 2. 9 - 2. 13) of trilobites from the Palaeozoic of England, Scotland and Wales.

(vi) A study of the relationship between generic duration and position on the marine palaeoslope utilising Ordovician genera from the Laurentian Province indicates that the longest duration genera appear to be the more eurytopic ones (Figure 2. 14). This wide geographical and environmental distribution probably enabled these genera to avoid localised factors which caused extinction in more endemic genera.

2. Based on a phylogenetic and morphometric analysis of the long duration shape conservative pterygometopid *Achatella* Delo, 1935, the following conclusions have been drawn:

(i) Nine species and one form under open nomenclature are recognised. They are: *A. achates* (Billings, 1860), Shermanian-Maysvillian of North America, the type species; *A. consobrina* Tripp, 1954, upper Caradoc, Girvan; *A. kuckersiana* (Schmidt, 1881), basal Caradoc, northern Estonia; *A. retardata* (Reed, 1914), upper Cautleyan-Hirnantian, Girvan and Oslo Region; *A. schmidti* (Warburg, 1925), Rawtheyan, central Sweden; *A. truncatocaudata* (Portlock, 1843),

Cautleyan, Co. Tyrone; *A.* cf. *truncatocaudata*, upper Cautleyan, Girvan; *A.* sp. nov. A, lower Caradoc, eastern Ireland; *A.* sp. nov. B, middle to upper Caradoc, Oslo Region; *A.* sp. nov. C, Shermanian, Wisconsin.

Three poorly known Llandeilian and Caradoc species were not available for study.

(ii) The total duration of the genus is upper Llanvirn-Hirnantian, approximately 22 myr. (time scale of Tucker *et al.* 1990) (Figure 5. 33).

(iii) The genus is characterised by mosaic patterns of states in characters which are superimposed on a conservative body plan, such that few of the species may be diagnosed on the possession of unequivocal apomorphies; rather they are recognised on unique patterns of possession of suites of character states (Figures 5. 7 - 5. 10). However, subclades on the cladogram do fall in correct stratigraphical order, suggesting that there is an underlying directional trend in the possession of character state complexes in the genus, upon which the mosaic pattern of states is superimposed.

(iv) It is tentatively suggested that *A. truncatocaudata* arose through a heterochronic process (possibly hypermorphosis) probably from *A. retardata.*

(v) *Achatella* demonstrates relatively high variation in some morphological characters, notably postocular length (Figure 5. 6), length of the L1 lateral glabellar lobe (Figure 5. 26) and pygidial segmentation (Figure 5. 28).

3. Based on a phylogenetic and morphometric analysis of the long duration shape conservative pterygometopid *Calyptaulax* Cooper, 1930, the following conclusions have been drawn:

(i) Phylogenetic analysis shows that the genus can be subdivided into two subgenera, defined as *Calyptaulax (Calyptaulax)* Cooper, 1930, and *Calyptaulax (Calliops)* Delo, 1935. The two subgenera are diagnosed on the basis of their pygidial morphology; the diagnoses therefore differ from the diagnoses of the pre-existing genera *Calyptaulax* Cooper and *Calliops* Delo. The total duration of the genus is about 25 myr., and the total duration of each of the two subgenera is about 20 myr. (timescale of Tucker *et al.* 1990).

(ii) Five species of *C. (Calyptaulax)* are recognised. They are: *C. (Calyptaulax) actonensis* Dean, 1961, upper Caradoc-Cautleyan, central and northern England;

C. (Calyptaulax) asteroideus (Reed, 1914), Rawtheyan, Girvan; *C. (Calyptaulax) foederatus* Tripp, 1962, Llanvirn-early Caradoc, Girvan; *C. (Calyptaulax) glabella* Cooper, 1930, late Caradoc-Rawtheyan, northern England, Wales, Oslo Region, Québec, the type species; *C. (Calyptaulax) hunteri* (Reed, 1914), early-middle Caradoc, Girvan.

(iii) Ten species of *C. (Calliops)* are recognised. They are: *Calyptaulax (Calliops) angusta* Cooper, 1953, middle Chazyan, Tennessee, Virginia, Alabama, Newfoundland; *Calyptaulax (Calliops) annulata* (Raymond, 1905), Chazyan, New York and Virginia; *Calyptaulax (Calliops) brevipostica* Cooper, 1953, late Chazyan-Blackriveran, Virginia; *Calyptaulax (Calliops) brongniartii* (Portlock, 1843), lower middle to upper Caradoc, Co. Tyrone, Girvan, Southern Uplands, Virginia; *Calyptaulax (Calliops) callicephala* (Hall, 1847), Shermanian-Maysvillian, North America, the type species; *Calyptaulax (Calliops) callirachis* (Cooper, 1953), late Chazyan-Blackriveran, Virginia, Tennessee, Northwestern Territories of Canada; *Calyptaulax (Calliops) cornwalli* Ross, 1967, middle Ordovician, Nevada; *Calyptaulax (Calliops) holstonensis* (Raymond, 1925), middle Chazyan-Blackriveran, Virginia, Tennessee, Alabama; *Calyptaulax (Calliops) larrabeei* (Slocum, 1913), Richmondian, Iowa; *Calyptaulax (Calliops) marginatus* (Tripp, 1962), Llanvirn, Girvan.

(iv) Another species, *Calyptaulax s.l. armatus* Ulrich and Delo, 1940, from the Blackriveran of Oklahoma could not be assigned to a subgenus.

(v) *C. (Calyptaulax)* is relatively well resolved on the cladogram, with subclades which occur in the correct stratigraphical order. Variations in relative lengths of the glabellar lobes, depth of the glabellar furrows, size of the eye and the associated number of lens files, are superimposed on an otherwise stable body plan.

(vi) *C. (Calliops)* is unresolved on the cladogram, due to a complex mosaic pattern of character states, such that species can only be diagnosed on the basis of unique patterns of possession of character states, rather than on possession of unequivocal apomorphies (Figures 6. 7 - 6. 8). This mosaic variation in superficial characters (nature of the genal angles, shape of the pygidium in dorsal and cross-sectional view, nature of the glabellar sculpture) is superimposed on an extremely stable body plan.

4. Based on a morphological study of the shape conservative phacopids *Acernaspis* Campbell, 1967 and *Ananaspis* Campbell, 1967, the following conclusions have been drawn:

(i) Eighteen species of *Acernaspis* are recognised. They are: *A. becsciensis* Lespérance and Letendre, 1982, Rhuddanian, Anticosti Island; *A. boltoni* Lespérance and Letendre, 1982, Rhuddanian-Telychian, Anticosti Island; *A. elliptifrons* (Esmark, 1833), Rhuddanian-Aeronian, Oslo Region, Girvan, Québec; *A. gaspensis* Lespérance and Letendre, 1982, Llandovery, Gaspé; *A. mimica* Lespérance and Letendre, 1982, Aeronian-Telychian, Anticosti Island; *A. orestes* (Billings, 1860), Llandovery, Anticosti Island; *A. quadrilineata* (Angelin, 1851), late Telychian, Gotland; *A. rubicundula* Ramsköld, 1985, Sheinwoodian, Gotland; *A. salmoensis* Lespérance, 1988, Rhuddanian, Anticosti Island; *A. skidmorei* (Lespérance, 1968), lower Llandovery, Gaspé; *A. sororia* Ramsköld, 1985, late Telychian, Gotland; *A. sufferta* (Lamont, 1947), ?late Aeronian-Telychian, Pentland Hills; *A. superciliexcelsis* Howells, 1982, Aeronian, Girvan; *A. woodburnensis* Clarkson, Eldredge and Henry, 1977, late Aeronian, Girvan; *A. xynon* Howells, 1982, Rhuddanian-Aeronian, Girvan; *A.* sp. nov. A, middle Llandovery, Girvan and Östergötland; *A.* sp. nov. B, late Aeronian - late Telychian, Oslo Region; *A.* sp. nov. C, Telychian, Co. Galway. The total duration of the genus is about 11 myr. (timescale of Harland *et al.* 1989).

A number of poorly known species were not available for study.

(ii) Four species of *Ananaspis* have been studied in order to test the hypothesis that this genus arose through neoteny from *Acernaspis*. They are: *A. amelangorum* Ramsköld, 1985, Homerian, Gotland; *Ananaspis fecunda* (Barrande, 1846), Ludlow, Barrandian, the type species; *A. stokesii* (Milne Edwards, 1840), Wenlock, Welsh Borderlands; *A.* sp. nov. A, Homerian, North Wales.

(iii) A phylogenetic analysis carried out by Ramsköld and Werdelin (1991) has demonstrated the occurrence of many convergences within *Acernaspis*, with mosaic patterns of character states resulting in a poorly resolved consensus tree for the clade. Thus, many species can only be diagnosed on unique possession of suites of character states rather than on unequivocal apomorphies. Vincular structures are of particular note in this respect. For example, a number of species occur in Llandovery strata of Anticosti Island, with very similar dorsal morphologies but differing greatly in their vincular morphologies. Some of these

species coexisted. Clearly the vincular structures were able to be very different in closely related species, and appear to have undergone rapid evolution.

(iv) It has been demonstrated that *Ananaspis* may have been derived from *Acernaspis* through a process of neoteny, as originally suggested by Ramsköld (1988). However, Ramsköld considered successively stratigraphically later *Ananaspis* species to be progressively more neotenic with respect to *Acernaspis*. Results obtained herein do not support this (Table 7. 3; p. 207). *Ananaspis* sp. nov. A appears to have arisen through neoteny from a species of *Acernaspis*, and then given rise to a radiation of *Ananaspis* species, with neoteny not necessarily playing the major role in the origination of the subsequent *Ananaspis* species. Ramsköld envisaged the species of *Ananaspis* as constituting a single anagenetic line, each species being successively more neotenic with respect to *Acernaspis*, whereas herein it is considered that the main neotenic event was that giving rise to *Ananaspis* sp. nov. A, and this species then gave rise to a clade, with neoteny playing a role of variable importance in the origination of the various subsequent species.

8. 2. General Conclusions on Stasis.

It is certainly not true to say that the shape conservative genera studied herein remained morphologically invariant throughout their existence. *Achatella*, *Calyptaulax* and *Acernaspis* all exhibit mosaic evolution with many convergences between species, as evidenced by the low consistency indices of the cladograms for stratigraphical samples (Figures 5. 7, 6. 5) and species (Figures 5. 9, 6. 7, 7. 3), and the character tracings through the cladograms (Figures 5. 8, 5. 10, 6. 6, 6. 8). This mosaic pattern occurs in what have been called "peripheral" characters herein; *i.e.* characters which can be thought of as being superficial to the main body plan of the organism. It is likely that this reflects the level of developmental canalisation in the organisms. The canalisation is sufficient to allow the "normal" phenotype (*i.e.* the "standard *Achatella* ", "standard *Calyptaulax* " or "standard *Acernaspis* " body plan) to be developed under a variety of environmental conditions, but loose enough to allow the abundant variation in "peripheral" characters which is seen between stratigraphical samples. It may be that different degrees of canalisation apply at different levels of phenotypic organisation. At the "body plan level", canalisation is strong, so that the *Calyptaulax (Calliops)* genome (for example) always produces a *Calyptaulax (Calliops)* phenotype under a wide variety of environmental conditions; but at the "peripheral level", canalisation is less strong, so that a variety of characters can be superimposed on the basic body plan: *C. (Calliops)* with fine glabellar sculpture, *C. (Calliops)* with coarse glabellar sculpture, *C. (Calliops)* with posteriorly produced genal angles, bigger *C. (Calliops)*, smaller *C. (Calliops)*, etc. This plasticity is envisaged as having a genetic basis; *i.e.* it is not considered to be purely

ecophenotypic variation. It may be that it is this genetically-based plasticity in "peripheral" characters which allows such genera to remain adapted to their various host environments without having to undergo more major and fundamental evolutionary changes.

Clearly wide geographical dispersal and eurytopic environmental requirements are also relevant in that they help to "protect" the organism from locally acting events which might cause extinction in more endemic organisms. It is probable that a combination of environment tracking, "generalist" morphology, and highly plastic "peripheral" phenotypic development serves to keep the organisms closely fitted to their environments.

A relatively high degree of developmental plasticity has been noted in Cambrian trilobites by a number of workers (Hughes 1991 and references therein). As was demonstrated in Chapter 2 herein, some Cambrian species have extremely long durations. It may therefore be that the Ordovician and Silurian genera studied herein, in maintaining stasis of their basic body plan through developmental plasticity at the "peripheral level", are exhibiting an evolutionary mode which was far more common in the Cambrian.

It will be noted that the summary diagrams at the end of each genus case study (Figs. 5. 33 - 5. 34, 6. 35 - 6. 36, and 7. 30 - 7. 31) give the impression of a punctuational pattern of speciation followed by stasis within species. Many of the species recognised herein are certainly stable entities in geological time, since they can be recognised from several stratigraphical samples which are widely separated in geological time. For example: *Achatella retardata* and *A. achates* on Figure 5. 34; *Calyptaulax (Calyptaulax) glabella, C. (Calyptaulax) foederatus, C. (Calliops) brongniartii, C. (Calliops) callicephala* on Figure 6. 36; *Acernaspis sufferta* on Figure 7. 31, to mention only a few. Some other species, while only being recognised from one or two of the stratigraphical samples used herein, are reliably reported from elsewhere in the literature, and therefore are also probably stable entities in geological time. For example: *Calyptaulax (Calliops) annulata* and *C. (Calliops) callirachis* on Figure 6. 36; *Acernaspis orestes, A. elliptifrons,* and *Ananaspis stokesii* on Figure 7. 31.

However, other species are recognisable only from single stratigraphical samples, or from only two or three very closely-spaced (in time and space) stratigraphical samples. For example: *Achatella* sp. nov. A, *A. schmidti, A. consobrina, A.* sp. nov. C on Figure 5. 34; *Calyptaulax (Calyptaulax) asteroideus, C. (Calliops) marginatus, C. (Calliops) armatus* on Figure 6. 36; *Acernaspis xynon, A. woodburnensis, A. quadrilineata, A. sororia, A. rubicundula, Ananaspis amelangorum* and *Ananaspis* sp. nov. A on Figure 7. 31, to mention a few. Such species may only be ephemera in continuously-varying

lineages (such as those shown in Figure 1. 1 for example). Application of Linnean taxonomy will tend to have the effect of obscuring such gradualistic patterns if they exist (Sheldon 1987). Such a gradualistic pattern of morphological evolution, possibly including reversals, could only be proved through detailed bed-by-bed sampling from individual stratigraphical sections; eg: from the Silurian of Anticosti Island (host to a number of *Acernaspis* species).

It could be further argued that not all such ephemera need be classed as separate species. There is no evidence for example that individuals identified herein as *Calyptaulax (Calliops) brongniartii, C. (Calliops) callicephala* and *C. (Calliops) larrabeei* would not be capable of interbreeding.

Throughout the three case studies herein, where statistically significant differences have been found between stratigraphically separate samples of fossils, these have been used in an attempt to define species. As mentioned above, it is always possible that animals which are slightly different are in fact two morphs of the same species (eg: *Calyptaulax (Calyptaulax) glabella* and *C. (Calyptaulax) actonensis* could represent morphs of a single species). Further, strongly allometric growth relationships can result in individuals of differing sizes, but belonging to the same species, having markedly different morphometric proportions. This observation is particularly apposite in the cases of *Achatella truncatocaudata* (Chapter 5) and *Acernaspis* sp. nov. A (Chapter 7). It is possible that *Achatella truncatocaudata* represents the same morphospecies as some other species of *Achatella* (? *A. retardata*) which is represented in the stratigraphical samples only by smaller individuals (see for example Figures 5. 21 - 5. 24 for the sizes of specimens of *A. truncatocaudata* as compared with those from other samples of *Achatella*). Localised hydrodynamic conditions may explain the absence of smaller specimens from the KILLEY stratigraphical sample. Similarly, the small specimens from the UCHAF stratigraphical sample for which *Ananaspis* sp. nov. A is erected may in fact be of the same species as *A. fecunda*, represented by much bigger specimens from the Ludlow of Bohemia (stratigraphical sample KOS-KOL-LOC), with which their morphometric similarity has already been noted (Section 7. 5, p. 237). The differences between them (*A.* sp. nov. A has fewer lenses on the visual surface, anterior face of the glabella which slopes less steeply, and more anteriorly-positioned point of maximum width of the cephalon) *may* be attributable to allometry. Again, localised hydrodynamic factors may explain the absence of larger specimens from the UCHAF stratigraphical sample. Further detailed exploration of the possibility of allometry in these samples could help to resolve these questions.

8. 3. Suggestions for Future Work.

1. The statistics on taxonomic ranges presented in Chapter 2 can probably be further analysed in order to relate taxonomic durations to the palaeoenvironments from which the taxa were drawn, if sufficient environmental data can be retrieved from the literature.
2. The morphometric results obtained herein should be compared with results describing intra- and interspecific variability in other, rapidly evolving trilobite taxa. Such comparison may eventually allow quantitative definitions of "stasis" and "non-stasis" in multivariate morphometric terms. Little morphometric data (and none as complete as that presented here) are currently available for trilobites, but the recent growth in the availability of equipment allowing for faster and more precise collection of morphometric data means that such data can now be collected far more easily. In allowing the rapid and accurate collection of data on amounts and patterns of variation in trilobites which evolved at varying rates, modern computer-based morphometrics will allow assessment of the data presented here in a much wider context.

REFERENCES

Allaby, A. and Allaby, M. (eds.) 1990. *The Concise Oxford Dictionary of Earth Sciences.* Oxford University Press. Oxford. 410 pp.

Angelin, N. P. 1851. *Palaeontologica Svecica. I: Iconographica crustaceorum formationis transitionis.* Fasc. 1, 1-24. Lund.

Aru, H. 1990. Ordovician trilobites. *In:* Kaljo, D. and Nestor, H. (eds.). *An excursion guidebook. IGCP project "Global Bioevents" Field Meeting, Estonia. Est. Acad. Sciences,* 72-73.

Ayrton, W. G., Berry, W. B. N., Boucot, A. J., Lajoie, J., Lespérance, P. J., Pavlides, L. and Skidmore, W. B. 1969. Lower Llandovery of the Northern Appalachians and adjacent regions. *Bull. Geol. Soc. Amer.*, **80**, 459-484.

Barnard, C. J. 1984. Stasis: a coevolutionary model. *J. Theor. Biol.*, **110**, 27-34.

Barnes, C. R. 1988. Stratigraphy and palaeontology of the Ordovician-Silurian boundary interval, Anticosti Island, Quebec, Canada. *Bulletin of the British Museum (Natural History)* (Geology), **43**, 195-219.

Barnes, C. R., Norford, B. S. and Skevington, D. 1981. The Ordovician system in Canada: correlation chart and explanatory notes. International Union of Geological Sciences Pub. no. 8, 27 pp., chart.

Barrande, J. 1846. *Notice préliminaire sur le systême Silurien et les Trilobites de Bohême.* 97pp. Leipsic.

Barrande, J. 1852. *Systême Silurien du centre de la Bohême. Iére partie. Recherches paléontologiques.* xxx+935pp. Prague and Paris.

Bassett, D. A., Ingham, J. K. and Wright, A. D. 1974. *Field Excursion Guide to Type and Classical Sections in Britain.* The Palaeontological Association Ordovician System Symposium. Birmingham, 1-66.

Bassett, D. A., Whittington, H. B. and William, A. 1966. The stratigraphy of the Bala district, Merionethshire. *Quart. J. Geol. Soc. London*, **122**, 219-271.

Bassett, M. G. 1974. Review of the stratigraphy of the Wenlock Series in the Welsh Borderland and South Wales. *Palaeontology*, **17**, 745-777.

Bassett, M. G. 1977. The articulate brachiopods from the Wenlock Series of the Welsh Borderland and South Wales. *Palaeontogr. Soc. Monogr.*, **4**, 123-176.

Bassett, M. G. and Cocks, L. R. M. 1974. A review of Silurian brachiopods from Gotland. *Fossils and Strata*, **3**, 1-56.

Becker, R. A., Chambers, J. M. and Wilks, A. R. 1988. The New S Language: a programming environment for data analysis and graphics. Wadsworth & Brooks / Cole Advanced Books & Software, Pacific Grove, California. 702pp.

Begg, J. L. 1943. Hypostomes of some Girvan trilobites and their relationship to the cephala. *Geological Magazine*, **80**, 56-65.

Begg, J. L. 1946. Some new fossils from the Girvan district. *Trans. Geol. Soc.*

Glasgow, **21**, 29-47.

Begg, J. L. 1951. Some new Girvan trilobites: with a note on the ventral aspect of *Phacops elliptifrons*. *Trans. Geol. Soc. Glasgow*, **21**, 362-370.

Billings, E. 1860. Description of some new species of fossils from the Lower and Middle Silurian rocks of Canada. *Canadian Naturalist & Geologist*, **5**, 49-69.

Bolton, T. E. 1971. Geological map and notes on the Ordovician and Silurian litho- and biostratigraphy, Anticosti Island, Québec. *Geol. Surv. Pap. Can., Ottawa*, **71-19**, 1-20.

Bolton, T. E. 1972. Geological map and notes on the Ordovician and Silurian litho- and biostratigraphy, Anticosti Island, Québec. *Geol. Surv. Canada Paper* 71-19, 20pp.

Bolton, T. E. 1981. Ordovician and Silurian biostratigraphy, Anticosti Island, Québec. *In:* Lespérance, P. J. (ed.) *Field meeting, Anticosti-Gaspé, Quebéc 1981, Vol. II (Stratigraphy and Palaeontology), Montréal (I.U.G.S. Subcommision on Silurian Stratigraphy Ordovician-Silurian Boundary Working Group)*, 41-59.

Bookstein, F. L. 1982. Foundations of morphometrics. *Ann. Rev. Ecol. Syst.*, **13**, 451-470.

Bookstein, F. L., Chernoff, B., Elder, R., Humphries, J., Smith, G. and Strauss, R. 1985. *Morphometrics in Evolutionary Biology*. The Academy of Natural Sciences of Philadelphia, Philadelphia.

Boucot, A. 1975. *Evolution and extinction rate controls*. Elsevier Scientific Publ. Co. Amsterdam, N.Y.

Bowring, S. A., Grotzinger, J. P., Isachsen, C. E., Knoll, A. H., Pelechaty, S. M. and Kolosov, P. 1993. Calibrating rates of Early Cambrian evolution. *Science*, **261**.

Bradley, J. H. 1930. Fauna of the Kimmswick Limestone of Missouri and Illinois. *Contributions from the Walker Museum*, University of Chicago, Chicago, IL, No. 2, 219-290.

Brenchley, P. J. and Cocks, L. R. M. 1982. Ecological associations in a regressive sequence: the latest Ordovician of the Oslo-Asker district, Norway. *Palaeontology*, **25**, 783-815.

Brenchley, P. J. and Newall, G. 1980. A facies analysis of Upper Ordovician regressive sequences in the Oslo Region of Norway - a record of glacio-eustatic changes. *Palaeogeog., Palaeoclimatol., Palaeoecol.*, **31**, 1-38.

Brett, C. E. and Baird, G. C. 1992. Coordinated stasis and evolutionary ecology of Silurian-Devonian marine biotas in the Appalachian basin. *Geol. Soc. America Abstracts with Programs*, **1992**, A140.

Brown, D. J. and Henderson, J. 1869. On the Silurian rocks of the Pentland Hills, with notes upon the Brachiopods by Thos. Davidson. *Trans. Edinb. Geol. Soc.*, **1**, 23-33.

Bunker, B. J., Witzke, B. J., Watney, W. L. and Ludvigson, G. A. 1988. Phanerozoic

history of the central midcontinent, United States. *In:* Sloss, L. L. (ed.). *The Geology of North America, Volume D-2. Sedimentary Cover - North American Craton: U.S. The Geological Society of America.* 243-260.

Campbell, K. S. W. 1967. Trilobites of the Henryhouse Formation (Silurian) in Oklahoma. *Bull. Oklahoma Geological Survey*, **115**, 1-68.

Campbell, K. S. W. 1977. Trilobites of the Haragan, Bois d'Arc and Frisco Formations (Early Devonian) Arbuckle Mountains Region, Oklahoma. *Bull. Oklahoma Geological Survey*, **123**, 1-227.

Charlesworth, B., Lande, R. and Slatkin, M. 1982. A neo-Darwinian commentary on macroevolution. *Evolution*, **36**, 474-498.

Chatterton, B. D. E. 1971. Taxonomy and ontogeny of Siluro-Devonian trilobites from near Yass, New South Wales. *Palaeontographica*, (A) **137**, 1-108.

Chatterton, B. D. E. 1980. Ontogenetic studies of middle Ordovician trilobites from the Esbataottine Formation, Mackenzie Mountains, Canada. *Palaeontographica*, (A) **171**, 1-74.

Chatterton, B. D. E. and Ludvigsen, R. 1976. Silicified Middle Ordovician trilobites from the south Nahanni River area, District of Mackenzie, Canada. *Palaeontographica*, (A) **154**, 1-106.

Chlupáč, I. 1972. New Silurian and Lower Devonian phacopid trilobites from the Barrandian area (Czechoslovakia). *Cas. Mineral. Geol.*, **17**, 4, 395-401.

Chlupáč, I. 1977. The phacopid trilobites of the Silurian and Devonian of Czechoslovakia. *Rozpravy Ústředního Ústavu Geologického*, **43**, 1-172.

Chlupáč, I. (ed.), Kodym, O., Suk, M., Halub, V., Eliáš, M., Cicha, I., Malkovsk ý, M., Tyŕaček, J., Menčík, E. and Buday, T. 1984. Stratigraphic development of the units. *In:* Suk, M. (ed.). *Geological History of the Territory of the Czech Socialist Republic.* Czechoslovak Academy of Sciences, Prague.

Clarke, J. M. and Hall, J. 1894. Report of the Department of Paleontology. *NY St. Geol. Annual Report*, **13**, 599-657; *NY State Museum Annual Report*, **47**, 793-851.

Clarke, J. M. 1897. The Lower Silurian trilobites of Minnesota. *In:* Geological and natural history survey of Minnesota, 3. *Geology of Minnesota*, 695-759.

Clarke, J. M. 1908. Early Devonic history of New York and eastern North America. *Mem. N.Y. State Mus.*, **9**, 1, 1-366.

Clarkson, E. N. K. 1988. The origin of marine invertebrate species: a critical review of microevolutionary transformations. *Proc. Geol. Ass.*, **9**, 153-171.

Clarkson, E. N. K., Eldredge, N. and Henry, J. -L. 1977. Some Phacopina (Trilobita) from the Silurian of Scotland. *Palaeontology*, **20**, 119-142.

Clarkson, E. N. K., Harper, D. A. T., Owen, A. W. and Taylor, C. M. 1992. Ordovician faunas in mass-flow deposits, southern Scotland. *Terra Nova*, **4**, 245-253.

Clarkson, E. N. K. and Tripp, R. P. 1982. The Ordovician trilobite *Calyptaulax brongniartii* (Portlock). *Trans. Roy. Soc. Edinburgh: Earth Sciences*, **72**, 287-294.

Cocks, L. R. M., Holland, C. H., and Rickards, R. B. 1992. *A revised correlation of Silurian rocks of the British Isles.* Geol. Soc. London, Special Report No. 21.

Cocks, L. R. M. and Toghill, P. 1973. The biostratigraphy of the Silurian rocks of the Girvan District, Scotland. *Quart. J. Geol. Soc. London*, **129**, 209-243.

Compston, W. and Williams, I. S. 1992. Ion probe ages for the British Ordovician and Silurian stratotypes. *In:* Webby, B. and Laurie (eds.). *Global perspectives on Ordovician Geology.* Balkema. Rotterdam.

Compston, W., Williams, I. S., Kirschvink, J. L., Zhang Zichao and Guogan, M. 1992. Zircon U-Pb ages from the Early Cambrian time-scale. *J. Geol. Soc. London*, **149**, 171-184.

Cooper, B. N. 1953. Trilobites from the Lower Champlainian formations of the Appalachian Valley. *Memoirs of the Geological Society of America*, no. 55, v+69pp.

Cooper, G. A. 1930. Upper Ordovician and Lower Devonian stratigraphy and paleontology of Percé, Quebec. Part II. New species from the Upper Ordovician of Percé. *American Journal of Science*, **20**, 365-392.

Cooper, J. A., Jenkins, R. J. F., Compston, W. and Williams, I. S. 1992. Ion-probe dating of a mid-Early Cambrian tuff in South Australia. *J. Geol. Soc. London*, **149**, 185-192.

Dalman, J. W. 1827. Om Palaeaderna eller de så kallade Trilobiterna. *Kungliga Svenska Vetenskapsacademiens Handlingar*, 1826 (2), 113-152, 226-294.

Darwin, C. 1859. *The Origin of Species by means of Natural Selection.* Murray. London.

Davis, J. C. 1986. *Statistics and Data Analysis in Geology* (Second Edition). John Wiley & Sons. New York. 646pp.

Dean, W. T. 1958. The faunal succession of the Caradoc Series of South Shropshire. *Bulletin of the British Museum (Natural History)* (Geology), **3**, 191-231.

Dean, W. T. 1959. The stratigraphy of the Caradoc Series in the Cross Fell Inlier. *Proc. Yorks. Geol. Soc.*, **32**, 185-228.

Dean, W. T. 1960. The Ordovician trilobite faunas of South Shropshire I. *Bull. Br. Mus. (Natural History)* (Geology), **4**, 71-143.

Dean, W. T. 1961. The Ordovician trilobite faunas of south Shropshire II. *Bulletin of the British Museum (Natural History)* (Geology), **5**, 313-358.

Dean, W. T. 1962. The trilobites of the Caradoc Series in the Cross Fell Inlier of northern England. *Bulletin of the British Museum (Natural History)* (Geology), **7**, 67-134.

Delo, D. M. 1935. A revision of the Phacopid trilobites. *J. Paleo.*, **9**, 402-420.

Delo, D. M. 1940. Phacopid trilobites of North America. *Special Papers. Geological Society of America*, no. **29**, 1-135.

DeMott, L. L. 1963. *Middle Ordovician trilobites of the upper Mississippi Valley.* Unpublished Ph.D. thesis, Harvard University, Cambridge, MA, 1-236.

Doyle, E. N. 1989. *The Biostratigraphy and Sedimentology of the Lower Silurian (Llandovery) Rocks of North Glaway.* Unpublished Ph.D. thesis, University College Galway.

Edgecombe, G. D. and Chatterton, B. D. E. 1987. Heterochrony in the Silurian radiation of encrinurine trilobites. *Lethaia*, **20**, 337-351.

Eldredge, N., and Gould, S. J. 1972. Punctuated equilibria: an alternative to phyletic gradualism. *In:* Schopf, T. J. M. (ed.). *Models in Paleobiology.* Freeman. San Francisco. 82-115.

Engel, B. A. and Morris, N. 1983. *Phillipsia-Weberphillipsia* in the early Carboniferous of eastern New South Wales. *Alcheringa*, **7**, 223-251.

Esmark, M. T. 1833. Om nogle nye Arter af Trilobiter. *Magazin Naturvidensk Christiania*, **11**, 268-270.

Fåhraeus, L. E. 1967. Upper Ludlovian deposits of Gotland defined by means of conodonts. *Geol. Fören. Stockholm Förh.*, **89**, 218-220.

Feist, R. and Clarkson, E. N. K. 1989. Environmentally controlled phyletic evolution, blindness and extinction in late Devonian tropidocorphine trilobites. *Lethaia*, **22**, 103-121.

Fisher, D. C. 1990. Rates of evolution - living fossils. *In:* Briggs, D. E. G. and Crowther, P. R. (eds.). *Palaeobiology: a synthesis.* Blackwell Scientific Publications, Oxford, 152-159.

Foerste, A. F. 1887. Notes on Illaeni. *Minn. Geol. Soc. Annual Report*, **15**, 478-481.

Foerste, A. F. 1919. Silurian fossils from Ohio, with notes on related species from other horizons. *Ohio Journal of Science*, **19**, 367-404.

Foote, M. 1988. Survivorship analysis of Cambrian and Ordovician trilobites. *Paleobiology*, **14**, 258-271.

Foote, M. 1989. Perimeter-based Fourier analysis: a new morphometric method applied to the trilobite cranidium. *J. Paleo.*, **63**, 880-885.

Foote, M. 1990. Nearest-neighbor analysis of trilobite morphospace. *Syst. Zool.*, **39**, 371-382.

Foote, M. 1991a. Morphologic patterns of diversification: examples from trilobites. *Palaeontology*, **34**, 461-485.

Foote, M. 1991b. Morphological and taxonomic diversity in a clade's history: the blastoid record and stochastic simulations. *Contributions from the Museum of Paleontology, University of Michigan*, **28**, 101-140.

Fortey, R. A. 1975. Early Ordovician trilobite communities. *Fossils and Strata*, **4**, 339-360.

Fortey, R. A. 1980. Genric longevity in lower Ordovician trilobites: relation to environment. *Paleobiology*, **6**, 24-31.

Fortey, R. A. 1985. Gradualism and punctuated equilibria as competing and complementary theories. *In:* Cope, J. C. W. and Skelton, P. (eds.). Evolutionary case histories from the fossil record. *Spec. Pap. Palaeont.*, **33**, 17-28.

Fortey, R. A., Harper, D. A. T., Ingham, J. K., Owen, A. W. and Rushton, A. W. A. In press. A revision of the Ordovician series and stages from the historical type area. *Geol. Mag.*

Fortey, R. A. and Owens, R. M. 1987. The Arenig Series in South Wales. *In:* The Arenig Series in South Wales: stratigraphy and palaeontology. *Bulletin of the British Museum (Natural History)* (Geology), **41**, 69-307.

Fortey, R. A. and Owens, R. M. 1990. Trilobites. *In:* McNamara, K. J. (ed.), *Evolutionary Trends.* Belhaven Press. London. 121-142.

Fortey, R. A. and Rushton, A. W. A. 1980. *Acanthopleurella* Groom 1902: Origin and life-habits of a miniature trilobite. *Bulletin of the British Museum (Natural History)* (Geology), **33**, 79-89.

Gingerich, P. D. 1983. Rates of evolution: effects of time and temporal scaling. *Science*, **222**, 159-161.

Goldring, R. and Stephenson, D. G. 1972. The depositional environments of three starfish beds. *N. Jb. Geol. Palaeont. H.*, **10**, 611-624.

Gould, S. J. and Eldredge, N. 1993. Punctuated equilibrium comes of age. *Nature*, **366**, 223-227.

Hall, J. 1847. *Paleontology of New York*, Vol. I. Albany. xiii + 338 pp.

Harland, W. B., Armstrong, R. L., Cox, A. V., Craig, L. E., Smith, A. G. and Smith, D. G. 1989. *A Geologic Time Scale.* Cambridge University Press. Cambridge. 263 pp.

Harper, D. A. T. 1981. The stratigraphy and faunas of the Upper Ordovician High Mains Formation of the Girvan district. *Scott. J. Geol.*, **17**, 247-255.

Harper, D. A. T. 1981a. The late Ordovician Lady Burn Starfish Beds of Girvan. *Proc. Geol. Soc. Glasgow*, **122/123**, 28.

Harper, D. A. T. 1982. The stratigraphy of the Drummuck Group (Ashgill), Girvan. *Geol. J.* **17**, 251-277.

Harper, D. A. T. 1988. Ordovician - Silurian junctions in the Girvan district, SW Scotland. *Bulletin of the British Museum (Natural History)* (Geology), **43**, 45-52.

Harper, D. A. T. and Ryan, P. D. 1990. Towards a statistical system for palaeontologists. *J. Geol. Soc. London*, **147**, 935-948.

Harper, J. C. 1952. The Ordovician rocks between Collon (Co. Louth) and Grangegeeth (Co. Meath). *Scientific Proceedings of the Royal Dublin Society,*

New Series, **26**, 85-112.

Haswell, G. C. 1865. *On the Silurian formation in the Pentland Hills.* 48pp. Edinburgh.

Hawle, I. and Corda, A. J. C. 1847. *Prodrom einer Monographie der böhmischen Trilobiten.* 176pp. Prague.

Hede, J. E. 1960. The Silurian of Gotland. *In:* Regnéll, G. and Hede, J. E. (eds.). The lower Palaeozoic of Scania; the Silurian of Gotland. *Excursion Guide 21st Intern. Geol. Congr., Copenhagen*, 1960. 44-89.

Helbert, G. J. 1985. *Silurian trilobites from Scandinavia.* Unpublished Ph.D. thesis, University of Keele.

Helbert, G. J., Lane, P. D., Owens, R. M., Siveter, D. J. and Thomas, A. T. 1982. Lower Silurian trilobites from the Oslo Region. *In:* Worsley, D. (ed.). *IUGS Subcommission on Silurian Stratigraphy. Field Meeting, Oslo Region. Paleont. Contr. Univ. Oslo 278*, 129-148.

Henderson, J. 1867. Short notice of three species of trilobites from the Silurian beds of the Pentland Hills. *Trans. Edinb. Geol. Soc.*, **1**, 21.

Henry, J. -L. 1980. Trilobites ordoviciens du Massif Armoricain. *Mém. Soc. géol. miner. Bretagne*, **22**, 1-250.

Henry, J. -L. and Clarkson, E. N. K. 1975. Enrollment and coaptations in some species of the Ordovician trilobite genus *Placoparia. Fossils and Strata*, **4**, 87-96.

Hoffman, A. 1982. Punctuated versus gradual mode of evolution: a reconsideration. *Evol. Biol.*, **15**, 411-436.

Hoffman, A. 1989. *Arguments on Evolution: a palaeontologist's perspective.* Oxford University Press. New York. 274 pp.

Holloway, D. J. 1980. Middle Silurian trilobites from Arkansas and Oklahoma, U.S.A. *Palaeontographica*, (A) **170**, 1-85.

Holtedahl, O. 1910. Über einige norwegischen Oleniden. *Norsk. Geologisk Tidsskrift*, (II) **2**, 1-24.

Howell, H. H. and Geikie, A. 1861. The Geology of the Neighbourhood of Edinburgh. *Mem. Geol. Surv. U.K.* 1-151.

Howells, Y. 1982. Scottish Silurian trilobites. *Monographs of the Palaeontographical Society*, 1-76.

Hughes, N. C. 1991. Morphological plasticity and genetic flexibility in a Cambrian trilobite. *Geology*, **19**, 913-916.

Hurst, J. M. 1979a. Evolution, succession and replacement in the type upper Caradoc (Ordovician) benthic faunas of England. *Palaeogeog., Palaeoclimatol., Palaeoecol.*, **27**, 189-246.

Hurst, J. M. 1979b. The stratigraphy and brachiopods of the upper part of the type Caradoc of south Salop. *Bulletin of the British Museum (Natural History)* (Geology), **32**, 183-304.

Ingham, J. K. 1978. Geology of a continental margin 2: middle and late Ordovician transgression, Girvan. *In:* Bowes, D. R. and Leake, B. E. (eds.). *Crustal evolution in northwestern Britain and adjacent regions.* Geol. J. Special Issue **10**, 163-176.

Ingham, J. K. 1992. Girvan foreshore. *In:* Lawson, J. D. and Weedon, D. S. (eds.). *Geological Excursions around Glasgow and Girvan.* Geological Society of Glasgow. Glasgow. 396-416.

Ingham, J. K., McNamara, K. J. and Rickards, R. B. 1978. The upper Ordovician and Silurian rocks. *In:* Moseley, F. (ed.). *The geology of the Lake District.* Yorks. Geol. Soc. occassional publication no. 3. W. S. Maney and Son. Leeds. 121-145.

Ingham, J. K. and Tripp, R. P. 1991. The trilobite fauna of the middle Ordovician Doularg Formation of the Girvan district, Scotland, and its palaeoenvironmental significance. *Trans. Roy. Soc. Edinburgh: Earth Sciences*, **82**, 27-54.

Isachsen, C. E., Bowring, S. A., Landing, E., Samson, S. A. 1994. New constraints on the division of Cambrian time. *Geology*, **22**, 496-498.

Jaanusson, V. 1953. Über die Fauna der oberordovizischen Slandrom-Kalksteines im Siljan-Gebiet, Dalarna. *Geol. För. Stockh. Förh.*, **75**, 97-105.

Jaanusson, V. 1982. The Siljan district. *In:* Bruton, D. L. and Williams, S. H. (eds.). *Field excursion guide. IV International Symposium on the Ordovician System. Paleont. Contr. Univ. Oslo 279*, 15-42.

Jaanusson, V., Laufeld, S. and Skoglund, R. (eds.). 1979. Lower Wenlock faunal and floral dynamics, Vattenfallet section, Gotland. *Sver. geol. Unders.* C **762**, 1-294.

Jaanusson, V and Ramsköld, L 1993. Pterygometopine trilobites from the Ordovician of Baltoscandia. *Palaeontology*, **36** (4), 743-770.

Jones, B. 1988. Paleoscene 8: biostatistics in paleontology. *Geoscience Canada*, **15**, 3-22.

Jones, B. G., Hall, C. G., Wright, A. J. and Carr, P. F. 1986. The geology of the Bungonia - Windellama area, New South Wales. *Proceedings Linn. Soc. NSW*, **108**, 267-286.

Kaufmann, R. 1933. Variations statistische Untersuchungen über die 'Artabwandlung' und 'Artumbildung' an der Oberkambrischen Trilobitengattung *Olenus* Dalm. *Abh., Geol.-Paläont. Inst. Univ. Griefswald*, **10**, 1-54.

Kay, G. M. 1943. Mohawkian Series on West Canada Creek, New York. *American Journal of Science*, **241**, 597-606.

Kitchell, J. A. 1990. Computer applications in palaeontology. *In:* Briggs, D. E. G. and Crowther, P. R. (eds.). *Palaeobiology: a synthesis.* Blackwell Scientific Publications, Oxford, 493-499.

Klasser, G. J., Mooi, R. D., and Locke, A. 1991. Consistency indices and random data.

Syst. Zool., **40**, 446-457.

Kneller, B. C., Scott, R. W., Soper, N. J., Johnson, E. W. and Allen, P. M. 1994. Lithostratigraphy of the Windermere Supergroup, northern England. *Geol. J.*, **29**, 219-240.

Kórts, A. and Einasto, R. 1990. Kohtla and Maidla quarries. *In:* Kaljo, D. and Nestor, H. (eds.). *An excursion guidebook. IGCP project "Global Bioevents" Field Meeting, Estonia. Est. Acad. Sciences,* 145-148.

Labandeira, C. C. and Hughes, N. C. 1994. Biometry of the later Cambrian trilobite genus Dikelocephalus and its implications for trilobite systematics. *J. Paleo.*, **68**, 492-517.

Laird, M. G. and McKerrow, W. S. 1970. The Wenlock sediments of north-west Galway, Ireland. *Geol. Mag.*, **107**, 297-317.

Lamont, A. 1947. Gala-Tarannon Beds in the Pentland Hills, near Edinburgh. *Geol. Mag.*, **84**, 193-208, 289-303.

Lamont, A. 1965. Gala-Tarannon trilobites and an ostracod from the Hagshaw Hills, Lanarkshire. *Scottish Journal of Science*, **1**, 33-46.

Lande, R. 1986. The dynamics of peak shifts and the pattern of morphological evolution. *Paleobiology*, **12**, 343-354.

Laufeld, S. 1974. Reference localities for palaeontology and geology in the Silurian of Gotland. *Sveriges Geologiska Undersökning*, Ser. C, No. 705, 1-172.

Leggett, J., McKerrow, W. S. and Eales, M. H. 1979. The Southern Uplands of Scotland: a lower Palaeozoic accretionary prism. *J. Geol. Soc.*, **136**, 755-770.

Lespérance, P. J. 1968. Ordovician and Silurian faunas of the Whitehead Formation, Percé region, Québec. *J. Paleo.*, **42**, 811-826.

Lespérance, P. J. 1985. Faunal distributions across the Ordovician-Silurian boundary, Anticosti Island and Percé, Québec, Canada. *Can. J. Earth Sci.*, **22**, 838-849.

Lespérance, P. J. 1988. Percé, Québec, Canada. *Bulletin of the British Museum (Natural History)* (Geology), **43**, 239-245.

Lespérance, P. J. 1991. Vincular furrows in some early Silurian and Devonian phacopidae (Trilobita), predominantly from North America. *J. Paleo.*, **65**, 276-294.

Lespérance, P. J. and Letendre, J. 1981. Phacopid trilobites of the Anticostian Series of Anticosti Island and of the Matapédia Group in Gaspé (Québec). *In:* Lespérance, P. J. (ed.). *Field meeting, Anticosti-Gaspé, Quebéc 1981, Vol. II (Stratigraphy and Palaeontology), Montréal (I.U.G.S. Subcommision on Silurian Stratigraphy Ordovician-Silurian Boundary Working Group),* 179-209.

Lespérance, P. J. and Letendre, J. 1982. Some early Silurian Phacopidae (Trilobita). *In:* Mamet, B. and Copeland, K. J. (eds.) *Proc. 3rd N. Amer. Palaeont. Conv. 2, 329-336.*

Levinton, J. S. 1983. Stasis in progress: the empirical basis of macroevolution. *Ann.*

Rev. Ecol. Syst., **14**, 103-137.

Ludvigsen, R. 1975. Ordovician formations and faunas, Southern Mackenzie Mts. *Can. J. Earth Sci.*, **12**, 663-697.

Ludvigsen, R. 1978. *Towards an Ordovician trilobite biostratigraphy of southern Ontario. Geology of the Manitoulin area.* Michigan Basin Geological Society, Special Paper 3, 73-84.

Ludvigsen, R. 1979. *Middle Ordovician trilobite biofacies, southern Mackenzie Mountains.* Geological Association of Canada, Special Paper 18, 1-37.

Ludvigsen, R. 1979a. A trilobite zonation of middle Ordovician rocks, SW District of Mackenzie. *Geol. Survey Canada, Bulletin*, 312.

Ludvigsen, R. and Chatterton, B. D. E. 1982. Ordovician Pterygometopidae (Trilobita) of North America. *Can. J. Earth Sciences*, **19** (11), 2179-2206.

Maksimova, Z. A. 1962. Trilobity ordovika i silura sibirskoy platformy. [Ordovician and Silurian trilobites of the Siberian platform.] *Trudy Vses. Nauch.-issled. Geol. Inst.* (VSEGEI) **76**. (In Russian).

Maksimova, Z. A. 1968. Srednepaleozoyskie trilobity tsentral'nogo Kazakhstana. (Middle Palaeozoic trilobites of central Kazakhstan.] *Trudy Vses. Nauch.-issled. Geol. Inst.* (VSEGEI) **165**. (In Russian).

Männil, R. 1958. [*Estoniops* - a new genus of Phacopidae (Trilobita)]. *Eesti NSV Teaduste Akadeemia Toimetised*, **6** [for 1957], 385-388. [In Russian with Estonian and English summaries].

Männil, R. 1970a. Estonian lower and middle Llandoverian trilobites of the genus *Acernaspis*. *Eesti NSV Teaduste Akadeemia Toimetised*, **19**, 156-165. [In Russian with English summary].

Männil, R. 1970b. Phacopid trilobites of the upper Llandoverian of Estonia. *Eesti NSV Teaduste Akadeemia Toimetised*, **19**, 342-349. [In Russian with English summary].

Männil, R. 1987. New phacopid trilobites from the Upper Silurian of the east Baltic. *Eesti NSV Teaduste Akadeemia Toimetised*, **36**, 113-120. [In English with Estonian and Russian summaries].

Männil, R. 1990. The Ordovician of Estonia. *In:* Kaljo, D. and Nestor, H. (eds.). *An excursion guidebook. IGCP project "Global Bioevents" Field Meeting, Estonia. Est. Acad. Sciences,* 11-20.

Manten, A. A. 1971. *Silurian Reefs of Gotland: typology, palaeoecology and stratigraphical implications.* Developments in Sedimentology 13. Elsevier. Amsterdam. 539pp.

Marcus, L. F. 1990. Traditional morphometrics. *In:* Rohlf, F. J. and Bookstein, F. L. (eds.). *Proceedings of the Michigan Morphometrics Workshop.* Special Publication no. 2, The University of Michigan Museum of Zoology, Ann Arbor. 77-122.

Marr, J. E. and Nicholson, H. A. 1888. The Stockdale Shales. *Quart. J. Geol. Soc. London*, **44**, 654-732.

Martinsson, A. 1962. Ostracodes of the family Beyrichiidae from the Silurian of Gotland. *Bulletin of the Geological Institution of Uppsala University*, **41**, 1-369.

Martinsson, A. 1967. The succession and correlation of ostracode faunas in the Silurian of Gotland. *Geol. Fören. Stockholm Förh.*, **89**, 350-386.

Maynard Smith, J. 1983. The genetics of stasis and punctuation. *Ann. Rev. Genet.*, **17**, 11-25.

Maynard Smith, J., Burian, R., Kauffman, S., Alberch, P., Campbell, J., Goodwin, B., Lande, R., Raup, D. and Wolpert, L. 1985. Developmental constraints and evolution. *Quart. Rev. Biol.*, **60**, 265-287.

Mayr, E. 1942. *Systematics and the Origin of Species.* Columbia University Press. New York.

Mayr, E. 1982. Speciation and macroevolution. *Evolution*, **36**, 1119-1132.

McBride, E. F. 1972. Flysch and associated beds of the Martinsburg Formation (Ordovician), central Appalachians. *J. Sed. Pet..*, **32**, 39-91.

McKerrow, W. S. 1979. Ordovician and Silurian changes in sea level. *J. Geol. Soc. London*, **136**, 137-145.

McKerrow, W. S. 1987. The Southern Uplands controversy. *J. Geol. Soc. London*, **144**, 735-736.

McKerrow, W. S., Leggett, J. K. and Eales, M. H. 1977. Imbricate thrust model of the Southern Uplands of Scotland. *Nature*, **267**, 237-239.

McLearn, F. H. 1918. Revision of some Phacopid genera. *Ottawa Naturalist*, **32**, 31-36.

McNamara, K. J. 1975. *Upper Ordovician stratigraphy and trilobites of the southern Lake District.* Thesis, University of Cambridge, Cambridge, 270 pp. (unpublished).

McNamara, K. J. 1978. Paedomorphosis in Scottish olenellid trilobites (Early Cambrian). *Palaeontology*, **21**, 53-92.

McNamara, K. J. 1979. Trilobites from the Coniston Limestone Group (Ashgill Series) of the Lake District, England. *Palaeontology*, **22**, 53-92.

McNamara, K. J. 1980. Evolutionary trends and their functional significance in chasmopine trilobites. *Lethaia*, **13**, 61-78.

McNamara, K. J. 1981. Paedomorphosis in middle Cambrian xystridurine trilobites from northern Australia. *Alcheringa*, **5**, 209-224.

McNamara, K. J. 1982. Heterochrony and phylogenetic trends. *Palaeobiology*, **8**, 130-142.

McNamara, K. J. 1983. Progenesis in trilobites. *Special Papers in Palaeontology*, **30**, 59-68.

McNamara, K. J. 1988a. Patterns of heterochrony in the fossil record. *Trends in*

Ecology and Evolution, **3**, 176-180.

McNamara, K. J. 1988b. The abundance of heterochrony in the fossil record. *In:* McKinney, M. L. (ed.) *Heterochrony in Evolution*. Plenum. 287-325.

McNamara, K. J. 1990. The role of heterochrony in evolutionary trends. *In:* McNamara, K. J. (ed.), *Evolutionary Trends*. Belhaven Press. London. 59-74.

McNamara, K. J. and Fordham, B. G. 1981. Mid. Cautleyan (Ashgill Series) trilobites and facies in the English Lake District. *Palaeogeog., Palaeoclimatol., Palaeoecol.*, **34**, 137-161.

Meek, F. B. 1873. *Descriptions of invertebrate fossils of the Silurian and Devonian systems.* Geological Survey of Ohio, Palaeontology, 1 (2), 243 pp.

Milici, R. C. and de Witt, W. Jr. 1988. The Appalachian Basin. *In:* Sloss, L. L. (ed.). *The Geology of North America, Volume D-2. Sedimentary Cover - North American Craton: U.S. The Geological Society of America.* 427-469.

Milne Edwards, H. 1840. *Histoire naturelle des Crustacés, comprenant l'anatomie, la physiologie et la classification de ces animaux.* **3**, 1-638, Paris.

Mitchell, W. I. 1977. The Ordovician Brachiopoda from Pomeroy, Co. Tyrone. *Monograph of the Palaeontographical Society*, 1-38.

Mitchell, C. E. and Bergström, S. M. 1991. New graptolite and lithostratigraphic evidence from the Cincinnati region, U.S.A., for the definition and correlation of the base of the Cincinnatian Series (Upper Ordovician). *In:* Barnes, C. R. and Williams, S. H. (eds.) *Advances in Ordovician Geology.* Geological Survey of Canada, Paper 90-9, 59-77.

Moore, R. C. (ed.). 1959. *Treatise on Invertebrate Paleontology. Part O. Arthropoda I.* University of Kansas Press and Meriden Gravure. Lawrence and Meriden. xix+560pp.

Morris, P. J., Ivany, L. C. and Schopf, K. M. 1992. Paleoecological stasis in evolutionary theory. *Geol. Soc. America Abstracts with Programs*, **1992**, A313.

Morris, S. F. 1988. A review of British trilobites, including a synoptic revision of Salter's monograph. *Monograph of the Palaeontographical Society* London. 1-316 (Pub. no. 574, part of vol. **140** for 1986).

Morris, S. F. and Tripp, R. P. 1986. Lectotype selections for Ordovician trilobites from the Girvan District, Strathclyde. *Bulletin of the British Museum (Natural History)* (Geology), **40**, 161-176.

Moseley, F. 1978. The geology of the English Lake District, an introductory review. *In:* Moseley, F. (ed.). *The geology of the Lake District.* Yorks. Geol. Soc. occassional publication no. 3. W. S. Maney and Son. Leeds. 1-16.

Murchison, R. I. 1839. *The Silurian System.* 786pp. London.

Murchison, R. I. 1859. *Siluria.* 3rd edition. xix+592pp. London.

Mykura, W. and Smith, J. D. D. 1962. Ordovician and Silurian. *In:* Mitchell, G. H. and Mykura, W. (eds.) *The geology of the Neighbourhood of Edinburgh.*

Memoirs of the Geological Survey of Scotland, 10-22.

Okulitch, V. L. 1942. New Pterygometopinae from the Ordovician of Ontario and Quebec. *Trans. Roy. Soc. Canada*, Section 4, **36**, 96-106.

Owen, A. W. 1981. The Ashgill trilobites of the Oslo Region, Norway. *Palaeontographica*, (A) **175**, 1-88.

Owen, A. W. 1986. The uppermost Ordovician (Hirnantian) trilobites of Girvan, SW Scotland with a review of coeval trilobite faunas. *Trans. Roy. Soc. Edinburgh: Earth Sciences*, **77**, 231-239.

Owen, A. W. and Bruton, D. L. 1980. Late Caradoc - early Ashgill trilobites from the central Oslo Region, Norway. *Paleont. Contr. Univ. Oslo*, *245*, 62pp.

Owen, A. W., Bruton, D. L., Bockelie, J. F. and Bockelie, T. G. 1990. The Ordovician successions of the Oslo Region, Norway. *Nor. geol. unders.* Special Publ. **4**, 3-54.

Owen, A. W. and Clarkson, E. N. K. 1992. Trilobites from Kilbucho and Wallace's Cast and the location of the Northern Belt of the Southern Uplands during the late Ordovician. *Scott. J. Geol.*, **28** (1), 3-17.

Owen, A. W., Harper, D. A. T., and Romano, M. 1992. The Ordovician biogeography of the Grangegeeth terrane and the Iapetus suture zone in eastern Ireland. *J. Geol. Soc. London*, **149**, 3-6.

Owen, A. W. and Ingham, J. K. 1988. The stratigraphic distribution and taxonomy of the trilobite Onnia in the type Onnian Stage of the uppermost Caradoc. *Palaeontology*, **31**, 829-855.

Owen, A. W. and Robertson, D. B. R. In press. Ecological changes during the end-Ordovician extinction. *Modern Geology.*

Peach, B. N. and Horne, J. 1899. The Silurian rocks of Britain. Vol. 1: Scotland. *Memoirs of the Geological Survey of the United Kingdom*, xviii+749pp.

Pillet, J. 1954. La classification des Phacopacea (Trilobites). *Bulletin de la Société géologique de France, série 6*, **3**, 817-839.

Piper, D. J. W. 1972. Sedimentary environments and palaeogeography of the late Llandovery and earliest Wenlock of North Connemara, Ireland. *J. Geol. Soc. London*, **128**, 33-51.

Portlock, J. E. 1843. *Report on the geology of the County of Londonderry, and parts of Tyrone and Fermanagh.* Dublin & London. xxxi+784 pp.

Poulsen, C. 1934. The Silurian faunas of North Greenland. 1. The fauna of the Cape Schuchert Formation. *Meddr. Grønland*, **72**, 2, (1).

Price, D. 1973. The age and stratigraphy of the Sholeshook Limestone of south-west Wales. Geol. J., 8, 225-246.

Price, D. 1974. Trilobites from the Sholeshook Limestone (Ashgill) of south Wales. *Palaeontology*, **17**, 841-868.

Price, D. 1980. The Ordovician trilobite fauna of the Sholeshook Limestone Formation

of South Wales. *Palaeontology*, **23**, 839-887.

Ramsköld, L. 1985. Silurian phacopid and dalmanitid trilobites from Gotland. *Stockholm Contrib. Geol.*, **40**, 1-62.

Ramsköld, L. 1988. Heterochrony in Silurian phacopid trilobites as suggested by the ontogeny of *Acernaspis*. *Lethaia*, **21**, 307-318.

Ramsköld, L. and Werdelin, L. 1991. The phylogeny and evolution of some phacopid trilobites. *Cladistics*, **7**, 29-74.

Raup, D. M. 1978. Cohort analysis of generic survivorship. *Paleobiology*, **4**, 1-15.

Raymond, P. E. 1905. The trilobites of the Chazy Limestone. *Annals of the Carnegie Museum*, **3**, 328-386.

Raymond, P. E. 1921. A contribution to the description of the fauna of the Trenton Group. *Geological Survey of Canada, Museum Bulletin* **31**, 1-64.

Raymond, P. E. 1925. Some trilobites of the lower Middle Ordovician of eastern North America. *Bulletin of the Museum of Comparative Zoology. Harvard*, no. **67**, 1-180.

Reed, F. R. C. 1905. The classification of the Phacopidae. *Geol. Mag.* (5) **2**, 172-178, 224-228.

Reed, F. R. C. 1906. The Lower Palaeozoic trilobites of the Girvan district, Ayrshire. *Monographs of the Palaeontographical Society*, 97-186.

Reed, F. R. C. 1914. The Lower Palaeozoic trilobites of Girvan. Supplement. *Monographs of the Palaeontographical Society*, 56 pp.

Reed, F. R. C. 1930. Notes on some new Ordovician trilobites from Girvan. *Annals and Magazine of Natural History*, (10) **6**, 193-201.

Reed, F. R. C. 1931. The Lower Palaeozoic trilobites of Girvan. Supplement No. 2. *Monograph of the Palaeontographical Society* , 30pp.

Reed, F. R. C. 1945. Notes on some Ordovician brachiopods and a trilobite from the Balclatchie Beds of Girvan. *Annals and Magazine of Natural History*, (11) **12**, 309-316.

Reed, F. R. C. 1952. Revision of certain Ordovician Fossils from County Tyrone. *Proc. Royal Irish Academy*, **55** (B), 95-136.

Robertson, D. B. R., Brenchley, P. J. and Owen, A. W. 1991. Ecological disruption close to the Ordovician-Silurian boundary. *Historical Biology*, **5**, 131-144.

Robertson, G. 1989. A palaeoenvironmental interpretation of the Silurian rocks in the Pentland Hills, near Edinburgh, Scotland. *Trans. Roy. Soc. Edinburgh: Earth Sciences*, **80**, 127-141.

Rohlf, F. J. 1982. Consensus indices for comparing classifications. *Math. Biosci.*, **59**, 313-344.

Romano, M. 1980. The stratigraphy of the Ordovician rocks between Slane (County Meath) and Collon (County Louth), eastern Ireland. *Journal of Earth Science, Royal Dublin Society*, **3**, 53-79.

Romano, M and Owen, A. W. 1993. Early Caradoc trilobites of eastern Ireland and their palaeogeographical significance. *Palaeontology*, **36** (3), 681-720.

Ross, R. J. 1967. Some Middle Ordovician brachiopods and trilobites from the Basin Ranges, Western US. *Prof. Pap. US geol. Surv.* no. 523-D, 1-43.

Ross, R. J. 1972. Fossils from the Ordovician bioherm at Meiklejohn Peak, Nevada. *Prof. Pap. US geol. Surv.* no. 685, 1-47.

Ross, R. J. and Shaw, F. C. 1972. Distribution of the Middle Ordovician Copenhagen Formation and its trilobites in Nevada. *Prof. Pap. US geol. Surv.* no. 749, 1-33.

Ross, R. J. R. Jr., Adler, F. J., Amsden, T. W., Bergstrom, D., Bergstrom, S. M., Carter, C., Churkin, M. Jr., Cressman, E. R., Derby, J. R., Dutro, J. T. Jr., Ethington, R. L., Finney, S. C., Fisher, D. W., Fisher, J. H., Harris, A. G., Hintze, L. F., Ketner, K. B., Kolata, D. L., Landing, E., Neuman, R. B., Pojeta, J. Jr., Potter, A. W., Rader, E. K., Repetski, J. E., Ross, J. R. P., Shaver, R. H., Sweet, W. C., Thompson, T. L. and Webers, G. F. 1982. The Ordovician System in the United States of America: correlation chart and explanatory notes. International Union of Geological Sciences Pub. no. 12, 73 pp., chart.

Safford, J. M. and Vogdes, A. W. 1889. Description of new species of fossil crustacea from the Lower Silurian of Tennessee, with remarks on others not well known. *P. Ac. Philad.* 166-168.

Salter, J. W. 1853. Figures and descriptions illustrative of British Organic Remains, Dec. 7. *Memoir of the Geological Survey of the United Kingdom*, 78pp.

Salter, J. W. 1864. A monograph of the British trilobites from the Cambrian, Silurian, and Devonian formations. *Monograph of the Palaeontographical Society* , 1-80.

Schmidt, F. 1881. Revisions der Ostbaltischen silurischen Trilobiten, Abteilung I. *Mémoires de l'' Académie Impériale des Sciences de St. Pétersbourg*, 7 serie, **30**, 1-237.

Schopf, T. J. M. 1981. Evidence from findings of molecular biology with regard to the rapidity of genomic change: implications for species durations. *In:* Niklas, K. J. (ed.). *Paleobotany, Paleoecology and Evolution, Vol. 1.* Praeger. New York. 135-192.

Schrank, E. 1972. Proetacea, Encrinuridae und Phacopina (Trilobita) aus silurischen Geschieben. *Geologie*, **21**, 1-117.

Scotford, D. M. 1965. Petrology of the Cincinnatian Series shales and environmental implications. *Bull. Geol. Soc. America*, **76**, 193-222.

Shaw, A. B. 1957. Quantitative trilobite studies II. Measurement of the dorsal shell of non-agnostidean trilobites. *J. Paleo.*, **31**, 193-207.

Shaw, F. C. 1968. Early middle Ordovician Chazy trilobites of New York. *Mem. N.Y. Mus. Nat. Hist.*, **17**, 1-163.

Shaw, F. C. 1974. Simpson Group (Middle Ordovician) trilobites of Oklahoma.

Memoir of the Paleontological Society, **6**, 1-54.

Shaw, F. C. and Fortey, R. A. 1977. Middle Ordovician facies and trilobite faunas in N. America. *Geol. Mag.*, **114**, 409-443.

Sheehan, P. M. and Coorough, P. J. 1990. Brachiopod zoogeography across the Ordovician-Silurian extinction event. *In:* McKerrow, W. S. and Scotese, C. R. (eds.). Palaeozoic Palaeogeography and Biogeography. *Geol. Soc. Mem. 12*, 181-187.

Sheldon, P. R. 1987. Parallel gradualistic evolution of Ordovician trilobites. *Nature*, **330**, 561-563.

Sheldon, P. R. 1988. Trilobite size-frequency distribution, recognition of instars, and phyletic size changes. *Lethaia*, **21**, 293-306.

Sheldon, P. R. 1990. Shaking up evolutionary patterns. *Nature*, **345**, 772.

Shimer, H. W. and Schrock, R. R. 1944. *Index fossils of North America.* M. I. T. Press, Cambridge, MA, 837pp.

Shrock, R. R. and Twenhofel, W. H. 1939. Silurian fossils from Northern Newfoundland. *J. Paleo.* **13**, 241-266.

Simpson, G. G. 1944. *Tempo and Mode in Evolution.* Columbia University Press. New York.

Simpson, G. G. 1953. *The Major Features of Evolution.* Columbia University Press. New York.

Sinclair, G. W. 1944. Some Ordovician trilobites from Ontario. *Trans. Roy. Canadian Institute*, **25**, 15-20.

Siveter, D. J. 1990. Photography. *In:* Briggs, D. E. G. and Crowther, P. R. (eds.). *Palaeobiology: a synthesis.* Blackwell Scientific Publications, Oxford, 505-508.

Skjeseth, S. 1963. Contributions to the geology of the Mjøsa District and the classical sparagmite area in Southern Norway. *Nor. geol. unders. Bull.*, **220**, 1-126.

Sloan, R. E. 1991. A chronology of North American Ordovician trilobite genera. *In:* Barnes, C. R. and Williams, S. H. (eds.) *Advances in Ordovician Geology.* Geological Survey of Canada, Paper 90-9, 165-177.

Slocum, A. W. 1913. New trilobites from the Maquoketa Beds of Fayette County, Iowa. *Publications of the Field Museum*, (Geology), **4** (3) (Publ. 171), 43-83.

Speldnæs, N. 1982. The Ordovician of the districts around Mjøsa. In: Bruton, D. L. and Williams, S. H. (eds.). *Field excursion guide. IV International Symposium on the Ordovician System. Paleont. Contr. Univ. Oslo 279*, 148-163.

Stanley, S. M. 1979. *Macroevolution - Pattern and Process.* Freeman. San Francisco.

Stanley, S. M. 1985. Rates of evolution. *Paleobiology*, **11**, 13-26.

Stearns, S. C. 1982. The role of development in the evolution of life-histories. *In:* Bonner, J. T. (ed.). *Evolution and Development.* Springer. Berlin. 237-258.

Stephens, G. C., and Wright, T. O. 1981. Stratigraphy of the Martinsburg Formation, West of Harrisburg in the Great Valley of Pensylvania. *American Journal of*

Science, **281**, 1009-1020.

Størmer, L. 1940. Early descriptions of Norwegian trilobites. *Norsk. Geologisk Tidsskrift*, **20**, 113-151.

Størmer, L. 1945. Remarks on the *Tretaspis (Trinucleus)* Shales of Hadeland. *Norsk. Geologisk Tidsskrift*, **25**, 379-426.

Størmer, L. 1953. The Middle Ordovician of the Oslo Region, Norway. 1. Introduction to stratigraphy. *Norsk. Geologisk Tidsskrift*, **31**, 37-141.

Svoboda, J. 1966. The Barrandian Basin. *In:* Svoboda, J. (ed.). *Regional geology of Czechoslovakia, Part 1: The Bohemian Massif.* Czech. Acad. Sciences. Prague. 281-342.

Sweet, W. C. 1984. Graphic correlation of upper middle and upper Ordovician rocks, North American Midcontinent Province, U.S.A. *In:* Bruton, D. L. (ed.). *Aspects of the Ordovician System. Paleont. Contr. Univ. Oslo 295*, 23-35.

Sweet, W. C. and Bergström, S. M. 1971. The American upper Ordovician standard: XIII. A revised time-stratigraphic classification of north American upper middle and upper Ordovician rocks. *Bull. Geol. Soc. Amer.*, **82**, 613-628.

Swofford, D. L. 1990. PAUP: phylogenetic analysis using parsimony. Version 3.0. Illinois Natural History Survey. i-iv+78pp.

Temple, J. T. 1975. Standardisation of trilobite orientation and measurement. *Fossils and Strata*, **4**, 461-467.

Temple, J. T. 1975a. Early Llandovery trilobites from Wales with notes on British Llandovery calymenids. *Palaeontology*, **18**, 137-159.

Temple, J. T. 1981. A numerical taxonomic study of Trinucleidae (Trilobita) from the British Isles. *Trans. Roy. Soc. Edinburgh: Earth Sciences*, **71**, 213-233.

Temple, J. T. 1982. Ordination of palaeontological data. *Misc. Pap. geol. Soc. London*, **14**, 224-236.

Temple, J. T. and Tripp, R. P. 1979. An investigation of the Encrinurinae (Trilobita) by numerical taxonomic methods. *Trans. Roy. Soc. Edinburgh: Earth Sciences*, **70**, 223-250.

Thomas, A. T. 1978-1981. British Wenlock trilobites. *Monographs of the Palaeontographical Society.* **I**, 1-56; **II**, 57-98.

Thomas, A. T., Owens, R. M., and Rushton, A. W. A. 1984. Trilobites in British stratigraphy. Geol. Soc. London, Special Report No. 16.

Tipper, J. C. 1975. Lower Silurian animal communities - three case histories. *Lethaia*, **8**, 287-299.

Tipper, J. C. 1976. The stratigraphy of the North Esk Inlier, Midlothian. *Scott. J. Geol.*, **12**, 15-22.

Titus, R. and Cameron, B. 1976. Fossil communities of the lower Trenton Group (middle Ordovician) of central and northwestern New York State. *J. Paleo.*, **50**, 1209-1225.

Tripp, R. P. 1954. Caradocian trilobites from mudstones at Craighead quarry, near Girvan, Ayrshire. *Trans. Roy. Soc. Edinburgh*, **62**, 655-693.

Tripp, R. P. 1962. Trilobites from the *confinis* Flags (Ordovician) of the Girvan District, Ayrshire. *Trans. Roy. Soc. Edinburgh*, **62**, 1-40.

Tripp, R. P. 1967. Trilobites from the Upper Stinchar Limestone (Ordovician) of the Girvan District, Ayrshire. *Trans. Roy. Soc. Edinburgh*, **67**, 7-93.

Tripp, R. P. 1980a. Trilobites from the Ordovician Balclatchie and lower Ardwell groups of the Girvan District, Scotland. *Trans. Roy. Soc. Edinburgh: Earth Sciences*, **71**, 123-145

Tripp, R. P. 1980b. Trilobites from the Ordovician Ardwell Group of the Craighead Inlier, Girvan District, Scotland. *Trans. Roy. Soc. Edinburgh: Earth Sciences*, **71**, 147-157.

Tripp, R. P. 1993. Review of the trilobites from the Middle Ordovician Barr Group, Girvan district, Scotland. *Trans. Roy. Soc. Edinburgh: Earth Sciences*, **84**, 87-102.

Tucker, R. D., Krogh, T. E., Ross, R. J. and Williams, S. H. 1990. Time-scale calibration by high-precision U-Pb zircon dating of interstratified volcanic ashes in the Ordovician and Lower Silurian stratotypes of Britain. *Earth and Planetary Science Letters*, **100**, 51-58.

Tunnicliff, S. P. 1980. *A catalogue of the Lower Palaeozoic fossils in the collection of Major-General J. E. Portlock, R.E., LL.D., F.R.S., F.G.S. etc.* Ulster Museum, Belfast, 111pp.

Twenhofel, W. H. 1928. Geology of Anticosti Island. *Geological Survey of Canada Memoir*, **154**, 481pp.

Twenhofel, W. H. 1954. Correlation of the Ordovician formations of North America. *Bull. Geol. Soc. America*, **65**, 247-298.

Van Valen, L. M. 1973. A new evolutionary law. *Evolutionary Theory*, **1**, 1-30.

Wake, D. B., Roth, G. and Wake, M. H. 1983. On the problem of stasis in organismal evolution. *J. Theor. Biol.*, **101**, 211-224.

Walcott, C. D. 1877. Descriptions of new species of fossils from the Chazy and Trenton limestones. *N.Y. State Mus., 31st Rept.*

Warburg, E. 1925. The trilobites of the Leptaena Limestone in Dalarne with a discussion of the zoological position and the classification of the Trilobita. *Bulletin of the Geological Institution of the University of Upsala*, no. 17, i-viii, 1-446.

Ward, P. D. 1992. *On Methuselah's Trail: living fossils and the great extinctions.* W.H. Freeman and Co. New York. 212 pp.

Warren, P. T., Price, D., Nutt, M. J. C., and Smith, E. G. 1984. Geology of the country around Rhyl and Denbigh. *Memoir of the British Geological Survey, Sheets 95 & 107.*

Weber, V. N. 1951. Verkhnesiluriyskie trilobity SSSR. [Upper Silurian trilobites of the U.S.S.R.] Trudy Vses. Nauch. -issled. Geol. Inst. (VSEGEI). [In Russian].

Whittington, H. B. 1950. Sixteen Ordovician genotype trilobites. *J. Paleo.*, **24**, 531-565.

Whittington, H. B. 1962-1968. A monograph of the Ordovician trilobites of the Bala area, Merioneth. *Monographs of the Palaeontographical Soc.* **I**, 1-32; **II**, 33-62; **III**, 63-92.

Whittington, H. B. 1965. Trilobites of the Ordovician Table Head Formation, western Newfoundland. *Bull. Mus. Comp. Zool. Harvard*, **132**, 275-442.

Williams, A. 1962. The Barr and Lower Ardmillan Series (Caradoc) of the Girvan district, south-west Ayrshire, with descriptions of the brachiopoda. *Memoir of the Geological Society of London*, **3**, 1-267.

Williams, A. 1963. The Caradocian brachiopod faunas of the Bala district, Merionethshire. *Bulletin of the British Museum (Natural History)* (Geology), **8**, 327-471.

Williams, A., Strachan, I., Bassett, D. A., Dean, W. T., Ingham, J. K., Wright, A. D. and Whittington, H. B. 1972. *A correlation of Ordovician rocks in the British Isles.* Geol. Soc. London, Special Report No. 3.

Williams, A., Lockley, M. G. and Hurst, J. M. 1981. Benthic palaeocommunities represented in the Ffairfach Group and coeval Ordovician successions of Wales. *Palaeontology*, **24**, 661-694.

Wilson, A. E. 1947. *Trilobita of the Ottawa Formation of the Ottawa - St. Lawrence Lowland.* Geological Survey of Canada, Bulletin 9, 1-86.

Wiman, G. 1908. Studien über das Nordbaltische Silurgebiet. *Bull. Geol. Inst. Univ. Uppsala*, **8**, 73-168.

Witzke, B. J. 1983. Ordovician Galena Group in Iowa subsurface. *In:* Delgado, D. J., (ed.). Ordovician Galena Group: deposition, submarine and later diagenesis, and paleoecology. *Society of Economic Paleontologists and Mineralogists, Great Lakes Section, 13th Annual Field Conference Guidebook*, p. D1-D26.

Worsley, D., Aarhus, N., Bassett, M. G., Howe, M. P. A., Mørk, A. and Olaussen, S. 1983. The Silurian succession of the Oslo Region. *Norges geologiske undersokelse*, **384**, 1-57.

Zhang, W. -T. and Meng, X. -S. 1986. Silurian trilobites from Xichuan, Henan. *Acta Palaeont. Sin.* **25**, 507-515. [In Chinese with English summary].

APPENDICES

APPENDIX ONE
COMPUTER PROGRAMS

This appendix gives details of two computer programs specially written to help in analysis and visualisation of taxonomic stratigraphical and chronostratigraphical range data for this Ph.D project (see Chapter 2 herein). Both programs were written to run under AT&T's "S" data analysis and graphics system operating on a Sun workstation. The programs were written in the "S" language (Becker *et al.* 1988). The two programs are:

(i) calibrator(): a user-defined S function which converts first and last appearance times of taxa in a stratigraphical section expressed in relative terms to absolute dates of first and last appearance in Ma with reference to a time scale.

(ii) rangeplotter(): an interactive user-defined S function which constructs stratigraphical range charts from either stratigraphical or chronostratigraphical data.

A1. 1. calibrator().

The function "calibrator()" takes an input file, which contains the appearance and disappearance times of a number of taxa, and outputs a file called "calibrated" which contains the absolute appearance and disappearance times of the taxa in Ma. calibrator() must have available to it a calibration file which is specified in the call to the function. The requirements for the files are:

The input file: must consist of two columns of numbers. The first column lists the times of appearance of the taxa (in relative terms); the second column lists the times of disappearance. The file can be of any length but must be terminated by a pair of "999" values.

The calibration file: must consist of two columns of numbers . The first column is a list of the key stratigraphical levels (*i.e.* all the levels which appear in the input file). The second column lists the absolute ages in Ma corresponding to the key levels listed in the first column. This file does not need to be terminated by 999s.

A1. 1. 1. Example Use of calibrator().

Example: to calibrate the file "strat_data", which contains the stratigraphical levels of appearance and disappearance of three taxa:

```
0     1
0     2
2     3
999   999
```

against the calibration file "time_scale", which gives the absolute ages of the relevant

stratigraphical levels:

0	600
1	500
2	400
3	300

Enter S in the normal way. Then give the following command (instructions typed by the user are in bold type; comments are in curly brackets):

> **calibrator(strat_data, time_scale)**
{This calls calibrator() and specifies the input and calibration files}

> **calibrated**

600	500	{S prints the output file "calibrated"}
600	400	
400	300	
999	999	

A1. 1. 2. Listing of calibrator().

```
function(file, calibration)
{
    calibrated <<- file
    col <- 1
    repeat {
        if(col == 3)
            break
        i <- 1
        repeat {
            if(file[i, col] == 999)
                break
            date <- calibration[, 2][calibration[, 1] == file[i, col]]
            calibrated[i, col] <<- date
            i <- i + 1
        }
        col <- col + 1
    }
}
```

A1. 2. rangeplotter().

The function "rangeplotter()" takes an input file, which contains the appearance and disappearance times of a number of taxa in a stratigraphical section, and constructs a stratigraphical range chart from the data. The input file must consist of two columns of numbers: the first column lists the times of appearance of the taxa in the section; the second column lists the corresponding times of disappearance. The file can be of any length but must be terminated by a pair of "999" values. The times of appearance and disappearance may be expressed in terms of absolute age in Ma, measured

stratigraphical height above some datum, or any other convenient metric.

A1. 2. 1. Example Use of rangeplotter().

Example: to construct a range chart from the data in the file "calibrated" produced by calibrator() above (NB rangeplotter() can draw a rangechart from any file containing two columns of numbers - it does not need to have been produced by calibrator()).

Enter S and specify the graphics device being used in the normal way. Then give the following command (instructions typed by the user are in bold type; comments are in curly brackets):

> **rangeplotter (calibrated)**
{This calls rangeplotter() and specifies the input file}

Range in Ma? y/n: **y** {rangeplotter() asks whether the data are absolute dates in Ma}
Y-axis starts at: **600** {rangeplotter() asks for the lowest and highest points on
Y-axis ends at: **300** the vertical axis to enable it to scale the vertical axis}
X-axis starts at: **1** {rangeplotter() asks how many taxa there are to enable it
X-axis ends at: **3** to scale the horizontal axis}
Give a title for the plot: **Example Range Chart**

S should now draw the range chart to the specified output device (usually the screen).

A1. 2. 2. Listing of rangeplotter().

```
function(file)
{
    cat("Range in Ma? y/n:")
    plottype <- readline()
    cat("Y-axis starts at:")
    ymin <- scan(n = 1)
    cat("Y-axis ends at:")
    ymax <- scan(n = 1)
    cat("X-axis starts at:")
    xmin <- scan(n = 1)
    cat("X-axis ends at:")
    xmax <- scan(n = 1)
    cat("Give a title for the plot:")
    name <- readline()
    if(plottype == "y" || plottype == "Y") {
        file[, 1] <- -file[, 1]
        file[, 2] <- -file[, 2]
        ymin <- -ymin
        ymax <- -ymax
    }
    x <- 0
    y <- 0
```

```
        plot(x, y, xlim = c(xmin, xmax), ylim = c(ymin, ymax), type = "n")
        i <- 1
        repeat {
            if(file[i, 1] == 999 || file[i, 1] == -999)
                break
            x <- c(xmin - 1 + i, xmin - 1 + i)
            y <- c(file[i, 1], file[i, 2])
            points(x, y, type = "l")
            i <- i + 1
        }
        title(main = name)
}
```

APPENDIX TWO
STRATIGRAPHICAL RANGE DATA FOR BRITISH TRILOBITE SPECIES AND GENERA

This appendix lists the data used in compiling the range charts and statistics on trilobite chronostratigraphical ranges presented in Chapter 2. The appendix is in five sections. Section A2. 1 lists the names of the trilobite species whose chronostratigraphical ranges are illustrated in Chapter 2. Section A2. 2 lists the names of the genera whose chronostratigraphical ranges are illustrated in Chapter 2. Section A2. 3 presents the data base "pal.final.alpha" which contains the raw specific range data on trilobites as extracted from Thomas *et al.* (1984). Section A2. 4 presents the data base "pal.gen.alpha" which contains the raw generic range data constructed from the specific range data. Finally, section A2. 5 presents the calibration file "GTS89" which was used in conjunction with the program "calibrator()" the convert times of first and last appearance of trilobite taxa expressed in biozone numbers into absolute dates (see Chapter 2 and Appendix 1). Because of the size of the data bases "pal.final.alpha" and "pal.gen.alpha" (971 rows x 10 columns and 359 rows x 6 columns respectively) they are presented on a separate computer disk.

A2. 1. Names of Trilobite Species from England, Scotland and Wales.

Listed below are the names of the 971 trilobites species from mainland Britain (*i.e.* England, Scotland and Wales) whose chronostratigraphical ranges are depicted in the range charts in Figures 2. 4 - 2. 8. The species are listed in the same order as that in which they appear on the charts (*i.e.* ascending stratigraphical order of appearance). Species denoted by * have a chronostratigraphical range greater than the 90% quantile value for the stratigraphical system in which they originated (equal to 4.5 myr for Cambrian species, 6.28 myr for Ordovician species, 7.99 myr for Silurian species, 2.25 myr for Devonian species and 13.0 myr for Carboniferous species).

Cambrian Species

[1,] "Hebediscus"	attleborensis*	[16,] "Pseudatops"	viola
[2,] "Callavia"	callavei*	[17,] "Calodiscus"	lobatus*
[3,] "Callavia"	hastata*	[18,] "Serrodiscus"	robustus*
[4,] "Triangulaspis"	annio	[19,] "Mohicana"	clavata
[5,] "Micmacca"	ellipsocephaloides	[20,] "Cobboldites"	comleyensis
[6,] "Olenellus"	hamoculus	[21,] "Strettonia"	comleyensis
[7,] "Strenuella"	strenuelloides	[22,] "Runcinodiscus"	index
[8,] "Olenelloides"	armatus*	[23,] "Latoucheia"	latouchei
[9,] "Serrodiscus"	bellimarginatus	[24,] "Protolenus"	morpheus
[10,] "Olenellus"	intermedius*	[25,] "Comluella"	platycephalum
[11,] "Olenellus"	lapworthi*	[26,] "Strenuella"	strenua
[12,] "Ladadiscus"	llarenai	[27,] "Serrodiscus"	ctenoa
[13,] "Strenuella"	pustulosa	[28,] "Cobboldites"	simplex
[14,] "Olenellus"	reticulatus*	[29,] "Condylopyge"	cambrensis
[15,] "Strenuella"	sabulosa	[30,] "Bailiella"	cobboldi*

[31,] "Acadoparadoxides" groomii
[32,] "Eccaparadoxides" harknessii
[33,] "Kootenia" lakei
[34,] "Bailiella" longifrons
[35,] "Bailiella" lyellii
[36,] "Bathyuriscus" pusillus*
[37,] "Metadiscus" sculptus
[38,] "Paradoxides" sedgwickii.sedgwicki
[39,] "Paradoxides" sjoegreni
[40,] "Ctenocephalus" solvensis
[41,] "Eodiscus" borealis
[42,] "Condylopyge" carinata
[43,] "Pleuroctenium" granulatum.pileatum
[44,] "Paradoxides" sedgwickii.porphyrus
[45,] "Paradoxides" aurora
[46,] "Liostracus" comleyensis
[47,] "Bailiaspis" dalmani
[48,] "Acadoparadoxides" salopiensis
[49,] "Diplagnostus" abbatiae
[50,] "Pleuroctenium" granulatum.granulatum
[51,] "Paradoxides" hicksii
[52,] "Tomagnostus" perrugatus*
[53,] "Condylopyge" rex
[54,] "Peronopsis" scutalis.tenuis*
[55,] "Ptychagnostus" triangulatus
[56,] "Bailiaspis" tuberculata
[57,] "Parasolenopleura" applanata*
[58,] "Ptychagnostus" davidis
[59,] "Liostracus" dubius*
[60,] "Parasolenopleura" elegans
[61,] "Peronopsis" fallax*
[62,] "Tomagnostus" fissus
[63,] "Pleuroctenium" granulatum.scanense
[64,] "Hartshillia" inflata
[65,] "Acadoparadoxides" intermedius
[66,] "Agraulos" longicephalus
[67,] "Ptychagnostus" longifrons
[68,] "Eodiscus" punctatus.scanicus
[69,] "Hypagnostus" truncatus
[70,] "Tomagnostus" corrugatus
[71,] "Phalagnostus" nudus.auctt
[72,] "Hypagnostus" parvifrons*
[73,] "Peronopsella" spinata
[74,] "Ptychagnostus" typicalis
[75,] "Condylopyge" globosa
[76,] "Holocephalina" incerta
[77,] "Tomagnostus" gracilis
[78,] "Ptychagnostus" barrandei
[79,] "Centropleura" pugnax
[80,] "Pleuroctenium" tuberculatum
[81,] "Phalagnostus" eskriggei
[82,] "Ptychagnostus" hybridus
[83,] "Clarella" impar
[84,] "Paradoxides" paradoxissimus
[85,] "Eodiscus" punctatus.punctatus
[86,] "Peronopsis" scutalis.scutalis
[87,] "Cotalagnostus" lens.lens
[88,] "Phalacroma" bibullatum
[89,] "Corynexochus" cambrensis
[90,] "Peronopsis" fallax.depressa
[91,] "Agraulos" illingi
[92,] "Bailiaspis" nicholasi
[93,] "Ptychagnostus" punctuosus
[94,] "Eccaparadoxides" pusillus
[95,] "Ptychagnostus" ciceroides
[96,] "Hartshillina" spinata
[97,] "Meneviella" venulosa
[98,] "Solenopleuropsis" variolaris
[99,] "Pleuroctenium" bifurcatum
[100,] "Liostracus" bruno
[101,] "Paradoxides" davidis
[102,] "Anopolenus" henrici
[103,] "Holocephalina" primordialis
[104,] "Doryagnostus" incertus
[105,] "Elrathia" pulchella
[106,] "Cotalagnostus" rotundus
[107,] "Peronopsis" scutalis.exarata
[108,] "Solenopleura" angustoria
[109,] "Ptychagnostus" lundgreni
[110,] "Hypagnostus" parvifrons.mammillatus
[111,] "Agaso" pococki
[112,] "Agaso" pringlei
[113,] "Agraulos" robustus
[114,] "Agaso" rushtonensis
[115,] "Dorypyge" rushtonensis
[116,] "Grandagnostus" falanensis
[117,] "Ptychagnostus" fumicola
[118,] "Hypagnostus" sulcifer
[119,] "Agnostus" pisiformis
[120,] "Cristagnostus" papilio
[121,] "Schmalenseeia" amphionura
[122,] "Proceratopyge" nathorsti
[123,] "Olenus" austriacus
[124,] "Olenus" gibbosus
[125,] "Homagnostus" obesus.obesus
[126,] "Glyptagnostus" reticulatus.reticulatus
[127,] "Olenus" transversus
[128,] "Olenus" truncatus
[129,] "Olenus" wahlenbergi
[130,] "Glyptagnostus" reticulatus.nodulosus
[131,] "Olenus" cataractes
[132,] "Olenus" micrurus
[133,] "Sulcatagnostus" securiger
[134,] "Olenus" mundus
[135,] "Proceratopyge" tullbergi
[136,] "Irvingella" nuneatonensis
[137,] "Homagnostus" obesus.laevis
[138,] "Parabolinoides" bucephalus
[139,] "Pseudagnostus" cyclopyge
[140,] "Parabolina" spinulosa

[141,] "Conocephalina" abdita
[142,] "Briscoia" celtica
[143,] "Leptoplastus" paucisegmentatus
[144,] "Leptoplastus" crassicornis
[145,] "Leptoplastus" raphidophorus
[146,] "Leptoplastus" intermedius
[147,] "Leptoplastus" ovatus
[148,] "Leptoplastus" angustatus
[149,] "Eurycare" explanatum
[150,] "Leptoplastus" neglectus
[151,] "Ctenopyge" postcurrens
[152,] "Ctenopyge" drytonensis
[153,] "Ctenopyge" flagellifera
[154,] "Ctenopyge" erecta
[155,] "Ctenopyge" modesta
[156,] "Ctenopyge" similis
[157,] "Ctenopyge" spectabilis
[158,] "Ctenopyge" tumidoides
[159,] "Ctenopyge" angusta
[160,] "Sphaerophthalmus" alatus
[161,] "Ctenopyge" tumida
[162,] "Ctenopyge" bisulcata
[163,] "Parabolinella" caesa
[164,] "Ctenopyge" directa
[165,] "Hedinaspis" expansa
[166,] "Ctenopyge" falcifera
[167,] "Sphaerophthalmus" humilis
[168,] "Pseudagnostus" obtusus
[169,] "Ctenopyge" pecten
[170,] "Micragnostus" rudis
[171,] "Peltura" scarabaeoides.scarabaeoides
[172,] "Ctenopyge" teretifrons
[173,] "Lotagnostus" trisectus
[174,] "Parabolinites" williamsonii
[175,] "Ctenopyge" fletcheri
[176,] "Richardsonella" invita
[177,] "Parabolinites" longispinus
[178,] "Sphaerophthalmus" major
[179,] "Peltura" scarabaeoides.westergaardi
[180,] "Parabolina" brevispina
[181,] "Shumardia" alata
[182,] "Niobella" homfrayi.homfrayi*
[183,] "Psilocephalinella" innotata
[184,] "Hysterolenus" toernquisti
[185,] "Neoagnostus" bilobus
[186,] "Parabolina" heres.heres
[187,] "Beltella" nodifer
[188,] "Dichelepyge" bicornis
[189,] "Parabolina" frequens
[190,] "Araiopleura" stephani

Ordovician Species

[191,] "Ciceragnostus" barlowii*
[192,] "Micragnostus" calvus*
[193,] "Beltella" depressa
[194,] "Boeckaspis" hirsuta
[195,] "Shumardia" curta
[196,] "Acanthopleurella" grindrodi
[197,] "Niobella" homfrayi.smithi
[198,] "Boeckaspis" mobergi
[199,] "Illaenus" inflatus
[200,] "Beltella" versimilis
[201,] "Geragnostus" callavei*
[202,] "Macropyge" chermi*
[203,] "Platypeltoides" croftii*
[204,] "Proteuloma" monile.praemonile
[205,] "Myindella" crux
[206,] "Micragnostus" dux*
[207,] "Micragnostus" latemarginalis*
[208,] "Leptoplastides" salteri*
[209,] "Parabolinella" argentinensis
[210,] "Hospes" clonograpti
[211,] "Lichapyge" cuspidata*
[212,] "Asaphellus" homfrayi*
[213,] "Proteuloma" monile.monile*
[214,] "Dichelepyge" phylax
[215,] "Asaphoon" pithogastron
[216,] "Geragnostus" sidenbladhi*
[217,] "Parabolinella" triarthra*
[218,] "Niobina" davidis
[219,] "Orometopus" elatifrons
[220,] "Anacheirurus" frederici*
[221,] "Dikelokephalina" furca
[222,] "Prospectatrix" genatenta
[223,] "Pseudokainella" impar
[224,] "Orometopus" praenuntius
[225,] "Shumardia" pusilla
[226,] "Apatokephalus" serratus
[227,] "Bienvillia" shinetonensis
[228,] "Orometopus" aridos
[229,] "Ceratopyge" forficula
[230,] "Peltocare" olenoides
[231,] "Anacheirurus" plutonis
[232,] "Orometopus" pyrus
[233,] "Angelina" sedgwickii
[234,] "Acanthopleurella" stipulae
[235,] "Ampyx" cetsarum
[236,] "Neseuretus" parvifrons*
[237,] "Neseuretus" grandior
[238,] "Neseuretus" brevisulcus*
[239,] "Placoparia" cambriensis.cambriensis*
[240,] "Neseuretus" complanatus*

[241,] "Myttonia" confusa*
[242,] "Ectillaenus" cunicularis*
[243,] "Bergamia" gibbsii*
[244,] "Ogyginus" hybridus*
[245,] "Selenopeltis" inermis.macropthalmus*
[246,] "Merlinia" major*
[247,] "Myttonia" multiplex*
[248,] "Neseuretus" murchisoni*
[249,] "Agerina" perplexa*
[250,] "Ampyx" salteri*
[251,] "Gog" scutatrix*
[252,] "Macrogrammus" scylfense*
[253,] "Merlinia" selwynii
[254,] "Anebolithus" simplicior*
[255,] "Ectillaenus" bergaminus
[256,] "Pricyclopyge" binodosa
[257,] "Segmentagnostus" hirundo
[258,] "Pricyclopyge" prisca
[259,] "Bergamia" rhodesi
[260,] "Megalaspidella" whittardi
[261,] "Seleneceme" acuticaudata
[262,] "Flexicalymene" aurora
[263,] "Gastropolus" brevicaudatum
[264,] "Bettonia" chamberlaini*
[265,] "Porterfieldia" convergens
[266,] "Stapeleyella" etheridgei
[267,] "Barrandia" homfrayi
[268,] "Illaenopsis" hopensis
[269,] "Ectillaenus" hughesi
[270,] "Stapeleyella" inconstans
[271,] "Dionide" jubata
[272,] "Ampyx" linleyensis
[273,] "Ormathops" llanvirnensis
[274,] "Ellipsotaphrus" monophthalmus
[275,] "Stapeleyella" murchisoni
[276,] "Microparia" nuda
[277,] "Cremastoglottus" occipitalis
[278,] "Ectillaenus" perovalis
[279,] "Protolloydolithus" ramsayi
[280,] "Placoparia" sedgwickii.shelvensis
[281,] "Microparia" shelvensis
[282,] "Illaenopsis" thomsoni
[283,] "Dionide" turnbulli
[284,] "Platycoryphe" vulcani
[285,] "Ogyginus" porcatus
[286,] "Barrandia" biannularis
[287,] "Segmentagnostus" caducus
[288,] "Cornovica" didymograpti
[289,] "Ogyginus" intermedius
[290,] "Corrugatagnostus" morea
[291,] "Ormathops" nicholsoni
[292,] "Barrandia" parabolica
[293,] "Pharostoma" pulchrum.pulchrum
[294,] "Ogygiocaris" seavilli
[295,] "Barrandia" tasgarensis
[296,] "Platycalymene" tasgarensis.tasgarensis
[297,] "Trinucleus" abruptus
[298,] "Ogyginus" corndensis*
[299,] "Protolloydolithus" neintianus
[300,] "Novakella" bergeroni
[301,] "Colpocoryphe" hughesi
[302,] "Cyclopyge" obtusicaudata
[303,] "Ogyginus" grandis
[304,] "Segmentagnostus" scoltonensis
[305,] "Metopolichas" patriarchus
[306,] "Marrolithus" primus
[307,] "Trinucleus" acutofinalis
[308,] "Ogygiocaris" bettonensis
[309,] "Marrolithus" inflatus.decipiens
[310,] "Remopleurides" ateuchetos
[311,] "Flexicalymene" cambrensis
[312,] "Marrolithus" craticulatus
[313,] "Ogygiocarella" debuchii*
[314,] "Whittardolithus" inopinatus
[315,] "Quinquecosta" stincharensis
[316,] "Basilicus" tyrannus
[317,] "Encrinuroides" autochthon
[318,] "Thulincola" barbara
[319,] "Illaenus" beggi
[320,] "Ceratocephala" confinis
[321,] "Barrandia" cordai
[322,] "Illaenus" devexus
[323,] "Ceraurinella" dispersa
[324,] "Sphaerexochus" eurys
[325,] "Barrandia" expansa
[326,] "Emmrichops" extensus
[327,] "Decoroproetus" fearnsidesi.pristinus
[328,] "Calyptaulax" foederatus
[329,] "Ampyx" harperi
[330,] "Raymondaspis" hermaion
[331,] "Whittardolithus" instabilis
[332,] "Whittardolithus" intertextus
[333,] "Xylabion" kirklandense
[334,] "Eobronteus" latus
[335,] "Lloydolithus" lloydi
[336,] "Calyptaulax" marginatus
[337,] "Marrolithus" maturus
[338,] "Segmentagnostus" mccoyii
[339,] "Lonchodomas" minuntionensis
[340,] "Cnemidopyge" nuda.nuda
[341,] "Bergamia" prima
[342,] "Remopleurides" procax
[343,] "Homalopteon" radians
[344,] "Protolloydolithus" reticulatus
[345,] "Sphaerocoryphe" saba
[346,] "Primaspis" simulatrix
[347,] "Isotelus" stincharensis
[348,] "Platycalymene" tasgarensis.simulata
[349,] "Cybeloides" terrigena
[350,] "Barrandia" ultima

[351,] "Primaspis" whitei
[352,] "Bergamia" whittardi
[353,] "Kirkdomina" williamsi
[354,] "Sphaerexochus" filius
[355,] "Calyptaulax" georgei
[356,] "Hemiarges" inghami
[357,] "Rorringtonia" kennedyi
[358,] "Dimeropyge" labrosa
[359,] "Crozonaspis" peachi
[360,] "Whittardolithus" radiatilis
[361,] "Ceratocephala" relativa
[362,] "Encrinuroides" stincharensis
[363,] "Remopleurides" vulgaris
[364,] "Metopolichas" contractus
[365,] "Marrolithus" lirellatus
[366,] "Marrolithus" magnificus
[367,] "Failleana" powisensis
[368,] "Atractopyge" williamsi
[369,] "Ogygiocarella" angustissima
[370,] "Marrolithus" anomalis
[371,] "Spirantyx" calvarina
[372,] "Platycalymene" duplicata.duplicata
[373,] "Marrolithus" favus.favus
[374,] "Cnemidopyge" nuda.granulata
[375,] "Sphaerocoryphe" akimbo
[376,] "Marrolithoides" arcuatus
[377,] "Cnemidopyge" bisecta
[378,] "Raymondaspis" brocklochensis
[379,] "Mesotaphraspis" circumflexa
[380,] "Pliomerella" craigensis
[381,] "Trinucleus" fimbriatus
[382,] "Rorringtonia" flabelliformis
[383,] "Marrolithus" inornatus
[384,] "Hemiarges" insolitus
[385,] "Ceraurinella" magnilobata
[386,] "Homalopteon" murchisoni
[387,] "Phorocephala" pelagia
[388,] "Alwynulus" peregrinus
[389,] "Encrinuroides" periops
[390,] "Encrinuroides" polypleura
[391,] "Nobiliasaphus" powysensis
[392,] "Ceraurus" proicens
[393,] "Illaenus" rectus
[394,] "Ceratocephala" sexpares
[395,] "Heliomeroides" teres.chipperfieldi
[396,] "Illaenus" transversus
[397,] "Lonchodomas" variabilis
[398,] "Raymondella" abundans
[399,] "Ampyxina" aldonensis
[400,] "Dubhglasina" aldonensis
[401,] "Gravicalymene" aldonensis
[402,] "Sphaerexochus" arcuatus
[403,] "Geragnostus" aspinosus
[404,] "Remopleurides" bertilloni
[405,] "Arthrorhachis" comes
[406,] "Cybelurus" expansus
[407,] "Pliomerella" girvanensis
[408,] "Telephina" girvanensis
[409,] "Sphaerocoryphe" hastata
[410,] "Lonchodomas" limbatus
[411,] "Atractopyge" petiolulata*
[412,] "Raymondaspis" reedi
[413,] "Ampyx" repulsus
[414,] "Miraspis" solitaria
[415,] "Telephina" subsecuta
[416,] "Remopleurides" superstes
[417,] "Yumenaspis" templei
[418,] "Nileus" teres
[419,] "Arthrorhachis" doulargensis
[420,] "Dimeropyge" hystrix
[421,] "Selenopeltis" inermis.inermis
[422,] "Telaeomarrolithus" intermedius
[423,] "Encrinuroides" obesus
[424,] "Lonchodomas" pernix
[425,] "Amphilichas" priscus
[426,] "Marrolithus" scalpriformis
[427,] "Bumastoides" scoticus
[428,] "Marrolithus" ventriculatus
[429,] "Hibbertia" whittingtoni
[430,] "Quinquecosta" williamsi
[431,] "Telaeomarrolithus" radiatus
[432,] "Flexicalymene" acantha
[433,] "Marrolithus" arenarius
[434,] "Marrolithus" bilinearis
[435,] "Brongniartella" caradociana
[436,] "Platycoryphe" dentata
[437,] "Costonia" elegans
[438,] "Decoroproetus" fearnsidesi.fearnsidesi
[439,] "Parabasilicus" powisii*
[440,] "Reacalymene" pusulosa
[441,] "Costonia" ultima
[442,] "Broeggerolithus" harnagensis
[443,] "Kloucekia" harnagensis
[444,] "Primaspis" harnagensis
[445,] "Gravicalymene" praecox
[446,] "Salterolithus" praecursor
[447,] "Reuscholithus" reuschi
[448,] "Smeathenia" smeathenensis
[449,] "Broeggerolithus" ulrichi
[450,] "Hemiarges" angustifrons*
[451,] "Cybellela" balclatchiensis
[452,] "Sphaerexochus" balclatchiensis
[453,] "Stenopareia" balclatchiensis*
[454,] "Robergia" barrandii*
[455,] "Teratorhynchus" bicornis*
[456,] "Sphaerexochus" bilobatus
[457,] "Calyptaulax" brongniartii*
[458,] "Porterfieldia" caecigenus
[459,] "Stenopareia" camladica
[460,] "Salterolithus" caractaci.paucus

[461,] "Raphiophorid.gen.indet" carrickensis
[462,] "Bronteopsis" concentricus
[463,] "Robergiella" correcta
[464,] "Mesotaphraspis" dalfaskensis
[465,] "Remopleurides" epimera*
[466,] "Dionide" euglypta.quadrata
[467,] "Arthrorhachis" girvanensis*
[468,] "Remopleurides" girvanensis*
[469,] "Ampyx" hornei
[470,] "Isotelus" instabilis*
[471,] "Decoroproetus" jamesoni
[472,] "Diacanthaspis" lalage
[473,] "Lonchodomas" macallumi
[474,] "Raymondella" macconochiei
[475,] "Parabasilicus" marstoni
[476,] "Illaenus" memorabilis
[477,] "Atractopyge" mitchelli*
[478,] "Robergiella" neteorum*
[479,] "Illaenus" peachii
[480,] "Sphaerocoryphe" pemphis*
[481,] "Amphilichas" planus*
[482,] "Salteria" primaeva
[483,] "Illaenus" richardsoni
[484,] "Pliomerella" serotina
[485,] "Pandaspinapyge" stubblefieldi
[486,] "Reedolithus" subradiatus*
[487,] "Nanillaenus" superstes*
[488,] "Toernquistia" translata*
[489,] "Nieszkowskia" unica
[490,] "Salterolithus" caractaci.caractaci*
[491,] "Reacalymene" limba
[492,] "Hemiarges" antelucanus
[493,] "Raymondaspis" ardmillanensis
[494,] "Hibbertia" balclatchiensis
[495,] "Lonchodomas" coagmentatus
[496,] "Encrinuroides" contentus
[497,] "Cybellela" dentata
[498,] "Illaenus" extans
[499,] "Calyptaulax" hunteri
[500,] "Diacanthaspis" hystrix
[501,] "Thulincola" immanis
[502,] "Physemataspis" mirabilis
[503,] "Proetus" owensi
[504,] "Amphilichas" panoplos
[505,] "Glaphurus" radialis
[506,] "Otarion(Aulacopleura)" reedi
[507,] "Telephina" salteri
[508,] "Mesotaphraspis" sola
[509,] "Lonchodomas" swindalensis
[510,] "Amphilichas" transversus
[511,] "Harpidella" tumida
[512,] "Rorringtonia" vetula
[513,] "Calyptaulax" vicinus
[514,] "Scotoharpes" youngi
[515,] "Broeggerolithus" broeggeri
[516,] "Decoroproetus" calvus*
[517,] "Amphilichas" fryi
[518,] "Brongniartella" minor.subcarinata
[519,] "Flexicalymene planimarginata*
[520,] "Broeggerolithus" soudleyensis*
[521,] "Hibbertia" flanaganni
[522,] "Isotelus" girvanensis
[523,] "Isotelus" grayi
[524,] "Amphilichas" hibernicus
[525,] "Brongniartella" minor.minor
[526,] "Kloucekia" apiculata
[527,] "Brongniartella" ascripta
[528,] "Scopelochasmops" cambrensis
[529,] "Broeggerolithus" globiceps
[530,] "Conolichas" melmerbiensis
[531,] "Broeggerolithus" nicholsoni
[532,] "Primaspis" semievoluta
[533,] "Estoniops" alifrons
[534,] "Brongniartella" bisulcata
[535,] "Flexicalymene" caractaci
[536,] "Flexicalymene" cobboldi
[537,] "Dindymene" duftonensis
[538,] "Toxochasmops" extensus
[539,] "Broeggerolithus" longiceps
[540,] "Harpidella" beggi
[541,] "Remopleurides" biaculeatus
[542,] "Achatella" consobrina
[543,] "Illaenus" convergens
[544,] "Xylabion" craigense
[545,] "Eobronteus" craigensis
[546,] "Remopleurides" craigensis
[547,] "Stenopareia" craigensis
[548,] "Amphilichas" declivis
[549,] "Diacanthaspis" elapsa
[550,] "Cyphoproetus" facetus
[551,] "Bumastoides" fornax
[552,] "Calymene" grayae
[553,] "Craigheadia" grayi
[554,] "Harpidella" isoplates
[555,] "Atractopyge" killochanensis
[556,] "Eobronteus" lamonti
[557,] "Encrinuroides" lapworthi
[558,] "Celtencrinurus" praecursor
[559,] "Sphaerocoryphe" psiles
[560,] "Flexicalymene" shirleyi
[561,] "Cybeloides" spinifera
[562,] "Encrinuroides" sublanceolatus
[563,] "Xylabion" susceptum
[564,] "Stenopareia" transmota
[565,] "Hibbertia" trippi
[566,] "Primaspis" caractaci
[567,] "Broeggerolithus" transiens
[568,] "Calyptaulax" actonensis
[569,] "Ampyxella" edgelli
[570,] "Onnicalymene" laticeps

[571,] "Remopleurides" latus
[572,] "Platylichas" laxatus
[573,] "Lonchodomas" pennatus
[574,] "Scopelochasmops" salopiensis
[575,] "Onnicalymene" salteri
[576,] "Remopleurides" warburgae
[577,] "Tretaspis" ceroides.favus
[578,] "Onnia" cobboldi
[579,] "Remopleurella" burmeisteri
[580,] "Onnia" gracilis
[581,] "Onnicalymene" onniensis
[582,] "Atractopyge" scabra
[583,] "Tretaspis" ceroides.alyta
[584,] "Cybeloides" girvanensis
[585,] "Onnia" superba.pusgillensis
[586,] "Onnia" superba.superba
[587,] "Brongniartella" bulbosa
[588,] "Tretaspis" colliquia
[589,] "Pseudosphaerexochus" densigranulatus
[590,] "Illaenus" fallax
[591,] "Tretaspis" hadelandica.convergens
[592,] "Gravicalymene" jugifera
[593,] "Acidaspis" magnospina
[594,] "Mucronaspis" mucronata.matutina
[595,] "Pseudosphaerexochus" octolobatus
[596,] "Decoroproetus" piriceps
[597,] "Calyptaulax" planiformis
[598,] "Pseudosphaerexochus" tectus
[599,] "Primaspis" evoluta
[600,] "Duftonia" lacunosa
[601,] "Tretaspis" moeldenensis.moeldenensis
[602,] "Brongniartella" sedgwicki
[603,] "Calymene" subdiademata
[604,] "Harpidella" tridens
[605,] "Atractopyge" verrucosa
[606,] "Toxochasmops" amphora
[607,] "Gravicalymene" convolva
[608,] "Phillipsinella" preclara
[609,] "Stenopareia" bowmanni
[610,] "Oedicybele" kingi
[611,] "Toxochasmops" marri
[612,] "Ascetopeltis" apoxys
[613,] "Pseudosphaerexochus" boops
[614,] "Pharostoma" cautleyense
[615,] "Flexicalymene" cavei
[616,] "Pseudosphaerexochus" conformis
[617,] "Encrinurus" cornutus
[618,] "Gravicalymene" deani
[619,] "Kloucekia" extensa
[620,] "Ceraurinella" intermedia
[621,] "Pseudosphaerexochus" juvenis
[622,] "Erratencrinurus" kingi
[623,] "Harpidella" lachrymosa
[624,] "Lichas" laciniatus
[625,] "Stygina" latifrons
[626,] "Primaspis" llandowrorensis
[627,] "Dindymene" longicaudata
[628,] "Calymene" marginata
[629,] "Platylichas" noctua
[630,] "Phillipsinella" parabola.aquilonia
[631,] "Lehua" princeps
[632,] "Sphaerocoryphe" punctata
[633,] "Paraharpes" ruddyi
[634,] "Encrinuroides" sexcostatus
[635,] "Gravicalymene" susi
[636,] "Arthrorhachis" tarda
[637,] "Diacanthaspis" turnbulli
[638,] "Paraharpes" whittingtoni
[639,] "Primaspis" bucculenta
[640,] "Staurocephalus" clavifrons
[641,] "Tretaspis" hadelandica.deliqua
[642,] "Calymene" prolata
[643,] "Diacanthaspis" sladensis
[644,] "Lonchodomas" drummuckensis
[645,] "Sphaerocoryphe" globiceps
[646,] "Paraharpes" hornei
[647,] "Celtencrinurus" lamonti
[648,] "Cryptolithus" latus
[649,] "Celtencrinurus" multisegmentatus
[650,] "Achatella" quarrellensis
[651,] "Achatella" truncatocaudata
[652,] "Tretaspis" caritus
[653,] "Illaenus" davisii
[654,] "Diacanthaspis" decacantha
[655,] "Calymene" emicata
[656,] "Ulugtella" galeata
[657,] "Duftonia" geniculata
[658,] "Platylichas" glenos
[659,] "Raphiophorus" gratus
[660,] "Tretaspis" hadelandica.brachystichus
[661,] "Dindymene" hughesiae
[662,] "Dindymene" ornata
[663,] "Gravicalymene" pontilis
[664,] "Lonchodomas" portlocki
[665,] "Amphitryon" radians
[666,] "Opsimasaphus" radiatus
[667,] "Liocnemis" recurvus
[668,] "Kloucekia" robertsi
[669,] "Pseudosphaerexochus" seabornei
[670,] "Lonchodomas" tumidus
[671,] "Whittingtonia" whittingtoni
[672,] "Calymene" drummuckensis
[673,] "Sphaerocoryphe" kingi
[674,] "Tretaspis" latilimbus.distichus
[675,] "Pharostoma" obtusum
[676,] "Decoroproetus" papyraceus
[677,] "Phillipsinella" parabola.parabola
[678,] "Gravicalymene" arcuata
[679,] "Paraproetus" girvanensis
[680,] "Mucronaspis" mucronata.olini

[681,] "Leonaspis" olini
[682,] "Gravicalymene" quadrata
[683,] "Decoroproetus" asellus
[684,] "Acidaspis" asteroidea
[685,] "Astroproetus" asteroideus
[686,] "Calyptaulax" asteroideus
[687,] "Remopleurides" asteroideus
[688,] "Proetus" berwynensis
[689,] "Flexicalymene" bigener
[690,] "Toxochasmops" bisseti
[691,] "Dindymene" cordai
[692,] "Platylichas" crescenticus
[693,] "Stenopareia" drummuckensis
[694,] "Pseudosphaerexochus" ekphyma
[695,] "Harpidella" elongata
[696,] "Stenopareia" fluvialis
[697,] "Hemiarges" geikiei
[698,] "Primaspis" girvanensis
[699,] "Remopleurides" hedstroemi
[700,] "Hadromeros" keisleyensis
[701,] "Stygina" latifrons.extensa
[702,] "Stenopareia" longicapitata
[703,] "Hemiarges" maccullochi
[704,] "Remopleurides" nicholsoni
[705,] "Tretaspis" persulcata
[706,] "Cryptolithus" praeterita
[707,] "Astroproetus" reedi
[708,] "Achatella" retardata
[709,] "Dionide" richardsoni
[710,] "Harpidella" rotunda
[711,] "Cyphoproetus" rotundatus
[712,] "Stenopareia" subcarinata
[713,] "Proceratocephala" terribilis
[714,] "Platylichas" thraivensis
[715,] "Illaenus" transversalis
[716,] "Panarchaeogonus" trigodus
[717,] "Celtencrinurus" trispinosus
[718,] "Raphiophorus" acus
[719,] "Mucronaspis" mucronata.brevispina
[720,] "Mucronaspis" mucronata.mucronata
[721,] "Tretaspis" sortita.sortita

Silurian Species

[722,] "Cyphoproetus" externus
[723,] "Opsypharus" maccallumi
[724,] "Astroproetus" scoticus
[725,] "Platylichas" scoticus
[726,] "Hemiarges" serus
[727,] "Encrinurus" squarrosus
[728,] "Stenopareia" thomsoni
[729,] "Calymene" ubiquitosa
[730,] "Kosovopeltis" cunctata
[731,] "Hadromeros" elongatus
[732,] "Decoroproetus" farragatus
[733,] "Stenopareia" glochin
[734,] "Harpidella" newlandensis
[735,] "Lichas" silvestris
[736,] "Acernaspis" superciliexcelsis
[737,] "Acernaspis" xynon
[738,] "Stenopareia" acymata
[739,] "Calymene" planicurvata
[740,] "Astroproetus" interjectus
[741,] "Youngia" morioides
[742,] "Encrinurus" newlandensis
[743,] "Globulaspis" prominens
[744,] "Ceratocephalina" reperta
[745,] "Miraspis" ultima
[746,] "Proromma" bregmops
[747,] "Eophacops" glaber
[748,] "Scotoharpes" judex
[749,] "Scotoharpes" willsi
[750,] "Raphiophorus" aloniensis
[751,] "Proromma" acanthodes
[752,] "Otarion" brachypygus
[753,] "Stenopareia" aemula
[754,] "Kosovopeltis" andersoni
[755,] "Stenopareia" arenacea
[756,] "Stenopareia" catathema
[757,] "Encrinurus" confusevarus
[758,] "Calymene" hadyardensis
[759,] "Proetus" haverfordensis
[760,] "Encrinurus" mullochensis
[761,] "Encrinurus" shelvensis
[762,] "Encrinurus" stateratus
[763,] "Dalmanites" tenuimucronatus
[764,] "Youngia" trispinosa
[765,] "Bumastus" vulsus
[766,] "Acernaspis" woodburnensis
[767,] "Leonaspis" acarescola
[768,] "Leonaspis" erinaceus
[769,] "Astroproetus" pseudolatifrons
[770,] "Cyphoproetus" pugionis
[771,] "Scotoharpes" volsellatus
[772,] "Cyphoproetus" binodosus
[773,] "Arctinurus" constrictus
[774,] "Encrinurus" diabolus
[775,] "Proetus" latifrons*
[776,] "Calymene" replicata
[777,] "Cheirurus" centralis
[778,] "Prantlia" grindrodi
[779,] "Acastocephala" macrops
[780,] "Sphaerexochus" mirus
[781,] "Encrinurus" onniensis
[782,] "Staurocephalus" susanae
[783,] "Encrinurus" tuberculatus
[784,] "Dalmanites" weaveri
[785,] "Warburgella" capetos

[786,] "Cyphoproetus" comitilis
[787,] "Anacaenaspis" dealgach
[788,] "Scotoharpes" domina
[789,] "Youngia" douglasi
[790,] "Encrinurus" expansus
[791,] "Calymene" frontosa
[792,] "Hemiarges" rolfei
[793,] "Podowrinella" straitonensis
[794,] "Acernaspis" sufferta
[795,] "Encrinurus" pagei
[796,] "Bumastus" barriensis
[797,] "Proetus" concinnus*
[798,] "Dalmanites" corrugatus
[799,] "Trimerus" cylindricus
[800,] "Cyphoproetus" depressus
[801,] "Planiscutellum" kitharos
[802,] "Proetus" oppidanus
[803,] "Cornuproetus" peraticus
[804,] "Anacaenaspis" phasganis
[805,] "Bumastus" phrix
[806,] "Dudleyaspis" portlockii
[807,] "Warburgella" scutterdinensis
[808,] "Radnoria" syrphetodes
[809,] "Tapinocalymene" volsoriforma
[810,] "Delops" nobilis.marri*
[811,] "Odontopleura" ovata*
[812,] "Raphiophorus" parvulus*
[813,] "Deiphon" barrandei
[814,] "Hemiarges" bucklandii
[815,] "Dalmanites" caudatus
[816,] "Acastoides" constricta
[817,] "Heliocephalus" coronatus*
[818,] "Leonaspis" deflexa
[819,] "Cyphaspis" elachopos
[820,] "Proetus" falcatus
[821,] "Platylichas" grayii
[822,] "Acanthopyge" hirsuta
[823,] "Eophacops" musheni
[824,] "Dalmanites" myops*
[825,] "Ktenoura" retrospinosa
[826,] "Dicranopeltis" salteri
[827,] "Hemiarges" scutalis
[828,] "Ananaspis" stokesii
[829,] "Acaste" subcaudata
[830,] "Encrinurus" variolaris
[831,] "Decoroproetus" wigwig
[832,] "Bumastus" xestos
[833,] "Cybantyx" anaglyptos
[834,] "Calymene" aspera
[835,] "Ceratocephala" barrandii
[836,] "Calymene" blumenbachii
[837,] "Acidaspis" brightii
[838,] "Leonaspis" coronata*
[839,] "Leonaspis" crenata.brutoni
[840,] "Trimerus" delphinacephalus
[841,] "Acaste" downingiae*
[842,] "Acaste" inflata*
[843,] "Trimerus" johannis
[844,] "Delops" nobilis.nobilis
[845,] "Tapinocalymene" nodulosa
[846,] "Dudleyaspis" quinquespinosa
[847,] "Decoroproetus" scrobiculatus*
[848,] "Warburgella" stokesii
[849,] "Cyphoproetus" strabismus
[850,] "Harpidella" aitholix
[851,] "Struveria" howgillensis
[852,] "Harpidella" maura
[853,] "Miraspis" mira
[854,] "Litotix" armata
[855,] "Delops" obtusicaudatus
[856,] "Calymene" tuberculosa
[857,] "Dalmanites" nexilis
[858,] "Scharyia" siceripotrix
[859,] "Proetus" astringens
[860,] "Homalonotus" knightii*
[861,] "Warburgella" ludlowensis*
[862,] "Acastella" minor*
[863,] "Proetus" odconicus*
[864,] "Calymene" lawsoni
[865,] "Encrinurus" rosensteinae
[866,] "Encrinurus" stubblefieldi
[867,] "Cheirurus" postremus
[868,] "Calymene" puellaris
[869,] "Acastella" spinosa
[870,] "Acastella" prima

Devonian Species

[871,] "Burmeisterella" bifurcata
[872,] "Burmeisterella" champernownei
[873,] "Scutellum" flabelliferum*
[874,] "Neometacanthus" stellifer
[875,] "Dechenella" setosa
[876,] "Cornuproetus" batillus
[877,] "Phacops" batracheus
[878,] "Scutellum" costatum.lummatonensis
[879,] "Scutellum" delicatum.delicatum
[880,] "Cyphaspis" ocellata
[881,] "Scutellum" pardalios
[882,] "Crotalocephalus" pengelli
[883,] "Cornuproetus" subfrontalis
[884,] "Harpes" whidbornei
[885,] "Scutellum" whidbornei
[886,] "Phacops.(Chotecops)" latifrons
[887,] "Proetus.(Gerastos)" audax
[888,] "Tropidocoryphe" champernowni
[889,] "Scutellum" delicatum.tigrinum
[890,] "Acanthopyge" devoniana
[891,] "Radiaspis" radiata
[892,] "Scutellum" costatum.costatum
[893,] "Asteropyge" laciniata
[894,] "Trimerocephalus" mastophthalmus
[895,] "Phacops.(Omegops)" accipitrinus
[896,] "Dianops" anopthalmus

[897,] "Phacops.(Phacops)" granulatus
[898,] "Calybole" ussheri
[899,] "Cryphops?" ensae
[900,] "Typhloproetus" subcarintiacus
[901,] "Phacops.(Phacops)" wedekindi
[902,] "Cryphops?" wocklumeriae

Carboniferous Species

[903,] "Carbonocoryphe" colei*
[904,] "Moschoglossis" decorata
[905,] "Namuropyge" discors*
[906,] "Archegonus.(Phillibole)" drewerensis
[907,] "Archegonus.(Phillibole)" duodecimae
[908,] "Brachymetopus" fryi
[909,] "Bollandia" globiceps*
[910,] "Archegonus.(Phillibole)" hercules
[911,] "Phillipsia" kellyi
[912,] "Brachymetopus" maccoyi*
[913,] "Phillipsia" ornata
[914,] "Archegonus.(Waribole)" porteri
[915,] "Eocyphinium" salteri
[916,] "Phillipsia" truncatula
[917,] "Brachymetopus" woodwardii
[918,] "Phillibolina" worsawensis*
[919,] "Archegonus.(Phillibole)" anglicus
[920,] "Cummingella" costabisulca
[921,] "Cyrtoproetus" mulesi
[922,] "Phillipsia" gemmulifera
[923,] "Bollandia" granulifera
[924,] "Cummingella" laticaudata*
[925,] "Eocyphinium" clitheroense
[926,] "Namuropyge" decora
[927,] "Carbonocoryphe.(Winterbergia)" hahnorum
[928,] "Archegonus.(Phillibole)" twistonensis
[929,] "Phillipsia" scabra
[930,] "Linguaphillipsia" matthewsi
[931,] "Phillipsia" holwellensis
[932,] "Griffithides" acanthiceps
[933,] "Namuropyge" acanthina
[934,] "Weania" anglica
[935,] "Paladin" bakewellensis
[936,] "Cummingella" carringtonensis
[937,] "Eocyphinium" castletonense
[938,] "Archegonus.(Phillibole)" coddonensis
[939,] "Cyrtoproetus" cracoensis
[940,] "Liobole" glabra
[941,] "Cummingella" insulae
[942,] "Cummingella" jonesi
[943,] "Namuropyge" kingi
[944,] "Griffithides" longiceps
[945,] "Spatulina" longispina
[946,] "Bollandia" obsoleta
[947,] "Brachymetopus" ouralicus
[948,] "Reediella" reedi
[949,] "Eocyphinium" seminiferum
[950,] "Spatulina" spatulata
[951,] "Eocyphinium" breve
[952,] "Griffithides" carinatus
[953,] "Griffithides" moriceps
[954,] "Archegonus.(Phillibole)" polleni
[955,] "Spatulina" spatulata.milleri
[956,] "Spinibole.(Vandergrachtia)" vandergrachtii
[957,] "Archegonus.(Phillibole) aprathensis
[958,] "Paladin" barkei
[959,] "Paladin" cuspidatus
[960,] "Paladin" glaber
[961,] "Kulmiella" leei
[962,] "Paladin" mucronatus.mucronatus
[963,] "Particeps" scoticus.minimus
[964,] "Particeps" scoticus.scoticus
[965,] "Paladin" angustipygus
[966,] "Typhloproetus" cephalispina
[967,] "Paladin" eakringensis
[968,] "Paladin" mucronatus.rotundatus
[969,] "Paladin" eichwaldi.parillis
[970,] "Paladin" lowickensis
[971,] "Paladin" eichwaldi.shunnerensis

A2. 2. Names of Trilobite Genera from England, Scotland and Wales.

Listed below are the names of the 359 trilobite genera from mainland Britain (*i.e.* England, Scotland and Wales) whose chronostratigraphical ranges are depicted in Figures 2. 9 - 2. 13. The genera are listed in the same order as that in which they appear on the charts (*i.e.* in ascending stratigraphical order of appearance). Genera denoted by * have a chronostratigraphical range greater than the 90% quantile value for the stratigraphical system in which they originated (equal to 11.96 myr for Cambrian

genera, 28.84 myr for Ordovician genera, 19.87 myr for Silurian genera, 17.45 myr for Devonian genera, and 29.6 myr for Carboniferous genera).

Cambrian Genera

[1,] "Callavia"*
[2,] "Hebediscus"
[3,] "Micmacca"
[4,] "Olenellus"*
[5,] "Strenuella"*
[6,] "Triangulaspis"
[7,] "Ladadiscus"
[8,] "Olenelloides"*
[9,] "Pseudatops"
[10,] "Serrodiscus"*
[11,] "Calodiscus"
[12,] "Cobboldites"
[13,] "Comluella"
[14,] "Latoucheia"
[15,] "Mohicana"
[16,] "Protolenus"
[17,] "Runcinodiscus"
[18,] "Strettonia"
[19,] "Acadoparadoxides"
[20,] "Bailiella"
[21,] "Bathyuriscus"
[22,] "Condylopyge"
[23,] "Ctenocephalus"
[24,] "Eccaparadoxides"
[25,] "Kootenia"
[26,] "Metadiscus"
[27,] "Paradoxides"
[28,] "Eodiscus"
[29,] "Pleuroctenium"
[30,] "Bailiaspis"
[31,] "Liostracus"
[32,] "Diplagnostus"
[33,] "Peronopsis"
[34,] "Ptychagnostus"*
[35,] "Tomagnostus"
[36,] "Agraulos"
[37,] "Hartshillia"
[38,] "Hypagnostus"
[39,] "Parasolenopleura"
[40,] "Peronopsella"
[41,] "Phalagnostus"
[42,] "Holocephalina"
[43,] "Centropleura"
[44,] "Clarella"
[45,] "Cotalagnostus"
[46,] "Corynexochus"
[47,] "Phalacroma"
[48,] "Hartshillina"
[49,] "Meneviella"
[50,] "Solenopleuropsis"
[51,] "Anopolenus"
[52,] "Doryagnostus"
[53,] "Elrathia"
[54,] "Agaso"
[55,] "Dorypyge"
[56,] "Solenopleura"
[57,] "Grandagnostus"
[58,] "Agnostus"
[59,] "Cristagnostus"
[60,] "Schmalenseeia"
[61,] "Proceratopyge"
[62,] "Glyptagnostus"
[63,] "Homagnostus"
[64,] "Olenus"
[65,] "Sulcatagnostus"
[66,] "Irvingella"
[67,] "Parabolinoides"
[68,] "Parabolina"
[69,] "Pseudagnostus"
[70,] "Briscoia"
[71,] "Conocephalina"
[72,] "Leptoplastus"
[73,] "Eurycare"
[74,] "Ctenopyge"
[75,] "Sphaerophthalmus"
[76,] "Hedinaspis"
[77,] "Lotagnostus"
[78,] "Micragnostus"*
[79,] "Parabolinella"*
[80,] "Parabolinites"
[81,] "Peltura"
[82,] "Richardsonella"
[83,] "Hysterolenus"
[84,] "Niobella"
[85,] "Psilocephalinella"
[86,] "Shumardia"*
[87,] "Beltella"
[88,] "Neoagnostus"
[89,] "Araiopleura"
[90,] "Dichelepyge"

Ordovician Genera

[91,] "Boeckaspis"
[92,] "Ciceragnostus"
[93,] "Acanthopleurella"
[94,] "Illaenus"*
[95,] "Geragnostus"*
[96,] "Macropyge"
[97,] "Platypeltoides"
[98,] "Proteuloma"
[99,] "Leptoplastides"
[100,] "Myindella"
[101,] "Asaphellus"
[102,] "Asaphoon"
[103,] "Hospes"
[104,] "Lichapyge"
[105,] "Anacheirurus"
[106,] "Apatokephalus"
[107,] "Bienvillia"
[108,] "Dikelokephalina"
[109,] "Niobina"
[110,] "Orometopus"
[111,] "Prospectatrix"
[112,] "Pseudokainella"
[113,] "Angelina"
[114,] "Ceratopyge"
[115,] "Peltocare"
[116,] "Ampyx"*
[117,] "Neseuretus"
[118,] "Agerina"
[119,] "Anebolithus"
[120,] "Bergamia"
[121,] "Ectillaenus"
[122,] "Gog"
[123,] "Macrogrammus"
[124,] "Merlinia"
[125,] "Myttonia"
[126,] "Ogyginus"
[127,] "Placoparia"
[128,] "Selenopeltis"
[129,] "Megalaspidella"
[130,] "Pricyclopyge"
[131,] "Segmentagnostus"
[132,] "Barrandia"
[133,] "Bettonia"
[134,] "Cremastoglottus"
[135,] "Dionide"*
[136,] "Ellipsotaphrus"
[137,] "Flexicalymene"*
[138,] "Gastropolus"
[139,] "Illaenopsis"
[140,] "Microparia"
[141,] "Ormathops"
[142,] "Platycoryphe"
[143,] "Porterfieldia"
[144,] "Protolloydolithus"
[145,] "Seleneceme"
[146,] "Stapeleyella"
[147,] "Cornovica"
[148,] "Corrugatagnostus"
[149,] "Ogygiocaris"
[150,] "Pharostoma"*

[151,] "Platycalymene"
[152,] "Trinucleus"
[153,] "Colpocoryphe"
[154,] "Cyclopyge"
[155,] "Novakella"
[156,] "Metopolichas"
[157,] "Marrolithus"
[158,] "Basilicus"
[159,] "Ogygiocarella"
[160,] "Quinquecosta"
[161,] "Remopleurides"*
[162,] "Whittardolithus"
[163,] "Calyptaulax"
[164,] "Ceratocephala"*
[165,] "Ceraurinella"
[166,] "Cnemidopyge"
[167,] "Cybeloides"*
[168,] "Decoroproetus"*
[169,] "Emmrichops"
[170,] "Encrinuroides"
[171,] "Eobronteus"
[172,] "Homalopteon"
[173,] "Isotelus"
[174,] "Kirkdomina"
[175,] "Lloydolithus"
[176,] "Lonchodomas"*
[177,] "Primaspis"*
[178,] "Raymondaspis"
[179,] "Sphaerexochus"*
[180,] "Sphaerocoryphe"
[181,] "Thulincola"
[182,] "Xylabion"
[183,] "Crozonaspis"
[184,] "Dimeropyge"
[185,] "Hemiarges"*
[186,] "Rorringtonia"
[187,] "Atractopyge"
[188,] "Failleana"
[189,] "Spirantyx"
[190,] "Alwynulus"
[191,] "Ceraurus"
[192,] "Heliomeroides"
[193,] "Marrolithoides"
[194,] "Mesotaphraspis"
[195,] "Nobiliasaphus"
[196,] "Phorocephala"
[197,] "Pliomerella"
[198,] "Ampyxina"
[199,] "Cybelurus"
[200,] "Dubhglasina"
[201,] "Gravicalymene"
[202,] "Miraspis"*
[203,] "Nileus"
[204,] "Raymondella"
[205,] "Telephina"
[206,] "Yumenaspis"
[207,] "Amphilichas"
[208,] "Arthrorhachis"
[209,] "Bumastoides"
[210,] "Hibbertia"
[211,] "Telaeomarrolithus"
[212,] "Brongniartella"
[213,] "Costonia"
[214,] "Parabasilicus"
[215,] "Reacalymene"
[216,] "Broeggerolithus"
[217,] "Kloucekia"
[218,] "Reuscholithus"
[219,] "Salterolithus"
[220,] "Smeathenia"
[221,] "Bronteopsis"
[222,] "Cybellela"
[223,] "Diacanthaspis"
[224,] "Nanillaenus"
[225,] "Nieszkowskia"
[226,] "Pandaspinapyge"
[227,] "Raphiophorid.gen.indet"
[228,] "Reedolithus"
[229,] "Robergia"
[230,] "Robergiella"
[231,] "Salteria"
[232,] "Stenopareia"*
[233,] "Teratorhynchus"
[234,] "Toernquistia"
[235,] "Glaphurus"
[236,] "Harpidella"*
[237,] "Otarion"
[238,] "Physemataspis"
[239,] "Proetus"*
[240,] "Scotoharpes"
[241,] "Conolichas"
[242,] "Scopelochasmops"
[243,] "Dindymene"
[244,] "Estoniops"
[245,] "Toxochasmops"
[246,] "Achatella"
[247,] "Calymene"*
[248,] "Celtencrinurus"
[249,] "Craigheadia"
[250,] "Cyphoproetus"
[251,] "Ampyxella"
[252,] "Onnicalymene"
[253,] "Platylichas"
[254,] "Tretaspis"
[255,] "Onnia"
[256,] "Remopleurella"
[257,] "Acidaspis"
[258,] "Mucronaspis"
[259,] "Pseudosphaerexochus"
[260,] "Duftonia"
[261,] "Phillipsinella"
[262,] "Oedicybele"
[263,] "Ascetopeltis"
[264,] "Encrinurus"
[265,] "Erratencrinurus"
[266,] "Lehua"
[267,] "Lichas"
[268,] "Paraharpes"
[269,] "Stygina"
[270,] "Staurocephalus"
[271,] "Cryptolithus"
[272,] "Amphitryon"
[273,] "Liocnemis"
[274,] "Opsimasaphus"
[275,] "Raphiophorus"
[276,] "Ulugtella"
[277,] "Whittingtonia"
[278,] "Leonaspis"
[279,] "Paraproetus"
[280,] "Astroproetus"
[281,] "Hadromeros"
[282,] "Panarchaeogonus"
[283,] "Proceratocephala"

Silurian Genera

[284,] "Opsypharus"
[285,] "Acernaspis"
[286,] "Kosovopeltis"
[287,] "Ceratocephalina"
[288,] "Globulaspis"
[289,] "Youngia"
[290,] "Eophacops"
[291,] "Proromma"
[292,] "Bumastus"
[293,] "Dalmanites"
[294,] "Arctinurus"
[295,] "Acastocephala"
[296,] "Cheirurus"*
[297,] "Prantlia"
[298,] "Anacaenaspis"
[299,] "Podowrinella"
[300,] "Warburgella"
[301,] "Cornuproetus"*
[302,] "Dudleyaspis"
[303,] "Planiscutellum"
[304,] "Radnoria"
[305,] "Tapinocalymene"
[306,] "Trimerus"
[307,] "Delops"
[308,] "Odontopleura"
[309,] "Acanthopyge"*
[310,] "Acaste"
[311,] "Acastoides"
[312,] "Ananaspis"
[313,] "Cyphaspis"*

[314,] "Deiphon"
[315,] "Dicranopeltis"
[316,] "Heliocephalus"
[317,] "Ktenoura"
[318,] "Cybantyx"
[319,] "Struveria"
[320,] "Litotix"
[321,] "Scharyia"
[322,] "Acastella"
[323,] "Homalonotus"

Devonian Genera

[324,] "Burmeisterella"
[325,] "Neometacanthus"
[326,] "Scutellum"
[327,] "Dechenella"
[328,] "Crotalocephalus"
[329,] "Harpes"
[330,] "Phacops"
[331,] "Radiaspis"
[332,] "Tropidocoryphe"
[333,] "Asteropyge"
[334,] "Trimerocephalus"
[335,] "Calybole"
[336,] "Dianops"
[337,] "Cryphops?"
[338,] "Typhloproetus"*

Carboniferous Genera

[339,] "Archegonus"*
[340,] "Bollandia"
[341,] "Brachymetopus"*
[342,] "Carbonocoryphe"
[343,] "Eocyphinium"*
[344,] "Moschoglossis"
[345,] "Namuropyge"
[346,] "Phillibolina"
[347,] "Phillipsia"
[348,] "Cummingella"
[349,] "Cyrtoproetus"
[350,] "Linguaphillipsia"
[351,] "Griffithides"
[352,] "Liobole"
[353,] "Paladin"
[354,] "Reediella"
[355,] "Spatulina"
[356,] "Weania"
[357,] "Spinibole"
[358,] "Kulmiella"
[359,] "Particeps"

A2. 3. Data Base "pal.final.alpha".

The data base "pal.final.alpha" contains the times of appearance and disappearance of the 971 trilobites species from mainland Britain (*i.e.* England, Scotland and Wales) used in the construction of the range charts and statistics presented in Chapter 2. The data were extracted from Thomas *et al.* (1984), and the appearance and disappearance times have been calibrated against the time scale of Harland *et al.* (1989) (see Chapter 2). Because of the size of "pal.final.alpha" (971 rows x 10 columns) it is presented on the accompanying 3 1/2 inch Macintosh format computer disk. The file is presented in two formats:

pal.final.alpha_xl: a Microsoft Excel version 4.0 document.

pal.final.alpha_txt: an ascii document which can be opened by any Macintosh application capable of reading text format documents.

The structure of pal.final.alpha is as follows: there are 971 rows, one for each species. The species are listed in alphabetical order by species name. Each row has ten fields:

Field 1: an identifying number (essentially a redundant field).

Field 2: genus name.

Field 3: species name.

Field 4: a letter indicating whether the species is known from the Anglo-Welsh area (A), Scotland (S) or both (B).

Field 5: a letter indicating whether the species has a finite stratigraphical range (R) or is only known from one locality (x).

Field 6: the species identification number used by Thomas *et al.* (1984). Thomas *et al.* did not normally assign numbers to species known only from single localities, so these have been assigned an "x" for field 6.

Field 7: the time of appearance of the species expressed as a biozone number (see Chapter 2).

Field 8: the time of disappearance of the species expressed as a biozone number (see Chapter 2).

Field 9: the time of appearance of the species in Ma B.P., obtained by calibrating the biozone number against Harland *et al.* (1989) (see Chapter 2).

Field 10: the time of disappearance of the species in Ma B.P., obtained by calibrating the biozone number against Harland *et al.* (1989) (see Chapter 2).

A2. 4. Data Base "pal.gen.alpha".

The data base "pal.gen.alpha" contains the times of appearance and disappearance of the 359 trilobite genera from mainland Britain (*i.e.* England, Scotland and Wales) used in the construction of the range charts and statistics presented in Chapter 2. See Chapter 2 for explanation of how the data base was constructed. Because of the size of the file (359 rows x 6 columns) it is presented on the accompanying 3 1/2 inch disk in two formats:

pal.gen.alpha_xl: a Microsoft Excel version 4.0 document.

pal.gen.alpha_txt: an ascii document which can be opened by any Macintosh application capable of reading text format documents.

The structure of pal.gen.alpha is as follows: there are 359 rows, one for each genus. The genera are listed in alphabetical order. Each row has six fields:

Field 1: an identifying number (essentially a redundant field).

Field 2: genus name.

Field 3: the time of appearance of the genus expressed as a biozone number (see Chapter 2).

Field 4: the time of disappearance of the genus expressed as a biozone number (see Chapter 2).

Field 5: the time of appearance of the genus in Ma B.P., obtained by calibrating the biozone number against Harland *et al.* (1989) (see Chapter 2).

Field 6: the time of disappearance of the genus in Ma B.P., obtained by calibrating the biozone number against Harland *et al.* (1989) (see Chapter 2).

A2. 5 Calibration file "GTS89".

Presented below is the calibration file "GTS89" which was used in conjunction with the program "calibrator()" to convert times of first and last appearence of trilobite taxa expressed in biozone numbers into absolute dates (Chapter 2). The file consists of two columns: the first lists the key stratigraphical levels at which trilobite taxa have first or last appearences in the fossil record, quoted in biozone numbers; the second lists the corresponding dates in Ma, as interpolated from the timescale given by Harland *et al.* (1989). See Chapter 2 for full description of how this was done.

	[,1]	[,2]
[1,]	0	570
[2,]	1.00	560
[3,]	1.50	557
[4,]	2.00	554
[5,]	2.25	549.5
[6,]	2.50	545
[7,]	2.75	540.5
[8,]	3.00	536
[9,]	3.50	535.04
[10,]	4.00	534.07
[11,]	4.50	533.1
[12,]	5.00	532.13
[13,]	5.50	531.17
[14,]	6.00	530.2
[15,]	6.25	529.66
[16,]	6.50	529.12
[17,]	6.70	528.68
[18,]	6.80	528.46
[19,]	7.00	528.03
[20,]	7.25	527.49
[21,]	7.50	526.95
[22,]	7.70	526.52
[23,]	7.80	526.3
[24,]	8.00	525.87
[25,]	8.50	524.79
[26,]	9.00	523.7
[27,]	9.50	522.62
[28,]	10.00	521.53
[29,]	11.00	519.37
[30,]	11.50	518.29
[31,]	11.75	517.74
[32,]	12.00	517.2
[33,]	12.25	516.81
[34,]	12.50	516.43
[35,]	12.75	516.04
[36,]	13.00	515.65
[37,]	13.10	515.5
[38,]	13.20	515.34
[39,]	13.30	515.19
[40,]	13.40	515.03
[41,]	13.50	514.88
[42,]	13.60	514.72
[43,]	13.75	514.49
[44,]	13.80	514.41
[45,]	13.90	514.26
[46,]	14.00	514.1
[47,]	14.25	513.93
[48,]	14.500	513.76
[49,]	14.750	513.59
[50,]	15.000	513.42
[51,]	15.100	513.35
[52,]	15.200	513.28
[53,]	15.300	513.21
[54,]	15.400	513.14
[55,]	15.500	513.08
[56,]	15.600	513.01
[57,]	15.800	512.87
[58,]	16.000	512.73
[59,]	16.330	512.5
[60,]	16.670	512.28
[61,]	17.000	512.05
[62,]	17.250	511.88
[63,]	17.375	511.8
[64,]	17.500	511.71
[65,]	17.750	511.54
[66,]	18.000	511.37
[67,]	18.250	511.2
[68,]	18.375	511.11
[69,]	18.500	511.03
[70,]	18.625	510.94
[71,]	19.000	510.68
[72,]	19.330	510.46
[73,]	19.500	510.34
[74,]	19.750	510.17
[75,]	20.000	510
[76,]	20.330	508.87
[77,]	20.500	508.3
[78,]	20.670	507.73
[79,]	21.000	506.6
[80,]	21.500	504.9
[81,]	22.000	503.2
[82,]	23.000	499.8
[83,]	23.500	498.1
[84,]	24.000	496.4
[85,]	24.500	494.7
[86,]	25.000	493
[87,]	26.000	489.62
[88,]	26.500	487.93
[89,]	27.000	486.24
[90,]	27.800	483.54
[91,]	28.000	482.86
[92,]	29.000	479.48
[93,]	30.000	476.1
[94,]	30.100	475.76
[95,]	30.30	475.08
[96,]	30.40	474.74
[97,]	30.50	474.4
[98,]	30.60	474.06
[99,]	30.70	473.72
[100,]	30.80	473.38
[101,]	30.90	473.04
[102,]	31.00	472.7
[103,]	31.20	471.88
[104,]	31.50	470.65
[105,]	31.60	470.24
[106,]	31.75	469.63
[107,]	32.00	468.6
[108,]	32.33	468.07
[109,]	32.50	467.8
[110,]	32.60	467.64
[111,]	32.67	467.53
[112,]	32.75	467.4
[113,]	33.00	467
[114,]	33.10	466.66
[115,]	33.20	466.31
[116,]	33.25	466.03
[117,]	33.30	465.97
[118,]	33.40	465.62
[119,]	33.50	465.05
[120,]	33.75	464.08
[121,]	33.90	463.9
[122,]	34.00	463.1
[123,]	34.10	462.3
[124,]	34.20	461.34
[125,]	34.25	460.86
[126,]	34.30	460.38
[127,]	34.40	459.42
[128,]	34.50	458.46
[129,]	34.60	457.5
[130,]	34.75	454.58
[131,]	34.80	453.6
[132,]	35.00	449.7
[133,]	35.10	448.83
[134,]	35.20	447.97
[135,]	35.25	447.54

	[,1]	[,2]
[136,]	35.30	447.1
[137,]	35.40	445.8
[138,]	35.50	444.5
[139,]	35.60	444.25
[140,]	35.70	444
[141,]	35.75	443.95
[142,]	35.80	443.89
[143,]	35.90	443.78
[144,]	36.00	443.66
[145,]	36.50	443.1
[146,]	37.00	442.27
[147,]	37.33	441.71
[148,]	37.50	441.44
[149,]	38.00	440.6
[150,]	38.10	440.5
[151,]	38.20	440.4
[152,]	38.25	440.35
[153,]	38.40	440.2
[154,]	38.50	440.1
[155,]	38.60	439.98
[156,]	38.70	439.86
[157,]	38.75	439.8
[158,]	38.90	439.62
[159,]	39.00	439.5
[160,]	40.00	439
[161,]	41.00	438.48
[162,]	42.00	437.95
[163,]	43.00	437.43
[164,]	43.50	437.17
[165,]	44.00	436.9
[166,]	44.50	436.19
[167,]	44.67	435.95
[168,]	45.00	435.47
[169,]	45.50	434.75
[170,]	46.00	434.03
[171,]	46.50	433.32
[172,]	47.00	432.6
[173,]	48.00	432.05
[174,]	49.00	431.5
[175,]	50.00	430.95
[176,]	50.50	430.68
[177,]	51.00	430.4
[178,]	52.00	429.68
[179,]	53.00	428.97
[180,]	54.00	428.25
[181,]	55.00	427.53
[182,]	56.00	426.82
[183,]	57.00	426.1
[184,]	57.50	425.75
[185,]	58.00	425.4
[186,]	59.00	424.7
[187,]	59.50	424.35
[188,]	60.00	424
[189,]	61.00	421.03
[190,]	62.00	418.07
[191,]	63.00	415.1
[192,]	64.00	412.9
[193,]	64.50	411.8
[194,]	65.00	410.7
[195,]	65.67	409.23
[196,]	66.00	408.5
[197,]	67.00	399.45
[198,]	68.00	390.4
[199,]	68.50	389.3
[200,]	69.00	388.2
[201,]	70.00	386
[202,]	71.00	383.4
[203,]	72.00	380.8
[204,]	73.00	379.95
[205,]	73.50	379.53
[206,]	74.00	379.1
[207,]	74.50	378.68
[208,]	75.00	378.25
[209,]	76.00	377.4
[210,]	77.00	372.2
[211,]	78.00	367
[212,]	79.00	365.88
[213,]	80.00	364.75
[214,]	81.00	363.63
[215,]	82.00	362.5
[216,]	82.50	356
[217,]	83.00	349.5
[218,]	83.50	347.25
[219,]	84.00	345
[220,]	84.50	343.9
[221,]	85.00	342.8
[222,]	85.50	341.1
[223,]	86.00	339.4
[224,]	86.50	337.7
[225,]	87.00	336
[226,]	87.50	334.45
[227,]	88.00	332.9
[228,]	88.50	332
[229,]	89.00	331.1
[230,]	89.50	329.7
[231,]	90.00	328.3

APPENDIX THREE
LIST OF LOCALITIES FOR SPECIMENS USED IN MORPHOMETRICS

The following is a list of the localities from which trilobite specimens have been sampled for use in morphometrics. The localities within each broad geographical area are listed in approximate stratigraphical order (although where several localities in the same stratigraphical formation are listed, the order in which they are listed does not imply ascending stratigraphical order within that formation) and the geographical areas are listed in the same order as that in which their successions are described in Chapter 3, *i.e.* arbitrarily in approximate order of increasing geographical remoteness from Glasgow. Localities at which collecting was carried out by the author are marked with an asterisk.

Girvan District, SW Scotland.

Ordovician localities:

1. Kirkdominae Hill *. [NX 250 921]. Confinis Fm. Decalcified pale-brown weathering mudstones exposed on the hillside of Kirkdominae Hill on the north side of the Stinchar Valley about 100m west of Struit Well. Williams (1962); Tripp (1962).
2. Minuntion *. [NX 221 911]. Confinis Fm. Brown weathering friable calcareous fine sandstones exposed along the path leading from the old limekiln to the quarry in Stinchar Limestone Fm., about 450m W of Minuntion Farm. Williams (1962); Tripp (1962).
3. Auchlewan Burn. In stream draining the S slopes of Baldowie Hill, W of Auchlewan Quarry (locality 5 below), although exact locality unclear. GLAHM catalogue information.
4. Bougang Quarry *. [NX 114 855]. Confinis Fm. Yellow weathering fine calcareous sandstones exposed in the east side of the water filled quarry about 300m SW of Bougang Farm. Considered by Williams (1962) to be transitional from Confinis Fm. to overlying Stinchar Limestone Fm. Williams (1962); Tripp (1962).
5. Auchlewan Quarry. [NX 233 921]. Stinchar Limestone Fm. Limestones exposed in quarry about 400m NNW of Auchlewan ruins. Tripp (1967).
6. Minuntion Quarry *. [NX 221 911]. Stinchar Limestone Fm. Bedded limestones in quarry above old limekiln, about 450m W of Minuntion Farm. Tripp (1962).
7. Separation Sandstone Bed. [NX 296 929]. Separation Sandstone Bed, Doularg Fm. About 15 cm of bedded calcareous silty mudstones in the middle part of the Doularg Fm. exposed in an excavation in the west bank of Plantation Burn on the north slope of Doularg Hill, ENE of Doularg Farm. Ingham and Tripp (1991).
8. Dow Hill *. [NX 192 960]. "Infra-Kilranny Greywackes and Mudstones".

Blue and green-grey nodular mudstones exposed on SW flanks of Dow Hill just below the summit. Williams (1962); Tripp (1980).

9. Penwhapple Bridge *. [NX 256 969]. Upper Balclatchie Gp. Green-grey mudstones exposed in roadside quarry about 135m WNW of Penwhapple Bridge. Williams (1962); Tripp (1980a).
10. Ardmillan *. [NX 169 938]. Ardwell Farm Fm., lower part. Blue-grey siltstones and mudstones exposed in a stream draining the north flank of Ardmillan Braes, about 600m south of Ardmillan House. Williams (1962); Tripp (1980a).
11. Pinmery. [NX 240 949]. Ardwell Farm Fm. middle part. Blue-grey mudstones exposed in the west bank of the small burn next to the entrance to Pinmery Farm. Williams (1962); Tripp (1980a).
12. Kiln Mudstone. [NS 234 013]. Kiln Mudstone, Craighead Fm. Calcareous brown and green mudstones with rare limestone nodules exposed at the foot of the SW wall of the old limekiln, Craighead Quarry. Tripp (1954, 1980b); Williams (1962).
13. East brow of Quarrel Hill *. [NS 260 041]. Quarrel Hill Fm. Green bedded mudstones outcropping in the burn draining the east brow of Quarrel Hill. Equates to Harper's (1982) localities Q9 to Q12 and Q14 to Q15. Harper (1982).
14. Crinoid Bed *. [NS 262 035]. Quarrel Hill Crinoid Bed, upper Quarrel Hill Fm. Coarse grained sandstone bed outcropping on the east brow of Quarrel Hill, at Harper's (1982) locality Q13. Harper (1982).
15. The Starfish Beds *. [NS 250 038]. Starfish Beds, near the summit of Farden Mbr., South Threave Fm. Famous fossil locality consisting of three coarse sandstone beds outcropping on the south bank of Lady Burn and recently re-excavated. Harper (1981a, 1982).
16. Trench at High Mains Farm *. [NS 266 039]. High Mains Fm. Trench excavated through sandstones of the High Mains Fm. in the field to the west of High Mains Farm, about 100m from the farmhouse. Harper (1981b, 1988); Owen (1986).

Silurian localities:

17. Locality 1 of Howells (1982) *. [NS 267 041]. Mulloch Hill Fm. Small cutting on the north side of the road running along the south foot of Kirk Hill. Howells (1982).
18. Locality 2 of Howells (1982) *. [NS 266 041]. Mulloch Hill Fm. Small cutting on the north side of the road running along the south foot of Kirk Hill, about 130m west of Howells' locality 1. Howells (1982).
19. Locality 3 of Howells (1982) *. [NS 265 042]. Mulloch Hill Fm. Quarry on the north side of the road running along the south foot of Kirk Hill, about 120m west

of Howells' locality 2. "Mulloch Hill High Road Quarry" of the Gray family. Howells (1982).

20. Locality 4 of Howells (1982). [NS 263 042]. Mulloch Hill Fm. Small excavation below Kirk Hill, about 150m NW of Howells' locality 3. Howells (1982).
21. Locality 5 of Howells (1982) *. [NS 262 042]. Mulloch Hill Fm. Bluff on north side of the road running along the south foot of Kirk Hill, about 300m west of Howells' locality 3. Howells (1982).
22. Locality 6 of Howells (1982). [NS 259 042]. Mulloch Hill Fm. Overgrown quarry on the north side of the road at the south foot of Craigens Hill about 250m from Howells' locality 5. "Craigens" of the Gray family. Howells (1982).
23. Locality 7 of Howells (1982) *. [NS 265 043]. Mulloch Hill Fm. Small excavations about 120m SW of the summit of Kirk Hill. Howells (1982).
24. Rough Neuk Quarry *. [NS 270 040]. Mulloch Hill Fm. Fine grained green sandstones exposed in the abandoned quarry in Ladywell Wood about 120m WSW of the derelict Rough Neuk cottage. Locality 8 of Howells (1982).
25. Woodland Point *. [NX 169 952]. Woodland Fm. Flaggy siltstones and shales exposed only at low tide about 430m west of Woodland Farm. Locality 18 of Howells (1982).
26. Newlands Farm *. [NS 278 043]. Newlands Fm. Yellow-buff fine sandstones exposed in small N-S ridge on E bank of burn about 150m E of Newlands Farm. Locality 14 of Howells (1982).
27. Camregan Wood Quarry. [NX 225 980]. Lower Camregan Grits. Small quarry on S side Camregan Hill. Locality 19 of Howells (1982).
28. Bargany Pond Burn *. [NX 250 986]. Wood Burn Fm. Exposures in banks of tributary of Lauchlan Burn, about 1000m SW of summit of Maxwellston Hill. Locality 21 of Howells (1982).
29. Penkill. [NX 236 983]. Wood Burn Fm. Exposure in E bank of Penkill Burn about 500m SE of Penkill Castle. Locality 22 of Howells (1982).

Northern Belt of the Southern Uplands of Scotland.

30. Duntercleuch. Fossiliferous conglomerates within the Kirkcolm Fm. "Duntercleuch Burn" of Peach and Horne (1899), exact locality unknown, but in region of grid ref. NT 832163 - NT 840145 (Clarkson *et al.* 1992). Fossils preserved in clasts of yellow goethitic mudstone.
31. Kilbucho. [NT 056 336]. Fossiliferous conglomerates within the Kirkcolm Fm. Coarse, quartzitic conglomerates exposed in two quarries on the S side of White Hill. The fossils occur in clasts of brown mudstone in the conglomerate. (Clarkson *et al.* 1992).

North Esk Inlier, Pentland Hills.

32. Deerhope Burn. [NT 149 580]. Upper Reservoir Fm. Small exposure of mudstones and shales in the S bank of Deerhope Burn, 20m below the coral bed. RSM catalogue information.
33. The Coral Bed, Deerhope Burn. Deerhope Fm. Highly fossiliferous siltstone bed exposed in S bank of Deerhope Burn, near the second tributary. RSM catalogue information.
34. Wether Law Linn *. [NT 148 586]. Wether Law Linn Fm. Shales exposed at top of scree slope on S bank of Deerhope Burn. Locality 41 of Howells (1982).

Lake District, NW England.

35. Garburn Nook. [NY 433 043]. Applethwaite Mbr, Kirkley Bank Fm. Exposure at side of Garburn road, about 2520m ENE of Troutbeck Church. SM catalogue information.
36. Till's Hole. [NY 481 050]. Applethwaite Mbr, Kirkley Bank Fm. Crags on W side of Longsleddale, about 410m W of Till's Hole. SM catalogue information.
37. Stumfell Howe. [NY 441 044]. Applethwaite Mbr, Kirkley Bank Fm. E side of crag at Stumfell Howe. SM catalogue information.
38. Torver Beck. [SD 276 962]. Applethwaite Mbr, Kirkley Bank Fm. Exposure in W bank of Torver Beck. SM catalogue information.

Cross Fell Inlier, NW England.

39. Locality A12 of Dean (1962). [NY 699 259]. Dufton Shale Fm. (Onnian). Exposure in Pus Gill, near Dufton. About 250 ft. ENE of the second wall crossing the stream NE of Hindriggs. Dean (1959, 1962: figure 2).
40. Locality B25 of Dean (1962). [NY 688 276]. Dufton Shale Fm. (Pusgillian). Exposure in Swindale Beck, near Knock. E bank of stream, immediately N of the bridge which crosses the stream about 400 ft. N of the confluence between Swindale Beck and Small Burn. Dean (1959, 1962: figure 3).

South Shropshire.

41. Quarry Field near Gretton. Acton Scott Fm. Soft yellow flaggy sandstones with shelly lenses in quarry near Cardington (now filled in). Dean (1958, 1960); Hurst 1979b.

Ashgill Successions of South Wales.

42. Sholeshook Farm. Sholeshook Limestone Fm. Old quarry about 300m NE of Sholeshook Farm, Haverfordwest, Pembrokeshire. SM catalogue information.
43. Prendergast Place. Sholeshook Limestone Fm. Prendergast Place, Haverfordwest, Pembrokeshire. SM catalogue information.

44. Mylet Farm. [SN 268 143]. Sholeshook Limestone Fm. Road section about 500m SW of Mylet Farm, Carmarthenshire. SM catalogue information.

Denbigh-Conway District.

45. Plas Uchaf. [SH 819 632]. Upper Mottled Mudstone, lower Nantglyn Flags Gp., exposed at roadside NE of Plas Uchaf. Horizontally cleaved mottled mudstones. (Warren *et al.* 1984).

Grangegeeth District, Eastern Ireland.

46. Grangegeeth Crossroads. Basal Knockerk House Sandstone Mbr. Knockerk Fm. Small quarry E of road, about 436m N of Grangegeeth crossroads. Romano and Owen (1993).
47. Collon Quarry. Basal Knockerk House Sandstone Mbr. Knockerk Fm. S end of large quarry about 554m at 175° from Collon crossroads. Romano and Owen (1993).

Pomeroy Inlier, Co. Tyrone.

48. South slopes of Craigbardahessiagh. Bardahessiagh Fm. Few exposures and abundant loose blocks of fine grained grey micaceous sandstones with coarse conglomerates on the S slopes of Craigbardahessiagh, about 0.5km from the summit. Mitchell (1977: text-fig. 2).
49. Little River. Killey Bridge Fm. Lead grey micaceous flaggy mudstones and siltstones exposed in the Little River, about 3.6km E of Pomeroy Square and about 160m E of Slate Quarry Bridge. Mitchell (1977: text-fig. 2).

Co. Galway.

50. Glenglosh. Kilbride Fm., middle part. Locality G.GS.1 of Doyle (1989).

Oslo Region.

Grid references are from Topografisk Kart 1:50 000 series.

Ordovician localities:

51. Furuberg, Mjøsa. [Hamar Sheet 1916 IV, PN 092 443]. Railway section exposing Furuberget and Mjøsa formations. Owen *et al.* (1990).
52. Bergevika, Mjøsa. [Østre Toten Sheet 1916 III, PN 101 364]. Mjøsa Fm., exposed at Bergevika south, Helgøya. Owen *et al.* (1990).
53. Kalvøya, Asker. [Asker Sheet 1814 I, NM 864 401]. Solvang Fm. Owen *et al.* (1990).
54. South Kuholmen, Asker. Solvang Fm. PMO catalogue information.
55. East Raudskjer, Asker. [Asker Sheet 1814 I, NM 864 347]. Solvang Fm. Owen *et al.* (1990).

56. Frognøya, Ringerike. [Hønefoss Sheet 1815 III, M 652 581 - 652 582]. Venstøp Fm., exposed at NW end of Frognøya. Owen *et al.* (1990).
57. North Langøyene, Oslo. Husbergøya Fm. PMO catalogue information.
58. NW Frognøya, Ringerike. [Hønefoss Sheet 1815 III, M 652 581 - 652 582]. Sørbakken Fm., exposed at NW end of Frognøya. Owen *et al.* (1990).
59. Borøya, Asker. Skjerholmen Fm. PMO catalogue information.
60. Lindøy, Asker. Sørbakken Fm. PMO catalogue information.
61. Terneholmen, Asker. Sørbakken Fm. PMO catalogue information.
62. Rokotjern, Hadeland. Lunner Fm. PMO catalogue information.
63. Grina, Hadeland. [Gran Sheet 1915 I, NM 845 874 - 845 872]. Lunner Fm. Present spelling Grinda, Owen *et al.* (1990).
64. Lunner Station, Hadeland. [Gran Sheet 1915 I, NM 877 862]. Kjørrven Fm., exposed in railway section. Owen *et al.* (1990).
65. Ringen, Hadeland. Kjørrven Fm. PMO catalogue information.
66. Lilleklostret, Skien-Langesund. Langøyene Fm. PMO catalogue information.

Silurian localities:

67. Skytterveien, Asker. [Asker Sheet 1814 I, NM 818 327]. Solvik Fm., "6cb". Helbert (1985).
68. Spirodden, Asker. [Asker Sheet 1814 I, NM 840 337]. Solvik Fm., "6b"-"6c". Helbert (1985).
69. "Malmøya", Oslo. Solvik Fm., "6b"-"6c". Probably referring to the locality at Solvik, NM 981 378. Worsley *et al.* (1983).
70. Malmøykalven, Oslo. [Oslo Sheet 1914 IV, NM 978 378]. Solvik Fm., "6b"-"6c". Myren and Padda members of Worsley *et al.* (1983). Also Helbert (1985).
71. Sjursøya, Oslo. [Oslo Sheet 1914 IV, NM 985 404]. Solvik Fm., "6a". Locality now covered by an industrial complex. Helbert (1985).
72. Ulvøya, Oslo. Rytteråker Fm., "7a"-"7b". Helbert (1985).
73. Bjerkøya, Oslo. Rytteråker Fm., "7a"-"7b". Helbert (1985).
74. Garntangen, Ringerike *. [Hønefoss Sheet 1815 III, NM 720 609]. Vik Fm., exposed in road section (E68) near Garntangen on coast of Steinsfjorden. Worsley *et al.* (1983).
75. Vik, Ringerike. [Hønefoss Sheet 1815 III, NM 715 609]. Vik Fm., exposed in road cuttings immediately E of Vik. Worsley *et al.* (1983).
76. Storøya, Ringerike. [Hønefoss Sheet 1815 III, NM 690 576 - 694 582]. Vik Fm., exposed in several outcrops on the W coast of Storøya. Worsley *et al.* (1983).

Gotland.

77. Norderstrand. Lower Visby Fm. NW coast of Gotland, vicinity of Visby. RM

catalogue information.

78. Kronviken. Lower Visby Fm. NW coast of Gotland, vicinity of Visby. RM catalogue information.
79. Rönnklint. Lower Visby Fm. NW coast of Gotland, vicinity of Visby. RM catalogue information.
80. Vattenfallsprofilen 1. [CJ 3800 9150]. Högklint Fm., unit b. About 1100m SW of Visby cathedral. Laufeld (1974).
81. Ireviken. [CK 5588 1409]. Högklint Fm., unit a-b. Cliff about 6970 W of Hangvar church. Laufeld (1974).
82. Kopparsvik 3. [CJ 9050 3715]. Högklint Fm., unit b. Section in cliff about 2425m SW of Visby cathedral. Ramsköld 1985.
83. Sudervik 1. [CJ 5176 2493]. Mulde Fm., undifferentiated. Shore exposure about 900m S of road junction at Kronvall, about 6875m WSW of Eksta church.

Barrandian Region, Bohemia.

84. Kosov Quarry. Kopanina Fm. (middle part). Quarry near Beroun, Barrandian Region. Chlupáč (1977).
85. Kolednik Quarry. Kopanina Fm. (middle part). Quarry near Beroun, Barrandian Region. Chlupáč (1977).
86. Lockhov Quarry. Kopanina Fm. (middle part). Quarry near Beroun, Barrandian Region. Chlupáč (1977).

Anticosti Island.

87. Jupiter Cliff. Jupiter Fm., West Jupiter Cliff, Anticosti Island, Québec. Bolton (1971), Barnes (1988).

Gaspé Peninsula, Québec.

88. Grande Coup. Matapédia Fm. Argillaceous light blue limestones and shales exposed on E side of Mt. Ste. Anne, about 1 mile N of Percé, E shore of peninsula. Locality F2 of Cooper (1930).
89. South Cove. Matapédia Fm. Thin bedded calcareous shales and limestones at South Cove, SE shore of peninsula. Locality F3 of Cooper (1930).
90. Priest's Road. Matapédia Fm. Slabs of grey limestone lying on the Priest's Road near the school, about 2.5 miles NW of Percé. Locality F1 of Cooper (1930).

New York State and Ontario.

91. Sloop Bay. Crown Point Fm., middle and upper part. Dark grey limestones exposed as ledges near the water in the middle of the shore, Sloop Bay, E shore of Valcour Island, New York State. Locality V114 of Shaw (1968).

92. Pebble Beach. Crown Point Fm. Alternating calcarenites and silty limestones exposed at the E end of Pebble Beach, S shore of Valcour Island, New York State. Locality PB81 of Shaw (1968).
93. Trenton Falls, N.Y. Dark, silty fossiliferous limestones of the Trenton Gp. exposed at Trenton Falls, West Canada Creek, New York State.
94. McCarthy Bros. Quarry, Ontario. Verulam Fm. Limestones at quarry about 1.5 miles NW of Gamebridge, Ontario.
95. Lakefield Quarry, Ontario. Verulam Fm. Abandoned quarry at the intersection of Smith Concession 5 and Highway 28, about 2 miles S of Lakefield, Ontario.
96. Canada Cement Co. Quarry, Ontario. Verulam Fm. Canada Cement Co. Quarry, about 1.6 miles NE of Lakefield Bridge, Ontario.
97. Little Current, Ontario. Lindsay Fm. Exposures on Highway 68 about 2.2 miles E of Little Current, Great Cloche Island, Ontario.

Central Midcontinent Region.

98. Duck Creek Quarry. Prosser Fm. (Trenton Gp.). Thin shales exposed about 25 feet above the base of Duck Creek Quarry, near Green Bay, Wisconsin.
99. Elkader Quarry. Upper Prosser Fm. (Trenton Gp.). Quarry just above the roadway following the river at Elkader, Iowa. Specimens from about 2 feet thickness of shales lying about 60 feet above river level.
100. Maquoketa Creek, Clermont. Maquoketa Gp. Shales exposed along Maquoketa Creek near Clermont, Iowa.
101. Ft. Atkinson. Maquoketa Gp. Bed E of Maquoketa section, about 1 mile NW of Fort Atkinson, Iowa.

Mackenzie Mountains District.

102. Esbataottine Mtn., Sunblood Mtn. Lower Esbataottine Fm. Specimens from sections on Esbataottine Mtn. and Sunblood Mtn., District of Mackenzie, North West Territories. Horizons A110, A115, A125, P1485 and P1512 of Chatterton and Ludvigsen 1976; Chatterton 1980).

APPENDIX FOUR
PAUP NEXUS FILES

This appendix presents the PAUP nexus files used in phylogenetic analysis of *Achatella* Delo (Chapter 5) and *Calyptaulax* Cooper (Chapter 6).

A4. 1. *Achatella.*

Phylogenetic analysis of *Achatella* was performed using a two stage process. In the first instance, the 20 stratigraphical samples were used as the operational taxonomic units (OTU's), and the resulting "sample-based" cladogram was used to identify a set of species. These species then became the OTU's for a second cladistic analysis (Chapter 5). The ancestor in both cases is *Pterygometopus sclerops* from the Arenig Expansus Limestone, Östergötland, Sweden (Chapter 5).

A4. 1. 1. Nexus File for Phylogenetic Analysis of *Achatella* Stratigraphical Samples.

```
#NEXUS
[!Achatella samples]

begin data;
        dimensions ntax = 21  nchar = 15;
        format labelpos = left  symbol = "012";
        matrix

PSCLEROPS       00000 00000 00000
HIGHMAIN        11111 01??? ?????
PROSSER         11000 011?0 10001
KNOCK           11011 00111 01000
QHILL           11111 0110? 00001
CINC            11000 011?2 10001
STARBED         11111 01102 00001
COBOURG         11000 011?2 11?01
CRINBED         11101 1?1?? ??00?
KILLEY          11001 11102 00101
TRENTON         11000 01112 11001
UTICA           11000 011?2 10001
VERULAM         11000 01112 11001
LORRAINE        11000 0110? 10001
HULL            11000 0111? 10?01
MJØSA           11000 00112 00??0
KILN            11000 00102 10001
KUKRUSE         11010 00011 00011
LANGØYENE       11111 0???? ?????
?BODA           11000 01110 00?01
FURUBERG        11000 0011? 00?01
        ;
end;

begin assumptions;
        typeset allunord = unord:all;
```

```
        ancstates allZero = 0:all;
end;

begin trees;
        translate
        1       P.SCLEROPS,
        2       HIGHMAIN,
        3       PROSSER,
        4       KNOCK,
        5       QHILL,
        6       CINC,
        7       STARBED,
        8       COBOURG,
        9       CRINBED,
        10      KILLEY,
        11      TRENTON,
        12      UTICA,
        13      VERULAM,
        14      LORRAINE,
        15      HULL,
        16      MJØSA,
        17      KILN,
        18      KUKRUSE,
        19      LANGØYENE,
        20      ?BODA,
        21      FURUBERG
        ;
end;

begin paup;
        set maxtrees = 1000;
end;
```

A4. 1. 2. Nexus File for Phylogenetic Analysis of *Achatella* Species.

```
#NEXUS
[!Achatella species]

begin data;
        dimensions ntax = 11  nchar = 15;
        format labelpos = left  symbol = "012";
        matrix

P.sclerops              00000 00000 00000
A.achates               11000 01112 11001
A.kuckersiana           11010 00011 00011
A.sp.A                  11011 00111 01000
A.sp.B                  11000 00112 00?01
A.consobrina            11000 00102 10001
A.truncatocaudata       11001 11102 00101
A.cf.truncatocaudata    11101 1?1?? ??00?
A.retardata             11111 01102 00001
A.schmidti              11000 01110 00?01
A.sp.C                  11000 011?0 10001
        ;
end;
```

```
begin assumptions;
        typeset allunord = unord:all;
        ancstates allZero = 0:all;
end;

begin trees;
        translate
        1       P.sclerops,
        2       A.achates,
        3       A.kuckersiana,
        4       A.sp.A,
        5       A.sp.B,
        6       A.consobrina,
        7       A.truncatocaudata,
        8       A.cf.truncatocaudata,
        9       A.retardata,
        10      A.schmidti,
        11      A.sp.C
        ;
end;

begin paup;
        set maxtrees = 1000;
end;
```

A4. 2. *Calyptaulax.*

Phylogenetic analysis of *Calyptaulax* was performed using a two stage process similar to that employed for *Achatella.* In the first instance, the 40 stratigraphical samples were used as the operational taxonomic units (OTU's), and the resulting "sample-based" cladogram was used to identify a set of species. These species then became the OTU's for a second cladistic analysis (Chapter 6). The ancestor in both cases is *Pterygometopus sclerops* from the Arenig Expansus Limestone, Östergötland, Sweden (Chapter 6).

A4. 2. 1. Nexus File for Phylogenetic Analysis of *Calyptaulax* Stratigraphical Samples.

```
#NEXUS
[!Calyptaulax samples]

begin data;
        dimensions ntax = 41  nchar = 11;
        format labelpos = left  symbol = "0123";
        matrix

P.SCLEROPS          00000 00000 0
CONFINIS_A          1200? 00112 1
CONFINIS_B          11000 01000 0
STINCHAR            12000 00112 1
DOULARG             120?? 0???? 1
DOW_HILL            11000 00000 1
BALCLATCHIE_A       11000 00000 1
BALCLATCHIE_B       320?? 02112 1
```

```
KIRKCOLM          11000 0??00  1
ARDMILLAN         11000 00000  1
PINMERY           320?? 02112  1
KILN              11000 00000  1
STARFISH          11001 12112  ?
BARDAHESSIAGH     11000 00000  1
CROWN_POINT       11000 01001  1
ESBATAOTTINE      11010 02101  2
DUCK              11010 00000  2
CANNON            11010 0????  2
TRENTON           11010 00000  2
ELKADER           11010 00000  2
ATHENS            110?0 02101  2
VERULAM           11010 00000  2
BELLEVILLE        1101? 0????  2
LINDSAY           11010 0????  2
FAIRMOUNT         1101? 0????  2
MAQUOKETA         11010 00000  1
FT.ATKINSON       11010 00000  1
MATAPEDIA         2200? 12112  1
ACTON             2210? 12112  1
DUFTON(ONN)       220?? 1?112  ?
DUFTON(PUS)       221?? 12112  1
APPLETHWAITE      221?? 12112  ?
SHOLESHOOK        220?? 12112  ?
RHIWLAS           220?? 12112  ?
DDOLHIR           22001 12112  1
SOLVANG           22001 12112  1
VENSTØP           2200? 12112  1
GAGNUM            2200? 12112  ?
SØRBAKKEN         2200? 12112  ?
KJØRRVEN          22001 12112  ?
HUSBERGØYA        22001 1????  ?
        ;
end;

begin assumptions;
        typeset allunord = unord:all;
        ancstates allZero = 0:all;
end;

begin trees;
        translate
        1       P.SCLEROPS,
        2       CONFINIS_A,
        3       CONFINIS_B,
        4       STINCHAR,
        5       DOULARG,
        6       DOW_HILL,
        7       BALCLATCHIE_A,
        8       BALCLATCHIE_B,
        9       KIRKCOLM,
        10      ARDMILLAN,
        11      PINMERY,
        12      KILN,
        13      STARFISH,
        14      BARDAHESSIAGH,
        15      CROWN_POINT,
        16      ESBATAOTTINE,
```

```
        17      DUCK,
        18      CANNON,
        19      TRENTON,
        20      ELKADER,
        21      ATHENS,
        22      VERULAM,
        23      BELLEVILLE,
        24      LINDSAY,
        25      FAIRMOUNT,
        26      MAQUOKETA,
        27      FT.ATKINSON,
        28      MATAPEDIA,
        29      ACTON,
        30      DUFTON(ONN),
        31      DUFTON(PUS),
        32      APPLETHWAITE,
        33      SHOLESHOOK,
        34      RHIWLAS,
        35      DDOLHIR,
        36      SOLVANG,
        37      VENSTØP,
        38      GAGNUM,
        39      SØRBAKKEN,
        40      KJØRRVEN,
        41      HUSBERGØYA
        ;
end;

begin paup;
        set maxtrees = 1000;
end;
```

A4. 2. 2. Nexus File for Phylogenetic Analysis of *Calyptaulax* Species.

```
#NEXUS
[!Calyptaulax species]

begin data;
        dimensions ntax = 12  nchar = 11;
        format labelpos = left  symbol = "0123";
        matrix

P.sclerops          00000 00000 0
C.foederatus        12000 00112 1
C.hunteri           320?? 02112 1
C.asteroideus       11001 12112 ?
C.glabella          22001 12112 1
C.actonensis        2210? 12112 1
C.marginatus        11000 01000 0
C.annulata          11000 01001 1
C.callirachis       11010 02101 2
C.brongniartii      11000 00000 1
C.callicephala      11010 00000 2
C.larrabeei         11010 00000 1
        ;
end;
```

```
begin assumptions;
        typeset allunord = unord:all;
        ancstates allZero = 0:all;
end;

begin trees;
        translate
        1       P.sclerops,
        2       C.foederatus,
        3       C.hunteri,
        4       C.asteroideus,
        5       C.glabella,
        6       C.actonensis,
        7       C.marginatus,
        8       C.annulata,
        9       C.callirachis,
        10      C.brongniartii,
        11      C.callicephala,
        12      C.larrabeei
        ;
end;

begin paup;
        set maxtrees = 1000;
end;
```

APPENDIX FIVE
MORPHOMETRIC DATA

This appendix contains the morphometric data obtained on *Achatella*, *Calyptaulax*, *Acernaspis* and *Ananaspis*. The appendix is in four parts. Section A5. 1 presents the measurements made on a single cephalon of *Calyptaulax (Calliops) brongniartii* and a single pygidium of *Ananaspis stokesii* in order to test the reproducibility of the methods used. Section A5. 2 presents morphometric data on *Achatella* Delo. Section A5. 3 presents morphometric data on *Calyptaulax* Cooper. Section A5. 4 presents morphometric data on *Acernaspis* Campbell and *Ananaspis* Campbell. Because of the size of the morphometric data bases on these three genera, they are presented on a separate computer disk.

A5. 1. Measurements made for Reproducibility Tests.

Ten measurements were made on each of 20 enlarged prints made from 20 photographs of a single cephalon of *Calyptaulax (Calliops) brongniartii* from the Kilbucho locality. The method is described in Chapter 4 and the measurements are defined in Chapter 6 (see Figure 6. 9 and Table 6. 4). The measurements b5, b32, C1 and C2 can be made on both the left and right hand sides of the cephalon; only the measurements made on the right hand side were used in the production of the summary given in Table 4. 1. All measurements are in mm.

	B	b5	b32	k5	k32	k21	k10	J	C1	C2
1st trial	8.16	4.03	2.52	7.39	7.16	4.55	3.74	11.53	4.08	8.73
2nd trial	8.12	4.01	2.55	7.36	7.08	4.58	3.73	11.47	4.01	8.64
3rd trial	8.16	4.03	2.52	7.31	7.13	4.61	3.75	11.49	4.08	8.69
4th trial	8.11	3.96	2.53	7.35	7.11	4.63	3.86	11.5	4.05	8.63
5th trial	8.12	3.94	2.47	7.41	7.17	4.6	3.9	11.48	3.99	8.6
6th trial	8.07	3.96	2.48	7.39	7.2	4.68	3.86	11.64	4.01	8.64
7th trial	8.02	3.94	2.52	7.4	7.16	4.6	3.84	11.58	3.99	8.64
8th trial	8.11	4.03	2.45	7.34	7.15	4.61	3.74	11.52	4.03	8.64
9th trial	8.12	4.02	2.45	7.41	7.17	4.58	3.77	11.52	4.02	8.69
10th trial	8.11	3.96	2.48	7.4	7.16	4.73	3.82	11.55	4.01	8.64
11th trial	8.12	4.01	2.53	7.4	7.16	4.68	3.72	11.55	4.06	8.64
12th trial	8.02	4.01	2.51	7.39	7.24	4.64	3.87	11.68	4.11	8.69
13th trial	8.06	4.01	2.53	7.45	7.16	4.67	3.72	11.51	4.05	8.64
14th trial	8.12	3.96	2.53	7.35	7.16	4.63	3.72	11.5	4.01	8.59
15th trial	8.11	3.98	2.5	7.4	7.2	4.66	3.75	11.57	4.03	8.69
16th trial	8.15	4	2.51	7.44	7.29	4.73	3.82	11.64	4.05	8.69
17th trial	8.12	4.09	2.49	7.44	7.2	4.56	3.85	11.57	4.09	8.7

18th trial	8.06	3.98	2.5	7.39	7.2	4.66	3.8	11.57	3.98	8.64
19th trial	8.11	4.01	2.49	7.52	7.27	4.79	3.86	11.77	4.06	8.74
20th trial	8.1	3.98	2.57	7.47	7.27	4.71	3.83	11.74	4.07	8.78

Four measurements were made on a single cephalon of *Ananaspis stokesii* from the Dudley locality. The pygidium was measured 20 times. The method is described in Chapter 4 and the measurements are defined in Chapter 7 (see Figure 7. 5 and Table 7. 2). All measurements are in mm.

	Y1	**Z1**	**W**	**X**		**Y1**	**Z1**	**W**	**X**
1st trial	3.6	4.45	10.8	3.1	11th trial	3.7	4.55	10.8	3.2
2nd trial	3.65	4.4	10.7	3.15	12th trial	3.65	4.5	10.85	3.2
3rd trial	3.65	4.5	10.75	3.15	13th trial	3.75	4.6	10.7	3.2
4th trial	3.65	4.55	10.8	3.1	14th trial	3.75	4.7	10.8	3.1
5th trial	3.7	4.6	10.75	3.05	15th trial	3.7	4.55	10.65	3.2
6th trial	3.65	4.45	10.8	3.15	16th trial	3.65	4.5	10.75	3.15
7th trial	3.7	4.55	10.7	3.05	17th trial	3.65	4.45	10.7	3.2
8th trial	3.7	4.6	10.8	3.2	18th trial	3.7	4.6	10.7	3.15
9th trial	3.7	4.55	10.75	3.1	19th trial	3.7	4.5	10.8	3.1
10th trial	3.8	4.65	10.85	3.2	20th trial	3.75	4.55	10.75	3.15

A5. 2. Morphometric Data on *Achatella* Delo.

The raw morphometric data on *Achatella* are presented on the accompanying 3 1/2 inch Macintosh format computer disk. There are four files of raw data for *Achatella.* They are:

Ach_cranid_xl: A Microsoft Excel version 4.0 document containing the measurements made on cephala and cranidia of *Achatella.*

Ach_cranid_txt: An ASCII format document containing the same data as Ach_cranid_xl, readable using any Macintosh application capable of opening text format documents.

Ach_pyg_xl: A Microsoft Excel version 4.0 document containing the measurements made on pygidia of *Achatella.*

Ach_pyg_txt: An ASCII format document containing the same data as Ach_pyg_xl.

All four files have the same format. There is one row of data for each specimen:

Field 1: specimen number.

Field 2: locality name.

Field 3: name of the stratigraphical sample to which the specimen is assigned.

Remaining fields: hold the morphometric data.

Missing values are represented by *. Measurements derived using axial symmetry of the specimen (*i.e.* where a structure is present on one side of the specimen but missing on the other) are in italics. All measurements are in mm. Refer to Figure 5. 11 and Table 5. 4 for definition of the measurement scheme.

A5. 3. Morphometric Data on *Calyptaulax* Cooper.

The raw morphometric data on *Calyptaulax* are presented on the accompanying 3 1/2 inch Macintosh format computer disk. There are four files of raw data for *Calyptaulax*. They are:

Caly_cranid_xl
Caly_cranid_txt
Caly_pyg_xl
Caly_pyg_txt

The format of the files is as for *Achatella*. All measurements are in mm. Refer to Figure 6. 9 and Table 6. 4 for definition of the measurement scheme.

A5. 4. Morphometric Data on *Acernaspis* Campbell and *Ananaspis* Campbell.

The raw morphometric data on *Acernaspis* and *Ananaspis* are presented on the accompanying 3 1/2 inch Macintosh format computer disk. There are four files of raw data for these two genera. They are:

AcAn_cranid_xl
AcAn_cranid_txt
AcAn_pyg_xl
AcAn_pyg_txt

The format of the files is as for *Achatella*. All measurements are in mm. Refer to Figure 7. 5 and Table 7. 2 for definition of the measurement scheme.

APPENDIX SIX
EIGENVALUE AND EIGENVECTOR OUTPUT FROM PRINCIPAL COMPONENT ANALYSES

This appendix presents the eigenvalue and eigenvector output from the principal component analyses performed on the study genera. Section A6. 1 presents output for analyses performed on *Achatella* Delo, Section A6. 2. presents output for analyses performed on *Calyptaulax*, and Section A6. 3 presents output for analyses performed on *Acernaspis* and *Ananaspis*. The associated principal component scores are presented in Appendix 7.

A6. 1. *Achatella*.

Three separate PCA analyses were done on *Achatella* : PCA on the "glabella data set", the "cephalon data set", and the "pygidium data set" (Chapter 5).

A6. 1. 1. Glabella Data Set.

Principal Component Analysis of Glabella Data Set
67 total cases of which 1 is missing

EigenValues	Values	Variance Proportion	Cumulative Variance Proportion
e1	22.321	89.3	89.3
e2	0.831	3.3	92.6
e3	0.539	2.2	94.8
e4	0.411	1.6	96.4
e5	0.176	0.7	97.1
e6	0.155	0.6	97.7
e7	0.126	0.5	98.2
e8	0.105	0.4	98.6
e9	0.082	0.3	98.9
e10	0.061	0.2	99.1
e11	0.051	0.2	99.3
e12	0.044	0.2	99.5
e13	0.022	0.1	99.6
e14	0.019	0.1	99.7
e15	0.016	0.1	99.8
e16	0.013	0.1	99.9
e17	0.008	0	99.9
e18	0.007	0	99.9
e19	0.005	0	99.9
e20	0.004	0	99.9
e21	0.003	0	99.9
e22	0.002	0	99.9
e23	0.001	0	99.9
e24	0	0	99.9
e25	0	0	99.9

EigenVectors

	V1	V2	V3	V4	V5
b5 left	-0.199	0.134	-0.325	-0.274	-0.015
b5 right	-0.195	0.135	-0.368	-0.307	-0.027
b32 left	-0.203	-0.152	0.061	0.028	-0.348
b32 right	-0.203	-0.124	0.08	0.069	-0.279
b21 left	-0.201	-0.118	-0.067	-0.092	0.222
b21 right	-0.2	-0.123	-0.14	-0.1	0.41
b10 left	-0.197	-0.287	-0.07	0.114	0.353
b10 right	-0.197	-0.279	-0.021	0.184	0.257
B	-0.21	-0.079	-0.11	-0.086	-0.096
k5	-0.205	0.17	0.084	-0.129	0.01
k32	-0.205	0.193	0.177	-0.027	-0.041
k21	-0.205	0.184	0.207	-0.017	0.033
k10	-0.204	0.181	0.24	0.031	0.044
k33	-0.202	0.193	0.191	-0.059	-0.065
k22	-0.205	0.191	0.205	-0.01	-0.022
k11	-0.204	0.166	0.254	0.082	0.071
k00	-0.201	0.211	0.261	0.037	0.118
b!5 left	-0.205	-0.009	-0.163	-0.289	-0.118
b!5 right	-0.204	-0.001	-0.2	-0.316	-0.113
b!32 left	-0.176	0.219	-0.439	0.539	-0.125
b!32 right	-0.184	0.272	-0.265	0.462	-0.035
b!21 left	-0.205	-0.136	0.101	-0.015	0.2
b!21 right	-0.2	-0.213	0.045	0.15	0.211
b!10 left	-0.193	-0.38	0.056	0.095	-0.281
b!10 right	-0.194	-0.348	0.111	0.055	-0.382

	V6	V7	V8	V9	V10
b5 left	-0.035	0.042	0.003	0.06	0.143
b5 right	-0.061	0.289	-0.044	0.266	0.05
b32 left	-0.257	-0.141	0.005	0.038	-0.412
b32 right	-0.155	-0.444	0.134	-0.255	-0.164
b21 left	0.428	-0.437	-0.208	-0.101	0.302
b21 right	0.364	-0.146	-0.014	-0.254	-0.379
b10 left	-0.204	0.273	0.271	-0.255	-0.138
b10 right	-0.103	0.357	0.168	-0.027	0.056
B	-0.045	-0.016	-0.061	0.049	-0.017
k5	-0.057	0.003	0.18	-0.212	0.306
k32	-0.041	-0.017	0.177	-0.16	0.188
k21	0.09	0.029	-0.028	0.044	-0.023
k10	0.135	0.106	-0.028	0.113	-0.252
k33	-0.094	-0.006	0.377	-0.246	0.244
k22	0.062	0.036	-0.079	0.048	0.062
k11	0.074	0.103	-0.09	0.172	-0.061
k00	0.112	0.109	-0.116	0.195	-0.288
b!5 left	-0.109	-0.023	-0.078	-0.048	-0.166
b!5 right	-0.032	-0.009	0.036	0.001	-0.131
b!32 left	0.264	-0.146	0.42	0.282	-0.03
b!32 right	-0.228	0.095	-0.585	-0.401	0.057
b!21 left	-0.313	-0.174	-0.216	0.21	0.155
b!21 right	-0.3	-0.296	-0.012	0.462	0.187
b!10 left	0.24	0.241	-0.126	0.025	0.26

b!10 right	0.305	0.202	-0.085	-0.001	0.067
	V11	**V12**	**V13**	**V14**	**V15**
b5 left	0.032	0.366	-0.129	0.031	0.311
b5 right	0.022	-0.203	-0.005	-0.104	-0.199
b32 left	-0.009	-0.464	0.108	-0.282	-0.113
b32 right	-0.17	0.417	-0.12	-0.027	0.096
b21 left	-0.432	-0.101	0.102	-0.108	-0.288
b21 right	0.48	-0.195	-0.096	-0.041	0.267
b10 left	0.015	0.211	-0.021	0.242	-0.519
b10 right	-0.509	-0.138	-0.014	-0.283	0.464
B	0	0.032	0.006	0.075	-0.006
k5	0.215	0.054	0.619	-0.311	0.014
k32	0.034	-0.1	-0.236	0.167	0.272
k21	-0.044	-0.107	-0.333	-0.017	-0.133
k10	-0.067	0.075	0.128	-0.129	0.08
k33	0.127	-0.226	-0.059	0.068	-0.128
k22	-0.048	-0.119	-0.321	0.074	-0.025
k11	-0.066	0.108	-0.115	-0.086	-0.167
k00	-0.032	0.326	0.331	0.09	0.002
b!5 left	-0.092	0.084	-0.003	0.013	-0.005
b!5 right	-0.15	0.038	-0.027	0.096	-0.067
b!32 left	-0.017	-0.054	0.076	0.141	-0.026
b!32 right	0.063	-0.016	0.006	-0.036	-0.001
b!21 left	0.004	-0.22	0.191	0.529	0.125
b!21 right	0.32	0.128	-0.108	-0.243	0.016
b!10 left	0.272	0.171	-0.192	-0.245	-0.126
b!10 right	0.066	-0.067	0.223	0.392	0.147
	V16	**V17**	**V18**	**V19**	**V20**
b5 left	0.086	0.097	0.114	0.052	0.209
b5 right	0.077	0.389	-0.056	0.011	0.086
b32 left	0.031	0.153	0.005	-0.027	-0.091
b32 right	0.185	0.277	0.012	-0.068	0.206
b21 left	-0.103	0.064	-0.04	0.079	-0.06
b21 right	0.007	0.065	0.085	-0.101	0.052
b10 left	0.15	-0.019	-0.066	0.068	-0.102
b10 right	-0.043	0.033	0.109	0.008	0.03
B	-0.095	-0.182	-0.012	-0.009	-0.064
k5	0.38	-0.115	0.038	-0.107	-0.108
k32	-0.13	0.053	-0.4	-0.144	-0.562
k21	0.32	-0.151	-0.077	0.243	0.182
k10	0.013	-0.31	-0.514	0.187	0.349
k33	-0.521	0.066	0.211	0.159	0.393
k22	0.414	0.112	0.293	0.188	-0.228
k11	-0.072	-0.187	0.358	-0.711	0.075
k00	-0.301	0.446	0.076	0.189	-0.228
b!5 left	-0.182	-0.41	0.153	0.131	-0.207
b!5 right	-0.127	-0.202	-0.153	-0.184	-0.075
b!32 left	0.048	-0.052	-0.031	-0.061	-0.029
b!32 right	-0.094	-0.044	0.008	0.062	0.022
b!21 left	0.113	0.107	-0.19	-0.239	0.249
b!21 right	-0.131	-0.182	0.107	0.257	-0.133
b!10 left	-0.101	0.171	-0.303	-0.161	0.04

b!10 right	0.068	-0.151	0.274	0.187	0.006
	V21	**V22**	**V23**	**V24**	**V25**
b5 left	0.295	-0.114	-0.555	0	0
b5 right	0.201	0.208	0.455	0	0
b32 left	0.184	-0.071	-0.402	0	0
b32 right	0.008	0.125	0.35	0	0
b21 left	0.172	-0.019	-0.087	0	0
b21 right	-0.05	0.012	0.084	0	0
b10 left	0.184	-0.053	-0.103	0	0
b10 right	-0.144	0.034	0.041	0	0
B	-0.149	-0.025	0.04	0.895	0.184
k5	-0.135	0.037	0.001	0	0
k32	0.283	0.167	0.017	0	0
k21	-0.288	0.598	-0.249	0	0
k10	0.288	-0.287	0.163	0	0
k33	-0.056	-0.106	0.015	0	0
k22	-0.125	-0.586	0.139	0	0
k11	0.216	0.079	0.014	0	0
k00	-0.21	0.089	-0.112	0	0
b!5 left	-0.096	0.033	0.125	-0.376	0.563
b!5 right	-0.394	-0.13	-0.006	-0.123	-0.664
b!32 left	-0.113	-0.035	-0.03	-0.075	0.112
b!32 right	0.009	0.024	0.032	-0.024	-0.129
b!21 left	-0.17	-0.067	-0.046	-0.127	0.189
b!21 right	0.098	0.058	0.116	-0.044	-0.237
b!10 left	-0.264	-0.141	-0.092	-0.129	0.193
b!10 right	0.265	0.178	0.093	-0.042	-0.224

A6. 1. 2. Cephalon Data Set.

Principal Component Analysis of Cephalon Data Set
67 total cases of which 22 are missing

EigenValues	**Values**	**Variance Proportion**	**Cumulative Variance Proportion**
e1	32.393	90	90
e2	1.101	3.1	93.1
e3	0.725	2	95.1
e4	0.461	1.3	96.4
e5	0.301	0.8	97.2
e6	0.191	0.5	97.7
e7	0.13	0.4	98.1
e8	0.114	0.3	98.4
e9	0.11	0.3	98.7
e10	0.084	0.2	98.9
e11	0.065	0.2	99.1
e12	0.056	0.2	99.3
e13	0.048	0.1	99.4
e14	0.042	0.1	99.5
e15	0.032	0.1	99.6
e16	0.026	0.1	99.7

e17	0.024	0.1	99.8
e18	0.019	0.1	99.9
e19	0.016	0	99.9
e20	0.013	0	99.9
e21	0.011	0	99.9
e22	0.009	0	99.9
e23	0.007	0	99.9
e24	0.006	0	99.9
e25	0.004	0	99.9
e26	0.004	0	99.9
e27	0.003	0	99.9
e28	0.002	0	99.9
e29	0.001	0	99.9
e30	0.001	0	99.9
e31	0.001	0	99.9
e32	0	0	99.9
e33	0	0	99.9
e34	0	0	99.9
e35	0	0	99.9
e36	0	0	99.9

EigenVectors

	V1	V2	V3	V4	V5	V6
b5 left	-0.165	-0.156	0.315	-0.001	0.084	0.084
b5 right	-0.164	-0.153	0.317	-0.025	0.239	0.076
b32 left	-0.168	0.151	0.01	-0.104	0.051	-0.311
b32 right	-0.168	0.141	0.01	-0.054	-0.179	-0.27
b21 left	-0.167	0.103	0.089	0.051	-0.139	0.397
b21 right	-0.166	0.14	0.148	-0.043	-0.156	0.389
b10 left	-0.161	0.316	0.044	-0.033	-0.082	-0.002
b10 right	-0.165	0.293	-0.058	0.006	-0.048	-0.077
b!5 left	-0.171	-0.02	0.221	-0.092	0.164	0.031
b!5 right	-0.17	-0.031	0.258	-0.081	0.164	0.03
b!32 left	-0.153	-0.159	0.152	0.312	-0.631	-0.129
b!32 right	-0.157	-0.165	0.01	0.361	-0.367	0.089
b!21 left	-0.169	0.184	-0.037	0.012	0.178	0.06
b!21 right	-0.166	0.226	-0.021	-0.003	-0.014	-0.026
b!10 left	-0.161	0.303	-0.043	-0.171	-0.156	-0.04
b!10 right	-0.162	0.283	-0.076	-0.219	-0.134	-0.078
k5	-0.17	-0.143	-0.023	0.013	0.131	-0.116
k32	-0.171	-0.149	-0.133	0.033	0.014	-0.192
k21	-0.171	-0.128	-0.167	-0.024	0.041	0.087
k10	-0.17	-0.119	-0.202	-0.056	0.006	0.182
k33	-0.169	-0.151	-0.097	0.025	0.089	-0.298
k22	-0.171	-0.136	-0.18	-0.029	0.031	0.025
k11	-0.17	-0.102	-0.233	-0.063	0.017	0.167
k00	-0.167	-0.137	-0.233	-0.081	0.027	0.277
B	-0.174	0.066	0.122	-0.047	0.021	0.006
J1	-0.17	0.056	-0.18	0.049	0.04	-0.026
J4	-0.166	-0.182	-0.194	0.1	0.068	-0.263
J5	-0.17	-0.067	-0.233	-0.079	-0.029	-0.068
Jb	-0.172	-0.018	-0.133	-0.068	0.012	-0.054
K	-0.166	-0.147	-0.241	-0.095	0.004	0.273
C1 left	-0.165	-0.225	0.21	-0.077	-0.001	-0.064

C1 right	-0.165	-0.218	0.242	-0.039	0.009	-0.131
C2 left	-0.172	-0.006	0.179	-0.191	-0.031	-0.024
C2 right	-0.172	0.003	0.172	-0.194	-0.03	-0.043
F left	-0.157	0.193	-0.014	0.507	0.28	-0.009
F right	-0.156	0.192	0.033	0.519	0.266	0.054

	V7	**V8**	**V9**	**V10**	**V11**	**V12**
b5 left	0.045	0.002	0.095	0.068	0.102	-0.236
b5 right	0.042	0.199	-0.066	-0.053	-0.111	-0.257
b32 left	-0.141	-0.066	-0.449	-0.218	-0.202	0.162
b32 right	-0.111	-0.404	-0.183	-0.043	0.141	-0.02
b21 left	0.273	-0.198	0.189	-0.043	-0.302	-0.089
b21 right	0.013	-0.112	0.252	-0.174	-0.067	0.496
b10 left	-0.279	-0.064	0.305	0.081	0.469	-0.04
b10 right	-0.04	0.095	0.168	0.032	0.342	-0.259
b!5 left	-0.097	-0.054	-0.131	-0.13	0.071	0.034
b!5 right	0.029	-0.059	-0.129	-0.162	0.082	-0.067
b!32 left	0.389	-0.128	-0.183	0.06	0.082	-0.072
b!32 right	-0.655	0.269	-0.026	-0.092	-0.194	-0.148
b!21 left	-0.084	-0.007	-0.075	0.372	-0.264	-0.208
b!21 right	0.015	-0.088	-0.073	0.68	-0.173	0.105
b!10 left	0.054	0.433	0.026	-0.043	-0.092	0.061
b!10 right	0.196	0.328	-0.068	-0.253	-0.038	0.071
k5	-0.115	-0.219	0.337	-0.102	-0.079	-0.016
k32	0.008	-0.059	0.076	0.015	-0.014	-0.054
k21	0.043	0.046	-0.053	-0.007	0.021	0.025
k10	-0.011	-0.018	-0.116	-0.087	0.131	0.102
k33	0.048	-0.217	0.192	-0.042	0.029	0.187
k22	0.036	0.069	-0.016	-0.017	-0.032	-0.057
k11	-0.019	0.028	-0.056	0.107	0.094	-0.028
k00	-0.08	-0.071	-0.166	0.045	0.223	0.046
B	-0.015	0.041	-0.101	-0.003	-0.02	-0.016
J1	-0.191	-0.196	0.13	-0.126	-0.351	0.095
J4	0.173	0.224	0.258	-0.036	0.023	0.027
J5	0.199	0.135	0.126	-0.007	-0.076	-0.177
Jb	0.069	-0.072	0.089	-0.015	-0.186	-0.144
K	0.027	-0.046	-0.306	0.02	0.205	-0.013
C1 left	-0.044	0.194	0.079	0.203	0.058	0.354
C1 right	-0.028	0.2	0.002	0.237	0.067	0.324
C2 left	-0.01	-0.091	0.043	-0.056	-0.016	-0.18
C2 right	0.024	-0.112	-0.012	-0.049	-0.053	-0.162
F left	0.116	0.016	-0.156	0.007	0.043	0.163
F right	0.13	0.062	-0.017	-0.167	0.123	0.001

	V13	**V14**	**V15**	**V16**	**V17**	**V18**
b5 left	0.037	0.272	0.051	0.198	-0.042	0.076
b5 right	-0.15	-0.059	-0.14	-0.049	0.151	-0.256
b32 left	-0.093	-0.168	0.034	-0.274	0.089	-0.041
b32 right	0.356	0.21	0.276	0.068	-0.031	0.042
b21 left	0.349	-0.383	0.166	-0.064	-0.216	0.049
b21 right	-0.265	0.125	0.125	-0.081	0.313	0.083
b10 left	-0.196	-0.244	0.027	0.169	0.152	-0.204
b10 right	-0.029	-0.101	-0.025	-0.428	-0.259	-0.046
b!5 left	0.002	-0.031	0.168	0.09	-0.021	0.29

b!5 right	-0.059	-0.045	0.1	0.079	0.015	0.06
b!32 left	-0.268	0.009	-0.227	-0.028	0.004	-0.068
b!32 right	0.079	-0.048	0.087	0.071	0.034	0.138
b!21 left	-0.286	-0.102	-0.092	-0.049	0.052	0.133
b!21 right	0.073	0.147	-0.074	0.029	0.179	0.187
b!10 left	0.294	0.169	-0.181	0.248	0.068	-0.186
b!10 right	-0.084	-0.017	-0.184	0.155	-0.197	0.277
k5	0.096	0.097	-0.524	0.068	-0.245	0.247
k32	0.009	-0.093	0.07	0.048	0.151	0.087
k21	0.151	-0.225	-0.063	-0.026	0.136	-0.146
k10	-0.092	0.082	-0.143	-0.248	-0.011	-0.007
k33	0.096	-0.266	-0.165	0.139	0.204	-0.037
k22	0.089	-0.231	-0.052	-0.09	0.242	-0.005
k11	0.143	-0.051	0.054	-0.154	0.002	-0.014
k00	-0.159	0.244	-0.024	-0.078	-0.231	0.133
B	-0.024	-0.002	0.013	0.086	0.012	0.139
J1	-0.175	0.185	-0.089	-0.021	-0.263	-0.304
J4	-0.22	0.074	0.269	0.057	0.129	0.288
J5	-0.002	0.062	0.362	-0.111	-0.056	0.085
Jb	-0.121	0.284	0.262	0.142	-0.002	-0.471
K	0.068	-0.03	-0.111	0.39	0.048	-0.108
C1 left	0.136	-0.051	0.026	-0.03	-0.159	-0.183
C1 right	0.097	0.011	0.083	-0.222	-0.267	-0.109
C2 left	0.016	0.068	-0.052	-0.028	0.035	-0.027
C2 right	-0.04	-0.02	-0.062	-0.09	0.036	-0.011
F left	-0.144	-0.205	0.134	0.313	-0.35	-0.073
F right	0.307	0.34	-0.127	-0.263	0.289	-0.025

	V19	**V20**	**V21**	**V22**	**V23**	**V24**
b5 left	0.072	0.28	-0.057	0.092	0.104	-0.134
b5 right	-0.007	-0.064	-0.208	-0.181	-0.023	0.084
b32 left	0.135	-0.154	-0.091	0.095	-0.18	0.142
b32 right	0.057	0.189	0.144	-0.208	0.004	0.031
b21 left	0.044	-0.221	-0.048	-0.203	0.081	0.06
b21 right	0.09	0.135	0.026	0.209	0.006	0.068
b10 left	-0.098	-0.046	-0.017	-0.181	-0.23	0.041
b10 right	0.055	-0.007	-0.017	0.188	0.221	0.018
b!5 left	-0.156	-0.043	-0.1	0.009	-0.064	-0.194
b!5 right	-0.277	-0.025	-0.06	0.07	-0.01	-0.113
b!32 left	-0.124	-0.003	-0.016	0.014	-0.116	-0.086
b!32 right	0.087	-0.097	-0.024	0.04	0.04	0.005
b!21 left	-0.023	-0.017	0.403	-0.021	0.125	-0.063
b!21 right	0.018	-0.023	-0.25	-0.012	-0.067	0.039
b!10 left	-0.078	0.017	-0.307	0.057	0.087	0.104
b!10 right	0.093	0.027	0.243	-0.138	0.042	-0.287
k5	0.157	0.007	-0.02	0.165	-0.388	0.142
k32	0.031	0.204	-0.027	0.198	0.514	-0.056
k21	0.118	0.35	-0.019	-0.31	-0.16	-0.111
k10	0.161	0.091	-0.128	0.082	0.247	0.045
k33	-0.054	-0.32	-0.19	0.046	0.286	-0.163
k22	0.053	0.47	0.094	-0.075	-0.161	0.026
k11	-0.147	-0.127	-0.054	0.298	-0.293	-0.539
k00	0.134	-0.175	-0.251	-0.364	0.066	0.028
B	-0.119	-0.023	-0.042	0.014	-0.007	-0.107

J1	-0.539	0.176	0.051	-0.184	0.114	-0.069
J4	0.019	-0.191	0.05	-0.344	-0.048	0.129
J5	-0.288	0.044	-0.054	0.297	-0.243	0.33
Jb	0.424	-0.193	0.023	0.079	-0.102	-0.248
K	-0.17	-0.203	0.294	0.161	0.072	0.372
C1 left	0.093	-0.121	0.462	0.061	-0.022	-0.042
C1 right	-0.117	0.064	-0.078	-0.104	0.044	0.113
C2 left	0.118	-0.045	0.124	0.043	0.07	0.158
C2 right	0.112	-0.012	0.048	0.003	0.026	0.199
F left	0.215	0.195	-0.129	0.173	-0.036	0.102
F right	-0.09	-0.159	0.221	-0.08	-0.009	-0.01

	V25	**V26**	**V27**	**V28**	**V29**	**V30**
b5 left	0.122	-0.252	-0.048	-0.068	-0.298	0.236
b5 right	-0.008	-0.034	0.074	-0.234	0.015	0.248
b32 left	-0.033	-0.075	0.152	-0.048	-0.18	0.112
b32 right	0.041	-0.027	-0.021	-0.092	-0.227	0.085
b21 left	0.058	0.006	0.153	0.013	-0.078	-0.067
b21 right	-0.167	-0.044	-0.053	0.049	-0.083	0.197
b10 left	0.201	0.196	0.193	-0.099	-0.004	-0.034
b10 right	-0.246	-0.285	-0.175	0.221	0.077	0.065
b!5 left	0.034	-0.001	-0.08	0.145	0.347	-0.143
b!5 right	-0.086	0.133	-0.067	0.201	-0.116	-0.339
b!32 left	-0.035	0.053	-0.001	0.01	-0.019	-0.073
b!32 right	0.046	-0.014	-0.114	0.032	0.062	0.04
b!21 left	0.052	0.214	-0.102	0.094	-0.421	0.001
b!21 right	0.054	-0.159	-0.016	-0.02	0.34	-0.014
b!10 left	-0.135	0.032	0.037	-0.004	-0.288	-0.234
b!10 right	0.147	0.079	-0.02	-0.057	0.189	0.26
k5	-0.032	0.125	0.131	0.127	-0.067	-0.012
k32	-0.197	0.363	0.499	-0.102	0.172	0.043
k21	0.085	0.031	-0.125	0.134	0.142	0.257
k10	0.685	-0.062	0.042	-0.03	-0.064	-0.343
k33	0.057	-0.037	-0.473	-0.039	-0.112	0.159
k22	-0.274	-0.066	-0.176	0.061	-0.014	-0.335
k11	-0.064	-0.199	0.308	-0.183	-0.141	0.106
k00	-0.376	0.268	-0.144	-0.223	-0.078	-0.002
B	-0.002	0.052	-0.055	0.097	0.051	-0.133
J1	-0.017	-0.213	0.033	-0.081	0.128	-0.018
J4	-0.014	-0.392	0.226	0.083	-0.126	-0.132
J5	0.183	0.305	-0.289	-0.215	0.048	0.152
Jb	0.012	0.146	-0.05	0.325	0.134	-0.087
K	-0.043	-0.183	0.089	0.247	0.069	0.185
C1 left	-0.075	-0.009	-0.106	-0.36	0.048	-0.242
C1 right	0.086	0.186	0.142	0.418	-0.054	0.216
C2 left	-0.01	-0.101	-0.012	-0.304	0.235	-0.085
C2 right	-0.048	-0.114	0.05	0.034	0.173	-0.035
F left	-0.026	-0.082	-0.016	-0.158	0.02	-0.033
F right	0.023	0.158	0.019	0.008	0.102	0.022

	V31	**V32**	**V33**	**V34**	**V35**	**V36**
b5 left	0.312	-0.389	0.139	0.08	0	0
b5 right	0.012	0.315	-0.354	-0.293	0	0
b32 left	0.219	-0.355	-0.02	0.111	0	0

b32 right	-0.123	0.303	-0.198	-0.196	0	0
b21 left	0.147	-0.089	-0.048	0.008	0	0
b21 right	-0.097	0.096	-0.087	-0.035	0	0
b10 left	0.173	-0.074	0.085	0.023	0	0
b10 right	-0.046	-0.069	-0.236	-0.074	0	0
b!5 left	0.029	-0.033	-0.098	-0.045	0.105	-0.662
b!5 right	-0.189	-0.068	-0.072	0.026	-0.529	0.402
b!32 left	-0.025	-0.046	-0.043	0.017	0.022	-0.136
b!32 right	-0.021	0.04	0.042	-0.009	-0.105	0.08
b!21 left	-0.157	0.062	0.019	0.056	0.036	-0.228
b!21 right	0.089	-0.05	-0.096	-0.057	-0.205	0.156
b!10 left	-0.168	-0.039	0.03	0.022	0.038	-0.241
b!10 right	0.191	0.122	0.03	-0.045	-0.185	0.14
k5	-0.048	-0.001	-0.161	-0.057	0	0
k32	0.004	-0.116	-0.08	-0.058	0	0
k21	-0.496	-0.361	-0.059	0.111	0	0
k10	-0.009	0.06	-0.072	-0.082	0	0
k33	0.056	0.104	0.119	0.028	0	0
k22	0.474	0.233	0.066	0.022	0	0
k11	-0.123	0.221	0.157	0.036	0	0
k00	0.058	-0.074	0.107	0.028	0	0
B	-0.05	-0.02	-0.049	-0.007	0.786	0.47
J1	0.057	-0.077	0.03	0.001	0	0
J4	-0.123	-0.016	-0.042	0.031	0	0
J5	0.005	-0.053	0.007	-0.058	0	0
Jb	0.109	0.018	-0.046	-0.002	0	0
K	0.094	-0.008	-0.088	-0.009	0	0
C1 left	-0.027	-0.237	-0.128	-0.216	0	0
C1 right	0.105	0.269	0.165	0.215	0	0
C2 left	-0.155	0.197	0.012	0.744	0	0
C2 right	-0.219	0.034	0.728	-0.395	0	0
F left	-0.118	0.156	0.116	0.036	0	0
F right	0.078	-0.053	0.124	0.033	0	0

A6. 1. 3. Pygidium Data Set.

Principal Component Analysis of Pygidium Data Set
103 total cases of which 44 are missing

EigenValues

	Values	Variance Proportion	Cumulative Variance Proportion
e1	3.379	84.5	84.5
e2	0.498	12.5	97
e3	0.086	2.2	99.2
e4	0.036	0.9	100.1

EigenVectors

	V1	V2	V3	V4
W	-0.494	-0.568	-0.08	-0.654
Z1	-0.514	-0.419	0.15	0.734
Axial Rings	-0.501	0.464	-0.728	0.064
Pleural Ribs	-0.492	0.535	0.664	-0.175

A6. 2. *Calyptaulax.*

Two separate PCA analyses were undertaken on *Calyptaulax* : PCA on the "cranidium data set" and the "pygidium data set" (Chapter 6).

A6. 2. 1. Cranidium Data Set.

Principal Component Analysis of Cranidium Data Set
192 total cases of which 39 are missing

EigenValues

	Values	Variance Proportion	Cumulative Variance Proportion
e1	29.163	85.8	85.8
e2	1.139	3.3	89.1
e3	0.792	2.3	91.4
e4	0.645	1.9	93.3
e5	0.557	1.6	94.9
e6	0.374	1.1	96
e7	0.289	0.9	96.9
e8	0.209	0.6	97.5
e9	0.167	0.5	98
e10	0.135	0.4	98.4
e11	0.105	0.3	98.7
e12	0.09	0.3	99
e13	0.064	0.2	99.2
e14	0.05	0.1	99.3
e15	0.044	0.1	99.4
e16	0.036	0.1	99.5
e17	0.028	0.1	99.6
e18	0.02	0.1	99.7
e19	0.02	0.1	99.8
e20	0.019	0.1	99.9
e21	0.011	0	99.9
e22	0.009	0	99.9
e23	0.007	0	99.9
e24	0.006	0	99.9
e25	0.006	0	99.9
e26	0.004	0	99.9
e27	0.003	0	99.9
e28	0.002	0	99.9
e29	0.002	0	99.9
e30	0.002	0	99.9
e31	0.001	0	99.9
e32	0.001	0	99.9
e33	0	0	99.9
e34	0	0	99.9

EigenVectors

	V1	V2	V3	V4	V5	V6
b5 left	-0.175	-0.166	0.119	0.215	0.187	-0.101
b5 right	-0.175	-0.155	0.141	0.206	0.19	-0.097

b32 left	-0.176	0.093	0.175	-0.184	0.044	0.092
b32 right	-0.177	0.086	0.11	-0.196	0.046	0.096
b21 left	-0.153	0.165	-0.27	0.365	-0.369	-0.212
b21 right	-0.153	0.153	-0.202	0.44	-0.333	-0.056
b10 left	-0.161	0.151	0.159	-0.317	-0.205	-0.435
b10 right	-0.159	0.132	0.18	-0.308	-0.126	-0.537
b!5 left	-0.179	-0.059	0.211	0.07	0.125	-0.044
b!5 right	-0.179	-0.066	0.207	0.06	0.126	-0.052
b!32 left	-0.172	0.01	-0.075	-0.075	0.085	0.154
b!32 right	-0.168	0.07	-0.105	-0.054	0.08	0.151
b!21 left	-0.169	0.269	-0.094	0.1	-0.031	-0.102
b!21 right	-0.173	0.192	-0.041	0.122	-0.002	-0.062
b!10 left	-0.143	-0.478	0.11	-0.069	-0.432	0.133
b!10 right	-0.145	-0.431	0.093	-0.078	-0.478	0.134
k5	-0.183	0.001	-0.058	0.049	0.047	0.084
k32	-0.183	0.068	-0.031	-0.032	0.01	0.115
k21	-0.181	0.126	-0.039	-0.003	-0.063	0.167
k10	-0.18	0.133	0.011	-0.09	-0.024	0.169
k33	-0.183	0.052	-0.053	-0.024	0.024	0.134
k22	-0.178	-0.012	-0.075	0.034	0.064	0.112
k11	-0.179	0.137	0.003	-0.105	-0.014	0.197
k00	-0.18	0.129	-0.038	-0.064	-0.021	0.171
B	-0.183	-0.051	0.116	0.038	0.035	-0.001
J	-0.183	0.018	-0.1	-0.06	0.046	0.013
J4	-0.177	0.034	-0.112	-0.109	-0.007	0.162
J5	-0.175	0.141	-0.03	-0.164	-0.065	0.142
C1 left	-0.175	-0.139	0.143	0.219	0.147	-0.049
C1 right	-0.167	-0.118	0.203	0.293	0.167	-0.103
C2 left	-0.181	-0.068	0.049	-0.009	0.068	-0.061
C2 right	-0.183	-0.055	0.087	0.033	0.081	-0.102
Pl	-0.136	-0.294	-0.548	-0.215	0.141	-0.271
Pr	-0.148	-0.279	-0.438	-0.107	0.243	-0.122

	V7	**V8**	**V9**	**V10**	**V11**	**V12**
b5 left	0.012	-0.166	0.099	0.06	0.03	-0.101
b5 right	0.008	-0.138	0.054	0.013	0.061	-0.09
b32 left	-0.08	0.113	-0.323	0.072	-0.044	0.339
b32 right	-0.119	0.137	-0.132	0.047	-0.021	0.408
b21 left	-0.181	-0.059	0.141	-0.209	0.334	0.336
b21 right	-0.051	-0.094	-0.539	0.103	-0.176	-0.189
b10 left	-0.04	0.047	-0.191	0.061	-0.155	-0.385
b10 right	-0.022	-0.064	0.226	-0.242	0.077	-0.027
b!5 left	0.028	-0.066	-0.163	0.028	0.144	0.158
b!5 right	0.047	-0.034	-0.163	0.026	0.1	0.175
b!32 left	-0.527	-0.015	0.092	0.068	-0.282	-0.104
b!32 right	-0.664	0.069	0.142	-0.045	0.058	-0.167
b!21 left	0.122	0.309	0.345	0.097	-0.093	0.175
b!21 right	0.209	0.036	0.174	0.24	-0.549	0.108
b!10 left	0.033	0.039	-0.004	0.019	-0.239	-0.014
b!10 right	-0.003	0.129	0.179	-0.001	0.106	0.062
k5	0.105	-0.016	0.095	-0.059	-0.011	-0.099
k32	0.084	0.027	-0.004	-0.021	-0.019	0.003
k21	0.095	0.076	0.018	0.01	0.154	-0.112
k10	0.157	0.11	-0.046	-0.028	0.213	-0.134

k33	0.073	0.043	-0.007	-0.02	0.017	-0.029
k22	0.164	0.012	0.292	-0.16	-0.256	0.026
k11	0.142	0.128	-0.04	0.028	0.186	-0.174
k00	0.127	0.118	-0.056	0.002	0.215	-0.203
B	-0.048	0.011	-0.03	0.046	-0.001	0.105
J	0.058	0.03	-0.054	-0.048	-0.105	0.035
J4	0.107	-0.445	0.104	0.015	0.033	-0.044
J5	0.086	-0.389	0.002	-0.093	0.075	-0.038
C1 left	-0.007	-0.159	0.123	-0.009	0.005	-0.22
C1 right	-0.016	0.471	0.011	-0.016	0.12	-0.18
C2 left	-0.041	-0.322	-0.029	0.034	-0.025	0.186
C2 right	-0.057	-0.051	-0.085	0.03	-0.019	0.131
Pl	0.041	0.045	0.004	0.594	0.227	0.021
Pr	0.094	0.146	-0.254	-0.63	-0.166	0.024

	V13	**V14**	**V15**	**V16**	**V17**	**V18**
b5 left	0.037	-0.053	0.152	0.168	0.128	-0.105
b5 right	-0.001	0.033	-0.094	0.039	-0.07	0.313
b32 left	-0.118	-0.087	-0.062	-0.012	-0.058	0.139
b32 right	0.118	0.068	0.175	0.06	0.157	-0.215
b21 left	-0.058	0.381	-0.069	-0.103	0.142	0.115
b21 right	-0.074	-0.339	0.205	0.076	-0.082	-0.122
b10 left	0.384	0.209	0.009	-0.11	0.28	0.272
b10 right	-0.439	-0.22	0.122	0.061	-0.282	-0.209
b!5 left	0.032	-0.011	0.046	0.078	0.033	-0.061
b!5 right	-0.059	0.037	-0.014	0.035	0.047	0.135
b!32 left	-0.473	-0.046	-0.166	-0.048	0.26	0.302
b!32 right	0.332	0.019	0.102	0.14	-0.266	-0.262
b!21 left	0.369	-0.293	-0.2	0.211	-0.097	0.152
b!21 right	-0.162	0.17	-0.249	0.176	0.004	-0.196
b!10 left	-0.011	0.445	-0.042	0.064	-0.309	-0.12
b!10 right	0.063	-0.498	-0.063	0.03	0.241	0.079
k5	-0.016	-0.042	-0.02	-0.364	-0.373	0.151
k32	0.027	-0.002	0.003	-0.299	-0.052	-0.024
k21	-0.104	0.107	0.153	0.078	0.084	0.13
k10	-0.14	0.066	-0.014	0.163	0.018	-0.063
k33	-0.026	-0.11	0.021	-0.317	-0.107	0.056
k22	-0.004	0.058	0.704	-0.06	0.257	0.053
k11	-0.083	0.088	0.068	0.162	-0.009	0.006
k00	-0.069	0.115	-0.064	0.303	-0.148	0.13
B	0.001	-0.007	-0.038	0.076	0.015	0.019
J	0.103	-0.026	-0.023	-0.377	-0.096	-0.15
J4	0.103	-0.094	-0.148	-0.049	-0.053	0.148
J5	0.065	-0.027	-0.299	-0.102	0.351	-0.447
C1 left	0.049	0.014	-0.083	0.155	0.076	-0.131
C1 right	-0.063	0.033	-0.178	-0.317	0.144	-0.241
C2 left	0.157	0.016	0.046	0.066	-0.162	0.138
C2 right	0.082	-0.004	0.077	-0.094	-0.137	0.011
Pl	-0.088	0.025	0.078	-0.031	0.035	-0.088
Pr	0.049	-0.035	-0.168	0.219	0.062	0.037

	V19	**V20**	**V21**	**V22**	**V23**	**V24**
b5 left	0.284	0.008	0.318	0.135	0.07	0.052
b5 right	-0.231	-0.299	0.03	0.111	-0.01	0.11

b32 left	-0.386	-0.117	-0.338	0.057	-0.104	0.009
b32 right	0.204	0.362	0.14	-0.166	0.037	-0.021
b21 left	0.054	0.044	-0.078	0.06	-0.061	0.074
b21 right	-0.07	0.007	0.049	-0.085	0.002	0.022
b10 left	0.038	0.063	0.013	0.092	-0.034	0.004
b10 right	-0.071	0.048	0.01	-0.042	0.021	0.004
b!5 left	-0.033	0.091	0.11	0.291	-0.242	-0.051
b!5 right	-0.096	0.038	0.316	-0.092	-0.167	0.061
b!32 left	0.146	-0.032	0.141	-0.2	0.003	0.038
b!32 right	-0.147	-0.038	-0.03	0.259	-0.051	-0.03
b!21 left	-0.15	-0.103	0.236	-0.323	0.051	0.091
b!21 right	0.112	0.06	-0.156	0.419	-0.003	-0.111
b!10 left	-0.178	-0.038	0.192	-0.192	0.068	0.112
b!10 right	0.174	-0.007	-0.162	0.209	-0.064	-0.102
k5	0.129	0.079	0.227	0.116	-0.29	-0.331
k32	0.037	0.203	-0.052	-0.07	0.075	0.043
k21	-0.222	0.062	0.111	-0.052	0.303	-0.663
k10	0.121	-0.141	0.114	-0.059	0.114	0.103
k33	-0.018	0.199	0.087	0.225	0.339	0.528
k22	-0.206	-0.166	-0.141	-0.002	-0.154	0.124
k11	0.148	-0.062	-0.072	0.061	0.115	0.113
k00	0.244	-0.054	-0.236	-0.029	-0.336	0.15
B	-0.046	0.026	0.148	0.076	-0.121	0.003
J	0.255	-0.217	-0.059	-0.248	-0.349	-0.076
J4	-0.204	0.383	-0.098	0.046	0.071	0.016
J5	-0.176	-0.367	0.137	-0.039	-0.019	0.004
C1 left	-0.058	0.376	-0.364	-0.433	-0.137	0.025
C1 right	-0.134	-0.001	-0.173	0.007	0.18	-0.067
C2 left	0.243	-0.167	-0.265	-0.092	0.324	-0.141
C2 right	0.269	-0.286	-0.157	-0.075	0.336	-0.041
P1	-0.107	-0.01	-0.016	-0.024	-0.041	0.015
Pr	-0.005	0.063	0.023	0.068	0.073	-0.05

	V25	**V26**	**V27**	**V28**	**V29**	**V30**
b5 left	0.019	0.195	0.124	0.365	0.017	-0.06
b5 right	-0.033	0.11	0.169	0.393	-0.079	-0.055
b32 left	0.174	-0.039	0.015	0.31	0.065	-0.054
b32 right	0.231	0.199	0.155	0.157	-0.07	-0.201
b21 left	0.028	-0.029	-0.042	0.089	0.019	-0.019
b21 right	0.056	0.081	-0.01	-0.024	-0.044	0.007
b10 left	0.059	-0.039	-0.012	0.006	0.043	0.009
b10 right	-0.056	0.07	0.023	0.002	-0.045	-0.014
b!5 left	-0.192	-0.138	-0.099	-0.244	0.022	0.106
b!5 right	-0.15	-0.065	-0.129	-0.284	-0.025	0.09
b!32 left	-0.005	0.02	-0.038	-0.097	-0.037	0.019
b!32 right	-0.066	-0.038	-0.032	-0.002	0.05	0.075
b!21 left	0.012	-0.002	-0.026	-0.049	-0.057	0.005
b!21 right	-0.059	-0.059	-0.002	0.017	0.06	0.015
b!10 left	-0.003	0.062	0.002	-0.013	-0.029	-0.024
b!10 right	-0.023	-0.062	0.01	0.038	0.022	0.022
k5	0.544	-0.167	-0.029	-0.004	-0.091	-0.076
k32	-0.206	-0.027	0.261	0.192	-0.321	0.73
k21	-0.306	-0.117	0.2	0.027	0.083	-0.181
k10	0.24	-0.057	-0.21	0.12	0.629	0.371

k33	-0.13	-0.308	0.156	-0.108	0.135	-0.341
k22	0.104	0.049	-0.027	-0.151	0.014	0.044
k11	-0.058	-0.073	-0.559	0.184	-0.541	-0.143
k00	-0.024	0.225	0.491	-0.273	-0.059	-0.105
B	-0.117	-0.064	-0.084	-0.17	0.005	0.073
J	-0.495	0.112	-0.185	0.202	0.23	-0.207
J4	-0.027	0.522	-0.205	-0.05	0.168	-0.018
J5	0.153	-0.102	0.167	-0.101	-0.177	-0.07
C1 left	0.064	-0.449	-0.023	0.101	0.067	-0.081
C1 right	0.13	0.374	-0.084	-0.228	-0.027	-0.028
C2 left	0.087	0.038	-0.153	-0.284	-0.094	0.062
C2 right	0.03	-0.119	0.158	-0.092	0.094	0.008
Pl	0.055	-0.047	0.014	-0.022	-0.017	0.023
Pr	0.01	-0.026	-0.006	0.011	-0.028	0.011

	V31	**V32**	**V33**	**V34**
b5 left	-0.31	-0.455	-0.004	0
b5 right	0.192	0.528	0.013	0
b32 left	-0.222	-0.34	-0.001	0
b32 right	0.142	0.357	0.003	0
b21 left	-0.019	-0.072	-0.001	0
b21 right	0.029	0.09	0	0
b10 left	-0.024	-0.02	0.002	0
b10 right	0	0.044	-0.001	0
b!5 left	0.081	0.014	0.703	-0.001
b!5 right	0.026	-0.038	-0.498	0.517
b!32 left	0.009	-0.027	0.188	0
b!32 right	0	0.019	-0.127	0.137
b!21 left	-0.028	-0.095	0.178	0
b!21 right	0.043	0.085	-0.121	0.129
b!10 left	-0.031	-0.081	0.137	0
b!10 right	0.032	0.079	-0.091	0.099
k5	0.007	-0.023	-0.009	0
k32	-0.055	-0.009	0.001	0
k21	-0.06	-0.007	-0.001	0
k10	-0.021	0.162	0.018	0
k33	-0.164	0.066	0.002	0
k22	0.025	-0.01	0	0
k11	0.135	-0.056	-0.002	0
k00	-0.051	-0.056	-0.016	0
B	0.027	0.002	-0.362	-0.829
J	-0.08	0.064	0.006	0
J4	0.229	-0.143	0.004	0
J5	-0.016	-0.004	-0.001	0
C1 left	0.025	-0.002	-0.007	0
C1 right	-0.068	0.003	0.014	0
C2 left	-0.507	0.243	0.019	0
C2 right	0.638	-0.32	-0.019	0
Pl	-0.002	0.017	0	0
Pr	0.01	-0.016	0	0

A6. 2. 2. Pygidium Data Set.

Principal Component Analysis of Pygidium Data Set
256 total cases of which 64 are missing

EigenValues

	Values	Variance Proportion	Cumulative Variance Proportion
e1	2.948	73.7	73.7
e2	0.884	22.1	95.8
e3	0.135	3.4	99.2
e4	0.033	0.8	100

EigenVectors

	V1	V2	V3	V4
W	0.539	-0.25	-0.804	-0.019
Z1	0.566	-0.144	0.407	0.702
Y1	0.57	-0.045	0.414	-0.708
Axial Rings	0.253	0.956	-0.129	0.067

A6. 3. *Acernaspis* and *Ananaspis*.

Three separate PCA analyses have been undertaken on *Acernaspis* and *Ananaspis* : PCA on the "cephalon data set", the "glabellar furrow data set", and the "pygidium data set" (Chapter 7).

A6. 3. 1. Cephalon Data Set.

Principal Component Analysis of Cephalon Data Set
171 total cases of which 58 are missing

EigenValues

	Values	Variance Proportion	Cumulative Variance Proportion
e1	25.158	86.8	86.8
e2	1.256	4.3	91.1
e3	0.694	2.4	93.5
e4	0.363	1.3	94.8
e5	0.329	1.1	95.9
e6	0.247	0.9	96.8
e7	0.212	0.7	97.5
e8	0.169	0.6	98.1
e9	0.103	0.4	98.5
e10	0.09	0.3	98.8
e11	0.082	0.3	99.1
e12	0.065	0.2	99.3
e13	0.055	0.2	99.5
e14	0.042	0.1	99.6
e15	0.026	0.1	99.7
e16	0.022	0.1	99.8
e17	0.02	0.1	99.9
e18	0.016	0.1	100

e19	0.01	0	100
e20	0.007	0	100
e21	0.007	0	100
e22	0.006	0	100
e23	0.005	0	100
e24	0.004	0	100
e25	0.003	0	100
e26	0.003	0	100
e27	0.002	0	100
e28	0.002	0	100
e29	0.001	0	100

EigenVectors

	V1	**V2**	**V3**	**V4**	**V5**	**V6**
B	-0.197	0.032	-0.01	-0.019	0.011	0.041
J	-0.197	0.039	-0.051	0.034	0.074	-0.14
J4	-0.197	0.089	-0.005	0	0.111	-0.073
J5	-0.195	0.089	0.001	0.029	0.139	-0.17
Pl	-0.159	-0.086	-0.604	-0.115	-0.297	-0.248
Pr	-0.167	-0.164	-0.49	-0.027	-0.146	-0.177
b21 left	-0.176	-0.188	0.236	-0.322	-0.434	0.051
b21 right	-0.173	-0.252	0.299	-0.224	-0.293	0.033
b!21 left	-0.172	-0.36	0.235	0.136	-0.142	-0.195
b!21 right	-0.175	-0.354	0.184	0.131	-0.135	-0.046
b10 left	-0.18	-0.014	0.055	0.606	0.009	0.122
b10 right	-0.18	-0.01	-0.032	0.526	-0.208	0.292
b!10 left	-0.17	0.396	-0.054	0.046	-0.332	0.14
b!10 right	-0.17	0.394	-0.043	-0.003	-0.332	0.073
k22	-0.195	-0.02	0.053	-0.111	0.114	0.107
k!22	-0.176	-0.027	-0.102	-0.324	0.142	0.675
k11	-0.197	-0.034	0.006	0.004	0.177	-0.052
k!11	-0.191	-0.073	0.067	-0.034	0.22	-0.159
k00	-0.195	-0.068	-0.025	-0.033	0.2	-0.056
K2	-0.197	0.067	-0.017	0.013	0.129	-0.099
K1	-0.196	0.09	0.023	-0.082	0.133	-0.117
K	-0.197	-0.027	-0.021	0.018	0.13	-0.077
k10	-0.196	-0.048	-0.017	-0.04	0.185	-0.041
C1 left	-0.195	0.025	-0.028	-0.059	0.111	0.155
C1 right	-0.195	0.033	-0.029	-0.078	0.113	0.123
C2 left	-0.194	-0.103	-0.076	0.026	0.071	0.119
C2 right	-0.195	-0.101	-0.079	0.03	0.055	0.124
Ramsk F left	-0.171	0.351	0.232	-0.041	-0.074	-0.211
Ramsk F right	-0.175	0.328	0.249	-0.089	-0.01	-0.201

	V7	**V8**	**V9**	**V10**	**V11**	**V12**
B	-0.137	-0.203	-0.081	0.134	-0.094	-0.001
J	0.003	-0.018	0.082	0.028	-0.007	-0.215
J4	-0.016	-0.041	0.094	0.12	0.056	-0.158
J5	0.044	-0.012	0.083	0.062	0.055	-0.17
Pl	0.148	-0.342	-0.13	-0.501	0.044	0.075
Pr	0.177	0.493	-0.127	0.572	0.004	0.021
b21 left	0.003	-0.09	0.184	0.152	0.408	-0.323
b21 right	-0.231	0.298	-0.333	-0.212	0.157	0.159
b!21 left	0.115	-0.183	0.135	0.062	-0.392	-0.242

b!21 right	0.145	0.005	0.045	-0.021	-0.385	0.393
b10 left	0.029	0.197	-0.522	-0.2	0.09	-0.336
b10 right	0.215	-0.131	0.403	0.074	0.359	0.274
b!10 left	-0.236	0.241	0.103	-0.053	-0.153	0.22
b!10 right	-0.261	0.047	0.135	-0.064	-0.243	-0.268
k22	0.063	0.162	0.019	-0.057	-0.266	0.07
k!22	0.474	0.068	-0.03	-0.14	-0.091	-0.163
k11	-0.042	0.14	0.201	-0.121	0.048	0
k!11	-0.033	0.037	-0.061	-0.101	0.395	0.066
k00	-0.127	0.137	0.185	-0.221	-0.011	0.057
K2	-0.028	-0.032	0.039	0.018	0.057	-0.049
K1	0.017	0.045	0.085	-0.029	-0.029	-0.011
K	-0.072	0.132	0.174	-0.153	0.015	0.016
k10	-0.04	0.175	0.182	-0.118	-0.001	0.028
C1 left	-0.181	-0.242	-0.178	0.242	0.013	0.244
C1 right	-0.168	-0.193	-0.195	0.2	0.052	0.183
C2 left	-0.218	-0.251	-0.102	0.082	-0.066	-0.052
C2 right	-0.213	-0.227	-0.105	0.115	-0.072	-0.056
Ramsk F left	0.42	-0.123	-0.208	0.083	-0.086	-0.055
Ramsk F right	0.287	-0.049	-0.151	0.004	0.102	0.314

	V13	**V14**	**V15**	**V16**	**V17**	**V18**
B	-0.045	0.087	0.199	0.086	-0.048	0.227
J	-0.09	0.288	-0.058	0.125	0.091	0.035
J4	-0.013	0.222	-0.196	0.075	-0.02	-0.151
J5	-0.086	0.3	-0.275	-0.172	-0.01	-0.123
Pl	-0.004	-0.044	-0.088	0.06	0.014	-0.05
Pr	0.003	-0.067	0.1	-0.038	-0.099	0.032
b21 left	0.032	-0.254	-0.199	0.053	0.294	0.157
b21 right	-0.301	0.311	0.121	0.043	-0.26	-0.199
b!21 left	0.171	-0.131	-0.033	-0.064	-0.332	-0.108
b!21 right	0.152	0.199	-0.095	-0.234	0.305	0.127
b10 left	0.034	-0.176	-0.202	0.003	0.098	0.11
b10 right	-0.136	0.059	0.147	0.142	-0.181	-0.149
b!10 left	0.19	0.119	-0.135	0.004	0.316	0.134
b!10 right	0.183	-0.096	0.19	-0.207	-0.327	-0.13
k22	0.128	-0.254	-0.062	0.737	0.056	-0.289
k!22	0.082	0.15	0	-0.202	-0.088	0.046
k11	-0.078	-0.203	0.124	-0.064	0.034	0.155
k!11	0.727	0.079	0.364	-0.063	0.033	-0.096
k00	-0.257	-0.274	0.091	-0.142	-0.118	0.019
K2	-0.032	0.252	-0.171	0.002	-0.06	-0.046
K1	0.018	0.214	-0.094	0.275	-0.079	0.179
K	-0.1	-0.091	-0.039	-0.198	0.215	-0.269
k10	-0.176	-0.21	0.043	-0.112	0.074	0.231
C1 left	-0.02	-0.192	-0.195	-0.112	0.057	-0.224
C1 right	0.038	-0.196	-0.228	-0.189	-0.069	-0.259
C2 left	-0.062	0.052	0.196	0.089	0.027	0.254
C2 right	-0.095	0.066	0.28	0.097	0.087	0.221
Ramsk F left	-0.26	-0.061	0.441	-0.063	0.344	-0.248
Ramsk F right	0.038	-0.175	-0.201	0.012	-0.386	0.416

	V19	**V20**	**V21**	**V22**	**V23**	**V24**
B	-0.056	-0.117	0.066	-0.298	0.318	0.035

J	-0.044	0.106	-0.225	-0.233	-0.422	0.211
J4	0.027	0.389	-0.108	-0.032	-0.369	-0.166
J5	0.146	0.123	0.608	-0.137	0.366	-0.108
Pl	0.054	-0.005	0.043	-0.015	-0.016	-0.003
Pr	-0.04	-0.005	-0.025	0.019	0.031	-0.001
b21 left	-0.121	-0.045	0.041	0.054	0.017	-0.051
b21 right	0.093	0.02	0.01	-0.048	-0.017	0.051
b!21 left	0.409	-0.037	-0.255	-0.012	0.128	0.028
b!21 right	-0.343	0.004	0.209	0.048	-0.203	-0.056
b10 left	-0.055	-0.072	0.009	-0.015	-0.017	-0.051
b10 right	0.003	-0.022	0.018	-0.025	0.007	-0.025
b!10 left	0.458	0.053	-0.192	0.056	0.114	-0.011
b!10 right	-0.369	-0.038	0.199	0.002	-0.141	-0.025
k22	-0.093	0.157	0.208	0.054	0.088	0.029
k!22	0.048	-0.001	-0.076	-0.016	0.02	0.017
k11	0.223	-0.219	0.321	0.009	-0.241	0.635
k!11	0.053	0.042	-0.004	-0.006	0.008	-0.101
k00	-0.054	0.022	-0.062	0.193	-0.103	-0.431
K2	-0.128	-0.184	-0.137	0.776	0.2	0.164
K1	-0.081	-0.668	-0.124	-0.189	-0.069	-0.246
K	-0.358	0.092	-0.418	-0.293	0.414	0.266
k10	0.216	0.13	0.027	-0.033	0.004	-0.279
C1 left	0.038	-0.241	-0.015	-0.12	-0.034	-0.139
C1 right	0.106	-0.037	0.001	0.02	-0.221	0.148
C2 left	-0.076	0.253	-0.016	0.169	0.088	0.074
C2 right	0.016	0.13	-0.016	0.044	0.025	-0.033
Ramsk F left	0.097	-0.08	-0.01	0.099	-0.043	-0.067
Ramsk F right	-0.136	0.261	-0.088	-0.056	0.062	0.118

	V25	**V26**	**V27**	**V28**	**V29**
B	0.298	-0.412	0.071	0.524	-0.057
J	-0.453	0.031	-0.287	0.334	-0.124
J4	0.597	-0.163	0.11	-0.164	0.123
J5	-0.234	-0.009	-0.019	-0.124	-0.002
Pl	0.063	0.012	0.007	0.007	0.018
Pr	-0.007	-0.024	-0.009	-0.044	-0.012
b21 left	-0.032	-0.054	0.015	0.011	0.003
b21 right	0.04	0.064	-0.028	-0.008	-0.013
b!21 left	-0.019	0.004	-0.035	-0.045	0.003
b!21 right	0.036	-0.018	0.039	0.037	0.008
b10 left	0.044	-0.036	0.01	0.014	0.007
b10 right	-0.032	0.047	0.029	0.017	-0.03
b!10 left	-0.07	-0.141	-0.011	-0.062	-0.014
b!10 right	0.02	0.174	-0.028	0.021	0.007
k22	-0.06	0.015	-0.012	0.073	0.005
k!22	-0.01	-0.039	-0.035	-0.009	0.008
k11	0.201	-0.113	-0.08	-0.171	0.076
k!11	-0.042	-0.007	-0.052	0.036	-0.018
k00	-0.254	-0.542	-0.083	-0.037	-0.005
K2	0.09	0.069	-0.071	0.245	0.068
K1	-0.011	0.117	0.242	-0.298	-0.056
K	0.038	0.057	0.091	-0.162	0.06
k10	0.184	0.604	0.093	0.363	-0.106
C1 left	0.132	0.128	-0.636	-0.066	0.03

C1 right	-0.236	-0.013	0.613	0.146	-0.098
C2 left	-0.017	0.078	-0.012	-0.399	-0.629
C2 right	-0.214	0.153	0.089	-0.157	0.719
Ramsk F left	0.012	0.001	0.049	-0.04	-0.064
Ramsk F right	-0.069	0.02	-0.074	-0.075	0.093

A6. 3. 2. Glabellar Furrow Data Set.

Principal Component Analysis
171 total cases of which 63 are missing

EigenValues

	Values	Variance Proportion	Cumulative Variance Proportion
e1	22.661	87.2	87.2
e2	1.052	4	91.2
e3	0.518	2	93.2
e4	0.395	1.5	94.7
e5	0.28	1.1	95.8
e6	0.246	0.9	96.7
e7	0.189	0.7	97.4
e8	0.158	0.6	98
e9	0.118	0.5	98.5
e10	0.093	0.4	98.9
e11	0.052	0.2	99.1
e12	0.049	0.2	99.3
e13	0.044	0.2	99.5
e14	0.04	0.2	99.7
e15	0.032	0.1	99.8
e16	0.019	0.1	99.9
e17	0.013	0.1	100
e18	0.011	0	100
e19	0.009	0	100
e20	0.007	0	100
e21	0.004	0	100
e22	0.004	0	100
e23	0.002	0	100
e24	0.001	0	100
e25	0.001	0	100
e26	0	0	100

EigenVectors

	V1	V2	V3	V4	V5	V6
b5 left	-0.204	0.091	0.072	-0.212	-0.162	-0.029
b5 right	-0.204	0.097	0.076	-0.215	-0.155	-0.021
b!5 left	-0.206	0.072	0.058	-0.194	-0.114	0.021
b!5 right	-0.207	0.058	0.054	-0.211	-0.101	0.006
b6 left	-0.207	0.074	0.085	-0.163	-0.087	-0.025
b6 right	-0.207	0.082	0.08	-0.178	-0.075	0.006
b!6 left	-0.206	0.05	0.113	-0.174	-0.119	-0.065
b!6 right	-0.206	0.059	0.089	-0.16	-0.096	-0.047
b32 left	-0.199	-0.043	0.081	-0.15	0.257	0.171
b32 right	-0.202	-0.015	0.088	-0.005	0.243	0.079

b!32 left	-0.197	0.078	0.077	0.031	0.279	0.485
b!32 right	-0.198	0.057	0.134	-0.006	0.186	0.468
b21 left	-0.183	-0.312	0.082	0.418	-0.152	0.25
b21 right	-0.177	-0.387	-0.039	0.148	-0.439	0.234
b!21 left	-0.179	-0.46	-0.113	-0.019	-0.021	-0.03
b!21 right	-0.181	-0.44	-0.097	0.044	0.068	-0.223
b10 left	-0.177	-0.03	-0.619	-0.279	0.004	-0.055
b10 right	-0.183	-0.016	-0.537	0.005	0.409	0.008
b!10 left	-0.182	0.353	-0.229	0.406	-0.149	-0.075
b!10 right	-0.18	0.378	-0.211	0.338	-0.241	0.083
k33	-0.208	0.039	0.036	0.002	0	-0.129
k!33	-0.207	0.026	0.053	0.052	-0.063	-0.161
k34	-0.206	0.037	0.052	0.084	-0.073	-0.206
k!34	-0.194	0.123	0.032	0.243	0.169	-0.04
k22	-0.203	-0.056	0.101	0.123	0.056	-0.292
k!22	-0.187	-0.025	0.304	0.223	0.378	-0.383

	V7	**V8**	**V9**	**V10**	**V11**	**V12**
b5 left	-0.046	0.184	0.051	-0.134	0.169	-0.294
b5 right	-0.004	0.146	0.052	-0.176	0.217	-0.29
b!5 left	-0.045	0.108	0.098	-0.061	-0.036	0.008
b!5 right	-0.031	0.089	0.102	-0.071	-0.043	-0.003
b6 left	-0.007	0.037	0.138	0.021	-0.146	0.177
b6 right	-0.035	0.041	0.118	0.025	-0.135	0.183
b!6 left	-0.052	0.027	0.027	0.082	-0.229	-0.012
b!6 right	-0.078	-0.022	0.092	0.044	-0.297	0.117
b32 left	-0.18	-0.226	-0.485	-0.236	-0.007	-0.215
b32 right	-0.288	-0.126	-0.327	0.171	-0.069	-0.287
b!32 left	0.141	-0.034	0.126	-0.2	-0.027	0.492
b!32 right	0.177	0.068	-0.058	0.23	0.279	0.042
b21 left	-0.09	0.305	0.154	0.377	-0.166	-0.229
b21 right	0.426	-0.11	-0.107	-0.338	0.08	-0.136
b!21 left	-0.341	-0.057	-0.013	0.177	-0.123	0.186
b!21 right	-0.226	-0.039	0.046	-0.415	0.04	0.223
b10 left	0.448	-0.128	-0.21	0.262	-0.243	-0.022
b10 right	-0.103	0.346	0.315	-0.076	0.222	-0.162
b!10 left	-0.137	0.017	-0.128	-0.249	0.072	0.108
b!10 right	-0.178	0.093	-0.252	-0.01	-0.217	0.074
k33	-0.027	-0.109	-0.029	0.165	0.19	0.075
k!33	0.035	-0.132	0.024	0.161	0.273	0.048
k34	0.068	-0.109	0.056	0.245	0.38	0.078
k!34	0.078	-0.628	0.5	-0.069	-0.203	-0.328
k22	0.116	-0.095	-0.191	0.148	0.246	0.227
k!22	0.416	0.385	-0.139	-0.133	-0.299	-0.073

	V13	**V14**	**V15**	**V16**	**V17**	**V18**
b5 left	-0.132	0.219	0.07	0.004	0.069	0.112
b5 right	-0.122	0.253	0.077	-0.08	0.188	0.123
b!5 left	-0.002	0.071	-0.055	0.266	0.149	-0.196
b!5 right	-0.04	0.065	-0.039	0.126	0.147	-0.263
b6 left	0.047	-0.056	-0.115	0.101	-0.158	0.069
b6 right	-0.031	-0.169	-0.075	-0.203	0.082	-0.007
b!6 left	0.114	-0.297	-0.159	-0.064	-0.224	0.226
b!6 right	0.26	-0.222	-0.013	-0.055	-0.075	-0.059

b32 left	0.032	-0.369	0.194	-0.325	0.257	-0.006
b32 right	0.311	0.347	-0.19	0.369	-0.303	0.006
b!32 left	0.212	0.294	0.285	0.04	0.11	0.072
b!32 right	-0.444	-0.102	-0.429	-0.087	-0.204	0.031
b21 left	0.248	0.088	-0.004	-0.264	0.293	0.036
b21 right	0.115	-0.212	0.045	0.236	-0.209	-0.101
b!21 left	-0.524	-0.009	0.159	0.125	0.022	-0.245
b!21 right	-0.004	0.248	-0.243	-0.2	-0.129	0.342
b10 left	0.007	0.253	-0.07	-0.165	0.102	0.053
b10 right	0.146	-0.355	0.085	0.177	-0.08	-0.023
b!10 left	0.056	0.059	-0.409	-0.254	0.027	-0.377
b!10 right	-0.27	-0.044	0.323	0.229	-0.07	0.357
k33	0.068	0.118	0.32	-0.187	-0.137	-0.371
k!33	0.091	0.017	0.243	-0.079	-0.321	-0.184
k34	0.058	-0.058	0.131	-0.155	-0.062	0.39
k!34	-0.188	0.006	-0.038	0.052	0.097	0.033
k22	0.105	-0.164	-0.204	0.415	0.547	0.079
k!22	-0.18	0.035	0.101	-0.032	-0.119	-0.084

	V19	**V20**	**V21**	**V22**	**V23**	**V24**
b5 left	0.153	-0.19	0.483	0.549	0.003	-0.141
b5 right	0.266	-0.146	-0.475	-0.389	-0.163	0.212
b!5 left	-0.433	0.27	0.246	-0.106	0.145	0.606
b!5 right	-0.323	0.233	-0.032	-0.232	-0.153	-0.719
b6 left	0.115	-0.03	-0.158	0.091	0.509	-0.017
b6 right	0.121	-0.093	-0.214	0.06	0.489	-0.113
b!6 left	0.079	0.12	0.047	0.008	-0.382	0.067
b!6 right	0.065	-0.241	0.063	0.011	-0.409	0.094
b32 left	-0.085	0.053	0.097	-0.051	0.133	0.009
b32 right	-0.043	-0.151	-0.137	0.001	0.091	-0.06
b!32 left	0.039	-0.165	0.067	0.003	-0.121	0.004
b!32 right	0.03	0.145	0.016	0.011	-0.111	0.029
b21 left	0.026	0.115	0.053	-0.032	0.07	-0.01
b21 right	-0.032	-0.077	-0.115	0.073	0.037	-0.018
b!21 left	0.002	-0.362	-0.006	-0.019	-0.083	0.054
b!21 right	0.003	0.325	0.043	-0.01	-0.022	-0.01
b10 left	0.003	0.015	0.064	-0.024	0.008	0.014
b10 right	0.032	-0.009	-0.063	0.021	0.008	-0.007
b!10 left	-0.045	-0.265	0.03	0.007	-0.036	0.042
b!10 right	0.032	0.233	-0.031	-0.025	0.002	-0.046
k33	0.025	0.396	-0.37	0.469	-0.14	0.096
k!33	0.345	0.089	0.449	-0.481	0.156	-0.045
k34	-0.597	-0.318	-0.061	-0.016	0.021	-0.034
k!34	0.02	0.042	0.005	0.029	0	0.007
k22	0.275	0.068	0.004	0.076	-0.074	-0.024
k!22	-0.075	-0.079	-0.005	-0.024	0.012	0.016

	V25	**V26**
b5 left	-0.016	0
b5 right	0.057	0
b!5 left	-0.097	0
b!5 right	0.057	0
b6 left	0.687	0
b6 right	-0.656	0

b!6 left	-0.033	-0.651
b!6 right	0.012	0.646
b32 left	0.163	0
b32 right	-0.163	0
b!32 left	-0.006	-0.191
b!32 right	0.008	0.191
b21 left	0.078	0
b21 right	-0.076	0
b!21 left	0.045	-0.147
b!21 right	-0.044	0.158
b10 left	0.021	0
b10 right	-0.021	0
b!10 left	0.072	-0.144
b!10 right	-0.056	0.137
k33	0.016	0
k!33	-0.041	0
k34	0.019	0
k!34	-0.006	0
k22	-0.004	0
k!22	-0.014	0

A6. 3. 3. Pygidium Data Set.

Principal Component Analysis
235 total cases of which 69 are missing

EigenValues

	Values	Variance Proportion	Cumulative Variance Proportion
e1	4.247	70.8	70.8
e2	0.98	16.3	87.1
e3	0.583	9.7	96.8
e4	0.123	2.1	98.9
e5	0.054	0.9	99.8
e6	0.013	0.2	100

EigenVectors

	V1	V2	V3	V4	V5	V6
W	-0.467	0.167	0.078	0.201	0.839	-0.06
X	-0.448	0.246	0.172	0.693	-0.479	0.014
Z1	-0.472	0.096	0.102	-0.502	-0.22	-0.677
Y1	-0.475	0.079	0.08	-0.456	-0.126	0.734
Axial Rings	-0.178	-0.876	0.438	0.095	0.012	-0.008
Pleural Ribs	-0.319	-0.359	-0.87	0.102	-0.051	-0.018

APPENDIX SEVEN
PRINCIPAL COMPONENT SCORE OUTPUT FROM PRINCIPAL COMPONENT ANALYSES

This appendix presents the principal component scores calculated from the morphometric data. Because of the size of the files, they are presented on the accompanying 3 1/2 inch Macintosh format computer disk.

A7. 1. PC Output for *Achatella*.

There are six files containing the PC score output for *Achatella*. They are:

Ach_glab_PC_xl: A Microsoft Excel version 4.0 document containing PC score output from PCA carried out on the glabella data set (see Section 5. 4. 2).

Ach_glab_PC_txt: An ASCII format document containing the same data as Ach_glab_PC_xl, readable using any Macintosh application capable of opening text format documents.

Ach_cranid_PC_xl: A Microsoft Excel version 4.0 document containing PC score output from PCA carried out on the cephalon data set (see Section 5. 4. 2).

Ach_cranid_PC_txt: An ASCII format document containing the same data as Ach_cranid_PC_xl.

Ach_pyg_PC_xl: A Microsoft Excel version 4.0 document containing PC score output from PCA carried out on the pygidium data set (see Section 5. 4. 2).

Ach_pyg_PC_txt: An ASCII format document containing the same data as Ach_pyg_PC_xl.

All six files have the same format. There is one row for each specimen:

Field 1: specimen number.

Field 2: locality name.

Field 3: name of the stratigraphical sample to which the specimen is assigned.

Remaining fields: hold the PC scores.

Some measurements used in the PCA calculation were unobtainable on some specimens due to quality of preservation, and these specimens therefore took no part in the PCA. They are represented by missing data characters (filled black circles).

A7. 2. PC Output for *Calyptaulax*.

There are four files containing the PC score output for *Calyptaulax*. They are:

Caly_cranid_PC_xl: A Microsoft Excel version 4.0 document containing PC score output from PCA carried out on the cranidium data set (see Section 6. 4. 2).

Caly_cranid_PC_txt: An ASCII format document containing the same data as Caly_cranid_PC_xl.

Caly_pyg_PC_xl: A Microsoft Excel version 4.0 document containing PC score output from PCA carried out on the pygidium data set (see Section 6. 4. 2).

Caly_pyg_PC_txt: An ASCII format document containing the same data as Caly_pyg_PC_xl.

The format of the files is as for *Achatella.*

A7. 3. PC Output for *Acernaspis* and *Ananaspis.*

There are six files containing the PC score output for *Acernaspis* and *Ananaspis.* They are:

AcAn_ceph_PC_xl: A Microsoft Excel version 4.0 document containing PC score output from PCA carried out on the cephalon data set (see Section 7. 4. 2).

AcAn_ceph_PC_txt: An ASCII format document containing the same data as AcAn_ceph_PC_xl.

AcAn_glab_PC_xl: A Microsoft Excel version 4.0 document containing PC score output from PCA carried out on the glabellar furrow data set (see Section 7. 4. 2).

AcAn_glab_PC_txt: An ASCII format document containing the same data as AcAn_glab_PC_xl.

AcAn_pyg_PC_xl: A Microsoft Excel version 4.0 document containing PC score output from PCA carried out on the pygidium data set (see Section 7. 4. 2).

AcAn_pyg_PC_txt: An ASCII format document containing the same data as AcAn_pyg_PC_xl.

The format of the files is as for *Achatella.*